Canadian Journal of Fisheries and Aquatic Sciences

Journal canadien des sciences halieutiques et aquatiques

Fisheries and Oceans
Pêches et Océans

Canada

Scientific Excellence • Resource Protection & Conservation • Benefits for Canadians

Excellence scientifique • Protection et conservation des ressources • Bénéfices aux Canadiens

The *Canadian Journal of Fisheries and Aquatic Sciences* has been published continuously since 1901, previously as *Contributions to Canadian Biology* 1901–25, *Contributions to Canadian Biology and Fisheries* 1926–34, *Journal of the Biological Board of Canada* 1934–37, and *Journal of the Fisheries Research Board of Canada* 1938–79.

Editorial Policy

The *Journal* publishes original research articles, critical reviews, perspectives (essays of opinion or hypothesis), and comments. Papers may concern cells, organisms, populations, ecosystems, or processes that affect aquatic production systems, and they should lead to identifiable conclusions or syntheses, which variously may amplify, modify, question, or redirect accumulated knowledge embodied in contemporary perceptions of a particular state of fisheries and aquatic sciences. They should demonstrate clearly a contribution to knowledge beyond the confirmation state. Originality should relate to more than the particular (a certain year, place, taxon, or chemical compound) such that existing understanding is reformulated or extended.

It would assist the Editors if prospective authors identified briefly by covering letter (a) aspects of their papers that meet the foregoing objectives, (b) potential referees, and (c) other manuscripts contemplated or in press containing the same or similar information.

Submissions in English or French are acceptable. The information must be original, that is, not copyrighted, published, or submitted elsewhere except in abstract form or unless by written consent of the Editor. The *Journal* accepts no responsibility for statements made by contributors. The use of proprietary names does not imply endorsement of the product or company.

A charge is made for manuscripts published. When submitting a manuscript, an author must state that the charge will be accepted.

Guides

Guides for authors and typists appear in the first issue of each volume and are available free from the *Journal*.

Subscriptions

The *Journal* is issued monthly to form annual volumes of twelve numbers plus Supplements. Orders and inquiries regarding subscriptions must be sent directly to Supply and Services Canada, Ottawa, Ontario, Canada K1A 0S9. Prepayment is required in Canadian funds to the order of "The Receiver General for Canada."

Microfilm

Issues from 1934 through the current volume can be purchased on 16- or 35-mm microfilm. Photocopies of individual articles or issues can be purchased from Xerox University Microfilms, 300 North Zeeb Road, Ann Arbor, Michigan 48106, USA.

Printed in Canada by: The Runge Press Limited, Ottawa

Imprimé au Canada par: The Runge Press Limited, Ottawa

Design: Ludvic Saleh & Associates, Ottawa

Conception graphique: Ludvic Saleh & Associates, Ottawa

Publié sans interruption depuis 1901, le *Journal canadien des sciences halieutiques et aquatiques* a paru sous plusieurs titres : *Contributions to Canadian Biology* 1901–1925, *Contributions to Canadian Biology and Fisheries* 1926–1934, *Journal of the Biological Board of Canada* 1934–1937 et *Journal de l'office des recherches sur les pêcheries du Canada* 1938–1979.

Politique de rédaction

Le *Journal* publie des articles fondés sur une recherche originale, des critiques, des essais portant sur une opinion ou une hypothèse (perspectives) et des commentaires. Les textes peuvent avoir trait aux cellules, aux organismes, aux populations, aux écosystèmes ou aux processus qui influent sur les systèmes de production aquatique. Ils doivent aboutir à des conclusions ou synthèses précises qui, de diverses façons, peuvent accroître, modifier, remettre en question ou réorienter le bagage actuel des connaissances et perceptions dans une discipline donnée des sciences aquatiques. Ils doivent clairement démontrer qu'ils contribuent aux connaissances en faisant plus que corroborer des faits. L'originalité doit dépasser le caractère particulier (une année, un endroit, un taxon ou un composé chimique donné) et tenir à une épuration ou à une reformulation des connaissances actuelles.

Les auteurs éventuels aideraient les rédacteurs s'ils identifiaient brièvement, dans une lettre d'accompagnement a) les aspects de leurs textes qui répondent particulièrement aux objectifs indiqués ci-dessus, b) des arbitres possibles et c) d'autres manuscrits envisagés ou sous presse, dont la teneur est identique ou se rapproche de celui qui est soumis.

Les contributions peuvent être en anglais ou en français. Elles doivent être originales, c.-à-d. qu'elles ne doivent pas avoir fait l'objet d'un copyright, avoir été publiées ou soumises ailleurs, sauf sous forme abrégée ou avec le consentement du rédacteur. Le *Journal* décline toute responsabilité quant aux énoncés des contributeurs. L'utilisation des noms de marques de commerce ne signifie aucunement une sanction du produit en question ou de la compagnie qui le fabrique.

Les manuscrits acceptés sont sujets à des frais de publication. Quand un auteur présente un texte, il doit préciser que ces frais seront acceptés. On trouvera dans une récente livraison du *Journal* les taux par page en vigueur.

Guides

Le guide des auteurs et celui des secrétaires d'auteurs paraissent dans la première livraison de chaque volume et sont offerts gratuitement par le *Journal*.

Abonnement

Le *Journal* paraît tous les mois, formant ainsi un volume de douze numéros, et offre en plus jusqu'à deux suppléments par année. On doit faire parvenir les commandes et demandes de renseignements concernant les abonnements à Approvisionnements et Services Canada, Ottawa (Ontario), Canada K1A 0S9. Les paiements doivent être faits à l'avance en devises canadiennes, à l'ordre du Receveur général du Canada.

Microfilms

On peut acheter sur microfilms de 16 ou 35 mm tous les numéros publiés depuis 1934. Des photocopies d'articles ou de numéros individuels sont aussi en vente auprès de Xerox University Microfilms, 300 North Zeeb Road, Ann Arbor, Michigan 48106, É.-U.

Canadian Journal of Fisheries and Aquatic Sciences

Journal canadien des sciences halieutiques et aquatiques

Volume 47, No. 7, July 1990

Volume 47, n° 7, juillet 1990

Scientific Publications/Publications scientifiques

D. G. Cook, Ph.D.	*Editor/Rédacteur*
J. Camp/G. J. Neville/C. Beaulac/ M. Milne	*Editorial and Publishing Services/Services de rédaction et d'édition*
P. E. K. Symons, Ph.D.	*Consulting Editor/Rédacteur-conseil (Victoria, B.C.)*

Associate Editors/Rédacteurs associés

J. R. M. Kelso, Ph.D.	*Department of Fisheries and Oceans, Sault Ste. Marie*
C. D. Levings, Ph.D.	*Department of Fisheries and Oceans, West Vancouver*
J. D. Neilson, Ph.D.	*Department of Fisheries and Oceans, St. Andrews*
P. Schwinghamer, Ph.D.	*Department of Fisheries and Oceans, St. John's*
N. H. F. Watson, Ph.D.	*Department of Fisheries and Oceans, Halifax*
D. J. Noakes, Ph.D.	*Department of Fisheries and Oceans, Nanaimo*

Editorial Board/Conseil de rédaction

P. V. Hodson	*Department of Fisheries and Oceans, Mont-Joli*	(1987–1990)
D. R. S. Lean	*Department of the Environment, Burlington*	(1987–1990)
R. M. Peterman	*Simon Fraser University*	(1987–1990)
R. A. Stein	*Ohio State University*	(1987–1990)
S. J. Smith	*Department of Fisheries and Oceans, Dartmouth*	(1988–1991)
J. C. Roff	*University of Guelph*	(1990–1992)
L. M. Dickie	*Department of Fisheries and Oceans, Dartmouth*	(1990–1992)

Editorial Office:

Department of Fisheries and Oceans
Communications Directorate
Scientific Publications
200 Kent Street, 14th Floor
Ottawa, Canada K1A 0E6
Telephone (613) 993–2209
FAX (613) 990-1866

Bureau de rédaction :

Ministère des Pêches et des Océans
Direction générale des communications
Publications scientifiques
200, rue Kent, 14e étage
Ottawa, Canada K1A 0E6
Numéro de téléphone (613) 993–2209
FAX (613) 990-1866

The *Journal* is abstracted or indexed in:/Le *Journal* est résumé ou signalé dans :

Aquatic Sciences and Fisheries Abstracts, Biological Abstracts, Chemical Abstracts, Current Awareness in Biological Sciences, Current Contents, FAO Freshwater and Aquaculture Contents Tables, FAO Marine Science Contents Tables, Oceanic Abstracts, and Science Citation Index

Particles in "Particle-free" Seawater: Growth of Ultraphytoplankton and Implications for Dilution Experiments

William K. W. Li

Department of Fisheries and Oceans, Biological Oceanography Division, Bedford Institute of Oceanography, Dartmouth, N.S. B2Y 4A2 Canada

Li, W. K. W. 1990. Particles in "particle-free" seawater: growth of ultraphytoplankton and implications for dilution experiments. Can. J. Fish. Aquat. Sci. 47: 1258–1268

Ultraphytoplankton cells were detected by flow cytometry in seawater that passed through filters of the finest pore size commonly used in aquatic research (0.22-μm Millipore®, 0.45-μm Millipore®, 0.2-μm Nuclepore®, Whatman® GF/F). Although the relative number of cells in freshly prepared filtrate was very small (generally less than 1% of the intact assemblage), the number of such cells increased rapidly during incubation. The implication of this apparent growth was investigated in dilution experiments where diluent was mixed with unfiltered seawater in varying proportions. Plots of apparent rate of change versus dilution factor were generally hyperbolic, with high rates at high dilutions. Simple calculations indicated that fluorometric measurements of bulk chlorophyll a would not have been able to detect these changes.

Des cellules d'ultraphytoplancton ont été décelées par cytométrie de flux dans de l'eau de mer filtrée au moyen de filtres à pores les plus fins utilisées couramment pour les recherches aquatiques (0,22 μm Millipore®, 0,45 μm Millipore®, 0,2 μm Nucleopore®, papier Whatman® GF/F). Même si le nombre relatif de cellules dans un filtrat fraîchement préparé était très petit (en général moins de 1% de l'assemblage intact), le nombre de ce type de cellules a augmenté rapidement pendant l'incubation. Les répercussions de cette croissance apparente ont été étudiées par des épreuves de dilution dans lesquelles le diluant a été mélangé dans différentes proportions à de l'eau de mer non filtrée. Les courbes du taux apparent de changement par rapport au facteur de dilution étaient en général hyperboliques, avec des taux élevés à fortes dilutions. De simples calculs ont montré que des mesures fluorométriques de la chlorophylle a en vrac n'auraient pas permis de déceler de tels changements.

Received February 20, 1990
Accepted March 28, 1990
(JA481)

Reçu le 20 février 1990
Accepté le 28 mars 1990

In the few years since Landry and Hassett (1982) introduced their protocol for estimating the grazing rate of marine microzooplankton, the so-called dilution technique, many researchers have adopted or adapted the method for their own studies (Table 1). In this type of experiment, a dilution series is established by mixing seawater containing the intact plankton assemblage with the same seawater from which all organisms have presumably been removed by filtration. Over several hours, there is often a substantial increase in the number of prey organisms in diluted samples; moreover, the apparent specific growth rate of the prey is inversely proportional to the percentage of the dilution that is unfiltered seawater. As dilution increases, the prey are thought to be able to grow at a rate more closely approaching their intrinsic rate because grazing pressure is relieved.

The method is attractive for at least four reasons: (1) the theoretical basis appears to be simple and crucial assumptions are amenable to direct tests (Tremaine and Mills 1987); (2) two important trophodynamic parameters are obtained for the prey from a single experiment (the rates of intrinsic growth and loss to grazing); (3) the abundance of prey can be quantified by any suitable method; (4) the experiment is simple to perform and the manipulation required to reduce grazing pressure (i.e. dilution with filtered seawater) would seem to be less harsh than methods such as physical separation (size fractionation) or chemical discrimination (selective inhibition).

TABLE 1. Types of filters used to prepare diluent in some published dilution experiments.

Filter type	Manufacturer	Reference
0.22 μm	Millipore®	Kirchman et al. 1982
0.22 μm	Millipore®	Ammerman et al. 1984
0.22 μm	Millipore®	Wright 1984
0.22 μm	Millipore®	Taylor and Haberstroh 1988
0.2 μm	Nuclepore®	Ferguson et al. 1984
0.2 μm	Nuclepore®	Landry et al. 1984
0.2 μm	Nuclepore®	Li and Dickie 1985
0.2 μm	Nuclepore®	Nagata 1987
0.2 μm	Nuclepore®	Tremaine and Mills 1987
0.2 μm	Nuclepore®	LaRock et al. 1988
0.2 μm	Nalgene®	Ducklow and Hill 1985
0.2 μm	Corning®	Campbell and Carpenter 1986
0.2 μm	Gelman®	Riemann et al. 1987
0.2 μm	Durapore®	Tranvik 1989
0.45 μm	Millipore®	Landry and Hassett 1982
0.45 μm	Millipore®	Geider 1989
GF/F	Whatman®	Paranjape 1987
GF/F	Whatman®	Gifford 1988
GF/F	Whatman®	Gallegos 1989
AE	Gelman®	Gallegos 1989
GF/C	Whatman®	Burkill et al. 1987

In dilution experiments on heterotrophic bacteria, Li and Dickie (1985) pointed out that a small number of cells was found in diluent freshly prepared by filtration through 0.2-μm Nuclepore® polycarbonate membranes. These cells grew rapidly and it was therefore difficult to interpret the results of a dilution experiment according to the Landry–Hassett scheme, which implicitly assumes a diluent free of all organisms. Confirmatory results were obtained by LaRock et al. (1988) who also monitored microbial activity in their diluent: they reported that up to 50% of activity could be associated with particles passing 0.2-μm Nuclepore® membranes. Li (1986) tested the efficacy of various commonly used filters to retain cells of three cyanobacterial cultures: although none of the filters proved completely effective under all conditions, a qualitative ranking in order of decreasing effectiveness is: 0.22-μm Millipore®>0.45 μm Millipore®>Whatman® GF/F>0.2-μm Nuclepore®. Taguchi and Laws (1988) recently confirmed and extended the observations of Phinney and Yentsch (1985) that GF/F fiilters do not completely retain all phytoplankton in natural samples. In addition, Stockner et al. (1990) demonstrated that not only picoplankton, but also nano- and micro-phytoplankton can pass through filters commonly used to prepare "particle-free" filtrates. In view of these results, it seems imperative to monitor possible growth of phytoplankton in the diluent of dilution experiments (Li 1986).

In this paper, flow cytometric analysis was used to follow the time course of growth for four ultraphytoplankton groups: cyanobacteria, cryptomonads, and two size-classes of algae that do not contain phycoerythrin. I show that seawater rendered "particle-free" by filtration in fact contained a small number of cells that grew rapidly during incubation, thereby affecting the interpretation of dilution experiments.

Materials and Methods

Experimental

Experiments were performed on board CSS *Baffin* (cruise 89-003, April–May 1989) and CSS *Hudson* (cruise 88-026, September 1988) at various sites in the north Atlantic (Table 2). Water was collected using Niskin bottles for the 1989 experiments and from a pump sampler system (Herman et al. 1984) for the single 1988 experiment. The Niskin bottles were custom designed (Crooks Mechanical Systems, Dartmouth) to circumvent possible toxicity from latex rubber (Price et al. 1986): the need for internal springs was avoided by adopting an external closing mechanism. Further, the closure seals were made of Teflon™. Diluent was prepared by filtering seawater at a vacuum pressure of 13.3 kPa through Millipore® 0.45-μm cellulose ester membranes (HAWP, 47-mm diameter). Membrane filters of this type contain Triton as a wetting agent (<5% by weight): to minimise possible contamination of the diluent by materials leaching from the filter, the initial 250–500 mL of filtrate was discarded (Brock 1983). Each dilution series consisted of 20-mL samples of the undiluted plankton, the diluent, and mixtures of the plankton and the diluent in ratios ranging from 1:99 to 75:25. The dilutions were placed into borosilicate glass scintillation vials which had screw-caps that were internally lined with coned-shaped plastic for secure, leak-proof closure. Incubations were carried out on deck under light intensity and temperature conditions simulating those in situ. Solar radiation was attenuated by neutral density perforated screens and temperature was maintained within about 2°C of that in situ using running seawater. In some experiments, the abundance of ultraphytoplankton was determined in time-course fashion over a duration of about 30 h: in other experiments, a single end-point measurement was made at 24 h. To minimise possible contamination of the vial contents by seawater used in the incubator for temperature control, each vial was thoroughly dried with paper towel and absorbent wipers (Kimwipes™) before being opened.

A time–course experiment was also performed to compare the growth (simulated in situ) of phytoplankton in filtrates of the following filters: Millipore® 0.22-μm and 0.45-μm cellulose ester membranes, Nuclepore® 0.2-μm polycarbonate membrane, and Whatman® GF/F glass-fibre filter. Additional unfiltered sample and 0.45-μm Millipore® filtrate were also incubated in darkened vials as a check for processes which do not depend on light.

The contribution of various size-classes to light and dark $^{14}CO_2$ uptake was determined in a time–course experiment in which, at each time of sampling, five replicate aliquots of radiolabelled plankton sample were separately filtered onto Nuclepore® membranes of the following nominal pore sizes: 0.1, 0.2, 1, 2, and 3 μm. The protocol and details of this experiment were similar to those described elsewhere (Li and Dickie 1990).

Analytical

Aliquots of no more 1.5 mL sample were removed from each vial for flow cytometric analysis performed according to protocols described elsewhere (Li and Wood 1988; Li 1989a). Because analysis was carried out on aliquots sampled directly from the vials, there was no need to collect cells on filters, as would be required for bulk pigment analysis or microscopy. In the present work, the sensitivity of the Coulter volume measurement was increased by changing the aperture current from 0.35 or 0.71 mA (used in earlier work) to 1.4 mA (Fig. 1). The sensitivity of the fluorescence measurements was also

TABLE

TABLE 2. Sampling dates, locations, depths, water temperature (T), and percent surface irradiance ($\%I_0$) for experiments shown in Figs. 3–9.

Station No.	Date	Latitude	Longitude	Depth (m)	Figure	T(°C)	$\% I_0$
65	05/12/89	44°53.7′N	41°31.0′W	5	3–5	12.4	42
56	05/10/89	44°48.6′N	41°23.3′W	5	6,7	11.6	39
18	04/28/89	40°37.4′N	47°10.8′W	10	8	15.0	30
18	04/28/89	40°37.4′N	47°10.8′W	45	8	15.0	1
23	04/29/89	40°31.9′N	47°10.2′W	10	8	15.4	40
23	04/29/89	40°31.9′N	47°10.2′W	45	8	15.3	2
38	05/03/89	39°56.7′N	47°01.4′W	10	8	14.9	37
38	05/03/89	39°56.7′N	47°01.4′W	45	8	14.9	1
440	09/11/88	35°59.5′N	64°06.8′W	60	9	25.4	10

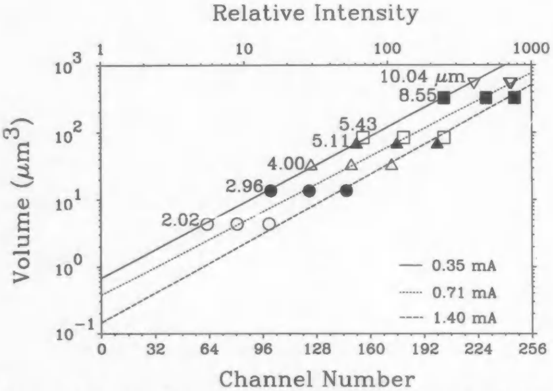

FIG. 1. Calibration of the Coulter volume sensor on the FACS® Analyser using suspensions of beads whose modal diameters are indicated (µm). Higher aperture currents (mA) increase the low-volume sensitivity.

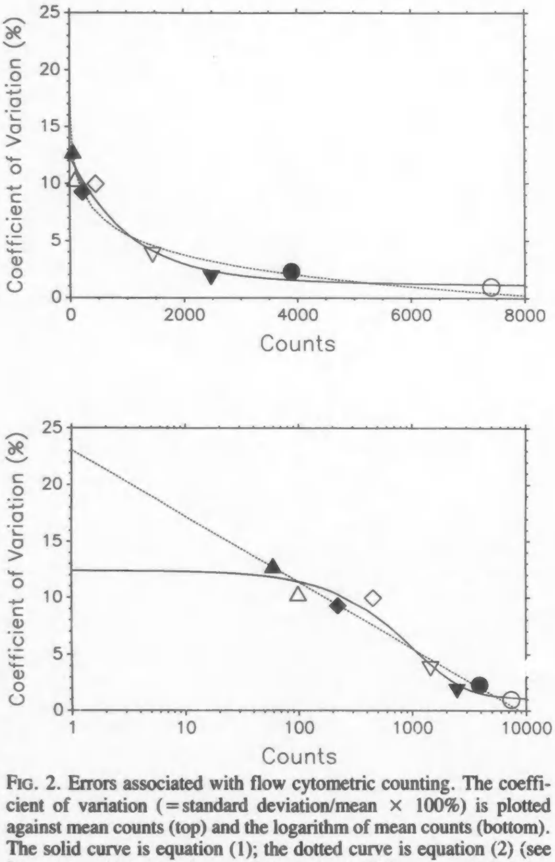

FIG. 2. Errors associated with flow cytometric counting. The coefficient of variation (= standard deviation/mean × 100%) is plotted against mean counts (top) and the logarithm of mean counts (bottom). The solid curve is equation (1); the dotted curve is equation (2) (see Materials and Methods for parameter values). Different symbol shapes identify different cell groups (see Fig. 3 and Results): circles = small greens; inverted triangles = small reds; triangles = large greens; diamonds = large reds. Filled and open symbols identify different plankton samples.

increased by changing photomultiplier voltages. Concerns about non-linear behaviour of logarithmic amplifiers (Olson 1989; Schmid et al. 1988) have been addressed (Li 1989b). As before (Li and Wood 1988; Li 1989a), short wavelength fluorescence ($<575 \pm 13$ nm) was ascribed to phycoerythrin and long wavelength fluorescence (>630 nm) was ascribed to chlorophyll *a*. This follows the convention used by others in similar applications (Olson et al. 1985; Wood et al. 1985) and is the basis for the ataxonomic analysis of phytoplankton by "colour groups" (Yentsch et al. 1986).

The errors associated with the counting procedure were assessed by the coefficient of variation (CV = standard deviation/mean × 100%) of replicate counts of selected samples. As shown in Fig. 2, CV decreased sharply from about 13% for a mean count of 60 to about 1% for a mean count of 7400. In order to extrapolate this relationship between CV (y) and counts (x), the data were fitted to the following two empirical equations:

(1) $y = A_1 \cdot \exp(-\alpha_1 x) + A_2 \cdot \exp(-\alpha_2 x)$

(2) $y = B + \beta \cdot \log(x)$

The parameters obtained by non-linear regression were as follows: $A_1 = 10.96 \pm 3.95$; $\alpha_1 = 0.00096 \pm 0.00067$; $A_2 = 1.44 \pm 4.31$; $\alpha_2 = 0.000031 \pm 0.00048$; $B = 23.09 \pm 1.88$; $\beta = -5.86 \pm 0.64$. Although it is seldom wise to extrapolate a relationship beyond the domain of the measured data, these two equations provide a rough indication of errors possible when counts are very large and very small, respectively. For the maximum count of 50 000 allowed by the Becton-Dickinson FACS® Analyser, equation (1) indicates a CV of 0.30% (equation (2) is not useful for large counts because it indicates CV = 0% at a count of 8715). For the minimum count of 1, equation (2) indicates a CV of 23.1% (equation (1) is not useful for small counts because it indicates an asymptotic approach to CV = 12.4% as the counts approach 0).

Results

Cytogram Signature

Ultraphytoplankton were classified according to an "allometric–ataxonomic" scheme (Yentsch et al. 1986; Li 1989a) that distinguished between "small" (<ca. 1 µm) and "large" (>ca. 1 µm, <ca. 10 µm) cells as well as between cells that contained phycoerythrin and those that did not (Fig. 3).

Group 1 cells (Fig. 3) were "small" and exhibited weak phycoerythrin fluorescence: they were almost certainly chroococcoid cyanobacteria (Johnson and Sieburth 1979; Waterbury et al. 1979, 1986). About 80% or more of group 1 cells were able to pass through 1-µm Nuclepore® membranes.

Group 2 cells (Fig. 3) were "large" and exhibited stronger phycoerythrin fluorescence: they were presumably cryptophytes (Chisholm et al. 1986; Yentsch et al. 1986; Li 1989a).

Group 3 cells (Fig. 3) were "small", without phycoerythrin, and exhibited weak chl *a* fluorescence: they presumably were the prochlorophytes (Chisholm et al. 1988) and may have also included the very small eukaryotic algae such as scaled, non-flagellated prasinophytes known to be abundant in these waters (Johnson and Sieburth 1982). About 90% or more of group 3 cells were able to pass through 1-µm Nuclepore® membranes.

Group 4 cells (Fig. 3) were "large", without phycoerythrin, and exhibited stronger chl *a* fluorescence: this group was clearly

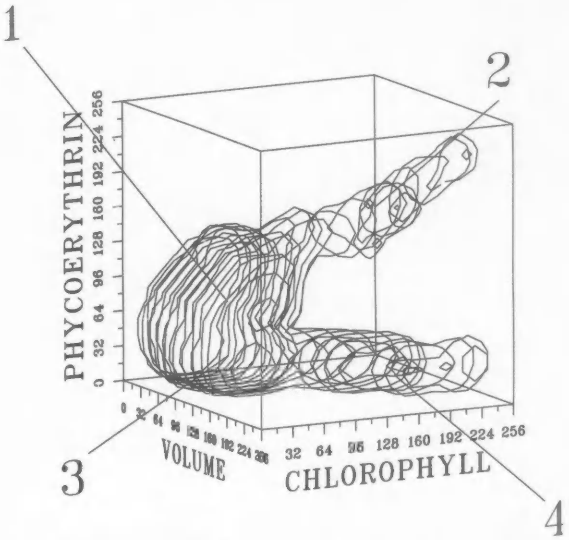

FIG. 3. Trivariate (volume, phycoerythrin, chlorophyll) density contours of a single ultraphytoplankton sample. Contour slices are taken along the volume axis. Coulter® volume and fluorescence intensity were recorded in relative units on logarithmic scales comprising 256 channels that spanned three orders of magnitude. Cells were classified into four groups which are described in the text.

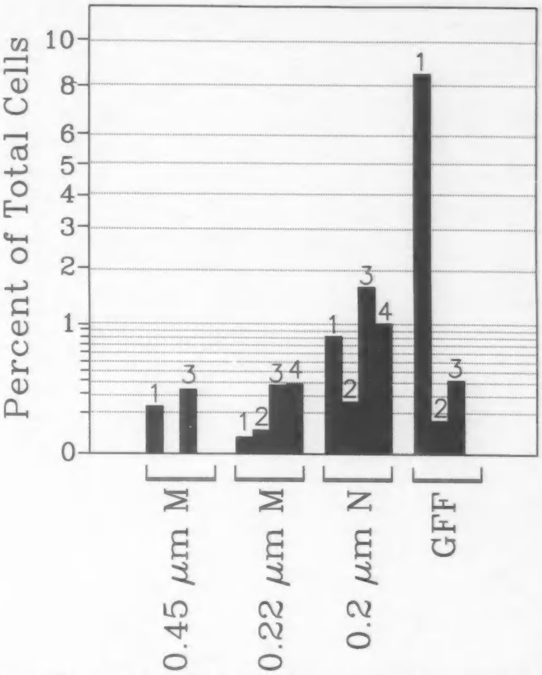

FIG. 4. The percentage of cells found in various filtrates. Cell groups are numbered as follows: 1 = small reds; 2 = large reds; 3 = small greens; 4 = large greens. Ordinate values are expressed in the angular transformation scale (arcsin $p^{1/2}$) which is appropriate for percentages (Sokal and Rohlf 1969). The growth of these filtered cells is shown in Fig. 5.

a mixed assemblage whose members were presumably from several taxa (Shapiro and Guillard 1986; Thomsen 1986).

To emphasize the nature of classification (by size and fluorescence colour), I refer to these four groups as small greens, large greens, small reds, and large reds, respectively. Note emphatically that "red" and "green" do not have taxonomic connotations; these terms refer to the colour of fluorescence used to indicate chl *a* and phycoerythrin, respectively.

Growth in Filtrates

None of the filters tested (0.22-μm and 0.45-μm Millipore®, 0.2-μm Nuclepore® and Whatman® GF/F) completely retained all cells (Fig. 4). The least effective filter was the 0.2-μm Nuclepore®: more cells passed through this filter than any other except for small reds which were found in substantial numbers in GF/F filtrate (Fig. 4).

Without exception, the small number of cells in each filtrate increased over time, with at most only a 4- to 6-h apparent lag (Fig. 5a–d) In view of the small number of cells initially found in the filtrates, we must be assured that the reported increases over time are statistically significant. As shown in Fig. 2, the coefficient of variation was possibly between about 13 to 23% for counts in the range 1 to 100. This degree of uncertainty was apparently not sufficient to obscure the time-dependent cell increase even in cases of very low counts. For example, cells of the large green group were counted in the GF/F filtrate (Fig. 5d) in the following numbers (incubation time (h) in parentheses): 0(0), 0(2), 1(4), 2(6), 6(8), 2(10), 9(12), 7(14), 6(20), 6(22), 8(24), 5(26), 4(28), 9(30). Even in this most extreme of examples, the correlation between counts and time was highly significant ($r = 0.69$, $\nu = 12$, $P < 0.01$). Electronic noise in the domain of the large green group could be disregarded as a contributing factor since the cytometer only accepted signals based on a threshold value of fluorescence (Li and Wood 1988; Li 1989a): counts of sheath fluid were made to confirm this.

Darkened cells in the 0.45-μm Millipore® filtrate also grew and exhibited the same "step" time progression as cells in ambient light. In other words, for small reds (Fig. 5a), large reds (Fig. 5b) and small greens (Fig. 5c), cell division occurred only during periods of the day when light was, or would have been present; although incubation in the dark reduced the rate of cell division, it did not abolish the apparently innate pattern of division — at least up to 30 h.

Dilution Experiments

Growth curves of small greens and small reds in dilutions ranging from $X = 1$ to $X = 0$ (where X is the proportion of unfiltered plankton sample) indicate rapid increase at high dilutions (low X values) (Fig. 6). Landry–Hassett plots (specific rate of change versus X) based on the amount of change after 24 h were highly non-linear (Fig. 7). In this experiment, one would have to disregard the data for $X < 0.1$ in order to obtain a satisfactory straight-line fit as required by the Landry–Hassett scheme.

Similar experiments on plankton taken from other stations and depths gave comparable results (Fig. 8). One exceptional case was the 10 m sample at station 38: growth rates of small reds at low X values, including $X = 0$, were lower than at high X values (Fig. 8c).

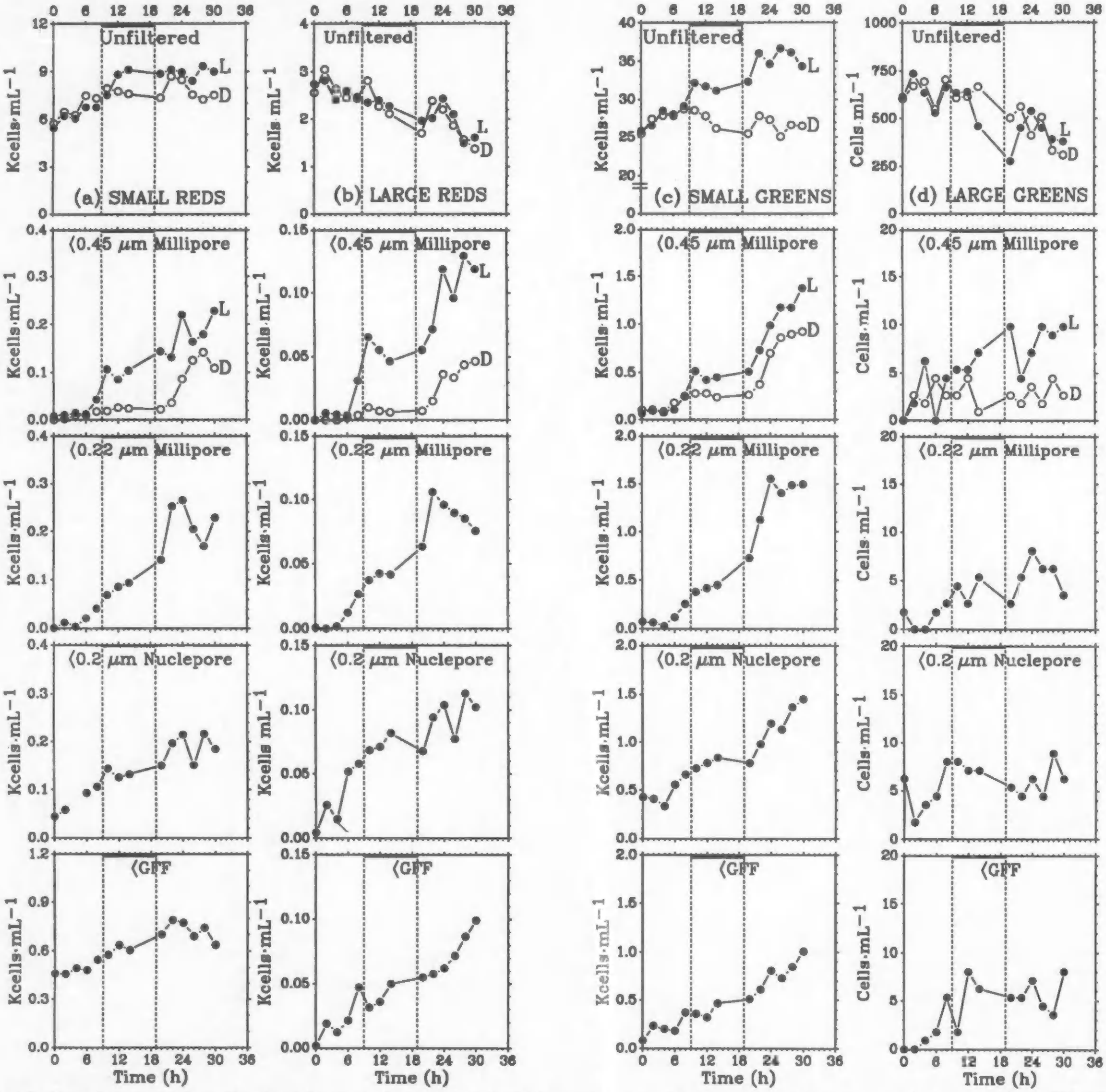

FIG. 5. Growth curves of small reds (column a), large reds (column b), small greens (column c), and large greens (column d) in unfiltered seawater (top row) and filtrates of 0.45-µm Millipore® (second row), 0.22 µm Millipore® (third row), 0. 2 µm Nuclepore® (fourth row), and Whatman GFF (bottom row) under simulated in situ conditions Dark period from 9 to 19 h is indicated by vertical dotted lines. Open symbols in the unfiltered sample and 0.45-µm Millipore® filtrate indicate samples incubated in dark vials.

Size-Fractionated ^{14}C

Figure 9 shows that in both light and dark bottles, the greatest portion of ^{14}C taken up was by the 0.2–1-µm size-class, followed by the 1–2-µm size-class and then the >3-µm size-class. Very little was taken up by the 2–3-µm size-class. There was virtually no difference in ^{14}C values measured on the 0.2- and 0.1-µm filters, indicating negligible uptake by organisms passing the 0.2-µm membrane. The "step" progression of ^{14}C in the light bottle (uptake only during the day and not at night) was typical of algal processes while the continuous exponential increase of ^{14}C in the dark bottle was suggestive of bacterial growth (Li and Dickie 1990).

Discussion

There is now little doubt that the filters commonly used in aquatic research do not completely and consistently retain all phytoplankton. The well-documented passage of cells through Whatman® GF/C filters (Sheldon 1972; Munawar et al. 1982; Yentsch 1983; Venrick et al. 1987) can be readily rationalised: these filters are rated by the manufacturer to retain particles of 1.2 µm so that they would allow passage of the picoplankters which have smaller diameters. However, it is less well-known that not only aquatic bacteria (Sheldon et al. 1967; Tabor et al. 1981; Torella and Morita 1981; MacDonell and Hood 1982; Li

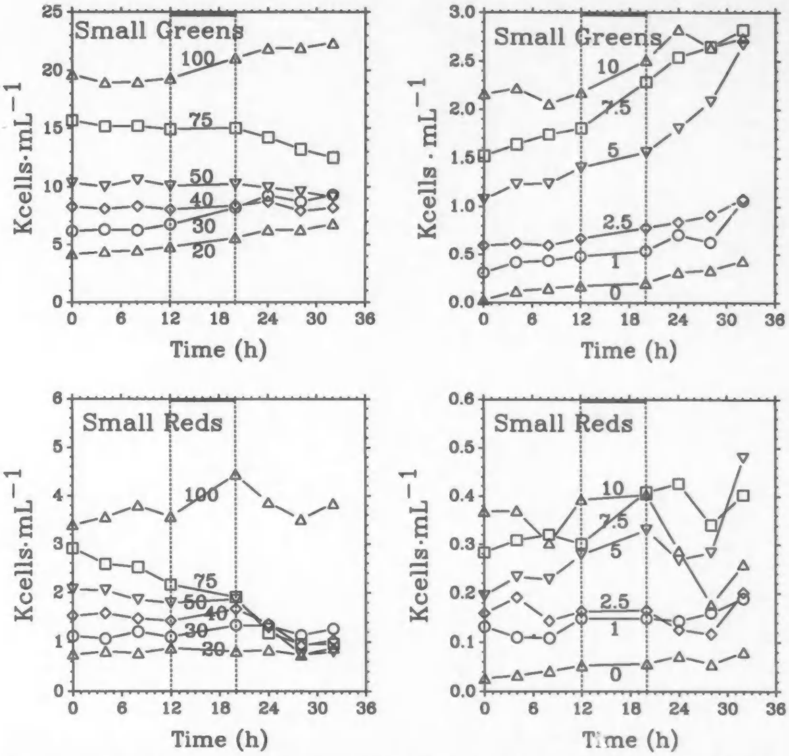

FIG. 6. Growth curves of small greens (upper panels) and small reds (lower panels) in a dilution series. Numbers adjacent to curves indicate the percentage of unfiltred plankton (i.e. 100× where X is the proportion of unfiltered plankton as defined in the text). Dark period from 12 to 20 h is indicated by vertical dotted lines.

and Dickie 1985) but also phytoplankton can pass through filters with even smaller rated pore sizes (Phinney and Yentsch 1985; Li 1986; Taguchi and Laws 1988). Recent photomicrographs of large holes in filters and of ultra-, nano-, and microplankton in filtrates (Stockner et al. 1990) should cast aside doubts that even 0.1-μm Nuclepore® filters can be "leaky".

A variety of filter types has been used in dilution experiments to date (Table 1). One would perhaps expect a small percentage of cells to pass through these filters simply because of the inevitable variation of pore size about the mean or rated values. For Whatman® glass microfibre filters, the rated "particle retention is expressed in terms of the particle size(μm) at which a retention level of 98% of the total number of particles initially challenging the filter is obtained" (Whatman Inc. undated). For Millipore® mixed cellulose esters membrane filters, there is pore size variation of ±0.04 and ±0.02 μm about the mean sizes of 0.45 and 0.22 μm, respectively (Millipore Corp. 1982). For Nuclepore® polycarbonate filters, the manufacturer states a tolerance range of +0 and −20% of the rated pore size (Nuclepore Corp. 1988) but Jones et al. (1989) indicate both positive and negative variations about a mode of 0.22 μm for nominal 0.2-μm Nuclepore® membranes. However, it seems likely that an important cause of "leaky filters" is the presence of large holes or pores, some up to seven to 10 times the nominal pore size (Stockner et al. 1990). It is also possible that large but flexible cells are drawn through the filters by the pressure differential (Azam and Hodson 1977; Murphy and Haugen 1985).

An implicit assumption of the Landry–Hassett dilution experiments is that the diluent be free of cells. Since this assumption can no longer be taken for granted, the interpretation of these experiments is now not so straightforward. In most cases, only a very small percentage of total cells is found in the filtrates (Li 1986 and Fig. 4), representing an even smaller percentage of total chl *a* or biomass (Venrick et al. 1897; Taguchi and Laws 1988). Although these cells would likely have little consequence on measurements of total primary production (Fig. 9), the present results show unequivocally that these cells grow very quickly (Fig. 5). The high growth rates achieved by these cells are not unrealistic, given the apparently favourable conditions in the filtrate: a presumed absence of predators and the virtual elimination of other cells competing for limiting resources. Specific growth rates in excess of $1.5 \cdot d^{-1}$ are not uncommon for undiluted ultraplankton (Wood 1989), even in the deep chlorophyll maximum layer where light is limiting (Iturriaga and Mitchell 1986).

An argument could be made for viewing the growth of cells in the filtrate as a direct measure of the intrinsic rate of increase which is given only as an unachievable extrapolation to $X=0$ in the Landry–Hassett scheme. There are at least four considerations that have an influence on this interpretation: the degree to which algae in the filtrate represent those in the original plankton sample, filtration-induced enrichment of nutrients,

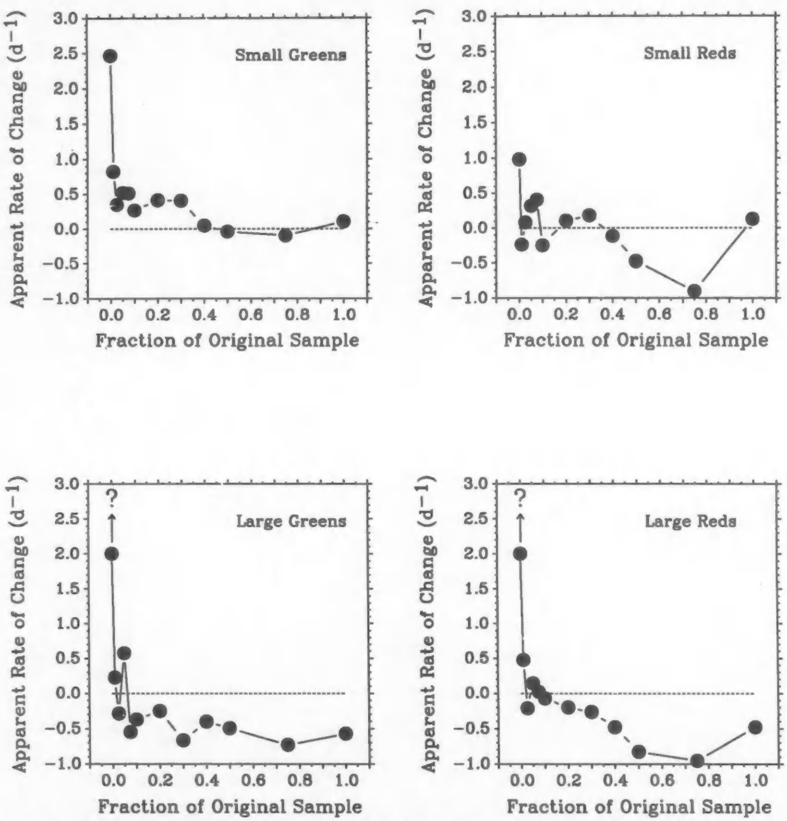

FIG. 7. Landry–Hassett plots for the experiment detailed in Fig. 6. Apparent rates of change calculated from initial and 24-h cell counts. Horizontal dotted lines indicate no net change over 24 h. For large greens and large reds, the rates of change at $X = 0$ were undefined (indicated by ?) because the number of cells in freshly prepared filtrate was below the level of detection.

effects of small incubation vessels, and contamination of the filtrate after preparation.

First, we know that cells do not go through the filters in the same proportion as they occur in the unfiltered seawater (Fig. 4). This means that if growth of the filtrate assemblage were measured using a bulk property (e.g. chl *a*), the rate so determined would not be indicative of the original plankton sample. Similarly, if growth of the filtrate phytoplankton were measured using methods capable of discriminating particular cell groups (e.g. microscopy, pigment HPLC, or flow cytometry), the rates so determined for each group would only be appropriate for those cells that were initially found in the diluent. In other words, even for cells within one group (e.g. small reds), it cannot be assumed that the sub-population found in the diluent is a representative sample of the original population. More likely, the sub-population would have a distribution skewed towards those cells which more easily go through filters (e.g. smaller, more flexible, etc.).

Second, there is the seemingly inevitable problem of nutrient enrichment of the diluent as a result of filtration-induced cell breakage (Ferguson et al. 1984; Fuhrman and Bell 1985; Goldman and Dennett 1985). However, as Tremaine and Mills (1987) showed by direct experimentation, it does not follow that the use of enriched diluents necessarily negates the validity of the dilution experiment. Whether or not cell growth is affected by the dilution treatment depends on the nature and severity of limitation (e.g. nutrient, grazing) and on the extent of filtration-induced nutrient enrichment. A simple calculation can be made as follows to set an upper bound for filtration-induced enrichment of inorganic nitrogen. The 5-m sample at station 65 (Table 2, Fig. 5) had a total particle volume of 1.9 $\mu L \cdot L^{-1}$ based on Coulter® counts in the range 0.6 to 128 μm (A. R. Longhurst, Bedford Institute of Oceanography, Canada — unpublished result using Coulter® model TA II). In a review, Wheeler (1983) stated that cellular pools of inorganic nitrogen in phytoplankton tend to be less than 100 mM. If we assume that all particles contained 100 mM inorganic nitrogen and that filtration caused all the particles to release this nitrogen into the filtrate, then the enrichment would be about 0.2 μM. This compares with a measured ambient concentration of 1.4 μM dissolved inorganic nitrogen (1.1 μM nitrate, 0.3 μM ammonium) for this sample. Clearly, even with the unrealistic assumptions that (i) all Coulter® particles were cells, (ii) that all cells were broken, and (iii) that all cells contained the non-representative concentration of 100 mM, the inferred enrichment would still only be a small fraction of the ambient nutrient level. Admittedly, the enrichment need not be very large to enhance the very few cells present in the diluent. The possibility

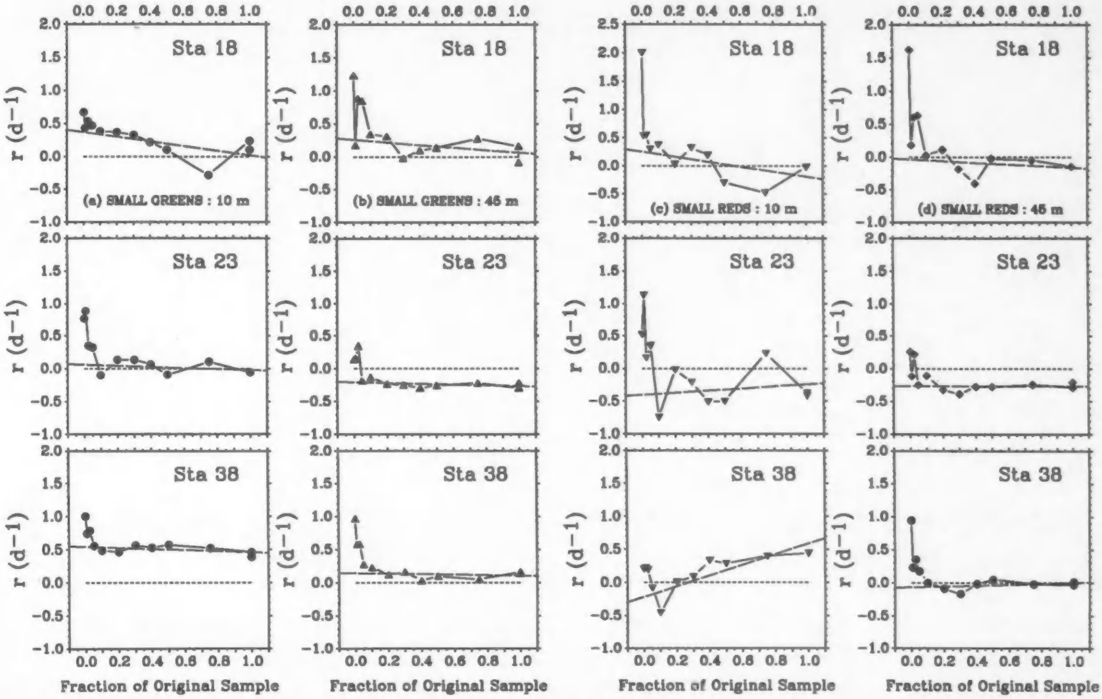

FIG. 8. Landry–Hassett plots for 10-m small greens at stations 18, 23, and 38 (column a), 45-m small greens at the same stations (column b), 10-m small reds at the same stations (column c), and 45-m small reds at the same stations (column d). Horizontal dotted lines indicate no net change over 24 h. Slanted dashed lines indicate linear regression of data omitting values for $X<0.1$.

that nutrient enrichment confounds the interpretation of dilution experiments in general remains problematic.

A third consideration is the effect, if any, of the small size (20 mL) of the incubation vial used here. Numerous studies have shown that algal productivity is not affected by the size of bottles (50 mL to 8 L) used for incubation (Qasim et al. 1972; Lewis 1974; Sharp et al. 1980; Li and Harrison 1982; Berger 1984). One study reported that production rate decreased with bottle size (Sheldon et al. 1973) but the authors attributed this to the supposition that small bottles contain few predators. Since the reduction of predators is the very principle of dilution experiments, the results of Sheldon et al. 1973) can be taken to mean the absence of bottle effects in dilution experiments. Li and Dickie (1987) showed no statistical difference in ^{14}C uptake rates using sample volumes of 10, 100, and 250 mL; rates were lower only when extremely small volumes were tested (1.5 and 2.5 mL). To my knowledge, only two studies (Gieskes et al. 1979; Brown 1982) have shown production rates to be higher in large bottles (hundreds to thousands of millilitres) than in bottles with capacities of a few tens of millilitres.

Fourth, although there is no absolute assurance that repeated sampling of the vial contents did not lead to contamination by algae in droplets of raw seawater (which was used for temperature regulation in the deck incubator), it is possible to defend the interpretation that the increase of cells in the filtrates was due to growth of the initial seed assemblage. Precautions were taken to ensure that each vial was individually dried before being opened (see Methods). Furthermore, the results of several experiments for which only a single end-point measurement was made (Fig. 8) were similar to those of the time–course incubations. If contamination is believed to explain the appearance and increase of cells in the filtrates, one might suppose that the dark incubation would be the control which monitored this artifact. If this were the case, we can calculate that at say 30 h, the measured concentration of "small red" cells in the dark 0.45-μm Millipore® filtrate (Fig. 5a) would have had to be introduced into the vial from the ambient seawater in a contaminating drop of close to 0.1 mL: this is clearly too large a volume to have gone unnoticed.

If we are reconciled that measurements of cell increase in the filtrates do in fact pertain to the growth of an initial seed assemblage, we must then reconsider the interpretation of the Landry–Hassett scheme. At high dilutions (low X values), it is likely that part of measured increase in prey population size is not due to the intended (i.e. X diluted) predator–prey interaction. At lower dilutions, the unintended effect should be lessened since the diluent cells, even though growing fast, account for only a small percentage of the entire prey population. Information pertaining to nonlinear feeding kinetics that rely on results at high dilutions (Gallegos 1989) may be confounded.

Since many dilution studies are based on measurements of chlorophyll *a* rather than cell counts, it is instructive to estimate the volume of sample required to detect (by fluorometric assay of bulk chlorophyll) the filtrate phytoplankton represented in the present experiments. We first assume the following values for carbon cell quotas: 250 fg cyanobacterium^{-1} (Kana and Glibert 1987), 60 fg prochlorophyte^{-1} and 7400 fg eukaryote^{-1}. The latter two values are based on 220 fg·μm^{-3} (Booth 1988) and spherical diameters of 0.8 μm for prochlorophytes (Chisholm et al. 1988) and 4 μm for eukaryotes (Li and Wood

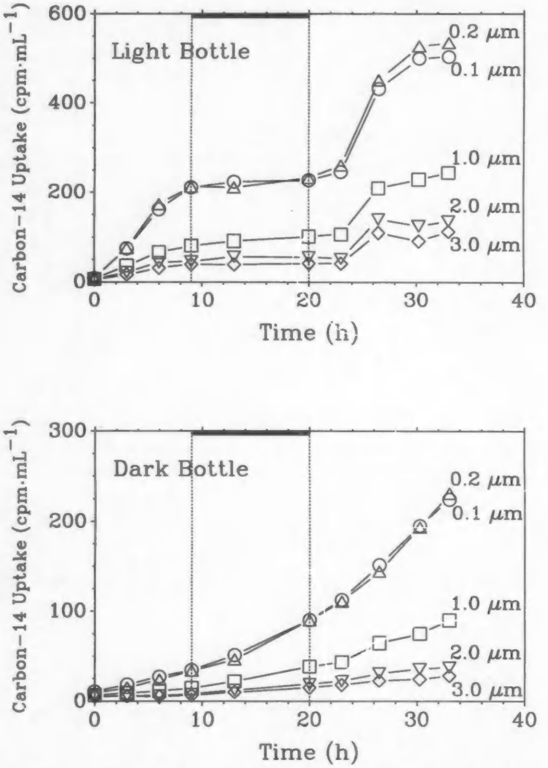

FIG. 9. Uptake of $NaH^{14}CO_3$ in light and dark bottles by size fractions of plankton collected on Nuclepore® membranes of various pore sizes as indicated. Dark period from 9 to 20 h is indicted by vertical dotted lines.

1988). If a C:Chl ratio of 50 is assumed, we infer that about 62 L of the freshly prepared 0.45-μm filtrate (station 65 sample, Fig. 4) would need to be filtered to achieve the limit of detection (Strickland and Parsons 1972). Clearly, it would be quite difficult to detect growth of filtrate cells in dilution experiments based on routine fluorometric measurements of Chl *a*.

As originally stated by Landry and Hassett (1982), an important assumption of the method is that predators consume prey in direct proportion to prey density. In other words, a plot of the apparent rate of change versus dilution factor (X) should yield a straight line with negative slope. This was explicitly verified by Tremaine and Mills (1987). Gallegos (1989) extended the theory of the dilution technique to encompass cases in which grazing is a nonlinear function of prey density. In these cases, plots of the apparent rate of change versus dilution factor are not straight lines but are curves whose first derivatives are negative. Visual inspection of these plots in Figs. 7,8 (present study), of figure 2 in Gifford's (1988) study and figure 3 in Gallegos' (1989) study indicates that over parts of the dilution range, the slope is positive and not negative as required by both Landry and Hassett (1982) and Gallegos (1989). From a statistical point of view, it would be possible to invoke random variation to explain the departure of data from a best-fitting straight line (or curve) with negative slope. However, it would be imprudent to dismiss the possibility that different patterns of trophic interactions characterise different parts of the dilution range. In future, we need experiments that are not only well-replicated at each dilution (e.g. Gifford 1988) but also closely-spaced throughout the entire dilution range.

In summary, the results of this study show, for the first time, the growth of phytoplankton that pass through filters of the finest pore size commonly used in aquatic research. These results, together with those on the growth of filtrate bacteria (Li and Dickie 1985; LaRock et al. 1988), indicate that the relatively few cells initially found in filtered seawater may multiply to form a substantial population in a short time. Earlier studies pointed to a similar conclusion (Sheldon et al. 1967) but the implications for dilution experiments have not been addressed heretofore. Clearly, it will be important that researchers not continue to regard the dilution techniques as the simple, straightforward protocol it once may seem to have been.

Acknowledgements

I thank Charles Gallegos for the privilege of reading his paper before publication, Paul Dickie for performing the ^{14}C experiment, and Alan Longhurst for an unpublished result. Drs. S. W. Chisholm, T. Platt, and W. G. Harrison offered comments on the manuscript.

References

AMMERMAN, J. W., J. A. FUHRMAN, Å. HAGSTRÖM, AND F. AZAM. 1984. Bacterioplankton growth in seawater: I. Growth kinetics and cellular characteristics in seawater cultures. Mar. Ecol. Prog. Ser. 18: 31–39.

AZAM, F., AND R. E. HODSON. 1977. Size distribution and activity of marine microheterotrophs. Limnol. Oceanogr. 22: 492–501.

BERGER, C. 1984. In situ primary production measured with 250 mL and 130 mL bottles. Hydrobiol. Bull. 18: 17–22.

BOOTH, B. C. 1988. Size classes and major taxonomic groups of phytoplankton at two locations in the subarctic Pacific Ocean in May and August, 1984. Mar. Biol. 97: 275–286.

BROCK, T. D. 1983. Membrane filtration: a user's guide and reference manual. Sci. Tech., Madison, WI. 381 p.

BROWN, P. C. 1982. A note on the effect of bottle size on phytoplankton production measurements. Fish. Bull. S. Afr. 16: 21–24.

BURKILL, P. H., R. F. C. MANTOURA, C. A. LLEWELLYN, AND N. J. P. OWENS. 1987. Microzooplankton grazing and selectivity of phytoplankton in coastal waters. Mar. Biol. 93: 581–590.

CAMPBELL, L., AND E. J. CARPENTER. 1986. Estimating the grazing pressure of heterotrophic nanoplankton on *Synechococcus* spp. using the seawater dilution and selective inhibitor techniques. Mar. Ecol. Prog. Ser. 33: 121–129.

CHISHOLM, S W., E. G. ARMBRUST, AND R. J. OLSON. 1986. The individual cell in phytoplankton ecology: cell cycles and applications of flow cytometry, p. 343–369. *In* T. Platt and W. K. W. Li [ed.] Photosynthetic picoplankton. Can. Bull. Fish. Aquat. Sci. 214.

CHISHOLM, S. W., R. J. OLSON, E. R. ZETTLER, R. GEORICKE, J. B. WATERBURY, AND N. A. WELSCHMEYER. 1988. A novel free-living prochlorophyte abundant in the oceanic euphotic zone. Nature (Lond.) 334: 340–343.

DUCKLOW, H. W., AND S. M. HILL. 1985. The growth of heterotrophic bacteria in the surface waters of warm core rings. Limnol. Oceanogr. 30: 239–259.

FERGUSON, R. L., E. N. BUCKLEY, AND A. V. PALUMBO. 1984. Response of marine bacterioplankton to differential filtration and confinement. Appl. Environ. Microbiol. 47: 49–55.

FUHRMAN, J. A., AND T. M. BELL. 1985. Biological considerations in the measurement of dissolved free amino acids in seawater and implications for chemical and microbiological studies. Mar. Ecol. Prog. Ser. 25: 13–21.

GALLEGOS, C. L. 1989. Microzooplankton grazing on phytoplankton in the Rhode River, Maryland: nonlinear feeding kinetics. Mar. Ecol. Prog. Ser. 57: 23–33.

GEIDER, R. J. 1989. Use of radiolabeled tracers in dilution grazing experiments to estimate bacterial growth and loss rates. Microb. Ecol. 17: 77–87.

GIESKES, W. W. C., G. W. KRAAY, AND M. A. BAARS. 1979. Current ^{14}C methods for measuring primary production: gross underestimates in oceanic waters. Neth. J. Sea Res. 13: 58–78.

Gifford, D. J. 1988. Impact of grazing by microzooplankton in the Northwest Arm of Halifax Harbour, Nova Scotia. Mar. Ecol. Prog. Ser. 37: 249–258.

Goldman, J. C., and M. R. Dennett. 1985. Susceptibility of some marine phytoplankton species to cell breakage during filtration and post-filtration rinsing. J. Exp. Mar. Biol. Ecol. 84: 47–58.

Herman, A. W., M. R. Mitchell, and S. W. Young. 1984. A continuous pump sampler for profiling copepods and chlorophyll in the upper oceanic layers. Deep-Sea Res. 31: 439–450.

Iturriaga, R., and B. G. Mitchell. 1986. Chroococcoid cyanobacteria: a significant component in the food web dynamics of the open ocean. Mar. Ecol. Prog. Ser. 28: 291–297.

Johnson, P. W., and J. McN. Sieburth. 1979. Chroococcoid cyanobacteria in the sea: a ubiquitous and diverse phototrophic biomass. Limnol. Oceanogr. 24: 928–935.

1982. In-situ morphology and occurrence of eucaryotic phototrophs of bacterial size in the picoplankton of estuarine and oceanic waters. J. Phycol. 18: 318–327.

Jones, S. E., S. A. Ditner, C. Freeman, C. J. Whitaker, and M. A. Lock. 1989. Comparison of a new inorganic membrane filter (Anopore) with a track-etched polycarbonate membrane filter (Nuclepore) for direct counting of bacteria. Appl. Environ. Microbiol. 55: 529–530.

Kana, T. M., and P. M. Glibert. 1987. Effect of irradiances up to 2000 $\mu E \cdot m^{-2} s^{-1}$ on marine *Synechococcus* WH7803-I. Growth, pigmentation, and cell composition. Deep-Sea Res. 34: 479–495.

Kirchman, D., H. Ducklow, and R. Mitchell. 1982. Estimates of bacterial growth from changes in uptake rates and biomass. Appl. Environ. Microbiol. 44: 1296–1307.

Landry, M. R., and R. P. Hassett. 1982. Estimating the grazing impact of marine micro-zooplankton. Mar. Biol. 67: 283–288.

Landry, M. R., L. W. Haas, and V. L. Fagerness. 1984. Dynamics of microbial plankton communities: experiments in Kaneohe Bay, Hawaii. Mar. Ecol. Prog. Ser. 16: 127–133.

LaRock, P. A., J. R. Schwarz, and K. G. Hofer. 1988. Pulse labelling: a method for measuring microbial growth rates in the ocean. J. Microbiol. Methods 8: 281–297.

Lewis, W. M., Jr. 1974. Primary production in the plankton community of a tropical lake. Ecol. Monogr. 44: 377–409.

Li, W. K. W. 1986. Experimental approaches to field measurements: methods and interpretation. *In* T. Platt, and W. K. W. Li [ed.] Photosynthetic picoplankton. Can. Bull. Fish. Aquat. Sci. 214: 251–286.

1989a. Shipboard analytical flow cytometry of oceanic ultraphytoplankton. Cytometry 10: 564–579.

1989b. Logarithmic amplification of optical signals on BIO BD-FACS. Signal and Noise 2:5.

Li, W. K. W., and P. M. Dickie. 1985. Growth of bacteria in seawater filtered through 0.2 μm Nuclepore membranes:implications for dilution experiments. Mar. Ecol. Prog. Ser. 26: 245–252.

1987. Temperature characteristics of photosynthetic and heterotrophic activities: seasonal variations in temperate microbial plankton. Appl. Environ. Microbiol. 53: 2282–2295.

1990. Light and dark carbon-14 uptake in dimly-lit oligotrophic waters: relation to bacterial activity. J. Plankton Res. 11: (In press).

Li, W. K. W., and W. G. Harrison. 1982. Carbon flow into the end-products of photosynthesis in short and long incubations of a natural phytoplankton population. Mar. Biol. 72: 175–182.

Li, W. K. W., and A. M. Wood. 1988. Vertical distribution of North Atlantic ultraphytoplankton: analysis by flow cytometry and epifluorescence microscopy. Deep-Sea Res. 35: 1615–1638.

MacDonell, M. T., and M. A. Hood. 1982. Isolation and characterization of ultramicrobacteria from a Gulf Coast estuary. Appl. Environ. Microbiol. 43: 566–571.

Millipore® Corporation 1982. A guide to membrane separation technology: catalogue and purchasing guide (MC579). Bedford, MA.

Munawar, M., I. F. Munawar, P. E. Ross, and A. Dagenais. 1982. Microscopic evidence of phytoplankton passing through glass-fibre filters and its implications for chlorophyll analysis. Arch. Hydrobiol. 94: 520–528.

Murphy, L. S., and E. M. Haugen. 1985. The distribution and abundance of phototrophic ultraplankton in the North Atlantic. Limnol. Oceanogr. 30: 47–58.

Nagata, T. 1987. Production rate of planktonic bacteria in the north basin of Lake Biwa, Japan. Appl. Environ. Microbiol. 53: 2872–2882.

Nuclepore® Corporation. 1988. Products for laboratory and process filtration (NC0887). Pleasanton, CA.

Olson, R. J. 1989. A note of caution regarding logarithmic amplifiers. Signal and Noise 2:1

Olson, R. J., D. Vaulot, and S. W. Chisholm. 1985. Marine phytoplankton distributions measured using shipboard flow cytometry. Deep-Sea Res. 32: 1273–1280.

Paranjape, M. A. 1987. Grazing by microzooplankton in the eastern Canadian arctic in summer 1983. Mar. Ecol. Prog. Ser. 40: 239–246.

Phinney, D. A., and C. S. Yentsch. 1985. A novel phytoplankton chlorophyll technique: toward automated analysis. J. Plankton Res. 7: 633–642.

Price, N. M., P. J. Harrison, M. R. Landry, F. Azam, and K. J. F. Hall. 1986. Toxic effects of latex and Tygon tubing on marine phytoplankton, zooplankton and bacteria. Mar. Ecol. Prog. Ser. 34: 41–49.

Qasim, S. Z., P. M. A. Bhattathiri, and V P. Devassy. 1972. Some problems related to the measurements of primary production using radiocarbon technique. Int. Rev. Gesanten. Hydrobiol. 57: 535–549.

Riemann, B., P. K. Bjørnsen, S. Newell, and R. Fallon. 1987. Calculation of cell production of coastal marine bacteria based on measured incorporation of [^{3}H]thymidine. Limnol. Oceanogr. 32: 471–476.

Schmid, I., P. Schmid, and J. V. Giorgi. 1988. Conversion of logarithmic channel numbers into relative linear fluorescence intensity. Cytometry 9: 533–538.

Shapiro, L. P., and R. R. L. Guillard. 1986. Physiology and ecology of the marine eukaryoyic ultraplankton, p. 371–389. *In* T. Platt and W. K. W. Li [ed.] Photosynthetic picoplankton. Can. Bull. Fish. Aquat. Sci. 214.

Sharp, J. H., M. J. Perry, E. H. Renger, and R. W. Eppley. 1980. Phytoplankton rate processes in the oligotrophic waters of the central North Pacific Ocean. J. Plankton Res. 2: 335–353.

Sheldon, R. S. 1972. Size separation of marine seston by membrane and glass-fiber filters. Limnol. Oceanogr. 17: 494–498.

Sheldon, R. W., T. P. T. Evelyn, and T. R. Parsons. 1967. On the occurrence and formation of small particles in seawater. Limnol. Oceanogr. 12: 367–375.

Sheldon, R. W., W. H. Sutcliffe, Jr., and A. Prakash. 1973. The production of particles in the surface waters of the ocean with particular reference to the Sargasso Sea. Limnol. Oceanogr. 18: 719–733.

Sokal, R. R., and F. J. Rohlf. 1969. Biometry. W. H. Freeman, San Francisco, CA. 776 p.

Stockner, J. G., M. E. Klut, and W. P. Cochlan. 1990. Leaky filters: a warning to aquatic ecologists. Can. J. Fish. Aquat. Sci. 47: 16–23.

Strickland, J. D. H., and T. R. Parsons. 1972. A practical handbook of seawater analysis. 2nd ed. Bull. Fish. Res. Board Can. 167: 310 p.

Tabor, P. S., K. Ohwada, and R. R. Colwell. 1981. Filterable marine bacteria found in the deep sea: distribution, taxonomy, and response to starvation. Microb. Ecol. 7: 67–83.

Taguchi, S., and E. A. Laws. 1988. On the microparticles which pass through glass fiber filter type GF/F in coastal and open waters. J. Plankton Res. 10: 999–1008.

Taylor, G. T., and P. R. Haberstroh. 1988. Microzooplankton grazing and planktonic production in the Bransfield Strait observed during the RACER program. Antarctic. J. U.S. 23: 126–128.

Thomsen, H. A. 1986. A survey of the smallest eucaryotic organisms of the marine phytoplankton, p. 121–158. *In* T. Platt and W. K. W. Li [ed.] Photosynthetic picoplankton. Can. Bull. Fish. Aquat. Sci. 214.

Torella, F., and R. Y. Morita. 1981. Microcultural study of bacterial size changes and microcolony and ultramicrocolony formation by heterotrophic bacteria in seawater. Appl. Environ. Microbiol. 41: 518–527.

Tranvik, L. J. 1989. Bacterioplankton growth, grazing mortality and quantitative relationship to primary production in a humic and a clearwater lake. J. Plankton Res. 11: 985–1000.

Tremaine, S. C., and A. L. Mills. 1987. Test of the critical assumptions of the dilution method for estimating bacterivory by microeucaryotes. Appl. Environ. Microbiol. 53: 2914–2921.

Venrick, E. L., S. L. Cummings, and C. A. Kemper. 1987. Picoplankton and the resulting bias in chlorophyll retained by traditional glass-fiber filters. Deep-Sea Res. 34: 1951–1956.

Waterbury, J. B., S. W. Watson, R. R. L. Guillard, and L. E. Brand. 1979. Widespread occurrence of a unicellular, marine, planktonic cyanobacterium. Nature (Lond.) 277: 293–294.

Waterbury, J. B., S. W. Watson, F. W. Valois, and D. G. Franks. 1986. Biological and ecological characterization of the marine unicellular cyanobacterium *Synechococcus*, p. 71–120. *In* T. Platt and W. K. W. Li [ed.] Photosynthetic picoplankton. Can. Bull. Fish. Aquat. Sci. 214.

Whatman Incorporated (undated). Laboratory product guide (900 LPG-A). Clifton, NJ.

Wheeler, P. A. 1983. Phytoplankton nitrogen metabolism, p. 309–346. *In* E. J. Carpenter, D. G. Capone, [ed.] Nitrogen in the marine environment. Academic Press, New York, NY.

Wood, A. M. 1989. Ultraphytoplankton community structure and evolution in the seasonal thermocline, p. 336–340. *In* T. Hattori, Y. Ishida, Y.

Maruyama, R. Y. Morita, and A. Uchida [ed.] Recent advances in microbial ecology. Japan Scientific Societies Press, Tokyo, Japan.

WOOD, A. M., P. K. HORAN, K. MUIRHEAD, D. A. PHINNEY, C. M. YENTSCH, AND J. B. WATERBURY. 1985. Discrimination between types of pigments in marine *Synechococcus* spp. by scanning spectroscopy, epifluorescence microscopy, and flow cytometry. Limnol. Oceanogr. 30: 1303–1315.

WRIGHT, R. T. 1984. Dynamics of pools of dissolved organic carbon, p. 121–154. *In* J. E. Hobbie and P. J. leB. Williams [ed.] Heterotrophic activity in the sea. Plenum Press, New York, NY.

YENTSCH, C. M., T. L. CUCCI, D. A. PHINNEY, AND J. A. TOPINKA. 1986. Real-time characterization of individual marine particles at sea: flow cytometry, p. 414–448. *In* M. Bowman, C. M. Yentsch, and W. T. Peterson [ed.] Tidal mixing and plankton dynamics. Lecture notes on coastal and estuarine studies 17. Springer-Verlag, New York, NY.

YENTSCH, C. S. 1983. A note on the fluorescence characteristics of particles that pass through glass-fiber filters. Limnol. Oceanogr. 28: 597–599.

Retention and Resuspension of Phosphorus, Nitrogen, and Iron in a Central Ontario Lake

P. J. Dillon

Ontario Ministry of the Environment, Dorset Research Centre, Bellwood Acres Road, P.O. Box 39, Dorset, Ont. Canada P0A 1E0

R. D. Evans

Trent University, Environmental Resource Studies Institute, P.O. Box 4800, Peterborough, Ont. K9J 7B8 Canada

and Lewis A. Molot

Department of Zoology, University of Toronto, 25 Harbord Street, Toronto, Ont. M5S 1A1 Canada

Dillon, P. J., R. D. Evans, and L. A. Molot. 1990. Retention and resuspension of phosphorus, nitrogen, and iron in a central Ontario lake. Can. J. Fish. Aquat. Sci. 47: 1269–1274.

Sediment traps were used to estimate the downward flux of total phosphorus, total Kjeldahl nitrogen, and iron in a small Precambrian shield lake for 4 yr. The flux as determined by the sediment trap method was much higher than the retention of the same elements as measured by mass balance methods (input–outflow). Total phosphorus (TP) sedimentation was about 17 times higher than retention while N was about three times higher and Fe was about 31 times higher. Very high N/P ratios in epilimnetic waters (36/1 by weight) and low N/P ratios in trap material (8/1) and surficial sediments (mean 8/1, range 4–11/1), in conjunction with high sedimentation to retention ratios, strongly suggest that resuspended sediment is a major component of trap material. Fe/TP ratios suggest that surficial sediment from shallow waters (<13 m) was the largest contributor to resuspended sediment. Large amounts of biologically available phosphorus originating with resuspended sediment may enter upper waters. The difference between N/P ratios in surficial sediments (4–11/1) and nutrients retained from mass balance calculations (50/1) is attributed to denitrification.

Des pièges à sédiments ont été utilisés pour évaluer l'écoulement descendant du phosphore total, de l'azote total Kjeldahl et du fer dans un petit lac du bouclier précambrien pendant quatre ans. L'écoulement tel qu'il a été déterminé par la méthode des pièges à sédiments était beaucoup plus élevé que la rétention des mêmes éléments mesurée par la méthodes des bilans massiques (apport–sortie). La sédimentation du phosphore total était environ 17 fois plus élevée que la rétention tandis que l'azote (N) était environ 3 fois plus élevé et le Fe environ 31 fois plus élevé. Des rapports très élevés N/P dans des eaux épilimnétiques (36/1 par poids) et des rapports faibles N/P dans le matériel des piège (8/1) et des sédiments de surface (moyenne de 8/1, étendue de 4-11/1), de concert avec des rapports sédimentation–rétention élevés, portent vivement à croire que les sédiments remis de nouveau en suspension constituent une composante importante du matériel des pièges. D'après les rapports Fe/TP, les sédiments de surface provenant d'eaux peu profondes (moins de 13 m) étaient les plus importants contribuables aux sédiments remis de nouveau en suspension. De grandes quantités de phosphore biologiquement disponible provenant des sédiments remis de nouveau en suspension peuvent pénétrer dans les eaux supérieures. La différence entre les rapports N/P dans les sédiments de surface (4-11/1) et les éléments nutritifs retenus à partir des calculs du bilan massique (50/1) est attribuée à la dénitrification.

Received August 10, 1989
Accepted February 8, 1990
(JA274)

Reçu le 10 août 1989
Accepté le 8 février 1990

Knowledge of the loss rate of material from the water column to the bottom of lakes is of prime importance in answering many limnological questions. The flux of material to the bottom sediments affects the biological communities of lakes (Rigler 1973) because the settling rate of particles can influence open water concentrations of elements including nutrients and toxicants. This can be either a negative or positive factor; that is, may correspond to a loss of elements attached to particles, or to an increase as falling particles accumulate at various depths and release associated components.

Loss rates to the sediments are often the most difficult parameter to measure in lake mass balance studies. Reckhow and Chapra (1983) reviewed the concept of a sedimentation coefficient as it relates to phosphorus dynamics in lakes. Because of the difficulty in accurately determining the sedimentation coefficient (especially if the gross coefficient is considered), the concept of retention, i.e. the net proportion of the input accumulated, has been used in mass balance work with nutrients (Kirchner and Dillon 1975; Reckhow and Chapra 1983) although retention is theoretically related to the sedimentation coefficient. The difficulties in accurately determining sedimentation rates from mass balance studies of eutrophic systems are reflected in the study of Rotsee, Switzerland (Vollenweider 1976; Bloesch 1977).

Despite the important role of sediments in lake processes, the sedimentary process is very poorly understood. This is not for lack of effort on the part of limnologists. It is, rather, in part because of the methodological problems involved in quantifying sedimentation over short periods of time. For changes in fluxes and accumulation over long periods of time (>10 yr), radiotracer and paleolimnological dating of sediment cores will usually suffice (Krishnaswami and Lal 1978; Evans 1980). These same techniques are not useful for shorter time periods, however. As a result, sediment traps are frequently used to measure fluxes and settling rates out of the water column over short time periods. However, there is a great deal of statistical uncertainty associated with short time periods and long-term studies are lacking.

A second difficulty in studies of sedimentary processes lies in the resuspension of bottom sediments, which can be significant even in small lakes (Davis 1968, 1973). Resuspended material can be significantly greater than material settling for the first time, such as zooplankton feces, senescent phytoplankton, inorganic material, etc., obscuring recycling processes.

This study quantifies the annual, whole-lake loss of nitrogen, phosphorus, and iron from the water column to the bottom sediments in a small, stratified, oligotrophic, P-limited lake. The goal was to quantify the contribution of resuspension to nutrient loading by measuring differences between sedimentation and retention rates of total phosphorus (TP), N, and total Fe in conjunction with epilimnetic and surficial sediment data over a 4-yr period. Fe/N/TP ratios were used to trace the origin of trap material.

Study Site

The study was conducted in Blue Chalk Lake (45°12′N, 78°56′W), a small, stratified, oligotrophic lake (average whole-lake TP concentration was 6.9 $\mu g \cdot L^{-1}$ 1977–81) located on the Precambrian shield in central Ontario (surface area 52.4 ha, mean depth 8.5 m, maximum depth 23 m). Approximately 31% of the sediment surface area lies in waters shallower than 4 m. Mean ice-free Secchi depth ranged from 5.8 to 7.3 m with a mean of 6.6 m during the study period (1977–81). The lake had a small zone of anoxia in the hypolimnion each summer, resulting in an average internal TP load of 6.5 $mg \cdot m^{-2} \cdot yr^{-1}$, about 16% of the external load (P. J. Dillon, unpubl. data).

Methods

Up to 11 sample stations were selected for sediment traps (Fig. 1). The exact number at any one time was variable as a result of upset traps and vandalism. The traps were exposed over four complete hydrologic years, commencing in April 1977 and finishing in April 1981.

Several reviews on the use and design of sediment traps have been published (Hargrave and Burns 1979; Bloesch and Burns 1980; Gardner 1980a,b). The proper design of a sediment trap has been refined to the point that we now accept that traps should be cylindrical in shape, have a height to diameter ratio (aspect ratio) of at least 5:1, preferably 10:1, and be suspended from a subsurface flotation device. Given this design, it is generally believed that traps can provide an accurate quantification of the downward flux of material at the trap location.

Two types of traps were used for comparative purposes in the initial phase of the study: negatively buoyant and positively buoyant. Both types of traps consisted of an open acrylic cylinder 50 cm tall with an inside diameter of 9.8 cm (aspect ratio = 5:1). The wall thickness was 0.6 cm. The negatively buoyant traps (Fig. 2), were suspended by a rope from a surface float which was permanently anchored to a cement block. A weight attached to the bottom of the traps gave them their negative buoyancy. Traps were pulled to the surface at a constant rate to obtain the sample. The positively buoyant traps (Fig. 2) were set by placing a wood and cement "tee" equipped with a pulley system on the lake bottom. The trap was attached by a line running through the pulleys to a float located just below the lake surface and then to a surface float. To raise the trap, the line attached to the subsurface float was loosened. A styrofoam collar on the trap brought it to the surface. This design

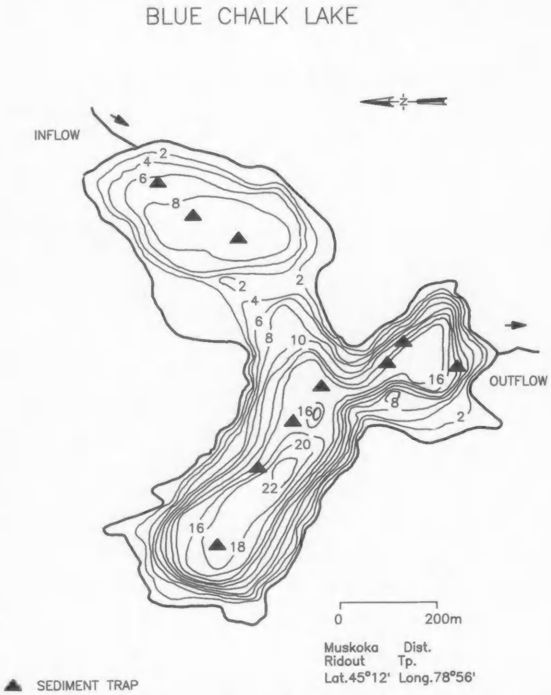

FIG. 1. Morphometric map of Blue Chalk Lake showing sediment trap locations.

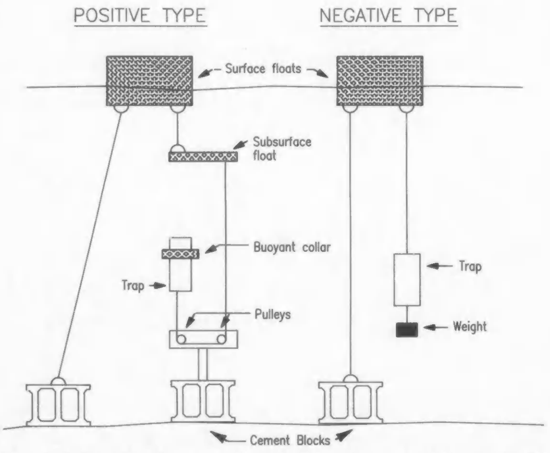

FIG. 2. Schematic diagrams of positively and negatively buoyant sediment traps.

is modified from that described by Kirchner (1975). Most of the traps were suspended approximately 1 m below the bottom of the thermocline. At two locations (20 and 14 m depth), duplicate traps were suspended 1 m off the bottom to check for variability in flux throughout the water column. After approximately 18 mo, all positively buoyant traps were replaced with negatively buoyant traps because the latter were much easier to use and resulted in less frequent loss of samples.

Traps were emptied at approximately 2-wk intervals except during ice cover. After fall turnover, traps were set and then left until the ice melted in the spring at which time they were recovered. Once retrieved, the total contents of the traps were emptied into a large pre-cleaned container. The sample volumes were measured and the contents homogenized and subsampled for analysis of suspended solids, TP, total Kjeldahl nitrogen (TKN) and Fe. Details of the analytical procedures are outlined elsewhere (Ontario Ministry of Environment 1983). Traps with identifiable contamination, such as live fish, were eliminated from the analysis.

At the same time as the traps were changed, the water column was sampled for TKN, TP, and Fe. In this way trap contents could be corrected for the mass present in the trap at the start of the exposure period and elemental ratios in the traps could be compared with the source of "new" production in the euphotic zone.

The major stream inflow and the lake outflow were fitted with hydrologic structures. Water level was continuously recorded and converted to discharge using a stage–discharge relationship derived from instantaneous measurements (Scheider et al. 1983). Each stream was sampled on a weekly basis (more frequently during spring runoff) for TKN, NO_3^-, TP, and Fe. At the same time, regular sampling and analysis of the precipitation in the vicinity of Blue Chalk Lake for these parameters was undertaken. From these data, detailed mass balance estimates of lake input, output, and retention (input–output) were calculated. There were no significant changes in the concentration of any of the three chemical parameters in the lake between years, simplifying the mass balance calculations. Specific details of the mass balance studies will be presented elsewhere.

Sixteen sediment cores were taken at lake depths ranging from 7.5 to 23 m in 1977–81 using a KB gravity corer with a 4.8-cm inside diameter core tube. One to three cores were obtained at each station. The cores were sectioned into 1-cm slices using an extruder and plastic collar. The replicate slices were combined, dried at 100°C to a constant mass (a minimum of 24 h) and then ground to a fine powder. Subsamples for nutrient determination were digested in hot sulfuric acid with the addition of potassium persulfate. TKN and TP were measured after elimination of interfering Fe by precipitation and filtration. Subsamples for analysis of Fe were digested overnight at 70°C in a 2:1 mixture of HCl and HNO_3, then diluted with deionized, distilled water. The ranges for the elemental ratios for the top 1 cm are reported in Table 2.

Results and Discussion

Spatial Variability

There was considerable variability in the amount of P, N, and Fe collected in the traps from site to site in any given sampling interval. There was, however, no consistent pattern. Spatial variability in sediment trap collections was a function of the water column depth of the sample site in Lake Erie (Bloesch 1982) and a function of the distance offshore in Lake Ontario (Rosa 1985). This was not the case in Blue Chalk Lake. Because of missing sample points, a detailed analysis of variance was not possible; however, an examination of several complete sampling intervals showed no consistent pattern to the variability.

TABLE 1. Annual trap sedimentation rates (S) and mass balance retention rates (R) of TP, TKN, and Fe ($mg \cdot m^{-2} \cdot yr^{-1}$) in Blue Chalk Lake.

Sampling period	Sedimentation	Retention	S/R Ratio
TP			
1977–78	641	56.5	11.3
1978–79	447	27.9	16.0
1978–80	457	27.5	16.6
1980–81	442	18.9	23.4
Nitrogen			
1977–78	6035[a]	1454[b]	4.2
1978–79	3756[a]	1720[b]	2.2
1979–80	3158[a]	2291[b]	1.4
1980–81	3717[a]	1117[b]	3.3
Fe			
1977–78	12134	265	45.8
1978–79	9381	373	25.2
1979–80	7276	345	29.7
1980–81	7086	318	22.3

[a] TKN
[b] TN(= TKN + NO_3)

No significant difference was observed between bottom traps and those in the upper water column at two locations where traps were exposed at 1 m below the thermocline and 1 m above the bottom on 27 separate occasions.

Annual Variability in Trap Catches

Because no consistent pattern of spatial variability was found, we have assumed that the average of all available samples was the best representation of the average sedimentation rate in the lake during the study period.

In Table 1, the annual sedimentation rates of each element are shown. TP sedimentation ranged from 442 $mg \cdot m^{-2} \cdot yr^{-1}$ in year 4 to 641 $mg \cdot m^{-2} \cdot yr^{-1}$ in year 1 with an average rate (± cv) of 497 (± 19%). The average TKN and Fe sedimentation rates were 4167 (± 31%) and 8970 (± 26%) $mg \cdot m^{-2} \cdot yr^{-1}$, respectively, with the highest rates also found in year 1.

Comparison of Sedimentation and Retention

Sedimentation and retention rates are compared on an annual basis for TP, TKN, and Fe in Table 1. It is clear that gross sedimentation rates as measured by traps are much greater than retention rates measured by mass balances. The sedimentation/retention ratios for TP, TKN, and Fe were approximately 17, 2.8, and 31, respectively. Fuhs (1973) found an almost equally large discrepancy between sediment trap collection and mass balances, with a ratio of 10 for TP in Canadarago Lake in New York. In another study, the ratios of trap flux to that calculated from surficial sediment chemistry and chronology were 3.2 for TKN and 1.1 for Fe using a trap with an aspect ratio of 2.7 just above bottom in the deepest part of Lake Windermere (Hamilton-Taylor and Willis 1984).

TABLE 2. Ratios of Fe/N/TP (by weight) in sediment trap material, surficial sediments, epilimnetic waters during summer stratification and material retained in mass balance calculations in Blue Chalk Lake 1977–81.

Sediment trap	18/8/1	(TKN)
Surficial sediments <13 m	16-29/4-10/1	(TKN)
>13 m	9-19/5-11/1	
Epilimnion	7/36/1	(TKN)
	7/34/1	(TON)
Retention	9/50/1	(TN)

Clearly, sedimentation and retention are not the same thing. It is extremely unlikely that our mass balance measurements missed over 90% of the incoming TP. Evans and Rigler (1980) and Cross and Rigler (1983) showed that retention of TP and permanent storage in the sediments were approximately equal in a small Canadian shield lake, which suggests that mass balance retention measurements provide a more realistic estimate of long-term accumulation than downward flux as measured by sediment traps.

It is possible that some feature of the trap design caused over-collection of material. Gardner (1980a) discussed the ''snow fence'' effect. In a fluid system where particles have some horizontal component of velocity, a boundary such as a sediment trap wall results in a decrease in the horizontal velocity. In such a situation, the particles lose their horizontal momentum and the result is an increase in the downward component of their velocity. In this situation, more particles will fall in the vicinity of the boundary. Work in experimental flumes (Gardner 1980a), however, has shown that at the minimal horizontal velocities experienced in the hypolimnia of lakes such as Blue Chalk, this phenomenon should be inconsequential.

Assuming that trap measurements provide a reasonable estimate of the downward flux of particulate material, i.e. of gross sedimentation rates, possible explanations for these differences are: (1) resuspension of bottom sediment and (2) rapid recycling of dissolved nutrients from bottom sediments into new production in the water column via entrainment as plausible rationales.

Resuspension should not be ignored as it is likely to be a common occurrence in lakes the size of Blue Chalk. Examples and explanations of resuspension in large and small lakes are reported by Bryson and Bunge (1956), Davis (1968, 1973), Serruya (1977), Stiller (1977), Wright et al. (1980), Bloesch (1982), Kortmann et al. (1982), Evans and Rigler (1983), Carper and Bachmann (1984), Peters and Cattaneo (1984), Rosa (1985), Kenney (1985), Hilton et al. (1986), Charlton and Lean (1987) and Lee et al. (1987).

Little or no sediment accumulates permanently above the bottom of the epilimnion in Blue Chalk Lake (Dillon and Evans 1982; P. J. Dillon, unpubl. data). Presumably, seston deposited in this region undergoes constant resuspension followed by redeposition in deeper waters. The distribution of net sediment accumulation rates with depth can be thought of as a probability distribution in which the probability of resuspension decreases with increasing depth (similar to Fee's (1979) description). As sediments are redeposited deeper and deeper, they will accumulate as they become less susceptible to resuspension; hence, the amount of resuspended sediment originating in deep waters should be minimal.

There was a trend towards increased sedimentation at fall turnover when resuspension was probably at its highest. Although the variability between samples makes analysis difficult, sedimentation would still grossly overestimate retention even if the fall overturn catch were eliminated. It is not surprising that material trapped over the relatively short overturn period was not a very large proportion of the annual catch in light of the work of Davis (1968) who continued to trap pollen during the winter in small, ice-covered Frains Lake. It appears that sufficient energy is imparted during turnover, even in small lakes, to maintain particles in suspension for long periods of time under quiescent conditions.

A clue as to the origin of trap material can be found by comparing elemental ratios. In Blue Chalk Lake, epilimnetic TKN/TP ratios were much higher than trap and surficial sediment ratios (Table 2), which probably rules out settling phytoplankton as a major component of trap material since much of the TKN and TP in the epilimnion is in the phytoplankton, and dissolved organic matter concentration is low. Trap material may, however, be derived from zooplankton feces. For example, a low N/P ratio of 2.6 was reported for fresh fecal pellets from a marine crustacean feeding on diatoms (Johannes and Satomi 1966).

Settling zooplankton feces and phytoplankton which are subjected to rapid loss of N (or P accumulation; Gächter and Mares 1985), although P accumulation runs counter to the argument that plankton P is rapidly recycled within the epilimnion (Golterman 1980; DePinto et al. 1986)) cannot be ruled out as a source of trap material with a low TKN/TP ratio. Unfortunately, we do not have estimates of annual community uptake rates of P, N, and Fe to compare with sedimentation rates. However, the similarity of trap and surficial sediment elemental ratios (Table 2) and the high sedimentation to retention ratios (Table 1) strongly suggests that resuspended surficial sediment is the major component of material collected in sediment traps in Blue Chalk Lake.

We attribute the discrepancy in N/P ratios in surficial sediments (7.7 (SD 1.7)/1) and in retained TN ($TKN + NO_3^-$) derived from mass balance calculations (50/1) to loss of N via denitrification. To compare retained TN to TKN stored in sediments, it must be assumed that storage of NO_3^- in sediments is negligible, a reasonable assumption for sediments 2 cm below the sediment/water interface. The TKN/TP ratios for 20 cm long cores were similar to surficial sediments; hence, over 80% of retained N is likely denitrified in Blue Chalk Lake.

Particulate N/P ratios were also low in P-limited Findley Lake, ranging from five to ten in trap material and 2.5–8.0 in surficial sediments (Hendrey and Welch 1974; Wissmar et al. 1977), similar to those in Blue Chalk Lake. Serruya (1977) estimated that 68% of material trapped on an annual basis in Lake Kinneret was resuspended bottom sediment by comparing alumino silicate concentrations in river inputs, bottom sediments and trap material. N/P ratios of trap material and bottom sediments were similar and were much lower than riverine inputs.

TN/TP ratios decreased with increasing turbulence in a large, shallow New Zealand lake (Hamilton and Mitchell 1988). Similarly, in Blue Chalk Lake, the average whole-lake TON/TP ratios (where $TON = TKN - NH_4^+$), which are estimates of particulate N/P ratios, were lower during turnover (~26) than in epilimnetic waters (~36) from April 1984 to July 1988. Hence, about 36% of suspended material was resuspended sediment during turnover in Blue Chalk Lake.

The proportion of trap material collected annually which is resuspended material was high in all of the lakes reported: 83%

in Frains Lake and 72–90% in Sayles Lake (Davis 1968, 1973), 91% in Canadarago Lake (Fuhs 1973) and 94% in Blue Chalk Lake. It is possible that large and variable amounts of resuspended P may account for some of the variability in published settling coefficients for TP in mass balance models (Frisk et al. 1981).

Fe/TP ratios suggest that surficial sediment from shallow waters (<13 m) was the largest contributor to resuspended sediment. The mean epilimnetic Fe/TP ratio was seven compared to 18 in trap material and 23 ± 5 (range 16–29) and 13 ± 3 (range 9–19) in surficial sediments from shallow and deep sites, respectively (Table 2). The decrease in the surficial sediment Fe/TP ratio with increasing depth may be related to the distribution of anoxic conditions.

The second alternative explanation of high sedimentation/retention ratios was rapid recycling of dissolved nutrients from bottom sediments into new production. While not excluding this possibility, the estimated internal P load during the study period of $6.5\ \mathrm{mg \cdot m^{-2} \cdot yr^{-1}}$ (P. J. Dillon, unpubl. data) was minor compared with the difference between the average sedimentation rate and the average retention rate of "new" TP which was $464\ \mathrm{mg \cdot m^{-2} \cdot yr^{-1}}$ (Table 1). Furthermore, recycling of dissolved nutrients from sediments does not explain the similarity in Fe/N/TP ratios between trap material and surficial sediments and the dissimilarity between trap material and epilimnetic ratios (Table 2) unless a P-enrichment mechanism such as that of Gächter and Mares (1985) is invoked. However, a successful enrichment model must account for both the fourfold increase in TP and the 10-fold increase in Fe relative to N in Blue Chalk Lake trap material; then the similarity in Fe/N/TP ratios between trap material and surficial sediments becomes a coincidence. Hence, recycling of dissolved nutrients from the sediment coupled to some mechanism which enriches "new" detrital material is not a likely explanation of the high sedimentation/retention ratio.

Clearly, the transport of nutrients from catchments and the atmosphere to the sediments of small lakes should not be considered unidirectional in stratified lakes because of repeated deposition and resuspension. Resuspension likely plays an important role in the nutrient dynamics of stratified lakes, especially oligotrophic lakes lacking significant diffusion of dissolved P from reduced sediments. Fitzgerald (1970) and Golterman (1977) showed that sediment supported algal growth under aerobic conditions in culture only when in direct contact with sediment whereas growth did not occur when sediment and algae were separated by dialysis membrane.

Large amounts of biologically available phosphorus (BAP) originating with resuspended sediment may enter the euphotic zone during turnover or from entrainment of hypolimnetic waters. The amount of resuspended BAP entering upper waters in Blue Chalk Lake may be five times larger than stream and atmospheric inputs of BAP assuming that 30% of the TP input from streams and bulk precipitation (Dillon and Reid 1981) and 10% of the resuspended TP is BAP (Young et al. 1985). Furthermore, particulate P may enter the pelagic food chain through grazing by strict heterotrophs as well as phagotrophic phytoflagellates (Bird and Kalff 1989).

We have shown using Fe/N/TP signatures from mass balance calculations, sediment traps, sediment cores and lake water chemistry during a relatively long term study period that sediment resuspension is a major process in a small, stratified, oligotrophic lake and that "new" detrital material is only a minor proportion of settling material. If "new" material is less than 10% of trap material but "new" material dominates the upper water column during stratification, then "new" material does not settle out — it must recycle efficiently in the water column, at least until fall turnover.

While steady state models can relate lake productivity to external load without direct reference to sediments, dynamic models of TP concentration and recycling will have to address the influence of resuspension.

Acknowledgements

We would like to thank R. Reid and B. Locke for helping with much of the field work, and Dr. G. Nürnberg for comments and discussion on the manuscript. This work was funded as part of the Lakeshore Capacity Study.

References

Bird, D. F., and J. Kalff. 1989. Phagotrophic sustenance of a metalimnetic phytoplankton peak. Limnol. Oceanogr. 34: 155–162.

Bloesch, J. 1977. Sedimentation rates and sediment cores in two Swiss lakes of different trophic status, p. 65–71. *In* H. L. Golterman [ed.] Interactions between sediments and freshwater. Proc. Int. Symp. Dr. W. Junk Publishers, Amsterdam, The Netherlands.

1982. Inshore–offshore sedimentation differences resulting from resuspension in the eastern basin of Lake Erie. Can. J. Fish. Aquat. Sci. 39: 748–759.

Bloesch, J., and N. M. Burns. 1980. A critical review of sedimentation trap technique. Schweiz. Z. Hydrol. 42: 15–55.

Bryson, R. A., and W. W. Bunge, Jr. 1956. The 'stress-drop' jet in Lake Mendota. Limnol. Oceanogr. 1: 42–46.

Carper, G. L., and R. W. Bachmann. 1984. Wind resuspension of sediments in a prairie lake. Can. J. Fish. Aquat. Sci. 41: 1763–1767.

Charlton, M. N., and D. R. S. Lean. 1987. Sedimentation, resuspension, and oxygen depletion in Lake Erie (1979). J. Great Lakes Res. 13: 709–723.

Cross, P. M., and F. H. Rigler. 1983. Phosphorus and iron retention in sediments measured by mass budget calculations and directly. Can. J. Fish. Aquat. Sci. 40: 1589–1597.

Davis, M. B. 1968. Pollen grains in lake sediments: redeposition caused by seasonal water circulation. Science (Wash., DC) 162: 796–799.

1973. Redeposition of pollen grains in lake sediment. Limnol. Oceanogr. 18: 44–52.

DePinto, J. V., T. C. Young, J. S. Bonner, and P. W. Rodgers. 1986. Microbial recycling of phytoplankton phosphorus. Can. J. Fish. Aquat. Sci. 43: 336–342.

Dillon, P. J., and R. D. Evans. 1982. Whole-lake lead burdens in sediments of lakes in southern Ontario, Canada. Hydrobiol. 91: 121–130.

Dillon, P. J., and R. A. Reid. 1981. Input of biologically available phosphorus by precipitation to Precambrian lakes, p. 183–198. *In* S. Eisenreich [ed.] Atmospheric pollutants in natural waters. Ann Arbor Science.

Evans, R. D. 1980. Measurement of sediment accumulation and phosphorus retention using lead-210 dating. Ph.D. thesis, McGill University, Montreal, Canada.

Evans R. D., and F. H. Rigler. 1980. Measurement of whole lake sediment accumulation and phosphorus retention using lead-210 dating. Can. J. Fish. Aquat. Sci. 37: 817–822.

1983. A test of lead-210 dating for the measurement of whole lake soft sediment accumulation. Can. J. Fish. Aquat. Sci. 40: 506–515.

Fee, E. J. 1979. A relation between lake morphometry and primary productivity and its use in interpreting whole-lake eutrophication experiments. Limnol. Oceanogr. 24: 401–416.

Fitzgerald, G. P. 1970. Aerobic lake muds for the removal of phosphorus from lake waters. Limnol. Oceanogr. 15: 550–555.

Frisk, T., J. S. Niemi, and K. A. I. Kinnunen. 1981. Comparison of statistical phosphorus-retention models. Ecol. Model. 12: 11–27.

Fuhs, G. W. 1973. Improved device for the collection of sedimenting matter. Limnol. Oceanogr. 18: 989–993.

Gächter, R., and A. Mares. 1985. Does settling seston release soluble reactive phosphorus in the hypolimnion of lakes? Limnol. Oceanogr. 30: 364–371.

Gardner, W. D. 1980a. Sediment trap dynamics and calibration. A laboratory evaluation. J. Mar. Res. 38: 17–39.

1980b. Field assessment of sediment traps. J. Mar. Res. 38: 41–52.

Golterman, H. L. 1977. Sediments as a source of phosphate for algal growth, p. 286–293. *In* H. L. Golterman [ed.] Interactions between sediments and freshwater. Proc. Int. Symp. Dr. W. Junk Publishers, Amsterdam, The Netherlands.

1980. Phosphate models, a gap to bridge. Hydrobiol. 72: 61–71.

Hamilton, D. P., and S. F. Mitchell. 1988. Effects of wind on nitrogen, phosphorus, and chlorophyll in a small New Zealand lake. Verh. Int. Ver. Limnol. 23: 624–628.

Hamilton-Taylor, J., and M. Willis. 1984. Depositional fluxes of metals and phytoplankton in Windermere as measured by sediment traps. Limnol. Oceanogr. 29: 695–710.

Hargrave, B. T., and N. M. Burns. 1979. Assessment of sediment trap collection efficiency. Limnol. Oceanogr. 24: 1124–1136.

Hendrey, G. R., and E. B. Welch. 1974. Phytoplankton productivity in Findley Lake. Hydrobiol. 45: 45–63.

Hilton, J., J. P. Lishman, and P. V. Allen. 1986. The dominant processes of sediment distribution and focusing in a small, eutrophic, monomictic lake. Limnol. Oceanogr. 31: 125–133.

Johannes, R. E., and M. Satomi. 1966. Composition and nutritive value of fecal pellets of a marine crustacean. Limnol. Oceanogr. 11: 191–197.

Kenney, B. C. 1985. Sediment resuspension and currents in Lake Manitoba. J. Great Lakes Res. 11: 85–96.

Kirchner, W. B. 1975. An evaluation of sediment trap methodology. Limnol. Oceanogr. 20: 657–660.

Kirchner, W. B., and P. J. Dillon. 1975. An empirical method of estimating the retention of phosphorus in lakes. Wat. Resour. Res. 11: 182–183.

Kortmann, R. W., D. D. Henry, A. Khether, and S. Kaufman. 1982. Epilimnetic material loading by metalimnetic erosion and resultant algal responses in Lake Waramaug, Conn. Hydrobiol. 92: 501–510.

Krishnaswami, S., and D. Lal. 1978. Radionuclide limnochronology, p. 153–177. *In* A. Lerman [ed.] Lakes — chemistry, geology, physics. Springer-Verlag, New York, NY.

Lee, C., J. A. McKenzie, and M. Sturm. 1987. Carbon isotope fractionation and changes in the flux and composition of particulate matter resulting from biological activity during a sediment experiment in Lake Greifen, Switzerland. Limnol. Oceanogr. 32: 83–96.

Ontario Ministry of Environment. 1983. Handbook of analytical methods for environmental samples. Vol. 1 and 2, Toronto, Ont., Canada.

Peters, R. H., and A. Cattaneo. 1984. The effects of turbulence on phosphorus supply in a shallow bay of Lake Memphremagog. Verh. Int. Ver. Limnol. 22: 185–189.

Reckhow, K. H., and S. C. Chapra. 1983. Engineering approaches for lake management. Vol. 1, Butterworth Publishers, Toronto, 340 p.

Rigler, F. H. 1973. A dynamic view of the phosphorus cycle in lakes, p. 539–572. *In* E. J. Griffith et al. [ed.] Environmental phosphorus handbook. John Wiley and Sons, New York, NY.

Rosa, F. 1985. Sedimentation and sediment resuspension in Lake Ontario. J. Great Lakes Res. 11: 13–25.

Scheider, W. A., C. M. Cox, and L. D. Scott. 1983. Hydrological data for lakes and watersheds in the Muskoka–Haliburton study area (1976–1980). Ont. Min. Environ. Data Rep. DR 83.6

Serruya, C. 1977. Rates of sedimentation and resuspension in Lake Kinneret, p. 48–56. *In* H. L. Golterman [ed.] Interactions between sediments and freshwaer. Proc. Int. Symp. Dr. W. Junk Publishers, Amsterdam, The Netherlands.

Stiller, M. 1977. Origin of sedimentation components in Lake Kinneret by their isotopic composition, p. 57–64. *In* H. L. Golterman [ed.] Interactions between sediments and freshwater. Proc. Int. Symp. Dr. W. Junk Publishers, Amsterdam, The Netherlands.

Vollenweider, R. A. 1976. Rotsee, a source, not a sink for phosphorus? A comment to and a plea for nutrient balance studies. Schweiz. J. Hydrol. 38: 29–34.

Wissmar, R. C., J. E. Richey, and D. E. Spyridakis. 1977. The importance of allochthonous particulate carbon pathways in a subalpine lake. J. Fish. Res. Board Can. 34: 1410–1418.

Wright, R. F., A. Matter, M. Schweingruber, and U. Siegenthaler. 1980. Sedimentation in Lake Biel, an eutrophic, hard-water lake in northwestern Switzerland. Schweiz. Z. Hydrol. 42: 101–126.

Young, T. C., J. V. DePinto, S. C. Martin, and J. S. Bonner. 1985. Algal-available particulate phosphorus in the Great Lakes Basin. J. Great Lakes Res. 11: 434–446.

Brood Mortality and Egg Predation by the Nemertean, *Carcinonemertes epialti*, on the Yellow Rock Crab, *Cancer anthonyi*, in Southern California

Jeffrey D. Shields[1], Robert K. Okazaki[2], and Armand M. Kuris

University of California, Department of Biological Sciences and the Marine Science Institute, Santa Barbara, CA 93106, USA

Shields, J. D., R. K Okazaki, and A. M. Kuris. 1990. Brood mortality and egg predation by the nemertean, *Carcinonemertes epialti*, on the yellow rock crab, *Cancer anthonyi*, in southern California. Can. J. Fish. Aquat. Sci. 47: 1275–1281.

Carcinonemertes epialti had a minimal impact on the egg mortality of a lightly infested population of a commercially important crab host, *Cancer anthonyi*. The nemertean had a high prevalence (>97%) but was found at low intensities (mean intensity = 86.5 worms/pleopod, mean density = 0.3 worms/1000 eggs). Egg mortality varied from 0.0–30.5%, and was highly correlated with both worm intensity, and the timing of crab embryogenesis (mean mortality = 5.7%). Separate sites within the pleopod experienced different causal mechanisms of mortality. Mortality at the base of the pleopod was correlated with the presence, abundance, and immigration of *C. epialti*. Mortality at the tip of the pleopod was less correlated with worm abundance and was most likely a result of abrasion to the eggs or egg mass. Infestations of *C. epialti* varied between seasons and between host species. The worm was more abundant on host species that bred year-round (*Cancer anthonyi* and *Hemigrapsus oregonensis*); hence, infestation dynamics varied markedly between host species. In southern California, *Cancer anthonyi* was virtually always infested with *C. epialti* and is the most important host for the worm in this area.

Carcinonemertes epialti avait peu d'effet sur la mortalité des oeufs d'une population peu infestée d'un crabe hôte à grande valeur commerciale *Cancer anthonyi*. Ce némertien avait une forte prévalence (97%) mais il a été trouvé à de faibles intensités (intensité moyenne = 86,5 vers par pléopode, densité moyenne = 0,3 vers par 1000 oeufs). La mortalité des oeufs variait de 0,0 à 30,5%, et elle était fortement correlée à l'intensité des vers et au moment de l'embryogenèse du crabe (mortalité moyenne = 5,7%). Des sites distincts à l'intérieur du pléopode présentaient différents mécanismes responsables de la mort. La mortalité à la base du pléopode était correlée à la présence, à l'abondance et à l'immigration de *C. epialti*. La mortalité à l'extrémité du pléopode était moins correlée à l'abondance du ver et elle était très probablement le résultat de l'abrasion des oeufs ou de la masse d'oeufs. Les infestations de *C. epialti* variaient d'une saison à l'autre et d'une espèce hôte à l'autre. Les vers étaient plus abondants chez les espèces hôtes qui se reproduisaient à l'année (*Cancer anthonyi* et *Hemigrapsus oregonensis*); donc, la dynamique de l'infestation variait de façon marquée d'une espèce à l'autre. Dans le sud de la Californie, *Cancer anthonyi* était presque toujours infesté par *C. epialti* et il s'agit de l'hôte le plus important du vers dans ce cas-ci.

Received October 9, 1978
Accepted February 27, 1990
(J9449)

Reçu le 9 octobre 1987
Accepté le 27 février 1990

Species of the nemertean genus *Carcinonemertes* are egg predators that may cause substantial brood mortality on their decapod crustacean hosts (Wickham 1979a; Wickham et al. 1985; Kuris and Wickham 1987; Shields and Kuris 1988a). The impact of these nemerteans on the broods of their hosts can be heavy with complete brood loss occurring in many instances (Wickham 1979a; Kuris and Wickham 1987; Shields and Kuris 1988a). Outbreaks of *Carcinonemertes* spp. on the Dungeness crab, *Cancer magister*, and the red king crab, *Paralithodes camtschatica*, may have contributed to the recent decline of certain stocks of these crabs (Wickham 1979a; Wickham et al. 1985). A related nemertean, *Pseudocarcinonemertes homari*, has been found at high intensities on the broods of *Homarus americanus*, and may be responsible for much egg mortality on that host (Aiken et al. 1985; Campbell and Brattey 1985).

Infestations of *Carcinonemertes epialti* occur on several crab species: *Cancer antennarius*, *Cancer anthonyi*, *Hemigrapsus oregonensis*, *Pachygrapsus crassipes*, and *Pugettia producta* (Kuris 1971, 1978; Roe 1979, 1984; Shields and Kuris 1988a). Past studies of *C. epialti* have focused on the relationship of the nemertean with its grapsid hosts; little work has been done on the impact of *C. epialti* on *Cancer anthonyi*.

The yellow rock crab, *Cancer anthonyi*, is a commercially harvested crab that is abundant at nearshore depths (≤100 m) in the Santa Barbara Channel, California. Annual landings of rock crabs (*C. antennarius*, *C. anthonyi*, and *C. productus*) along the California coast were valued at over 2.0 million dollars in 1985, (Preliminary Notes of Commercial Fish Landings by Region; Resource Agency of California, California Fish and Game, 245 Broadway, Suite 350, Long Beach, CA). The Santa Barbara fishery represents between 24–67% of the total landings (1981–86), and *C. anthonyi* is the largest contributor to this fishery in southern California (Carroll and Winn 1988).

---

[1] Present address: University of Queensland, Department of Parasitology, St. Lucia, Brisbane, 4067, Qld., Australia.

[2] Present address: University of South Alabama, Department of Biological Sciences, Life Sciences Building, Mobile, AL. 36688, USA.

Studies of *Carcinonemertes* spp. on other commercially harvested hosts have examined the effects of outbreaks of high worm abundance on crab egg mortality. Since it has been suggested that such outbreaks may be associated with the fishery (Wickham 1979a; Kuris and Wickham 1987; but see Shields and Kuris 1988a), we undertook the examination of a lightly infested population of commercially harvested crabs.

We develop refinements in sampling procedures to account for spatial variation in mortality within the crab egg mass. The infestation parameters examined include prevalence, worm intensity, and worm density. Egg mortality and the effects of predation on egg natality were analyzed in relation to crab embryogenesis, seasonality, and worm abundance. We compare the dynamics of *Carcinonemertes epialti* infestations on *Cancer anthonyi* with infestations on other crab species.

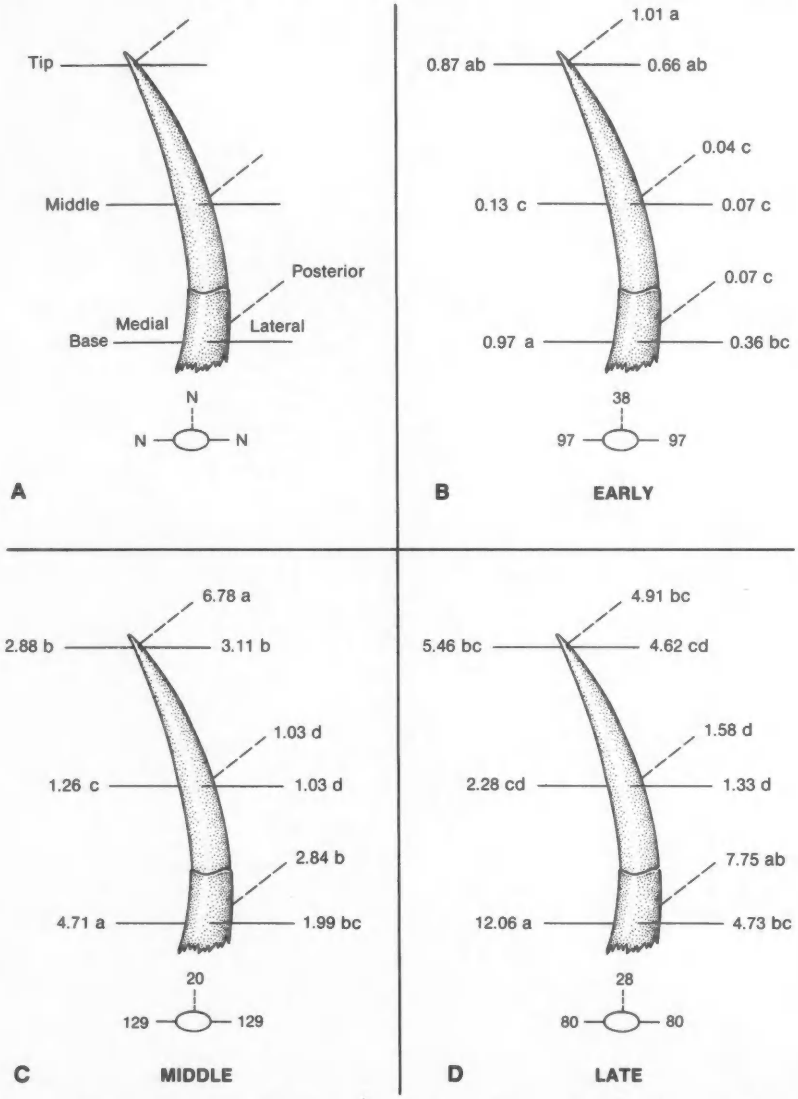
Tip
Middle
Posterior
Medial
Lateral
Base
N
N
N
A
1.01 a
0.87 ab
0.66 ab
0.04 c
0.13 c
0.07 c
0.07 c
0.97 a
0.36 bc
38
97
97
B
EARLY
6.78 a
2.88 b
3.11 b
1.03 d
1.26 c
1.03 d
2.84 b
4.71 a
1.99 bc
20
129
129
C
MIDDLE
4.91 bc
5.46 bc
4.62 cd
1.58 d
2.28 cd
1.33 d
7.75 ab
12.06 a
4.73 bc
28
80
80
D
LATE

FIG. 1. Mean egg mortality (%) by site in the egg mass of the left second pleopod of *Cancer anthonyi* over the course of embryogenesis. *N* is the number of crabs sampled at the respective locations within the egg mass. Pleopods are illustrated schematically as seen from their anterior surface (which, in situ, is appressed against the thoracic sternites). Ovals at the base of each figure represent cross sections of the pleopods with summed sample sizes (*N*). Means with different letters are significantly different from each other, within the pleopod (ANOVA, Bonferroni's inequality, $P<0.05$). (A) Key to locations; (B) early EDS I–II; (C) middle EDS III–IV; (D) late EDS V–VII.

Materials and Methods

Ovigerous crabs were collected by commercial fishermen from the Santa Barbara Channel, between Summerland Gaviota, California (approximately 34°23′–34°25′, 119°34′–120°12′). Crabs were obtained at nearshore depths of 10–100 m. Random samples of 20 to 25 crabs were obtained at monthly or bimonthly intervals for 2 yr (November 1981–November 1983). A total of 345 *Cancer anthonyi* were sampled with the clutches of 311 crabs fully processed. The entire second left pleopod was excised and stored in 5% formalin in seawater (5% FSW) for further analyses. Crabs were either released or maintained in flowing seawater aquaria.

Egg mortality was estimated by sub-sampling different locations on the ovigerous pleopod. The sub-samples (setae with intertwined eggs) were taken from the following sites on the pleopod (Fig. 1A): medial, lateral, and posterior surfaces at the tip of the pleopod; medial, lateral, and posterior surfaces at the middle of the pleopod; and medial, lateral, and posterior surfaces at the base of the pleopod. A preliminary analysis showed that the middle region of the egg mass had a relatively low and uniform degree of egg mortality in the middle and late developmental stages (developmental stages of embryogenesis — EDS classes), thus, we ceased to sample the middle region after August 1982. In 1982–83, the base sites were replicated, and the three middle sites and all of the posterior sites were no longer sampled. At least 100 eggs were counted from each site and the number of live and dead eggs were recorded. Dead eggs persisting as empty egg membranes were attributed to worm predation as in Wickham (1979a); and this was further substantiated by personal observations (Shields and Kuris 1988b). The numbers of worms and worm egg strings found on these sub-samples were also recorded.

To determine the extent of egg mortality along the length of the pleopod and to correct for bias in our sub-sampling, 12 pleopods were divided into 10 equal length pieces and the medial sites were examined. Egg mortality, worm number, and the number of brooded eggs were analyzed along the lengths of each of these pleopods. Since these data compared favorably with those from the site-specific sub-sampling routine, the data were grouped according to region (base, middle, and tip) for statistical analyses.

To correct for variation within the egg mass, the overall mean percentage of egg mortality for each crab was estimated by summing the dead eggs from each sub-sample and dividing by the sum of the total number of eggs in each sub-sample. Egg mortality was then expressed as the percentage of eggs that were dead. A constant mortality estimate was factored into total egg mortality values for each crab sampled after August 1982, since the middle sites were no longer sampled after that date. Egg mortality could not be reliably estimated when hatching was imminent (approximately 40 d post-oviposition) because hatched eggs could not be distinguished from dead eggs. Thus, clutches at or near hatching (EDS stage VIII, see below) were excluded from the statistical analyses.

Crab embryogenesis was quantified as the number of days since oviposition and was based on the mean cumulative time to reach the midpoint of the developmental stage of the eggs (EDS, see Fig. 4). These times were based on daily observations of crabs observed throughout the brood period. Embryogenesis was split into three periods (early development, I–II; middle development, III–V; and late development, VI–VII) for some statistical analyses.

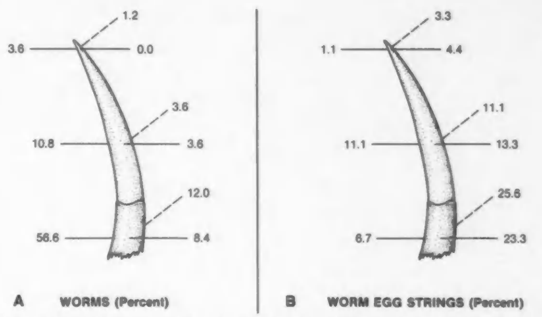

FIG. 2. Distribution of *Carcinonemertes epialti* found at different sites in sub-samples of crab eggs: (A) Worms ($N = 83$ sub-samples); (B) worm egg strings ($N = 90$ sub-samples).

Egg mortality was projected through the developmental period using mortality estimates from clutches in early and middle stages of development (Stages I–IV). Projections were estimated by dividing the proportion of dead eggs in a sub-sample by the cumulative time to the midpoint of the EDS, then multiplying the result by 40, the average number of days in the embryogenic period.

Nemerteans were collected by agitating the complete pleopod (minus the sub-samples) in 400–500 mL of seawater for a minimum of three 1-min washes. After decanting, the worms were transferred to a petri dish and counted under a dissecting microscope. The worms were then stored in 5% FSW.

Nemertean abundance was measured in terms of prevalence, the proportion of infected hosts, and mean intensity, the mean number of worms per infested host (Margolis et al. 1982). Worm intensity was split into four classes (1–30, 31–60, 61–120, and 121+ worms/pleopod) for statistical analyses. Where appropriate, worm intensity was transformed into worm density, defined as the number of worms per 1000 eggs after Wickham (1979a,b; Margolis et al. 1982).

The number of eggs per pleopod was assessed as per Shields and Kuris (1988a). In addition, the total number of eggs per crab was determined for 12 crabs (96 pleopods). The proportion of eggs on each pleopod and the number of worms on each pleopod were also assessed for these crabs.

Results

Site-Specific Mortality

Mortality varied between sites on the pleopod throughout embryogenesis. The base and tip regions exhibited significantly greater egg mortality than the middle region (Fig. 1B–D; ANOVA, Bonferroni's inequality, $P<0.05$).

The distributions of the worms and worm egg strings within the pleopod showed distinctive patterns. Worms were found throughout the pleopod but they were more frequently found in the base sites, especially the medial base site (Fig. 2A). The prevalence and intensity of worms on the individual lengths of the pleopod were significantly lower in the tip region than in the middle and base regions (Table 1). The base region also contained significantly more worm egg strings than the other region (Fig. 2). The egg strings were not, however, markedly abundant at the medial base site where worm numbers and egg mortality were relatively high.

The distribution of the worms was related to the distribution of eggs in the brood (Table 2). Significantly more worms were

TABLE 1. Distribution of *Carcinonemertes epialti* within regions of the pleopod and associated crab egg mortality. The proportion of eggs in each region of the pleopod is also shown, $N = 12$ crabs.

	Mean proportion of eggs on pleopod	Prevalence of worms in separate lengths(%)	Worm number by region	Proportion of worms in regions	Mean intensity	Mean mortality (%)
Tip	0.295	22/48[a] (45.8)	50	0.107	4.2 ± 3.3	1.0
Middle	0.424	31/36 (86.1)	127	0.273	10.6 ± 7.7	0.7
Base	0.281	34/36 (94.4)	290	0.620	24.2 + 19.4[b]	3.2
Total	1.000	87/120 (72.5)	467	1.000	38.9 ± 27.6	1.6

[a] $P<0.05$, $G_H = 30.6$, $d.f. = 2$, significantly different from other regions.

[b] $P<0.05$, ANOVA, Bonferroni's inequality, significantly different from other regions.

TABLE 2. Distribution of *Carcinonemertes epialti* and crab eggs on individual pleopods of *Cancer anthonyi*. The mean total fecundity was approximately 2 608 000 eggs per crab (Shields, Okazaki, and Kuris, unpubl. data). Means with different letters are significantly different from each other (ANOVA, Bonferroni's inequality, $P<0.05$). $N = 12$ crabs, 2858 worms, 96 pleopods. Fecundity and worm data were arcsin-square root transformed for the analysis.

Pleopod pair	Percentage of total fecundity (± SE)	Percentage of total worm abundance (± SE)	Worm density (worms/1000 eggs) mean (± SE)
One	27.4AB (0.3)	34.2A (1.6)	0.111 (0.024)
Two	31.5A (0.4)	29.4A (2.7)	0.093 (0.029)
Three	24.6B (0.7)	20.1B (1.1)	0.085 (0.019)
Four	16.4C (0.5)	16.1C (0.8)	0.087 (0.019)
Total	100.0	100.0	0.093 (0.010)

TABLE 3. Correlation statistics for egg mortality at the tip and base of the pleopod in relation to worm intensity during different developmental periods. Mortality data were arcsin-square root transformed for the analysis. R represents the Pearson product–moment correlation coefficient, N, number of pleopods.

		Worm intensity	
Site	Developmental period	R	N
Tip	Early	0.079	85
	Middle	0.271[a]	120
	Late	0.218	76
Base	Early	0.142	85
	Middle	0.281[a]	120
	Late	0.641[b]	76

[a] $P<0.025$, correlation coefficient significantly different from zero.

[b] $P<0.0001$, correlation coefficient significantly different from zero.

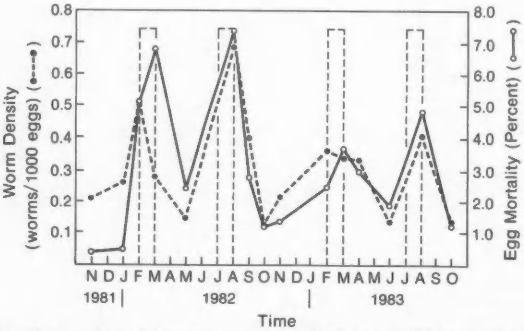

FIG. 3. Density of *Carcinonemertes epialti* (worms/1000 eggs) and egg mortality of *Cancer anthonyi* through time. Winter and summer values (reference bar) were significantly greater than spring and fall values for both density and mortality.

TABLE 4. Relationship between worm intensity and egg mortality. N is the number of pleopods sampled. Means (and standard deviations) with different letters represent significantly different groups (ANOVA, Bonferroni's inequality $P<0.05$.), after arcsin-square root transformation of egg mortality data. Egg mortality is the number of dead eggs per total number of eggs in sub-samples.

Worms/pleopod	N	Egg mortality (%)
0	3	0.7 + 0.3A
1–30	55	1.1 ± 1.5A
31–60	72	1.7 ± 2.0A
61–120	95	3.2 ± 3.5B
121 +	63	5.2 ± 5.9B

found on the first and second pairs of pleopods (those adjacent and closest to the thoracic sternites) than on the other pleopods.

Mortality at the base of the pleopod was highly correlated with worm intensity during the middle and late embryogenic periods (Table 3). Mortalities at the base and tip sites were not correlated with worm intensity during early embryogenic stages, as nemerteans would, as yet, have had little time to effect egg mortality. Projections of egg mortality from crabs having low intensity infestations (1–30 worms/pleopod) indicate that the tip region may experience a relatively constant egg mortality of approximately 4.0–6.0% (for projections see Shields 1987). Since worms were infrequently recovered from the tip sites (Fig. 2), other mortality factors appear to have operated there. Further, a significant correlation was found between mortality at the tip of the pleopod and worm intensity only for clutches in the middle of embryogenesis (Table 3).

Overall Mean Egg Mortality

Carcinonemertes epialti exhibited seasonal variation in mean density on *Cancer anthonyi*, with winter and summer peaks in both years (Fig. 3). The winter and summer peaks in both worm density and total egg mortality were significantly greater than the spring and fall values (ANOVA, Bonferroni's inequality, $P<0.05$). In both years, the total percentage of egg mortality coincided with the July–August peak in worm density, but lagged slightly behind the February–March peaks. The seasonal pattern for mean intensity (not shown) was similar to that for mean density since prevalence was 100% for 13 of the 15 months sampled.

Egg mortality ranged from 0.0–30.5% of the clutch. On individual crabs, egg mortality varied with worm intensity (Table 4), being significantly greater at 61–120 and 121+ worms than at lower intensities (ANOVA, Bonferroni's inequality, $P<0.05$). Two-way ANOVA between egg mortality, and the class variables, intensity, and EDS, showed significant variation in egg mortality with intensity and with EDS ($F=23.67$, *d.f.* $=9$ and 287, $P<0.0001$), but no significant interaction was found between intensity and EDS ($F=0.79$, *d.f.* $=3$ and 6, $P<0.715$).

Time since oviposition, as indicated by EDS, was highly correlated with egg mortality ($R=0.603$, $P<0.0001$, *d.f.* $=283$, $Y=0.040+0.006\ X$). Egg mortality rose from a mean of less than 0.2% (2.5 d post-oviposition) to over 6.0% (37.5 d post-oviposition) over the duration of embryogenesis (Fig. 4a).

Worm density was highly correlated with EDS ($R=0.407$, $P<0.0001$, *d.f.* $=283$, $Y=0.327+0.010\ X$). Worm density varied from 0.01–2.83 worms/1000 eggs or 1–765 worms per pleopod (Fig. 4b). Significant increases in worm density were detected at 21.5 d after oviposition and at 34 d after oviposition when compared with 2.5 and 7.5 d after oviposition (ANOVA, Bonferroni's inequality, $P<0.05$).

Discussion

Carcinonemertes epialti had little effect on the broods of *Cancer anthonyi*. The nemertean never reached the high intensities observed on other decapod species and egg mortality resulting from *C. epialti* rarely exceeded 10% of the clutch. Since rock crab landings have steadily increased over the past 6 yr (Carroll and Winn 1988; Preliminary Notes of Commercial Fish Landings by Region; Resource Agency of California, California Fish and Game, 245 Broadway, Suite 350, Long Beach, CA, 1981–86, unpubl. data) and the intensities of *C. epialti* have remained low, *C. epialti* has at present a minimal impact on the rock crab fishery in southern California.

This analysis documents two causes of site-specific egg mortality in *Cancer anthonyi*. Firstly, egg mortality at the base of the pleopod was strongly associated with the abundance of *C. epialti*, and may result primarily from egg predation. Mechanical damage to the egg mass is unlikely at the base sites of the pleopod and cannot account for the relatively high mortality observed there (see below). Relatively high egg mortality in the basal portion of the clutch may be caused by the continued immigration and feeding of these worms at this site from oviposition to eclosion.

Secondly, egg mortality may be produced by abiotic means. A relatively constant egg mortality of 4.0–6.0% was projected for the tip of the pleopod when worm intensity was low. The mortality at the tip site may be due to exposure resulting in mechanical damage; the abdomen of *Cancer anthonyi* does not completely enclose the distal portion of the egg clutch. Abrasion to the egg mass may occur when female crabs bury and rebury themselves (Wild 1983).

Worm egg strings were located in sites adjacent to the most heavily infested medial base site. Wickham (1979b; 1980) found that the egg strings of *C. errans* were distributed evenly within the egg mass of *Cancer magister* in relation to the distribution of the mature worms (>40 d post-host oviposition in a 90-d embryogenic period). Since an increase in egg mortality may increase the abundance of fouling micro-organisms (Fisher and Wickham 1976), eggs oviposited away from the most heavily affected sites would not be adversely affected by the fouling community.

Carcinonemertes epialti was most abundant on the first and second pairs of pleopods. These pleopods contain the largest proportion of the clutch, and may also be more protected than the other pleopods. They are closest to the thoracic sternites, and worms may move to the sternites prior to host oviposition (Kuris 1978). *Pseudocarcinonemertes homari* behaves in an analogous manner. That is, it avoids the more exposed pleopods (inner and outer pairs) of its lobster host (Campbell and Brattey

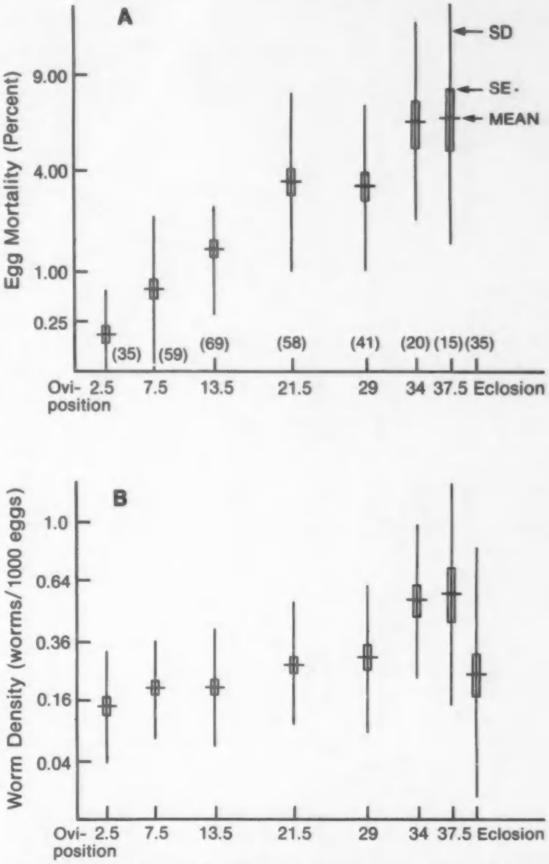

FIG. 4. Mean egg mortality of *Cancer anthonyi*, and mean worm density of *Carcinonemertes epialti* over the course of crab egg embryogenesis. *N* is the number of crabs sampled. Key to egg development stages (cumulative time to midpoint of developmental stage, in days): I, one-cell stage through blastulation (2.5); II, gastrulation through development of tagmata (7.5); III, limb buds evident through buds well developed (13.5); IV, development of eye placodes and eyes, faint heartbeat in live eggs (21.5); V, completed eyes, yolk in four distinct lobes, strong heartbeat in live eggs (29.0); VI, yolk reduced to a band or two lobes (34.0); VII, yolk reduced to two small masses (37.5); VIII, hatching (40). (A) Mean egg mortality of *Cancer anthonyi* through embryogenesis. Egg mortality data were arcsin-square root transformed for the analysis. (B) Mean worm density of *C. epialti* through crab embryogenesis. Density data were square root transformed for the analysis.

TABLE 5. Mean worm densities (worms/1000 eggs) of various species of *Carcinonemertes* on their decapod hosts and projected host egg mortalities.

Host species	Worm species	Mean density	Projected mortality (%)	Reference
Cancer anthonyi	*C. epialti*	0.3	5.7	Present study
Hemigrapsus oregonensis	*C. epialti*	1.4	8.1	Shields and Kuris 1987
		≈40.0	100.0	
H. oregonensis	*C. epialti*	0.5	6.9–7.5	Kuris and Wickham 1987
		1.0–3.1	17.4–19.0	
Cancer magister	*C. errans*	1.8	10.6	Wickham 1979b; 1980
		4.0	30.0	
		8.6	50.3	
		14.6	63.3	
Paralithodes camtschatica	*C. regicides*[a]	39.7	65.4	Wickham et al. 1985
		140.2	96.9	
Homarus americanus	*P. homari*	2.4	34.0–39.0	Campbell and Brattey 1986

[a] Described as *Carcinonemertes regicides* Shields, Wickham, and Kuris 1989.

1985). *Pseudocarcinonemertes homari* is centrally located within the lobster egg mass, residing primarily on those pleopods in the middle of the clutch.

The increase in worm density with increasing EDS showed that worms immigrated into the crab egg clutch throughout the embryogenic period. In contrast, Kuris (1978) found that the prevalence and intensity of *C. epialti* on ovigerous *Hemigrapsus oregonensis* increased through the early and middle stages of crab embryogenesis, but decreased during the late stages of embryogenesis. Campbell and Brattey (1985) found that the prevalence of *Pseudocarcinonemertes homari* declined with EDS but worm intensity was not correlated with EDS. Since *P. homari* undergoes direct development on its host, *Homarus americanus* (Uhazy et al. 1985), it is surprising that prevalence and intensity were not positively correlated with EDS. However, lobsters clean their egg masses of dead eggs and thus, reduce the number of worms found in the clutch (Aiken et al. 1985). For crabs, selective larval settlement (Bauman 1984; Wickham and Roe 1987), or contact transmission of juvenile worms to the ovigerous crabs (Kuris 1978) may account for the increase in worm density late in the embryogenic period.

Carcinonemertes epialti may be found on its hosts throughout the year, but the seasonal pattern of infestation varies with each host species. The yellow rock crab, *Cancer anthonyi*, experiences two seasonal peaks in the abundance of *C. epialti*. The shore crabs, *Hemigrapsus oregonensis* and *Pachygrapsus crassipes*, experience a single fall peak in the abundance of *C. epialti* (Kuris 1978; Roe 1979; Shields and Kuris 1988a). Both *Cancer anthonyi* and *H. oregonensis* produce multiple broods per year (Kuris 1971; 1978; J. D. Shields, R. K. Okazaki, and A. M. Kuris, unpubl. data), whereas *P. crassipes* generally produces a single brood per year with few females producing eggs during other seasons (Hiatt 1948; Roe 1979). Seasonal peaks in worm abundance precede the onset of the winter reproductive period of *H. oregonensis* (Roe 1979; Shields and Kuris 1988a) but are unrelated to the spring–summer reproductive period of *P. crassipes* (Roe 1979).

Carcinonemertes epialti is frequently found on *Hemigrapsus oregonensis* and *Pachygrapsus crassipes* in northern and central California (Kuris 1978; Roe 1979), but it is rarely found on these species in southern California (Kuris 1971; A. M. Kuris unpubl. data). Ovigerous *Cancer anthonyi* may be found year-round in southern California (Reilly 1987), and thus, may supply a suitably large, continuous resource of eggs for these predatory nemerteans. *Cancer anthonyi* is virtually always infested with *C. epialti*, hence it is the most important host for *C. epialti* in southern California.

Infestations of *C. epialti* on *Cancer anthonyi* did not reach the outbreak levels observed for other carcinonemertids on the more heavily fished populations of Dungeness and red king crabs (Table 5). Outbreaks of *C. errans* on *Cancer magister* in central California have resulted in nearly complete brood loss in this stock for several years (Wickham 1986). Episodic outbreaks of a new species, *C. regicides* (Shields et al. 1989) and an unidentified form (nemertean form #4, Wickham and Kuris 1988) on the red king crab, *Paralithodes camtschatica*, have caused complete brood loss in localized nidi in several geographically distinct areas of Alaska (Wickham et al. 1985; A. M. Kuris et al. unpubl. data). Outbreaks of *Pseudocarcinonemertes homari* on *Homarus americanus* can attain high levels, and may result in a moderate degree of egg mortality on this host (Aiken et al. 1985; Campbell and Brattey 1985). While nemerteans have been implicated in causing massive declines in fishery stocks, their role has yet to be determined.

Acknowledgments

We thank J. Crisp and T. Matelson for help in collecting and collating the data, and J. E. Shields and N. Barthelemy-Okazaki for moral support. We acknowledge Gil Crabbe for his able fishing and collection of crabs. Drs. R. Trench, I. Ross, W. Clark, G. Conan, and two anonymous reviewers improved the manuscript. This work is a result of research sponsored in part by NOAA, National Sea Grant College Program, Department of Commerce, under grant number NA80AA-D-00120, project number R/F-75, through the California Sea Grant College Program, and in part by the California State Resources Agency. The United States government is authorized to reproduce and distribute for governmental purposes.

References

AIKEN, D. E., S. L. WADDY, AND L. S. UHAZY. 1985. Aspects of the biology of *Pseudocarcinonemertes homari* and its association with the American lobster, *Homarus americanus*. Can. J. Fish. Aquat. Sci. 42: 351–356.

BAUMAN, L. 1984. Aspects of the larval ecology of *Carcinonemertes epialti*. Wasmann J. Biol. 42: 27–39.

CAMPBELL, A., AND J. BRATTEY. 1985. Egg loss from the American lobster, *Homarus americanus*, in relation to nemertean, *Pseudocarcinonemertes homari*, infestation. Can. J. Fish. Aquat. Sci. 43: 772–780.

CARROLL, J. C. AND R. N. WINN. 1988. Species profiles: life histories and environmental requirements of coastal fishes and invertebrates (Pacific Southwest) — rock crabs: brown, red, and yellow crabs. U.S. Fish. Wildl. Serv. Biol. Rep. 82, U.S. Army Corps of Engineers, TR EL-82-4.

FISHER, W. S., AND D. E. WICKHAM. 1976. Mortality and epibiotic fouling of eggs from wild populations of the Dungeness crab, *Cancer magister*. U.S. Fish Bull. 74: 201–207.

HIATT, R. W. 1948. The biology of the lined shore crab, *Pachygrapsus crassipes* Randall. Pac. Sci. 2: 135–213.

KURIS, A. M. 1971. Population interactions between a shore crab and two symbionts. Ph.d. thesis, University of California, Berkeley, CA.

1978. Life cycle, distribution and abundance of *Carcinonemertes epialti*, a nemertean egg predator of the shore crab, *Hemigrapsus oregonensis*, in relation to host size, reproduction and molt cycle. Biol. Bull. 154: 121–137.

KURIS, A. M., AND D. E. WICKHAM. 1987. Effect of nemertean egg predators on crustaceans. Bull. Mar. Sci. 41: 151–164.

MARGOLIS, L., G. W. ESCH, J. C. HOLMES, A. M. KURIS, AND G. A. SCHAD. 1982. The use of ecological terms in parasitology (report of an ad hoc committee of the American Society of Parasitologists). J. Parasitol. 68: 131–133.

REILLY, P. N. 1987. Population studies of rock crab, *Cancer antennarius*, yellow crab, *C. anthonyi*, and Kellet's whelk, *Kelletia kelletii*, in the vicinity of Little Cojo Bay, Santa Barbara County, California. Calif. Fish Game 73: 88–98.

ROE, P. 1979. Aspects of development and occurrence of *Carcinonemertes epialti* (Nemertea) from shore crabs in Monterey Bay, California. Biol. Bull. 156: 130–140.

1984. Laboratory studies of feeding and mating in species of *Carcinonemertes* (Nemertea:Hoplonemertea). Biol. Bull. 167: 426–436.

SHIELDS, J. D. 1987. The dynamics and mechanisms of egg mortality in *Cancer anthonyi* (Decapoda). Ph.D. thesis, University of California, Santa Barbara, CA.

SHIELDS, J. D., AND A. M. KURIS. 1988a. Temporal variation in abundance of the egg predator *Carcinonemertes epialti* (Nemertea) and its effect on egg mortality of its host, the shore crab, *Hemigrapsus oregonensis*. Hydrobiologia 156: 31–38.

1988b. An *in vitro* analysis of egg mortality in *Cancer anthonyi*: the role of symbionts and temperature. Biol. Bull. 174: 267–275.

SHIELDS, J. D., D. E. WICKHAM, AND A. M. KURIS. 1989. *Carcinonemertes regicides* n. sp. (Nemertea), a symbiotic egg predator on the red king crab, *Paralithodes camtschatica*, from Alaska. Can. J. Zool. 67: 923–930.

UHAZY, L. S., D. E. AIKEN, AND A. CAMPBELL. 1985. Morphology and systematics of the nemertean *Pseudocarcinonemertes homari* (Hoplonemertea: Monostilifera) from the American lobster, *Homarus americanus*. Can. J. Fish. Aquat. Sci. 42: 342–350.

WICKHAM, D. E. 1979a. Predation by *Carcinonemertes errans* on eggs of the Dungeness crab, *Cancer magister*. Mar. Biol. 55: 45–53.

1979b. *Carcinonemertes errans* and the fouling and mortality of eggs of the Dungeness crab, *Cancer magister*. J. Fish. Res. Board Can. 36: 1319–1324.

1980. Aspects of the life history of *Carcinonemertes errans* (Nemertea: Carcinonemertidae), an egg predator of the crab, *Cancer magister*. Biol. Bull. 159: 247–257.

1986. Epizootic infestations by nemertean brood parasites on commercially important crustaceans. Can. J. Fish. Aquat. Sci. 43: 2295–2302.

WICKHAM, D. E., S. F. BLAU, AND A. M. KURIS. 1985. Preliminary report on egg mortality in Alaskan king crabs caused by the egg predator *Carcinonemertes*, p. 265–270. *In* Proceedings of the International King Crab Symp. Ser., Alaska Sea Grant Rep. 85–12.

WICKHAM, D. E., AND KURIS, A. M. 1988. Diversity among nemertean egg predators of decapod crustaceans. Hydrobiologia 156: 23–30.

WICKHAM, D. E., AND P. ROE. 1987. Selectivity in transmission to crab hosts by the symbiotic nemertean, *Carcinonemertes epialti*. J. Parasitol. 73: 697–701.

WILD, P. W. 1983. The influence of seawater temperature on spawning, egg development, and hatching success of the Dungeness crab, *Cancer magister*, p. 197–214. *In* P. W. Wild and R. N. Tasto [ed.] Life history, environment, and mariculture studies of the Dungeness crab, *Cancer magister*, with emphasis on the central California fishery resource, Fish Bull. 172 p.

A Stratified Random Transect Design for Acoustic Surveys of Fish Stocks

G. M. Jolly

38 Silverknowes Terrace, Edinburgh, EH4 5HJ United Kingdom

and I. Hampton

Sea Fisheries Research Institute, Private Bag X2, Rogge Bay, Cape Town, Republic of South Africa

Jolly, G. M., and I. Hampton. 1990. A stratified random transect design for acoustic surveys of fish stocks. Can. J. Fish. Aquat. Sci. 47: 1282–1291.

The differences between design-based and model-based inference are examined briefly, and some recent applications of model-based procedures in fishery surveys are discussed. It is shown that valid estimates of mean and variance can be obtained by taking a stratified random sample, where the primary sampling units in each stratum are parallel transects randomly-spaced within certain non-critical limits. The strata are defined on the basis of the expected fish density or the expected variance in fish density within the region. Formulae are developed for the optimum allocation of transects to strata according to the density or variance in density within each stratum. To illustrate that such designs are entirely feasible, an example is given of a stratified random acoustic survey of South African anchovy (*Engraulis capensis*), in which the strata were defined on the basis of anchovy distribution encountered on previous surveys of the region. Through a two-phase approach, the transect allocation was adjusted during the survey for differences between the expected and observed distributions. It is demonstrated that in this survey, stratification, with uniform allocation of effort between strata, would have increased precision by an estimated factor of 2.4 compared with an unstratified random sample, while optimising effort within strata gave a further potential increase of 1.4. The coefficient of variation actually achieved was 16%.

Les différences entre une inférence fondée sur un théorie et une inférence fondée sur un modèle ont été étudiées brièvement, et certaines applications récentes des procédés fondés sur un modèle utilisés pour les relevés dans le domaine des pêches ont été analysées. Les auteurs ont montré qu'il est possible d'obtenir des estimations valables de la moyenne et de la variance en utilisant un échantillon aléatoire stratifié dans lequel les premières unités d'échantillonnage de chacune des strates sont des transects parallèles espacés aléatoirement dans certaines limites non critiques. Les strates sont définies selon la densité probable de poissons ou de la variance probable de la densité de poissons dans la région. Des formules sont élaborées en vue de l'allocation optimale des transects aux strates en fonction de la densité ou de la variance de la densité dans chacune des strates. Afin de montrer que ces conceptions sont entièrement faisables, on donne un exemple de relevé acoustique aléatoire stratifié concernant l'anchois du Cap (*Engraulis capensis*) dans lequel les strates ont été définies d'après la répartition des anchois enregistrée lors de relevés effectués précédemment dans la région. Par le biais d'une approche en deux étapes, l'allocation de transect a été ajustée pendant le relevé de façon à tenir compte des différences entre les répartitions probables et les répartitions observées. Dans ce relevé, on a montré que la stratification, avec une allocation uniforme de l'effort entre les strates, aurait accru la précision d'un facteur évalué de 2,4 par rapport à un échantillon aléatoire non stratifié, tandis que l'effort d'optimisation à l'intérieur des strates a donné une autre augmentation potentielle de 1,4. Le coefficient de variation obtenu présentement était de 16%.

Received April 10, 1989
Accepted February 27, 1990
(JA129)

Reçu le 10 avril 1989
Accepté le 27 février 1990

1. Introduction

The literature contains numerous descriptions of sample surveys in marine research. Also, a wealth of theory has been developed over the past few decades capable of being applied to any sampling problem. However, Jolly and Hampton (1990) present evidence to show how, in their opinion, these two fields of study are not yet sufficiently integrated to provide generally coherent strategies for marine surveys. The choice of sampling method is often governed more by tradition than logic, leading to insuperable difficulties in the statistical analyses. Also, dubious assumptions may be involved resulting in varying degrees of invalidity.

In Section 2 we discuss the implications of recent papers on model-based procedures. Thereafter the design and analysis of an acoustic survey to estimate anchovy (*Engraulis capensis*) biomass on the South African continental shelf will be described to show that the application of established sampling theory to an acoustic survey is entirely practicable.

2. Model-Based Estimation

Attention was drawn by Jolly and Hampton (1990) to the fact that unbiased estimation of mean and variance by conventional sampling methods requires no distributional assumptions. If, however, the data were to follow one of a number of specific (infinite) distributions, there is a theoretical possibility of obtaining an estimate of greater precision. One such distribution which has been assumed by Pennington (1983, 1986) for fish and plankton net surveys and by MacLennan and MacKenzie (1988) for fish acoustic surveys is the Δ-distribution, which is a lognormal with allowance for zero observations.

R. A. Myers and P. Pepin (Department of Fisheries and Oceans, St. John's, Nfld., unpubl. data) have demonstrated from simulations that when the data contain even small and possibly undetectable deviations from a sample from a true Δ-distribution, serious bias and loss of information can occur in the estimation of the mean. On this basis they do not recommend the method. These findings have been confirmed by Jolly and Smith (1989) from an acoustic survey of anchovy and a haddock trawl survey. In the first example, an overall positive bias of 50% in abundance and a 72% loss of information was found on comparison with conventional estimation procedures. In the second example, both bias and efficiency fluctuated inconsistently among the four strata.

Smith (1990) explains the essential differences between model-based and design-based inference. Difficulties can result from the former approach when the expectation of the model-based estimator does not equal the finite population mean. The Δ-distribution is an example of this, whereas in the normal, Poisson and negative binomial distributions the model-based estimate and the finite population mean are identical.

There is no advantage in using a model-based approach to estimate the mean for the latter three distributions. In contrast, estimates of the finite population mean based on the Δ-distribution are not robust to deviations from the assumed model. This lack of robustness will lead to possible bias of the estimated mean as well as loss of efficiency relative to the design-based estimates.

The second purpose of Smith (1990) is to illustrate the successful application of a predictive type model relating the variate of interest to associated covariates. In this situation, as sample size increases, the expectation of the estimator of the mean can be shown to approach the finite population mean asymptotically, independently of the model used (the property of Asymptotic Design Consistency). As an example, he uses a generalised Poisson model to relate catches of 4-yr-old cod to three covariates (temperature, salinity, and depth). All three variates contributed to a substantial reduction in variance of the predicted mean, while tests showed the fit of the Poisson model to be very good after the inclusion of quadratic terms.

We suggest strongly that any model whose estimator of the mean is different from the sample mean should be tested for bias and efficiency against the appropriate design-based estimator, using real data. We are not aware of any model, other than the predictive model of Smith (1990), having been so tested and found acceptable for estimation of abundance in fisheries surveys. We stress the use of real data, since, although simulated data may succeed in detecting non-robustness, failure in this respect could be caused by the inability of the simulations to represent the idiosyncracies of a real population.

Another form of a model-based estimate known as "kriging" has been used by Guillard et al. (1990) to estimate abundance of larvae and fish. This procedure fits a surface taking account of local correlations and is described by Ripley (1981). Although the estimate can be equated to the sample mean, we believe that a comparison with conventional design-based procedures is necessary for the following reasons. First, while positional effects may be eliminated from the sampling error at least as well as by stratification, the absence of formal strata does not allow for the increased efficiency resulting from relatively high sampling intensities in areas of known high fish density. Second, we do not know of any comparison having been made with design-based methods to demonstrate any gain of information from the assumptions underlying the surface fitting, and which would offer some justification for the complexity of the method.

3. Background to Anchovy Survey

In 1983, acoustic surveys of anchovy spawner biomass were introduced by the Sea Fisheries Research Institute, Cape Town, as an aid to managing the resource, which is one of the most important commercially in South African waters. A major requirement of these surveys is to assess the biomass with minimum sampling error consistent with available ship's time. Minimisation and valid estimation of sampling error is important in the management as well as the scientific sense, as the sampling error is taken into account directly in making quota recommendations from the survey estimates (e.g. Armstrong and Butterworth 1986).

The spawning fish occupy an area in the region of 10^5 km^2, predominantly on the Agulhas Bank (marked by the 200-m isobath east of Cape Point in Fig. 1). The population has to be surveyed from a single vessel, which is usually available for a continuous period of about 20 d. Gross movement of the population over such a period is not thought to occur, although, on a smaller scale, movement might be substantial.

The first survey from which valid biomass estimates were obtained was conducted in November 1984 (Hampton 1987). As mapping of the distribution was considered to be of prime importance at that time, a non-stratified systematic sample was taken in which the sampling units were equally-spaced lines running approximately normal to the coastline. The survey grid and the fish density contours derived therefrom are shown in Fig. 1. The distribution agreed well with that found in a pilot acoustic survey the previous November (Hampton 1987) and with that inferred from earlier egg and larval surveys (Shelton 1986). The distribution was therefore regarded as sufficiently typical to be used in designing a further survey of the spawning population in November 1985. In this case, a stratified random sampling design was adopted, using the 1984 information on distribution to pre-stratify the area and allocate sampling intensity in the different strata. Details of the theoretical basis of the design and the stratification criteria are given in Section 5 and 6, respectively.

4. Acoustic Methods

Estimates of acoustic back-scattering intensity were made with a 38-kHz echo-sounder, calibrated by the standard sphere method (Foote et al. 1981), and a custom-built digital echo-integrator (Anon. 1986). Fish density estimates were obtained by integrating echo intensity continuously along short sections of transect (termed intervals) separated by egg-collection stations. Trawl samples were taken as circumstances allowed throughout the survey to identify acoustic targets and partition the back-scattered intensity among the different pelagic species present. Identification of anchovy was facilitated by their characteristic shoaling behaviour pattern, the presence or absence of anchovy eggs in the vicinity, and the fact that they were the most abundant pelagic fish present in the survey area.

Standard echo-integration theory (e.g. Forbes and Nakken 1972) was used to convert measurements of back-scattering intensity to estimates of fish density. Target strengths needed

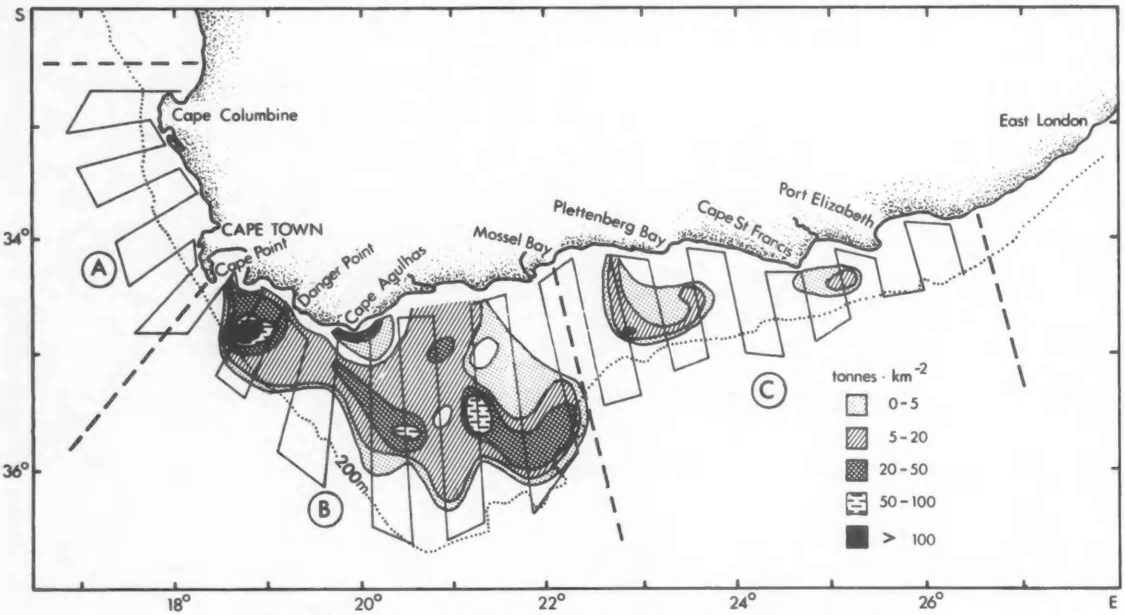

FIG. 1. Anchovy distribution in November 1984 deduced from acoustic survey.

in this conversion were estimated from the length distribution of fish in the trawl samples, through a relationship between length and target strength at 38-kHz obtained by Halldorsson and Reynisson (1983) for North Atlantic herring (*Clupea harengus*). The procedures are described in detail by Hampton (1987) and need not concern us further here.

Since this paper is concerned only with sampling error, we make no attempt here to assess potential biases in the density estimates arising, for example, from systematic errors in calibration constants or in the target strength expression used. We note however that there is evidence from a contemporaneous egg survey in 1985 to support the absolute acoustic estimate of anchovy spawning biomass in that year (Hampton et al. 1990). No comparable egg estimate is available for 1984.

It should be appreciated that random factors such as equipment instability, variation in species composition, and variations in the relationship between target strength and length are automatically accounted for in our analysis, as they appear as variations in the density estimates and are therefore reflected in the sampling error.

5. Survey Design and Estimation Procedure

The survey area was first stratified according to the anticipated anchovy density based on experience of previous years. This process will be described in Section 6. Within each stratum a selection of parallel transects was made by a two-stage random procedure which will be described later in this section. Each transect covered the full distance between stratum boundaries, the direction of transects being chosen with the aim of minimizing variance among transects. Since the main variation within a stratum was likely to be associated with distance from the shore, transects were approximately at right angles to the shoreline.

The mean weight, ρ_{ij}, of anchovy beneath a unit area for the jth transect within stratum i is estimated from

$$\hat{\bar{\rho}}_{ij}=\frac{b_{ij}}{L_{ij}},$$

where b_{ij} is the observed biomass of anchovy, and L_{ij} the length, for the jth transect.

The mean density, $\bar{\rho}_i$, for the ith stratum is then estimated by the ratio estimate (Cochran 1977)

$$(1)\quad \hat{\bar{\rho}}_i=\frac{1}{n_i}\sum_{i=1}^{n_i} w_{ij}\,\hat{\bar{\rho}}_{ij},$$

where $w_{ij}=L_{ij}/\bar{L}_i$, L_{ij} $(j=1,2,\ldots n_i)$ are the lengths of the n_i sample transects, and

$$\bar{L}_i=\frac{1}{n_i}\sum_{j=1}^{n_i} L_{ij}.$$

Weighting by stratum area, A_i, gives the final density estimate

$$(2)\quad \hat{\bar{\rho}} = \frac{\sum_i A_i\,\hat{\bar{\rho}}_i}{\sum_i A_i}$$

This corresponds to the "separate" ratio estimate of Cochran (1977; Chap. 6) in which separate densities are assumed for different strata and the knowledge is utilised of the stratum areas which can be measured accurately from a map.

With completely random selection of transects within strata, the variance of $\hat{\bar{\rho}}$ is estimated as

$$(3)\quad \mathrm{Var}(\hat{\bar{\rho}}) = \frac{\sum_i A_i^2 \,\mathrm{Var}(\hat{\bar{\rho}}_i)}{\left(\sum_i A_i\right)^2},$$

where

$$\mathrm{Var}\,(\hat{\bar{\rho}}_i) = \frac{\sum_{j=1}^{n_i} w_{ij}^2 \,(\hat{\bar{\rho}}_{ij} - \hat{\bar{\rho}}_i)^2}{n_i\,(n_i - 1)}.$$

If the transects are not randomly selected, no fully valid estimate of sampling error can be made from a single survey unless the population is randomly distributed (Jolly and Hampton (1990)). On the other hand, completely random selection of transects within a stratum may by chance result in a very uneven distribution of sampling effort, and a region of suspected high density being left unsurveyed. This is more likely to happen with small sample sizes, say with less than 10 transects in a stratum. In the present survey a compromise was made between regular spacing and complete randomisation by a two-stage sampling procedure. Each stratum was divided notionally into a number of strips of equal width running parallel to the direction of the transects. These strips were designated first-stage units and transects became second-stage units. The theory was to select strips at random within the stratum, and one transect at random within each selected strip.

We first consider the general case of n_{ij} random transects selected from the jth strip. Using suffix k to denote individual sampled transects within a strip, the mean density of the jth strip is estimated as

$$(4)\quad \hat{\bar{\rho}}_{ij} = \frac{1}{\mathrm{n}_{ij}} \sum_{k=1}^{n_{ij}} w_{ijk}\, \hat{\bar{\rho}}_{ijk},$$

where $w_{ijk} = L_{ijk}/\bar{L}_{ij}$ and $\bar{L}_{ij} = \sum_{k=1}^{n_{ij}} L_{ijk}/\mathrm{n}_{ij}$. Thus equation (4) is a ratio estimate within a second-stage unit, similar to equation (1) in single stage sampling.

The stratum mean is then estimated likewise as a weighted mean of the $\bar{\rho}_{ij}$, that is,

$$(5)\quad \hat{\bar{\rho}}_i = \frac{1}{\mathrm{n}_i} \sum_{j=1}^{n_i} w_{ij}\, \hat{\bar{\rho}}_{ij},$$

where $w_{ij} = \bar{L}_{ij}/\bar{L}_i$, and $\bar{L}_i = \sum_{j=1}^{n_i} \bar{L}_{ij}/n_i$.

The estimated variance of $\hat{\bar{\rho}}_i$ is

$$(6)\quad \mathrm{Var}(\hat{\bar{\rho}}_i) = \frac{1-f_{1i}}{n_i} \sum_{j=1}^{n_i} \frac{w_{ij}^2(\hat{\bar{\rho}}_{ij} - \hat{\bar{\rho}}_i)^2}{n_i - 1} + \frac{1}{n_i N_i} \sum_{j=1}^{n_i} \frac{(1-f_{2ij}) w_{ij}^2 s_{2ij}^2}{n_{ij}},$$

where f_{1i} is the first-stage sampling fraction, n_i/N_i, N_i is the total number of strips in the stratum, and s_{2ij}^2 the within-strips mean square given by

$$s_{2ij}^2 = \frac{1}{n_i - 1} \sum_{k=1}^{n_{ij}} w_{ijk}^2\, (\hat{\bar{\rho}}_{ijk} - \hat{\bar{\rho}}_{ij})^2.$$

The formula is a generalisation of equation 11.30 of Cochran (1977). The second-stage sampling fraction, f_{2ij}, is the ratio of n_{ij} to N_{ij}, the total number of possible transects in the jth strip. Because of the negligible width of a transect, f_{2ij} is effectively zero. For the method of sampling used in the 1985 survey, $n_{ij} = 1$ for all j. Writing s_{1i}^2 for the mean square among strips, i.e.

$$s_{1i}^2 = \frac{1}{n_i - 1} \sum_{j=1}^{n_i} w_{ij}^2\, (\hat{\bar{\rho}}_{ij} - \hat{\bar{\rho}}_i)^2,$$

and s_{2i}^2 for the average contribution within strips, with $n_{ij} = 1$ i.e.

$$s_{2i}^2 = \frac{1}{n_i} \sum_{j=1}^{n_i} w_{1j}^2\, s_{2ij}^2,$$

equation (6) becomes

$$(7)\quad \mathrm{Var}(\hat{\bar{\rho}}_i) = \frac{1}{n_i}\{(1 - f_{1i}) s_{ij}^2 + f_{1i}\, s_{2i}^2\}$$

Since $n_{ij} - 1 = 0$, s_{2i}^2 is not estimable. However, s_{2i}^2 is likely to be only slightly less than s_{1i}^2 on the assumption that each stratum is reasonably homogeneous. Thus, if f_{1i} does not exceed, say, about, 0.3, the first term of equation (7) will dominate, and a reasonable estimate of the variance could be obtained by equating s_{2i}^2 to its probable upper limit of s_{1i}^2 to give

$$\mathrm{Var}(\hat{\bar{\rho}}_i) \sim s_{1i}^2/n_i$$

Thus, equations (2) and (3) may be used for the population estimate and its variance, respectively.

For most strata the width of a strip was chosen to give an anticipated first-stage sampling fraction of about 0.3, this determining the likely "spread" of the sample over the stratum. There still remained a chance, although now greatly reduced, of two sample transects occurring very close to each other, and therefore because of currents, fish movement or navigational error possibly sampling the same fish. Therefore a rule was made to discard any transect lying within a specified distance of a previously selected transect. In the present survey this distance was one strip width, but a shorter distance could have been chosen. This rule will have negligible effect on theoretical considerations.

Finally, regarding use of the ratio estimate in equation (1), Cochran (1977) notes that in general the estimate has a bias of order $1/n$ where n is the sample size. However, the cause of bias is independent variation in the denominator, and this circumstance does not arise when the ratio is, for example, a biomass divided by the length of transect to which the biomass relates. In other words, for any given length of transect, the biomass estimate is unbiassed. More formally, Cochran quotes the exact bias in a ratio estimate, $\hat{R} = \bar{y}/\bar{x}$, as

$$-\mathrm{Cov}(\hat{R},\bar{x})/\bar{X},$$

where $\bar{X}$ is the population mean of x. In our situation, since we can safely assume fish density to be unassociated with the length of transect involved, we have $\mathrm{Cov}(\hat{R},\bar{x}) = 0$.

6. Stratification and Optimisation of Effort

In 1984 a clear density pattern had emerged (see Fig. 1). As in the pilot study the previous November (Hampton 1987), no anchovy were detected north of Cape Point (Stratum A), while between Cape Point and Mossel Bay (Stratum B) anchovy density was estimated as 14.5 g/m^2 compared with 2.0 g/m^2 in Stratum C to the east of this (Hampton 1987). This suggested at least two strata in 1985. Also, there was some evidence from the high density area in 1984 of consistent differences between individual transects at corresponding points along their length. Since the longest of these extended to around 220 km offshore, some gain in precision might be expected from a splitting of this stratum by an east–west line to allow independent randomisation in the two strata so formed.

Because of the differences in density expected between strata, an optimal strategy was required for the numbers of transects to be sampled in each stratum. The first step was to estimate the relative numbers of sample transects, assuming particular densities, $\bar{\rho}_i$, for the two strata. The actual numbers would then depend on the steaming time available after allowing for the fixed distance travelled in an east–west direction between transects.

Since optimum allocation will depend only marginally on whether sampling is two-stage random or completely random, we shall assume the latter. Equation (3) can therefore be applied except that, in the place of "Var" to denote an "estimated variance", "V" will be used to signify the "true" variance. Thus,

$$V(\bar{\rho}) = \frac{\sum_i A_i^2 \, \mathrm{V}(\hat{\bar{\rho}}_i)}{\left(\sum_i A_i\right)^2} .$$

Before a formula for optimum allocation can be developed, A_i has to be linked to the other parameters in $V(\bar{\rho})$. Since $A_i \alpha N_i\bar{L}_i$, taking $\bar{L}_i$ as approximately the mean length of all possible transects in the stratum, and N_i as the number of strips in the stratum,

$$\text{(8)} \quad V(\bar{\rho}) \,\alpha\, \sum_i (N_i \bar{L}_i)^2 \, V(\bar{\rho}_i)$$
$$= \sum_i \frac{1}{n_i} (N_i \bar{L}_i)^2 S_{\rho i}^2 ,$$

where $S_{\rho i}^2$ is the expectation of the mean square among transects of the $\hat{\bar{\rho}}_{ij}$, that is,

$$S_{\rho i}^2 = E\left\{\frac{1}{n_i - 1} \sum_{j=1}^{n_i} w_{ij}^2 \, (\hat{\bar{\rho}}_{ij} - \hat{\bar{\rho}}_i)^2\right\}.$$

Using the method of Lagrange multipliers to minimise $V(\hat{\bar{\rho}})$ conditional on $\sum_i n_i\bar{L}_i$ (which is set by the time available for steaming transects), the condition for optimum allocation in each stratum is

$$\frac{(N_i\bar{L}_i)^2 S_{\rho i}^2}{n_i^2} = \bar{L}_i \times \text{constant.}$$

This gives the relationship for f_{1i}, the first-stage sampling fraction for stratum i, as

$$f_{1i} = \frac{n_i}{N_i} \,\alpha\, \sqrt{\bar{L}_i}\, S_{\rho i} .$$

The optimum proportion of the total number of transects that should be allocated to stratum i is then

$$\text{(9)} \quad \frac{n_i}{\sum_i n_i} = \frac{A_i S_{\rho i}}{\sqrt{\bar{L}_i} \sum_i A_i S_{\rho i} / \sqrt{\bar{L}_i}} .$$

If estimates of $S_{\rho i}^2$ are available from previous sampling, these can be substituted in equation (9). Otherwise, a reasonable speculation might be that the distribution of the biomass of a transect is approximately Poisson, in which case the variance of a transect total would be roughly proportional to the weight of fish insonified on the transect, that is, to $\bar{\rho}_i \bar{L}_i$. Since $S_{\rho i}^2$ refers to a mean per unit area, this is equivalent to

$$\text{(10)} \quad S_{\rho i}^2 \propto \bar{\rho}/\bar{L}_i ,$$

$$f_{1i} \propto \sqrt{\bar{\rho}_i} ,$$

and

$$\text{(11)} \quad \frac{n_i}{\sum_i n_i} = \frac{A_i \sqrt{\bar{\rho}_i}}{\bar{L}_i} \Big/ \sum_i \frac{A_i \sqrt{\bar{\rho}_i}}{\bar{L}_i}$$

If, as is likely, the variance of the biomass of a transect exceeds the Poisson variance, equation (10) will still apply provided the constant of proportionality is approximately the same in all strata.

A retrospective examination of the high and low density strata in the 1984 survey gave the results in Table 1. Note that the mean transects length ($\bar{L}$) is the weighted mean of the $\bar{L}_i$ values, weighting by $N_i = A_i/\bar{L}_i$. The alternatives (a) and (b) in the last two columns correspond to the allocations of equations (9) and (11), respectively. They show close agreement for this set of data, indicating that in this case the Poisson assumption was probably not unreasonable. It is worth noting in passing that the actual allocation in 1984 was far from optimum, with far too many transects in Stratum C.

If a stratum has too few sample transects, the estimate of variance for that stratum will tend to be unreliable. This will tend to occur in the lightly sampled low-density strata in particular. A method for combining these strata to give a single estimate of density, $\hat{\bar{\rho}}_i$, with variance, without losing the advantages of the original stratification, was therefore devised and is presented in Appendix A. In the survey analysis a group of strata combined in this way can then be treated as a single stratum with density $\hat{\bar{\rho}}_i$.

7. Implementation

The results in Table 1 were used as a basis for the survey in 1985, on the assumption that the geographic limits and density structure of the population would be roughly similar to those in 1984. Although no anchovy were expected on the West Coast (i.e. north of Cape Town), the survey was extended as far north as Cape Columbine (see Fig. 4) to check for the presence of drifted anchovy eggs in the region. The formal design of the acoustic survey was however restricted to the South Coast.

To allow some adjustment for differences in the pattern of fish density between the two years, the area was surveyed in two phases. In the first, an outward-going (eastward) phase, transects were allocated according to the expected density structure, while in the return (westward-going) phase, they were allocated according to the actual density structure found in the first phase. Slight increase of sampling error might result if there were rapid movement of shoals in a direction across the transects such that large aggregations had a chance of being either missed or sampled twice. Since the effect would be automatically taken account of in the estimate of sampling error, bias would not result. As noted in Section 3, gross movement of anchovy is not expected during the period of the survey.

TABLE 1. Anchovy density structure, optimum sampling fractions and optimum number of transects for Strata B and C in the 1984 survey, applying (a) equation (9) and (b) equation (11).

Stratum	A_i (km$^2 \times 10^{-3}$)	$\bar{\rho}_i$ (g/m^2)	$\bar{L}_i$ (km)	$S_{\rho_{i_2}}$ (g/m^2)	$n_i/\Sigma n_i$ (a)	$n_i/\Sigma n_i$ (b)	$(n_{opt})_i$ (a)	$(n_{opt})_i$ (b)	n_i (actual)
B	68.9	14.5	90.9	11.85	0.84	0.78	15	14	11
C	32.8	2.0	56.4	3.71	0.16	0.22	3	4	11
Means/Totals, both strata	101.7	10.5	75.9	1.95	1.00	1.00	18	18	22

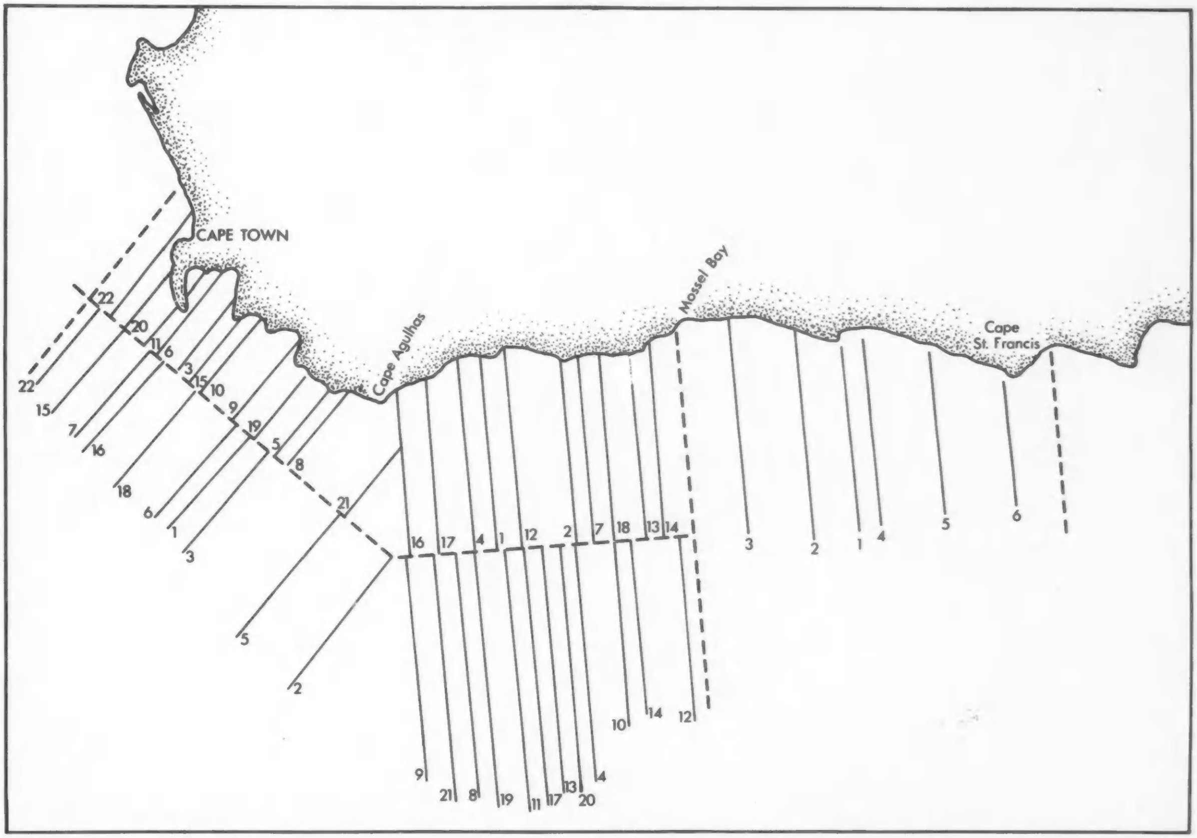

FIG. 2. Initial transect plan for South Coast acoustic survey in November 1985, showing transect ranking.

As a starting point, 78% of the transects were initially placed west of Mossel Bay, based on Method (b) in Table 1. (Method (b) was preferred to Method (a), as it was felt that the density structure was more likely to be similar between the two years than the variance structure). The transects (50 in number) were randomised as described in Section 5, the transects west of Mossel Bay being independently randomised in inshore and offshore strata as described in Section 6. The full transect plan for the South Coast survey is shown in Fig. 2.

More transects were originally selected than could be surveyed in the time available. Approximately three-quarters of the anticipated final number were then selected at random for surveying in Phase 1. On completion of Phase 1, a sub-set of the remainder were selected as Phase 2 transects, to be allocated according to the time remaining, using on-the-spot estimates of $\bar{\rho}_i$ obtained from the Phase 1 transects and equation (11). Random selection of transects was simplified by assigning to each a serial number (ranking) within strata at the time of the original selection to determine the order of selection for survey. These rankings are given in Fig. 2.

The survey grid actually steamed, showing both Phases, is shown in Fig. 3, and the anchovy distribution (contoured from the Phase 1 transects only) in Fig. 4. As a marked reduction in density had been noted east of Cape Agulhas during Phase 1 (see Fig. 4), the inshore and offshore high-density strata (as defined in Section 6) were further subdivided for the purposes of Phase 2 by a line running approximately north/south through a point to the east of Cape Agulhas. Together with the low-density area east of Mossel Bay, this defined the five strata shown in Figs. 3 and 4 and referred to in Tables 2 and 3. The Phase 2 transects were drawn from the same original random set in the order of the rankings.

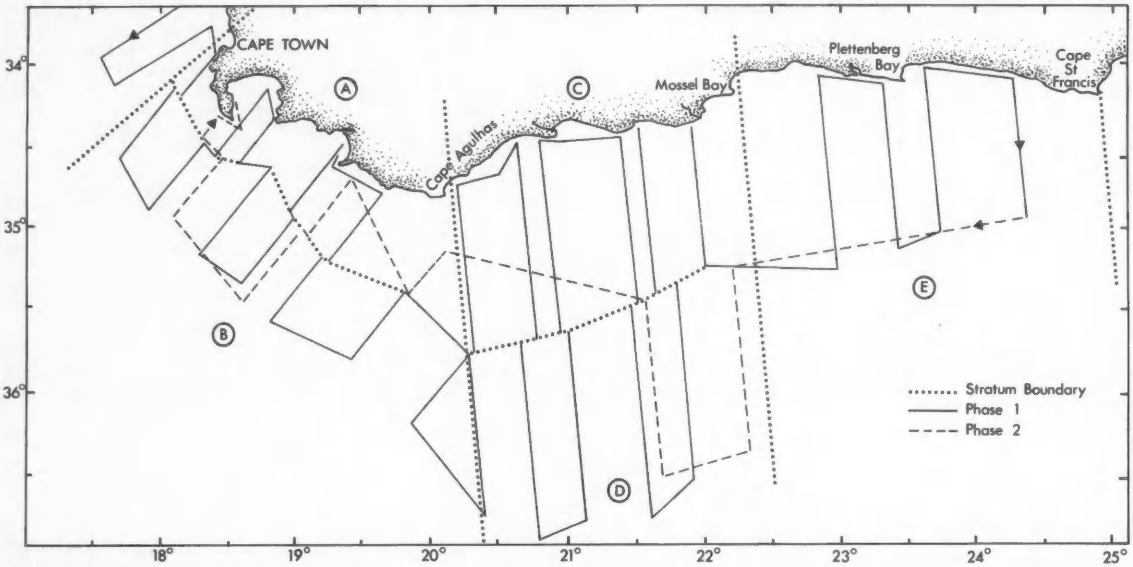
CAPE TOWN
Mossel Bay
Plettenberg Bay
Cape St Francis
Cape Agulhas
A
B
C
D
E
34°
35°
36°
18°
19°
20°
21°
22°
23°
24°
25°
Stratum Boundary
Phase 1
Phase 2

FIG. 3. Final survey grid for South Coast acoustic survey in November 1985, showing both first and second phase transects and definition of Strata A to E.

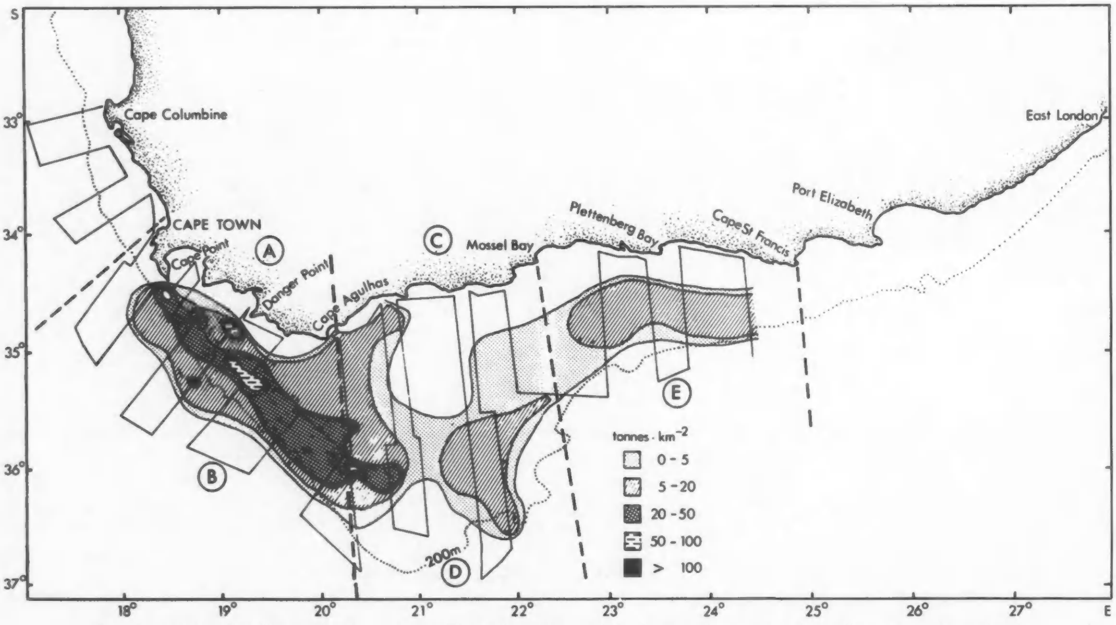
S
Cape Columbine
East London
CAPE TOWN
Cape Point
Danger Point
Cape Agulhas
Mossel Bay
Plettenberg Bay
Cape St Francis
Port Elizabeth
A
B
C
D
E
200m
tonnes · km^{-2}
0 - 5
5 - 20
20 - 50
50 - 100
> 100
33°
34°
35°
36°
37°
18°
19°
20°
21°
22°
23°
24°
25°
26°
27°
E

FIG. 4. Anchovy distribution in November 1985 deduced from Phase 1 acoustic survey. Only Phase 1 transects shown.

In all, 34 transects (27 in Phase 1 and 7 in Phase 2) were surveyed on the South Coast from a population of 120 notional strips, over a period of 16 d. Thirteen of these were spent on Phase 1 and three on Phase 2. Three of the Phase 1 transects were ultimately discarded (one in Stratum A and two in Stratum E) as fish in their vicinity were too shallow to be detected reliably. A breakdown of the first-stage sampling fractions and the number of transects for all designated strata is given in Table 2. The values in parenthesis are the numbers of usable transects remaining in strata where transects were discarded.

The last two columns in Table 2 give the optimum transect allocations estimated from the Phase 1 transects, using equations (9) and (11), respectively. It can be seen that the actual allocation came close to realising the theoretical optimum based on equation (11). The slight over-sampling of strata C and D compared with the other three strata is largely due to the placing

TABLE 2. First stage sampling fractions and actual numbers of sample transects in each of the designated strata in the 1985 survey, also optimal allocations applying (a) equation (9) and (b) equation (11).

	Phase 1		Phase 2		Phase 1 and 2		Optimal allocations predicted from Phase 1	
Stratum	f_{1i}	n_i	f_{1i}	n_i	f_{1i}	n_i	(a)	(b)
A	0.23	6 (5)	0.12	3	0.35	9 (8)	12	10
B	0.27	8	0.08	2	0.35	10	10	11
C	0.21	5	0	0	0.21	5	4	4
D	0.21	4	0.08	2	0.29	6	7	5
E	0.20	4 (2)	0	0	0.20	4 (2)	1	4
All strata	0.22	27 (24)	0.06	7	0.28	34 (31)	34	34

TABLE 3. Estimated mean and standard error of anchovy density in each of the designated strata in the 1985 acoustic survey, together with optimum theoretical transect allocations applying (a) equation (9), (b) equation (11), and the actual allocations.

Stratum	A_i ($\text{km}^2 \times 10^{-3}$)	$\bar{\rho}_i$ (tonnes/km^2)	S.E. ($\bar{\rho}_i$) (tonnes/km^2)	C.V. ($\bar{\rho}_i$)	Biomass (tonnes $\times 10^{-3}$)	$\bar{L}_i$ (km)	$(n_{\text{pol-}})_i$ (a)	$(n_{\text{opt}})_i$ (b)	n_i (actual)
A	15.98	21.30	8.02	0.38	340.4	25.6	19	13	9 (8)
B	27.84	13.53	3.00	0.22	376.7	40.0	10	11	10
D	19.60	6.29	1.79	0.29	123.3	62.6	3	4	6
C+E	42.50	3.17	0.42	0.13	134.7	*	2	6	9 (7)
Means/Totals, all strata	105.92	9.20	1.49	0.16	975.1	*	34	34	34 (31)

of too many transects in these strata in Phase 1, which in turn is a consequence of the difference in density structure between the 1984 and 1985 surveys. Also, an extra Phase 2 transect was included in Stratum D for an oceanographic study not directly related to the acoustic survey.

Although more complex than a systematic design, this design did not prove to be too difficult to implement in practice. The chief difficulty lay in the occasional back-tracking required in transitting between inshore and offshore transects as a result of the independent randomisation and rankings in the two strata. Back-tracking was kept within reasonable bounds by occasionally upsetting rankings where this enabled a substantial saving in steaming time to be made.

8. Results

Comparison of Figs. 1 and 4 show that the broad-scale distribution of anchovy in 1984 and 1985 was similar, justifying the use of the 1984 density structure in the design of the 1985 survey. As expected, no anchovy were detected north of Cape Town in 1985 and, as in 1984, there was a marked reduction in density on the eastern side of the Agulhas Bank.

Table 3 shows the values of A_i and $\bar{L}_i$, and estimates of $\bar{\rho}_i$ and biomass for each of the strata, A, B, and D, on the South Coast, using the data from both phases. Values are likewise given for a combination (as in Appendix A) of strata C and E, in both of which the number of transects was considered to be too low for reliable estimation of their individual variances. The mean density and total biomass over all strata are given. The standard errors of the density estimates are the square roots of Var ($\hat{\bar{\rho}}_i$) and Var ($\hat{\bar{\rho}}$) defined in equation (3). Table 3 also gives the optimum defined in equation (3). Table 3 also gives the optimum transect allocations estimated from the transects in both phases using the alternative formulae of equations (9) and (11), while the actual allocation (in Table 2) is repeated in the final column for comparison.

TABLE 4. Standard errors in mean density (g/m^2)$^-$expected from different allocations of sampling effort in the 1985 survey; (c) = equation (9).

Stratum	Unstratified (a)	Stratified (Numbers of transects in brackets)		
		(b) Uniform	(c) Optimum	(d) Actual
A	Total of 34 transects	8.51 (8)	5.52 (19)	8.02 (9)
B		3.16 (9)	3.00 (10)	3.00 (10)
C		0.64 (6)	1.57 (1)	0.79 (5)
D		1.96 (5)	2.53 (3)	1.79 (6)
E		0.48 (6)	1.18 (1)	0.59 (4)
S.E. ($\bar{\rho}$)	2.40	1.54	1.30	1.49
Coefficient of variation (%)	26.10	16.7	14.1	16.1
Relative precision	1.00	2.43	3.41	2.59

Table 4 compares the standard errors that would be expected on the basis of the 1985 results from a sample of 34 transects allocated to the five strata in the following ways:

(a) at random, ignoring strata,
(b) stratified with a uniform sampling fraction,
(c) stratified with optimal allocation based on equation (9) using the stratum variances from the 1985 survey,
(d) stratified with the actual allocation used in 1985.

(Note that since the present discussion is framed within the context of a single-stage sample, the term "sampling fraction" here is not synonymous with the "sampling fractions" in Table 2. The two are equivalent in the sense of differing by a constant factor only if the first-stage units (strips) used in the selection of sample transects are of the same width in all strata.)

The method of estimating variances for the unstratified sample from the data of the stratified sample is given in Appendix

B. The coefficients of variation are the standard errors of $\hat{\bar{\rho}}$ divided by their respective mean densities. The estimates of relative precision are relative to the unstratified sample; thus the relative precision for (b) is $(2.40)^2/(1.54)^2 = 2.43$.

The allocation for (c) is based on equation (9), using the best available estimates of the stratum variances, this being more relevant for present purposes than the more predictive allocation of equation (11) (which depends on an assumed relationship between variance and density).

Not surprisingly, the most substantial gain is in the comparison between stratified and unstratified sampling. The allocation of the actual sample has turned out to be much closer to that of the uniform than to that of the optimal (see Section 9), but the potential gain of the optimum over the uniform is indicated by a relative precision of $3.41/2.43 = 1.40$, that is, a gain in efficiency of 40%.

9. Discussion

We hope to have shown that stratified random designs are both appropriate and practicable for acoustic surveys. Sometimes an initial stratification may be somewhat speculative — though still valid — if prior information is limited. Other examples would include populations which, as in the present case, are found by observation to have a similar distribution from one survey to the next, or whose distribution can be predicted from environmental features (e.g. surface temperature, chlorophyll fronts, egg distribution).

The greater difference between the theoretical allocations given by equations (9) and (11) in 1985 compared with 1984 (cf. Tables 1 and 3), indicates that the distribution in 1985 departed further from the distributional assumption implied in equation (11) than was the case in 1984. As illustrated in Table 4, a gain in precision would have been achieved by allocating more of the transcects to Strata B and C. The scope for doing so was however limited by the need to have a reasonable number of transects in all the strata during Phase 1. However, if after more surveys, this pattern is found to persist, it may be advisable to reach some compromise which allocates more transects to the expected high-density regions than indicated by equation (11), while retaining a basic minimum coverage of the regions where the density is expected to be low. Small numbers of transects in the low-density strata will not be disadvantageous if the allocation is thereby brought closer to the optimum, especially as these strata can subsequently be combined as was done in the 1985 survey.

A recent investigation, looking at more extensive anchovy survey data, suggests that the variance of stratum mean density may be more nearly proportional to the square of density than to density itself. Thus, a more realistic appraisal might be a replacement of $\bar{\rho}_i^2$ for $\bar{\rho}_i$ in equation (10) with a corresponding removal of the square root signs in equation (11).

The value or otherwise of the two-phase approach depends on the degree of confidence in the prestratification, and the extent to which the distribution may change during the survey, making allocations based on the first phase inappropriate to the second.

A balance needs to be found between having sufficient Phase 2 transects in hand to adjust for differences between the anticipated and observed distributions in Phase 1, while retaining sufficient transects in Phase 1 to determine the density structure and allocate the Phase 2 transects optimally.

In situations where there is very little prior information on distribution, it would probably be advisable to decrease the proportion of transects in Phase 1.

Where there is a substantial movement of fish causing major changes in distribution between strata during the course of the survey, the two-phase approach may be inappropriate and wasteful. One way to counteract this in situations such as ours, where there is a clear density gradient in the direction normal to the transects, would be to conduct the Phase 1 survey in the direction of anticipated density increase (in our case from east to west), to minimise the time difference between the Phase 1 and Phase 2 surveys of the high-density regions.

Acknowledgements

We wish to thank Mr. Stephen J. Smith and two anonymous referees for their helpful comments, also Professor George Seber, University of Auckland, and Dr. Chris Francis, Ministry of Agriculture and Fisheries, Wellington, New Zealand, for kindly drawing our attention to specific points.

References

ANONYMOUS 1986. Research ship Africana. Spec. Rep. Sea Fish. Res. Inst. S. Afr. 3: 80 p.

ARMSTRONG, M. J., AND D. S. BUTTERWORTH. 1986. Estimates of yield for the South African anchovy resource in ICSEAF Division 1.6 Collect. Sci. Pap. Int. Comm. SE. Atl. Fish. 13(1): 45–53.

COCHRAN, W. G. 1977. Sampling techniques. 3rd ed. John Wiley and Sons, New York, NY. 428 p.

FOOTE, K. G., H. P. KNUDSEN, G. VESTNES, R. BREDE, AND R. L. NIELSEN. 1981. Improved calibration of hydroacoustic equipment with copper spheres. Coun. Meet. Int. Coun. Explor. Sea 1981 B(20): 18 p. (mimeo).

FORBES, S. T., AND O. NAKKEN [ED.] 1972. Manual of methods for fisheries resource survey and appraisal. FAO Man. Fish. Sci. 2: 138 p.

GUILLARD, J., D. GERDEAUX, AND J. M. CHAUTRU. 1990. The use of geostatistics for abundance estimation in lakes: the example of Lake Annecy. J. Cons. Int. Explor. Mer (In press)

HALLDORSSON, O., AND P. REYNISSON. 1983. Target strength measurements of herring and capelin *in situ* at Iceland. *In* O. Nakken and S. C. Venema [ed.] Symposium on Fisheries Acoustics. Selected Papers of the ICES/FAO Symposium on Fisheries Acoustics. Bergen, Norway. June 1982. FAO Fish. Rep. 300: 78–84.

HAMPTON, I. 1987. Acoustic study on the abundance and distribution of anchovy spawners and recruits in South African waters. *In* A. I. L. Payne, J. A. Gulland and K. H. Brink [ed.] The Benguela and comparable ecosystems. S. Afr. J. Mar. Sci. 5.

HAMPTON, I., M. J. ARMSTRONG, G. M. JOLLY, AND P. A. SHELTON. 1990. Assessment of anchovy spawner biomass off South Africa through combined acoustic and egg-production surveys. *In* Proceedings of the 1987 International Symposium on Fisheries Acoustics, Seattle, WA, USA.

JOLLY, G. M., AND I. HAMPTON. 1990. Some problems in the statistical design and analysis of acoustic surveys to assess fish biomass. *In* Proceedings of the 1987 International Symposium on Fisheries Acoustics, Seattle, WA, USA.

JOLLY, G. M., AND S. J. SMITH. 1989. A note on the analysis of marine survey data. *In* Progress in Fisheries Acoustics, Proceedings of the Institute of Acoustics. MAFF Fisheries Laboratory, Lowestoft, England 11(3): 195–201.

MACLENNAN, D. N., AND I. G. MACKENZIE. 1988. Precision of acoustic fish stock estimates. Can. J. Fish. Aquat. Sci. 45: 605–616.

PENNINGTON, M. 1983. Efficient estimators of abundance for fish and plankton surveys. Biometrics 39: 281–286.

1986. Some statistical techniques for estimating abundance indices from trawl surveys. Fish. Bull. 84: 519–525.

RIPLEY, B. D. 1981. Spatial statistics. John Wiley and Sons, New York, NY. 252 p.

SHELTON, P. A. 1986. Fish spawning strategies in the variable southern Benguela Current region. Ph.D. thesis, University of Cape Town, South Africa. (vi) + 327 p.

SMITH, S. J. 1990. The use of statistical models for the estimation of abundance from groundfish trawl survey data. Can. J. Fish. Aquat. Sci. 47: 894–903.

Appendix A

Combination of Strata with few Sample Transects

Since strata with few sample transects are most likely to occur in the less intensively sampled, low-density areas, they can reasonably be combined into a single group of strata having a mean density and a variance averaged over the within-stratum variances. The procedure follows that of Cochran (1977, p. 165) for the combination of ratio estimates. The only minor difference is that we replace Cochran's N_i by its estimate $\alpha A_i/\bar{L}_i$, the constant of proportionality cancelling out in the formation of the combined ratio, $\hat{\hat{\rho}}_c$.

First, we define the variable $y_{ij} = L_{ij}\,\hat{\hat{\rho}}_{ij}$, with stratum mean given by

$$\bar{y}_i = \frac{1}{n_i}\sum_{j=1}^{n_i} L_{ij}\,\hat{\hat{\rho}}_{ij},$$

where n_i is the number of sample transects in the ith stratum. A weighted mean over the strata of $\bar{y}_i$ and $\bar{L}_i$ (the unweighted mean transect length in stratum i) is then formed, with weights $A_i/\bar{L}_i$. The estimated mean density for the combined strata, $\hat{\hat{\rho}}_c$, is then

$$\text{(A.1)}\quad \hat{\hat{\rho}}_c = \sum_i \frac{A_i\bar{y}_i}{\bar{L}_i} \Big/ \sum_i \frac{A_i\bar{L}_i}{\bar{L}_i} = \frac{\sum_i A_i\,\hat{\hat{\rho}}_i}{\sum_i A_i}.$$

The variance of $\hat{\hat{\rho}}_c$ is estimated as

$$\text{(A.2)}\quad \mathrm{Var}(\bar{\rho}_c) = \sum_i \frac{A_i^2 S_i^2 / n_i\bar{L}_i^2}{\left(\sum_i A_i\right)^2},$$

where

$$S_i^2 = S_{iy}^2 - 2\hat{\hat{\rho}}_i S_{iyL} + \hat{\hat{\rho}}_i^2 S_{iL}^2,$$

S_{iy}^2, S_{iL}^2 and S_{iyL} being the mean squares and products of y_{ij} and L_{ij} within stratum i. Note that since $\mathrm{Var}(\hat{\hat{\rho}}_c)$ is still based on within-stratum variation, the advantage of the original stratification is retained in full.

In the survey analysis, a group of strata combined according to the above procedure is treated as a single stratum with density $\hat{\hat{\rho}}_c$.

Appendix B

Variance of an Unstratified Random Sample estimated from data from a Stratified Sample

The problem is to discover the correct weighting to be assigned to the variance components estimated from a stratified random sample for the purpose of obtaining an unbiased estimate of variance appropriate to an unstratified random sample from the same population.

For a single variate, y, Cochran (1977, section 5A.11) quotes a result with a proof. In present notation his equation (5A.44) gives

$$\text{(B.1)}\quad \mathrm{Var}_{ran}(\bar{y}) = \frac{N-n}{n(N-1)}\left[\frac{1}{N}\sum_i \frac{N_i}{n_i}\sum_{j=1}^{n_i} y_{ij}^2 - \bar{y}_{st}^2 + \mathrm{Var}(\bar{y}_{st})\right],$$ [1]

as the estimated variance for the mean, $\bar{y}$, of an unstratified random sample of size n, where $\mathrm{Var}(\bar{y}_{st})$ is the estimated variance of $\bar{y}_{st}$, the estimated mean from the stratified sample, n_i, N_i, n and N are the numbers of sampling units in the sample and in the population, with i referring to strata and j to different units within the same stratum.

To express $\mathrm{Var}_{ran}(\bar{y})$ in terms of mean squares within and among strata, we have

$$\sum_{j=1}^{n_i} y_{ij}^2 = \sum_{j=1}^{n_i} (y_{ij}-\bar{y}_i)^2 + n_i\bar{y}_i^2 = (n_i-1)S_{yi}^2 + n_i\bar{y}_i^2,$$

where

$$S_{yi}^2 = \sum_{j=1}^{n_i} (y_{ij}-\bar{y}_i)^2/(n_i-1) \text{ and } \bar{y}_i = \frac{1}{n_i}\sum_j y_{ij}.$$

Substituting in equation (B-1) gives

$$\mathrm{Var}_{ran}(\bar{y}) = \frac{N-n}{n(N-1)}\left[\sum_i \frac{N_i}{N}\left\{1-\frac{1}{n_i}+\frac{N_i}{Nn_i}-\frac{1}{N}\right\} S_i^2 + \sum_i \frac{N_i}{N}(\bar{y}_i-\bar{y}_{st})^2\right].$$

Since N_i and N are very large and n_i and n small, we can make the approximations

$$1-\frac{1}{N} \simeq 1 \text{ and } \frac{N-n}{N-1} \simeq 1,$$

giving,

$$\text{(B.2)}\quad \mathrm{Var}_{ran}(\bar{y}) = \frac{1}{n}\sum_i \frac{N_i}{N}\left[\left\{1-\frac{1}{n_i}\left(1-\frac{N_i}{N}\right)\right\} S_{yi}^2 + (\bar{y}_i-\bar{y}_{st})^2\right].$$

Defining y_{ij} as the biomass of the jth transect of the ith stratum and x_{ij} as the transect length, the covariance, $\mathrm{Cov}_{ran}(\bar{x},\bar{y})$, between $\bar{x}$ and $\bar{y}$ is given by a formula similar to (B.2) with the mean product S_{xyi} replacing S_{yi}^2 and $(\bar{x}_i-\bar{x}_{st})(\bar{y}_i-\bar{y}_{st})$ replacing $(\bar{y}_i-\bar{y}_{st})^2$. Applying the standard formula of Cochran (1977) for the variance of the estimated ratio, $\bar{y}/\bar{x}$, we have for the variance of the mean density, $\hat{\hat{\rho}}$,

$$\mathrm{Var}_{ran}(\hat{\hat{\rho}}) = Var_{ran}\left(\frac{\bar{y}}{\bar{x}}\right) = \frac{1}{n\,\bar{x}^2}\sum_i \frac{N_i}{N}\{\mathrm{Var}_{ran}(\bar{y}) - 2\,\hat{\hat{\rho}}\,\mathrm{Cov}_{ran}(\bar{x},\bar{y}) + \hat{\hat{\rho}}^2\mathrm{Var}_{ran}(\bar{x})\}.$$

On substitution, equating x_{ij} to L_{ij} and $\bar{y}_{st}/\bar{x}_{st}$ to $\hat{\hat{\rho}}$ (these ratios having the same expectation), this reduces to

$$\text{(B.3)}\quad \mathrm{Var}_{ran}(\hat{\hat{\rho}}) = \frac{1}{n}\sum_i \frac{N_i}{N}\left\{\left(n_i-1+\frac{N_i}{N}\right)\mathrm{Var}(\hat{\hat{\rho}}_i) + \left(\frac{\bar{L}_i}{\bar{L}}\right)^2(\hat{\hat{\rho}}_i-\hat{\hat{\rho}})^2\right\},$$

where $\mathrm{Var}(\hat{\hat{\rho}}_i)$ is the variance in equation (3) in the main text.

---

[1] Note that, in Cochran's notation, his "V_{ran}" in equation (5A.44) should read "v_{ran}".

Metabolic Effects of Bovine Growth Hormone and Genetically Engineered Rainbow Trout Growth Hormone in Rainbow Trout (*Oncorhynchus mykiss*) Reared at a High Temperature

Roy G. Danzmann[1]

John Hopkins University, Chesapeake Bay Institute, Shady Side, MD 20764 USA

Glen J. Van Der Kraak,

University of Guelph, Department of Zoology, Guelph, Ont. N1G 2W1 Canada

Thomas T. Chen, and Dennis A. Powers[2]

John Hopkins University, Chesapeake Bay Institute, Shady Side, MD 20764. USA,
and John Hopkins University, Department of Biology, Baltimore, MD 21218 USA
and University of Maryland, Center of Marine Biotechnology, Baltimore, MD 21202 USA

Danzmann, R. G., G. J. Van Der Kraak, T. T. Chen, and D. A. Powers. 1990. Metabolic effects of bovine growth hormone and genetically engineered rainbow trout growth hormone in rainbow trout (*Oncorhynchus mykiss*) reared at a high temperature. Can. J. Fish. Aquat. Sci. 47: 1292–1301.

The growth promoting ability of bovine growth hormone purified from natural sources (bGH) and genetically engineered rainbow trout growth hormone (rtGH) were compared in rainbow trout (*Oncorhynchus mykiss*) reared at 17.0°C. Fish were fed high (on-demand feeding) and low (2.8–4.6% of body weight/d) rations. On both rations, length specific growth rates were significantly higher in bGH treated fish than in all other treatments. No significant differences in weight specific growth rates were detected between treatments. Testosterone levels in fish fed the high ration and treated with 1.0 μg/g rtGH or bGH were significantly elevated compared with controls as were 17-β-estradiol levels in females. bGH significantly reduced condition factors of low ration fish, and bGH and rtGH significantly depressed hepatosomatic indicies of high ration fish compared with controls. In a second experiment, weight and length specific growth rates were higher in rtGH and bGH injected fish than in saline controls but these differences were not significant. DNA standardized RNA levels were higher in rtGH and bGH treated fish than in saline control fish and these differences were significant in bGH treated fish. Results indicate that at high rearing temperatures GH administration does not have a major influence on growth but does stimulate steroidogenic and metabolic activity.

La capacité de favoriser la croissance de l'hormone de croissance d'origine bovine purifiée de sources naturelles (bGH) et de l'hormone de croissance provenant de la truite arc-en-ciel (rtGH) obtenue par génie génétique a été comparée chez la truite arc-en-ciel (*Oncorhynchus mykiss*) élevée à 17,0°C. Les poissons ont reçu des rations alimentaires élevées (à la demande) et faibles (2,8 à 4,6% du poids par jour). Dans le cas des deux types d'alimentation, le taux de croissance spécifique en fonction de la longueur était significativement plus élevée chez les poissons auxquels on a administré l'hormone de croissance d'origine bovine que chez les poissons auxquels on a administré tous les autres traitements. Aucune différence significative n'a été décelée au niveau du taux de croissance spécifique en fonction du poids entre les différents traitements administrés aux poissons. Le taux de testostérone chez les poissons ayant reçu une ration élevée et auxquels on a administré une dose de 1,0 μg/g de rtGH ou de bGH était significativement plus élevé par rapport aux poissons témoins tout comme le taux de 17β-estradiol chez les femelles. L'administration de bGH a abaissé significativement le coefficient de condition des poissons auxquels on a administré une ration faible, et l'administration de bGH et de rtGH a abaissé significativement les indices hépatosomatiques des poissons ayant reçu une portion élevée par rapport aux poissons témoins. Dans une deuxième expérience, le taux de croissance spécifique en fonction du poids et de la longueur était plus élevé chez les poissons auxquels on a injecté de la rtGH et de la bGH que chez les témoins auxquels on a administré une solution physiologique, mais ces différences n'étaient pas significatives. Le taux d'ARN normalisé par rapport à l'ADN était plus élevé chez les poissons ayant reçu de la rtGH et de la bGH que chez les poissons témoins auxquels on a administré une solution physiologique et ces différences étaient significatives chez les poissons ayant reçu de la bGH. D'après les résultats obtenus, à température élevée, l'administration d'hormone de croissance n'a pas d'effet important sur la croissance mais elle stimule la stéroïdogenèse et le métabolisme.

Received August 23, 1989
Accepted February 27, 1990
(JA290)

Reçu le 23 août 1989
Accepté le 27 février 1990

---

[1] **Present address: University of Guelph, Department of Zoology, Guelph, Ont. N1G 2W1 Canada.**

[2] **Present address: Stanford University, Hopkins Marine Station, Department of Biological Sciences, Pacific Grove, CA. 93950–3094 USA.**

In recent years there have been several studies examining the growth promoting abilities of growth hormone (GH) in salmonid fishes (Higgs et al. 1975, 1976, 1977, 1978; Clarke et al. 1977; Markert et al. 1977; Donaldson et al. 1979; Gill et al. 1985; Sekine et al. 1985; Kawauchi et al. 1986; Agellon et al. 1988; Down et al. 1988, 1989). The GH used in these studies was either purified from mammalian or piscine sources, or synthetically produced from cloned mammalian or piscine growth hormone genes. Generally, all of these studies have documented an increased growth rate of salmonid fishes in response to GH administration.

Agellon et al. (1988) reported that recombinant rainbow trout GH (rtGH) at a dosage of 1.0 μg/g was the most effective in stimulating growth in rainbow trout (*Oncorhynchus mykiss*) reared at 13–15°C. In other studies, bovine GH (bGH) at dosages of 1.0 μg/g body weight or higher were necessary to elicite significant growth enhancement in coho salmon reared at 10°C (Higgs et al. 1977, 1978). In contrast, bGH administered at a dose of 0.25 μg/g body weight significantly enhanced growth rates in sockeye salmon (*O. nerka*) reared at 17.5°C (Clarke et al. 1977). These results indicate that the dosage of bGH necessary to affect growth rates may be reduced in salmonids reared at warmer temperatures.

Most studies investigating the effects of GH on growth have been conducted at lower temperatures than the thermal optimum for growth. In this study we examine how GH administration effects growth rates in rainbow trout reared at the thermal optimum for growth (17–18°C). Two types of GH were used: (1) a recombinant rainbow trout GH (rtGH) (Agellon and Chen 1986) and; (2) natural bGH. When food is not limiting, salmonid growth rates are directly proportional to environmental temperature (up to the thermal optimum for the species) (Brett et al. 1969; Weatherley 1972). It was of interest, therefore, to determine if rtGH also has enhanced growth promoting ability at warmer temperatures and to compare the growth promoting ability of rtGH and bGH at temperatures where growth is maximally stimulated. In addition, the interaction between ration size (high and low) and GH administration on growth rate was examined.

Materials and Methods

Source of the Fish

Experiment 1: the Reynoldsdale strain of rainbow trout was used in this work. Gametes were obtained from the Reynoldsdale State Fish Hatchery, Fishertown, Pennsylvania, on June 3, 1987. Approximately equal proportions of gametes from 16 females and 27 males were mixed separately and then pooled together to make a large pooled cross. Embryos were raised at the Chesapeake Bay Institute in vertical FAL incubating trays at 12–14°C until hatching. The fish were then acclimated to summer well water temperatures at the Institute (16–18°C) prior to experimentation. The experiment was initiated January 25, 1988, when the fish were 236 d old, post-fertilization.

Experiment 2: juvenile Reynoldsdale rainbow trout obtained on July 28, 1987, were acclimated at 16–18°C at the Chesapeake Bay Institute for approximately 2 mo prior to the initiation of the experiment on September 21.

Experimental Protocols

Experiment 1 was conducted to measure the influence of GH on weight and length specific growth rates, physiological changes, and steroidogenic activity in individual fish. Experiment 2 was conducted to measure the influence of GH on length and weight specific growth rates and nucleic acid levels in individual fish.

Experiment 1: 2 wk prior to the initiation of the experiment, lots of 20 fish each were weighed and measured. Each lot of 20 fish was housed in a circular 30 gallon tank on a 12:12 light:dark cycle. Twenty experimental lots (400 fish) were used for the experiment. The fish were divided into high and low feeding rations (200 fish in each). Fish were either: (1) fed using on-demand feeding hoppers or; (2) fed a hatchery ration calculated from tables of feeding rations for salmonid fishes (Bardach et al. 1972). According to the tables, fish were fed a ration which was approximately 4.6% of body weight at the beginning of week 1. This ration was gradually decreased to 2.8% of body weight after week 6. Rations were recalculated at each weighing and adjusted for any mortalities. Low ration fish were fed once daily. The diet fed was Martins 3/32″ 84G pellets (40% protein; 10% fat; 3% fibre) from Martins Feed Mills, Elmira, Ont.

Five treatments were used for each feeding ration: (1) an uninjected control; (2) an injected control group receiving an extract of bacterial protein from strain HB101 (the bacterial strain used to clone rtGH); (3) a bGH treatment receiving (USDA-bGH-B1) from the National Hormone and Pituitary Program, at a concentration of 1.0 μg/g body weight; (4) a rtGH treatment receiving a dose of 1.0 μg/g body weight; and (5) a rtGH treatment receiving a dose of 0.1 μg/g body weight. RtGH was prepared according to the protocols outlined in Agellon and Chen (1986) and Agellon et al. (1988).

All fish were measured (fork length) and weighed, and injected (if needed according to treatment) intraperitoneally weekly at the beginning of week 1, 2, 3, 4, and 6. Doses were recalculated according to the weights of each individual fish at these times. Fish were not fed on the day of these measurements. The fish were anaesthetized with 2-phenoxyethanol (Sigma Chemical Co.) at a 1:2000 dilution to facilitate handling. The experiment was terminated at the end of week 8. At this time, a blood sample was obtained from 15 fish in the uninjected control, bGH, and rtGH (1.0 μg/g) treatments, for measurements of circulating testosterone and 17-β-estradiol levels. The average weight and length of the fish at the beginning of the experiment was 11.79 g (range: 4.79–30.03 g) and 9.25 cm (range: 7.1–12.9 cm), respectively. Mortalities throughout the course of the experiment were low, ranging from 0 to 3.75% of the fish in a treatment, averaged over both feeding rations.

Experiment 2: 36 fish were randomly assigned to one of three treatment groups consisting of: (1) a saline control; (2) bGH; or (3) rtGH. Fish were measured (fork length), weighed, and injected 4 × at 8-d intervals, and the experiment was terminated on day 32. At this time, a muscle sample was excised from each fish and immediately frozen in liquid nitrogen for nucleic acid determinations. Fish were fed ad libitum twice daily with Martins 84G pellets.

Fish in the saline control received 200 μL of 0.8% saline at each injection, while bGH treated fish received 15 μg of hormone in 150 μL of saline at each injection. rtGH treated fish received 200 μL of recombinant protein extract which was initially estimated (using an immunoblot analysis) to be an equivalent dosage to the bGH treatment, but was subsequently shown to contain 10 μg of rtGH. Therefore, rtGH treated fish received a lower dose of GH than bGH treated fish. The initial starting

TABLE 1. Final mean weights (g) and percent increases in weight based upon the initial mean starting weight of fish in the different treatments in experiment 1.

Feeding ration	Treatment Normal control	HB101 control	bGH 1.0 μg/g	rtGH 1.0 μg/g	rtGH 0.1 μg/g
High	49.68	48.29	55.68	47.82	47.01
± SE	3.26	2.56	3.81	3.22	3.14
Sig.	+	+	+	+	+
Low	44.50	39.85	45.17	41.70	41.08
± SE	3.01	2.35	2.53	3.00	2.93
Sig.	+	+	+	+	+
Percentage increase in weight since the beginning of the experiment					
High (%)	316	309	368	297	297
Low (%)	288	263	266	261	241

[a]Results from a GT-2 pairwise multiple comparison test. Treatments are not significantly different from one another (across rows) if underscored by the same symbol.

weight of the fish in each treatment were: (saline control; mean = 40.00 g; range = 27.07–54.87 g), (bGH; mean = 39.21 g; range = 31.89–60.27 g), (rtGH; mean = 39.27; range = 20.09–81.00 g). Corrected for mortalities, the initial starting weights were: (saline control; N = 8; mean = 38.02 g; range = 27.07–47.61 g), (bGH; N = 8; mean = 41.78 g; range = 33.92–60.27 g), (rtGH; N = 6; mean = 44.32 g; range = 33.03–81.00 g).

Biochemical Analyses

For nucleic acid measurements, 0.1-g samples (approximate weight) were homogenized by sonication in 4 mL of cold phosphate buffered saline (PBS). After centrifugation, an 800 μL aliquot was removed and further diluted to 4 mL in cold PBS. All samples were analyzed in duplicate for both RNA and DNA content, using the methods of Karsten and Wollenberger (1972; 1977). Total nucleic acids (RNA + DNA) were measured, and DNA levels were determined by treating replicate samples with RNase using the protocol described by Ferguson and Drahushchak (1990). Protein determinations were made using the Lowry method (Lowry et al. 1951).

For the analysis of steroid levels, plasma samples were extracted with ether and the testosterone and 17-β-estradiol content determined by RIA as previously described (Van Der Kraak et al. 1984).

Statistical Analyses

Experiment 1: differences in length and weight specific growth rates between treatments over the course of the experiment were compared using a two-factorial ANOVA based upon replicate means (Sokal and Rohlf 1981). The five treatments were considered the first factor and feeding ration the second factor. Within each feeding level 200 fish were divided between five treatments, such that each treatment consisted of four replicates divided between two tanks with 10 fish in each replicate. Ten fish within each tank were caudal fin branded and 10 fish were unmarked. Replicates were moved to a new experimental tank after each weighing to minimize environmental and social influences upon the growth dynamics of the fish. However, only fish of one treatment class were housed together.

TABLE 2. Mean weight specific growth rates[a] (Day 1–56) of replicates ($N = 4$) in the different experimental treatments used in experiment 1.

Feeding ration	Treatment Normal control	HB101 control	bGH 1.0 μg/g	rtGH 1.0 μg/g	rtGH 0.1 μg/g
High	2.701	2.713	2.932	2.653	2.659
± SE	0.167	0.037	0.137	0.016	0.120
Sig.[a]	+	+	+	+	+
Low	2.511	2.399	2.347	2.339	2.229
± SE	0.072	0.047	0.039	0.052	0.054
Sig.	+	+	+	+	+

[a]Specific growth rates calculated as: $\frac{\ln wt_2 - \ln wt_1}{t_2 - t_1} \times 100$, where wt_1 is the mean weight of fish in the group at time t_1 and wt_2 is the mean weight of fish in the same group at time t_2.

[b]Results from a GT-2 pairwise multiple comparison test. Treatments are not significantly different from one another (across rows) if underscored by the same symbol.

TABLE 3. Final mean lengths (mm) and percent increases in length based upon the initial mean starting length of fish in the different treatments in experiment 1.

Feeding ration	Treatment Normal control	HB101 control	bGH 1.0 μg/g	rtGH 1.0 μg/g	rtGH 0.1 μg/g
High	151.2	150.3	157.3	148.9	147.5
± SE	3.30	2.84	3.43	3.43	3.26
Sig.[a]	+	+	+	+	+
Low	144.8	140.3	149.5	142.2	142.5
± SE	3.30	2.91	2.47	3.38	3.31
Sig.	+	+	+	+	+
Percentage increase in length since the beginning of the experiment					
High (%)	61.5	60.1	72.3	62.4	61.3
Low (%)	55.3	52.1	59.3	55.9	53.2

[a]Results from a GT-2 pairwise multiple comparison test. Treatments are not significantly different from one another (across rows) if underscored by the same symbol.

For the analysis of final lengths, weights, hepato-somatic indices (HSIs), initial condition factors (CF), and serum steroid levels, individual fish were considered replicates within each experimental treatment to meet the assumptions of homogeneity of variance. Values for serum steroid levels were square-root transformed. Differences in final CF between treatments were tested using non-parametric procedures as variances between treatments were refractory to normalization using several transformations. A Kruskal-Wallis test was used to test for significant differences between treatments. If significance was detected, pair-wise comparisons between treatments were made using a Wilcoxon two-sample test (Sokal and Rohlf 1981). An alpha-level of $0.05/2c$, where c is the number of pair-wise comparisons, was considered significant. This correction was adopted to minimize type I error.

Experiment 2: length and weight specific growth rates and CF were calculated for the fish as described in experiment 1. Differences in the means between treatments were compared using a one-way ANOVA. RNA/DNA ratios were reciprocally transformed (1/value) to meet the assumptions of homogeneity of variances between treatments. Protein values were analyzed

TABLE 4. Mean length specific growth rates (Day 1–56) of replicates ($N=4$) in the different experimental treatments used in experiment 1.

	Treatment				
Feeding ration	Normal control	HB101 control	bGH 1.0 μg/g	rtGH 1.0 μg/g	rtGH 0.1 μg/g
High	0.917	0.905	1.036	0.934	0.921
± SE	0.050	0.010	0.043	0.011	0.007
Sig.[a]	+	+	*	+,*	+,*
Low	0.814	0.779	0.848	0.808	0.776
± SE	0.019	0.015	0.006	0.017	0.016
Sig.	+	+	+	+	+

[a] Results from a GT-2 pairwise multiple comparison test. Treatments are not significantly different from one another (across rows) if underscored by the same symbol.

using a non-parametric Kruskal-Wallis test, since it was not possible to satisfactorily transform these data.

Results

Experiment 1

Weight

While no significant differences in final weights ($P=0.166$), or weight specific growth rates ($P=0.240$) were detected between treatments, highly significant differences in final weights ($P<0.001$), and weight specific growth rates ($P<0.001$) were evident between feeding rations (Tables 1 and 2). When treatments within feeding rations were compared using a one-way ANOVA, no significant differences were detected within either the high or low feeding ration (Table 1).

Length

As expected, feeding ration had a very pronounced stimulatory effect upon the final lengths attained by the experimental fish ($P<0.001$). When comparisons were made between treatments within feeding rations (one-way ANOVA), no significant differences were detected between treatments (Table 3).

Significant differences were detected in the length specific growth rates, between both rations ($P<0.001$), and treatments ($P=0.004$). Length specific growth rates in bGH treated fish were significantly higher ($P<0.02$) than in all other treatment groups (two-way ANOVA). All other comparisons were not significant. When comparisons were made between treatments within feeding rations (one-way ANOVA), it was observed that bGH treated fish in the high feeding ration had significantly higher rates of length increase than either normal control fish, or fish in the HB101 protein extract control treatment. All other comparisons between treatments at the high feeding ration were not significant. No significant differences were detected between treatments at the low feeding ration (Table 4).

Condition factor

No significant differences in CF were detected between treatments at the high feeding ration. However, bGH treated fish had significantly lower CFs than normal control fish ($P<0.001$), and HB101 control fish ($P<0.001$), at the low feeding ration. No significant differences were detected in other pair-wise comparisons at the low feeding ration (Table 5).

Liver weight

Significant differences in HSI were detected between treatments ($P<0.001$), and feeding ration ($P<0.001$). In addition a significant interaction effect between treatment and feeding ration was observed ($P=0.003$). At the high feeding ration, HSIs of bGH treated fish, and rtGH treated fish (1.0 and 0.1 μg/g) were significantly lower than HSIs of normal control ($P<0.001$; $P=0.004$; and $P=0.049$, respectively), and HB101 control fish ($P<0.001$; $P<0.001$; and $P<0.001$, respectively). HSIs of bGH treated fish were also significantly lower than HSIs of rtGH (0.1 μg/g) treated fish ($P=0.009$). Other pairwise comparisons were not significant (Table 6). At

TABLE 5. Initial and final mean condition factors[a] of fish in the different treatments in experiment 1[b].

	Treatment				
Feeding ration	Normal control	HB101 control	bGH 1.0 μg/g	rtGH 1.0 μg/g	rtGH 0.1 μg/g
High – Initial	13.001	13.089	13.360	13.214	13.230
± SE	0.178	0.134	0.159	0.172	0.177
Sig.	+	+	+	+	+
High – Final	13.640	13.732	13.515	13.606	13.875
± SE	0.136	0.153	0.142	0.138	0.220
Sig.	+	+	+	+	+
Prob.[c]	<0.01	<0.01	NS	NS	<0.05
Low – Initial	13.091	13.285	13.309	13.818	13.242
± SE	0.145	0.171	0.134	0.167	0.176
Sig.	+	+	+	+	+
Low – Final	13.876	13.814	13.081	13.569	13.375
± SE	0.137	0.161	0.123	0.094	0.148
Sig.	+	+	*	+,*	+,*
Prob.	<0.001	<0.05	NS	NS	NS

[a] Condition factor was calculated using: $(W/L^3) \times 1000$, where W = weight (mg) and L = length (mm).

[b] Results from a T-method pairwise multiple comparison test for initial condition factors and pairwise Wilcoxon two-sample tests (alpha $=0.05/2c$) for final condition factors. Treatments are not significantly different from one another (across rows) if underscored by the same symbol.

[c] Results from a students *t*-test or Wilcoxon two-sample test comparing initial and final condition factors within treatments.

TABLE 6. Final mean hepato-somatic indices (HSIs)[a] of fish in the different treatment and feeding rations in experiment 1[b].

	Treatment				
Feeding ration	Normal control	HB101 control	bGH 1.0 μg/g	rtGH 1.0 μg/g	rtGH 0.1 μg/g
High	1.795	1.883	1.526	1.628	1.679
± SE	0.042	0.033	0.032	0.040	0.035
Sig.[b]	+	+	*	*, –	–
Low	2.059	1.997	1.933	1.994	2.031
± SE	0.052	0.046	0.037	0.030	0.054
Sig.	+	+,*	*	+,*	+,*

[a] Hepato-somatic index (HSI) was calculated using: (liver weight (g)/body weight(g)) × 100.

[b] Results from a GT-2 pairwise multiple comparison test. Treatments are not significantly ($P > 0.05$) different from one another (across rows) if underscored by the same symbol.

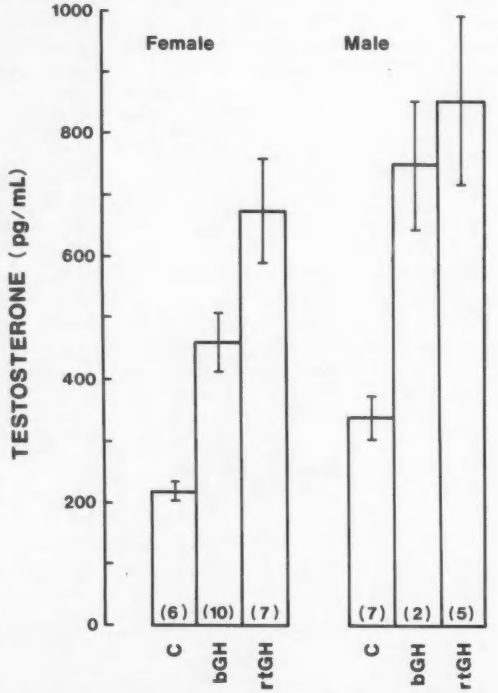

FIG. 1. Mean testosterone levels (pg/mL) in males and females fed a high ration in experiment 1. Normal control (C), bGH, and rtGH treated fish are compared. Bars represent the standard error of the mean. Sample sizes are in parentheses.

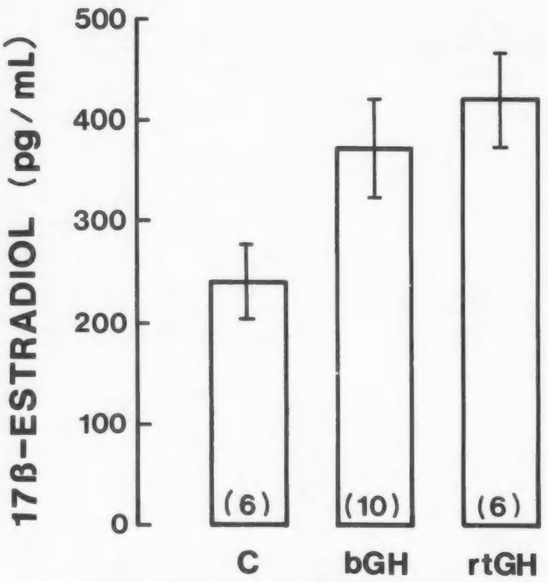

FIG. 2. Mean 17-β-estradiol levels (pg/mL) in females fed a high ration in experiment 1. Normal control (C), bGH, and rtGH treated fish are compared. Bars represent the standard error of the mean.

the low feeding ration, bGH treated fish had significantly lower HSIs than normal control fish ($P = 0.032$). All other comparisons were not significant (Table 6).

Generally, two observations can be made using these data: (1) the HSIs of rtGH treated fish were intermediate to the HSIs observed in control and bGH treated fish; and (2) HSIs increased in all treatments at the low feeding ration, accounting for the significant interaction effect observed. This results because liver weight tends to increase at a proportionately lower rate compared with muscle mass or carcass weight (i.e. expresses negative allometry) in rainbow trout larger than 10–15 g (Weatherley and Gill 1983). Since low-ration fish have slower rates of weight increase compared with high-ration fish, liver weights will represent a proportionately greater percentage of body weight in low-ration fish.

If liver demonstrates negative growth allometry, HSIs may be lower in heavier or bigger fish simply because liver weights are proportionately lower in heavier fish. However, since weight specific growth rates (Table 2) and final weights (Table 1) (within feeding rations) were not significantly different between treatments, it is unlikely that our HSI estimates were biased

To ensure that liver weights were indeed proportionately lower in GH treated fish, regardless of body weight, we performed an analysis of co-variance (ANCOVA) which tests for equality of y-intercepts (liver weights) when body weight is held constant. This analysis was conducted within feeding levels. At the high feeding level, the results from ANCOVA and a one-way ANOVA of HSIs are identical. bGH treated, rtGH (1.0 μg/g), and rtGH (0.1 μg/g) treated fish have significantly lower liver weights than normal control fish ($P < 0.001$; $P = 0.001$; and $P = 0.023$, respectively), and HB101 control fish ($P < 0.001$; $P < 0.001$; and $P < 0.001$, respectively). bGH treated fish also had significantly lower liver weights than rtGH (0.1 μg/g) treated fish ($P = 0.013$). No significant differences were detected between bGH and rtGH (1.0 μg/g) treated fish or between both rtGH treatments. No significant difference were detected between treatments at the low feeding level. Therefore, the differences in HSIs observed between treatments are physiologically meaningful and do not result from differential growth allometries.

Food conversion efficiencies

Food conversion efficiencies were higher in the low-ration fish (range: 0.7830–0.8958) than in the high-ration treatment (range: 0.5862–0.6947). This reflects the wastage of food asso-

TABLE 7. Mean initial and final weights, lengths, condition factors (CF), and weight and length specific growth rates of fish in the different treatments used in experiment 2[a].

Variable	Treatment		
	Saline control	bGH	rtGH
Weight(g) (Day 1)	38.03	41.78	44.32
± SE	2.47	3.40	7.41
Sig.	+	+	+
Weight(g) (Day 33)	66.14	84.32	80.92
± SE	8.29	9.13	14.99
Sig.	+	+	+
Length(mm) (Day 1)	149.4	152.5	150.6
± SE	3.2	4.4	8.3
Sig.	+	+	+
Length(mm) (Day 33)	172.8	185.8	178.5
± SE	5.9	5.6	9.7
Sig.	+	+	+
Weight specific growth rate (Day 1–33)	1.629	2.140	1.835
± SE	0.260	0.168	0.161
Sig.	+	+	+
Length specific growth rate (Day 1–33)	0.446	0.616	0.531
± SE	0.059	0.053	0.054
Sig.	+	+	+
CF (Day 1)	11.33	11.69	12.59
± SE	0.39	0.37	0.36
Sig.	+	+	+
CF (Day 33)	12.40	12.80	13.59
± SE	0.29	0.25	0.38
Sig.	+	+,*	*

[a] Results from a GT-2 pairwise multiple comparison test. Treatments are not significantly ($P>0.05$) different from one another (across rows) if underscored by the same symbol.

TABLE 8. Mean RNA/DNA ratios and protein levels in white muscle of the fish used in experiment 2.

Variable	Treatment		
	Saline control	bGH	rtGH
DNA (μg/g)	104.89	102.77	110.51
± SE	5.85	9.12	7.18
Sig.	+	+	+
RNA (μg/g)	457.69	597.49	566.39
± SE	34.29	43.68	41.56
Sig.	+	*	+,*
RNA/DNA	4.394 (0.236)	6.212 (0.179)	5.203 (0.199)
± SE	0.017	0.022	0.017
Sig.[a]	+	+	+
Protein (mg/g)	89.76	93.99	91.37
Sig.[b]	+	+	+

[a] Results are based upon a one-way ANOVA of reciprocally transformed RNA/DNA ratios (ratio given in parentheses).

[b] Results from a Kruskal-Wallis test. Treatments are not significantly ($P>0.05$) different from one another (across rows) if underscored by the same symbol.

TABLE 9. Correlation coefficients[a] between body size or specific growth rates, and nucleic acid or protein levels in the fish from all treatments in experiment 2.

	DNA	RNA	RNA/DNA	Protein
Body weight (Day 33)	−.222	.389	.428[b]	.104
Weight specific growth rate (Day 1–33)	−.091	.543[c]	.507[b]	.240
Weight specific growth rate (Day 17–33)	−.109	.537[c]	.478[b]	.126
Body length (Day 33)	−.256	.424[b]	.488[b]	.129
Length specific growth rate (Day 1–33)	−.001	.563[c]	.456[b]	.127
Length specific growth rate (Day 17–33)	−.141	.594[c]	.542[c]	.111
Condition factor	−.004	.189	.112	.150
Protein	.142	.448[b]	.317	

[a] Pearson product–moment correlation coefficients (20 df) are indicated between all pairwise variables except with Protein where Spearman rank correlation coefficients are shown.

[b] $P<0.05$.

[c] $P<0.01$.

ciated with using on-demand feeders to feed fish. No food wastage was observed in the low-ration treatments. Food conversion efficiencies are generally closer to 0.9 or greater with salmonid fishes (Gill et al. 1985), but were slightly lower in this study. The high water temperature in the present experiment would increase metabolic rates in the fish thereby decreasing food conversion efficiencies.

Sexual maturation

Precocious sexual maturation was observed in 23% (42 of 182) of the males. No significant differences were evident between treatments in the relative number of males showing precocious sexual maturation in either the high or low feeding ration (contingency χ^2 tests: data not shown).

Significant differences in testosterone levels were evident between treatments in both males ($P<0.001$), and females ($P<0.001$). Testosterone levels obtained from males showing precocious gonadal maturation were not included in the analysis, because they were elevated. bGH treated males had significantly higher testosterone levels than control males ($P=0.006$), as did rtGH treated males ($P<0.001$). No significant differences were evident between bGH and rtGH treated males ($P=0.201$). Control females had significantly lower testosterone levels than bGH ($P=0.001$) and rtGH ($P<0.001$) treated females. Also, testosterone levels in rtGH treated females were significantly higher ($P=0.001$) than in bGH treated females (Fig. 1).

Significant differences in 17-β-estradiol levels in females were detected between treatments ($P=0.041$). Control females had significantly lower levels of 17-β-estradiol than did rtGH ($P=0.016$) and bGH ($P=0.046$) treated fish (Fig. 2). No significant differences were detected between GH treated females ($P=0.418$) (Fig. 2).

Testosterone levels and gonadal somatic indices (GSIs) were positively correlated ($r_s=0.607$; $P=0.07$). Testosterone levels in the precocious males sampled ranged from 18.820 ng/mL to 3.550 ng/mL, while in immature males, values were less than 1 ng/mL. GSIs ranged from 2.46 to 6.50% in precocious males and were less than 0.2% in immature males.

Experiment 2

Weight and length

No significant differences in weight were detected between the treatments at the beginning ($P=0.609$), or end ($P=0.419$) of the experiment. Similarly, no significant differences in weight specific growth rates were detected between treatments

($P = 0.221$) during the 33-d experimental period (Table 7). In addition, no significant differences in length were detected between treatments at the beginning ($P = 0.910$) or end ($P = 0.392$) of the experiment, or in length specific growth rates (Day 1–33) between the treatments ($P = 0.108$) (Table 7).

Condition factor

No significant differences in CF were initially detected between treatments ($P = 0.097$). However, by the end of the experiment, the CFs of the rtGH treated fish were significantly greater than those of the saline control fish ($P = 0.013$). CFs of the bGH and rtGH treated ($P = 0.083$), and bGH treated and saline control fish ($P = 0.335$) did not significantly differ. CFs of all groups significantly increased ($P < 0.02$) during the course of the experiment from initial values (Table 7).

Nucleic acid and protein levels

No significant differences were detected between treatments in DNA levels ($P = 0.782$), protein levels ($P = 0.827$), or RNA/DNA ratios ($P = 0.121$). Significant differences were, however, detected between treatments in RNA levels ($P = 0.048$) (Table 8). bGH treated fish had significantly higher ($P = 0.019$) RNA levels than saline control fish, but not rtGH treated fish ($P = 0.602$). No significant differences were detected between rtGH treated and saline control fish ($P = 0.080$) (Table 8).

RNA and RNA/DNA ratios were significantly, and positively associated with increased fish size and higher length and weight specific growth rates (Table 9). Protein levels were also significantly higher in fish with increased RNA content (Table 9). DNA levels and growth rates in fish were not associated (Table 9). There was a tendency for DNA levels in larger fish to be slightly lower, however, as evidenced by the negative correlation coefficients between weight or length at Day 33, and DNA. However, there were no significant differences between treatments in weight standardized DNA levels ($P = 0.743$) or length standardized DNA levels ($P = 0.799$) when the final weights and lengths of the fish were used as covariates.

Discussion

The present experiments demonstrate that bGH and rtGH have limited growth promoting ability in rainbow trout reared at elevated water temperatures, compared to results obtained at equivalent dosages of hormone when fish are reared in colder water. Despite this lack of effect on somatic growth, both growth hormone preparations are active in physiologically influencing condition factors, liver metabolism (hepatosomatic index), and RNA levels. In addition, these hormones influenced gonadal function by causing an elevation in circulating sex steroid levels in male and female trout. This paradoxical action of GH is consistent with recent studies on *Fundulus* (Singh et al. 1988) and goldfish (*Carassius auratus*) (Van Der Kraak et al. 1990), showing that GH exerts a direct effect on the gonad leading to enhanced steroidogenic activity. Furthermore, the results indicate that rtGH is more potent in stimulating both higher testosterone and 17-β-estradiol production than bGH. bGH appears to stimulate more somatic growth than rtGH, while rtGH preferentially enhances gonadal maturation when administered at an equivalent dosage.

Temperature

If food is not limiting, each species exhibits a thermal optimum for growth. At temperatures above or below this optimum, growth will be depressed. In sockeye salmon the thermal optimum for growth has been reported to be 15°C (Brett et al. 1969), and may be even higher in rainbow trout. Iwama and Tautz (1981) reported that growth rates for hatchery strains of rainbow trout were directly proportional to water temperatures up to 18°C, the highest temperature recorded.

The growth rates of the control fish in experiment 1 were higher than those reported for control fish in other studies examining the effect of GH administration in salmonids (Table 10). This is partially because of the age of the fish, but primarily because of the warm rearing temperature used. Weight specific growth rates during the first year of growth in hatchery strains of rainbow trout reared under colder environmental temperatures have been reported to range from 1.14 to 1.45%/d (Kincaid 1981) compared with rates exceeding 2.5%/d in the present study.

If salmonids are growing at, or close to, the thermally mediated maximum growth rate for the species, GH administration may have little effect on growth rates, but could alter other physiological processes in the fish because of a re-allocation of mobilized energy reserves. It would appear that in rainbow trout reared at a high temperature, GH administration influences gonadal and other metabolic functions to a greater extent than growth rates.

Physiology: CF and HSI

The results indicate pronounced physiological responses associated with the administration of GH which are 'type' and 'dose' dependent such that bGH(1.0 μg/g)>rtGH(1.0 μ/g) >rtGH(0.1 μg/g). In experiment 1, rtGH administration at a dose of 1.0 μg/g depressed CFs in rainbow trout but to a lesser degree than the equivalent dosage of bGH. A significant decrease in CFs has been recorded in coho salmon after bGH administration (Higgs et al. 1975, 1976, 1977, 1978; Markert et al. 1977; Gill et al. 1985; Down et al. 1988, 1989). Also, the HSIs of GH treated fish were significantly different from the HSIs of control fish and these differences paralleled the changes observed in CF. For example, the largest decrease in both CF and HSI was observed in bGH treated fish. rtGH (1.0 μg/g) treated fish also had low HSI levels and depressed CF but not to the same degree as bGH treated fish. rtGH (0.1 μg/g) treated fish had final CFs and HSI levels that were intermediate between control fish and rtGH (1.0 μg/g) treated fish. The large decreases in HSIs observed in the GH treated fish is likely the result of the lipolytic action of GH which has been reported in several species of fish (Clarke 1976; Higgs et al. 1975, 1976, 1977; Kayes 1977; Leatherland and Nutti 1981; Markert et al. 1977; Sheridan 1986). Liver lipolysis would decrease somatic HSIs.

In experiment 2, rtGH treated fish showed a significant increase in CFs compared with control fish. Interestingly, Agellon et al. (1988) reported that CFs increased in rainbow trout after the administration of rtGH. Higgs et al. (1978) also reported that chinook salmon pituitary extracts enhanced CFs in coho salmon. This effect may have been due to other hormones or releasing factors present in the extract which could have had a stimulatory role on weight increase. It is not believed that GH administration directly influenced the CFs of the fish in experiment 2, as CFs of fish in all the treatments significantly increased throughout the course of the experiment. All fish initially showed signs of stress after being transferred from the hatchery to the Chesapeake Bay Institute. Therefore, the large

TABLE 10. Weight specific growth rates (WGR) and length specific growth rates (LGR) of coho salmon and rainbow trout reared at different temperatures and administered different GH treatments.[a]

Species and treatment	Rearing temperature (°C)	Initial x̄ weight (g)	Initial x̄ length (cm)	WGR	LGR	Source
Coho salmon	10					Higgs et al. (1975)[b]
Control		11.37	10.30	0.574	0.171	
bGH (10 μg/g)		10.61	10.07	1.511	0.550	
bGH (100 μg/g)		9.85	9.92	1.591	0.554	
Coho salmon	10					Higgs et al. (1976)[b]
Control		8.40	8.99	0.504	0.155	
Control (inj.)		7.43	8.74	0.467	0.144	
bGH (5 μg/g)		7.20	8.61	2.320	0.782	
Coho salmon	10–10.4					Higgs et al. (1977)[b]
Control		12.27	10.26	0.708	0.225	
Control (inj.)		12.79	10.36	0.650	0.198	
bGH (10 μg/g)		12.65	10.23	1.850	0.674	
Coho salmon	10					Markert et al. (1977)[b]
Control (hp–lr)		22.74	12.78	0.654	0.229	
Control (lp–lr)		24.78	13.08	0.750	0.250	
Control (hp–hr)		19.51	12.15	1.040	0.336	
Control (lp–hr)		22.49	12.73	0.906	0.297	
bGH(10 μg/g) (hp–lr)		24.43	13.17	0.857	0.349	
bGH(10 μg/g) (lp–lr)		25.35	13.22	1.000	0.404	
bGH(10 μg/g) (hp–hr)		22.78	12.79	1.400	0.522	
bGH(10 μg/g) (lp–hr)		22.13	12.65	1.530	0.549	
Coho salmon	10					Higgs et al. (1978)[b]
Control		14.30	NA	0.877	NA	
Control (inj.)		15.00		0.666		
bGH (0.1 μg/g)		14.20		0.747		
bGH (0.32 μg/g)		14.70		0.915		
bGH (1.0 μg/g)		15.10		1.010		
bGH (3.2 μg/g)		15.10		1.100		
bGH (10 μg/g)		13.30		1.410		
Coho salmon	10–11					Gill et al. (1985)[c]
Control		4.00	7.40	1.580	NA	
Control (inj.)		"	"	1.480		
bGH (1 μg/g)		"	"	2.040		
bGH (5 μg/g)		"	"	2.260		
rbGH (1 μg/g)		"	"	2.200		
rbGH (5 μg/g)		"	"	2.380		
rcGH (1 μg/g)		"	"	2.000		
rcGH (5 μg/g)		"	"	2.360		
Rainbow trout	13–15					Kawauchi et al. (1986)[d]
(Exp. 1)						
Control (inj.)		9.70	9.16	0.573	0.098	
csGH (0.01 μg/g)		10.26	9.06	1.093	0.376	
csGH (0.1 μg/g)		10.86	9.36	1.711	0.549	
(Exp. 2)						
Control (inj.)		16.54	10.27	0.509	0.067	
csGH (0.1 μg/g)		16.54	10.07	1.052	0.251	
Rainbow trout	15					Agellon et al. (1988)[c]
Control		77.04	NA	1.001	NA	
Control (inj.)		"		1.025		
rtGH (0.2 μg/g)		"		1.746		
rtGH (1.0 μg/g)		"		1.779		
rtGH (2.0 μg/g)		"		1.432		
Coho salmon	7.40					Down et al. (1988)[d]
Control		129.30	NA	0.24	0.11	
Control (inj.)		"		0.26	0.10	
22K rbGH (0.5 μg/g)		"		0.59	0.25	
22K rbGH (5.0 μg/g)		"		0.69	0.25	

TABLE TABLE 10. (*continued*)

Species and treatment	Rearing temperature (°C)	Initial x̄ weight (g)	Initial x̄ length (cm)	WGR	LGR	Source
Coho salmon	10.80					Down et al. (1989)[d]
Control		2.60	6.30	2.16	0.67	
Control (inj.)		"	"	2.11	0.65	
22K rbGH (0.2 μg/g)		"	"	2.17	0.70	
22K rbGH (2.0 μg/g)		"	"	2.30	0.76	
21K rbGH (0.2 μg/g)		"	"	2.34	0.76	
21K rbGH (2.0 μg/g)		"	"	2.60	0.83	
Rainbow trout	16.75					Present study
Control (hr)		11.94	9.36	2.701	0.917	
Control (lr)		11.51	9.33	2.511	0.814	
Control (inj.) (hr)		11.81	9.38	2.713	0.905	
Control (inj.) (lr)		10.98	9.22	2.399	0.779	
bGH (1.0 μg/g) (hr)		11.90	9.13	2.932	1.036	
bGH (1.0 μg/g) (lr)		12.34	9.38	2.347	0.848	
rtGH (1.0 μg/g) (hr)		12.05	9.16	2.653	0.934	
rtGH (1.0 μg/g) (lr)		11.54	9.12	2.339	0.808	
rtGH (0.1 μg/g) (hr)		11.82	9.14	2.659	0.921	
rtGH (0.1 μg/g) (lr)		12.06	9.30	2.229	0.776	

[a] The treatment symbols used throughout are: control = uninjected control; control (inj.) = injected control (see paper for details); bGH = naturally purified bGH; rbGH = recombinant bGH; rcGG = recombinant chicken GH; csGH = chum salmon GH; hp = high protein; lp = low protein; hr = high ration; lr = low ration.

[b] Initial weights and lengths calculated from the regression equations of $\log_e$ transformed growth data.

[c] Initial weights and lengths obtained from graphical representations (approximate values given).

[d] Initial weights and lengths given in text.

increases in CF observed likely reflects increasing adaptation of these fish to their aquatic environment, accompanied by increasing appetites.

Physiology: Nucleic Acid Levels

Results from the analysis of nucleic acids indicate that rtGH and bGH stimulate metabolic activity in rainbow trout. RNA levels in bGH treated fish were significantly elevated compared with saline control fish, and were also higher in rtGH treated fish. RNA levels, calculated on a per wet or dry weight basis, have been reported to be higher in fish with faster growth rates, while DNA levels remain fairly constant (Goolish et al. 1984; Bulow 1987). Therefore, higher RNA/DNA ratios are generally indicative of faster growth rates. However Wilder and Stanley (1983) have reported that RNA level alone may be a better predictor of growth in salmonid fishes than RNA/DNA ratio when fish are reared in a common thermal environment. This was subsequently confirmed by Ferguson and Danzmann (1990) who suggested that an ANCOVA using DNA as a co-variate is the best method for assessing metabolic differences between treatments. When differences in RNA levels between treatments were compared using an ANCOVA with DNA as a co-variate, significant differences between treatments were observed ($P = 0.05$). RNA levels in bGH treated fish (adjusted mean = 600.50 μg/g) were significantly higher than in saline control fish (adjusted mean = 458.5 μg/g) ($P = 0.018$). No significant differences were evident between rtGH treated (adjusted mean = 561.3 μg/g) and saline control ($P = 0.101$), or bGH treated ($P = 0.521$) fish.

The results from this study clearly indicate that RNA levels and RNA/DNA ratios are accurate predictors of rainbow trout growth rates. Furthermore, weight or length specific growth rates were more strongly correlated with either RNA or RNA/DNA, than were absolute sizes of the fish (Table 9). These data support Bulow's (1987) contention that RNA/DNA ratios more accurately reflect recent growth, and may not necessarily be indicative of the absolute size of the fish.

GH treated fish in experiment 2 exhibited a greater somatic growth rate than fish used in experiment 1, even though fish in experiment 1 were administered higher GH dosages. On average, the dosages of bGH and rtGH administered to each fish at the beginning and end of experiment 2 ranged from 0.36–0.18 μg/g for bGH treated fish and 0.23–0.12 μg/g for rtGH treated fish. The discrepancy in response to GH administration between fish in the two experiments is not understood but may result from differences in responsivity of large and small fish to GH stimulation. D. Rollo, (McMaster University, Hamilton, Ont., pers. comm.) has reported that larger rainbow trout appear to be more responsive to rtGH stimulation. Since growth rates are lower in larger fish, GH administration may increase metabolic rates and subsequently accelerate growth rates. The initial sizes of fish used in experiment 2 were approximately 4 × larger than those used in experiment 1, and therefore these fish may have been more responsive to GH stimulation.

Dosage

It is possible that higher doses of bGH and rtGH would have been more stimulatory in promoting growth. Higgs et al. (1978) reported that growth rates of coho salmon were proportional to bGH dosages up to 10 μg/g body weight (the highest dosage used) when fish were reared at 10°C. Agellon et al. (1988), however, reported that dosages of rtGH higher than 2.0 /μg/g were detrimental to growth. Therefore, we decided not to use dosages exceeding 1.0 μg/g. The current results indicate that GH dosages up to 1.0 μg/g are not very effective in stimulating rainbow trout weight growth when reared at 16.75°C. However, length enhancement was noted with bGH when accompanied by a high feeding ration. It would appear bGH stimulates length increase preferentially to weight increase and may only stimulate a weight increase if surplus energy is available. At lower temperatures, more energy will be available to stimulate an increase in weight as well as length, because routine metabolic costs will be lower. Therefore, the dosages of rtGH and bGH used in this study may only be effective in stimulating growth at lower temperatures.

Acknowledgements

We wish to thank the late Mr. Ken Corl, former Director of the Pennsylvania Fish and Game Commission and Mr. Richard Pugh of the Reynoldsdale Fish Hatchery for their support and generous assistance. We also wish to thank Mr. William Kennedy and Mr. Walter Bair of the Benner Springs Fish Hatchery for providing us with fish from the Wytheville strain of rainbow trout, which were used in earlier phases of this research. Without the fish and gametes obtained from these Pennsylvania State Fish Hatcheries this research program would not have been possible. We also thank the National Hormone and Pituitary Program, Baltimore, Maryland, for their gift of bovine growth hormone.

References

AGELLON, L. B., AND T. T. CHEN. 1986. Rainbow trout growth hormone: molecular cloning and expression in *Escherichia coli*. DNA 5: 463–471.

AGELLON, L. B., C. J. EMERY, J. M. JONES, S. L. DAVIES, A. D. DINGLE, AND T. T. CHEN. 1988. Promotion of rapid growth of rainbow trout (*Salmo gairdneri*) by a recombinant fish growth hormone. Can. J. Fish. Aquat Sci. 45: 146–151.

BARDACH, J. E., J. H. RYTHER, AND W. O. MCLARNEY. 1972. Aquaculture: the farming and husbandry of freshwater and marine organisms. Wiley-Interscience, New York, NY. p. 416–417.

BRETT, J. R., J. E. SHELBOURN, AND C. T. SHOOP. 1969. Growth rate and body composition of fingerling sockeye salmon, *Oncorhynchus nerka*, in relation to temperature and ration size. J. Fish. Res. Board Can. 26: 2363–2394.

BULOW, F. J. 1987. RNA–DNA ratios as indicators of growth in fish: a review, p. 45–64. *In* R. C. Summerfelt and G. E. Hall [ed.]. The age and growth of fish. Iowa State University Press, Ames, IA.

CLARKE, W. C. 1976. Effect of prolactin and growth hormone on growth, lipid content and seawater adaptation in juvenile sockeye salmon. Reg. Conf. Comp. Endocrinol. Oregon State University, Corvalis, OR. Abstr. No. 38.

CLARKE, W. C., S. W. FARMER, AND K. M. HARTWELL. 1977. Effect of teleost pituitary growth hormone on growth of *Tilapia mossambica* and on growth and seawater adaptation of sockeye salmon (*Oncorhynchus nerka*). Gen. Comp. Endocrinol. 33: 174–178.

DONALDSON, E. M., U. H. M. FAGERLUND, D. A. HIGGS, AND J. R. MCBRIDE. 1979. Hormonal enhancement of growth in fish. p. 455–597. *In* W. S. Hoar, D. J. Randall, and J. R. Brett [ed.] Fish physiology, Vol. VIII. Academic Press, New York, NY.

DOWN, N. E., E. M. DONALDSON, H. M. DYE, T. C. BOONE, K. E. LANGLEY, AND L. M. SOUZA. 1989. A potent analog of recombinant bovine somatotropin accelerates growth in juvenile coho salmon (*Oncorhynchus kisutch*). Can. J. Fish. Aquat. Sci. 46: 178–183.

DOWN, N. E., E. M. DONALDSON, H. M. DYE, K. LANGLEY, AND L. M. SOUZA. 1988. Recombinant bovine somatotropin more than doubles the growth rate of coho salmon (*Oncorhynchus kisutch*) acclimated to seawater and ambient winter conditions. Aquaculture 68: 141–155.

FERGUSON, M. M., AND R. G. DANZMANN. 1990. RNA/DNA ratios in white muscle as predictors of growth in rainbow trout held at different temperatures. Can. J. Zool. (In press)

FERGUSON, M. M., AND L. R. DRAHUSHCHAK. 1990. Effects of tissue collection and storage methods on nucleic acid determinations in white muscle of fishes. Trans. Am. Fish. Soc. (In press)

GILL, J. A., J. P. SUMPTER, E. M. DONALDSON, H. M. DYE, L. SOUZA, T. BERG, J. WYPYCH AND K. LANGLEY 1985. Recombinant chicken and bovine growth hormones accelerate growth in aquacultured juvenile pacific salmon *Oncorhynchus kisutch*. Bio/Technology 3: 643–646.

GOOLISH, E. M., M. G. BARRON, AND I. R. ADELMAN. 1984. Thermoacclimatory response of nucleic acid and protein content of carp muscle tissue: influence of growth rate and relationship to glycine uptake by scales. Can. J. Zool. 62: 2164–2170.

HIGGS, D. A., E. M. DONALDSON, H. M. DYE, AND J. R. MCBRIDE. 1975. A preliminary investigation of the effect of bovine growth hormone on growth and muscle composition of coho salmon (*Oncorhynchus kisutch*). Gen. Comp. Endocrinol. 27: 240–253.

HIGGS, D. A., E. M. DONALDSON, J. R. MCBRIDE, AND H. M. DYE. 1978. Evaluation of the potential for using chinook salmon (*Oncorhynchus tshawytscha*) pituitary extract versus bovine growth hormone to enhance the growth of coho salmon (*Oncorhynchus kisutch*). Can. J. Zool. 56: 1226–1231.

1976. Influence of bovine growth hormone and *L*-thyroxine on growth, muscle composition, and histological structure of the gonads, thryroid, pancreas, and pituitary of coho salmon (*Oncorhynchus kisutch*). J. Fish. Res. Board Can. 33: 1585–1603.

HIGGS, D. A, U. H. M. FAGERLUND, J. R. MCBRIDE, H. M. DYE, AND E. M. DONALDSON. 1977. Influence of combinations of bovine growth hormone, 17–methyltestosterone, and *L*-thyroxine on growth of yearling coho salmon (*Oncorhynchus kisutch*). Can. J. Zool. 55: 1048–1056.

IWAMA, G. K., AND A. F. TAUTZ. 1981. A simple growth model for salmonids in hatcheries. Can. J. Fish. Aquat. Sci. 38: 649–656.

KARSTEN, U., AND A. WOLLENBERGER. 1972. Determination of DNA and RNA in homogenized cells and tissues by surface fluorometry. Anal. Biochem. 46: 135–148.

1977. Improvements in the ethidium bromide method for direct fluorometric estimation of DNA and RNA in cell and tissue homogenates. Anal. Biochem. 77: 464–470.

KAWAUCHI, H., S. MORIYAMA, A. YASUDA, K. YAMAGUCHI, K. SHIRAHATA, J. KUBOTA, AND T. HIRANO. 1986. Isolation and characterization of chum salmon growth hormone. Archiv. Biochem. Biophys. 244: 542–552.

KAYES, T. 1977. Effects of temperature on hypophyseal (growth hormone) regulation of length, weight, and allometric growth and total lipid and water concentrations in black bullhead (*Ictalurus melas*). Gen. Comp. Endocrinol. 33: 382–393.

KINCAID, H. L. 1981. Trout strain registry. Publication of the National Fisheries Center, Kearneysville, WV. 25430. USA.

LEATHERLAND, J. F., AND R. N. NUTTI. 1981. Effects of bovine growth hormone on plasma FFA concentrations and liver, muscle and carcass lipid content in rainbow trout, *Salmo gairdneri* Richardson. J. Fish. Biol. 20: 487–497.

LOWRY, O. H., N. J. ROSEBROUGH, A. L. FARR, AND R. J. RANDALL. 1951. Protein measurement with the folin phenol reagent. J. Biol. Chem. 193: 265–275.

MARKERT, J. R., D. A. HIGGS, H. M. DYE, AND D. W. MACQUARRIE. 1977. Influence of bovine growth hormone on growth rate, appetite, and food conversion of yearling coho salmon (*Oncorhynchus kisutch*) fed two diets of different composition. Can. J. Zool. 55: 74–83.

SEKINE, S., T. MIZUKAMI, T. NISHI, Y. KUWANA, A. SAITO, M. SATA, S. ITOH, AND H. KAWAUCHI. 1985. Cloning and expression of cDNA for salmon growth hormone in *Escherichia coli*. Proc. Natl. Acad. Sci. USA 82: 4306–4310.

SHERIDAN, M. A. 1986. Effects of thyroxin, cortisol, growth hormone and prolactin on lipid metabolism of coho salmon, *Oncorhynchus kisutch*, during smoltification. Gen. Comp. Endocrinol. 64: 220–238.

SINGH, H., R. W. GRIFFITH, A. TAKAHASHI, H. KAWAUCHI, P. THOMAS AND J. STEGMAN. 1988. Regulation of gonadal steroidogenesis in *Fundulus heteroclitus* by recombinant salmon growth hormone and purified salmon prolactin. Gen. Comp. Endocrinol. 72: 144–153.

SOKAL, R. R., AND F. J. ROHLF. 1981. Biometry, 2nd ed. W. H. Freeman and Co., San Francisco, CA.

VAN DER KRAAK, G., H. M. DYE, AND E. M. DONALDSON. 1984. Effects of LH–RH and das GLY^{10} [*D*-Ala^{6}] LH-RH ethylamide on plasma sex steroid profiles in adult female coho salmon (*Oncorhynchus kisutch*).Gen. Comp. Endocrinol. 55: 36–45.

VAN DER KRAAK, G., P. ROSENBLUM AND R. E. PETER. 1990. Growth hormone dependent potentiation of gonadotropin stimulated steroid production by ovarian follicles of the goldfish. Gen. Comp. Endocrinol. (In Press)

WEATHERLEY, A. H. 1972. Growth and ecology of fish populations. Academic Press, Inc., London, UK. 294 p.

WEATHERLEY, A. H., AND H. S. GILL. 1983. Relative growth of tissues at different somatic growth rates in rainbow trout *Salmo gairdneri* Richardson. J. Fish Biol. 22: 43–60.

WILDER, I. B., AND J. G. STANLEY. 1983. RNA–DNA ratio as an index to growth in salmonid fishes in the laboratory and in streams contaminated by carbaryl. J. Fish Biol. 22: 165–172.

Pumping Rates, Water Pressures, and Oxygen Use in Eight Species of Marine Bivalve Molluscs from British Columbia

F. R. Bernard[1] and D. J. Noakes

Department of Fisheries and Oceans, Biological Sciences Branch, Pacific Biological Station, Nanaimo, British Columbia V9R 5K6 Canada

Bernard, F. R., and D. J. Noakes. 1990. Pumping rates, water pressures, and oxygen use in eight species of marine bivalve molluscs from British Columbia. Can. J. Fish. Aquat. Sci. 47: 1302–1306.

Pumping characteristics and oxygen utilization for *Solemya reidi, Yoldia thraciaeformis, Chlamys hastata, Mytilus edulis, Crassostrea gigas, Clinocardium nuttallii, Saxidomus giganteus*, and *Mya truncata* were studied. Pressures were recorded using a Yale A79 spinal tap needle inserted in the pallial cavity or siphonal aperture. Pumping volumes were determined through particulate analysis using a Model B Coulter counter and oxygen consumption by standard Winkler titration modified for small samples. The species chosen were selected to represent progressive increases in gill complexity and siphon length. The minimum pressure differential across the gill (20 Pa) was observed for *Y. thraciaeformis* while the maximum pressure gradient (600 Pa) was recorded for *M. truncata*. Pumping rates varied from $1.41\ \mathrm{L \cdot h^{-1} \cdot g^{-1}}$ (*Y. thraciaeformis*) to $4.71\ \mathrm{L \cdot h^{-1} \cdot g^{-1}}$ (*C. hastata*) and species with siphons tended to pump at lower rates. The deeply burrowing *M. truncata* consumed 3.5 times as much oxygen ($0.63\ \mathrm{mL\ O_2 \cdot h^{-1} \cdot g^{-1}}$) as *S. reidi* ($0.18\ \mathrm{mL\ O_2 \cdot h^{-1} \cdot g^{-1}}$) which inhabits anoxic environments. For all species, the metabolic cost of pumping was less than 1% of the total oxygen uptake.

Les caractéristiques du pompage et l'utilisation de l'oxygène ont été étudiées chez *Solemya reidi, Yoldia thraciaeformis, Chlamys hastata, Mytilus edulis, Crassostrea gigas, Clinocardium nuttallii, Saxidomus giganteus* et *Mya truncata*. Les pressions ont été enregistrées au moyen d'une aiguille à ponction lombaire Yale A79 introduite dans la cavité palléale ou l'ouverture du siphon. Les volumes de pompage ont été mesurés par l'analyse des particules au moyen d'un compteur de Coulter modèle B et la consommation d'oxygène par la technique de titration standard de Winkler modifiée pour les petits échantillons. Les espèces choisies ont été sélectionnées afin de représenter une augmentation progressive de la complexité des branchies et de la longueur du siphon. La différence de pression minimale dans les branchies (20 Pa) a été observée chez *Y. thraciaeformis* tandis que le gradient de pression maximale (600 Pa) a été enregistré chez *M. truncata*. La vitesse de pompage variait de $1{,}41\ \mathrm{L \cdot h^{-1} \cdot g^{-1}}$ (*Y. thraciaeformis*) à $4{,}71\ \mathrm{L \cdot h^{-1} \cdot g^{-1}}$ (*C. hastata*) et la vitesse de pompage avait tendance à être plus lente chez les espèces dotées de siphons. L'espèce *M. truncata* à enfouissement profond consommait 3,5 fois plus d'oxygène ($0{,}63\ \mathrm{mL\ O_2 \cdot h^{-1} \cdot g^{-1}}$) que *S. reidi* ($0{,}18\ \mathrm{mL\ O_2 \cdot h^{-1} \cdot g^{-1}}$) qui vit dans un milieu anoxique. Chez toutes les espèces, le bilan métabolique du pompage correspondait à moins de 1 pour cent de la capture totale d'oxygène.

Received August 10, 1989
Accepted February 27, 1990
(JA272)

Reçu le 10 août 1989
Accepté le 27 février 1990

The majority of bivalve molluscs pump water through the pallial cavity by means of ciliated gills. Many bivalves have modified the mucociliary cleansing mechanism of the gill to collect suspended nutritious particles and convey them to the mouth. These animals pump a volume of water much in excess of that required for respiration. The simplest type of gill, present in the palaeotaxodont bivalves, is not adapted to particle collection. These detrivours use oral appendages to collect nutritious particles from the sediment. However, in suspension feeders, the gill filaments have become greatly elongated and folded on themselves, effectively increasing the surface area by a factor of four. The effective area of the gill has also been increased in some species by plication of the gill axis. In addition, invasion of the clastic sediment habitat resulted in the progressive fusion of the mantle margins in some species, thereby isolating the pallial cavities from possible entrance of sediments. This has led to the development of siphons of increasing length to accommodate the deep infaunal habitat. These structural changes affect both the volume of water transported and the pumping pressures required to maintain the necessary flow in the system.

Gills transport water by means of special cilia situated on the lateral parts of the filaments. Hypertrophy of filaments, enlargement of gill surface area, and increasing hydrostatic pressures generated by limited openings to the pallial chamber, together with frictional losses because of the siphon walls, significantly increase the pressure gradient across the gill. Mechanical integrity of the gill is maintained by progressive series of adaptations involving mutual fusion of the filaments, the appearance of lateral plates of tissues, and the development of strengthening rods. Eventually, the gill consists of a solid sheet of tissue, pierced by numerous small ostia, rather than a comb-like series of unconnected filaments. Descriptions of the various gill structures encountered in bivalve molluscs can be found, for example, in Jorgensen (1966), Wilbur (1983a,b), and Yonge and Thompson (1976).

The bivalve pumping configuration comprises inhalant and exhalant areas of relatively small size, leading to a chamber separated by a large area of gill bearing numerous ciliated slits or pores between gill filaments which act as a series of pumps.

---

[1] Deceased.

TABLE 1. List of species examined along with their feeding and gill type.

Species	Feeding type	Gill type
Solemya reidi (Bernard 1980)	Autotrophic	Protobranch
Yoldia thraciaeformis (Storer 1838)	Detrivour	Protobranch
Chlamys hastata (Sowerby 1843)	Suspension	Isofilibranch
Mytilus edulis (Linne 1758)	Suspension	Filibranch
Crassostrea gigas (Thunberg 1793)	Suspension	Filibranch
Clinocardium nuttallii (Conrad 1837)	Suspension	Filibranch
Saxidomus giganteus (Deshayes 1839)	Suspension	Filibranch
Mya truncata (Linne 1758)	Suspension	Filibranch

The gill can be considered to consist of a large number of pumps in parallel, so that pressure is equivalent to a single pump, but the total flow is proportional to the total number of pumps (Fox 1974). This structure allows flow to increase with area while pressure remains relatively constant. Maximum pressure occurs just posterior to the gill openings, but it is not practical to obtain readings in this area. The general pattern of bivalve pumping is the drawing in of the inhalant stream at low velocity, its passage between the gill filaments, and its ejection at higher velocity through the exhalant aperture or siphon. Published differences between inhalant and exhalant pressure have varied from less than 100 Pa (100 Pa $\approx$ 1.0197 mm H_2O) for bivalves with short siphons (Foster–Smith 1976a), to as much as 230 Pa measured in the exhalant siphon (Jones and Allen 1986).

In this paper, we measure the pressure and volume of water pumped by eight species of bivalves, representative of progressively more complex gill structures and the presence of siphons of increasing length. These observations are used together with measured physical characteristics to estimate friction losses in the inhalant and exhalant siphons. The costs of complex gill structures and longer siphons are discussed in terms of increased pressure in the system and oxygen utilization.

Materials

Eight species of bivalves from the Oregonian Province of the northeast Pacific Ocean (Bernard 1983a) were collected in the shallow water and intertidal zones of Vancouver Island, British Columbia. Species were selected to represent a variety of gill types, siphonal development, and methods of feeding (Table 1).

Solemya reidi maintains an anterior to posterior ventilatory current through siphonless openings in the mantle margins. The protobranch gills are proportionately large and thickened. This organism has no alimentary canal and nutrition is by chemautotrophic commensal bacteria housed in the gill tissue. *Yoldia thraciaeformis* is also a protobranch, but feeds on nutritious particles collected by elongated oral appendages from the bottom sediment. The gill is small and the ventilatory current is through narrow siphons.

Chlamys hastata has an open pallial chamber, controlled by a hypertrophied mantle fold, forming a pallial curtain. Temporary and ever changing openings are left in the pallial curtain to accommodate the ventilatory currents. The gill is filibranch and much larger than in the protobranch configuration. The few temporary cross-connections between the filaments and the plicated gill axis result in a large very porous gill.

Mytilus edulis lacks siphons, but the inhalant and exhalant openings are delimited. The filibranch gill is similar to that of *Chlamys*, but is not plicated. *Crassostrea gigas* has no siphons and the mantle is widely open. Its gills have complex cross-attachments and the interfilamental openings are reduced to oval ostia. The free ends of the filaments are united to the mantle, effectively separating the inhalant and exhalant chambers.

The other three species were selected for increasing length of siphons. *Clinocardium nuttallii* has a widely open mantle with two short siphons, and its gills are plicated and fused posteriorly to a siphonal septum. *Saxidomus giganteus* has an extensively fused mantle, two siphons of medium length, and plicated gills. *Mya truncata* has a fully fused mantle, plicated gills with complex fusion structures, and long siphons.

Methods

Bivalves were collected in summer, while animals were in an active metabolic phase, and performance was estimated within 3 d of collection. Subjects were kept in a flow-through aquarium. Epifaunal species were placed in a petri dish. Burrowers were buried in washed coarse sand in a small battery jar or beaker. Observations were carried out in a large enclosed flow-through system held at near ambient temperature and salinity, as described in Bernard (1983b).

Pressure was recorded by the insertion of a Yale A79 spinal tap needle in the pallial cavity or siphonal aperture. The tip of the needle was modified by the formation of a side-opening in order to reduce any artifacts due to flow (Burton 1965). The spinal tap needle was connected by 2 mm polyethylene tubing to a Statham P20BB physiological pressure transducer. The pressure was monitored by a Beckman Type R dynograph fitted with a 9890 Strain Gauge Coupler.

Pumping volume was estimated by the interception and collection of the exhalant stream in a constant level tank. Because direct volume estimation is inaccurate due to mechanical constraints, the pumping rates of the filter-feeding bivalves was estimated from the difference between particle populations in the inhalant and exhalant stream, using a Model B Coulter Electronic Particle Counter, following the method of Sheldon and Parsons (1976). Oxygen consumption was monitored using a portion of the sample removed for particle counts, using the standard Winkler titration modified for small samples (Strickland and Parsons 1968).

After the determinations were made, bivalves were relaxed in a 2% chloral hydrate solution in sea water, the gills were dissected and their surface area measured. Interfilamental or ostial openings were measured under a microscope and the extent of plication of the gill axis estimated. These data were used to calculate the gill porosity. Total area of the pallial and siphonal openings was estimated photographically with a square millimetre grid. Tissues were then dried to constant weight at 10°C to calculate weight-specific data.

Results

Shell lengths differed by nearly a factor of 2 while dry weights and siphon lengths varied by an order of magnitude (Table 2). The ratio of the inhalant to exhalant aperture areas ranged from 1.6 to 1.9 for species with measurable and distinct siphons (*Y. thraciaeformis*, *C. nuttallii*, *S. giganteus*, and *M. truncata*) and from 1.9 to 2.8 for species with distinct but siphonless entry and exit openings (*S. reidi*, *C. hastata*, *M. edulis*, and *C. gigas*). The measured gill area was three to four times the estimated porosity for all species considered with the exception of *M. truncata* where the ratio was 1.6:1.

The lowest hydrostatic pressure differential, −13.7–12.7 Pa, was recorded for *Y. thraciaeformis* while maximum values, −123.6 − 483.5 Pa, were observed for *M. truncata* (Table 3). Although pressure differentials increased with siphon length, gill complexity also appeared to have a significant influence on observed pressures in the system. For instance, the pressure differential for *C. gigas* which has no siphon but has a complex gill structure was third highest, −16.7–321.7 Pa, among the species considered in this study.

The lowest pumping rates were observed for the two species with protobranch gills, *S. reidi* and *Y. thraciaeformis*, and the highest in *C. hastata* and *C. gigas* (Table 4). The observed pumping rates and physical characteristics of the inhalant and exhalant siphons were used to estimate the velocity of the exhalant stream and head loss in the siphons. Exit velocity was calculated as the observed pumping rate over the exhalant cross-sectional area. The velocity of the exhalant stream is important because the loss in kinetic energy as this stream enters the surrounding water is proportional to this velocity squared. In some cases, these losses can be roughly of the same order of magnitude as those due to friction (Table 4). These combined losses mean additional work is required to pump water through the system. This is illustrated by the weight specific oxygen consumptions and the metabolic costs of pumping 1 L of water (Table 5) which generally increased with gill complexity and siphon length. Reynolds numbers for the inhalant and exhalant streams ranged from less than 200 to about 1000 indicating the flows were laminar.

Frictional losses calculated using the Hagen–Poiseuille equation (Jorgensen and Riisgard 1988) were comparable to measured pressure differences between the gill and exits reported in Table 3. For example, the mean observed pressure differences between the gill and the exits for *M. truncata's* inhalant and exhalant siphons were 53.0 (123.6–70.6) and 147.1 Pa (483.5–336.4), respectively (Table 3). The estimated head losses using the Hagen–Poiseuille equation are 74.5 and 182.4 Pa, respectively (Table 4). These losses were the largest recorded with frictional losses for the other species typically being less than 50 Pa.

Discussion

Jorgensen (1966) and Winter (1969) suggest that bivalve molluscs with siphons display lower pumping rates than bivalves without siphons. Taking into account differences in feeding behaviour, our data tend to support this observation (Table 4). *S. reidi* and *Y. thraciaeformis* are not suspension feeders, have relatively small gills, and pumped at rates considerably lower than the other species considered in this study. Within this group, the *Y. thraciaeformis* which has a siphon pumped at a lower rate than *S. reidi* which has no siphon. Among suspension feeders, two species without siphons, *C. hastata* and *C. gigas*, produced the highest pumping rates. *M. edulis*, which also has no siphon, pumped at a slightly lower rate reflecting its smaller gill and inhalant opening. Pumping rates generally decreased with siphon length for the remaining three suspension feeders. The exception was *M. truncata* whose pumping rate increased slightly due in part to its extremely large porous gill.

Taking into account differences in the physical characteristics of the specimens, the pumping rates and exit velocities observed for *M. edulis* in this study were similar to those reported by Jorgensen et al. (1986a, 1988). Using an exhalant opening of 14 mm^2, Jorgensen et al. (1988) estimated a pumping rate of about 35 $mL\cdot min^{-1}$ or 2.1 $L\cdot h^{-1}$. Assuming a dry tissue weight of about 1 g, Jorgensen's et al. (1988) estimated pumping rate is comparable with our estimate of 2.49 $L\cdot h^{-1}\cdot g^{-1}$. Similarly, Jorgensen et al. (1986a) employed an exhalant velocity of 62.5 $mm\cdot s^{-1}$, a flow rate of 1 $mL\cdot s^{-1}$ (3.6 $L\cdot h^{-1}$), and an exhalant cross-sectional area of 16 mm^2 in determining system characteristics of the mussel pump. Adjusting for the differences in flow rate (2.49 $L\cdot h^{-1}\cdot g^{-1}$ to 3.6 $L\cdot h^{-1}\cdot g^{-1}$) and cross-sectional area (14 mm^2 to 16 mm^2), our estimate of exhalant velocity increases from 49.9 $mm\cdot s^{-1}$ to a comparable 63.1 $mm\cdot s^{-1}$.

Weight specific oxygen consumption values observed for *M. edulis* in this study are also similar to estimates obtained by other researchers. Jorgensen et al. (1986b) and Widdows et al. (1979), for instance, found the weight specific oxygen consumption for *M. edulis* to be in the order of 0.45 mL $0_2\cdot h^{-1}\cdot g^{-1}$ (i.e. 7.5 $\mu L\cdot g^{-1}\cdot min^{-1}$) and 0.42 mL $0_2\cdot h^{-1}\cdot g^{-1}$, respectively. These values compare with our estimate of 0.47 mL $0_2\cdot h^{-1}\cdot g^{-1}$.

Comparisons are also possible between our observations for *M. truncata* and those presented by Jorgensen and Riisgard (1988) for *M. arenaria*. These authors reported mean pumping rates for *M. arenaria* of 3 $L\cdot h^{-1}\cdot g^{-1}$ which was about 30% higher than our observed rate of 2.27 $L\cdot h^{-1}\cdot g^{-1}$ for *M. truncata*. Estimated frictional head losses in *M. arenaria*'s inhalant and exhalant siphons were 20.6 (0.21 mm H_2O) and 37.3 (0.38 mm H_2O) Pa, respectively, for the assumed pumping rate of 1 $mL\cdot s^{-1}$ and the cross-sectional areas presented in their study (Jorgensen and Riisgard 1988). Adjusting for differences in flow rate, siphon length, and cross-sectional areas, the losses reported for *M. arenaria*'s inhalant and exhalant siphons would scale to 72.6 and 171.6 Pa, respectively. These scaled esti-

TABLE 2. Shell lengths, tissue dry weights, siphon lengths, and measured and estimated pallial areas of the eight bivalve species considered in the study. The estimated porosity was calculated from the surface area, amount of plication, and size of openings.

Species	Length (mm)	Dry weight (g)	Siphon (mm)	Inhalant (mm^2)	Exhalant (mm^2)	Gill area (mm^2)	Porosity (mm^2)
S. reidi	35	1.73	0	61	22	561	130
Y. thraciaeformis	31	1.94	29	23	12	306	75
C. hastata	48	2.20	0	63	25	2576	825
M. edulis	41	1.01	0	27	14	1928	608
C. gigas	46	3.02	0	142	51	4099	1358
C. nuttallii	56	5.79	12	57	32	5277	1422
S. giganteus	47	6.72	43	66	40	5992	1530
M. truncata	40	8.81	145	58	37	6760	4259

TABLE 3. Measured hydrostatic pressure (Pa above ambient) reported as mean and standard deviation. The exit measurement was obtained from just inside the aperture or siphon with the probe positioned for maximum reading. Gill measurement location was inside the pallial chamber as close as possible to gill. N is the number of observations. 100 Pa ≈ 1.0197 mm H_2O

		Inhalant			Exhalant		
Species	N	Exit	Gill	Differential	Exit	Gill	Differential
S. reidi	6	-10.8 ± 5.9	-5.9 ± 2.9	4.9	99.0 ± 40.2	104.0 ± 36.3	4.9
Y. thraciaeformis	14	-13.7 ± 2.0	-8.8 ± 3.9	4.9	8.8 ± 4.9	12.7 ± 5.9	3.9
C. hastata	27	-25.5 ± 8.8	-20.6 ± 6.9	4.9	99.0 ± 37.3	104.0 ± 28.4	4.9
M. edulis	33	-43.1 ± 10.8	-47.1 ± 8.8	3.9	134.4 ± 40.2	137.3 ± 42.2	2.9
C. gigas	25	-12.7 ± 6.9	-16.7 ± 4.9	3.9	295.2 ± 79.4	321.7 ± 64.7	26.5
C. nuttallii	21	-52.0 ± 30.4	-64.7 ± 22.6	12.7	216.7 ± 61.8	265.8 ± 52.0	49.0
S. giganteus	25	-59.8 ± 46.1	-90.2 ± 37.3	30.4	272.6 ± 56.9	334.4 ± 36.3	61.8
M. truncata	12	-70.6 ± 38.2	-123.6 ± 24.5	53.0	336.4 ± 59.8	483.5 ± 55.9	147.1

TABLE 4. Observed pumping rates determined by comparing particulate counts in the inhalant and exhalant streams. Exhalant velocities were calculated using the observed pumping rate and cross-sectional area of the exhalant siphon. Frictional head losses were estimated using the Hagen–Poiseuille equation.

Species	Calculated exhalant velocity $mm \cdot s^{-1}$	Exhalant Kinetic Head Loss (Pa)	Frictional Loss Inhalant	Frictional Loss Exhalant	Observed volume pumped $L \cdot h^{-1} \cdot g^{-1}$
S. reidi	36.2	–	–	–	1.66
Y. thraciaeformis	63.3	19.6	12.7	47.1	1.41
C. hastata	115.1	–	–	–	4.71
M. edulis	49.9	–	–	–	2.49
C. gigas	59.5	–	–	–	3.62
C. nuttallii	126.2	79.4	4.9	14.7	2.51
S. giganteus	96.6	47.1	11.8	32.4	2.07
M. truncata	150.1	112.8	74.5	182.4	2.27

TABLE 5. O_2 uptake calculated on the basis of dry weight of meat and metabolic cost observed by direct collection of exhalant stream.

Species	O_2 uptake $mL\ O_2 \cdot h^{-1} \cdot g^{-1}$	Metabolic cost $mL\ O_2 \cdot (L\ H_2O)^{-1}$
S. reidi	0.18	0.11
Y. thraciaeformis	0.25	0.18
C. hastata	0.38	0.08
M. edulis	0.47	0.19
C. gigas	0.51	0.14
C. nuttallii	0.55	0.22
S. giganteus	0.41	0.20
M. truncata	0.63	0.28

mates are similar to our observed, 53.0 and 147.1 Pa, and estimated, 74.5 and 182.4 Pa, losses for *M. truncata*.

For species with long siphons, such as *M. truncata*, frictional losses in the siphons may be relatively large (Table 4). To overcome these additional losses, greater energy is required per unit pumped. This is consistent with the findings of Foster–Smith (1976b) who showed that forms with siphons operate at higher hydrostatic pressure. This metabolic cost associated with increased siphon length is reflected in the upward trend in metabolic cost in $mL\ O_2 \cdot (L\ H_2O)^{-1}$ for bivalves with siphons (Table 5).

Volume and pressure measurements may be used to calculate the energy requirement for pumping water (Jorgensen 1955). For example, the observed hydrostatic head for *M. truncata* was about 500 Pa and the weight specific pumping rate was $2.27\ L \cdot h^{-1} \cdot g^{-1}$. These figures translate to 0.11 J utilized per gram of dry weight. Accepting the oxycaloric coefficient of 5 calories (thermochemical) or 20.92 J per mL O_2 (Winberg 1956; Paloheimo and Dickie 1966), then this work or energy would require an uptake of $0.0053\ mL\ O_2 \cdot h^{-1} \cdot g^{-1}$. This corresponds to less than one percent of the observed O_2 uptake of $0.63\ mL\ O_2 \cdot h^{-1} \cdot g^{-1}$ for *M. truncata*. Calculations for the other species yield similar results.

This is a low value, but is comparable with the work of Bidder (1937) on the primitive sponge *Leucandra*. These estimates are, however, based on minimum energy requirements in a frictionless system with perfect energy transfer. Ludwig (1931) calculated a 2% energy transfer efficiency for ciliated cells, so oxygen usage may be high in relation to work done. As indicated by the large pressure differential across the *C. gigas* gill (Table 3), significant losses must be sustained as water passes through the pallial cavities where large angular changes of direction occur. Frictional losses in the inhalant and exhalant siphons may also be considerable in some species (Tables 3 and 4). Therefore, it may be concluded that actual oxygen requirements for pumping water are at least an order of magnitude greater than the theoretical value estimated in a frictionless system.

The oxygen cost of pumping (Collier 1959; Djours 1972) is one possible method for comparing the efficiency of various gill and siphon configurations. Such comparisons, however, should be viewed with caution. McLusky (1973) showed that this was not a fixed ratio and depended on the metabolic state of the organism (Bernard 1983b). Verduin (1969), for instance, estimated that 0.3 mL O_2 was required for each litre pumped at low rates by *Mercenaria mercenaria* while at high pumping rates, the requirement increased five fold to 1.5 mL O_2. In our study, the oxygen cost of pumping ranged from 0.08 to 0.28 $mL\ O_2 \cdot (L\ H_2O)^{-1}$ pumped for *C. hastata* and *M. truncata*, respectively. Assuming all specimens were in a similar metabolic state, then the metabolic costs presented in Table 5 provide a reasonable assessment of the relative performance of the various gill and siphon combinations.

The direct application of mechanistic models to the hydrodynamics of bivalve pumping is difficult, and the performance is dependent on ever-changing relationships between muscle tone of the gill, mucus production, size of pallial openings, and extension of the siphons. All surfaces lack sharp boundaries and are coated with mucus. In the simplest situation, the pumping gill is suspended in a chamber with a straight-through flow. In more advanced bivalves, both the inhalant and exhalant openings are situated posterior, so that the pumped stream must move through large angles. Mucus may reduce friction drag (Toms 1948; Daniel 1981) as demonstrated for fish in turbulent flow (Rosen and Cornford 1971). In this study, estimated friction losses were in general agreement with observed values. Losses in the gill may be significant for some species, but because of its complex structure, it may be difficult to develop a mechanistic model beyond simply mimicking the inputs and outputs to the gill.

Acknowledgements

We thank Drs.Neil Bourne, Glen Jamieson, Dan Quayle, and two anonymous referees for their review of an earlier draft of this manuscript. Their comments were useful and appreciated.

References

Bernard, F. R. 1980. A new *Solemya s. str.* from the northeastern Pacific. (Bivalvia: Cryptodonta). Venus Jpn. J. Malacol. 39: 17–23, fig.

1983a. Catalogue of the living bivalvia of the eastern Pacific Ocean: Bering Strait to Cape Horn. Can. Spec. Publ. Fish. Aquat. Sci. 61: 102 p.

1983b. Physiology and the mariculture of some northeastern Pacific bivalve molluscs. Can. Spec. Publ. Fish. Aquat. Sci. 63: 24 p.

Bidder, G. D. 1937. The perfection of sponges. Proc. Linn. Soc. Lond. 149: 119–146.

Burton, A. C. 1965. Physiology and biophysics of the circulation. Year Book Medical Publishers, Chicago, IL 226 p.

Collier, A. 1959. Some observations on the respiration of the American oyster, *Crassostrea virginica* (Gmelin). Publ. Inst. Mar. Sci. Univ. Tex. 6: 92–108.

Conrad, T. A. 1837. Description of new marine shells from upper California, collected by Thomas Nuttall, Esq. J. Acad. Nat. Sci. Phil. 7: 227–268.

Daniel, T. L. 1981. Fish mucus: in situ measurements of polymer drag reduction. Biol. Bull. 160: 376–382.

Deshayes, G. P. 1839. Nouvelles espèces de mollusques, provenant des côtes de la Californie, du Mexique, de Kamtschatka, et de Nouvelle-Zéland. Rev. Zool. Soc. Cuvierienne. 3: 356–361.

Djours, P. 1972. Comparison of gas transport by convection among animals. Respir. Physiol. 14: 96–104.

Foster-Smith, R. L. 1976a. Pressure generated by the pumping mechanism of some ciliary filter-feeders. J. Exp. Mar. Biol. Ecol. 25: 199–206.

1976b. Some mechanisms for the control of pumping activity in bivalves. Mar. Behav. Physiol. 4: 41–60.

Fox, J. A. 1974. An introduction to engineering fluid mechanics. Macmillan Press Ltd., London, UK 385 p.

Jones, H. D., and J. R. Allen. 1986. Inhalant and exhalant pressures in *Mytilus edulis* L. and *Cerastoderma edule* (L.). J. Exp. Mar. Biol. Ecol. 98: 231–240.

Jorgensen, C. B. 1955. Quantitative aspects of filter feeding in invertebrates. Biol. Rev. 30: 391–454.

1966. Biology of Suspension Feeding. Pergamon Press, Oxford, UK 357 p.

Jorgensen, C. B., P. Famme, H. S. Kristensen, P. S. Larsen, F. Mohlenberg, and H. U. Riisgard. 1986a. The bivalve pump. Mar. Ecol. Prog. Ser. 34: 69–77.

Jorgensen, C. B., P. S. Larsen, F. Mohlenberg, and H. U. Riisgard. 1988. The mussel pump: properties and modelling. Mar. Ecol. Prog. Ser. 45: 205–216.

Jorgensen, C. B., F. Mohlenberg, and O. Sten-Knudsen. 1986b. Nature of relation between ventilation and oxygen consumption in filter feeders. Mar. Ecol. Prog. Ser. 29: 73–88.

Jorgensen, C. B., and H. U. Riisgard. 1988. Gill pump characteristics of the soft clam *Mya arenaria*. Mar. Biol. 99: 107–109.

Linne, C. von. 1758. Systema naturae per regna tria naturae...editio decima, reformata. Stockholm. Vol. I. Regnum animale. 824 p.

Ludwig, W. 1931. Zur Theorie de flimmergewegung (Dynamik, Nutzeffeht, Energeibilanz). Z. Vgl. Physiol. 13: 397–205.

McLusky, D. S. 1973. The effect of temperature on the oxygen consumption and filtration rate of *Chlamys (aequipecten) opercularis* (L.) (Bivalva). Ophelia 10: 141–154.

Paloheimo, J. E., and L. M. Dickie. 1966. Food and growth of fishes. 2. Effects of food and temperature on the relationship between metabolism and body weight. J. Fish. Res. Board Can. 23: 869–908.

Rosen, M. W., and N. E. Cornford. 1971. Fluid friction of fish slimes. Nature 234: 49–51.

Sheldon, R. W., and T. R. Parsons. 1967. A continuous size spectrum for particulate matter in the sea. J. Fish. Res. Board Can. 24: 909–915.

Sowerby, G. B., iii. 1843. Thesaurus conchyliorum, or monographs of genera shells. London, 5 vol. (issued in 44 parts).

Storer, D. H. 1838. Description of a new species of *Nucula* from Massachusetts Bay. J. Nat. Hist. 2: 122–123.

Strickland, J. D. H., and T. R. Parsons. 1968. A practical handbook of seawater analysis. Bull. Fish. Res. Board Can. 167: 311 p.

Thunberg, C. P. 1793. Techning och beskifning pa en ostronsort ifram. Japon. K. Sven. Vetenskapsakad. Handl. 14: 140–142.

Toms, B. A. 1948. Some observations on the flow of linear polymer solutions through straight tubes at large Reynolds numbers. Proc. Int. Rheol. Congr. Holland 2: 135–141.

Verduin, J. 1969. Hard clam pumping rates: energy requirements. Science (Wash., DC) 166: 1309–1310.

Widdows, J., B. L. Bayne, D. R. Livingstone, R. I. E. Newell, and P. Donkin. 1979. Physiological and biochemical responses of bivalve molluscs to exposure to air. Comp. Biochem. Physiol. 62A: 301–308.

Wilbur, K. M. [ed.] 1983a. The Mollusca, Vol. 4, Physiology, Part 1. Academic Press, New York, NY 523 p.

1983b. The Mollusca, Vol. 5, Physiology, Part 2. Academic Press, New York, NY 500 p.

Winberg, G. G. 1956. Rate of metabolism and food requirements of fishes. Nauch. Tr. Beloruss. Govar, Univ. I Lenina. Minsk. 253 p. (Fish. Res. Board Can. Translation #194)

Winter, J. 1969. On the influence of food concentration and other factors on filtration rates and food utilization in the mussels *Arctica islandica* and *Modiolus modiolus*. Mar. Biol. 4: 87–135.

Yonge, C. M., and T. E. Thompson. 1976. Living marine molluscs. William Collins Sons and Co. Ltd., London. 288 p.

Temperature-Dependent Growth of Juvenile Red King Crab (*Paralithodes camtschatica*) and its Effects on Size-at-Age and Subsequent Recruitment in the Eastern Bering Sea

Bradley G. Stevens

National Marine Fisheries Service, Kodiak Island Laboratory, P.O. Box 1638 Kodiak, AK 99615 USA

Stevens, B. G. 1990. Temperature-dependent growth of juvenile red king crab (*Paralithodes camtschatica*), and its effects on size-at-age and subsequent recruitment in the eastern Bering Sea. Can. J. Fish. Aquat Sci. 47:1307–1317.

A temperature-based growth relationship was derived for juvenile red king crab (*Paralithodes camtschatica*) from published data. Growth of annual cohorts of crab was simulated at various locations in Bristol Bay, AK, using long-term water temperature observations, and the resulting mean sizes were compared with those observed by the annual National Marine Fisheries Service eastern Bering Sea crab survey. Results indicate that mean age-at-recruitment is 3–5 yr greater than previously estimated, and has decreased from 9.5 to 7.5 yr over the past decade as a result of increasing sea temperature. Single year-classes require 3–5 yr for complete recruitment to the 'mature' size interval, and recruitment in any year may consist of crabs from four to five year-classes. The high landings and subsequent crash of the Bering Sea red king crab population during the late 1970's probably originated from one or more adjacent strong year-classes in the late 1960's which recruited over a period of several years, followed by a period of recruitment failure and high mortality. Future stock–recruitment studies should account for the effects of multi-year recruitment and year-class overlap.

Un rapport de croissance basé sur la température a été établi pour des juvéniles de crabe royal (*Paralithodes camtschatica*) à partir de données publiées. La croissance de cohortes annuelles de crabes a été simulée à différents endroits dans la baie Bristol, AK, à l'aide d'observations à long terme de la température de l'eau, et les tailles moyennes obtenues ont été comparées à celles enregistrées par le NMFS lors du relevé annuel des crabes dans l'est de la mer de Béring. D'après les résultats, le recrutement moyen selon l'âge est de 3 à 5 ans de plus que l'âge estimé antérieurement, et l'âge est passé de 9,5 ans à 7,5 ans au cours de la dernière décennie à la suite de l'augmentation de la température de l'eau de mer. Il faut de 3 à 5 ans aux classes d'âge unique pour atteindre un recrutement complet au niveau de l'intervalle de la taille mature, et le recrutement au cours d'une année quelconque peut comprendre des crabes des classes d'âge 4 et 5. Les débarquements élevés et l'effrondement subséquent de la population de crabe royal de la mer de Béring à la fin des années 1970 proviennent probablement d'une ou de plusieurs fortes classes d'âge adjacentes à la fin des années 1960 qui ont été recrutées pendant plusieurs années, suivis par une période de non recrutement et de mortalité élevée. Les prochaines études sur le stock et le recrutement devraient tenir compte des effets du recrutement pluriannuel et du chevauchement des classes d'âge.

Received June 19, 1989
Accepted February 27, 1990
(JA199)

Reçu le 19 juin 1989
Accepté le 27 février 1990

The red king crab (RKC), *Paralithodes camtschatica*, comprises one of the most valuable fisheries in the United States. Since 1971, the majority of the landings have come from the Bristol Bay stock, in the eastern Bering Sea (EBS) (ADFG 1988). Peak landings of 84 000 t occurred in 1980, when it was the most valuable single-species fishery in the United States, valued at $168.7 million (United States Department of Commerce 1981). Landings declined precipitously to 1362 t in 1982, and the Bristol Bay fishery was closed in 1983; since 1984, landings have gradually increased to 5 600 t, valued at $49 million in 1987 (ADFG 1988).

The EBS king crab fishery is managed by harvest guidelines, based on annual stock abundance surveys conducted by the National Marine Fisheries Service (NMFS) (Stevens and MacIntosh 1989). In addition, a ricker-type stock–recruitment (S–R) model has been proposed by Reeves and Marasco (1980) who defined recruits as the estimated number of males in the size range 95–109 mm carapace length (CL) and assigned them an age of 5 yr, based on studies by Powell (1965) and Weber (1967). One management goal based on this S–R model is the maximization of recruitment by maintaining the abundance of fertilized females in the range of 24–47 million crabs, a level that has not occurred since 1982.

The application of S–R models (which were developed for fish populations) to a crustacean population has inherent problems due to fundamental differences in the biology of crabs and fish, which were not addressed by Reeves and Marasco (1980). Assumptions required by the S–R relationship include: (1) parameters describing growth and mortality rates are not age-specific; (2) the abundance of recruits, as defined above, can be estimated with a reasonable degree of accuracy; (3) the age of recruits is known; (4) the abundance of recruits can be specified to an abundance of spawners which produced them. Virtually all of these assumptions are violated by crustacean populations.

Age of crustaceans cannot be directly determined due to the lack of permanent hard body parts, so most growth studies have relied on length–frequency analysis. Estimates of age versus length for RKC vary greatly with location of study; mean size of 3-yr-old crabs was estimated to be 17 mm in the EBS (INPFC 1959), 22 mm in the eastern Sea of Okhotsk (Vinogradov 1968), 60 mm at Unalaska, AK (Weber 1967), and 61 mm at Kodiak, AK (Powell 1965). Despite these contradictory findings, the age–size relationships described by Weber (1967) and Powell (1965) for Unalaska and Kodiak, respectively, have been routinely assumed to apply to EBS populations of RKC (Balsiger 1974; Reeves and Marasco 1980). These disparate conclusions may be the result of differing water temperature regimes in the study locations.

Within a specific zone of tolerance, crustacean growth is primarily a function of temperature. Kurata (1960, 1961, 1962) demonstrated that the intermolt periods for larval and early postlarval RKC were a constant product of days·degrees (days-Celsius or dC), and estimated the entire period of larval development to require 460 dC. Studies of RKC growth by Nakanishi (1987) supported Kurata's conclusions. This phenomenon of temperature-dependent growth has been generalized to most crustacea (Hartnoll 1982). Increasing temperature usually causes a decrease in the intermolt period, with little effect on the molt increment (Hartnoll 1982).

This study was conducted to determine if a relationship existed between published growth rates of RKC (Weber 1967) and water temperature, with the goals of estimating more precisely the age of crabs captured in the NMFS surveys of the EBS, predicting their age at recruitment to the mature adult population, and improving estimates of year-class success.

Methods

This investigation consisted of four phases: (1) the establishment of a temperature-based growth equation based on previously collected growth data for juvenile RKC; (2) the creation of a chronological temperature matrix for inner Bristol Bay, AK, and simulated growth of crabs at gridpoints of that matrix via the growth equation; (3) analysis of data from the NMFS EBS crab stock survey to detect large catches of small RKC in Bristol Bay and estimate their mean size: and (4) estimation of the age of crabs observed by the NMFS crab survey by comparison to the mean size calculated by the simulation model.

Temperature–Growth Relationship

Weber (1967) conducted a study of juvenile king crab growth at Unalaska, AK in the period 1958–59. Mean carapace lengths of modes depicted in that paper (primarily from his figures 20 and 21) were estimated by eye, and corresponding dates were noted (Table 1). Only clearly distinct modes with mean lengths up to 60 mm were used because observations of larger crabs were scarce. Weber (1967) concluded that the mean date of occurrence of the first postlarval crab (C1) was approximately 1 July. Since larval development requires approximately 2 mo (Haynes 1974) I assumed that hatching occurred around 1 May.

Mean monthly Unalaska surface temperatures (UST) were obtained from the National Oceanographic Atmospheric Administration (NOAA) National Ocean Survey. Missing data (19 values) were estimated via regression of UST on monthly mean air temperature at Cold Bay, AK, (CBA) lagged 0 and 1 mo, for the period January 1956 to December 1962 (Table 2). Degree-days (days Celsius, or dC) for each month in this period were calculated as (days in month)·UST.

Since Weber's (1967) sampling periods covered 1—2 wk, and UST was available only on a monthly basis, the total degree days for each length–frequency mode observed by Weber (1967) were calculated from presumed hatching dates of 1 May 1956, 1957, or 1958 to the first day of the month nearest the date of observation. An additional point representing the first postlarval stage (C1) was added (Table 1), with mean length of 1.75 mm (Kurata 1962), and temperature requirement of 460 dC (Kurata 1960). A temperature-based growth equation was calculated by regression of the natural log (ln) of mean CL against the natural log of cumulative degree-days for each mode.

TABLE 1. Mean size of modes (estimated by eye) and date observed by Weber (1967), and number of degree-days accumulated from an estimated hatching date of 1 May. Unalaska surface temperatures obtained from NOAA/NOS. Date is first day of month nearest actual sampling date.

Date	Mean CL (mm)	Cumulative degree-days	Probable year-class
7/01	2[a]	475	
10/01/58	5	1312	1958
03/01/59	8	1873	,,
06/01/59	11	2140	,,
05/01/58	13	2257	1957
10/01/58	18	3570	,,
,,	22	3570	,,
05/01/58	36	4142	1956
03/01/59	36	4131	1957
06/01/59	42	4398	,,
03/01/59	61,63	6015	1956

[a] First postlarval stage, not observed by Weber, requires a minimum of 460 degree-days (Kurata 1960), but has accumulated 475 by 1 July.

Growth Model

Long-term (30 yr) monthly mean surface and bottom water temperatures, and deviations from those means for each month of the 30-yr period, were obtained from Ingraham (1983), who integrated the data to a 24 by 24 gridpoint matrix covering the EBS. A sub-matrix of 28 gridpoints which lay within Bristol Bay was utilized for the present study (Fig. 1).

Data were missing for many of the winter months in the period 1953–82, the majority of observations occurring from May to October. Missing data were estimated by regressing mean monthly surface and bottom water temperature on Cold Bay air temperature lagged 0 and 1 mo, as was done for Unalaska water temperatures (Table 2). Only months with at least 16 valid gridpoints were used.

Crab growth was simulated at the 28 temperature matrix gridpoints under the following assumptions:

(A) Larval development to stage C1 was assumed to require 460 dC (Kurata 1960) and to occur at a single sampling station.

(B) Juvenile crabs were assumed to be non-migratory up to 60 mm CL, as indicated by Dew (1990), and were subject to the bottom temperature at the same station as A above.

(C) Growth up to 60 mm CL was assumed to follow the regression on cumulative dC. Larger crabs tend to molt annually and growth increment stabilizes at approximately 15 mm per molt (Weber 1967; Weber and Miyahara 1962). Subsequent temperature changes, or movement from the original station were assumed to have no further effect upon growth rates.

(D) Growth of king crabs was assumed to occur only at temperatures above 0°C, as indicated by Kurata (1961). There-

TABLE 2. Parameters of regression equations utilized in the growth model. UST_m = mean Unalaska surface temperature (°C, month_m), BBST_m = mean Bristol Bay surface temperature (°C, month_m), BBBT_m = mean Bristol Bay bottom temperature (°C, month_m), CBA_m = mean Cold Bay air temperature (°C, month_m), SD = standard deviation of mean carapace length (CL).

Dependent variable	Constant	Coefficients 1	Coefficients 2	r^2	n
UST_m	3.37	$0.565 \cdot \mathrm{CBA}_m$	$0.0722 \cdot \mathrm{CBA}_{m-1}$	0.959	64
BBST_m	0.0687	$0.246 \cdot \mathrm{CBA}_m$	$0.6541 \cdot \mathrm{CBA}_{m-1}$	0.904	45
BBBT_m	0.6144	$0.0114 \cdot \mathrm{CBA}_m$	$0.6266 \cdot \mathrm{CBA}_{m-1}$	0.855	33
SD	0.04	$0.075 \cdot \mathrm{CL}$		0.41	37

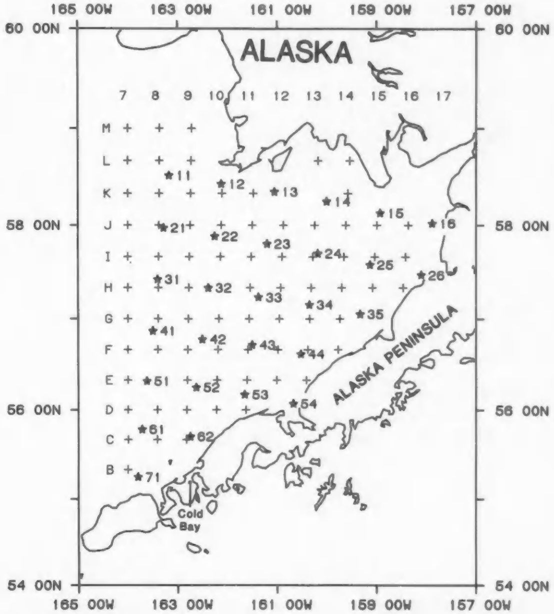
165 00W
163 00W
161 00W
159 00W
157 00W
60 00N
58 00N
56 00N
54 00N
ALASKA
ALASKA PENINSULA
Cold Bay
7 8 9 10 11 12 13 14 15 16 17
M
L
K
J
I
H
G
F
E
D
C
B
11
12
13
14
15
16
21
22
23
24
25
26
31
32
33
34
35
41
42
43
44
51
52
53
54
61
62
71

FIG. 1. Chart of Bristol Bay, Alaska, showing the NMFS survey station pattern (crosses), and the temperature matrix gridpoints (stars) within that region. Both grid patterns extend west and north beyond the Bristol Bay region. See text for explanation of grid labels.

fore, all negative water temperatures were converted to 0°C, to prevent the model from predicting negative growth at negative temperatures. Accumulated positive temperatures are referred to as growing-degree-days.

(E) No allowance was made for skip-molting since the probability of this is very low below sizes of 100 mm CL (Balsiger 1974).

(F) A 'normal' hatch date of 1 May was assumed. However timing of RKC embryo hatching appears to depend on water temperatures (NMFS, unpubl. data). Therefore, hatching date was assumed to vary ± 1 mo depending on June EBS bottom temperature, as described below.

Input data for the growth model consisted of: two 28:12[1] matrices containing the 12 long-term (30-yr) monthly mean surface or bottom temperatures (MMST and MMBT), for each of the 28 Bristol Bay gridpoints; two 1:12 vectors of long-term mean monthly surface or bottom temperatures (LTMST or LTMBT), averaged over 30 yr and all 28 gridpoints; and a 30:12 matrix of 360 mean monthly air temperatures at Cold Bay (CBA) representing the years 1955–87.

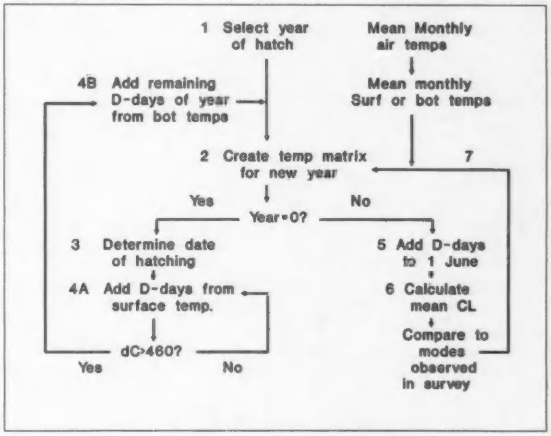
1 Select year of hatch
Mean Monthly air temps
Mean monthly Surf or bot temps
4B Add remaining D-days of year from bot temps
2 Create temp matrix for new year
7
Yes
No
Year=0?
3 Determine date of hatching
4A Add D-days from surface temp.
dC>460?
Yes
No
5 Add D-days to 1 June
6 Calculate mean CL
Compare to modes observed in survey

FIG. 2. Flowchart of growth model.

The growth model was written in APL, and operated in the following manner (Fig. 2):

(1) A hatching year (1967 to 1983), was selected and designated as year 0.

(2) Mean surface and bottom temperature (MST and MBT) over all 28 gridpoints were calculated for month_m of year_y via the regression equations using CBA (example given only for surface temperature):

$$\mathrm{MST}_{ym} = a + b_1(\mathrm{CBA}_{ym}) + b_2(\mathrm{CBA}_{y,m-1}) \quad [1]$$

A single-value surface or bottom temperature anomaly was calculated for month_m of year_y (STANOM or BTANOM) as the difference between calculated mean (MST) and long-term mean (LTMST):

$$\mathrm{STANOM}_{ym} = \mathrm{MST}_{ym} - \mathrm{LTMST}_{.m}, \quad [2]$$

where $\mathrm{LTMST}_{.m}$ implies monthly temperatures averaged over years. Estimated monthly surface or bottom temperatures (EMST and EMBT) for each gridpoint (labeled as $_{ij}$ in Fig. 1) were calculated by addition of the anomaly (STANOM) to the long term gridpoint means (MMST or MMBT):

$$\mathrm{EMST}_{ymij} = \mathrm{MMST}_{.mij} + \mathrm{STANOM}_{ym}, \quad [3]$$

---

[1] Dimensions of matrices and vectors are given as Z:Y:X or Y:X, respectively, corresponding to the number of elements in each of the Z, Y, or X dimensions. Similarly, gridpoints of the geographic temperature matrix were given two-digit labels corresponding to their row and column (Y and X) coordinates in the matrix; gridpoint 11 is at the upper left corner (Fig. 1).

Note that the same anomaly value was added to all gridpoints in any month. Individual anomalies for each gridpoint could not be calculated due to missing data, so the relative geographic distribution of temperatures was not varied between years, i.e. the relative temperature distribution in June was assumed to be similar for all years. Degree-days were then calculated for each gridpoint in each month of year$_y$:

[4] $dC_{ijym} = EMST_{ijym} \cdot days_m$

(3) A hatching date of 1 May was assumed if STANOM for June (actual data from the survey) was > -1.0°C and < 1.0°C. Hatching dates of 1 April or 1 June were assumed if STANOM was above or below this range, respectively.

(4) (A) At each gridpoint, degree-days were accumulated from the hatching date on a monthly basis, using the estimated surface temperatures (EMST) until 460 dC were accumulated.

(B) Degree-days for the remaining months of the year were accumulated using estimated bottom temperatures (EMBT), which were used for all further growth.

(5) A temperature matrix for the year following hatching (year 1) was then created as above, and degree-days were further accumulated using bottom temperatures (EMBT) until 1 June, the approximate starting date for the annual NMFS crab survey.

(6) Mean CL was calculated at all gridpoints using the accumulated degree-days and the temperature-based growth equation.

(7) The remaining degree-days in the year were accumulated, a new temperature matrix was calculated for year 2, and degree-days accumulated to 1 June, at which point mean CL were again calculated for all gridpoints. For those gridpoints with estimated CL>60 mm at this point, further growth was simulated by adding 15 mm per year. Step 7 was repeated through year 10.

(8) The entire process was repeated for the next hatching year.

King Crab Recruitment in Bristol Bay

The NMFS has conducted a trawl survey of commercially exploited crab and groundfish resources in the EBS annually since the late 1960's at predesignated intervals of 20 nmi (Fig. 1), each station representing a 400 nmi^2 square (See Otto 1986 for procedures). All crabs were removed from the catch, sorted by species and sex, and weighed in aggregate. Large catches were subsampled so that approximately 300 king crabs were measured per tow. King crabs were measured to the nearest 1.0 mm from the rear of the right eyesocket to the center of the rear margin of the carapace.

Population abundance was calculated by the area-swept method (Alverson and Pereyra 1969) and expressed as crab density (crabs/nmi^2) for each sex, using a stratified systematic technique (Cochran 1963). The abundance of male crabs in the size interval 95–109 mm CL was used as an index of recruitment to the adult population for consistency with Reeves and Marasco (1980), because male king crabs mature at approximately 103 mm CL (Somerton 1980), and because king crab appear to be not fully recruited to the trawl gear at smaller sizes (abundance estimates typically increase with size up to this interval, then decline at larger sizes, e.g. Stevens and MacIntosh 1989).

Individual stations sampled from 1972 to 1987 were examined for the presence of small crabs in either of the size groups 0–50 mm CL, or 51–75 mm CL; earlier data were not available. This division of sizes was necessary because larger crabs were almost always more abundant and tended to mask the abundance of smaller ones. A valid mode was defined as a group of at least 25 crabs with a distinct quasi-normal size frequency distribution, observed at a given station and date. Stations with fewer crabs generally did not form a well defined mode, and calculation of mean CL and standard deviation (SD) was meaningless for those data. Stations were analyzed individually, rather than being grouped geographically, because of the non-migration assumption, and because temperatures between adjacent stations could be quite different.

Length frequency data, weighted by the proportion subsampled, were analyzed with a mode separation technique (program NORMSEP; adapted from MacDonald and Pitcher 1979) to determine the mean CL, SD, and number of crabs in each mode, and were plotted for visual verification. Initial estimates of mean, SD, and number of modes (usually only one per station) were iteratively recalculated to produce a predicted length frequency distribution. This was compared with the original distribution, the lowest chi-squared value indicating the best fit. The calculated SD of each mode was then regressed on mean CL to determine the relationship between these two parameters (Table 2).

Estimation of Age of Observed Crabs and Number Recruiting

Each of the 28 model gridpoints represented growth at 3 or 4 of the 92 survey trawl stations in Bristol Bay. For those years when small crabs were found, the observed mean carapace length (CL_0) was compared with the predicted mean CL (CL_p) at the gridpoint nearest where it was observed, or to the average CL predicted at two to four equidistant gridpoints, comparing different possible model hatching years in an iterative fashion. The model year which produced a CL_p closest to CL_0 was selected as the most probable year of hatching. The year in which this cohort subsequently 'recruited' into the mature size interval (95–109 mm CL) was designated year R. The predicted mean size (CL_p) at which it recruited was recorded, and the predicted variance (V_p) of CL_p was calculated from the regression of SD on mean CL. For example 95% of the crabs in a mode with mean $CL = 100$, and $SD = 7.54$, would lie between 85 and 115 mm (mean $\pm 2 \cdot SD$), a range of 30 mm.

Because each mode required several years to fully recruit, the proportion of crabs from each mode recruiting in year $R-1$ through year $R+1$, a period of 3 yr, was determined. Each mode was assumed to be a normal curve with parameters (CL_p, V_p) and the proportion within the recruitment size interval (95–109 mm CL) was calculated from a table of areas of the normal curve (table P of Rohlf and Sokal 1969). This value was then multiplied by the original number of crabs in the mode to determine the number recruiting in that year. This procedure was repeated for each mode separately. All crabs recruiting in a given year from different modes were summed up and plotted as an index of relative recruitment (modal index).

Mortality Scenarios

Since the largest mode of crabs captured appeared to be an outlier (see Discussion), and since smaller crabs required several years more than larger ones to recruit, five different scenarios covering a range of mortality conditions were examined:

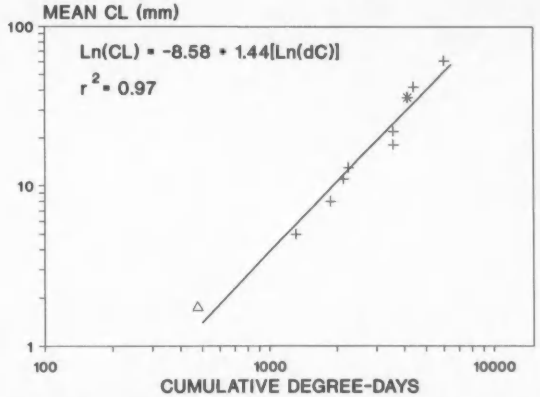

FIG. 3. Regression of ln mean carapace length (CL) on ln of cumulative degree-days (dC) for 10 modes of crab length frequency (+) observed by Weber (1967), and estimated length of first instar (triangle; Kurata 1961). Asterisk denotes two overlapping points.

(1) No mortality applied.

(2) Equal annual mortality (A) of 0.1 (Balsiger 1974) applied to all modes in all years.

(3) No mortality, but the abundance of the largest mode (1984/H13) was reduced from 7547 to 365 (the number actually sampled).

(4) Differential annual mortality applied. $A = 0.1$ for all modes in all years except 1983–86, when $A = 0.5$. The years 1983–1985 were identified as years of possible higher mortality because of the relatively high incidence of diseases reported for RKC sampled in 1983–84 (Sparks and Morado 1985), as well as the discrepancies between observed and predicted recruitment for those years.

(5) Differential annual mortality, as in Scenario 4, but abundance of mode 1984/H13 reduced as in scenario 3.

Calculation of appropriate variances, proportion and number recruiting, relative recruitment index, and mortality scenarios were all accomplished with a spreadsheet program on a desktop microcomputer.

Results

The natural log (ln) of CL of Unalaska RKC (Weber 1967) was positively related to ln of cumulative degree days for Unalaska surface temperatures ($r^2 = 0.97$; Fig. 3). Both air and sea surface temperatures in Bristol Bay (Fig. 4) were above the 30-yr mean in the late 1960's, well below average from 1971 through 1976, and above average again from 1977 through 1986, excluding 1982. Average annual growing-degree-days calculated by the model ranged from a high of 1646 dC at nearshore gridpoints, to a low of 583 dC further offshore (Fig. 5).

From 15 yr of data, parameter estimates were produced for 59 modes which met the validity criteria. Figure 6 shows four examples covering a range from the smallest to the largest mode analyzed. Differences between CL_0 and CL_p were usually less than 10% (Fig. 7).

Large catches of crabs <50 mm CL occurred repeatedly at four different groups of adjacent stations (Fig. 1): B07-08, and C09 (7 yr); D10-11, E11-12, and F12 (8 yr); G15 (3 yr); and J15-16 (6 yr). All four groups are within 30 nmi of a major estuary and all except for the first group are less than 45 m in depth. Small crabs occurred at a fifth group of shallow offshore stations (I11-15 and H11-14) in 8 yr, but usually at larger sizes (50–80 mm CL).

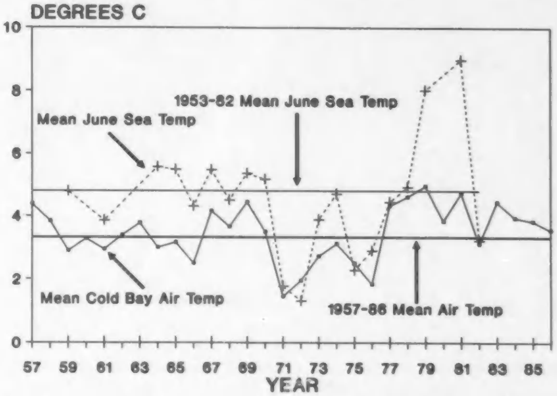

FIG. 4. Annual and long-term (1957–86) mean air temperature (°C) at Cold Bay, AK, and mean sea surface temperature of Bristol Bay in June (annual and long term).

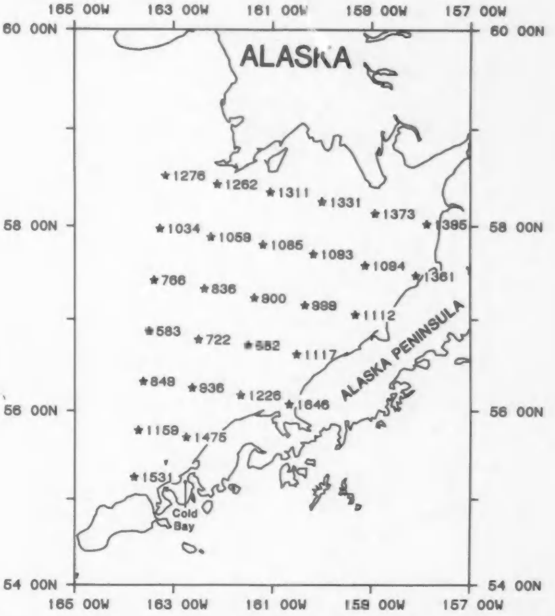

FIG. 5. Average annual growing degree days (sum of dC≥0) for each gridpoint of Bristol Bay temperature matrix, calculated from 30-yr mean monthly temperatures, 1953–82.

Two modes appeared to remain in place for two consecutive years (YC 1970, station B07, and 1976/F12). A third, apparently hatched in 1968, appeared first at station I15 at age 5, then at station I14 at age 6, a distance apart of 20 nmi. Generally, crabs were first captured by the survey gear at the age of 5 or 6, occasionally at age 4, and only rarely (2 occasions), at age 3, both times at a very shallow inshore station (G15).

Recruitment to the Adult Size Interval

Predicted mean age at recruitment to the 95–109 mm CL size-interval ranged from 7 to 12 yr (Fig. 8), and was generally

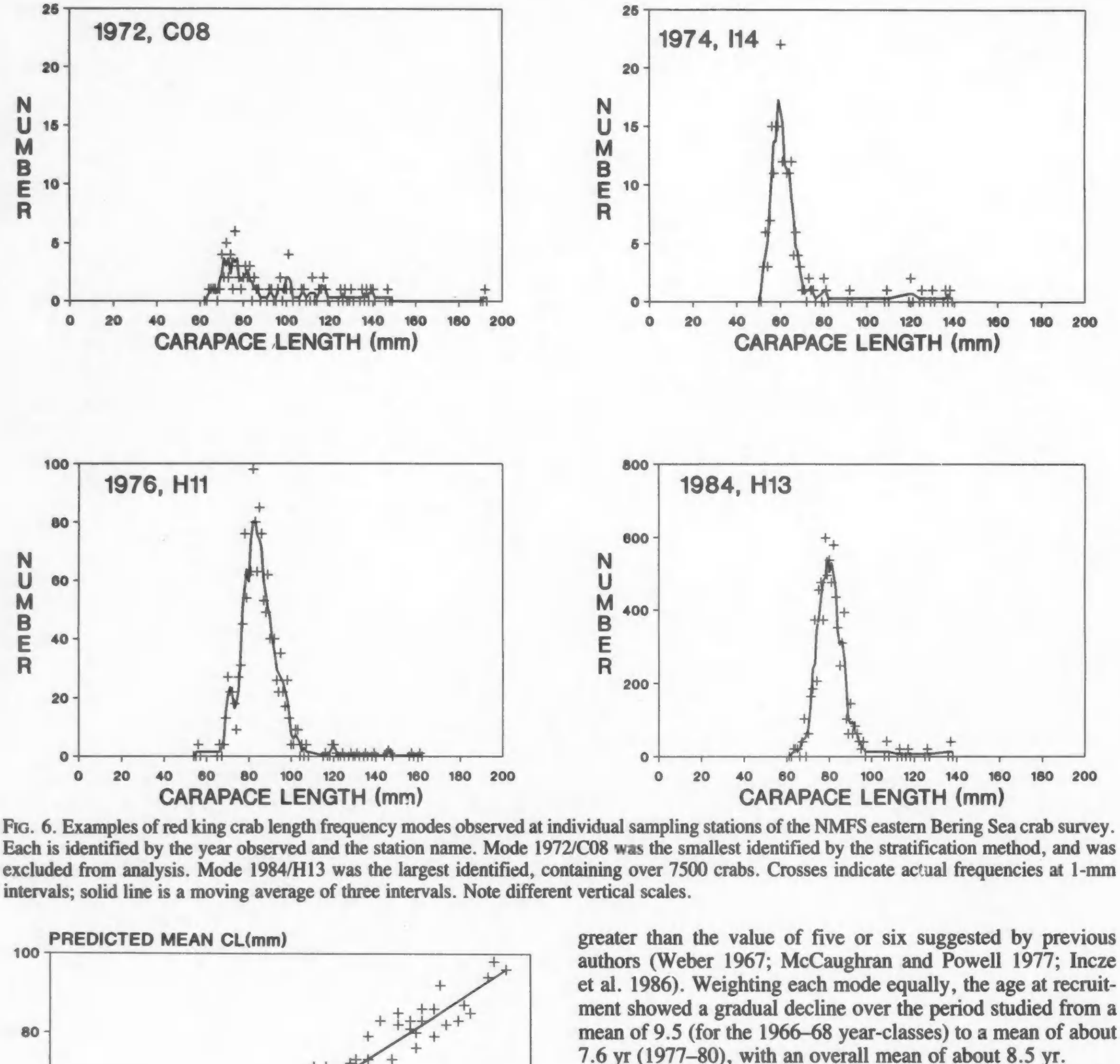

FIG. 6. Examples of red king crab length frequency modes observed at individual sampling stations of the NMFS eastern Bering Sea crab survey. Each is identified by the year observed and the station name. Mode 1972/C08 was the smallest identified by the stratification method, and was excluded from analysis. Mode 1984/H13 was the largest identified, containing over 7500 crabs. Crosses indicate actual frequencies at 1-mm intervals; solid line is a moving average of three intervals. Note different vertical scales.

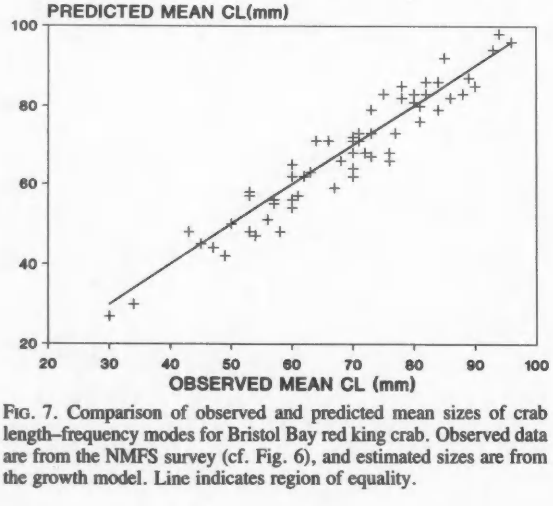

FIG. 7. Comparison of observed and predicted mean sizes of crab length–frequency modes for Bristol Bay red king crab. Observed data are from the NMFS survey (cf. Fig. 6), and estimated sizes are from the growth model. Line indicates region of equality.

greater than the value of five or six suggested by previous authors (Weber 1967; McCaughran and Powell 1977; Incze et al. 1986). Weighting each mode equally, the age at recruitment showed a gradual decline over the period studied from a mean of 9.5 (for the 1966–68 year-classes) to a mean of about 7.6 yr (1977–80), with an overall mean of about 8.5 yr.

Since the 95% confidence interval for recruitment modes enclosed approximately 30 mm of CL, several years were required for complete recruitment to a 15-mm interval. The leading edge of the mode (crabs in the right tail of a normal distribution) reached this interval 1 or 2 yr earlier than the mean (in year $R-1$ or $R-2$), and the trailing edge (the left tail) reached it 1 or 2 yr later than the mean (year $R+1$ or $R+2$). Although complete recruitment of a mode could require 4–5 yr, 97.5% of the observed crabs recruited during the 3-yr period from year $R-1$ to $R+1$, according to the model.

Crabs were grouped together according to their estimated hatching and recruiting years, and the number recruiting in each year was summed (Table 3). Table 3 shows the results of scenario 1 (no mortality applied), and indicates that recruitment in any single year, e.g. 1982, may consist of crabs from up to six different year-classes (YC), e.g. 1971 through 1976. A corollary result is that crabs from a single YC, e.g. 1967, growing at different locations and temperatures, may recruit over 4–

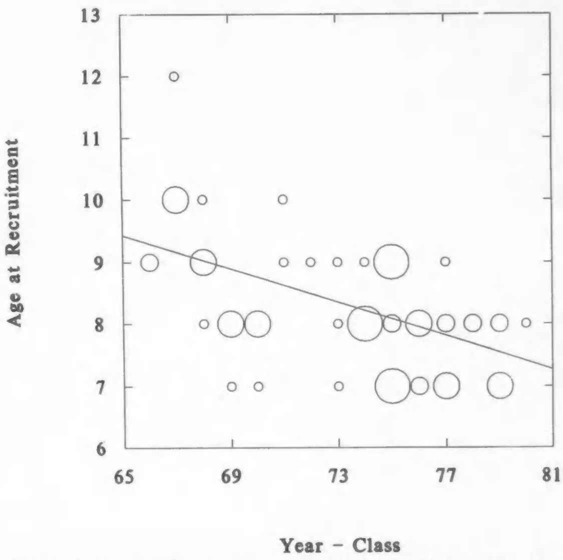

FIG. 8. Age at recruitment of each mode to the 95–109 mm CL interval, by year-class. Radius of circle is proportional to number of modes at each locus (range/1–4; total/59). Linear regression line indicates trend in data.

5 yr or more (1976–80). Vertical summation of crabs recruiting in each year provided a crude 'modal recruitment index,' and horizontal summation provided an index of year-class success. The proportion of each year-class which was predicted to recruit in any year (the recruit-class) can be easily calculated from Table 3. For example, 16.5% (332/2015) of the 1970 YC was predicted to recruit in 1979, but these crabs comprised 58% (332/572) of the 1979 recruit-class.

An extremely large mode of crabs ($n = 7547$, mean CL = 80 mm) was observed at station H13 in 1984, and predicted to contribute substantially to recruitment over the period 1984–86. However, this large mode was not observed in the previous or following years, suggesting that subsampling error, extreme aggregation of crabs (e.g. podding), substantially increased mortality, or some combination of factors had occurred. Therefore, this mode was treated as an outlier in mortality scenarios 3 and 5 (see Methods), and its abundance was reduced by the subsampling factor of 21 employed at that station, to a value of 365, the number of crabs actually sampled. This was one of the largest subsampling factors ever employed in the king crab survey; most catches were not subsampled, but when done, factors in the range of two to four were more typical.

Results similar to Table 3 were produced for each of the five scenarios described, but the major differences in predicted recruitment occurred ony for the 1975–77 year-classes, so complete tables are not given. Results for scenarios 1–5 are compared in Fig. 9, which shows the predicted year-class success (rightmost column of Table 3, 'YC Sum,' and its equivalent from each scenario). Reduction of mode 1984/H13 in scenarios 3 and 5 significantly reduced the predicted success of the 1977 YC. Application of mortality in scenarios 2, 4, and 5 reduced all predictions of YC success by 13–32%, whereas higher mortality in the years 1983–86 (scenarios 4 and 5) reduced the contribution of 5 YC's, from 1974 to 1979.

Scenario 5 gave the best fit between the predicted recruitment (modal index) and the observed recruitment (adult index) and indicates that a dominant group of crabs (1977 recruits) is reasonably represented by both techniques (Fig. 10). Over the period of time analyzed, three periods of strong recruitment were detected, occurring in 1975–77, 1981–82, and 1984. In all cases, the modal index predicted both the timing and magnitude of recruitment relatively well. The three outstanding recruitment years (1977, 1982, and 1984) all consisted of multiple, relatively successful YC's. In 1977, four relatively strong adjacent YC's (1967–70) appeared to recruit simultaneously, and none contributed more than 31% of the total recruitment. The 1982 and 1984 recruitment years consisted primarily of crabs from the 1975 and 1976 YC's, but in neither case did the

TABLE 3. Results of recruitment scenario 1, as described in text. Values are numbers of crab from each year-class (YC) recruiting to the 95–109 mm CL interval in each recruitment year (RY). Vertical sums (RY sum) are cumulative numbers of observed crabs from all YC surviving to recruitment in each recruitment year and constitute a modal recruitment index. Horizontal sums (YC sum) are numbers of crabs from each YC which survive to recruitment, i.e. an index of YC success. No mortality applied in this scenario.

	Year of recruitment																
YC	1974	1975	1976	1977	1978	1979	1980	1981	1982	1983	1984	1985	1986	1987	1988	1989	YC sum
1966	15	108	38														161
1967			87	893	427	128	123										1658
1968		7	229	599	206	12											1053
1969		7	147	828	308												1290
1970			44	575	1064	332											2015
1971						80	369	132	10								591
1972							6	181	123								310
1973						20	123	402	375	45							965
1974								180	354	210	33						777
1975								199	1157	1125	1457	371					4309
1976									118	884	1098	620					2720
1977										200	1543	4463	3659	28			9893
1978												141	598	160			899
1979												109	359	146	7		621
1980														5	220	180	405
RY sum	15	122	545	2895	2005	572	621	1094	2137	2464	4131	5704	4616	339	227	180	27667

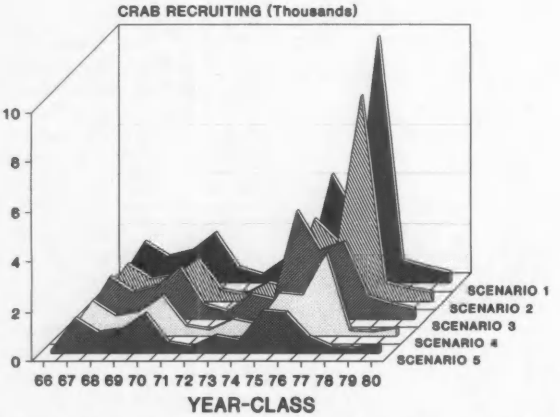

FIG. 9. Comparison of results of recruitment/mortality scenarios 1–5. Values are number of crabs surviving to recruitment to the 95–109 mm CL interval. Scenario 1 values represent the rightmost column of Table 3 ('YCsum'). All other scenarios follow same format.

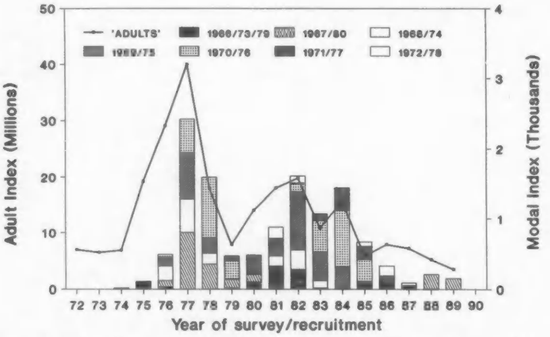

FIG. 10. Recruitment scenario 5: comparison of adult recruitment index (observed numbers of crab in 95–109 mm CL interval; solid line) with modal recruitment index (predicted numbers of crab recruiting to the 95–109 mm CL interval; vertical bars). Modal index shows the relative recruitment from specific year-classes. This scenario incorporates annual mortality of 0.5 in 1983–86, and 0.1 in all other years. Station H13 (1977 YC) has been reduced to a value of 365.

predominant YC contribute more than 56% of the total recruitment. In fact, no single YC stands out above the others over the period considered (Fig. 9), except perhaps 1975, if mortality is assumed constant (scenarios 1–3), and perhaps 1977, if the high value at station H13 is retained (scenarios 1, 2, and 4).

The index of YC success ranged from 9893 to 161 in scenario 1 (Table 3), a ratio of 61:1, or from 1755 to 131 in scenario 5, a ratio of 13.4:1. The modal recruitment index values also lie within this range. Over this same period, the adult recruitment index has varied from 40 million crabs in 1977 to 3.4 million in 1989, a ratio of 11.8:1, and the estimates of legal-sized male crabs from 1.5 to 46.6 million, a ratio of 31:1. Years of weak recruitment appear to consist primarily of the overlapping of extreme tail ends of strong cohorts which recruited at intervals of 3–5 yr or more (Fig. 10). Over the period analyzed, there has not been a long enough gap between strong cohorts to determine if this baseline level of weak recruitment would approach 0 in the absence of additional strong recruitment, but since 1984, the last year in which a recruitment pulse was observed, the adult recruitment index has declined to a new record low of 3.42 million crabs in 1989 (Stevens and MacIntosh 1989).

The years 1974–76 lack proper representation in this analysis because of the 3–5 yr lag times required between first observation of the modes (1973) and subsequent recruitment (1977). Although survey data through 1987 were analyzed, essentially no significant numbers of small crabs have been observed since 1984, implying either that no detectable year-classes have been produced since about 1980, or that year-classes produced since that time have gone undetected by the survey.

Discussion

Weber's (1967) conclusions regarding age and growth for Unalaska crabs up to about 60 mm (3 yr of age) were probably accurate. However, he expected the age–length relationship of Bristol Bay RKC to be similar to Unalaska crabs, despite an acknowledged mean annual temperature difference of about 3°C. Balsiger (1974) perpetuated this assumption, and concluded that the age–size relationship for Bristol Bay RKC was identical to that for Kodiak RKC. Management policies have incorporated this conclusion ever since. In contrast, length frequency data from Bristol Bay (INPFC 1959) indicate much slower growth than for Kodiak (Powell 1965) or Unalaska crabs, with mean sizes of about 4, 9, and 17 mm CL at probable ages of 1, 2, and 3 yr.

Prior attempts to develop a stock–recruitment model for the EBS king crab stock (Reeves and Marasco 1980; Reeves 1985) were made without adequate knowledge of the age structure of the population. Thus the implicit assumption was made that lag times between spawners and recruits were constant, i.e. that recruitment in consecutive years resulted from consecutive YC's recruiting at a constant age. A corollary assumption was that a one-to-one relationship existed between the parent stock index (*P*) and a subsequent recruitment index (*R*), such that for each estimate of *P*, only one *R* existed, and vice versa. These assumptions are probably invalid for EBS king crab. According to the model, at least six YC's recruited in 1982, and the 1967 YC recruited over a 5-yr period. Future stock–recruitment analyses should attempt to incorporate the effects of multiple year-class and multi-age recruitment, with improved estimates of lag time (age at maturity).

The results of this analysis allow some insight into the causes of the rise and fall of the EBS RKC population in the late 1970's. The strong recruitment pulse of 1975–77 was apparently composed of multiple year-classes collectively comprising a 'functional cohort' which recruited more-or-less synchronously over a period of at least 3 (and probably more) yr. The gradual rise in recruitment over the period 1975–77, rather than representing several increasingly successful consecutive year-classes, actually represents the successive partial sampling of a strong functional cohort as it first entered, then passed through, and finally left the recruitment size-interval. For a geographically dispersed crustacean population such as the red king crab, the simultaneous recruitment of individuals from multiple year-classes and nursery areas seriously inhibits the capacity to distinguish year-class modes from the combined length–frequency data in any survey year. For this reason it was necessary to examine individual catches to identify those grounds that were most productive of juveniles, and model growth at those locations to predict the probable age structure which would exist at the time of recruitment to the adult population.

The rapid decline in abundance of legal-sized (>135 mm CL) RKC which occurred from 1980 to 1982 was primarily the result of several factors, including the natural decline of a dominant cohort, compounded by poor recruitment and higher than expected mortality. The latter can be partially explained by the results of this investigation, if mortality is a function of age, as opposed to size. Otto (1986) developed a model to predict the abundance of legal male RKC in the EBS 1 and 2 yr in advance, based on observed numbers of sublegal (110–135 mm CL) males, expected growth and harvest rates, and transition matrices of size-specific mortality and molting probabilities (Balsiger 1974). Predicted abundances of legal males underestimated observed abundances by 25–50% while the population was increasing (1976–78), were fairly precise as the population peaked in 1978–80, and overestimated abundance by 100–200% during the period of rapid population decline (1981–84). In the case of a strong functional cohort recruiting to the population, as occurred in the late 1970's, the initial increase in legal-sized crabs would consist of those which grew most rapidly and were therefore younger than average, thus exhibiting below-average mortality rates. Crabs recruiting to the legal size group might have ranged in age from 8 to 13 yr, due both to normal variation in growth and the convergence of several age classes due to spatial and temporal variation in temperatures. When the last, and hence slowest growing, crabs of this dominant cohort recruited to the legal population in the early 1980's, their mean age and size-specific mortality rates would have been well above average, and the decline in abundance which occurred was therefore more rapid than expected.

Strong year-classes of RKC have occurred sporadically over the 15-yr range of RKC data examined. Only four YC's (1970, 1975, 1976, and perhaps 1977) produced modal indices of year-class success exceeding the mean value of 1845 (Table 3), and of those four, 1977 is questionable since it's predicted success was dependent upon crabs from a single catch. Success of RKC year-classes appears to have varied greatly between years, perhaps by factors up to 60. This conclusion is consistent with the observation of Hennemuth et al. (1980) that the frequency distribution of YC strength in many fishery stocks is lognormal.

The results of this analysis suggest that *Paralithodes camtschatica* has the capacity to rebuild a diminished population with a single very strong YC. However, strong recruitment may be more often the result of the overlap of several YC of moderate strength recruiting in the same or consecutive years. The magnitude of observed recruitment is therefore not only a function of YC success but of the chronological spacing of strong YC's, and the stochastic geographic distribution of larval settlement. Two strong YC's occurring in consecutive years (e.g. 1967–70) would produce a stronger recruitment pulse than two equally strong YC's occurring two or more years apart, because of the overlapping of the tails of the size distribution from each YC. Additionally, temperature variation over the geographic range of the stock would insure that growth rates varied enough to spread recruitment over a period of several years. Thus, recruitment estimates can be highly modified by environmental variation and do not necessarily reflect YC strength directly.

The remoteness and size of the EBS region makes it extremely difficult to efficiently sample a large area for juvenile RKC, which apparently require specific habitats in their first few years. Unfortunately, the standard NMFS survey is not designed to sample juvenile RKC, so estimates of YC strength cannot be produced without improved knowledge of habitat requirements for juvenile RKC, and dedicated sampling with alternative gear types such as dredges and beam trawls (e.g. McMurray et al. 1986) or artificial habitat-type collecting devices (Freese and Babcock 1990). Additionally, the sparsity of temperature records, and the discontinuation of Ingraham's (1983) data series prohibits extrapolating the results of this particular model further than its present status. Despite the value of demersal fisheries in the EBS region, there has been no concerted effort to obtain year-round bottom temperature records for any location. Such data would be invaluable for calibrating this model and developing others.

The assumption of non-migratory larvae is contentious, since Haynes (1974) showed that RKC larvae could be transported 160 km or more during development. Tidal currents flowing eastward along the north side of the Alaska Peninsula often approach several knots, but net transport is only about 1–5 cm/s (0.02–0.10 knots; Kinder and Schumacher 1981), which is still enough to transport larvae 50 to 250 km over a 40–60–d period of development, if they remained stationary relative to the water mass. Although RKC larvae are not strong swimmers, they can swim vertically in response to certain environmental factors. (T. Shirley, College of Fisheries and Science, University of Alaska, Juneau, AK 99810, pers. comm.) Such behavior could allow them to take advantage of different current regimes at different depths, which could just as easily result in transport over long distances as it could in retention of larvae in a given region. This argument has also been developed by Armstrong et al. (1981).

The assumption that RKC remain non-migratory until reaching a size of 60 mm CL is supported by a variety of evidence. Crabs below this size can be retained by the survey trawl gear but are usually not caught except in years of apparently high abundance, perhaps due to spillover from even higher density nursery areas farther inshore which were not adequately sampled. McMurray et al. (1986) also found higher abundances of very small king crabs (<30 mm CL) in nearshore habitats which were dominated by bivalve shell debris and bryozoans. Juvenile king crabs of 20–60 mm CL are known to aggregate into pods of hundreds to thousands of individuals, which remain essentially localized for long periods of time (Powell and Nickerson 1965). Two such pods were continuously observed in a small area of Women's Bay, Kodiak Island, AK, during the winters of 1987 and 1988 (Dew 1990). Thus, there may be a behavioral change, e.g. cessation of podding, occurring at about 60 mm CL which causes king crabs to become more vulnerable to the trawl gear.

Certain nearshore locations seem to be more productive of juvenile crabs. McMurray et al. (1986) suggested that good habitats for juvenile RKC existed as scarce "islands" of hard substrate in an otherwise sandy–mud environment, and that only those post-larvae which settled in such habitats providing adequate shelter and food would survive their first year. Aggregation of small RKC into pods reduces the probability of their capture or predation, but produces very large catches when encountered. At sizes above 60 mm CL, their tendency to aggregate decreases, and they are less vulnerable to predation, so they spread into offshore environments where they are encountered by the NMFS trawl survey.

It is interesting to note that the four areas where the smallest crabs have been collected by the NMFS survey are all near estuaries. The presence of these geographic features might contribute to survival or settlement of RKC postlarvae, perhaps as sources of gravel or other hard substrates and/or localized water currents which might contribute to good habitat for crabs or their prey/cover species, or by providing a source of lower-salinity water which may have some positive physiological or behavioral effect on the settling crabs. Estuaries may also contribute nutrients and food sources to immediately adjacent offshore areas, adding to the attractiveness or quality of these habitats for juvenile RKC.

Temperature has a strong influence on the intermolt period of decapod crustaceans, but less of an effect on growth increment (Hartnoll 1982; Kurata 1960, 1961, 1962; Nakanishi 1987). By relating temperature to mean size of individual cohorts of crab, the present model incorporates both intermolt period and growth increment implicitly. It does not account for the apparent loss of temperature dependence at sizes >60 mm CL, nor does it account for skip-molting, which has a relatively low probability among the size-classes studied, but increases steeply above 100 mm CL (Balsiger 1974). However, the existence of both of these phenomena is predicated upon the assumption that large male crabs should molt annually. Although female RKC must molt annually in order to spawn, the periodicity of adult male molting is less well understood, and males may not molt simultaneously like females do. The decrease in molting probability with age for adult male RKC is consistent, though, with an increase in intermolt period, and therefore may be related to cumulative degree days, as is growth of juvenile crabs. The variance of CL becomes so large with age, however, and molting events become so asynchronous and staggered in time, that modes of adult male RKC are essentially unidentifiable, so this type of modal analysis is untenable for older crabs. Only long-term studies of individual crabs will be likely to unravel the entertwined phenomena of age, growth, and temperature.

Acknowledgements

This investigation benefitted greatly from many discussions with Dr. Robert Otto, National Marine Fisheries Service (NMFS), Kodiak, and Dr. David Armstrong, University of Washington. Some of the conclusions presented herein grew from ideas developed and refined during conversations with them. I would also like to thank Drs. Jerry Reeves and Bernard Megrey, NMFS, Alaska Fisheries Center, Seattle, for their careful review and comments on an early draft of this manuscript, as well as two anonymous reviewers.

References

Alaska Department of Fish and Game. (ADFG). 1988. Westward region shellfish report to the Alaska board of Fisheries. ADFG, 211 Mission Rd., Kodiak, AK, 99615, USA.

Alverson, D. L., and W. T. Pereyra. 1969. Demersal fish in the Northeastern Pacific Ocean – an evaluation of exploratory fishing methods and analytical approaches to stock size and yield forecasts. J. Fish. Res. Board Can. 26: 1985–2001.

Armstrong, D. A., L. S. Incze, D. L. Wencker, and J. L. Armstrong. 1981. Distribution and abundance of decapod crustacean larvae in the southeastern Bering Sea with emphasis on commercial species. Final Report to Outer Continental Shelf Environmental Assessment Program, Office of Marine Pollution Assessment, National Oceanographic and Atmospheric Administration, U.S. Dept. Comm. 373 p.

Balsiger, J. W. 1974. A computer simulation model for the eastern Bering Sea king crab population. Ph.D. thesis, University of Washington, Seattle, WA. 198 p.

Cochran, W. G. 1963. *Sampling techniques*. 2nd ed. John Wiley and Sons, Inc., New York, NY. 413 p.

Dew, C. B. 1990. Behavioral ecology of podded red king crabs, *Paralithodes camtschatica*. Can. J. Fish. Aquat. Sci. 47: (In press).

Freese, J. L., and M. M. Babcock. 1990. The use of artificial substrate collectors to determine the time and location of setting of first benthic stages of red king crab (*Paralithodes camtschatica*) in Auke Bay, Alaska. *In* B. Melteff [ed.] Proc. Internat. Symp. on King and Tanner Crabs, November 28–30, 1989, Anchorage, AK. University of Alaska Sea Grant Program, Fairbanks, AK, 99775, USA.

Hartnoll, R. G. 1982. Growth. Chap. 5 *in* D. Bliss [ed.] *The biology of crustacea, Vol. II: embryology, morphology, and genetics*. Academic Press, New York, NY, 440 p.

Haynes, E. B. 1974. Distribution and relative abundance of larvae of the king crab, *Paralithodes camtschatica*, in the southeastern Bering Sea, 1969–1970. Fish. Bull. 72(3): 804–812.

INPFC (International North Pacific Fisheries Commission). 1959. Report of research on king crabs from the eastern Bering Sea. Annual Report 1959, International North Pacific Fisheries Commission, p. 72–78.

Hennemuth, R. C., J. E. Palmer, and B. E. Brown. 1980. A statistical description of recruitment in eighteen selected fish stocks. J. Northwest Atl. Fish. Sci. 1: 101–111.

Incze, L. S., R. S. Otto, and M. K. McDowell. 1986. Recruitment variability of juvenile red king crab, PC, in the southeastern Bering Sea. *In* G. S. Jamieson and N. Bourne [ed.] North Pacific Workshop on stock assessment and management of invertebrates. Can. Spec. Publ. Fish. Aquat. Sci. 92: 370–378.

Ingraham, W. J., jr. 1983. Temperature anomalies in the eastern Bering Sea, 1953–1982, for the Dynumes 24×24 ecosystem model grid. Processed Rep. 83–21. Northwest and Alaska Fisheries Center, NMFS/NOAA, 7600 Sand Point Way, Seattle, WA 98115, USA. 348 p.

Kinder, T. H., and J. D. Schumacher. 1981. Circulation over the continental shelf of the southeastern Bering Sea. Chap. 5. *In* D. W. Hood and J. A. Calder [ed.] The eastern Bering Sea Shelf: oceanography and resources. NOAA, Office of Marine Pollution Assessment. University of Washington Press, Seattle, WA.

Kurata, H. 1960. Studies on the larvae and postlarvae of *Paralithodes camtschatica*. III. The influence of temperature and salinity on the survival and growth of the larvae. Bull. Hokkaido Region. Fish. Res. Lab. 21: 9–14.

1961. Studies on the larvae and postlarvae of *Paralithodes camtschatica*. IV. Growth of the postlarvae. Hokkaido Fish. Exp. Stn. Month. Rep. 18(1):1–9.

1962. Studies on the age and growth of crustacea. Bull. Hokk. Region Fish. Res. Lab. 24: 1–115.

MacDonald, P. D. M., and T. J. Pitcher. 1979. Age groups from size-frequency data: a versatile and efficient method of analyzing distribution mixtures. J. Fish. Res. Board Can. 36: 987–1001.

McCaughran, D. A., and G. C. Powell. 1977. Growth model for Alaska king crab (*Paralithodes camtschatica*). J. Fish. Res. Board Can. 34: 989–995.

McMurray, G., A. H. Vogel, P. A. Fishman, D. A Armstrong, and S. C. Jewett. 1986. Distribution of larval and juvenile red king crabs (*Paralithodes camtschatica*) in Bristol Bay. Final Report to Outer Continental Shelf Environmental Assessment Program, NOAA Office of Marine Pollution Assessment, Vol. 53, December 1986. 186 p.

Nakanishi, T. 1987. Rearing condition of eggs, larvae, and postlarvae of king crab. Bull. Jpn. Sea Region. Fish. Res. Lab. 37: 57–161.

Otto, R. S. 1986. Management and assessment of eastern Bering Sea king crab stocks, p. 83–106. *In* G. S. Jamieson and N. Bourne [ed.] North Pacific Workshop on stock assessment and management of invertebrates. Can. Spec. Publ. Fish. Aquat. Sci. 92: 83–106.

Powell, G. C. 1965. Growth of king crabs in the vicinity of Kodiak Island, Alaska. Alaska Department of Fish and Game Informational Leaflet 92. Alaska Fish and Game, 211 Mission Rd., Kodiak, AK, 99615, USA. 106 p.

Powell, G. C., and R. B. Nickerson. 1965. Aggregations among juvenile king crabs (*Paralithodes camtschatica*, Tilesius) Kodiak, Alaska. Anim. Behav. 13(2–3): 374–380.

Reeves, J. 1975. Computation and interpretation of biological characteristics of fish populations. Bull. Fish. Res. Board Can. 191. 382 p.

1985. Expected stock status and catch for Bristol Bay red king crab. Report to the North Pacific Fisheries Management Council, March 1985. Northwest and Alaska Fisheries Center, 7600 Sand Point Way, Seattle, WA 98115, USA. 9 p.

Reeves, J., and R. Marasco. 1980. An evaluation of alternative management options for the southeastern Bering Sea king crab fishery. Processed Report 80–6. Northwest and Alaska Fisheries Center, 7600 Sand Point Way, Seattle, WA, 98115, USA. 85 p.

Rohlf, F. J., and R. R. Sokal. 1969. Statistical tables. W. H. Freeman and Co., San Francisco, CA. 233 p.

Sparks, A., and F. Morado. 1985. A preliminary report on the diseases of Alaska king crabs, 333–340. *In* B. Melteff [ed.] Proceedings of the international king crab symposium, Anchorage, AK, Jan. 22–24 1985. University of Alaska, Alaska Sea Grant Rep. No. 85–12, November 1985. 507 p.

SOMERTON, D. A. 1980. A computer technique for estimating the size of sexual maturity in crabs. Can. J. Fish. Aquat. Sci. 37: 1488–1494.

STEVENS, B. G., AND R. A. MACINTOSH. 1989. Report to Industry on the 1989 eastern Bering Sea crab survey. Processed Report 89–18. Kodiak Island Facility, Northwest and Alaska Fisheries Center, NMFS, NOAA, P.O. Box 1638, Kodiak, AK, 99615, USA. 47 p.

UNITED STATES DEPARTMENT OF COMMERCE, NMFS/NOAA. 1981. Fisheries of the United States, 1980. April 1981. 119 p.

VINOGRADOV, L. G. 1968. The crab population in Kamchatka. Priroda 7: 43–50.

WEBER, D. D. 1967. Growth of the immature king crab *Paralithodes camtschatica* (Tilesius). International North Pacific Fisheries Commission. Bull. 21. p. 21–53.

WEBER, D. D., AND T. MIYAHARA. 1962. Growth of the adult male king crab *Paralithodes camtschatica* (Tilesius). Fish. Bull. U.S. Fish Wildl. Serv. 62(200): 53–75.

Relationships between Acidity and Benthic Invertebrates of Low-Order Woodland Streams in the Adirondack Mountains, New York[1]

Michael E. Smith,[2] Barbara J. Wyskowski, Carol M. Brooks, Charles T. Driscoll, and Christina C. Cosentini

Department of Civil Engineering, Syracuse University, Syracuse, NY 13244-1190 USA

Smith, M. E., B. J. Wyskowski, C. M. Brooks, C. T. Driscoll, and C. C. Cosentini. 1990. Relationships between acidity and benthic invertebrates of low-order woodland streams in the Adirondack Mountains, New York. Can. J. Fish. Aquat. Sci. 47: 1318–1329.

Benthic invertebrates were collected during January, April, July, and October 1985 from three low-order woodland streams in the Adirondack Mountains, New York to evaluate relationships between acidity and stream invertebrates. Total invertebrate generic richness, generic diversity, Ephemeroptera density and richness, collector–gatherer richness, and scraper density and richness were positively correlated to stream pH. Ephemeroptera and Naididae (Oligochaeta) were absent from the acidic sampling site. Enchytraeid oligochaetes and Turbellaria were collected at all sites, but in significantly higher densities at the acidic site. Elmid beetles (*Optioservus ovalis, Oulimnius latiusculus, Promoresia tardella*), mayflies (*Cinygmula* and *Baetis*) and caddisflies (*Glossosoma, Apatania*, and *Micrasema*) were abundant at the sites where pH was highest and were absent from other sampling locales. Total invertebrate density was not decreased at the acidic site when compared with most other sampling sites. Multiple regression analyses revealed that pH and benthic organic matter were the two most important measured stream parameters in describing the variance of invertebrate communities in the three study streams.

Des invertébrés benthiques ont été prélevés pendant les mois de janvier, avril, juillet et octobre 1985 dans trois ruisseaux sylvestres d'importance secondaire des Adirondaks (New York) afin d'évaluer le rapport entre l'acidité et les invertébrés dans les ruisseaux. La diversité totale des genres d'invertébrés, la densité des Éphéméroptères et leur diversité, la diversité des collecteurs, et la densité et la diversité des organismes sur le grattoir présentaient une corrélation positive avec le pH du ruisseau. Le lieu d'échantillonnage acide ne contenait pas d'Éphéméroptères ni de Naïdidae (Oligochètes). Des Enchythrées et des Turbellaria ont été prélevés dans tous les points d'échantillonnage, mais les densités étaient significativement plus fortes dans les lieux acides. Les Dryopidés (*Optioservus ovalis, Oulimnius latiusculus, Promoresia tardella*), des éphémères communes (*Cinygmula* et *Baetis*) et des phryganes (*Glossosoma, Apatania* et *Micrasema*) abondaient dans tous les lieux à pH élevé et étaient absents des autres lieux. La densité totale des invertébrés n'a pas diminué au lieu acide par rapport à la plupart des autres points d'échantillonnage. Des analyses de régression multiple ont montré que le pH et la matière organique benthique étaient les deux paramètres les plus importants mesurés dans le ruisseau pour décrire la variance des communautés d'invertébrés dans les trois ruisseaux à l'étude.

Received March 18, 1987
Accepted February 8, 1990
(J9185)

Reçu le 18 mars 1987
Accepté le 8 février 1990

Acidification of freshwater lakes and streams has become a serious environmental problem in several areas of the world including Scandinavia (Almer et al. 1974; Overrein et al. 1980), parts of Canada (Dillon et al. 1980), and in the northeastern United States (Likens et al. 1979; Driscoll and Newton 1985). Atmospheric deposition of strong acids such as H_2SO_4 and HNO_3 from fossil fuel combustion has been implicated in surface water acidification in the northeastern United States (Likens et al. 1979). Acid-sensitive watersheds in this region generally are underlain by granitic bedrock and have small pools of readily available (exchangeable or easily weatherable) basic cations (Ca^{2+}, Mg^{2+}, Na^+, K^+). These watersheds also have limited capacity to retain strong acidic anions (SO_4^{2-}, NO_3^-); therefore, high loadings of strong acids without a sufficient release of basic cations results in incomplete neutralization and subsequent transport of acidic cations (H^+, metals such as inorganic monomeric aluminum, Al^{n+}) and trace metals (Mn^{2+}, Zn^{2+}) from the soil to surface waters (Baker 1982; Driscoll and Newton 1985).

Increased concentrations of H^+ and trace metals in fresh waters resulting from acidification can be detrimental to all trophic levels (Haines 1981), including benthic invertebrates (Allan and Burton 1986; Allard and Moreau 1986, 1987; Burton et al. 1985; Kimmel et al. 1985; Simpson et al. 1985). There are, however, differences in results between these studies as to the extent of specific invertebrate parameters altered at acidic sites (e.g. total invertebrate density and biomass, feeding group composition and abundance). Lack of agreement between these studies may be a result of several factors: differences in experimental approach, viz. acidification of natural (Hall et al. 1980, 1982, 1985) or artificial (Burton et al. 1985) aquatic systems; comparison of existing acidic and nonacidic aquatic systems (Kimmel et al. 1985; Mackay and Kersey 1985; Simpson et al. 1985); differences in monitoring of water chemistry parameters deemed important in altering benthic parameters, viz. pH only (Kimmel et al. 1985; Mackay and Kersey 1985; Allan and Burton 1986); pH and trace metals, especially aluminum (Hall et al. 1980; Burton et al. 1985; Simpson et al. 1985; Allard and Moreau 1986, 1987). Additionally, species information may vary based on the geographic region studied.

---

[1] Contribution number 93 of the Upstate Freshwater Institute.

[2] Author to whom correspondence should be addressed. Present address: Department of Biology, Valdosta State College, Valdosta, GA 31698, USA.

Clearly then, there is a need for further process-level information of the relationships between acidity and benthic invertebrates as well as an understanding of regional variations in these relationships. Thus, we undertook a year-long study of three low-order woodland streams in the Adirondack Mountain region of New York, an area known to be heavily impacted by atmospheric acid inputs (Driscoll and Newton 1985) and where only a single previous study of low-order streams has been conducted (Simpson et al. 1985). Our objectives were to compare benthic invertebrate parameters between three streams of differing acidity and to examine relationships between stream chemistry and these invertebrate parameters.

Study Sites

The three study streams were located in the western Adirondack Mountains, New York, USA (Fig. 1) and were chosen because they exhibited a continuum in water chemistry parameters such as pH, ANC and Al. Pancake-Hall Creek (43°50′N 74°52′W) generally had the lowest pH and ANC, and highest Al concentrations. Moss Lake Inlet (43°47′N 74°50′W) had intermediate values and Beaver Brook (43°43′N 74°22′W) had highest pH and ANC, and lowest Al concentrations. Watershed areas for Pancake-Hall Creek, Moss Lake Inlet, and Beaver Brook are 74, 220, and 770 ha, respectively.

Watersheds for all three study streams contain primarily second-growth deciduous stands (*Acer saccharum*, *Fagus grandifolia*, *Betula alleghaniensis*) with small, interspersed coniferous stands (*Picea rubens*, *Abies balsamea*, *Tsuga canadensis*). Beaver activity and/or bog conditions are present in portions of each watershed and are characteristic of low-order streams in the Adirondacks.

Sampling sites, like the study streams, were selected based on the relative continuity of their water chemistry parameters (Table 1) and were located in first or second-order reaches of each stream. Three sampling sites were chosen for study in Pancake-Hall Creek. PAT was located at the confluence of two first-order tributaries to Pancake-Hall Creek, PA2 was located immediately downstream of a beaver impoundment and PA3 was furthest downstream (Fig. 1). Moss Lake Inlet had two first-order sampling sites, MO2 and MO3 (Fig. 1). Beaver Brook had three sampling sites. BE1 was situated in a high elevation first-order stream reach; BE2 and BE3 were located in lower elevation second-order stream reaches (Fig. 1). Substrate at each site was similar, consisting primarily of cobbles overlying gravel and sand. Mean current velocities for PAT, PA2, PA3, MO2, MO3, BE1, BE2, and BE3 were 0.21, 0.27, 0.39, 0.35, 0.36, 0.34, 0.39, and 0.37 m · s^{-1}, respectively.

Materials and Methods

Benthic invertebrates were collected quarterly from January to October 1985 using a modified Hess sampler (0.1 m^2;

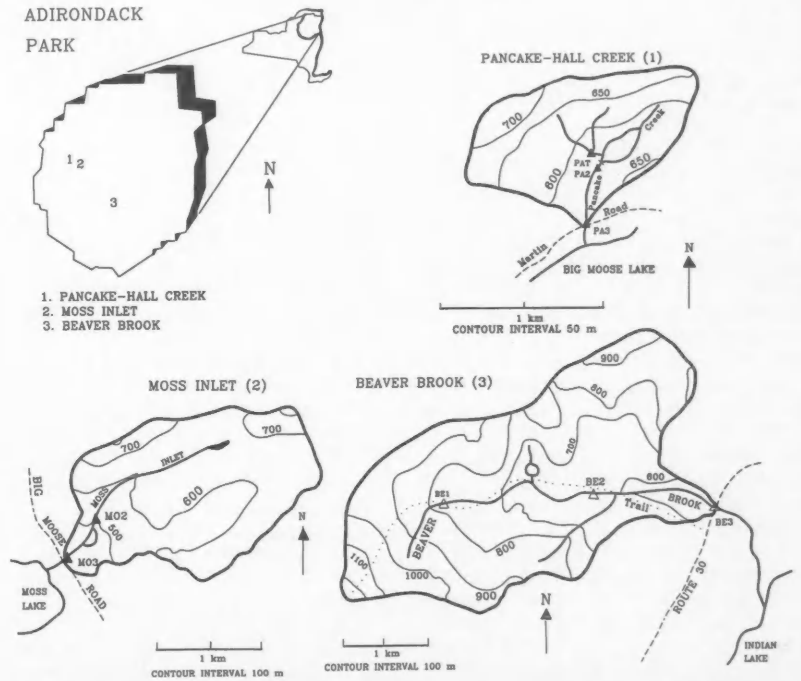

FIG. 1. Adirondack Park showing location of the three streams sampled and individual study streams with sampling sites.

TABLE 1. Analytical methods used in the Adirondack stream study

SO_4^{2-}, NO_3^-, Cl^-	Ion chromatography	Small et al. 1975
NH_4^+	Phenate colorimetry; autoanalyzer	U.S. EPA 1983
Ca^{2+}, Mg^{2+}, K^+, Na^+	Atomic absorption spectrophotometry (AAS)	Slavin 1968
pH	Potentiometrically with glass electrode, field measurement	Standard methods for the analysis of water and wastewater 1985
Acid neutralizing capacity (ANC)	Strong acid titration with Gran plot analysis	Gran 1952
Dissolved organic carbon (DOC)	Filtration, ampulation, persulfate oxidation, syringe stripping of CO_2 and detection by gas chromatography	Menzel and Vaccaro 1964
Dissolved silica	Heteropoly blue complex colorimetry; autoanalyzer	U.S. EPA 1983
Total F	Potentiometrically with ion selective electrode after TISAB addition	Orion instruction manual 1976
Total Al	Acid digestion (1 h, pH 1), 8-hydroxyquinoline extraction into methyl isobutyl ketone (MIBK), analysis by AAS, graphite furnace	Barnes 1976; Driscoll 1984
Monomeric Al	Field extraction by 8-hydroxyquinoline into MIBK, analysis by AAS, graphite furnace	Barnes 1976
Nonlabile monomeric Al	Fractionation by ion exchange column, analysis for monomeric Al	Driscoll 1984
Specific conductance	Conductivity bridge	Standard methods for the analysis of water and wastewater 1985
Fe, Mn, Zn	AAS with graphite furnace	Slavin 1978
Dissolved oxygen	Winkler titration	Standard methods for the analysis of water and wastewater 1985
Temperature	Thermistor	

250-μm mesh size) in shallow riffle areas of comparable substrate type. Five replicates were collected at each site and immediately preserved in 95% ethanol. Invertebrates were handpicked in the laboratory, identified (usually to genus) and counted. Organisms were then assigned to appropriate functional feeding groups using Merritt and Cummins (1984) or by analysis of gut contents. Benthic organic matter (BOM; >250 μm) was measured from samples by loss on combustion (450°C for 24 h) after invertebrates were removed.

Water samples were collected monthly and concurrently with biological samples during quarterly periods for chemical analysis. Twenty-one water chemistry parameters were measured as well as temperature at each sampling site (Table 1). Procedures for water collection and analysis are found in Driscoll et al. (1987). Briefly, water samples were collected from midwater column in acid-washed polyethylene bottles. Samples were measured for temperature in the field. The pH measurements and monomeric Al extractions were conducted on refrigerated samples within 12 h to minimize transformations (e.g. changes in temperature and degassing of CO_2) that might alter these determinations. All other refrigerated water samples were then transported to Syracuse University, stored at 4°C and analyzed as soon as possible, usually within 72 h. Analytical methods used in this study are summarized in Table 1. Aluminum was fractionated using the procedure of Driscoll (1984). Labile monomeric Al is an estimate of inorganic species of aqueous Al. Nonlabile monomeric Al is thought to represent Al complexed with organic solutes.

Two-way analysis of variance (ANOVA) and Duncan's multiple range test (DMRT) were used on unpooled data ($n = 20$) to determine significant differences between sampling sites in density and percentage community composition of invertebrate taxa and functional feeding groups. All DMRT were run at the $P < 0.05$ significance level only. Regression analyses were performed using the least squares method with monthly means to correlate water chemistry with benthic invertebrate parameters. All statistical analyses were done using SAS (SAS Institute Inc. 1985). Density and percentage data were transformed prior to statistical analysis using $\log (x+1)$ (Elliot 1977) and arcsin (Sokal and Rohlf 1981) transformations, respectively, so that parametric statistics could be used. Generic diversity index values were calculated at each site using the machine formula of the Shannon–Weiner index (Weber 1973).

Results

Acid neutralizing capacity (ANC) of all streams was low (less than 150 $\mu eq \cdot L^{-1}$), but only PAT was acidic (mean ANC ≤ 0 $\mu eq \cdot L^{-1}$). Mean pH values were lowest at PAT and highest at BE3. Significant ($P < 0.0001$, $r^2 = 0.34$) correlations

TABLE 2. Yearly means (ranges) of water chemistry parameters from January 1985 to January 1986, except Fe, Mn, and Zn which are from January 1985 to October 1985.

	PAT	PA2	PA3	MO2	MO3	BE1	BE2	BE3
pH	4.9 (4.5–5.8)	5.3 (4.7–5.9)	5.4 (4.7–6.4)	5.4 (4.9–6.1)	5.8 (5.1–6.6)	5.8 (5.0–6.6)	6.2 (5.4–6.9)	6.2 (5.4–7.0)
Acid neutralizing capacity (ANC) (μeq · L^{-1})	−6 (−18–22)	25 (−12–120)	18 (−11–72)	11 (−2–43)	39 (6–142)	32 (−4–131)	47 (3–115)	57 (6–114)
Total monomeric Al (mg Al · L^{-1})	0.52 (0.09–0.91)	0.27 (0.08–0.46)	0.27 (0.08–0.49)	0.20 (0.07–0.45)	0.12 (0.007–0.31)	0.11 (0.01–0.38)	0.06 (0.02–0.14)	0.04 (0.010–0.18)
Labile monomeric Al (mg Al · L^{-1})	0.38 (0.04–0.63)	0.15 (0.03–0.24)	0.14 (0.03–0.30)	0.10 (0.02–0.27)	0.06 (0.002–0.20)	0.05 (0–0.08)	0.007 (0.004–0.18)	0.007 (0.002–0.16)
Nonlabile monomeric Al (mg Al · L^{-1})	0.14 (0.05–0.28)	0.12 (0.06–0.21)	0.12 (0.05–0.19)	0.11 (0.05–0.18)	0.06 (0.01–0.12)	0.06 (0.02–0.29)	0.05 (0.01–0.33)	0.05 (0.01–0.34)
Basic cations (C_B) (μeq · L^{-1})	149 (99–202)	154 (95–200)	164 (109–212)	185 (127–260)	223 (152–306)	195 (151–268)	214 (135–290)	228 (153–287)
SO_4^{2-} (mg SO_4^{2-} · L^{-1})	7.3 (6.7–8.7)	5.6 (2.1–7.9)	5.9 (2.5–7.8)	6.9 (5.3–10.0)	6.8 (4.7–8.5)	6.4 (5.6–7.8)	6.0 (5.0–7.6)	6.2 (5.2–7.5)
NO_3^- (mg NO_3^- · L^{-1})	0.50 (0.09–1.30)	0.28 (0.02–0.92)	0.40 (0.08–1.19)	0.38 (0.07–0.83)	0.45 (0.14–0.85)	0.39 (0–0.94)	0.44 (0–1.02)	0.40 (0–0.92)
Dissolved organic carbon (DOC) (mg C · L^{-1})	3.6 (2.4–4.6)	6.6 (3.7–12.3)	5.9 (3.3–12.0)	4.4 (3.7–6.2)	3.2 (1.9–4.6)	2.0 (0.32–3.0)	2.3 (1.6–3.0)	2.1 (1.5–2.8)
Fe (mg Fe · L^{-1})	0.14 (0.03–0.71)	0.85 (0.23–1.66)	0.38 (0–1.03)	0.08 (0.01–0.16)	0.13 (0.05–0.27)	0.12 (0–0.78)	0.11 (0–0.45)	0.03 (0–0.15)
Mn (mg Mn · L^{-1})	0.08 (0.06–0.19)	0.12 (0.06–0.40)	0.10 (0–0.34)	0.04 (0.007–0.07)	0.05 (0.02–0.11)	0.02 (0–0.05)	0.02 (0.005–0.06)	0.01 (0–0.03)
Zn (mg Zn · L^{-1})	0.05 (0–0.09)	0.06 (0.01–0.31)	0.03 (0–0.09)	0.04 (0.02–0.15)	0.03 (0.003–0.05)	0.03 (0.002–0.05)	0.03 (0.006–0.14)	0.01 (0.003–0.03)

between pH, and ANC, Ca, Al, Mn, and Zn were calculated by combining data from all sampling sites. Thus, water samples with low pH exhibited coincident low Ca and ANC and elevated Al, Mn, and Zn concentrations (Table 2).

ANOVA tests revealed statistically significant ($p<0.001$) differences between sampling sites in density, percentage of total density, generic richness, and percentage of total generic richness for all insect orders and functional feeding groups tested. PA2 had significantly (DMRT, $p<0.05$) higher total density ($6012 \cdot m^{-2}$) than all other sites primarily due to large numbers of Chironomidae. MO2 and MO3 had significantly (DMRT, $p<0.05$) higher total densities than all other sites, except PA2. Beaver Brook (BE1, BE2, BE3) exhibited the lowest total invertebrate densities (Fig. 2).

BE2 and BE3 had significantly (DMRT, $p<0.05$) higher densities of Coleoptera than other sampling sites due to the presence of Elmidae (*Optioservus ovalis*, *Oulimnius latiusculus*, and *Promoresia tardella*). Beetles were absent at MO2 and were present in low densities at other sites, never exceeding a mean yearly density of $32 \cdot m^{-2}$ (Fig. 2). Additionally, Coleoptera represented less than 3% of total invertebrate density at all sites; thus, they were excluded from percentage of total density analyses. Elmidae were collected only at Beaver Brook sites. Dytiscid beetles, *Agabus*, *Hydaticus*, and *Oreodytes*, were present at all sampling sites.

Diptera were present in high densities at most sites and represented at least 30% of total invertebrate density at each site (Figs. 2 and 3). Chironomidae were the dominant Diptera; the fauna consisted of Orthocladiinae, Chironomini, Tanytarsini, and Tanypodinae. Simuliidae (*Simulium*, *Prosimulium*), Ceratopogonidae, Empididae (*Chelifera*, *Oreogeton*), Chironomidae, and Tipulidae (*Antocha*, *Dicranota*, *Limnophila*, *Ormosia*) were present at all sites including PAT.

Ephemeroptera were absent at PAT and represented a significantly higher (DMRT, $p<0.05$) percentage of total density at BE2 and BE3 compared with other sites (Figs. 2 and 3). Ephemeroptera collected from other sampling sites included *Ephemerella (Eurylophella) funeralis*, *Epeorus*, *Cinygmula*, *Baetis*, *Ameletus*, and *Leptophlebia*. *Ephemerella* were collected at all sites except PAT and PA2 where minimum pH values were as low as 4.7 and labile monomeric Al concentrations as high as 0.30 mg Al · L^{-1}. *Cinygmula* and *Baetis* were collected only at Beaver Brook (BE2, BE3) sites where mean (minimum) pH values were 6.2(5.4), and 6.2(5.4) for BE2 and BE3, respectively. Additionally, Al concentrations were low at BE2, BE3 (Table 2).

Density of Plecoptera was significantly higher (DMRT, $p<0.05$) at MO2 and MO3 (Fig. 2), reaching densities of 1980 and $1730 \cdot m^{-2}$, respectively. The percentage of total density represented by Plecoptera showed highest values at sites of intermediate pH (Fig. 3). *Peltoperla arcuata*, *Strophopteryx*, and *Acroneuria* were collected in low densities from Beaver Brook sites only. Nemourid stoneflies (*Amphinemura*, *Ostrocerca*) were present at all sites, as were *Leuctra* and *Suwallia*/*Sweltsa*. *Leuctra* was the dominant stonefly at all sites.

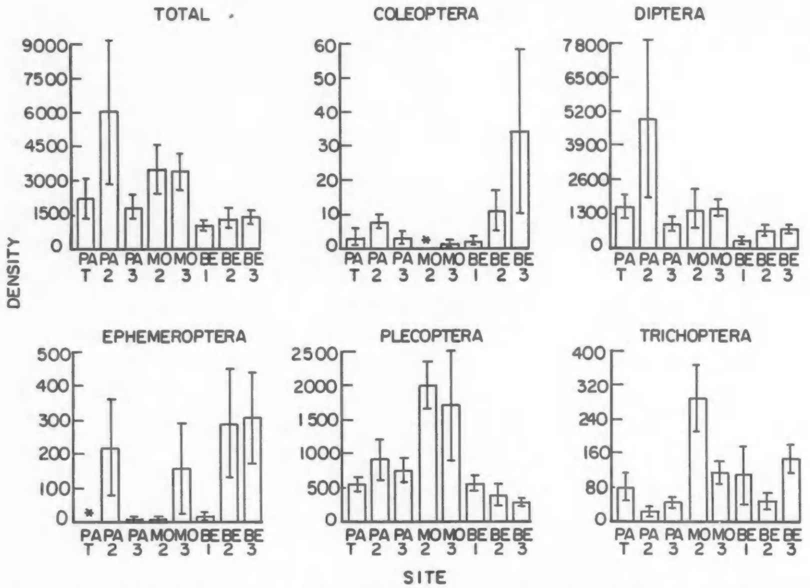

FIG. 2. Mean density (numbers · m^{-2}) for total invertebrates and insect orders collected at each sampling site over the study period. Data are overall means from means of each sampling period, $N = 4$. Error bars represent ± 1 SE. * = no organisms collected.

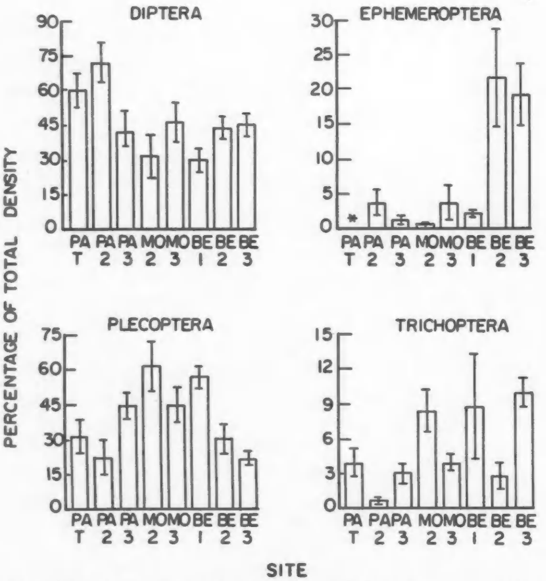

FIG. 3. Mean percentage of total invertebrate density represented by the insect orders at each sampling site. Data are overall means from means of each sampling period, $N = 4$. Error bars are ± SE. * = no organisms collected.

Trichoptera mean yearly density never exceeded 286 · m^{-2}, and did not represent more than 10% of total density at any site (Figs. 2 and 3). Many caddisflies were collected at PAT and thus, were tolerant of acidic conditions. These included *Cyrnellus fraternus, Polycentropus, Parapsyche apicalis, Rhyacophila, Palaeagapetus celsus, Oligostomis ocelligera, Lepidostoma, Hydatophylax*, and *Psilotreta*. The hydrospsychid caddisflies *Hydropsyche* and *Diplectrona modesta* were collected at all sites except PAT. *Glossosoma, Apatania*, and *Micrasema* were collected in high densities and *Pycnopsyche* and *Triaenodes* in low densities only at Beaver Brook sites.

Non-insect fauna also exhibited differences in density between sampling sites. Turbellaria density was significantly higher (DMRT, $p<0.05$) at PAT than other sites. Oligochaeta were collected at all sites and included the families Naididae, Enchytraeidae, and Lumbriculidae, but differences existed between sampling sites in composition of the oligochaete fauna. Naididae were absent from PAT, but were present at all other sites. Species collected at other sites included *Chaetogaster diastrophus, Nais communis, Nais elinguis, Nais simplex, Nais variabilis, Pristina aequiseta*, (morph *foreli*), *Pristina leidyi, Pristinella osborni, Pristinella jenkinae, Slavina appendiculata, Specaria josinae*, and *Vejdovskyella comata*. Enchytraeidae were present at all sites, but significantly higher (DMRT, $p<0.05$) densities were collected at PAT.

Total generic richness (excluding Chironomidae) was depressed at low pH sites (Fig. 4). PA2 richness was significantly lower (DMRT, $p<0.05$) than other sites. Beaver Brook sites had a significantly (DMRT, $p<0.05$) lower percentage of total richness represented by Diptera and significantly (DMRT, $p<0.05$) higher percentage of Ephemeroptera, (BE2, BE3 only) compared with other sampling sites (Fig. 4). Pancake-Hall Creek sites showed few differences from other sites except for an absence of Ephemeroptera at PAT and a significantly ($p<0.05$) reduced proportion of total fauna represented by Plecoptera and Trichoptera at PA2 (Fig. 4).

Collector–filterer density, percentage of total density, and percentage of total generic richness were highest at sites of intermediate pH (PA3, MO2, MO3) (Figs. 5, 6, and 7).

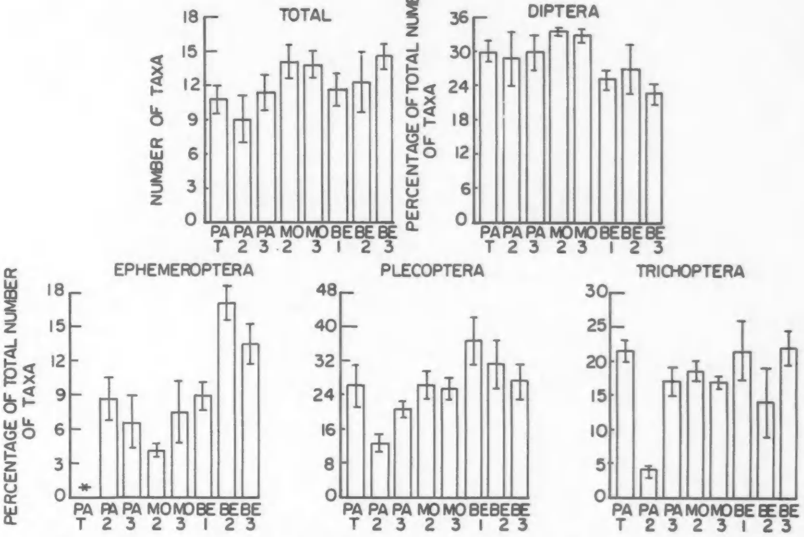

Fig. 4. Mean generic richness (excluding Chironomidae) for total invertebrates and mean percentage of total richness represented by insect orders. Diptera values are excluding Chironomidae. Data are overall means from means of each sampling period, $N=4$. Error bars are ± 1 SE. * = no organisms collected.

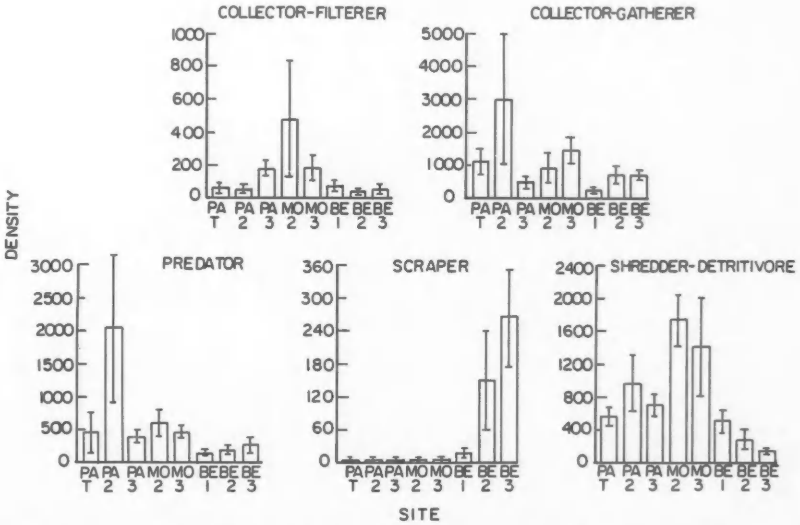

Fig. 5. Mean density (numbers · m^{-2}) of insect feeding groups collected at each sampling site. Data are overall means from means of each sampling period, $N=4$. Error bars represent ± SE.

Collector–gatherer percentage of total density was significantly (DMRT, $p<0.05$) less at PA3, MO2, and BE1 compared with other sites, representing 24, 21, and 25%, respectively (Fig. 6). Alternatively, collector–gatherer percentages were 49% at BE3 and 50% at BE2. The percentage of total richness represented by collector–gatherers at the acidic site, PAT, was significantly (DMRT, $p<0.05$) less than at other sampling sites. The percentage of total richness represented by predators was significantly (DMRT, $p<0.05$) less at Beaver Brook sites compared with other sites (Fig. 7). Scrapers were present in significantly (DMRT, $p<0.05$) greater abundance and richness at Beaver Brook sites (BE2, BE3); Pancake-Hall Creek and Moss Lake Inlet had low scraper density, percentage of total density, and percentage of total richness (Figs. 5, 6, and 7). Scraper importance increased at downstream sites (i.e. BE3>BE2>BE1) in Beaver Brook. Shredder–detritivore density was highest at sites

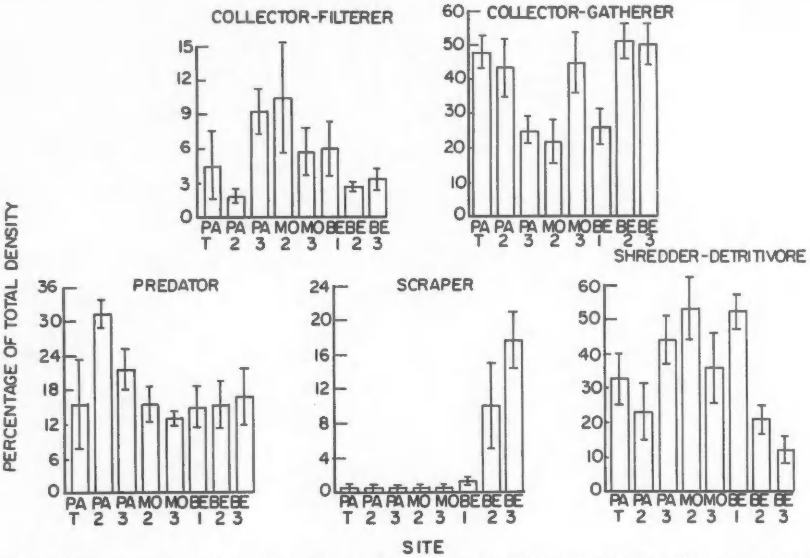

FIG. 6. Mean percentage of total invertebrate density represented by each insect feeding group. Data are overall means from means of each sampling period, $N=4$. Error bars are ±SE.

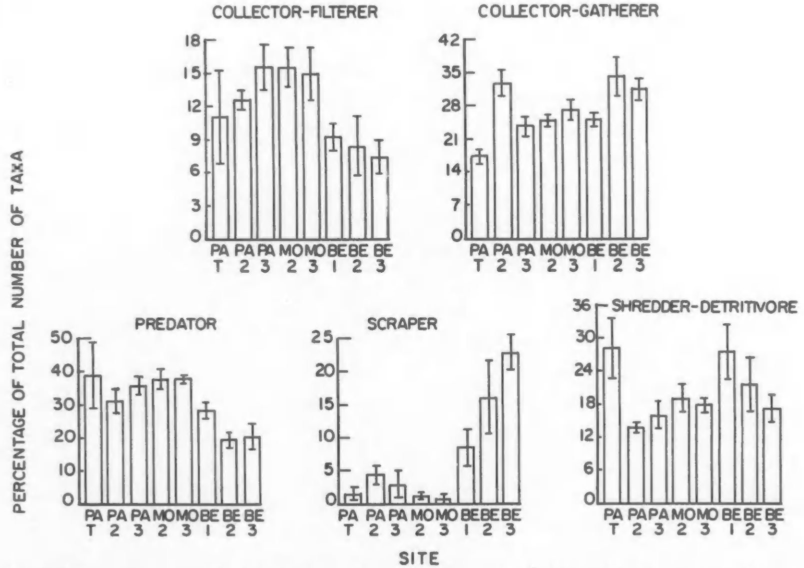

FIG. 7. Mean percentage of total generic richness represented by each insect feeding group. Data are overall means from means of each sampling period, $N=4$. Error bars are ±SE.

MO2 ($1786 \cdot m^{-2}$) and MO3 ($1520 \cdot m^{-2}$); significant (DMRT, $p<0.05$) differences existed between MO2 and MO3 and all other sites (Fig. 5). The percentage of total density represented by shredder–detritivores was higher at some sites, representing 54, 52, and 44% at sites MO2, BE1, and PA3 respectively. These sites had significantly (DMRT, $p<0.05$) higher percentages than all other sites. The percentage of total richness represented by shredder–detritivores was significantly (DMRT, $p<0.05$) higher at PAT, (27%) and BE1 (26%) when compared with the other sampling sites.

Ephemeroptera density ($p<0.0001$, $r^2=0.52$), percentage of total density ($p<0.0001$, $r^2=0.50$), richness ($p<0.0001$, $r^2=0.58$), and percentage of total richness ($p<0.0001$, $r^2=0.38$) were all positively correlated to stream pH (Fig. 8). Total richness also showed a significant ($p<0.0001$, $r^2=0.29$) positive correlation to stream pH (Fig. 8).

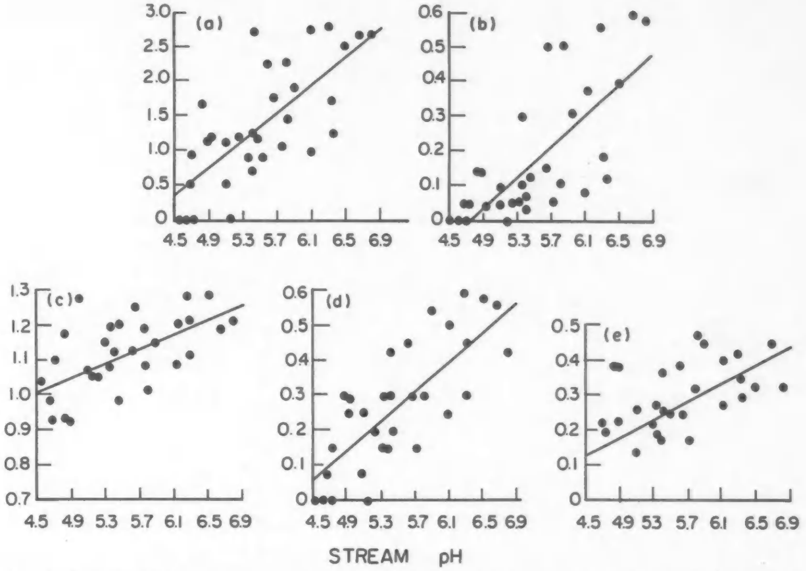

FIG. 8. Relationship between stream pH and five invertebrate community parameters. (a) Density (numbers · m^{-2}) of Ephemeroptera, $y=1.00x-4.16$, $r^2=0.52$, $p<0.0001$. (b) Percentage of total density represented by Ephemeroptera, $y=0.21x-0.98$, $r^2=0.50$, $p<0.0001$. (c) Total number of taxa, $y=0.09x+0.65$, $r^2=0.29$, $p<0.001$. (d) Number of Ephemeroptera taxa, $y=0.21x-0.89$, $r^2=0.58$, $p<0.0001$. (e) Percentage of total number of taxa represented by Ephemeroptera, $y=0.13x-0.46$, $r^2=0.38$, $p<0.001$. Data are means of monthly samplings.

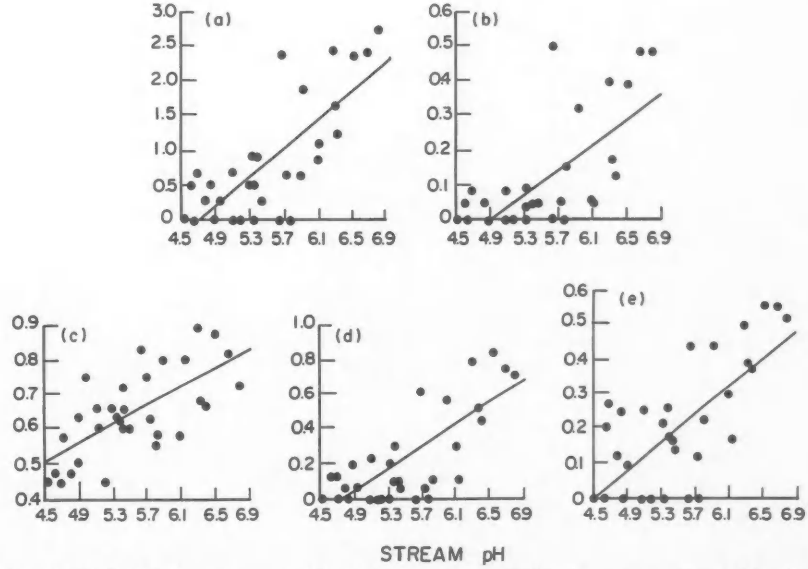

FIG. 9. Relationship between stream pH and five invertebrate feeding group parameters. (a) Density (numbers · m^{-2}) of scrapers, $y=1.05x-4.96$, $r^2=0.58$, $p<0.0001$. (b) Percentage of total density represented by scrapers, $y=0.18x-0.88$, $r^2=0.48$, $p<0.0001$. (c) Number of collector–gatherer taxa, $y=0.13x-0.09$, $r^2=0.43$, $p<0.0001$. (d) Number of scraper taxa, $y=0.32x-1.50$, $r^2=0.56$, $p<0.0001$. (e) Percentage of total taxa represented by scrapers, $y=0.20x-0.88$, $r^2=0.47$, $p<0.0001$. Data are means of monthly samplings.

TABLE 3. Results of stepwise multiple regression analyses on invertebrate density for which regression models accounted for at least 40% of variation in invertebrate parameters. BOM = benthic organic matter >250 μm, DIC = dissolved inorganic carbon.

Density	Environmental parameter	Cumulative percent variation explained	Probability	Relationship
Total Invertebrates	BOM	60.5	<0.0001	Positive
Diptera	BOM	60.1	<0.0001	Positive
Ephemeroptera	pH	52.1	<0.0001	Positive
Plecoptera	BOM	45.7	<0.0001	Positive
	Nonlabile monomeric Al	50.8	0.0918	Positive
	DIC	57.3	0.0490	Negative
Trichoptera	DIC	12.7	0.0451	Negative
	SO_4^{2-}	43.8	0.0141	Positive
Collector–gatherer	BOM	45.3	<0.0001	Positive
Predator	BOM	58.1	<0.0001	Positive
Scraper	pH	57.9	<0.0001	Positive
	Labile monomeric Al	65.2	0.0198	Negative
	Nonlabile monomeric Al	71.0	0.0255	Negative
	BOM	74.9	0.0483	Negative
Shredder–Detritivore	BOM	42.0	<0.0001	Positive
	Nonlabile monomeric Al	53.6	0.0120	Positive

TABLE 4. Results of stepwise multiple regression analyses on number of invertebrate taxa for which regression models accounted for at least 40% of variation in invertebrate parameters. BOM = benthic organic matter >250 μm, DIC = dissolved inorganic carbon, C_B = basic cations.

Number of taxa	Environmental parameter	Cumulative percent variation explained	Probability	Relationship
Total Diptera	BOM	29.7	0.0013	Positive
	DIC	66.9	<0.0001	Negative
	C_B	68.7	0.2180	Positive
	Nonlabile monomeric Al	75.8	0.0088	Positive
Ephemeroptera	pH	57.5	<0.0001	Positive
Plecoptera	DIC	41.6	<0.0001	Negative
Trichoptera	DIC	19.4	0.0117	Negative
	SO_4^{2-}	44.7	0.0011	Positive
Collector–Gatherer	pH	43.4	<0.0001	Positive
	Nonlabile monomeric Al	52.6	0.0251	Negative
Predator	BOM	35.6	0.0003	Positive
	DIC	53.7	0.0021	Negative
Scraper	pH	55.5	<0.0001	Positive
	BOM	64.4	0.0116	Negative
	Labile-monomeric Al	69.0	0.0508	Negative
	Nonlabile monomeric Al	73.2	0.0443	Negative

Scraper density ($p<0.0001$, $r^2=0.58$), percentage of total density ($p<0.0001$, $r^2=0.48$), richness ($p<0.0001$, $r^2=0.56$) and percentage of total richness ($p<0.0001$, $r^2=0.47$) were all positively correlated to stream pH (Fig. 9). Collector–gatherer richness also exhibited a significant ($p<0.0001$, $r^2=0.43$) positive correlation to stream pH (Fig. 9).

Benthic organic matter and pH were the most important environmental parameters correlated to invertebrate density and richness (Tables 3 and 4). Benthic organic matter and pH were the environmental variables that generally explained most of the variation in invertebrate parameters from the multiple regression models.

Diversity index values also exhibit significant positive correlations to stream pH for all dates combined ($p<0.01$, $r^2=0.22$) (Fig. 10) and during each quarterly sampling period: January ($p<0.0001$, $r^2=0.86$), April ($p<0.05$, $r^2=0.16$), July ($p<0.0001$, $r^2=0.83$), October ($p<0.001$, $r^2=0.32$).

Discussion

PAT was the only acidic site in our study (ANC ≤ 0 $\mu eq \cdot L^{-1}$). This site had lowest pH, C_B and highest concentrations of monomeric Al; these conditions can potentially limit invertebrate populations (see review by Haines 1981). Labile monomeric Al concentrations were elevated at PAT. This Al fraction has been

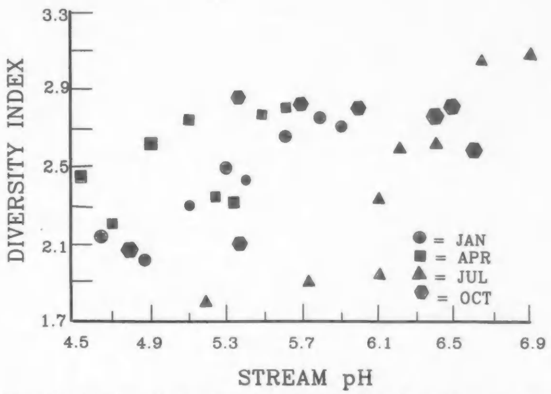

FIG. 10. Relationship between invertebrate diversity and stream pH. All sampling dates combined, $y=0.26x+0.98$, $r^2=0.22$, $p<0.01$. January samplings only, $y=0.54x-0.45$, $r^2=0.86$, $p<0.0001$. April samplings only, $y=0.25x+1.26$, $r^2=0.16$, $p<0.05$. July samplings only, $y=0.87x-2.96$, $r^2=0.83$, $p<0.0001$. October samplings only, $y=0.29x+0.91$, $r^2=0.32$, $p<0.001$. Data are means of monthly samplings.

implicated in toxicity to aquatic organisms (Driscoll et al. 1980). pH was correlated to ANC, C_B, Al, Mn, and Zn in our study; therefore, it follows that correlations of various invertebrate parameters with pH also correlate to these water chemistry parameters.

Total invertebrate density was not significantly (DMRT, $p<0.05$) lower at our acidic site (PAT) when compared with most other sites. Only one other study (Simpson et al. 1985) has shown similar results from natural stream systems, although it should be noted that this study was only conducted during summer (two samplings, July and September).

Contradictory observations regarding the relationship between total invertebrate density and pH have been reported by Kimmel et al. (1985) and Townsend et al. (1983). Townsend et al. (1983) sampled 34 streams in England once during October only. They correlated pH to total invertebrate density. The study by Kimmel et al. (1985) was a year-long quarterly sampling of Pennsylvania streams. Water chemistry analyses were not complete; they measured only pH. Trace metals, notably Al, were not measured and may contribute to changes in invertebrate communities (Haines 1981). Thus, comparisons between our study and the results of Kimmel et al. (1985) are tenuous.

Generic richness and diversity were correlated with pH in our study, but were not significantly ($p>0.05$) lower at PAT than most of the sites. Other studies have shown decreased richness and diversity at low pH sites (Kimmel et al. 1985; Mackay and Kersey 1985; Townsend et al. 1983; Simpson et al. 1985) for streams in Europe and North America. Site PA2 had significantly (DMRT, $p<0.05$) lower invertebrate richness and diversity than other sampling sites and is presumably due to its location downstream of a beaver impoundment. Humic material often covered the substrate at this site and discharge regimes may have differed from other sites. Additionally, Fe, Mn, and Zn concentrations were highest at this site.

Ephemeroptera were absent at our acidic sampling site (PAT). Mayflies are sensitive to acidification, exhibiting either reduced density, diversity, or richness (Sutcliffe and Carrick 1973; Fiance 1978; Friberg et al. 1980; Townsend et al. 1983; Aston et al. 1985; Mackay and Kersey 1985; Peterson et al. 1985; Simpson et al. 1985) at sites with low pH. Our study indicates that *Baetis* and certain heptageniid mayflies (*Cinygmula*) are only found in streams with higher pH (annual minimum $\geqslant$5.4). *Baetis* is reported to be intolerant of low pH (Sutcliffe and Carrick 1973; Fiance 1978; Aston et al. 1985; Peterson et al. 1985; Simpson et al. 1985). Ours is the first report of *Cinygmula* distribution relative to pH and other water chemistry parameters such as ANC, C_B, Al, Mn, and Zn. *Ephemerella (Eurylophella) funeralis* was the mayfly most tolerant of lower pH in our study streams. *Ephemerella funeralis* has been collected at acidic sites (pH 4.9; Fiance 1978) and other locations where pH ranged from 5.3–6.2 (Mackay and Kersey 1985), or where pH values were never below 5.5 (Simpson et al. 1985). The study by Simpson et al. (1985) was the only one of these to monitor Al concentrations; labile (inorganic) monomeric Al concentrations never exceeded 0.04 mg $\mathrm{Al \cdot L^{-1}}$ at the site where *Ephemerella funeralis* were collected. *Ephemerella funeralis* were found at lower pH in our study (4.7) and at labile (inorganic) monomeric Al concentrations of 0.30 mg $\cdot$ $\mathrm{L^{-1}}$.

Elmid beetles were only present in neutral pH, Beaver Brook. Townsend et al. (1983) could find no correlation of elmid density to stream pH in English streams. Conversely, Simpson et al. (1985) collected *Oulimnius latiusculus* from a site where pH values were always above 5.5 and labile (inorganic) monomeric Al concentrations never exceeded 0.04 mg $\mathrm{Al \cdot L^{-1}}$, *O latiusculus* was not found at sites with lower pH and higher Al concentrations.

Plecoptera were generally well represented at all our sampling sites. *Leuctra* were abundant at several sites, including PAT. *Leuctra* have been abundant at acidic sites in other studies also (Townsend et al. 1983; Simpson et al. 1985). *Peltoperla arcuata*, *Strophopteryx* and *Acroneuria* were the Plecoptera least tolerant of low pH in our study, they were only collected at Beaver Brook sites. Kimmel et al. (1985) collected *Peltoperla sp.* from a neutral pH (6.1–7.4) site only; the same stonefly was absent from the low pH site (values ranging from 4.6–6.0). Ours are the first data for the distribution of *Strophopteryx* and *Acroneuria* relative to pH and concomitant water chemistry parameters. Trichoptera were collected from all sites in our study, but distribution differences existed between genera. Several genera were only present at our high pH sites and seem to be intolerant of lower pH conditions. (e.g. *Glossosoma, Apatania, Pycnopsyche, Micrasema, Triaenodes*). *Hydropsyche sp.* and *Diplectrona modesta*, both hydropsychid caddisflies, may be good indicators of acidic conditions as they were present at all sites except our acidic site, PAT. Many of the Trichoptera collected in our study were also present in the Hubbard Brook Experimental Forest in New Hampshire where low-order acidic streams are numerous (McConnochie and Likens 1969).

Turbellaria were tolerant of low pH in our study. No other data exist on the response of this group to pH but it appears they can reach significantly higher densities in acidic streams. Naidid oligochaetes were absent from our acidic site; conversely, Enchytraeidae were present at all sites and in significantly higher densities at PAT, reflectng their tolerance to acidic conditions. Little is known of the response of Naididae to low pH. Simpson et al. (1985) collected only one species, *Nais elinguis*, in low numbers (1) at sites of low ANC (-40 to -15 $\mu\mathrm{eq \cdot L^{-1}}$) and pH values of 4.4–4.7. Enchytraeidae were also collected by Simpson et al. (1985) and have been found in acidic waters (Stephenson 1930). Based on findings in our study, these non-insect groups may be excellent indicators of acidity and should be carefully examined in future research. Collection of oligochaetes may be facilitated by using a small mesh net (≤250 μm maximum size) due to their small size.

Collector–filterer richness, density and percentage of total density were found by Townsend et al. (1983) and Townsend and Hildrew (1984) to be positively correlated with stream pH. We found that collector–filterer parameters were not correlated to stream pH or other stream chemical factors; rather, this feeding group was most abundant and comprised the greatest percentage of total richness at sites of intermediate pH. Perhaps increased filterer abundance at MO2 and MO3 was a result of factors not measured in our study, such as transported particulate organic matter and not directly related to water chemistry. Collector–gatherer richness was positively correlated with stream pH in our study. Similar results have been observed by Townsend et al. (1983). Predators were well represented at all sites in our study, including the acidic site, PAT. Townsend et al. (1983) found that predator richness was positively correlated with stream pH; these findings were coincident with a positive correlation of total invertebrate density (potential prey) to stream pH. Thus, decreases in predator parameters such as richness may be more a reflection of prey availability then response to low pH and concomitant water variables. In our study, we did not observe significant decreases in total invertebrate density or predator community parameters at PAT when compared with most other sites.

Decreases in scraper communities have been documented for acidic streams (Sutcliffe and Carrick 1973; Townsend et al. 1983; Townsend and Hildrew 1984; Winterbourn et al. 1985). We found several scraper community parameters to be positively correlated with stream pH. Shredder–detritivores were one of the most dominant feeding groups along with collector–gatherers at most sites in our study, which is typical of low-order woodland streams in North America (Vannote et al. 1980). Increases in shredder abundance is often evident with decreasing pH (Friberg et al. 1980; Townsend et al. 1983; Townsend and Hildrew 1984) and often shredders are dominant in acidic streams (Simpson et al. 1985).

Multiple regression analyses revealed several stream parameters which were correlated to invertebrate density and/or richness. Benthic organic matter (BOM, >250 μm) was correlated with several orders and functional feeding groups such as total invertebrates, Diptera, Plecoptera, collector–gatherers, predators, and shredder–detritivores. This stream parameter is seldom monitored but may be involved with invertebrate distribution or abundance patterns as noticed in our study. Ephemeroptera, collector–gatherers, and scrapers were correlated with pH and Al concentrations, both of which appear to be toxic to aquatic invertebrates and as such may limit their distribution or abundance in stream systems (Bell and Nebeker 1969; Bell 1971; Hall et al. 1980; Cook and Haney 1984; France 1984; Hall et al. 1985).

Acknowledgments

This study was funded by the Electric Power Research Institute as part of the aluminum stream study (ALSS). We would like to thank Dr. and Mrs. Steinhauser and the Big Moose Lake Association for their cooperation, and J. Elwood and D. Porcella for their encouragement in this investigation.

References

ALLAN, J. W., AND T. M. BURTON. 1986. Size-dependent sensitivity of three species of stream invertebrates to pH depression, p. 54–66. *In* B. G. Isom, S. D. Dennis, and J. M. Bates [ed.] Impact of acid rain and deposition on aquatic biological systems, ASTM STP 928. American Society for Testing and Materials, Philadelphia, PA.

ALLARD, M., AND G. MOREAU. 1986. Influence of acidification and aluminum on the density and biomass of lotic benthic invertebrates. Water Air Soil Pollut. 30: 673–679.

1987. Effects of experimental acidification on a lotic macroinvertebrate community. Hydrobiologia 144: 37–49.

ALMER, B., W. DICKSON, C. EKSTRÖM, E. HORNSTRÖM, AND U. MILLER. 1974. Effects of acidification on Swedish Lakes. Ambio 3: 30–36.

ASTON, R. J., K. SADLER, A. G. P. MILNER, AND S. LYMAN. 1985. The effects of pH and related factors on stream invertebrates. Cent. Elect. Gen. Board, England. TPRD/L/2792/N84:8 p.

BAKER, J. P. 1982. Effects on fish of metals associated with acidification, p. 165–176. *In* R. E. Johnson [ed.] Acid rain/fisheries. American Fisheries Society, Bethesda, MD.

BARNES, R. B. 1976. The determination of specific forms of aluminum in natural waters. Chem. Geol. 15: 177–191.

BELL, H. L. 1971. Effect of low pH on the survival and emergence of aquatic insects. Water Res. 5: 313–319.

BELL, H. L., AND A. V. NEBEKER. 1969. Preliminary studies on the tolerance of aquatic insects to low pH. J. Kans. Entomol. Soc. 42: 230–236.

BURTON, T. M., R.M. STANFORD, AND J. W. ALLAN. 1985. Acidification effects on stream biota and organic matter processing. Can. J. Fish. Aquat. Sci. 42: 669–675.

COOK, W., AND J. HANEY. 1984. The acute effects of aluminum and acidity upon nine stream insects. Tech. Comp. Rep. 46, Water Resource Research Center, University of New Hampshire, Durham, NH. 33 p.

DILLON, P. J., D. S. JEFFRIES, W. A. SCHEIDER, AND N. D. YAN. 1980. Some aspects of acidification in southern Ontario, p. 212–213. *In* D. Drablos and A. Tollan [ed.] Ecological impact of acid precipitation. SNSF Project, Oslo, Norway.

DRISCOLL, C. T. 1984. A procedure for the fractionation of aqueous aluminum in dilute acidic waters. Int. J. Environ. Anal. Chem. 16: 267–284.

DRISCOLL, C. T., J. P. BAKER, J. J. BISOGNI, AND C. L. SCHOFIELD. 1980. Effects of aluminum speciation on fish in dilute, acidified waters. Nature (Lond.) 284: 161–164.

DRISCOLL, C. T., AND R. M. NEWTON. 1985. Chemical characteristics of Adirondack Lakes. Environ. Sci. Technol. 19: 1018–1024.

DRISCOLL, C. T., B. J. WYSKOWSKI, C. C. COSENTINI, AND M. E. SMITH. 1987. Processes regulating temporal and longitudinal variations in chemistry of a low-order woodland stream in the Adirondack region of New York. Biogeochemistry 3: 225–241.

ELLIOT, J. M. 1977. Some methods for the statistical analysis of samples of benthic invertebrates. Freshwater Biol. Assoc. Sci. Pub. 25. 2nd ed. Freshwater Biological Association, Ambleside, UK. 160 p.

FIANCE, S. B. 1978. Effects of pH on the biology and distribution of *Ephemerella funeralis* (Ephemeroptera). Oikos 31: 332–339.

FRANCE, R. L. 1984. Comparative tolerance to low pH of three life stages of the crayfish *Orconectes virilis*. Can. J. Zool. 62: 2360–2363.

FRIBERG, F. C., C. OTTO, AND B. SVENSSON. 1980. Effects of acidification on the dynamics of allochthonous leaf material and benthic invertebrate communities in running waters, p. 304–305. *In* D. Drablos and A. Tollan [ed.] Ecological impact of acid precipitation. SNSF Project, Oslo, Norway.

GRAN, G. 1952. Determination of the equivalence point in potentiometric titration. Int. Congress Analyt. Chem. 77: 661–671.

HAINES, T. 1981. Acidic precipitation and its consequences for aquatic ecosystems: a review. Trans. Am. Fish. Soc. 110: 669–707.

HALL, R. J., C. T. DRISCOLL, G. E. LIKENS, AND J. M. PRATT. 1985. Physical, chemical, and biological consequences of episodic aluminum additions to a stream. Limnol. Oceanogr. 30: 212–220.

HALL, R. J., G. E. LIKENS, S. B. FIANCE, AND G. R. HENDREY. 1980. Experimental acidification of a stream in the Hubbard Brook Experimental Forest, New Hampshire. Ecology 61: 976–989.

HALL, R. J., J. M. PRATT, AND G. E. LIKENS. 1982. Effects of experimental acidification on macroinvertebrate drift diversity in a mountain stream. Water Air Soil Pollut. 18: 273–287.

KIMMEL, W. G., D. J. MURPHEY, W. E. SHARPE, AND D. R. DEWALLE. 1985. Macroinvertebrate community structure and detritus processing rates in two southwestern Pennsylvania streams acidified by atmospheric deposition. Hydrobiologia 124: 97–102.

LIKENS, G. E., R. F. WRIGHT, J. N. GALLOWAY, AND T. J. BUTLER. 1979. Acid rain. Sci. Am. 241: 43–51.

MACKAY, R. J., AND K. E. KERSEY. 1985. A preliminary study of aquatic insect communities and leaf decomposition in acid streams near Dorset, Ontario. Hydrobiologia 122: 3–11.

McConnochie, K., and G. E. Likens. 1969. Some Trichoptera of the Hubbard Brook Experimental Forest in central New Hampshire. Can. Field-Nat. 83: 147–154.

Menzel, D. W., and R. F. Vaccaro. 1964. The measurement of dissolved organic and particulate carbon in seawater. Limnol. Oceanogr. 9: 138–142.

Merritt, R. W., and K. W. Cummins [ed.]. 1984. An introduction to the aquatic insects of North America. 2nd ed. Kendall/Hunt Publishing Company, Dubuque, Iowa, 722 p.

Orion Instruction Manual. 1976. Fluoride electrodes. Orion Research Inc., Cambridge, Massachusetts. 35 p.

Overrein, L. N., H. M. Seip, and A. Tollan. 1980. Acid precipitation — effects on forest and fish. Final report of the SNSF Project 1972-1980. SNSF Research Report 19/80, Oslo, Norway.

Peterson, R. H., D. J. Gordon, and D. J. Johnston. 1985. Distribution of mayfly nymphs (Insecta: Ephemeroptera) in some streams of eastern Canada as related to stream pH. Can. Field-Nat. 99: 490–493.

SAS Institute, Inc. 1985. SAS user's guide: statistics. SAS Institute, Inc., Cary, NC.

Simpson, K. W., R. W. Bode and J. R. Colquhoun. 1985. The macroinvertebrate fauna of an acid-stressed headwater stream system in the Adirondack Mountains, New York. Freshwater Biol. 15: 671–681.

Slavin, W., 1968. Atomic absorption spectroscopy. John Wiley Interscience, New York.

Small, H., T. S. Stevens, and W. C. Bauman. 1975. Novel ion exchange chromatographic method using conductimetric detection. Analyt. Chem. 47: 1801–1809.

Sokal, R. R., and F. J. Rohlf. 1981. Biometry: the principles and practice of statistics in biological research. 2nd ed. W. H. Freeman and Company, San Francisco, CA. 859 p.

Standard Methods for the Analysis of Water and Wastewater. 1985. 16th ed. American Public Health Association, Washington D. C. 1192 p.

Stephenson, J. 1930. The Oligochaeta. Clarendon Press, Oxford, 978 p.

Sutcliffe, D. W., and T. R. Carrick. 1973. Studies on mountain streams in the English Lake District. I. pH, calcium and the distribution of invertebrates in the River Duddon. Freshwater Biol. 3: 437–462.

Townsend, C. R., and A. G. Hildrew. 1984. Longitudinal pattern in detritivore communities of acid streams: a consideration of alternative hypotheses. Verh. Int. Ver. Limnol. 22: 1953–1958.

Townsend, C. R., A. G. Hildrew, and J. Francis. 1983. Community structure in some southern English streams: the influence of physicochemical factors. Freshwater Biol. 13: 521–544.

U.S. EPA. 1983. Methods for chemical analysis of water and wastes. Environmental Monitoring and Support Laboratory, Cincinnati, Ohio. EPA-600/4-79-020.

Vannote, R. L., G. W. Minshall, K. W. Cummins, J. R. Sedell, and C. E. Cushing. 1980. The river continuum concept. Can. J. Fish. Aquat. Sci. 37: 130–137.

Weber, C. I. [ed.] 1973. Biological field and laboratory methods for measuring the quality of surface waters and effluents. EPA-670/4-73-001. United States Environmental Protection Agency, Cincinnati, OH.

Winterbourn, M. J., A. G. Hildrew, and A. Box. 1985. Structure and grazing of stone surface organic layers in some acid streams of southern England. Freshwater Biol. 15: 363–374.

Estimating the Density and Mortality of Juvenile Western Rock Lobsters (*Panulirus cygnus*) in Nursery Reefs

Bruce F. Phillips

CSIRO Marine Laboratories, Division of Fisheries, P.O. Box 20, North Beach, W.A. 6020, Australia

Phillips, B.F. 1990. Estimating the density and mortality of juvenile western rock lobsters (*Panulirus cygnus*) in nursery reefs. Can. J. Fish. Aquat. Sci. 47: 1330–1338.

Studies of juvenile rock lobsters (*Panulirus cygnus*) in the nursery reefs of Western Australia indicated that density-dependent processes on the reefs were the major determinant of year-class strengths of recruitment to the fishery. Reassessment of early data, plus additional information, indicates that these estimates may have been inaccurate. Alternative methods of estimating juvenile densities were examined; application of length–frequency analysis to calculate the age-classes; visual estimates, and single-night trapping. Length–frequency analysis indicated that either immigration onto the test reefs had occurred, or the data were inaccurate. Visual estimates and single-night trapping were more rapid and used less manpower and resources than mark–recapture methods, but the estimates were of unknown accuracy. No truly satisfactory method of making reliable estimates of either the density of natural mortality rate of juveniles in the nursery reefs is yet available. Nevertheless, the data on the levels of larval settlement and subsequent catches, suggest that density dependent processes probably have a significant effect on the levels of recruitment to the fishery, although the upper level to this recruitment has not been reached over the past 20 yrs.

Des études sur les langoustes juvéniles dans les récifs nourriciers de l'Australie-Occidentale ont montré que des processus dépendant de la densité dans les récifs étaient le principal déterminant des effectifs des classes annuelles exploitables. Une réévaluation des premières données, plus d'autres informations, indiquent que ces estimations ont pu être imprécises. D'autres méthodes d'estimation des densités de juvéniles ont été étudiées: l'analyse de la fréquence des longueurs pour calculer les classes d'âge; les estimations visuelles et les prises au casier au cours d'une seule nuit. D'après les résultats de l'analyse de la fréquence des longueurs, il y a eu immigration vers les récifs à l'étude ou les données étaient imprécises. Les estimations visuelles et les prises au casier pendant une seule nuit étaient des méthodes plus rapides et nécessitaient moins de main-d'oeuvre et de ressources que les méthodes de marquage et de recapture, mais la précision des estimations était inconnue. On ne dispose pas encore de méthode vraiment satisfaisante pour effectuer des estimations valables de la densité des juvéniles ou du taux de mortalité naturelle des juvéniles dans les récifs nourriciers. Néanmoins, il semble d'après les données sur le taux de fixation des larves et les prises subséquentes, que les processus dépendant de la densité ont probablement un effet important sur le taux de recrutement pour la pêche bien que le niveau supérieur de ce recrutement n'ait pas été dépassé au cours des 20 dernières années.

Received September 30, 1988
Accepted February 8, 1990
(J9888)

Reçu le 30 septembre 1988
Accepté le 8 février 1990

The western rock (spiny) lobster, *Panulirus cygnus* George, is Australia's most valuable single-species fishery, with landings valued at more than $A190 million in 1987/88. This lobster is found on the west coast of Australia from approximately North West Cape to Augusta (Sheard 1962) (Fig. 1).

Studies of the juveniles in the nursery reefs by Chittleborough (1970, 1974, 1975, 1976) and Chittleborough and Phillips (1975) indicated that density-dependent effects on growth and survival, probably caused primarily by a shortage of food or shelter, limit recruitment to the fishable stock.

Chittleborough and Phillips (1975, 1979) and Chittleborough (1979) suggested that, owing to the restricted holding capacity of the shallow nursery reefs, in most years the level of larval settlement was above the holding capacity of the reefs. Density-dependent mortality would reduce most year-class strengths of juvenile densities to approximately the same level prior to recruitment to the fishery, at approximately 4 yr of age. It was therefore thought that only a particularly weak year-class could be traced through from the time of puerulus settlement at the end of the larval phase to recruitment into the fishery. This was in accord with the observed correspondence between the very low level of puerulus settlement in 1969/70 and the low catch of 1973/74, 4 yr after settlement (Chittleborough and Phillips 1975). Catch being equated to population size although it is recognized that there are a number of potential biases in the catch data including interannual variation in effective effort.

The conclusions concerning the strong effect of density-dependent mortality on the juveniles in the nursery reefs were unchallenged until a high level of larval settlement in 1974/75 was subsequently reflected in the high commercial catch of 1978/79, and the even higher level of settlement in 1978/79 gave the high commercial catch of 1982/83. These data and data from other years revealed that the level of larval settlement in any year so closely parallels the level of recruitment to the fishery 4 yr after settlement that it can be used to predict the catch of recruits and also the size of the total annual catch (Phillips 1986). The holding capacity of the nursery reefs was apparently not fully limiting within the range of the observed levels of puerulus settlement and existing environmental conditions, and therefore post settlement mortality did not restrict juvenile recruitment to a strict upper limit.

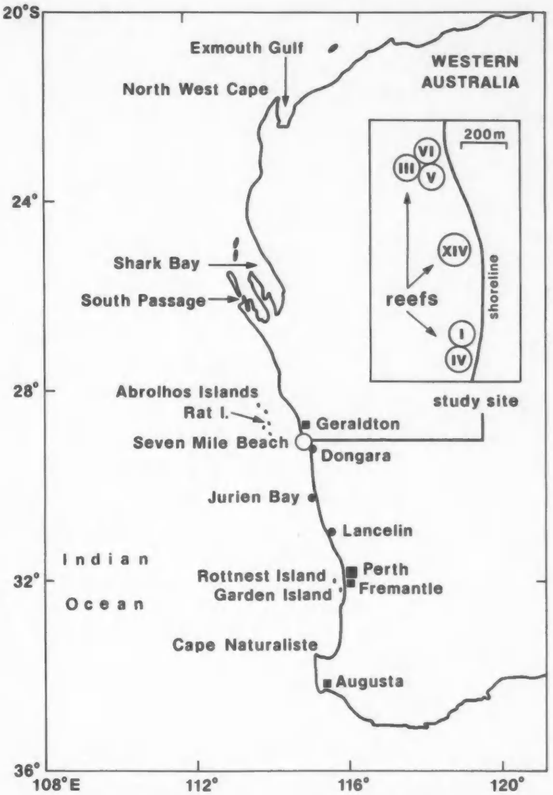

FIG. 1. Location of the sites mentioned in the text. The distribution and numbering of the test reefs at Seven Mile Beach is given in the insert.

In view of these anomalies it is appropriate to reassess the accuracy of the data on the juvenile densities of *P. cygnus*, and the conclusions made from these data. In this paper the methods of estimating larval settlement, juvenile densities, age structure and mortality are described, and the data obtained are reexamined. Alternative methods for calculating the age-classes and estimating juvenile densities are also considered. The implications of these data are discussed in relation to the estimates of juveniles in the nursery reefs.

Reappraisal of Previous Methods of Estimating Larval Settlement, Juvenile Densities, Age Structure and Natural Mortality

Levels of larval settlement were estimated using the number of pueruli caught on collectors. Mark–recapture techniques using baited traps had produced data that suggested that juvenile densities, at least of those aged 2 and 3 yr, reflected the levels of larval settlement. Additional data now indicates that there is no relationship between the levels of larval settlement and subsequent juvenile densities of any age-class. However, the mark–recapture estimates may be inaccurate and the estimates of density and also natural mortality may therefore also be inaccurate.

Larval Settlement

Levels of puerulus settlement were estimated by counting the number of pueruli settling in collectors of artificial seaweed (Phillips 1972). The catches of six collectors (mean catch/collector/year) at Seven Mile Beach (Fig. 1) since 1969 were used as an index of the level of annual larval settlement of the western rock lobster population. The catches of the collectors at this site correlate closely with the number of recruits to the fishery and the total catch of the fishery, 4 yr later (Morgan et al. 1982; Phillips 1986).

Test Reefs

Test reefs were selected at sites where juveniles were known to occur in considerable numbers.

Reefs at Jurien Bay, Garden Island, and Seven Mile Beach (Fig. 1), were selected by Chittleborough (1970). The test reefs selected were shallow reefs on which good numbers of rock lobsters (usually more than 100) could be captured in one or two nights. At Garden Island, three sections of reef (numbered A, B, and C) in water up to 5 m deep, were selected. At Seven Mile Beach six reefs were selected (Fig. 1). Reefs I and IV are parallel to the shore and 745 m south of reefs III, V, and VI. Reefs V and VI are 32 m apart and parallel to the shore, while reef III is approximately 63 m further offshore from reef V. Water depths at low tide are 2–3 m around reefs I, V, and VI and 3–5 m around reef III.

Population Estimates

The population size and density of the juveniles on the test reefs were estimated at Garden Island and Jurien Bay from 1962 to 1977 and at Seven Mile Beach from 1970-86 as described by Chittleborough (1970) and Chittleborough and Phillips (1975).

The single mark–recapture estimate of Bailey (1951) was used to calculate estimates of population sizes for January and August each year. Densities were obtained by dividing these estimates of population size by the measured area of the test reef, or reefs, around which the baited traps were set.

Estimates of Age Structure

In order to follow the strength of individual year-classes, it is necessary to separate the estimates of total density into individual age groups.

Chittleborough (1970) found that at Garden Island, it was possible to separate those aged 2 and 3 yr by means of the polymodal size composition of the catches, but older groups were not often distinguishable at this site. However, juvenile rock lobsters 2 yr of age were poorly represented in the catches upon which the estimates of population density were made. This was due to dominance by larger juveniles in competition for food, as shown experimentally by Chittleborough (1974).

To overcome these problems, Chittleborough and Phillips (1975) produced estimates of the 2-, 4-, and 5-yr-old juveniles at Garden Island, Jurien Bay, and Seven Mile Beach using the presumed natural mortality rate (based on changes in density between January/February and August/September) observed in the combined data for the 3 yr and older juveniles. Chittleborough and Phillips (1975), back-calculated to estimate the density of 2-yr-olds in the previous year. Similarly, the density of the 4-yr-olds was calculated by applying the natural mortality coefficient of those 3 yr and over to the density of 3-yr-olds of the earlier year; the density of 5-yr-olds was calculated by applying the mortality coefficient of those 3 yr and older to the estimated density of 4-yr-olds of the earlier year.

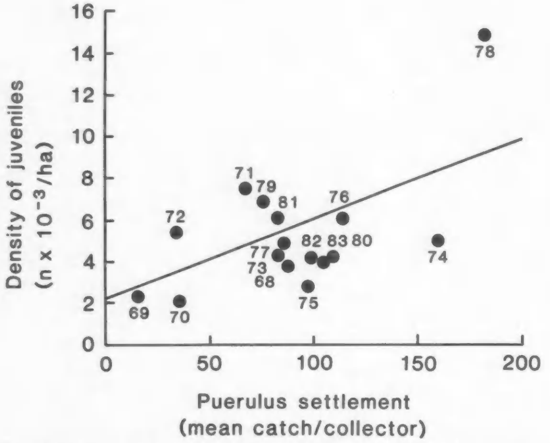

FIG. 2. The annual level of puerulus settlement of *Panulirus cygnus* at Seven Mile Beach from 1968 to 1983, plotted against the density of 3-yr-old juveniles arising from this settlement and located on reef I. The year shown is the year of puerulus settlement.

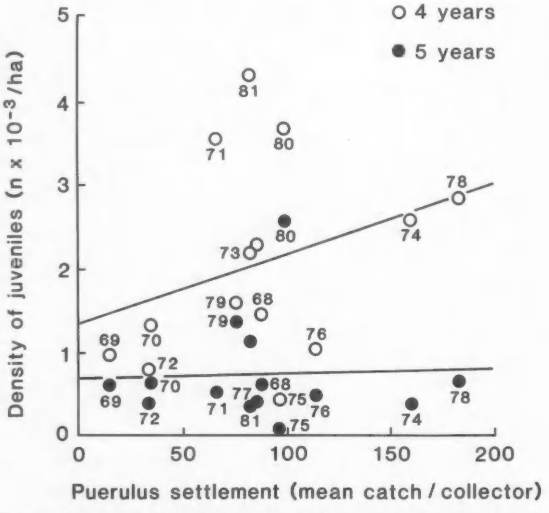

FIG. 3. The annual level of puerulus settlement of *Panulirus cygnus* at Seven Mile Beach from 1968 to 1981, plotted against the density of 4- and 5-yr-old juveniles arising from this settlement and located on reef I. Densities calculated using the method of Chittleborough (1970) and Chittleborough and Phillips (1975). The year shown is the year of puerulus settlement.

Larval Recruitment and Juvenile Density

Examination of both earlier and recent data has revealed no evidence of a relationship between patterns of larval settlement and year-class densities of juveniles.

Chittleborough (1974, 1979), Chittleborough and Phillips (1975), and Morgan et al. (1982) related the levels of larval settlement to the densities of the various age-classes of juveniles arising from this settlement on test reefs at Garden Island, Jurien Bay, and Seven Mile Beach. The estimates of relative year-class strengths obtained by Chittleborough and Phillips (1975), and Morgan et al. (1982) from the puerulus collectors were consistent with those derived from estimates of the density of juveniles aged 2 or 3 yr. However, the densities of the later age groups (4 and 5 yr of age) on the nursery reefs did not mirror the pattern of puerulus settlement and therefore did not give a good indication of the number of recruits to the fishery.

Sampling at Garden Island and Jurien Bay ended in 1977, and no additional data are available from these areas. However, sampling was continued at Seven Mile Beach until 1986. The Seven Mile Beach data on 3-yr-old juveniles to 1986 and the level of larval settlement from which they arose (Fig. 2) is correlated ($r=0.568$, $p<0.05$), but this correlation is heavily influenced by the single high data point on the right-hand side of Fig. 3 and without this point the correlation is not significant ($r=0.255$, $p>0.20$). Analysis of the Seven Mile Beach data on 4- and 5-yr-olds (Fig. 3) shows a wide scatter: in the data on 4-yr-olds, ($r=0.337$, $p>0.20$) and similarly on 5-yr-olds, ($r=0.055$, $p>0.50$). It must be pointed out that the lack of correlation between the levels of larval settlement and later juvenile densities is inconclusive because the data may have a non-linear relationship. This has not been tested as the distribution of both variables, most points in the middle, means that the fitting of any relationship will be unconvincing.

Nevertheless, the earlier conclusion by Chittleborough and Phillips (1975, 1979) and Chittleborough (1979) that the densities of 3-yr-olds correlate with the level of larval settlement is now in doubt, suggesting that there may also be a sampling problem with the 3-yr-olds.

Natural Mortality Estimates

Reductions in the juvenile densities between year-classes were attributed solely to natural mortality. Chittleborough (1970) reported that rock lobsters in segments of a reef at Garden Island remained there for several years, rarely moving even from one part of a reef on to another. Chittleborough also reported that the populations of juveniles on the reefs were not subject to emigration and immigration between January and October each year and virtually closed until the juveniles reached 4 to 6 yr of age. In November to December each year these larger animals emigrated from the inshore reefs as 'whites' and recruited into the fishery.

From subsequent studies it was concluded that, as the population on a test reef is virtually closed between January and October and as the test areas are not open to fishing, any decrease in density during that period would be due to natural mortality. On this premise, the coefficient of natural mortality for that closed period could then be detected from the change in density with time.

The baited-trap technique used in these studies is biased against younger juveniles. Rock lobsters are not caught in traps until they are around 25 to 30 mm carapace length (CL) (between 1 and 2 yr old); hence the 1- and 2-yr age-groups are poorly sampled by baited traps (Chittleborough and Phillips 1975). Estimates of juvenile natural mortality coefficients made by Chittleborough (1970), for Garden Island based on the rate of decline in total population density during that part of the year when migration was minimal, are suspect because of the poor representation of those 1 and 2 yr of age. The baited-trap technique appeared to adequately sample the juvenile rock lobsters 3 yr and older, so estimates of their densities are more reliable (Chittleborough and Phillips 1975). Because of the problem of biased trapping, Chittleborough and Phillips (1975) based their

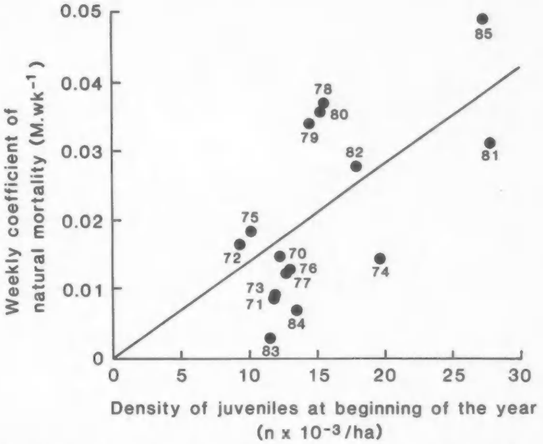

FIG. 4. Relation between natural mortality coefficient (per week) during a year, to the population density of juvenile *Panulirus cygnus* on reef I in January, from 1970 to 1985 at Seven Mile Beach on Reef I.

estimates of natural mortality on changes in the combined density of the 3-yr and older juveniles in the population.

Chittleborough (1970) reported that at Garden Island there was a direct relationship between initial population density of juveniles (all age groups combined), in January, in each year and subsequent mortality during the year. Using the same method, a regression of similar data for Seven Mile Beach from 1970 to 1985 (Fig. 4) shows that the relationship ($r=0.66$, $P>0.05$) between the estimate of the natural mortality rate during the year and the density of the population at the beginning of the year is also significant at this site. These data clearly suggest a decline in numbers on the test reefs related to density, but did these animals die or disperse? Chittleborough (1970) argued that this decline in numbers at Garden Island was not the result of premature emigration of juveniles to deeper waters, but was attributable to density-dependent natural mortality. However, evidence to support this conclusion was not available.

Reliability of the Population and Natural Mortality Estimates

A likely reason for the estimates of juvenile densities not reflecting the level of larval settlement is that the former are inaccurate. The estimates of density (and on these the estimates of natural mortality) were calculated from catches taken by baited traps and are subject to the usual problems associated with mark–recapture techniques.

The method of estimating density and natural mortality rates was validated on test reefs at Garden Island (Chittleborough 1970). Using this same technique, juvenile populations were later examined at other locations, including Jurien Bay (1971–74) and Seven Mile Beach (1970–86). No attempt was made to revalidate the assumptions of the mark–recapture techniques at these latter sites.

In establishing the method, Chittleborough (1970) examined how well the five main assumptions on which the population estimates are based were met at Garden Island. Each of these assumptions will now be re-examined.

(1) That the marked individuals are distributed at random throughout the population on that reef,
(2) that the marking itself does not increase mortality significantly,
(3) that all marked individuals recaptured are recognized and reported,
(4) that marked and unmarked individuals are equally likely to be captured during the second (recapture) phase of each experiment,
(5) that there is no dispersal or emigration or immigration during the interval between marking and recapture.

No additional data are available to test the first three assumptions, but Chittleborough's (1970) examination of these assumptions, including laboratory tests for the effects of marking, was adequate and his assurance, that these are satisfied is acceptable. However, assumptions (4) and (5) must now be questioned in the light of recent information.

(4) *That marked and unmarked animals are equally liable to recapture.*

The tests carried out by Chittleborough (using a double-marking experiment, with two methods of capture) showed that 1 wk after marking, marked individuals were more likely than unmarked animals to enter baited traps. After 4 wk, the number of marked animals caught was slightly higher, but the difference in the probability of recapture of marked and unmarked animals was not statistically significant.

However, when Morgan (1974a) examined this question for legal-sized *P. cygnus* at the Abrolhos Islands, he reported that marked animals had a higher probability of capture than unmarked animals, even after 4 wk. Morgan suggested that Chittleborough's data may have been based on too small a sample for this bias to have emerged clearly.

As the success of mark–capture technique relies on the validity of this assumption, the estimates derived from using this technique must be questioned.

(5) *That there is no significant emigration or immigration during the interval between marking and recapture.*

For this assumption to be tenable, certain conditions must be met during the censusing operations. The population on a reef should be closed (ie. gains and losses from the population should be negligable) for the 1-mo period (January/February or August/September) in which the census is taken. It should also be closed for a full year to give estimates of mortality rates within that year, and be closed for several years to calculate the mortality rates of each year-class.

Chittleborough (1970) sampled juveniles on different reefs at Garden Island in January/February and August/September each year and concluded that the population on each reef had few immigrants from January to October. The larger (older) individuals emigrated to deeper water in November and December each year. Although, as Chittleborough (1970) pointed out, the apparently high mortality of the juveniles might be attributable to premature emigration, the number of individuals recaptured over several years on the same reef was sufficient to suggest the population was relatively static. However, it is the animals that were not recaptured that pose a problem: did they emigrate? or did they die? Chittleborough (1970) quoted the similarity of the estimates of natural mortality calculated for the total population and for the 3-yr-old juveniles between January and October 1967 as additional evidence in support of his hypothesis. However, since the estimates of the mortality for the total population were based largely on recaptures of the dominant 3-yr-old age-group, this evidence is inconclusive.

The disappearance of lobsters at Garden Island during the year was not, Chittleborough (1979) thought, due to premature dispersal (emigration) of the larger animals to other reefs, for he observed few movements of marked rock lobsters between reefs and found that the percentage of rock lobsters marked in January in the trap catches on each reef remained almost constant to the following October. These findings were taken to indicate that there was no significant dispersal from the reefs, for that would have the effect of reducing the proportion of tagged animals in the population. However, if tagged and untagged animals are equally likely to disperse (and there is no reason to suspect that they are not) the proportion of tagged to untagged animals would not change during the year; Chittleborough's conclusion that dispersal does not occur, based on these data, may not therefore, be correct.

Accuracy of the Population Estimates

Possibly the number of animals sampled to produce the density estimates did not provide sufficiently accurate results to permit useful comparisons of the estimates.

Seber (1982) discussed the accuracy of the mark–recapture methods of the single mark–recapture estimate used in this paper and pointed out that many applications of the method were unsatisfactory because too few individuals were marked, so that too few were recaptured. Robson and Regier (1964) developed a method of determining the accuracy (*A*) of the estimate, based on the number marked, the number in the population, and the number examined for marks. Three standard levels for *A* were suggested:

(i) $A = 0.50$; recommended for preliminary studies or management surveys where only a rough idea of population size is needed.
(ii) $A = 0.25$; recommended for more accurate management work.
(iii) $A = 0.10$; recommended for careful research into population dynamics.

The number of rock lobsters marked at Garden Island each January and August sampling period ranged between 157 and 840 and those examined for the presence of marks in February and September between 158 and 540. At Seven Mile Beach the number marked ranged between 72 and 540 marked and those examined for marks ranged between 84 and 491.

Based on these numbers, at Garden Island, the mean accuracy of the estimates over the 13 yr from 1965 to 1977 was 0.18 (range 0.09–0.34). At Seven Mile Beach the mean accuracy of the estimates over the 17 yr from 1970 to 1986 was 0.89 (range 0.45–1.0). Using the levels of accuracy defined by Robson and Regier (1964), at Garden Island the level was at the level required for accurate management work, but less than for research into population dynamics. However, the level of accuracy at Seven Mile Beach was below that required even for preliminary surveys, where only a rough idea of population size is needed.

The accuracy of the single census estimate, used in the present study, is also in doubt. Morgan (1974b) found that at the Abrolhos Islands single-census estimates, using Bailey's (1951) technique over-estimated the population size of legal sized (>76 mm) *P. cygnus* in some months and grossly underestimated it in others.

Alternative Methods of Estimating Population Density and Natural Mortality

New methods of data analysis were used to estimate the year-class strengths of the juveniles. In addition, visual estimates made by divers and single-night trapping were investigated as alternative techniques to obtain estimates of the total population on the test reefs. However, all of these techniques were found to have deficiencies.

Application of New Assessment Techniques for Age Structure

Re-examination of the density estimates for Garden Island and Seven Mile Beach using new methods to separate age-groups indicated that either animals do move between reefs in some years, or that the estimates are inaccurate.

Length–frequency distributions of animals older than 3 yr of age did not enable Chittleborough (1970) to distinguish these age-groups with confidence at Garden Island. In the present study, new estimates of the relative densities of the year-classes of juveniles were made for Garden Island and Seven Mile Beach by calculating the percentage of each age-class directly from the length–frequency data and then calculating the density from the estimated population size on the reefs. The data from Jurien Bay were not re-examined because, as Chittleborough and Phillips (1975) pointed out, the relatively low intensity of sampling makes the data from that locality less reliable.

The problem of separating these data for the older age-groups was reapproached using the maximum likelihood method of MacDonald and Pitcher (1978) to estimate the age-group parameters using the personal computer software MIX (version 2.3). In addition to distinguishing the 2- and 3-yr-old groups, this new technique indicated that there were two modal groups of larger animals, although the size range of the largest group varied considerably from year to year and the picture was clearer at Seven Mile Beach than at Garden Island. Chittleborough and Phillips (1975) suggested that on the nursery reefs the animals that were older than 3 yr of age, were 4, 5, and 6 yr old, with a few possibly 7 yr old. The two modal groups were treated as the 4- and 5-yr-olds, as the small number in the larger modal group made the distinction of the older age-classes (e.g. 5, 6, and 7) relatively unimportant.

Estimates of the density of 3-, 4-, and 5-yr-old juveniles on Garden Island from 1962 to 1977 are given in Table 1; those for Seven Mile Beach made from 1967 to 1983 are given in Table 2. The year of the estimate of the 3-yr-old density was 3 yr after the year of puerulus settlement. Estimate 1 was derived by the method described by Chittleborough and Phillips (1975); the second, estimate 2, was derived by using the method of MacDonald and Pitcher (1978) to separate the age-classes. On both reefs, estimate 2 gives the density of 4-yr-olds in some years as exceeding that of 3-yr-olds in the previous year (at Garden Island, in 9 yr out of 15, and at Seven Mile Beach in 5 yr out of 16). If estimate 2 is correct, immigration of juveniles onto the test reefs at Garden Island and Seven Mile Beach occurred in those years. However, there is always an element of subjectivity in all methods of length–frequency analysis, and these results should be viewed with caution.

Visual and Single-Night Trapping Estimates of Population

Visual and single-night trapping estimates of juvenile numbers are of similar precision but unknown accuracy.

Visual estimates made by divers for *P. cygnus* were developed by Ford et al. (1988) to obtain an index of the number of 3-yr and older juveniles (>40 mm CL) under reefs.

The visual estimates of the number of juveniles present on test reefs I, III, V, and XIV during the day were compared with the number caught that night by trapping on the reef (Fig. 5).

TABLE 1. Mean density of juvenile *Panulirus cygnus* on test reefs A, B, and C (combined) in January each year at Garden Island, arising from single year-classes of puerulus settlement. Standard errors in parentheses. Estimate 1, using techniques described by Chittleborough and Phillips (1975); estimate 2, after analysis of the length frequency data, using the technique of Macdonald and Pitcher (1978).

Year of puerulus settlement	3 yr olds		Density (no./ha) 4-yr-olds		5-yr-olds	
	Estimate 1	Estimate 2	Estimate 1	Estimate 2	Estimate 1	Estimate 2
1959	3245 (75)	3170 (79)	921 (49)	965 (52)	697 (29)	292 (12)
1960	1070 (57)	1106 (60)	810 (34)	1576 (65)[a]	178 (10)	129 (7)
1961	3324 (138)	3300 (110)	730 (39)	1283 (69)	401 (18)	292 (13)
1962	317 (17)	343 (18)	174 (8)	733 (33)[a]	128 (7)	318 (18)
1963	265 (12)	257 (12)	195 (11)	650 (37)[a]	152 (9)	197 (12)
1964	875 (49)	901 (47)	685 (40)	1057 (62)[a]	424 (19)	36 (2)
1965	537 (32)	520 (17)	333 (15)	1032 (46)[a]	217 (15)	316 (23)
1966	92 (4)	91 (5)	60 (3)	581 (42)[a]	28 (4)	159 (22)
1967	971 (69)	1002 (56)	448 (61)	468 (63)	304 (21)	256 (18)
1968	1200 (163)	1170 (150)	813 (56)	812 (56)	443 (29)	343 (23)
1969	274 (19)	319 (18)	149 (101)	553 (36)[a]	91 (7)	146 (11)
1970	1053 (69)	1096 (71)	646 (47)	1038 (76)[a]	366 (20)	102 (6)
1971	765 (56)	748 (51)	311 (17)	686 (38)[a]	205 (20)	141 (14)
1972	969 (53)	974 (51)	638 (62)	321 (31)	618 (71)	184 (22)
1973	630 (61)	625 (52)	611 (70)	161 (18)		
1974	1300 (149)	1310 (140)				

[a] Higher than density of the 3-yr-old age-class in the previous year.

TABLE 2. Density of juvenile *Panulirus cygnus* on test reef I in January each year at Seven Mile Beach, arising from single year-classes of puerulus settlement. Standard errors in parentheses. Estimate 1, using techniques described by Chittleborough and Phillips (1975); estimate 2, after analysis of the length–frequency data, using the technique of MacDonald and Pitcher (1978).

Year of puerulus settlement	Index of puerulus settlement	3-yr-olds		Density (no./ha) 4-yr-olds		5-yr-olds	
		Estimate 1	Estimate 2	Estimate 1	Estimate 2	Estimate 1	Estimate 2
1967		5779 (389)	5680 (270)	3540 (226)	4901 (321)	1352 (104)	426 (56)
1968	88.2	3825 (245)	3906 (230)	1461 (112)	4670 (359)[a]	616 (33)	644 (35)
1969	15.2	2318 (178)	2226 (163)	978 (54)	2847 (156)[a]	613 (28)	916 (41)
1970	35.0	2135 (117)	2146 (108)	1339 (60)	3663 (165)[a]	621 (25)	546 (20)
1971	67.3	7591 (342)	7363 (274)	3522 (143)	2615 (105)	509 (18)	569 (20)
1972	33.7	5460 (219)	5509 (179)	789 (27)	1861 (64)	397 (15)	820 (30)
1973	83.2	4316 (149)	4299 (135)	2174 (80)	2463 (97)	1127 (49)	483 (21)
1974	159.8	5012 (184)	4988 (179)	2598 (113)	3448 (150)	397 (20)	755 (38)
1975	97.3	2828 (128)	2906 (121)	433 (21)	1682 (85)	73 (3)	383 (17)
1976	114.3	6145 (309)	6001 (296)	1039 (45)	1902 (83)	475 (41)	842 (72)
1977	86.0	4986 (218)	4890 (211)	2218 (24)	5115 (437)[a]	435 (32)	215 (16)
1978	182.8	14803 (1775)	13976 (1656)	2828 (206)	1288 (94)	644 (38)	383 (22)
1979	76.2	6978 (509)	6952 (1499)	1590 (93)	2491 (146)	1360 (121)	1203 (107)
1980	78.8	4287 (251)	4301 (249)	3668 (326)	4520 (402)	2553 (357)	1567 (219)
1981	83.0	6154 (547)	6097 (482)	4285 (600)	9976 (1397)[a]	345 (22)	1811 (115)
1982	40.3	5193 (727)	5203 (698)	419 (27)	2569 (164)		
1983	105.3	4085 (261)	4071 (249)				

[a] Higher than density of the 3-yr-old age-class in the previous year.

A close relationship between the data ($r = 0.860$, $p < 0.001$) is apparent and the regression line is not significantly different from the bisector line slope with zero intercept. We can conclude that the two methods (visual estimates and single-night trapping) give comparable counts. However, it is not possible to say whether the animals counted in the visual estimates are the same as those caught in the baited traps or whether some of the latter had come from other reefs.

To eliminate migration between reefs, and to test the accuracy of visual estimates, reefs XIV and IV were fenced on four occasions with a net from the bottom to the surface. Prior to shooting the net, visual estimates were made of the juvenile densities. After the net was in position, baited traps were set overnight within the enclosure in numbers sufficient to ensure saturation trapping. The catches on the four occasions the net was around reefs IV and XIV are also indicated on Fig. 5. They show a close fit to the other data; visual estimates and single-night trapping therefore provide estimates of similar precision at Seven Mile Beach.

The close relationship between the visual estimate and the number caught on the first night of trapping could suggest that the majority of animals present on the reef are caught on the first night. However, if trapping is continued for more than a single night significant numbers of animals are caught on the

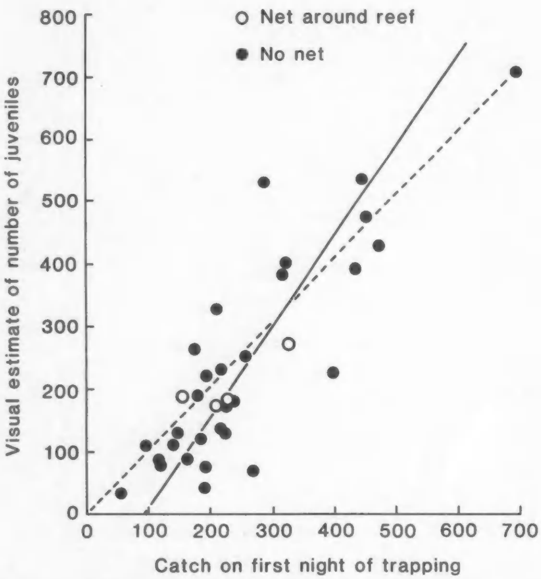

FIG. 5. Visual estimates of the number of juvenile *Panulirus cygnus* present on the test reefs I, III, V, and XIV at Seven Mile Beach compared with the number caught on the single night of trapping. The bisector line is indicated.

later nights. For example, two night trapping carried out on Reef I for 15 yr from 1971 to 1985 showed that 45.3% (range 31.6–58.7%) of the animals were caught on the second night. Obviously the source of the animals caught by the trapping was unknown.

Discussion

Migration or Natural Mortality

Although the full extent of the foraging and other movements between reefs is undetermined, it must be concluded that populations of juveniles on the reefs are not closed to migration during the mark–recapture period in January/February, or between January and October, and are therefore not closed between years. The assumption that there is no dispersal or migration must be rejected, which casts doubts on the estimates of density and also of natural mortality.

Previous mark–recapture studies suggested that the test reefs were closed to immigration and emigration, and that the foraging area of the juveniles was very limited. The juveniles in each segment of the Garden Island reefs apparently remained there for several years, rarely changing their home reef or foraging far from it (Chittleborough 1970, 1974). Their foraging range, as determined by Chittleborough (1974) from trapping studies, did not exceed a radius of 15 m during the year, although he found the maximum radius at Seven Mile Beach to be 50 m.

All the recent data indicate that rock lobsters are more mobile than was previously believed. Phillips et al. (1984) showed that *P. cygnus* had natural foraging ranges up to 105 m at Seven Mile Beach. Jernakoff et al. (1987) found that some juvenile *P. cygnus* at Seven Mile Beach travelled 600–803 m among the reefs whilst foraging in a single night and B. F. Phillips (unpubl. data) observed 39 animals to move from Reef I to Reefs III and V during January 1984, a straight line distance of 745 m. In addition, Jernakoff and Phillips (1988) have shown that juveniles are attracted and enter baited traps from at least 120 m. Obviously lobsters can easily move between reefs, or to traps, over considerable distances.

The movements of juveniles between reefs observed at Seven Mile Beach may be part of the continuous transition of animals from shallow to deeper habitats. Juveniles often moved alongshore, but also offshore, from reefs V and VI (depth 2–3 m) to the slightly deeper (3–5 m) reef III. A similar movement of juveniles was observed from reef V to reef III in 1981/82 (R.F. Ford, Dept. of Biology, San Diego State University, San Diego, CA, pers. comm.). Joll (1984) recorded an offshore movement of juveniles from reefs close to the shore at Cliff Head (about 30 km south of Seven Mile Beach), apparently as a response to high summer temperatures. It is interesting that test reefs used by Chittleborough (1970) at Garden Island were surrounded by water up to 5 m deep and were therefore most like reef III at Seven Mile Beach.

The possibility that all or some of the movements of the tagged juveniles may be a response to the trapping, handling, and tagging, (including variations in tagging methods between studies) can neither be supported nor refuted from the data available.

Fallibility of the Mark–Recapture Technique

The estimates of juvenile densities of *P. cygnus* made by the mark–recapture of animals caught with baited traps, as presently practised, are not suitable for studies of the population dynamics of *P. cygnus*.

Many factors, such as changes in the catchability of lobsters with annual fluctuations in temperature and salinity (Morgan 1974b), may influence the density estimates, but the strongest evidence against the mark–recapture method that has been identified, is that an unknown number of animals moved between reefs at Seven Mile Beach, and that a proportion of such movements occurred during the January/February mark–recapture sampling period. In addition the number of animals marked and subsequently examined for marks was small in proportion to the estimated size of the population, which means that the accuracy of the estimates was low.

The estimates of year-class strengths of juveniles made by Chittleborough (1970) at Garden Island and Chittleborough and Phillips (1975) at Garden Island, Jurien Bay, and Seven Mile Beach are probably all invalid. Furthermore, since the data used for calculating the new estimates for Garden Island and Seven Mile Beach given in this paper were obtained from the same samples, the new estimates are probably also unreliable. Because the mortality estimates depend on the density estimates and because of the emigration of animals to other reefs, the natural mortality rates, at least at Seven Mile Beach, are inaccurate and probably over-estimate the mortality of the juveniles.

The conclusion is unavoidable that estimates of juvenile densities of *P. cygnus* made by the mark–recapture of animals caught with baited traps, as previously practised, are not suitable for studies of the population dynamics of *P. cygnus*.

Baited traps can provide, by single-night sampling, some measure of abundance and they can also provide data on the size structure and sex composition of the juveniles. However, the age-classes are not represented in relation to their true abundance and the source reef of the animals is generally unknown, these samples are also biased.

Visual Estimates

The visual estimates of the number of juveniles are of unknown accuracy.

The visual estimates described in this paper are of similar precision to those obtained by single-night trapping, are rapid, and can be undertaken with fewer personnel and resources. It should be possible to obtain an index of juvenile density on a large number of reefs in a short time. However, the divers must have clear water (Ford et al. 1988) and the technique gives no indication of year-class strengths in the population.

It has not as yet been possible to relate the estimates obtained either by single-night trapping or visual estimates to larval settlement, or any other factor, and hence their accuracy as measures of the actual density of lobsters on the test reefs is unknown.

Regional Differences in Population Behavior

The movements of animals between test reefs which were observed at Seven Mile Beach, but not by Chittleborough (1970) at Garden Island, suggest possible differences between the behavior of the juveniles at these two sites.

The test reefs at Garden Island contain relatively low densities of juveniles compared wih those at Seven Mile Beach (Chittleborough and Phillips 1975), which is nearer the centre of the range of *P. cygnus*. The emigration of juveniles from the reefs at Seven Mile Beach may be caused by the increased density of juveniles in that area, but other factors such as annual variations in food supply or increased water temperatures in summer might also contribute to, or stimulate, such movements.

The levels of larval settlement at Garden Island are much lower than at Seven Mile Beach, the latter being more typical of those found elsewhere along the coast of Western Australia, e.g. Jurien Bay and Rat Island (Abrolhos Islands); and the levels of larval settlement at Seven Mile Beach are reflected in the catches of the western rock lobster fishery (Morgan et al. 1982; Phillips 1986). The behavior pattern of the juveniles at Seven Mile Beach is therefore more likely to represent the general juvenile population than the pattern of those at Garden Island.

Predation or Emigration

Studies of predation of *P. cygnus* suggest that predation by fish in the nursery reefs is most intense from puerulus settlement up to about 2 yr of age (Howard 1988). Reductions in density observed between the 3- and 4-yr-old rock lobsters in the nursery reefs may thus reflect emigration rather than mortality.

Zimmer-Faust et al. (1985) who showed that *Panulirus interruptus* (Randall) colonizes previously unoccupied habitats, also pointed out that nocturnal den-switching without associated foraging activity has been observed in *Panulirus argus* (Latreille) (Herrnkind et al. 1975). Zimmer-Faust et al. (1985) suggest these activities are part of a complex behavior that reduces the vulnerability of individual rock lobsters to predation. It is likely that this behavior increases survival by providing better resource utilization, particularly under conditions of high density.

The movement of juvenile *P. cygnus* between reefs presumably reflects a similar behavior leading to reduced predation or better resource utilization. In either case, when high levels of larval settlement occur, it is probable that reefs which are underutilized, or not normally used by juvenile *P. cygnus*, become occupied. Those reefs provide additional shelter and/or access to food supplies, which would result in a rate of survival higher than previously estimated. At Seven Mile Beach, the movements of juvenile *P. cygnus* suggested a directional component, with the animals moving offshore in a similar manner to that of the "whites" at the time of recruitment to the fishery. Phillips (1983) suggested that this inshore–offshore movement is into less densely populated areas and may provide a mechanism to allow greater survival of the juveniles. Both this directional movement and that between reefs may be different aspects of the same behavior leading to improved resource utilization.

Density Dependence

The studies by Chittleborough (1970, 1974, 1975, and 1976) and Chittleborough and Phillips (1975) lead to the conclusion that density-dependent processes on the reefs, with an upper threshold to juvenile density, were the major determinant of year-class strengths of recruitment to the fishery. The upper level to this recruitment has not been reached over the past 20 yr.

The demonstrated methodological inaccuracies and inadequacies in the estimates of population density and natural mortality cast doubt on these conclusions. However, ignoring the inaccuracies in the estimates and accepting them as rough guides, examination of the data relating densities of juveniles at 3 yr of age (Fig. 2) and 4 and 5 yr of age (Fig. 3) indicates that survival decreases with initial year-class strength of puerulus settlement. In addition the variance of year-class strength decreased at each successive age-group.

A similar picture emerges from examination of the levels of larval settlement and the catch of the fishery. The levels of larval settlement at Seven Mile Beach between 1969 and 1980, ranged from 15.2 to 182.8 pueruli/collector/season, while the total catch from 1973 to 1984 ranged from only 6.7 to 12.4 10^6 kg (Phillips 1986). However, the principal determinant of the level of recruitment to the fishery is the level of larval settlement and the upper level to this recruitment has not been reached within the observed levels of settlement and environmental conditions over the past 20 yr.

Taken together these data suggest that although density-dependent processes may not be the only ones occurring in the nursery reefs, they probably have a significant effect on the levels of recruitment to the fishery. Strong (1986) has suggested that a better term for this type of relationship between density and recruitment would be density vagueness. Density-dependent effects probably occurring as the result of extremes of high and low levels of larval settlement, while density-independent processes operate at the intermediate levels of settlement.

Improvement of Census Technique

Despite the present criticism of the mark–recapture technique, no truly satisfactory alternative has been developed.

The solution to producing reliable estimates of *P. cygnus* population density suitable for studying the dynamics of the populations may partly lie in the scale of the reef area selected. As already described, the test reefs were selected because they gave high numbers of recaptures over one or two nights of sampling. They were therefore "good" reefs, with extensive undercuts that provided shelter for the rock lobsters during the day and surrounding seagrass beds in which they foraged during the night. Other "less suitable" reefs, providing poorer shelter and not surrounded by seagrass beds, also exist in each test area.

The best approach may be to examine the rock lobsters on a group of test reefs covering a range of habitats, including different depths, at each locality. A combination of mark–recapture on some reefs and visual estimates on a larger number of reefs could be the solution. A similar approach to assess the population of *Panulirus argus* (Latreille) in Florida has been suggested by Davis (1977). For these mark–recapture estimates it would be necessary to mark, and then examine for marks, a considerably larger proportion of the populations than in the earlier studies of Chittleborough (1970) and Chittleborough and Phillips (1975). As pointed out by Roff (1973) and Seber (1982), if the number of animals are similar and if density estimates of an accuracy of 10%, which is the recommendation of Robson and Regier (1964) for research into population dynamics, are to be obtained, it will be necessary to mark at least 50% of the population.

It would be a number of years before we had sufficient data to confirm the validity of this approach in *P. cygnus* and because of the necessity for considerable resources to undertake such a study, it has not been attempted.

Obviously neither trapping nor visual estimates adequately samples the very young (post-puerulus) juveniles between 1 and 2 yr of age, <40 mm CL, because of the different behavior of these animals. Unfortunately, a knowledge of the density and mortality rates of these young juveniles is essential if we are to understand the ecology of the nursery reefs. No solution to this problem has yet been found, but investigations are continuing.

Acknowledgements

The author acknowledges Nick Caputi, Tom Ebert, Donald Hancock, Graham Harris, Roy Harden Jones, Peter Jernakoff, Lindsay Joll, Vivienne Mawson, Paulette McWilliam, and Keith Sainsbury for helpful comments in preparation of the manuscript.

References

BAILEY, N. T. J. 1951. On estimating the size of mobile populations from recapture data. Biometrika 38: 293–306.

CHITTLEBOROUGH, R. G. 1970. Studies on recruitment in the Western Australian rock lobster *Panulirus longipes cygnus* George: density and natural mortality of juveniles. Aust. J. Mar. Freshwater Res. 21: 131–148.

1974. Home range, homing and dominance in juvenile western rock lobsters. Aust. J. Mar. Freshwater Res. 25: 227–234.

1975. Environmental factors affecting growth and survival of juvenile western rock lobster. Aust. J. Mar. Freshwater Res. 26: 277–296.

1976. Growth of juvenile *Panulirus longipes cygnus* George on coastal reefs compared with those reared under optimal environmental conditions. Aust. J. Mar. Freshwater Res. 27: 279–295.

1979. Natural regulations of the population of *Panulirus longipes cygnus* George and responses to fishing pressure. Rapp. P.-V. Reun. Cons. Int. Explor. Mer 175: 217–221.

CHITTLEBOROUGH, R. G., AND B. F. PHILLIPS. 1975. Fluctuations of year-class strength and recruitment in the western rock lobster *Panulirus longipes* (Milne-Edwards). Aust. J. Mar. Freshwater Res. 26: 317–328.

1979. Recruitment to the catchable stock of the western rock lobster *Panulirus longipes cygnus* George. Rapp. P. -V. Reun. Cons. Int. Explor. Mer 175: 139–142.

DAVIS, G. E. 1977. Effects of recreational harvest on a spiny lobster, *Panulirus argus* population. Bull. Mar. Sci. 27: 223–276.

FORD, R. F., B. F. PHILLIPS, AND L. M. JOLL. 1988. Experimental manipulation of population density and its effects on growth and mortality of juvenile western rock lobsters, *Panulirus cygnus* George. U.S. Fish. Bull. 86: 000–000.

HERRNKIND, W. F., J. VANDER WALKER, AND L. BARR. 1975. Population dynamics, ecology and behavior of spiny lobsters, *Panulirus argus*, of St. John, U.S.V. I: (III) Habitation, patterns of movement and general behavior. Sci. Bull. Nat. Hist. Mus., Los Angeles City 20: 31–45.

HOWARD, R. K. 1988. Fish predators of the western rock lobster (*Panulirus cygnus* George) in a nearshore nursery habitat. Aust. J. Mar. Freshwater Res. 39: 307–316.

JERNAKOFF, P., AND B. F. PHILLIPS. 1988. The effect of a baited trap on the foraging movements of juvenile western rock lobsters. Aust. J. Mar. Freshwater Res. 39: 185–192.

JERNAKOFF, P., B. F. PHILLIPS, AND R. A. MALLER. 1987. A quantitative study of nocturnal foraging distances of the West Australian Rock Lobster, *Panulirus cygnus* George. J. Exp. Mar. Biol. Ecol. 113: 9–21.

JOLL, L. M. 1984. Natural diet and growth of juvenile western rock lobsters, *Panulirus cygnus* George. Ph.D. thesis, University of Western Australia, Australia.

MACDONALD, P., AND T. PITCHER. 1978. Age-groups from size frequency data: a versatile and efficient method of analysing distribution mixtures. J. Fish. Res. Board Can. 36: 987–1001.

MORGAN, G. R. 1974a. Aspects of the population dynamics of the western rock lobster, *Panulirus cygnus* George. I. Estimation of population density. Aust. J. Mar. Freshwater Res. 25: 235–248.

1974b. Aspects of the population dynamics of the western rock lobster, *Panulirus cygnus* George. II. Seasonal changes in the catchability coefficient. Aust. J. Mar. Freshwater Res. 25: 249–259.

MORGAN G. R., B. F. PHILLIPS, AND L. M. JOLL. 1982. Stock and recruitment relationships in *Panulirus cygnus*, the commercial rock (spiny) lobster of Western Australia. Fish. Bull. 80(3): 475–486.

PHILLIPS, B. F. 1972. A semi-quantititative collector of the puerulus larvae of the western rock lobster *Panulirus cygnus* George (Decapoda:Palinuridae). Crustaceana 22: 147–54.

1983. Migrations of pre-adult western rock lobsters, *Panulirus cygnus* in Western Australia. Mar. Biol. 76: 311–318.

1986. Prediction of commercial catches of the western rock lobster *Panulirus cygnus* George. Can. J. Fish. Aquat. Sci. 43: 2126–2130.

PHILLIPS, B. F., L. M. JOLL, AND D. C. RAMM. 1984. An electromagnetic trading system for studying the movements of rock (spiny) lobster. J. Exp. Mar. Biol. Ecol. 79: 9–18.

ROBSON, D. S., AND H. A. REGIER. 1964. Sample size in Petersen mark–recapture experiments. Trans. Am. Fish. Soc. 93: 215–226.

ROFF, D. A. 1973. On the accuracy of some mark–recapture estimators. Oecologia 12: 15–34.

SEBER, G. A. F. 1982. The estimation of animal abundance in related parameters. Macmillan Publishing Co., New York, NY. 654 p.

SHEARD, K. 1962. The Western Australian crayfishery 1944–1961. Paterson Brokensha, Perth, Australia. 107 p.

STRONG, D. R. 1986. Density vagueness: abiding the variance in the demography of real populations, p. 257–268. *In* J. Diamond and T. J. Case [ed.] Community ecology. Harper and Row, New York, NY.

ZIMMER-FAUST, R. K., J. E. TYRE, AND J. F. CASE. 1985. Chemical attraction causing aggregation in the spiny lobster, *Panulirus interruptus* (Randall), and its probable ecological significance. Biol. Bull. 169: 106–118.

Use of Extant Populations of Scaled Chrysophytes for the Inference of Lakewater pH

Peter A. Siver

Department of Botany, Connecticut College, New London, CT 06320 USA

and Josephine S. Hamer

Department of Mathematics, Western Connecticut State University, Danbury, CT 06810 USA

Siver, P. A., and J. S. Hamer. 1990. Use of extant populations of scaled chrysophytes for the inference of lakewater pH. Can. J. Fish. Aquat. Sci. 47: 1339–1347.

Abundance of living populations of scaled chrysophytes were used to develop multiple regression models for inferring lakewater pH. Until now, all such inference models had been prepared with surface sediment remains and used to reconstruct historical (down-core) changes. We demonstrate that highly significant models can be prepared from living populations of scaled-chrysophytes which could be valuable for monitoring chronic, episodic and/or long-term changes in lakewater pH. Average weighted-mean pH and a cluster analysis technique were used to divide 33 taxa found in 26 Connecticut lakes into groups according to their distribution along a pH gradient. Two calculations of average weighted-mean pH were made; one based on data from this study and one from literature records. Inference models were developed using a single sample from each lake as well as for multiple samples collected throughout the year. The best model based on a single discrete sample yielded an $R^2=0.58$ ($p<0.05$); multiple samples from each lake yielded significantly higher R^2 values, (between 0.75 and 0.83). Scaled chrysophytes appear to be a very valuable assemblage of indicator organisms for the long-term monitoring of lakes.

L'abondance des populations vivantes de chrysophycées à écailles a été utilisée afin de développer des modèles de régression multiple pour déduire le pH de l'eau de lac. Jusqu'à maintenant, tous ces modèles d'inférence avaient été établis au moyen de vestiges de sédiment de surface et utilisés pour reconstituer les changements antérieurs. Nous démontrons qu'il est possible de préparer des modèles très significatifs à partir de populations vivantes de chrysophycées à écailles, qui peuvent être utiles pour surveiller les changements chroniques, épisodiques et (ou) à long terme du pH de l'eau de lac. Un pH moyen à moyenne pondérée et la technique de l'analyse des amas ont été utilisés pour répartir 33 taxons présents dans 26 lacs du Connecticut en groupes selon leur répartition dans un gradient de pH. On a effectué deux calculs du pH moyen à moyenne pondérée; un calcul fondé sur les données tirées de la présente étude et un autre à partir des données tirées de la littérature. Des modèles d'inférence ont été élaborés à partir d'un seul échantillon prélevé dans chacun des lacs de même que pour des échantillons multiples prélevés au cours de l'année. Le meilleur modèle fondé sur un seul échantillon discret a produit un $R^2 = 0,58$ ($p<0,05$): des valeurs R^2 significativement plus élevées ont été obtenues avec des échantillons multiples provenant de chacun des lacs (entre 0,75 et 0,83). Il semble que les chrysophycées à écailles constituent un assemblage d'organismes indicateurs de valeur pour la surveillance à long terme des lacs.

Received February 1, 1989
Accepted February 27, 1990
(JA041)

Reçu le 1 février 1989
Accepté le 27 février 1990

Long-term biological monitoring programs, using living organisms in conjunction with routine chemical measurements to detect contemporary shifts in lakewater pH are currently being developed in the United States and Canada (Thornton et al. 1987). The goal of such a program is to enhance the effectiveness of physical methods of detecting changes in lakewater pH through the addition of a biological component. Periodic fluctuations in lakewater pH, caused by such factors as a storm, spring snowmelt, or a shift in primary productivity could go undetected or mask more subtle long term changes in a program relying solely on yearly or seasonal chemical measurements.

The use of fossil microalgae to reconstruct the paleo-record has been of considerable interest for inferring historical pH levels (e.g. Charles 1985; Charles and Norton 1986; Charles and Smol 1988; Dixit et al. 1988a,b). Mostly, emphasis has been placed on using fossil diatom assemblages to develop inference models (e.g. Battarbee et al. 1986; Davis and Anderson 1985; Charles 1985; Dixit et al. 1988b), the methods of which are well established (see Davis and Anderson 1985; Charles 1985). Surface sediment diatom assemblages from a group of lakes, referred to as the calibration set, are correlated with contemporary lakewater pH to develop an inference model for sediment cores that can be applied downcore to reconstruct pH through time. Such an approach has been successfully applied to different lake regions (e.g. the Adirondacks — Charles 1984; Charles 1985; Sudbury — Dixit et al. 1988b; and New England/Norway — Davis et al. 1983) and models with values for $R^2 \pm \text{SE}$ as high as 0.94 ± 0.28 have been developed (Charles 1985).

However, several characteristics of diatom ecology suggest that they may not always be the most reliable and accurate group for reconstructing historical lakewater pH. First, in some regions, lakes with a pH <5.5 have few planktonic diatoms

(Almer et al. 1974; Battarbee 1984; Charles 1985). Second, because fossil diatom assemblages include both planktonic and benthic forms, they represent organisms that may have lived under different pH regimes.

Algal taxa in the families Paraphysomonadaceae of the class Chrysophyceae (Preisig and Hibberd 1983) and Mallomonadaceae of the class Synurophyceae (Andersen 1987), herein referred to as scaled chrysophytes, are strictly planktonic organisms each covered with species-specific siliceous scales. Like diatom frustules, the siliceous remains of scaled chrysophytes are preserved as microfossils in lake sediments and present a useful group for paleolimnological reconstructions (Smol 1986).

Recently, the distribution of scaled chrysophytes as a group (Roijackers and Kessels 1986; Smol et al. 1984; Charles and Smol 1988; Dixit et al. 1988a; Siver and Hamer 1989) and at species and subspecific levels (Siver and Hamer 1989; Siver 1989c) has been shown to be strongly influenced by lakewater pH. As well the distributions of many species along a pH gradient have been identified (see Siver 1989a for a summary). Thus, it is no surprise that methods for reconstructing pH based solely on scaled chrysophyte microfossils (e.g. Dixit et al. 1988; $R^2 = 0.74$), or on both chrysophytes and diatoms (e.g. Charles and Smol 1988; $R^2 = 0.88$ to 0.94) have yielded significant models.

In a program incorporating a biological component, alterations in the composition of living taxa are used to document shifts in lakewater pH. The usefulness of scaled chrysophytes in monitoring programs is, in part, dependent on whether inference models for lakewater pH, similar to those derived from fossil assemblages, can be developed using data from living populations. The purpose of the current study is to determine if significant pH inference models can be produced using data from discrete samples of living populations.

Materials and Methods

A total of 288 collections from 45 waterbodies were made between September 1983 and September 1986 and analyzed with scanning electron microscopy (SEM) and light microscopy (LM) for scaled chrysophyte populations. Discrete water samples taken from the center of the lake at a depth of 1 m or at 0.5 m along shore were used for all quantitative analyses. Samples were always made at the same location. In general, lakes with boat access were sampled from the center, whereas more remote lakes were sampled close to, or at, the outlet. For 26 lakes a minimum of four collections were made, one during each of the spring, summer, fall, and winter seasons (Table 1). Plankton net samples (6- or 10-μm mesh) were also made by pulling a net 5 to 10 m horizontally at approximately the same depth from which the discrete water samples were taken. During the winter months water was poured through the net. The concentrated net samples were used solely to aid in the identification of taxa with scanning electron microscopy (SEM); they were not used in any quantitative analyses. Additional water samples used for pH determinations were taken from the same depth as the plankton samples and placed into vials with polyseal lined caps to avoid contamination with air. Measurements were made in the field or immediately upon return to the laboratory with a Fisher Accumet model 640A pH meter.

Sample preparation in the laboratory consisted of a series of washings to dissociate scales and remove other debris. Two hundred millilitres from each discrete water sample, fixed with Lugol's solution, were concentrated by centrifugation at 2000 rpm and resuspended in 5 to 10 mL. A 1-mL portion of the concentrate was air dried on aluminium foil for SEM analysis. An equal amount of H_2SO_4 and a pinch of potassium dichromate was added to the remainder of each concentrated sample and allowed to stand for a minimum of 48 h. Each sample was then washed in distilled water and reconcentrated by centrifugation approximately six times. A 1-mL aliquot from each concentrate was then pipetted onto a glass coverslide, air dried, and used to prepare a burnt mount according to Wee (1983). For each collection with scaled chrysophytes present, 300 scales were identified and enumerated by inspecting random fields on the burnt mount preparations. Additional burnt mounts were prepared for samples with few scales.

Before a count of scales was made, a list of the taxa present and qualitative estimates of their relative abundances were prepared by examination wth SEM. For SEM, the aluminum foil sample was washed (Siver 1987), trimmed, mounted onto an aluminum stub with Apiezon wax, coated with gold for 4.5 min using a Polaron ES 100 sputter coater and observed with a Coater and Welter scanning electron microscope at 15 to 20 kV.

Undigested samples were used for SEM analysis, allowing whole cells, whole colonies, or groups of intact scales to be used for identification purposes. For taxa which could not be separated using isolated scales with light microscopy (LM), proportional estimates were made during the SEM analysis and the LM counts subsequently separated using the proportional estimates. Species of the genus *Spiniferomonas* presented the most difficult problem since isolated scales may not yield sufficient information to identify the scale to the species level with either LM or SEM. This was not generally a problem since most collections had only one or no species of *Spiniferomonas*. For collections where two or more species of *Spiniferomonas* were present, proportional estimates were made with SEM by counting whole cells. By using whole cells as the proportional estimator, each species of *Spiniferomonas* was treated the same regarding the number of scales per cell; that is, it was assumed that each species has the same number of scales per cell. It is unlikely that this assumption is true. However, since the range in the number of scales per cell for species of *Spiniferomonas* is much less than for species of *Mallomonas* (P. A. Siver, unpubl. data), and since species of *Spiniferomonas* are all relatively small, the above estimation method was believed to be a good approximation. It should also be remembered that the resultant models are based on the relative abundances of scales and not cells and assume an equal number of scales per cell for all taxa.

Weighted mean pH values for each taxon were calculated according to the following equation:

$$\text{WMpH} = \sum_{i=1}^{9} P_i\,(X_i) / \sum_{i=1}^{9} P_i,$$

where WMpH = weighted mean pH; P_i = frequency of occurrence of the taxon in the ith pH interval and; X_i = pH midpoint of the ith interval. The pH intervals were <5, >8.5, and the seven 0.5 unit intervals between 5 and 8.5. A total of 207 collections surveyed from the literature were also used to calculate weighted mean pH values for taxa using the above formula (Siver 1989a). Only studies where identification of species was made with electron microscopy and the presence–absence of the taxa observed reported for each collection were used for

TABLE 1. Locations within the State of Connecticut, the ranges of pH and the arithmetic mean pH for 26 lakes used to prepare inference models for lakewater pH. The position from which each lake was sampled is also noted: C = center; S = deep area along shore; O = outlet.

Lake	Town	pH		Sampling location
		Range	Mean	
Bigelow	Union	5.5–6.6	6.1	C
Breakneck	Union	5.5–6.5	6.0	S
Chamberlain	Woodstock	5.6–7.3	6.2	C
Black	Woodstock	5.9–7.3	6.6	C
Kenosia	Danbury	7.0–8.1	7.3	C
Waubeeka	Danbury	6.7–8.0	7.1	C
Forest	New Fairfield	5.6–6.8	6.2	C
West	Danbury	7.5–8.0	7.8	S
Crystal	Ellington	6.45–6.7	6.5	C
Stateline	Stafford	5.6–6.3	6.0	O
Wonoscopomuc	Salisbury	7.6–9.1	8.6	S
Twin East	Salisbury	7.5–8.6	8.2	C
Long	Ledyard	6.5–7.0	6.9	S
Fullers	Kent	7.0–8.2	7.7	O
Dog	Goshen	7.1–9.2	7.6	C
Tyler	Goshen	6.9–8.7	7.6	C
Westside	Goshen	7.0–8.0	7.3	C
Ford	Salisbury	7.2–9.0	7.8	O
Trout	Grandby	6.4–6.8	6.6	O
Emmons	Hartland	4.3–4.8	4.5	O
Avery	Preston	6.9–7.0	6.9	O
Putnam Park	Redding	6.8–7.8	7.2	S
Hemlock	Easton/Fairfield	7.1–7.7	7.3	S
Squantz	New Fairfield/Sherman	7.8–8.8	8.0	C
Crescent	Enfield	6.4–6.5	6.5	C
Shaker	Enfield	6.4–7.5	6.7	O

quantitative purposes. The studies utilized in this manner are listed in the note to Table 2.

Three methods were used to divide the taxa into four groups (Table 2). First, organisms were divided based on their weighted mean pH (WMpH) values as calculated from this study. The groups are designated: WMpH group 1, taxa with WMpH$\leq$6.0; WMpH group 2, taxa with 6.0$<$WMpH$\leq$6.5; WMpH group 3, taxa with 6.5$<$WMpH$\leq$7.0 and; WMpH group 4, taxa with WMpH$>$7.0. The boundaries were selected with an attempt to produce groups with equal numbers of taxa as proposed by Charles and Smol (1988). Second, the taxa were separated on the basis of their WMpH calculated from literature records; these were designated literature groups 1–4 and had the same pH boundaries as the WMpH groups (Table 2). Siver and Hamer (1989) separated the taxa in this data set into five clusters using principal component (PC) scores as a distance measure. Since lakewater pH strongly dominated the first PC axis and the clusters were well separated along a pH gradient, these clusters were used as a third way to separate the taxa. Since one cluster (Group 3 in Siver and Hamer 1989) consisted of a single species, *Mallomonas tonsurata* Teiling em. Kreiger, this species was moved into cluster 5, the cluster of closest affinity. These groups are referred to as PC groups 1, 2, 4, and 5, using the original numbers assigned (Siver and Hamer 1989).

Thirty-three of the 60 taxa of scaled chrysophytes identified from the study lakes were used in the multiple regression analysis (Table 2). These 33 taxa accounted for over 95% of the total number of scales counted. The remaining taxa are rare and have too few distributional records to calculate weighted mean pH values. Rarely did a taxon not used in the analysis account for more than 3% of the total scales counted for a given sample. The results of PCA for *Mallomonas alpina* Pascher and Ruttner em. Asmund and Kristiansen and *Mallomonas paludosa* Fott, completed subsequent to an earlier paper (Siver and Hamer 1989), were included in this study. Although pH records were available for all populations observed of *Mallomonas papillosa* Harris and Bradley, *Mallomonas transsylvanica* Péterfi and Momeu, and *Chrysosphaerella brevispina* Korsh. em. Harris and Bradley to enable weighted pH means to be calculated, PCA was not done because of incomplete data records for other variables. Data records from this study and the literature survey were combined for *Mallomonas paludosa, Mallomonas hindonii* Nicholls, *Mallomonas canina* Kristiansen, and *Mallomonas transsylvanica* for the calculation of weighted mean pH values (Table 2). Too few records were available from the literature to calculate weighted mean pH values for *Mallomonas acaroides* v. *muskokana* Nicholls, *Mallomonas galeiformis* Nicholls, *Mallomonas portae-ferreae* Péterfi and Asmund, *Mallomonas pseudocoronata* Prescott and *Mallomonas pugio* Bradley.

Multiple regression models for inferring lakewater pH (dependent variable), based on the percentages of scales from taxa within each pH group (independent variables), were derived using three different combinations of the data, herein referred to as methods 1, 2, and 3. Since there were also three ways by which the taxa were divided into groups, nine models were developed (Table 3). The stepwise regression procedure in SPSSX (Norušis 1985) was used on a VAX 8550 mainframe computer to develop each model. In this procedure each of the four independent variables are added into the model in the order of their importance in describing lakewater pH (i.e. the percentage of the variance explained); variables are added to the

TABLE 2. Weighted mean pH values and group assignments for 33 taxa of scaled chrysophytes. Weighted mean pH scores were calculated using data from this study and using records from the literature. The WMpH and literature group assignments were based on the taxon's weighted mean pH from this study and the literature survey, respectively. The following categories were used: Group 1 ≤ 6.0; 6<Group 2≤6.5; 6.5<Group 3≤7.0 and; Group 4>7.0. The PC group designations were as reported by Siver and Hamer (1989).

	Weighted mean pH		Group assignment		
Taxon	This study	Literature survey[c]	WMpH	PC	Literature
Mallomonas					
acaroides v. *acaroides*	8.1	8.4	4	5	4
acaroides v. *muskokana*	5.3	—	1	2	—
akrokomos	6.5	6.7	2	4	3
alpina	7.7	8.0	4	5[b]	4
canina/hindonii	4.9[a]	4.9[a]	1	2	1
caudata	6.7	6.6	3	1	3
corymbosa	7.7	7.0	4	5	3
crassisquama	6.9	6.6	3	1	3
elongata	6.9	6.8	3	5	3
galeiformis	6.3	—	2	4	—
hamata	5.9	6.4	1	4	2
heterospina	6.3	6.3	2	4	2
paludosa	5.1[a]	5.1[a]	1	2[b]	1
papillosa	6.4	6.6	2	—	3
portae-ferreae	7.1	—	4	5	—
pseudocoronata	7.3	—	4	5	—
pugio	4.9	—	1	2	—
punctifera	5.9	6.8	1	2	3
tonsurata	7.6	8.1	4	5	4
transsylvanica	6.4[a]	6.4[a]	2	—	2
Synura					
echinulata	6.0	5.9	1	2	1
petersenii	6.2	7.0	2	1	3
sphagnicola	5.3	5.4	1	2	1
spinosa	6.1	6.5	2	1	2
uvella	6.6	6.4	3	1	2
Spiniferomonas					
bilacunosa	6.5	6.6	2	1	3
bourrellyi	6.1	6.1	2	1	2
coronacircumspina	6.7	6.6	3	1	3
trioralis	6.7	6.8	3	1	3
serrata	6.4	6.9	2	1	3
Chrysosphaerella					
brevispina	6.2	6.8	2	—	3
longispina	5.9	6.3	1	1	2

[a] Data from this study and the literature survey combined in order to calculate the average weighted mean pH.

[b] Analysis completed since the paper by Siver and Hamer (1989).

[c] Note: literature records included data from Cronberg and Kristiansen (1980); Dürrschmidt (1982, 1984); Eloranta (1985); Green (1979); Gretz et al. (1979, 1983); Kristiansen (1978); Roijackers (1981); Roijackers and Kessels (1981, 1986); Skogstad (1982); Wujek and Hamilton (1972, 1973); and Wujek et al. (1975, 1977).

model provided that they result in a significant change ($\alpha = 0.05$) in the F-ratio statistic for the regression model.

Method 1

In this method each collection was treated as an independent sample in the regression analyses, regardless of the season or lake. The percentages of scales of all taxa within each pH group were regressed against the observed lakewater pH at the time of collection.

Methods 2 and 3

In Methods 2 and 3 results from all collections from a given lake were first combined and then used in the regression analyses. The dependent variable in both methods was the simple arithmetic mean of all lakewater pH values made from a given lake (Middleton and Rovers 1976). Only lakes ($n = 26$) where a minimum of four collections, one from each of the spring, summer, fall, and winter seasons, were used (Table 1). In method 2 all collections from a given lake were weighted

TABLE 3. Multiple regression equations for inferring lakewater pH based on live populations of scaled chrysophytes. The data were combined for analysis in each of three ways, herein referred to as methods 1, 2, and 3. Also, three approaches, referred to as WMpH groups, PC groups and literature groups, were used to separate the taxa into each of four categories. See text for details.

Equation	Taxon grouping method	R^2	SE
Method 1[a]			
(1.) $\mathrm{pH}=5.85+2.59\,G_4+1.86\,G_3-0.43\,G_1$	WMpH	0.57	0.46
(2.) $\mathrm{pH}=5.86+3.18\,G_3-0.71\,G_2+0.67\,G_1$	PC	0.42	0.54
(3.) $\mathrm{pH}=-4.5+13.48\,G_4+9.95\,G_1+10.1\,G_2$	Literature	0.30	0.57
Method 1[b]			
(4.) $\mathrm{pH}=5.72+2.05\,G_3+2.51\,G_4$	WMpH	0.58	0.37
(5.) $\mathrm{pH}=5.79+3.68\,G_3+0.57\,G_1$	PC	0.42	0.44
(6.) $\mathrm{pH}=-14.19+23.97\,G_1+19.6\,G_2+20.1\,G_3+20.7\,G_4$	Literature	0.30	0.49
Method 2			
(7.) $\mathrm{pH}=7.5-3.09\,G_1+1.19\,G_4-1.12\,G_2$	WMpH	0.82	0.37
(8.) $\mathrm{pH}=7.25-2.99\,G_2+1.79\,G_3-3.65\,G_4$	PC	0.83	0.39
(9.) $\mathrm{pH}=7.48-3.59\,G_1-2.73\,G_2+1.71\,G_4$	Literature	0.75	0.48
Method 3			
(10.) $\mathrm{pH}=6.22-2.32\,G_1+2.32\,G_4+1.05\,G_3$	WMpH	0.82	0.40
(11.) $\mathrm{pH}=5.47-1.33\,G_2+3.73\,G_3+1.58\,G_1$	PC	0.79	0.45
(12.) $\mathrm{pH}=7.46-3.93\,G_1+2.34\,G_4-2.24\,G_2$	Literature	0.77	0.47

[a] Using only collections with five or more species of scaled chrysophytes ($n=144$).

[b] Using only collections with more than six species of scaled chrysophytes ($n=74$).

equally. That is, the percentages of scales from taxa within each pH group were calculated separately for each collection made from a given lake. Then, the mean percentages of scales per group were calculated and used in the regression analyses. In method 3, scale counts were first tallied for all samples from a given lake, and the tallied counts used to calculate the percentages of scales per pH group. If the numbers of scales counted per collection were equal for a given lake then the percentages obtained via methods 2 and 3 would be the same.

Results

Method 1

Method 1 was used to derive a pH inference model using only those collections where five or more species of scaled chrysophytes were found (144 of 288 collections). The best relationship, obtained using the WMpH groups, yielded an R^2 and standard error of 0.57 and 0.46, respectively (Table 3). In this model WMpH groups 4, 3, and 1 were entered stepwise into the model; since WMpH group 2 did not result in a significant change in the F-statistic ($\alpha=0.05$), it was not included. Although multiple regression models based on the PC groups and literature groups yielded significant relationships, correlation coefficients of only 0.42 and 0.30, respectively, were obtained (Table 3). Analyses using only collections with greater than six species ($n=74$) yielded models with essentially identical R^2 values but smaller standard error estimates (Table 3). Here again, the best model was developed using the abundances of taxa within the WMpH groups; however, only WMpH groups 3 and 4 were entered into the model; entering WMpH groups 1 and 2 did not significantly increase the F-statistic.

Method 2

Data from all collections for each of 26 lakes were combined according to method 2 and used in multiple regression analyses to prepare pH inference models (Table 3). Highly significant inference equations, each with a much larger R^2 than obtained in method 1 were found for each of the three groupings of taxa (Table 3; Fig. 1a–c). Correlation coefficients of 0.83, 0.82, and 0.75 and standard error values of 0.39, 0.39, and 0.48 were obtained using the PC, WMpH, and literature groupings, respectively.

Each of the predictive equations consisted of three of the four categories of taxa. In each case using a stepwise procedure, the grouping of taxa with the lowest weighted mean pH scores was entered into the model first, usually followed by the group with the highest mean pH scores.

Method 3

Method 3 yielded inference equations with identical correlation coefficients and similar standard error values as method 2 when the WMpH and literature groupings of organisms were used (Table 3; Fig. 2a–c). A slightly smaller R^2 value was obtained for the model based on PC groups (0.79 versus 0.83). As was found using method 2, only three of the four groups were entered into each model; the groupings of taxa representing the extremes of the pH gradient were the most important.

Discussion

Multiple regression models for pH inference based solely on the remains of scaled chrysophytes from surface sediments have yielded correlation coefficients of 0.70 for lakes in the Adirondacks (Charles and Smol 1988) and 0.74 for lakes near Sudbury, Ontario (Dixit et al. 1988a). It is evident from this study, where

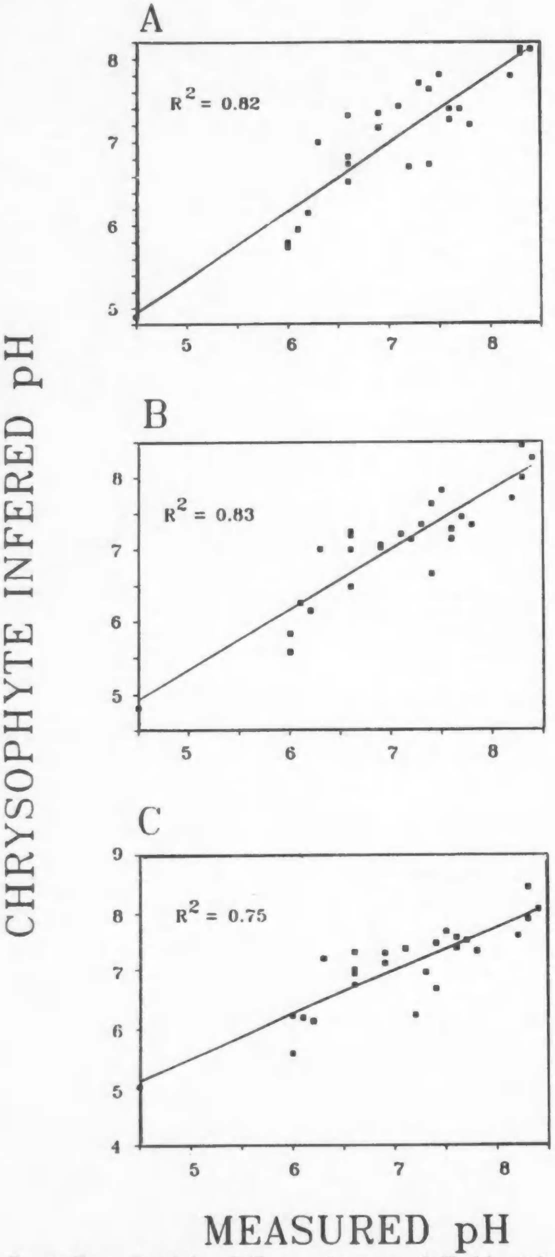

FIG. 1. Chrysophyte inferred pH versus the measured pH of the study lakes using method 2. A = WMpH groups; B = PC groups; and C = literature groups.

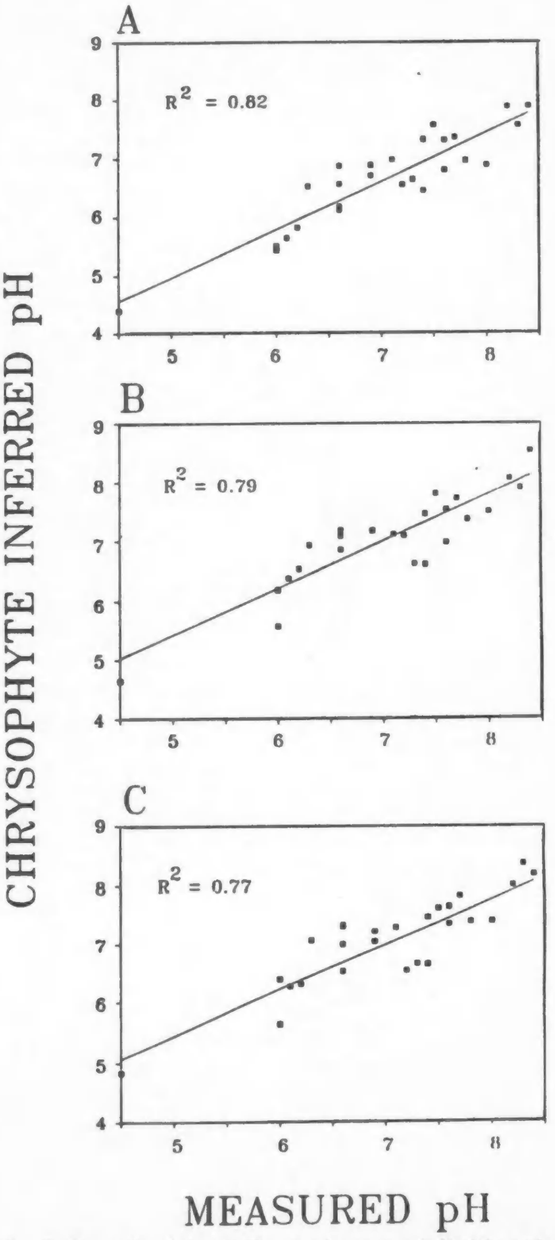

FIG. 2. Chrysophyte inferred pH versus the measured pH of the study lakes using method 3. A = WMpH groups; B = PC groups; and C = literature groups.

correlation coefficients over 0.80 were obtained, that statistically significant models can also be developed for inferring lakewater pH using collections of living organisms made throughout the year. In addition, the standard error values for models where $R^2 > 0.8$ ($0.37 \leq \text{SE} \leq 0.45$) were within the ranges reported by Charles and Smol (1988) and Dixit et al. (1988a). Therefore, models based on a minimum of four collections made throughout the year (methods 2 and 3) would be valuable components of a long-term monitoring program and in estimating potential effects due to hypothetical changes in pH.

Somewhat surprising was the fact that a statistically significant model, although with an R^2 and standard error of only 0.58 and 0.37, respectively, was obtained based on a single discrete sample (method 1). It seems appropriate that since a discrete sample may very well yield valuable information, provided sufficient numbers of species are present, that a series of samples taken over closely spaced time intervals may provide insights into short-term changes (e.g. episodic events such as spring snowmelt).

The successful development of valid pH inference models based on either extant populations or on microfossil remains should not be surprising because both types of assemblages have been used to illustrate the importance of pH in controlling the distribution of scaled chrysophytes (Smol et al. 1984; Roijackers and Kessels 1986; Siver 1989c; Siver and Hamer 1989; Charles and Smol 1988; Dixit et al. 1988a). In addition, Siver (1989a) showed that the average weighted mean pH values for many taxa of scaled chrysophytes calculated using living populations were strikingly similar to those obtained from surface sediment remains.

It should be emphasized that pH inference models derived from living versus microfossil assemblages would be used for different purposes and, as such, do not represent opposing methods. Models based on living populations, such as in this study, could be used for monitoring contemporary changes in lakewater conditions or to predict potential changes in community structure from postulated changes in pH. Models based on surface sediment assemblages would be used for modelling historical (down core) changes. Some of the sources of error incorporated into models developed using each method are similar; however, each method also incorporate different biases. Thus, there are advantages and disadvantages in developing pH inference models using either living populations or a paleolimnological approach. Clearly, one advantage of using surface sediments is that they integrate over time and the whole water column. Thus, provided dissolution of scales is not a problem (see Davis and Smol 1986) and the disarticulated remains can be identified, most taxa are integrated into the model. In reality, some taxa cannot be identified to the species level using sediment remains and other, more fragile taxa, are presumably lost. On the other hand, by using samples from discrete positions within the water column, short lived taxa present only between sampling events as well as those residing in deeper metalimnetic or hypolimnetic strata (Fee 1976; Healy 1983; Pick et al. 1984) could be overlooked. The degree to which missing taxa are a problem depends, in part, on the questions "How many taxa are needed to develop a model?," and, "To what degree do missing taxa significantly affect the ratio of organisms within each pH category (e.g. WMpH groups)?." The assumption could be made that the organisms not accounted for would be equally distributed between all pH categories, and, therefore do not effect the resultant ratios.

In their survey of the surface sediments of 47 lakes in the Adirondacks, Charles and Smol (1988) reported that most lakes had between five and 15 species of scaled chrysophytes; a few lakes had only one or two taxa. In this study 6% of the discrete samples lacked species of scaled chrysophytes, however, up to 17 taxa per collection were found in others. An average of 6.5 taxa per collection was found for samples between a pH of 5.5 and 8.0. Based on a review of the literature of studies utilizing EM to identify scaled chrysophytes, Siver (1989b) reported an even greater number of taxa per collection. Integrating over all samples for a given lake between five and 25 different species were found in each of the 26 lakes. Thus, the number of taxa per lake used in the present study to develop statistical inference models were within, or greater than, the range reported by Charles and Smol (1988).

In paleolimnological studies surface sediment assemblages, which represent organisms accumulated over the whole year, are commonly correlated with the pH taken at a specific time of the year (e.g. Dixit et al. 1988a) or are averaged over a portion of the year (e.g. Smol et al. 1984; Charles 1985; Davis and Smol 1986; Charles and Smol 1988). Thus, in constructing a model based on surface sediments, the same pH is used for taxa that originally grew in the epilimnion versus those restricted to deeper strata as well as for those that grew in warmer versus cooler periods of the year. Presumably, this would result in some error in the model. On the other hand, the use of living samples enables the investigator to correlate the abundance of a given taxon with the specific pH taken at the time of collection; in this case differences in lakewater pH measured during the year are recognized and utilized in the model.

Deepwater strata of phytoplankton are commonly found in clearwater lakes during periods of density stratification (Baker and Brook 1971; Fee 1976; Pick et al. 1984). In dilute clearwater lakes of the Canadian Shield, the strata are often dominated with chrysophytes (Pick et al. 1984). Similar metalimnetic strata have been observed in a few of the lakes in Connecticut, however, the strata are commonly dominated with Cyanophyceae (P. A. Siver, unpubl. data). The pH of the lakewater at a given stratum is often different than that of the epilimnion. If organisms that are restricted to deepwater strata are incorporated into pH inference models, the pH of the strata should be considered as well.

When developing an inference model utilizing living collections additional taxa of scaled chrysophytes that can't be identified from their disarticulated components in the sediment, but can be identified in live samples, can be incorporated into the data set. For example, because the morphological characteristics of scales and spines of many species of *Spiniferomonas* are similar, the taxa can't be identified from their isolated components. However, with living populations, the species can be identified and their abundances estimated before the cells become disarticulated. Also, using living populations, identifications can be made using intact cells. The identification of some species of scaled chrysophytes, even using EM, can be difficult when based on isolated scales, and virtually impossible using LM. For example, isolated scales of *Mallomonas alpina*, *M. corymbosa* Asmund and Hilliard, *M. portae-ferreae* and *M. tonsurata* could be virtually impossible to separate with LM and even difficult with EM (see Asmund and Kristiansen 1986). However, identifications based on whole cells can be unequivocally made.

In an earlier paper (Siver and Hamer 1989) the taxa used in this study were divided into groups using cluster analysis based on mean principal component scores (i.e. the PC groups). In that paper, we concluded that the groupings were strongly related to the distribution of the taxa along a pH gradient which, in turn, prompted us to use these groupings in the current study. This conclusion is further supported since inference models prepared using the PC groups yielded similar R^2 and standard error values as ones based on the WMpH groups. In general, the concordance of all three methods for grouping the taxa indicates that each is closely tied to the distribution of the organisms along a pH gradient.

Significant inference models ($R^2 = 0.75$) were also prepared using the literature groupings. It is very likely that a more significant inference model would have been developed using the literature groups if the taxa for which too few records were available to calculate weighted mean pH values (e.g. *M. aca-*

roides v. *muskokana*) were included. Using data from the literature, one may introduce at least two additional sources of error. First, different researchers were involved in the pH measurements and taxonomic identifications. Second, and perhaps more importantly, are regional differences in the distributions of selected species along environmental gradients. Some regional differences in the distribution of species, for example *Mallomonas acaroides* (Siver 1989c), have been demonstrated to be of a taxonomic nature. Yet, for other species, such as *Mallomonas punctifera* Korshikov which has been reported as having a maximum in alkaline (Kristiansen 1986; Dixit et al. 1988a) as well as acidic (Siver and Hamer 1989; Charles and Smol 1988) water, it is unclear if txonomic differences exist or not (Charles and Smol 1988).

It is a generally accepted policy that inference models should be developed from calibration sets made from lakes within the region of interest and not with data from outside of the region (Smol 1986; Davis and Smol 1986; Davis and Anderson 1985; Dixit et al. 1988a). Although more precise models would be developed using regional calibration data sets, this study emphasizes the fact that models prepared from the literature utilizing scaled chrysophytes are highly significant and of considerable value. The fact that highly significant models can be developed using literature records not only indicates the robustness of the method for preparing the models, but also suggests the applicability of the models to a wide range of geographical regions. In addition, a literature-based inference model could be used in a specific region to identify potential problem areas while a more regional based model is being developed.

In summary, highly significant inference models for use in monitoring contemporary changes in lakewater pH and in predicting effects from postulated changes in pH can be developed using data from living populations of scaled chrysophytes. Such models will be invaluable in long-term monitoring programs. Although some of the sources of error in developing models based on living populations are similar to those produced using sediment assemblages, others are different. Both methods will ultimately yield more sophisticated models as they are finetuned through improvements in taxonomy, sampling, and statistical procedures. There is little question that the two approaches could and would compliment each other within the framework of a given program, such as a long-term biological monitoring program.

Acknowledgements

We would like to extend special thanks to Jim Romano and Alan Wachtell at the University of Connecticut for use of and assistance with SEM facilities; Regina Jones for help with fieldwork and Kate Duff who assisted in the preparation of the manuscript. This work was supported in part by a grant from the United States Department of the Interior (14-08-0001-G1412-04) and a 1988 CSU-AAUP grant to P. A. Siver.

References

ALMER, B., W. DICKSON, C. EKSTRÖM, E. HÖRNSTRÖM, AND U. MILLER. 1974. Effects of acidification on Swedish lakes. Ambio 3: 30–36.

ANDERSEN, R. A. 1987. Synurophyceae classis nov., a new class of algae. Am. J. Bot. 74: 337–353.

ASMUND, B., AND J. KRISTIANSEN. 1986. The genus *Mallomonas* (Chrysophyceae). Opera Botanica 85: 1–128.

BAKER, A. C., AND A. J. BROOK. 1971. Optical density profiles as an aid to the study of microstratified phytoplankton populations in lakes. Arch. Hydrobiol. 69: 214–233.

BATTARBEE, R. W. 1984. Diatom analysis and the acidification of lakes. Philos. Trans. R. Soc. Lond. Ser. B305: 451–477.

BATTARBEE, R. W., J. P. SMOL, AND J. MERILÄINEN. 1986. Diatoms as indicators of pH: an historical review, p. 5–17. *In* J. P. Smol, R. W. Battarbee, R. B. Davis, and J. Meriläinen [ed.] Diatoms and lake acidity. Dr. W. Junk Publishers, Dordrecht, The Netherlands.

CHARLES, D. F. 1984. Recent pH history of Big Moose Lake (Adirondack Mountains, New York, U.S.A.) inferred from sediment diatom assemblages. Verh. Int. Ver. Limnol. 22: 559–566.

1985. Relationships between surface sediment diatom assemblages and lakewater characteristics in Adirondack lakes. Ecology 66: 994–1011.

CHARLES, D. F., AND S. A. NORTON. 1986. Paleolimnological evidence for trends in atmospheric deposition of acids and metals, p. 335–431. *In* Acid deposition: long-term trends. National Academy Press.

CHARLES, D. F., AND J. P. SMOL. 1988. New methods for using diatoms and chrysophytes to reconstruct past lakewater pH. Limnol. Oceanogr. 33: 1451–1462.

CRONBERG, G., AND J. KRISTIANSEN. 1980. Synuraceae and other Chrysophyceae from Central Smoland, Sweden. Bot. Not. 133: 595–618.

DAVIS, R. B., AND D. S. ANDERSON. 1985. Methods of pH calibration of sedimentary diatom remains for reconstructing history of pH in lakes. Hydrobiol. 120: 69–87.

DAVIS, R. B, S. A. NORTON, C. T. HESS, AND D. F. BRAKKE. 1983. Paleolimnological reconstruction of the effects of atmospheric deposition of acids and heavy metals on the chemistry and biology of lakes in New England and Norway. Hydrobiol. 103: 113–123.

DAVIS, R. B., AND J. P. SMOL. 1986. The use of sedimentary remains of siliceous algae for inferring past chemistry of lake water — problems, potential and research needs, p. 291–299, *In* J. P. Smol., R. W. Battarbee, R. B. Davis, and J. Meriläinen [ed.] Diatoms and lake acidity. Dr. W. Junk Publishers, The Netherlands.

DIXIT, S. S., A. S. DIXIT, AND R. D. EVANS. 1988a. Scaled chrysophytes (Chrysophyceae) as indicators of pH in Sudbury, Ontario lakes. Can. J. Fish. Aquat. Sci. 45: 1411–1421.

1988b. Sedimentary diatom assemblages and their utility in computing diatom-inferred pH in Sudbury, Ontario lakes. Hydrobiologia 169: 135–148.

DÜRRSCHMIDT, M. 1982. Studies on the Chrysophyceae from South Chilean inland waters by means of scanning and transmission electron microscopy. II. Arch. Hydrobiol. Suppl. 63: 121–163.

1984. Studies on scale-bearing Chrysophyceae from the Giessen area. Federal Republic of Germany. Nord. J. Bot. 4: 123–143.

ELORANTA, P. 1985. Notes on the scaled chrysophytes (Synuraceae, Chrysophyceae) in small lakes in and near Salamajarvi National Park, Western Finland. Mem. Soc. Fauna Flora Fenn. 61: 77–83.

FEE, E. J. 1976. The vertical and seasonal distribution of chlorophyll in lakes of the Experimental Lakes Area, northwestern Ontario. Implications for primary production estimates. Limnol. Oceanogr. 21: 767–783.

GREEN, R. B. 1979. Scale-bearing Chrysophyceae from seven lakes on Vancouver Island. Syesis 12: 155–162.

GRETZ, M. R., M. R. SOMMERFELD, AND D. E. WUJEK. 1979. Scaled Chrysophyceae of Arizona: a preliminary survey. J. Ariz. — Nev. Acad. Sci. 14: 75–80.

GRETZ, M. R., D. E. WUJEK, AND M. SOMMERFELD. 1983. Scaled Chrysophyceae of Arizona: further additions to the aquatic flora. J. Ariz. — Nev. Acad. Sci. 18: 17–21.

HEALY, F. P. 1983. Effect of temperature and light intensity on the growth rate of *Synura sphagnicola*. J. Plankton Res. 5: 767–774.

KRISTIANSEN, J. 1978. Studies on the Chrysophyceae of Bornholm. II. Bot. Tidsskr. 73: 71–85.

1986. Silica-scale bearing Chrysophytes as environmental indicators. Br. Phycol. J. 21: 425–436.

MIDDLETON, A. C., AND F. A. ROVERS. 1976. Average pH. J. Water Pollut. Control Fed. 48: 395–396.

NORUŠIS, M. J. 1985. SPSSX: advanced statistics guide. McGraw-Hill Publishers.

PICK, F. R., C. NALEWAJKO, AND D. R. S. LEAN. 1984. The origin of a metalimnetic chrysophyte peak. Limnol. Oceanogr. 29: 125–134.

PREISIG, H. R., AND D. J. HIBBERD. 1983. Ultrastructure and taxonomy of *Paraphysomonas* (Chrysophyceae) and related genera. 3. Nord. J. Bot. 3: 695–723.

ROIJACKERS, R. M. M. 1981. Chrysophyceae from freshwater localities near Nijmegen, the Netherlands. Hydrobiologia 76: 179–189.

ROIJACKERS, R. M. M., AND H. KESSELS. 1981. Chrysophyceae from freshwater localities near Nijmegen, the Netherlands. II. Hydrobiologia 80: 231–239.

1986. Ecological characteristics of scale-bearing Chrysophyceae from the Netherlands. Nord. J. Bot. 6: 373–383.

Siver, P. A. 1987. The distribution and variation of *Synura* species (Chrysophyceae) in Connecticut, U.S.A. Nord. J. Bot. 7: 107–116.

1989a. The distribution of scaled chrysophytes along a pH gradient. Can. J. Bot. 67: 2120–2130.

1989b. A critical literature review on the usefulness of chrysophytes to detect lake chronic or episodic acidification and/or recovery in the context of a long term monitoring program. U.S. Environmental Protection Agency, Corvallis, Corvallis, OR. (In press)

1989c. The separation of *Mallomonas acaroides* v. *acaroides* and v. *muskokana* (Synurophyceae) along a pH gradient. Beiheft zur Nova Hedwigia 95: 111–117.

Siver, P. A., and J. S. Hamer. 1989. Multivariate statistical analysis of the factors controlling the distribution of scaled chrysophytes. Limnol. Oceanogr. 34: 368–381.

Skogstad, A. 1982. Synuraceae-Floraen I 27 Lokaliteter I Oslo-Omrodet, En Lysmikros Kopisk Og Elektronmikroskopisk Undersokelse. Institute of Marine Biology and Limnology, University of Oslo. 128 p.

Smol, J. P. 1986. Chrysophycean microfossils as indicators of lakewater pH. *In* J. P. Smol, R. W. Battarbee, R. B. Davis, and J. Meriläinen [ed.] Diatoms and lake acidity. Dr. W. Junk Publishers, Dordrecht, The Netherlands.

Smol, J. P., D. F. Charles, and D. R. Whitehead. 1984. Mallomonadacean (Chrysophyceae) assemblages and their relationships with limnological characteristics in 38 Adirondack (New York) lakes. Can. J. Bot. 62: 911–923.

Thornton, K. W., F. E. Payne, J. Ford, and D. H. Landers. 1987. The concept of TIME. U.S. Environmental Protection Agency, Environmental Research Laboratory, Corvallis, Corvallis, OR.

Wee, J. L. 1983. Specimen collection and preparation for critical light microscope examination of Synuraceae (Chrysophyceae). Trans. Am. Micros. Soc. 102: 68–76.

Wujek, D. E., and R. Hamilton. 1972. Studies on Michigan Chrysophyceae. I. Mich. Bot. 11: 51–59.

1973. Studies on Michigan Chrysophyceae. II. Mich. Bot. 12: 118–122.

Wujek, D. E., R. Hamilton, and J. Wee. 1975. Studies on Michigan Chrysophyceae III. Mich. Bot. 14: 91–94.

Wujek, D. E., M. Gretz, and M. G. Wujek. 1977. Studies on Michigan Chrysophyceae. IV. Mich. Bot. 16: 191–194.

Vertical Fine Structure of Particulate Matter and Nutrients in Sea Ice of the High Arctic

Ralph E. H. Smith

Department of Biology, University of Waterloo, Waterloo, Ont. N2L 3G1 Canada

and W. Glen Harrison, Leslie R. Harris, and Alex W. Herman

Department of Fisheries and Oceans, Biological Sciences Branch, Bedford Institute of Oceanography, Dartmouth, N.S. B1Y 4A2 Canada

Smith, R. E. H., W. G. Harrison, L. R. Harris, and A. W. Herman. 1990. Vertical fine structure of particulate matter and nutrients in sea ice of the high arctic. Can. J. Fish. Aquat. Sci. 47: 1348–1355.

The vertical fine structure of particulate matter and inorganic nutrients through the bottom layers of sea ice was determined at a site in the Canadian high arctic. Intense vertical gradients of chlorophyll a, nitrate, ammonium, nitrite, phosphate, and silicate developed in the lower 6 cm of the ice as ice algae attained standing crops of 250 $mg\cdot m^{-2}$ (up to 60 $mg\cdot L^{-1}$) of chlorophyll a. Pigment and inorganic nutrient concentrations were closely correlated, and pools of inorganic nutrient were shown to exist in the particulate matter, suggesting that the extremely high dissolved nutrient concentrations in the bottom ice (e.g. up to 400 $\mu mol\cdot L^{-1}$ nitrate) were derived at least in part from leakage of algal intracellular pools. Nitrogen and phosphorus were present in excess of algal needs, but silicon may not have been. The ratios of particulate organic carbon to chlorophyll a and to particulate organic nitrogen increased from the ice–water interface upwards, consistent with a physiological response of the ice algae to the strong corresponding gradient of light availability. Although spatially compact, the assemblage of algae in the bottom ice inhabits a highly stratified environment.

La structure verticale fine des particules et des éléments nutritifs inorganiques dans les couches de fond de la glace de mer a été établie à un endroit dans l'Arctique canadien. Des gradients verticaux prononcés de chloropylle a, de nitrate, d'ammoniac, de nitrite, de phosphate et de silicate se sont développés dans les 6 derniers cm de glace alors que les algues contenues dans la glace atteignaient des teneurs en chlorophylle a de 250 $mg\cdot m^{-2}$ (jusqu'à 60 $mg\cdot L^{-1}$). Il existait une corrélation étroite entre les concentrations de pigment et d'éléments nutritifs inorganiques dans les particules, ce qui porte à croire que les concentrations élevées d'éléments nutritifs dissous dans la glace de fond (par ex. jusqu'à 400 μ molaire de nitrate) provenaient en partie, du moins, de fuite de réserves intracellulaires des algues. Les quantités d'azote et de phosphore étaient supérieures aux besoins des algues, mais peut être pas le silicone. Les rapports de carbone organique particulaire et de chlorophylle a et d'azote organique particulaire ont augmenté à partir de l'interface eau-glace vers le haut, conformément à une réaction physiologique des algues dans la glace au fort gradient correspondant de lumière disponible. L'assemblage d'algues dans la glace de fond, bien que spatialement dense, occupe un milieu fortement stratifié.

Received September 18, 1989
Accepted February 8, 1990
(JA310)

Reçu le 18 septembre 1989
Accepté le 8 février 1990

Communities of algae, bacteria, protozoa, and invertebrate animals colonize sea ice in polar regions and are known collectively as the ice biota (Horner et al. 1988). In the Antarctic, ice biota colonize varying types of ice, and may occur in abundance in the bottom ice (i.e. the lower 20 cm or so), on top of the ice, or in intermediate layers and cracks in the ice (Horner 1985; Horner et al. 1988). In the Arctic, ice biota are currently known to be widely abundant only in the bottom ice, where algae form layers of exceptionally high concentration compared to other marine habitats (Smith et al. 1988; Welch et al. 1988; Welch and Bergmann 1989). Most studies to date, whether in the Arctic or the Antarctic, have sampled the bottom ice biota as a whole with little attempt to resolve the vertical structure of the populations within the ice. The compact vertical distribution, compared to those familiar from planktonic systems, of the bottom ice biota invites such treatment. There is every reason to believe, however, that environmental conditions vary strongly through even the limited vertical extent of the bottom ice community.

The supply of light, attenuated by passage through snow and ice, frequently limits production of bottom ice algae (Gosselin et al. 1986; Grossi et al. 1987; Smith et al. 1988; Welch and Bergmann 1989). At the high concentration of algal pigment commonly observed at sites in the high Arctic and McMurdo Sound in Antarctica, light can be attenuated from saturating levels at the top of the algal layer to less than compensation values at the bottom (Smith et al. 1988) and its spectral quality heavily modified, from blue-green at the top of the algal layer to predominantly green at the bottom (Palmisano et al 1987; SooHoo et al. 1987). Compared to phytoplankton in a mixed water column, ice algae are relatively fixed in vertical position, although some may at times move at rates as high as a few centimetres per day as the ice sheet thickens (Welch and Bergmann 1989). Such relatively small rates of movement should expose ice algae to comparatively sustained differences in light quantity and quality along vertical gradients.

Bottom ice algae in Hudson Bay may be limited by the supply of inorganic nitrogen, phosphorus, or silicon when light availability improves in late spring, depending on the salinity and accompanying chemical regime of the underlying water (Maestrini et al. 1986; Gosselin et al. 1989). In the high arctic, the vertical transport of inorganic nutrients to the bottom ice algae may limit ice algal productivity when algal crops are large and their nutrient demand high (Cota et al. 1987; Cota and Horne 1989). However, high inorganic nutrient concentrations have been reported from bottom ice communities (Cota et al. 1990), and the algae also appear to possess relatively large pools of intracellular free amino acids (Smith et al. 1989). The algae may enrich the bottom ice by concentrating nutrients from the water column (Cota et al. 1989), but we know little of the distribution of nutrients within the community. Except in the extreme lower portions of the ice sheet, ice algae are presumed to inhabit brine channels and pockets which are largely isolated from the underlying seawater, and may be extensively modified in salinity and nutrient concentrations (Maykut 1985; Horner 1985; Grossi and Sullivan 1985). We may therefore anticipate strong vertical gradients in the chemical, as well as light, environment.

Assemblages of ice algae from bottom ice in the Antarctic develop species-specific vertical distributions, on the scale of 5–20 cm, suggesting that ice algae are influenced by the expected gradients of growth conditions (Grossi and Sullivan 1985). Species-specific vertical distributions have also been reported for arctic ice communities (Hsiao 1980). As yet, there are no published data that would resolve distributions within the bottom layer, typically 5 cm thick or less (Smith et al. 1988; Welch and Bergman 1989), that commonly includes the bulk of the algal community in high arctic annual ice.

The purpose of the present work was to determine the vertical profiles of ice algal pigment, chemical composition, and inorganic nutrient concentrations at a site in the high arctic in order to characterize the vertical structure of ice algal populations and their light and nutrient environment. Such information is basic to any mechanistic understanding of ice algal growth and productivity. Conventional sampling methods, which involve coring the ice from the surface downwards, may distort the apparent vertical structure through selective loss of material from the lower and softer parts of the ice (Welch et al. 1988). We were able to use a novel under-ice sampler to minimize such problems, and obtain an accurate characterization of the growth and vertical development of an intense algal bloom from its beginning to its decline.

Materials and Methods

The sampling sites were in Resolute Passage (part of the Northwest Passage), approximately 3 km offshore from the settlement of Resolute (74°40′ N, 90°0′ W). Water depth was aproximately 100 m. The area is described more fully in Cota et al. (1987) and Welch and Bergman (1989).

Cores were obtained from the underside of the ice using a new in situ incubator/sampler, except for the routine sampling for pigment in 1986 (see below). The in situ sampler was deployed from the surface through a 25.4 cm (10″) auger hole. The underside of the ice was inspected using a video camera before implanting the cylindrical chamber (12.5 cm diameter) of the sampler to its normal depth of about 60 mm penetration into the ice. A heating element on the rim of the chamber allowed implantation within about 2 min without significant melting of the adjacent ice. The samples described here were collected in the course of primary production experiments, which required the chamber to remain implanted in the ice for 1–1.5 h before retrieval. A heated cutter was triggered from the surface to cut free the chamber, which was retrieved together with its captive ice core and rushed to a darkened tent for processing within minutes of retrieval.

The core recovered from the sampler chamber was cut into sections using an electric meat cutter, with a circular stainless steel blade capable of making sections of 2 mm or more thickness. In some cases, the sections were allowed to melt, taking care that they did not warm to more than a few degrees above zero (low salinity treatment). In other cases, filtered seawater (30‰) was added to the ice sections before they melted to prevent the salinity experienced by organisms in the sections from falling below 27‰ (high salinity treatment). Previous measurements have shown that, without added seawater, the melted ice sections range from about 6 to 10‰ depending on distance from the ice–water interface.

Within about 1 h of melting the sections, aliquots were filtered and frozen pending analysis for chlorophyll *a* and pheopigments by a fluorometric method (Yentsch and Menzel 1963; Smith et al. 1989). All filtering used glass fibre filters, GF/F grade. The filters were extracted with acetone (containing 10% distilled water by volume) for 18–24 h at −20°C before reading on the fluorometer. Replicability of chlorophyll *a* and pheopigment analyses by this method has been excellent, with average 95% confidence intervals of ±5% of the mean or less for triplicates collected at various times over 3 yr of sampling (R. E. H. Smith, unpubl. data).

Filtrate was collected and frozen pending analysis of inorganic nutrients. Nitrate, nitrite, phosphate, and silicate were determined using a Technicon automated analyzer. Ammonium was analyzed by the phenolhypochlorite method (Solorzano 1969). The nutrients were not analyzed until after several months of frozen storage, so ammonium concentrations would be suspect if initial concentrations were low (Parsons et al. 1984). However, the typical nutrient concentrations in the ice samples and the patterns of variation indicated that contamination during storage had little influence on the very high nutrient levels in the ice samples.

Additional aliquots were collected on filters and frozen pending extraction and analysis of inorganic nutrients from the particulate matter. To extract nutrients, the filters were placed in boiling distilled water for 10 min, and then the extract was filtered again (through GF/F) before analysis (Thoresen et al. 1982). Blanks were run to assess contributions from the distilled water and filters, which were negligible compared to the samples.

Precombusted filters were used to collect aliquots for analysis of particulate organic carbon (POC) and particulate organic nitrogen (PON) by elemental analyzer (Smith et al. 1989).

Seasonal chlorophyll *a* data for 1986 were based on routine sampling using a SIPRE corer operated from the surface (Smith et al. 1988). While the surface coring method may not recover all the pigment present in the undisturbed ice (Smith et al. 1988, Welch et al. 1989) the results confirmed that the 1986 nutrient samples, like the 1987 samples, were taken at or soon after the seasonal peak in algal biomass. The 1986 nutrient samples (collected May 21), like those for 1987 (collected May 9 and 13), were taken using the in situ sampler.

We assume that our sampling methods provided relatively quantitative recovery of the microbial community, including algae and bacteria. By contrast, the recovery of protozoa and larger fauna was probably incomplete due to avoidance reac-

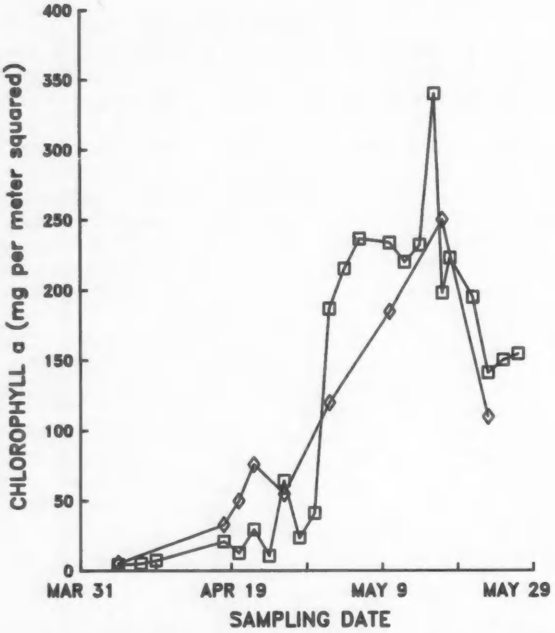

FIG. 1. The seasonal dynamics of chlorophyll *a* concentration observed in 1987 (squares) and 1986 (diamonds) in the lower 60 mm (1987) or 40 mm (1986) of annual sea ice covered by 0–4 cm of snow. Each point is the mean of duplicate determinations on a single SIPRE core.

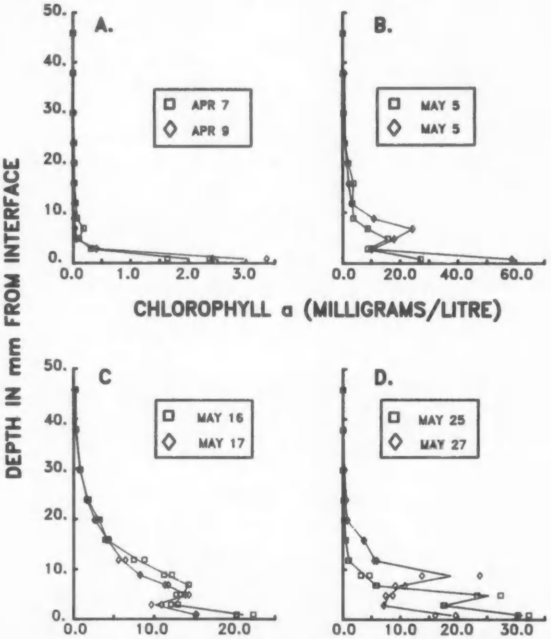

FIG. 2. The vertical profiles of chlorophyll *a* concentration at different times from the beginning of the bottom ice algal bloom to its decline in 1987. Each point represents an individual determination.

TABLE 1. Summary of regression models relating particulate matter and inorganic nutrients (μmol·L^{-1})) to chlorophyll *a* concentrations (μg·L^{-1}) in the lower 5 cm of arctic sea ice. All models are of the form log $(Y) = a + b \cdot \log(X)$, and were based on seven measured profiles totalling 69 individual samples for POC (particulate organic carbon), PON (particulate organic nitrogen), and Pheo (pheopigment). Sample size was 18 for NH_4 and 34 for the other nutrients. Slopes significantly different from unity ($P<0.05$) are indicated by *.

Y	*a*	*b*	SE (*b*)	R^2
POC	1.384	0.700*	0.026	0.91
PON	0.0426	0.815*	0.021	0.96
Pheo	−0.844	0.965	0.040	0.90
NO_3	−1.373	0.831*	0.041	0.93
NH_4	−0.869	0.534*	0.086	0.69
PO_4	−1.147	0.635*	0.044	0.88
SiO_3	0.480	0.248*	0.073	0.29

tions and destruction during sample processing (Garrison and Buck 1986). Thus, the results should be viewed as describing primarily the algal and bacterial communities (and associated nutrient conditions).

Results

Progress of the Algal Bloom

Sampling commenced in early April, 1987, and continued to late May. Chlorophyll *a* concentrations integrated over the bottom 6 cm of the ice increased from initial values of less than 5 mg·m^{-2} to a sustained peak greater than 200 mg·m^{-2} in mid-May (Fig. 1). In the latter half of May, chlorophyll *a* concentrations began to decline. However, the bottom ice was still noticeably coloured as late as the end of June (L. R.Harris, unpubl. data), indicating that substantial algal populations remained even then. Consistent with previous years' observations, visible pigment was routinely restricted to the lower few centimetres of the ice.

Less intensive sampling (using surface coring) in 1986 revealed a broadly similar pattern of seasonal pigment dynamics, although the last sample taken suggested an earlier and greater decline in pigment concentrations than in 1987 (Fig. 1). The chlorophyll dynamics in 1986 and 1987 indicated that our samples for particulate matter composition and nutrient concentrations were taken at or shortly after the peak of ice algal abundance in both years. In both years, the samples were taken before sloughed algae began to appear in the water column beneath the ice.

The profiles of chlorophyll *a* concentration within the ice in 1987 revealed substantial modification throughout the onset, peak, and early decline of the bloom. At the outset, the layer of high chlorophyll *a* concentrations (more than 1 mg·L^{-1}) was restricted approximately to the bottom 2 mm of the ice (Fig. 2A). As the bloom progressed, high chlorophyll concentrations were found progressively higher in the ice (Fig. 2B,2C,2D). For much of the bloom period, the profile of chlorophyll concentrations with depth was roughly exponential, with peak concentrations occurring within the lower 4 mm of the ice sheet. The greatest concentrations, in the range 50–60 mg·L^{-1}, were attained in early May in the lowest sections (e.g. Fig. 2B), and were not surpassed or even equalled later in the bloom.

Although the chlorophyll *a* profiles in 1987 were roughly exponential in form, a distinct bimodal pattern was superimposed from the time of the bloom's peak in early May to the end of our sampling period (Fig. 2B,2C,2D). The secondary peak occurred variously between 5 and 10 mm from the ice–water interface. By late May, during the bloom's early decline, the concentration of chlorophyll *a* in the secondary peak rivalled that in the primary peak in the lower 4 mm (Fig. 2D). At the same time, a banding of colour in the ice cores became obvious to the naked eye, consistent in location and occurrence with the secondary peak of chlorophyll *a* concentration.

The chlorophyll *a* concentration averaged over all the profiles measured during April, 1987, was significantly greater ($P<0.05$, *t*-test) at 1 mm depth than at any greater depths from the ice–water interface. For the averaged May profiles, the concentration at 1 mm was not significantly different from the concentrations at 5 or 7 mm depth, but was significantly greater than the concentration at all other depths, including 3 mm (at the 0.05 level, *t*-test). Although crude, such tests reinforce the impression of a late-developing secondary maximum in chlorophyll *a* concentration as suggested both by the individual profiles (Fig. 2) and the appearance of the cores in the field.

The pigment profiles measured in 1986 lacked secondary peaks but otherwise resembled those measured at the peak of the algal bloom in 1987.

Particulate Matter Composition

Pheopigment concentrations vaied directly with chlorophyll *a* concentrations, forming roughly exponential profiles in parallel with those for chlorophyll *a*. About 90% of the variation in pheopigment concentrations was explained by a double log-linear regression on chlorophyll *a* concentrations (Table 1). The exponent of the relationship was not significantly different from unity, suggesting a direct, linear relationship. The abundance of pheopigment relative to chlorophyll *a* increased slightly with distance from the interface above 2 cm from the ice–water interface. However, the ratio of pheopigment to chlorophyll *a* was less than 0.25 even in the upper sections, averaging 0.135 (±0.035, 95% C.I.) in the 30–60 mm sections. By comparison, the ratio was 0.125 (±0.017, 95% C.I.) over the entire depth of ice sampled.

Profiles of POC and PON concentrations were measured only during the peak of the 1987 bloom, May 1–13. Like pheopigments, POC and PON also showed roughly exponential profiles, covarying with chlorophyll *a* concentrations. Both POC and PON were closely related to chlorophyll *a* in double log-linear regression models and the exponents of both regressions were significantly less than unity (Table 1). Profiles of the ratios of POC to chlorophyll *a* and to PON (Fig. 3) showed generally increasing values, from the ice–water interface upwards. Regression analysis demonstrated that both ratios were related to depth by a highly significant exponential model, with R^2 values of 78% for the POC:chlorophyll *a* ratio and 76% for the POC:PON ratio (Fig. 3). The ratios actually observed in the lowest section, 0–2 mm, were somewhat higher than expected from the regression model (Fig. 3).

Inorganic Nutrients

Measured near the peak of the ice algal bloom (before major sloughing of algae), the profiles of dissolved inorganic nutrient concentration (Fig. 4) often resembled the approximately exponential chlorophyll *a* profiles, but the profiles did vary significantly among nutrients, sampling dates, and with sample processing methods, as described below. Nitrate closely followed an exponential function of depth, with R^2 values ranging between 92 and 98% for individual profiles, and a highly significant pooled relationship. At the opposite extreme, silicate followed an exponential model for only one profile. Phosphate and ammonium were intermediate in adherence to the exponential model, with R^2 values ranging between 50 and 90% for individual profiles. Nonetheless, it was clear that the nutrients, with the possible exception of silicate, frequently displayed

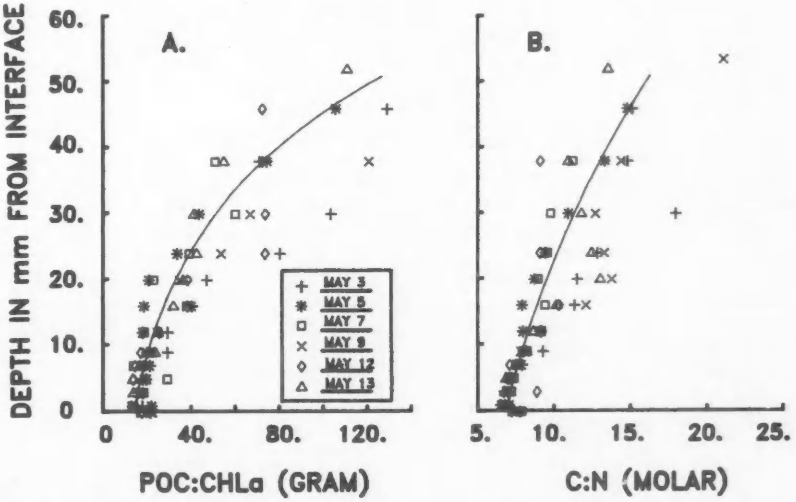

FIG. 3. The vertical profiles of particulate matter composition ratios observed at different times during the peak of the bloom of bottom ice algae in 1987. (A) Particulate organic carbon:chlorophyll *a* (POC:Chl *a*). The fitted line is log (POC:Chl *a*) = 1.182 + 0.0188·Depth. (B) Particulate organic carbon: particulate organic nitrogen (POC:PON). The fitted line is log (POC:PON) = 0.846 + 0.00744·Depth.

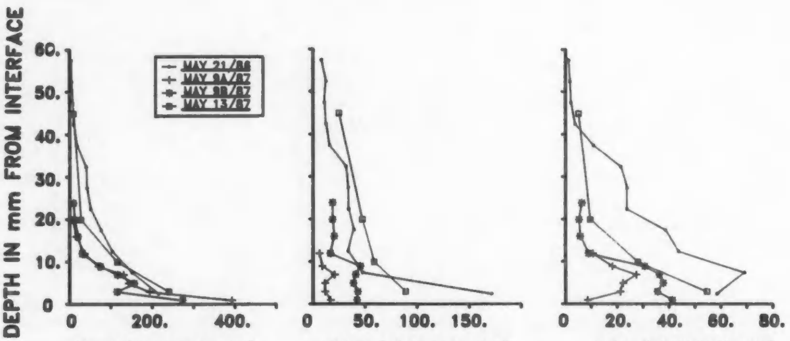

FIG. 4. The profiles of dissolved inorganic nutrient concentrations observed in bottom ice in 1986 and 1987. Samples were melted with added seawater (high salinity treatment) on May 9 (B) and May 13, 1987, but without added seawater (low salinity treatment) on May 21, 1986 and May 9 (A), 1987.

TABLE 2. Inorganic nutrient extracted in distilled water from particulate matter in samples of annual sea ice at different depths from the ice–water interface. The values are percentages of the total inorganic nutrient (dissolved plus extracted) and thus depict the proportion of the inorganic pool (particulate and dissolved) which was extractable; the ranges are 95% C.I. (i.e. twice the standard error) and brackets enclose the sample number. Results for all nutrients except nitrate are pooled over high and low salinity treatments. Missing data indicated by na.

Depth (mm)	NH_4	NO_2	NO_3 Low	NO_3 High	Si	PO_4
0–10	37.2	82.4	3.3	19.3	13.1	37.0
	±11.5	±18.1	±1.1	±6.7	±15.5	±15.4
	(11)	(11)	(5)	(6)	(11)	(11)
10–20	30.8	87.4	21.2	24.9	na	37.0
	±5.2	±25.1	±14.4	±6.7		±11.4
	(5)	(5)	(3)	(4)		(5)
20–45	19.1	92.9	41.5	37.0	na	32.4
	±11.3	±8.9	na	±8.4		±14.6
	(5)	(5)	(1)	(4)		(5)

TABLE 3. The average concentration of inorganic nutrient as a percentage of the concentration of the same element in particulate form over the entire thickness of ice (0–6 cm from ice–water interface) sampled in this study, pooling the results from four profiles collected over 2 yr. TIN denotes the sum of the inorganic N fractions.

	NH_4	NO_2	NO_3	TIN	Si[1]	PO_4[2]
Percent inorganic	3.01	1.12	5.73	9.81	4.96	23.3
95% C.I.	±2.22	±1.32	±1.17	±3.26	±8.01	±3.62
Sample number	(20)	(9)	(20)	(9)	(8)	(17)

[1] Particulate silica estimated as 10 times chlorophyll *a* (weight/weight) (Cota et al. 1987).

[2] Particulate phosphorus estimated as (1/106) times carbon (mole/mole) (Parsons et al. 1983).

extremely steep gradients of concentration over very limited vertical distances. The peak concentrations, observed in the lowest sections, were extraordinarily high for marine systems, greater than 200 μmol·L^1 for nitrate and greater than 50 μmol·L^1 for phosphate.

Much of the variation in nutrient profiles among sampling dates could be explained by variations in the chlorophyll *a* profiles. Dissolved nitrate and phosphate concentrations varied closely and directly with chlorophyll *a* in a double log-linear regression model of the pooled data (Table 1). The lack of pattern in residuals suggested that the regression models were not only good predictors but also quite accurate in functional form for nitrate and phosphate. Ammonium was less closely related to chlorophyll *a*, while silicate was poorly related to chlorophyll *a* concentration (Table 1).

Significant amounts of inorganic nutrient could be extracted from the particulate matter using distilled water (Table 2). The proportion extractable varied with salinity treatment only for nitrate (Table 2), and only in the lower 10 mm of the ice. The extractable proportion of ammonium, nitrite and phosphate was also higher in the high salinity treatment in the lower 10 mm, but not significantly so. Salinity treatment had no significant effect on the extractable proportion in higher sections for any nutrient, so the results were pooled across treatments except for nitrate (Table 2). The extractable proportion was determined only on samples from 1987, but confidence intervals were still large (Table 2), reflecting substantial variability even within narrow vertical zones within one season.

Among nutrients, the outstanding difference was the consistently high extractable proportion of nitrite compared to other nutrients (Table 2). Oher differences were specific to depth class. The extractable proportion for nitrate was significantly lower than for other nutrients in the lower 10 mm, especially in the low salinity treatment. Ammonium and phosphate yielded the smallest extractable proportions in the 20–45 mm depth range. The extractable proportion of silicate was small, but was measured only in the lower 10 mm.

The ratio of total inorganic nutrient (dissolved plus extractable) to particulate nutrient was greatest for phosphate and least for nitrite, over the entire sampled algal layer (Table 3). Except for silicate, there was little or no vertical pattern. By contrast, the ratio of inorganic silicate (dissolved only) to estimated particulate concentrations was minimal in the lower 10 mm (1.09%, ±0.47 95% C.I.), and increased to a maximum in the highest sections (17.8%, ±7.81, 95% C.I. in the 40–60 mm depth range).

The composition of inorganic nitrogen changed substantially from the ice–water interface upwards (Fig. 5). The dissolved

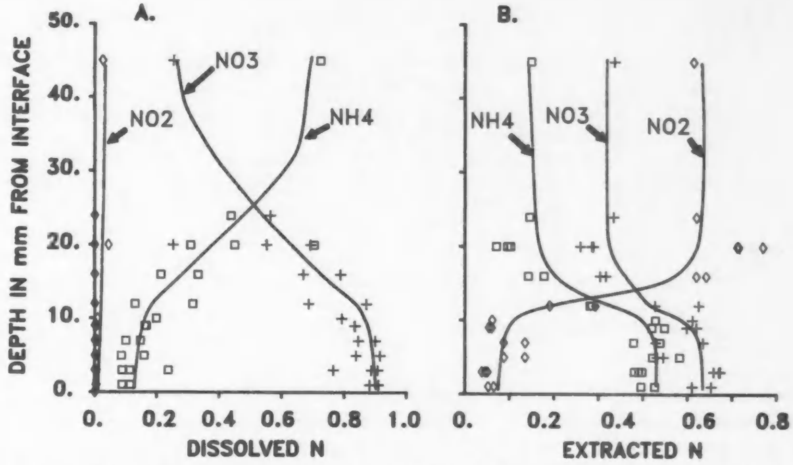

FIG. 5. The vertical profiles of inorganic nitrogen pools measured on May 9 and 13, 1987, as proportion of total inorganic nitrogen in dissolved form (A) or extractable form (B). The lines were fitted by eye to data smoothed by a running mean for NO_3 (+), NO_2 (◇), and NH_4 (□).

fraction was dominated by nitrate in the lower sections, but ammonium became equally or more abundant than nitrate in the upper sections. In the extractable fraction, nitrate and ammonium were of comparable importance in the lower sections, where nitrite was usually undetectable. However, nitrite became the dominant pool in the extractable fraction of the upper sections (Fig. 5).

Discussion

Algal pigment is largely restricted to the lower 5 or 10 cm of annual sea ice throughout the high Arctic according to published reports (Hsiao 1980; Cota et al. 1987; Welch and Bergmann 1989). Our results showed strong gradients in pigment concentration through the bottom 5 cm and peak concentrations within the lower centimetre (Fig. 2). The pattern was maintained even though the ice itself grew approximately 20 cm in thickness over the sampling period. The algae might have moved downward with the ice to maintain the observed pigment profiles (Welch and Bergmann 1989) or may have grown preferentially in the lower sections (Meguro et al. 1967; Hsiao 1980; Grossi and Sullivan 1985). The dominant algae in the bottom ice near Resolute are usually large, non-motile, colonial forms (Smith et al. 1988; and R. E. H. Smith, unpubl. data) but might conceivably be redistributed by brine drainage and associated convective motions of the interstitial water (Maykut 1985) as the ice grows.

Without cell counts and accurate measurements of ice growth rate we cannot be sure whether some algal movement and/or differential growth of populations occurred. However, pigment concentrations at 20 cm from the interface at the peak of the bloom in early–mid May were no lower, and often higher, than the concentrations at the interface in early April when the ice was about 20 cm thinner. This suggests that the algae were at least preserved as the ice grew past and may have continued to grow in isolated brine pockets (cf. Grossi and Sullivan 1985). The secondary peak of pigment concentration, at 6–10 mm distance from the interface, developed and intensified in May as self-shading slowed algal photosynthesis at the interface below to near the compensation point (R. E. H. Smith, unpubl. data; and Fig. 2). This too suggests that algae can be trapped by growing ice but continue to survive and grow, in this case even better than cells closer to the interface but at lower light levels. Clearly, however, conditions for algal growth over the whole bloom period are best close to the ice–water interface (within a cm), unless very substantial vertical movement of cells takes place. Since light availability should always favour populations growing higher in the ice (Smith et al. 1988) some other factor must be operating. The osmotic stress of increasing brine concentrations and the diminishing volume of interstitial liquid available for algal growth are often cited as the factors involved (Meguro et al. 1967; Horner 1985). If so, these aspects of the ice habitat must change dramatically over very small vertical scales, of only a few centimetres, in the ice in our study area.

The ratios POC:Chl *a* and POC:PON increased with distance from the ice-water interface (Fig. 3). Such variation is consistent with a physiological response of the algae to increasing light with increasing distance from the interface (Morris 1981; Grossi and Sullivan 1985; Smith et al. 1989). Light was attenuated by 80–95% in passage through the bottom 5 cm of ice from May 1 to the end of our observation period (unpubl. data), as expected from previous measurements of under-ice light in the area (Smith et al. 1988; Welch and Bergmann 1989). Not only the quantity but also the spectral quality of light would be expected to change in passage through highly concentrated algal assemblages like those described here (Palmisano et al. 1987; SooHoo et al. 1987), possibly prompting additional changes in biosynthesis and composition. However, self-shading and spectral modification by the algae themselves cannot explain all the observed changes in composition, because major changes in composition ratios were observed in the upper sections, above the major part of the algal layer (e.g. Fig. 3). Our results (Fig. 3) indicate that, even if algal cells can move as the ice grows, they are not mixed at a rate sufficient to maintain vertical uniformity of chemical composition even over spatial scales as small as a few centimetres.

The gradients of chemical composition could also reflect an increasing proportion of senescent or detrital cells and material with increasing distance from the ice–water interface, as found in studies of some other bottom ice communities in the Arctic (Hsiao 1980), Antarctic (Grossi and Sullivan 1985), and Gulf of St. Lawrence (Demers et al. 1984). The increasing concentrations of ammonium and nitrite relative to nitrate with distance from the interface (Fig. 5) might be consistent with such an interpretation but could have other explanations as well. We observed little change of the pheopigment to chlorophyll *a* ratio with depth, suggesting that algal-derived detrital matter did not accumulate to a significant degree in the upper sections. The vertical gradients of chemical composition may therefore be determined more by algal physiology and/or qualitative changes in the populations comprising the community of ice biota (Grossi and Sullivan 1985; Hsiao 1980) than by degradation of algae trapped in the ice.

Dissolved inorganic nutrients are known to attain high concentrations in the bottom layers of annual sea ice inhabited by ice algal populations (Grainger 1977; Cota et al. 1987, 1990) but the present results offer much greater vertical resolution than any previous. Probably as a consequence, we observed the highest volumetric chlorophyll and inorganic nutrient concentrations yet reported for bottom ice. Although very high, our measured chlorophyll values yield reasonable assimilation numbers when compared to contemporaneous measurements of ice algal photosynthesis (Smith and Herman, pers. observ.) and support estimates of in situ standing crops consistent with those reported by others working in the area (Welch and Bergmann 1989). The nitrate and phosphate concentrations in the lower centimetre of the ice (Fig. 4) are among the highest to be found in any coastal marine environment. Because the peak concentrations are found in the bottom few millimetres, where contact with the surface seawater is good, it seems highly unlikely that the nutrients result from freezing out (Meguro et al. 1967; Maykut 1985). The nutrient distributions are instead more consistent with the accumulation of nutrients from the water column within ice algae (Cota et al. 1987, 1990). The close correlation between chlorophyll concentration and the concentration of nitrate, phosphate, and to a lesser extent ammonium (Table 1) also suggests that much of the "dissolved" nutrient is derived from the algae (Cota et al. 1989).

The presence of significant amounts of water-extractable inorganic nutrient in the particulate matter (Table 2) showed that particulates, probably algal cells, could indeed be a source of dissolved nutrients. Ice samples for determination of inorganic nutrients are routinely melted before filtration, subjecting the ice biota in the sample to an osmotic shock that might be expected to promote leakage of cell contents, including nutrients (Garrison and Buck 1986; Cota et al. 1990). We expected that by reducing the shock with added seawater, we would greatly reduce the apparent dissolved concentrations but increase the extractable concentration. However, only nitrate, and then only in the bottom-most sections of ice, behaved as expected (Table 2). Phosphate, ammonium and nitrate may be very easily released from ice algae, by small changes in osmotic, temperature, or other conditions, or by the stresses of filtration. The extractable nutrient that we measured, even with our attempt to protect the cells against osmotic shock, was probably only a residual portion of the intracellular pools. Ice algae remain photosynthetically competent for periods of hours to at least a few days in melted seawater suspensions (Bates and Cota 1986; Smith et al. 1987, 1988), so whatever causes leakage of nutrients does not apear to seriously impair physiology. A likely agent might therefore be the filtration step itself (Goldman and Dennett 1985).

The apparent intracellular pools of inorganic nitrogen and phosphorus were large but within the known limits for nutrient-sufficient microalgae (Cembella et al. 1984; Wheeler 1983; Dortch et al. 1984) if we assume that the dissolved as well as the extractable nutrients originated from intracellular pools in the algae (Table 3). There was no indication that either nutrient might become more limiting with distance from the ice–water interface. The present results join previous evidence (Smith et al. 1989; Cota et al. 1990) that nitrogen and phosphorus are available in excess of algal need. Even the extractable pools alone would argue against any limitation by nitrogen or phosphorus.

Of the three nutrients studied here, silicon has been suggested to be closest to limiting ice algal growth in the vicinity of Resolute (Cota et al. 1990). Ice algae in Hudson Bay, which are sometimes limited by nitrogen or phosphorus in lower salinity waters, tend towards silicon limitation in the open waters of the bay where salinities are more comparable to those at our high arctic site (Gosselin et al. 1989). The relatively low ratio of reactive silicate to estimated particulate silica in our samples (Table 3) suggested that silicate was indeed in shortest supply. We found only a very small extractable pool (Table 3), consistent with expectation if diatoms are unable to accumulate substantial intracellular pools of reactive silicate (Paasche 1980), and indicating the lack of reserves comparable to those found for nitrogen or phosphorus. Relative availability of silicate was minimal in the lowest sections, where algal biomass concentration was greatest. Unfortunately, silicon requirements of diatoms are highly variable among species (Paasche 1980) and unknown for the species in our samples. Further study of silicon requirements of ice diatoms is needed to assess the possibility that silicon, together with light, is a controlling factor of ice algal growth in the high arctic.

Although vertically compact, the bottom-ice algal assemblage at our study site was highly structured and was associated with steep gradients in light, inorganic nutrient concentration, and particulate matter composition. We know little about the physiological state of populations from different points along the strong and persistent vertical gradients. Future studies of the physiological ecology of ice algae may have to recognize the likelihood that bottom ice assemblages like those near Resolute are composed of populations adapted to greatly differing growth conditions. On a coarser scale, vertical differences in species composition and the conditions and mechanisms of growth have already been recognized in different types of ice community (Meguro et al. 1967; Hoshiai 197; Garrison et al. 1983; Grossi and Sullivan 1985). Our results indicate that homogeneity of populations and growth conditions is an unwise assumption even within one type of community, over very small spatial scales.

References

BATES, S. S., AND G. F. COTA. 1986. Fluorescence induction and photosynthetic responses of arctic ice algae to sample treatment and salinity. J. Phycol. 22: 421–429.

CEMBELLA, A. D., N. J. ANTIA, AND P. J. HARRISON. 1984. The utilization of inorganic and organic phosphorus compounds as nutrients by eukaryotic microalgae: a multidisciplinary perspective. Part 2. CRC Crit. Rev. Microbiol. 11: 12–81.

COTA, G. F., AND E. P. W. HORNE. 1989. Physical control of arctic ice algal production. Mar. Ecol. Prog. Ser. (In press)

Cota, G. F., J. L. Anning, L. R. Harris, W. G. Harrison, and R. E. H. Smith. 1990. The impact of ice algae on inorganic nutrients in seawater and sea ice in Barrow Strait, NWT, Canada during spring. Can. J. Fish. Aquat. Sci. 47: 1402–1415.

Cota, G. F., S. J. Prinsenberg, E. B. Bennett, J. W. Loder, M. R. Lewis, J. L. Anning, N. H. F. Watson, and L. R. Harris. 1987. Nutrient fluxes during extended blooms of arctic ice algae. J. Geophys. Res. 92: 1951–1962.

Demers, S., J. C. Therriault, and C. Descolas-Gros. 1984. Biomasse et composition spécifique de la microflore des glaces saisonnières: influence de la lumière et de la vitesse de congélation. Mar. Biol. 78: 185–191.

Dortch, Q., J. R. Clayton, jr., S. S. Thoresen, and S. I. Ahmed. 1984. Species difference in accumulation of nitrogen pools in phytoplankton. Mar. Biol. 81: 237–250.

Garrison, D. L., and K. R. Buck. 1986. Organism losses during melting: a serious bias in sea ice community studies. Polar Biol. 6: 237–239.

Garrison, D. L., S. F. Ackley, and K. R. Buck. 1963. A physical mechanism for establishing algal populations in frazil ice. Nature (Lond.) 306: 363–365.

Goldman, J. C., and M. R. Dennett. 1985. Susceptibility of some marine phytoplankton species to cell breakage during filtration and post-filtration rinsing. J Exp. Mar. Biol. Ecol. 86: 47–58.

Gosselin, M., L. Legendre, J. C. Therriault, and S. Demers. 1989. Light and nutrient limitation of sea ice microalgae in arctic waters. J. Phycol. (In press)

Gosselin, M., L. Legendre, J. C. Therriault, S. Demers, and M. Rochet. 1986. Physical control of the horizontal patchiness of sea ice microalgae. Mar. Ecol. Prog. Ser. 29: 289–298.

Grainger, E. H. 1977. The annual nutrient cycle in sea ice, p. 225–300. *In* M. J. Dunbar [ed.] Polar oceans. Arctic Institute of North America, Calgary, Alta.

Grossi, S. M., and C. W. Sullivan. 1985. Sea ice microbial communities. V. The vertical zonation of diatoms in an antarctic fast ice community. J. Phycol. 21: 401–409.

Grossi, S. M., S. T. Kottmeier, R. L. Moe, G. T. Taylor, and C. W. Sullivan. 1987. Sea ice microbial communities VI. Growth and primary production in bottom ice under graded snow cover. Mar. Ecol. Prog. Ser. 35: 153–164.

Horner, R. A. 1985. Ecology of sea ice microalgae, p. 83–103. *In* R. A. Horner [ed.] Sea ice biota. CRC Press. Boca Raton, FL.

Horner, R., E. E. Syvertsen, D. P. Thomas, and C. Lange. 1988. Proposed terminology and reporting units for sea ice algal assemblages. Polar Biol. 8: 249–253.

Hoshiai, T. 1977. Seasonal change of ice communities in the sea ice near Syowa Station, Antartica, p. 307–317. *In* M. J. Dunbar [ed.] Polar oceans. Arctic Institute of North America, Calgary, Alta.

Hsiao, S. I. C. 1980. Quantitative composition, distribution, community structure and standing stock of sea ice microalgae in the Canadian arctic. Arctic 33: 768–793.

Maestrini, S. Y., M. Rochet, L. Legendre, and S. Demers. 1986. Nutrient limitation of the bottom ice microalgal biomass (southeastern Hudson Bay, Canadian Arctic). Limnol. Oceanogr. 31: 969–982.

Maykut, G. A. 1985. The ice environment, p. 22–82. *In* R. A. Horner [ed.] Sea ice biota. RC Press, Boca Raton, FL.

Meguro, H., K. Ito, and H. Fukushima. 1967. Ice flora (bottom type): a mechanism of primary production in polar seas and the growth of diatoms in sea ice. Arctic 20: 114–133.

Morris, I. 1981. Photosynthesis products, physiological state, and phytoplankton growth, p. 83–102. *In* T. Platt [ed.] Physiological bases of phytoplankton ecology. Can. Bull. Fish. Aquat. Sci. 210 p.

Paasche, E. 1980. Silicon, p. 259–284. *In* I. Morris [ed.] The physiological ecology of phytoplankton. Blackwell Scientific Publications, London, UK.

Palmisano, A. C., J. B. SooHoo, R. L. Moe, and C. W. Sullivan. 1987. Sea ice microbial communities. VII. Changes in under-ice spectral irradiance during the development of antarctic sea ice microalgal communities. Mar. Ecol. Prog. Ser. 35: 165–173.

Parsons, T. R., Y. Maita, and C. M. Lalli. 1984. A manual of chemical and biological methods for seawater analysis. Pergamon Press. Oxford, UK. 173 p.

Parsons, T. R., M. Takahashi, and B. Hargrave. 1983. Biological oceanographic processes. 3rd ed. Pergamon Press. Oxford, UK. 330 p.

Smith, R. E. H., J. Anning, P. Clement, and G. F. Cota. 1988. The abundance and production of ice algae in Resolute Passage, Canadian Arctic. Mar. Ecol. Prog. Ser. 48: 251–263.

Smith, R. E. H., P. Clement, G. F. Cota, and W. K.W.Li. 1987. Intracellular photosynthate allocati and the control of arctic marine ice algal production. J. Phycol. 23: 124–132.

Smith, R. E. H., P. Clement and E. J. Head. 1989. Biosynthesis and photosynthate allocation patterns of arctic ice algae. Limnol. Oceanogr. 34: 591–605.

Solorzano, L. 1969. Determination of ammonia in natural waters by the phenolhypochlorite method. Limnol. Oceanogr. 14: 799–801.

SooHoo, J. B., A. C. Palmisano, S. T. Kottmeier, M. P. Lizotte, S. L. SooHoo, and C. W. Sullivan. 1987. Spectral light absorption and quantum yield of photosynthesis in sea ice microalgae and a bloom of *Phaeocystis* from McMurdo Sound, Antarctic. Mar. Ecol. Prog. Ser. 39: 175–189.

Thoresen, S. S., Q. Dortch, and S. I. Ahmed. 1982. Comparison of methods for extracting intracellular pools of inorganic nitrogen from marine phytoplankton. J. Plankton Res. 4: 695–704.

Welch, H. E., and M. A. Bergmann. 1989. The seasonal development of ice algae and its prediction from environmental factors near Resolute, N.W.T., Canada. Can. J. Fish. Aquat. Sci. 46: 1793–1804.

Welch, H. E., M. A. Bergmann, J. K. Jorgenson, and W. Burton. 1988. A subice suction corer for sampling epontic algae. Can. J. Fish. Aquat. Sci. 45: 562–568.

Wheeler, P. A. 1983. Phytoplankton nitrogen metabolism, p. 309–346. *In* E. J. Carpenter and D. G. Capone [ed.] Nitrogen in the marine environment. Academic Press, New York, NY.

Yentsch, C. S., and D. W. Menzel. 1963. A method for the determination of phytoplankton chlorophyll and phaeophytin by fluorescence. Deep Sea Res. 10: 221–231.

A Possible Eddy Retention Mechanism for Ichthyoplankton in Hecate Strait

William R. Crawford,

Department of Fisheries and Oceans, Institute of Ocean Sciences, Sidney, B.C. V8L 4B2 Canada

Albert V. Tyler,

Department of Fisheries and Oceans, Pacific Biological Station, Nanaimo, B.C. V9R 5K6 Canada

and Richard E. Thomson

Department of Fisheries and Oceans, Institute of Ocean Sciences, Sidney, B.C. V8L 4B2 Canada

Crawford, W. R., A. V. Tyler, and R. E. Thomson. 1990. A possible eddy retention mechanism for Ichthyoplankton in Hecate Strait, Can. J. Fish. Aquat. Sci. 47: 1356–1363.

The cause of the high rate of production of groundfish in Hecate Strait is uncertain. It is likely that the large, shallow areas of the Strait contribute to the high productivity because of their suitability as juvenile habitat. In winter, however, when many groundfish species spawn, a strong current flows northward through the Strait into Dixon Entrance and likely carries many of the pelagic larvae out of the Strait. A recent study shows that the recruitment rate of Pacific cod varies inversely with this current, which is to be expected if the larvae are swept out of the Strait by the flow. We examine current and wind data from a variety of field programs in Hecate Strait, and find evidence for a return flow toward the southwest in Hecate Strait, counter to the wind-driven transport. This return flow is driven by the set-up of sea level along the Strait by the wind, and its strength increases with the intensity of southeast storm winds. We believe the return flow will recirculate a significant fraction of the larvae in the Strait, increasing their residence time sufficiently to allow settling out, thus enhancing recruitment.

La cause du taux de production élevé de poissons de fond dans le détroit d'Hécate est incertaine. Il semble que les vastes zones d'eau peu profonde du détroit contribuent à la productivité élevée parce qu'elles conviennent comme habitat pour les juvéniles. En hiver, toutefois, lorsque de nombreuses espèces de poissons de fond frayent, un fort courant traverse le détroit pour se diriger dans l'entrée Dixon vers le nord et il transporte vraisemblablement un bon nombre de larves pélagiques hors du détroit. D'après une étude récente, le taux de recrutement de la morue du Pacifique varie inversement avec ce courant, ce qui est logique si les larves sont entraînées hors du détroit par le courant. Nous étudions les données sur le courant et les vents provenant de divers programmes expérimentaux réalisés dans le détroit d'Hécate, et des indications montrent qu'il existe un écoulement inverse vers le sud-ouest dans le détroit d'Hécate, opposé au transport aérien. Cet écoulement inverse est conditionné par le réglage du niveau de la mer par le vent le long du détroit, et sa force augmente avec l'intensité des vents de tempête du sud-est. Nous pensons que l'écoulement inverse remet en circulation une fraction importante des larves dans le détroit, ce qui prolonge suffisamment leur temps de séjour pour leur permettre de se déposer, et augmente ainsi le recrutement.

Received August 28, 1989
Accepted January 30, 1990
(JA292)

Reçu le 28 août 1989
Accepté le 30 janvier 1990

Hecate Strait is known as an important area for commercial fisheries on the west coast of Canada. Of the 45160 metric tonnes of groundfish (excluding halibut) landed in 1985, 6683 t came from this region. In 1975, 9833 t of groundfish were landed from the Strait, a significant portion of the 24000 t landed from the entire Canadian west coast (Leaman 1986). In addition to groundfish production, Hecate Strait has large concentrations of Pacific herring (Haist and Stocker 1984; McCarter and Hay 1985). A recent multi-investigator project in the Strait has led to new understanding of the complexities of the animal community (Tyler 1989).

The biological and physical oceanographic reasons for the fisheries production in Hecate Strait are unclear. The fact that the Strait is a shallow continental shelf region, most of it being less than 80 m in depth and well mixed most of the year, is conducive to high productivity. Moresby Gully extends into the Strait, providing deep-water habitat at depths to 497 m. On the other hand, the development of a strong northward current during the winter spawning season is expected to reduce the productivity. With non-tidal velocities of up to 50–75 $\mathrm{cm \cdot s^{-1}}$, this current has the potential to transport most of the ichthyoplankton out of the Strait, and indeed, out of Canadian waters. North of Hecate Strait is Dixon Entrance and the narrow waterways of the archipelago of the Alaska Panhandle, where the species dominant in Hecate Strait (several flatfish species, Pacific cod (*Gadus macrocephalus*) give way to other (rockfish (*Sebastes* sp.); Anon. 1985). In this paper we describe a newly discovered winter current that could act as an egg and larval retention mechanism.

Hypotheses Regarding Retention of Young Fish in Hecate Strait

In the 1950's, variability in recruitment was studied by Ketchen (1956) who postulated that English sole must spawn in the southern part of the Strait in order to overcome the effects of the northward advection. He suggested that the development time for the pelagic eggs was just short enough that the young would metamorphose and settle to the bottom before they were swept out of the Strait. Of course, current strength would vary, and so in some years there would be less settlement than in others. At best, the retention of eggs and larvae seemed to be tenuous, and the high biomass of English sole in the Strait, and the concentrations of young in the shallows revealed by surveys (Fargo and Westerheim 1986), was surprising in the face of the winter current. Others postulated that the Strait was particularly suited to fishes such as Pacific cod and rock sole (*Lepidopsetta bilineata*) that deposit their eggs on or near the bottom (Hart 1973). Though this makes sense, a recent statistical study of Pacific cod recruitment showed that northward advection during the first quarter of the year, when the newly hatched year-class is in the larval stage, accounts for most of the variance in the year-class strength (Tyler and Westrheim 1986). Apparently, currents still influence bottom spawners. A more positive retention mechanism would have to be postulated to account for the fishery potential.

Description of the Non-Tidal Current Patterns

Current meter data

Crawford et al. (1988) examine the transport of water through Hecate Strait, as observed during the period May 1983–April 1984 using current meters deployed along three lines across the Strait (Fig. 1). An interesting feature of these currents during winter is that the net transport toward the north is more accurately measured by a single mooring on R-line in the north than by the seven moorings along M-line in the south. This is because the net flow across M-line is determined by the relatively small difference between strong opposing flows on either side of the Strait, whereas moorings along line R are in a region of unidirectional flow. Relatively small uncertainties in these opposing flows at M-line contribute to large uncertainties in the net flow there. The current vectors in Fig. 1 show strong flow to the northwest along the eastern and extreme western side of M-line, and at all surface moorings on W-line and the bottom meter on R-line. The interesting features here for fisheries biologists are the return flow toward the southwest found in mooring M04, and the weak bottom currents in some regions. Both features can permit the retention of eggs and larvae within the Strait, particularly if the return flow gives rise to eddy recirculation.

Another view of this current is presented in Fig. 2. Hatched areas represent regions of southward transport across M-line. At the 50-m level this flow is as strong as the northward flow at mooring M01, while at bottom this flow is the strongest observed on M-line. The historical view of winter circulation, which described a simple current flowing through Hecate Strait into Dixon Entrance, is clearly not correct. Much of the water crossing M-line in the east turns across Hecate Strait and returns to Queen Charlotte Sound and southern Hecate Strait.

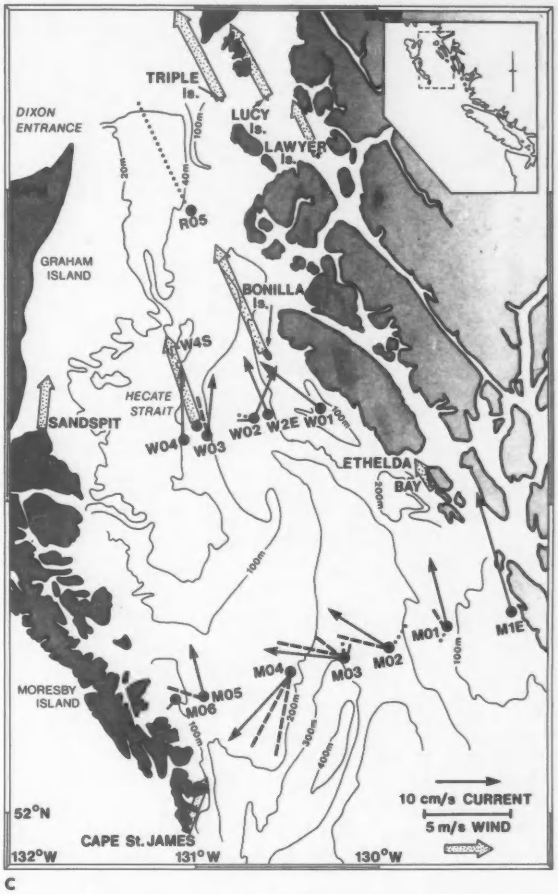

FIG. 1. Average currents and winds in Hecate Strait, 20 January 1984–4 April 1984. Solid arrows represent currents 50 m below the surface, dotted lines, currents within 15 m of the bottom and dashed lines, currents at intermediate depths. Wide shaded arrows represent winds (from Crawford et al. 1988).

The net northward transport across W- and R-lines is wind-driven. The stipled arrows in Fig. 1, representing the average wind, are all directed to the north or northwest. Crawford et al. (1988) describe how both the net transport to the north and fluctuations in transport to the north are predominately wind-driven, but do not address the return flow to the south.

Our hypothesis here is that a large fraction of the eggs and larvae are not swept into Dixon Entrance by this wind-driven transport in winter, but are either carried around the southern Strait in the return flow in the vicinity of M04, or drift slowly across the Strait and to the south in the bottom-water flow near W02 and M01.

Geostrophic currents

No current meters have been deployed in winter to the south of M-line so we have no direct measurement of the proposed winter recirculation at the southern entrance to Hecate Strait. The winter current-meter records used by Thomson and Wilson

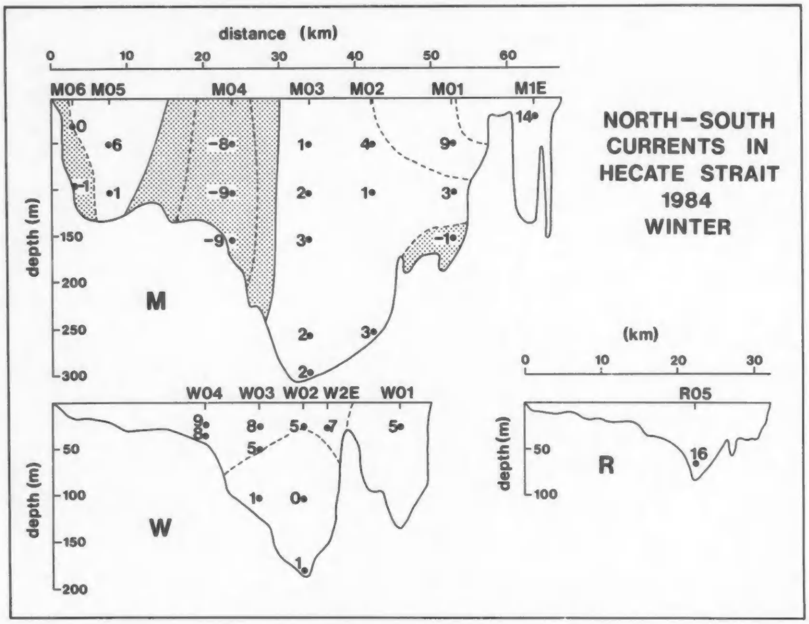

Fig. 2. Average currents across M-, W-, and R-lines, 20 January, 1984 – 4 April, 1984. Hatched areas show southward currents. Speeds are in cm·s^{-1}.

(1987) to investigate the tidally generated eddy to the west of Cape St. James are outside the recirculation region. In an attempt to extend our coverage of the currents further south, we have searched the literature for water-property survey data that could be used to determine the winter-time geostrophic flow in the region. Unfortunately, there have been few oceanographic surveys in southern Hecate Strait in winter. The earliest water-bottle surveys were begun by the Pacific Oceanographic Group (Nanaimo) in the mid 1950's and continued into the 60's (mainly in non-winter months). A summary of these data is provided by Dodimead (1980). Monthly CTD surveys were conducted by the Pacific Biological Station (Nanaimo) from January to April 1980 (Mason et al. 1981a, 1981b). This was followed by a sequence of eight large-scale water property surveys in the vicinity of the Queen Charlotte Islands during the Northern Coastal Oceanic Dynamics Experiment (NCODE) from May 1983 to December 1985 (Thomson et al. 1988). Of these surveys, only that of January 1984 occupied winter stations at the southern end of Hecate Strait.

Based on the available physical oceanographic data, the most extensive winter-time geostrophic current maps for the southern strait were obtained for the winters of 1955 (Pacific Oceanographic Group 1955), 1980 (Mason et al. 1981a, 1981b) and 1984 (Thomson et al. 1988). Additional hydrographic data are available for some of the intervening years, but survey coverage is too sparse to permit adequate resolution of the flow structure. The near-surface (10 m) geostrophic currents relative to 100-m depth obtained from the survey of February 1955 (Fig. 3a) indicate the presence of recirculation at the southern end of the Strait with especially strong baroclinic flow (20 cm·s^{-1}) to the east and west of the central Strait. The April map for 1955 (Figure 3b) shows that the strong northward flow on the west side of the southern Strait has weakened and only the relatively strong baroclinic flow along the eastern side persists. The 4-mo sequence beginning in January 1980 (Fig. 4a–d) is consistent with the notion of recirculation in the southern Strait in that eddy-like recirculation is confined to the entrance to Queen Charlotte Strait while weak baroclinic flow persists throughout much of the southern region of Hecate Strait. The map of the surface geostrophic current relative to 100 m for January 1984 (Fig. 5) provides further evidence for at least partially closed recirculation in this area. In this instance, the recirculation appears to be centered near the head of Moresby Trough leading into Hecate Strait to the east of Cape St. James.

The calculated geostrophic currents give the baroclinic component of the flow based on the assumption of no net motion relative to 100 m depth. As such, the current maps in Fig. 3–5 do not represent absolute currents and therefore do not reveal the full picture of the recirculation in the southern Hecate Strait. They do, however, supplement the absolute flow derived from the subsurface current meter observations by providing information on the current shear in the upper 100 m of the water column. The fact that the winter geostrophic currents near surface relative to 100 m are generally weak suggests that the subsurface measurements from the current meters, most lying at 50 m below surface, are representative of the flow in the upper 50 m. However, there are times when a strong baroclinic flow develops over the Strait in winter. As in January 1984, the recirculation associated with the barotropic flow may be significantly modified by the presence of a baroclinic flow which may in turn lead to interannual variations in groundfish recruitment in the region.

Satellite-tracked drifters

Additional information on the near-surface winter flow south of M-line is provided by satellite-tracked drifters, drogued at

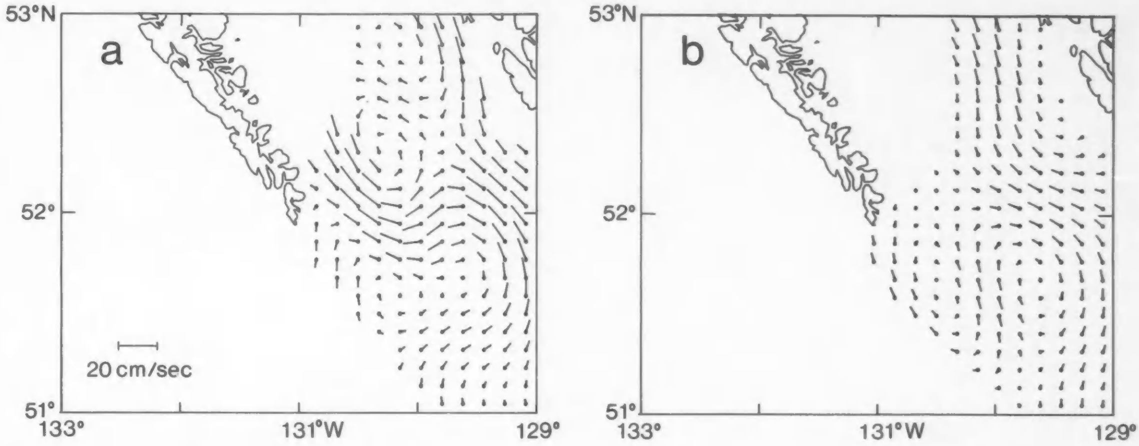
53°N
a
b
52°
51°
133°
131°W
129°
20 cm/sec

FIG. 3. Geostrophic currents at 10-m depth relative to 100-m level of no motion. Currents are directed away from the dots (vector origins) with speeds given by the velocity scale. Motions are assumed to have along- and cross-strait correlation scales of 50 and 25 km, respectively. (a) February 6–10, 1955 (17 stns.); (b) April 14–16, 1955 (16 stns).

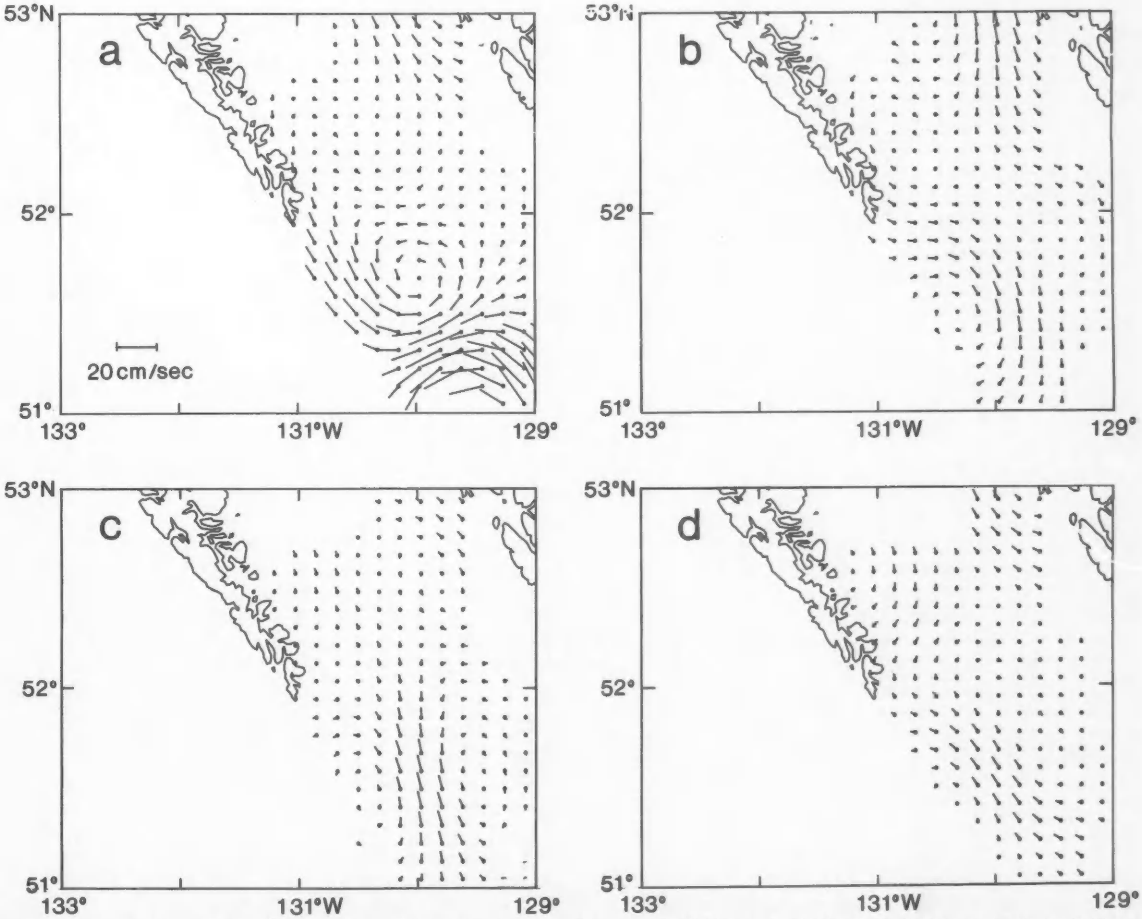
53°N
a
b
c
d
52°
51°
133°
131°W
129°
20 cm/sec

FIG. 4. As in Fig. 3 except for 1980. (a) January 21–23 (17 stns.); (b) February 18–20 (11 stns.); (c) March 18–20 (12 stns.); (d) April 15–23 (11 stns.).

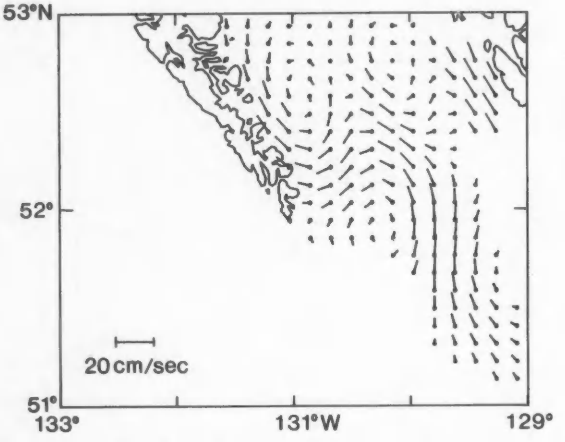

FIG. 5. As in Fig. 3. except for 1984. January 13–20 (38 stns.).

10-m depth, and deployed to the east of Cape St. James during early March 1986 (figures 12a in Thomson and Wilson, 1987). They were deployed during an extended period of strong (10 $m \cdot s^{-1}$) southerly winds characteristic of winter conditions over the Queen Charlotte Sound — Hecate Strait region prior to the spring transition. Over a 4-d period, the drifters released at the southern end of Hecate Strait moved seaward, counter to the direction of the prevailing winds. Therefore, the drifters demonstrate the tendency for winter flow to be southward along the western side of Hecate Strait. In this particular instance, larvae and eggs would have been caught in the quasi-permanent eddy that frequently forms off the southeast coast of Moresby Island (Thomson and Wilson 1987) or carried directly along the west coast of Queen Charlotte Islands. At other times, the flow may recirculate.

A short time-series of drifters tracked between 12 and 20 March 1986, (Fig. 6) presents a less conclusive view of currents off Cape St. James. This cluster remained in the region, neither leaving nor entering the Sound.

Satellite thermal images

Movement of surface water southward on the western side of the Strait, and northward through the center of the Strait can be seen in a set of satellite images made on three consecutive days, February 11, 12, and 13, 1986 (Fig. 7). The downward pointing triangle shows a cool-water feature (darker grey) moving very slowly to the south, while the upward pointing triangle shows a cool-water feature moving more rapidly northward during this period. The directions are consistent with the observations made by current meters.

Mixing due to strong winds in winter eliminates most of any vertical density gradient; therefore the thermal imagery as measured by satellite represents water masses tens of metres thick.

Analysis

To examine the behavior of the return flows observed in the current-meter data, we employ empirical orthogonal function (EOF) analysis to determine basin-wide features of currents and winds. This analysis is described by Crawford et al. (1985).

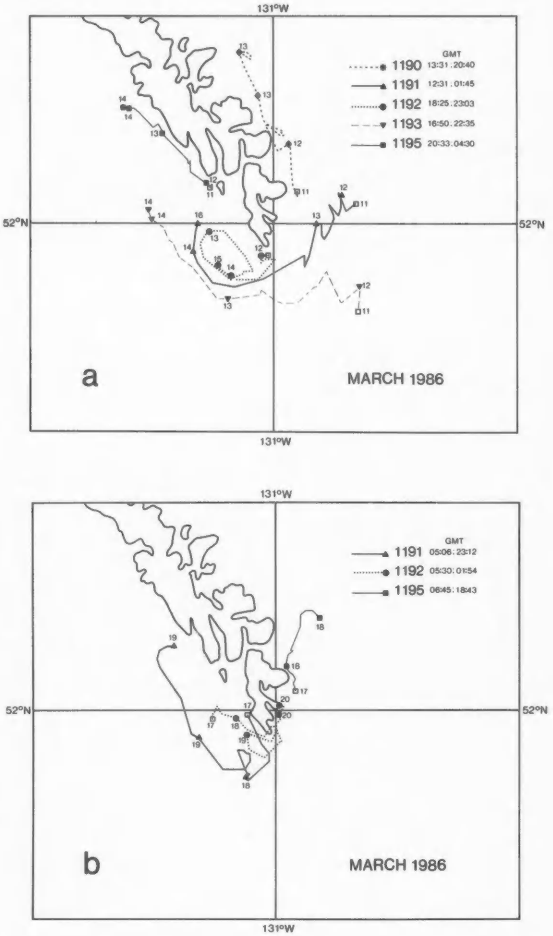

FIG. 6. Drifter tracks for the period 12–20 March, 1986. Symbols show approximate position of the buoys within ±2 h of 0000 GMT on specified day. Deployment and recovery times for the first and last day on a given track are listed to the right of the buoy ID (from Thomson and Wilson, 1987).

Briefly, it is a statistical technique that permits current-meter time-series to be separated into dominant spatial patterns or modes. The mathematical procedure is similar to that of principal component analysis.

We began with hourly time series of winds and currents. To remove the influence of tides on this analysis, only 2-d low-pass-filtered currents were considered, and for consistency, winds were passed through the same filter. Both series were subsampled at 6-h intervals and the means and trends of each time series were removed. To prevent one or two energetic time series from dominating the modes, each series was normalized by dividing by its standard deviation. Each signal of wind and current contributes two time series, one for each of the east–west and north–south components.

Three products are output by the analysis: eigenvalues λ_j, eigenvectors ϕ_{ij}, and expansion coefficients E_{jk}. The eigenval-

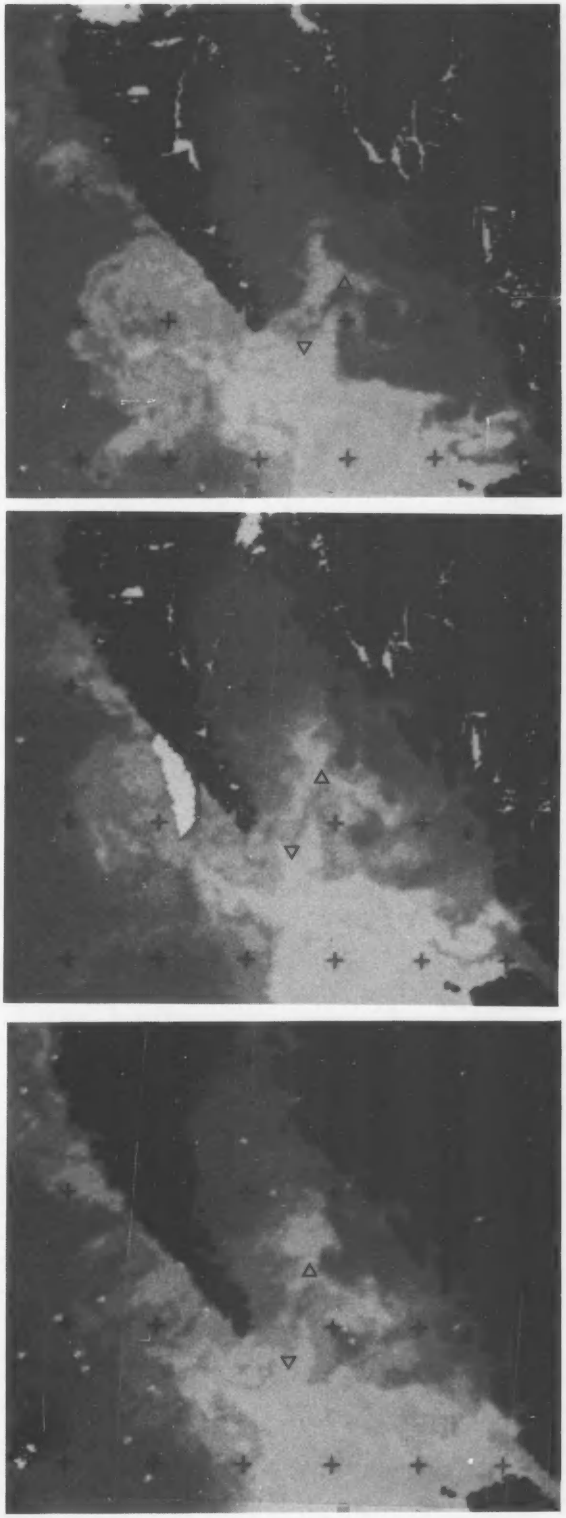

ues λ_j give the variance in a particular mode j. The analysis ranks the modes in order of decreasing variance, with the first mode having most variance. With these data we consider only the first mode, whose eigenvalue is λ_1.

The time series of the first mode is represented by E_{1k}, where the subscript k indicates the time of the observation, and the contribution of the first mode to any particular series is given by the eigenvector ϕ_{i1}, where i denotes the particular east–west or north–south time series.

We use these three products as follows. The eigenvalue tells us how effective the first mode is at "capturing" all the variance. For the Hecate Strait data, 24% of the current energy and 49% of the wind energy are in the first mode.

We use the expansion coefficients to compare the wind and currents. The expansion coefficient is defined mathematically by

$$E_{jk} = \sum_{i=1}^{N} U_{ik}\,\phi_{ij} \tag{1}$$

where U_{ik} is the observed, normalized east–west or north–south time series. The symbol E_{jk} denotes the magnitude of the jth mode at time k. The time series of E_{jk} represents the temporal variations of mode j. To compare the dominant patterns of fluctuation of winds and currents we compare the separate E_{1k} of the current and wind EOF analysis. Results are presented in the next section.

The eigenvectors are used to examine the spatial patterns of the first modes of wind and current at particular current meter and anemometer sites. To do this we recover V_i, the dimensional root-mean-square component of current or wind of the first mode at any site by means of the formula

$$\begin{aligned} V_i &= \lambda_1^{1/2}\sigma_i\phi_{i1} \\ V_{i+1} &= \lambda_1^{1/2}\sigma_{i+1}\phi_{i+1,\,1} \end{aligned} \tag{2}$$

where σ_i is the standard deviation of the east–west time series i; σ_{i+1} is the standard deviation of the north–south times series $_{i+1}$ at the same site. ϕ_{i1} is the eigenvector of mode 1 for time series i, and $\phi_{i+1,1}$ follows the same convention as σ_{i+1}.

Separate analyses were run for currents and winds, with only the first modes of each considered. The east–west and north–south vectors were computed using (2) and combined into one vector at each site, and plotted in Fig. 8, with the scale shown at the bottom right. Near-surface, mid-depth, and bottom currents follow the convention of Fig. 1. These vectors represent fluctuations in the currents and winds; therefore, the vectors could all be rotated 180 degrees. The present direction is chosen because it conforms to the pattern of the average currents and winds.

The fluctuations of mode 1 are all in phase, as required by this analysis, and confined along the direction of the vectors in Fig. 8. These fluctuations are, in fact, remarkably similar to the averages in Fig. 1. When the northward flow intensifies at M01 and M02, the return flow at M04 increases. A few differences emerge: fluctuations at M03 are directed to the southwest while the average current is to the east and north, and a very weak fluctuating flow to the west is observed at W03.

FIG. 7. Satellite thermal images of the Hecate Strait area (north at top). The images were made on three consecutive days, February 11, 12, and 13, 1986, top, middle, and bottom, respectively. The triangle pointing upward on the right was drawn at the northern edge of a northward-moving cool feature.

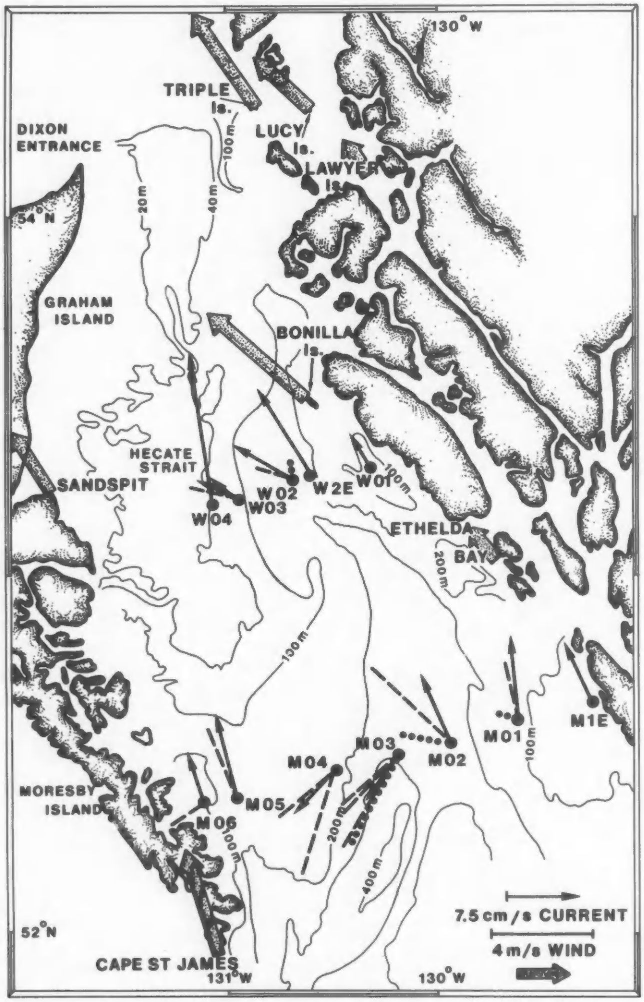
130°W
TRIPLE Is.
DIXON ENTRANCE
LUCY Is.
LAWYER Is.
100 m
20 m
40 m
54°N
GRAHAM ISLAND
BONILLA Is.
HECATE STRAIT
SANDSPIT
W02
W2E
W01
W03
W04
100 m
ETHELDA BAY
200 m
100 m
M1E
M01
100 m
M02
M03
M04
M05
M06
MORESBY ISLAND
100 m
200 m
400 m
7.5 cm/s CURRENT
4 m/s WIND
52°N
CAPE ST JAMES
131°W
130°W

FIG. 8. Vectors of the empirical orthogonal functions for the period 20 January–4 April, 1984. Both east–west and north–south eigenvectors at a site have been converted to dimensional eigenfunctions before forming the vectors for plotting. Scales are shown at bottom right.

Discussion

Over the 29 time series of currents, which comprise 58 time series in the EOF analysis, the mode 1 currents comprise 23% of the total energy. Among 8 series of winds, the first mode accounts for 49%, as noted earlier. (The wind at Langara Is., not shown in Fig. 8, is included. Its contribution to mode 1 is small.) A coherence analysis between these two modes of currents and winds, using E_{jk} as defined in (1), is illustrated in Fig. 9. The coherence is high, and winds lead the currents. We conclude that the fluctuations represented by the mode 1 currents are predominately wind-driven, and both winds and currents have basin-wide patterns which dominate the fluctuations. The mode 1 fluctuations in both winds and currents are similar to the averages, leading us to conclude that the average currents in winter are also wind-driven. We draw support for this last conclusion from the observation of Crawford et al. (1988) that the average currents and winds in summer are very much different from the pattern revealed in Fig. 2, and the time of transition between summer and winter currents is close to the time of shift in the nature of winds.

In winter, the strong flow through Hecate Strait along the eastern side of M-line bifurcates into one branch which continues through the Strait and another which turns to the southeast. In addition, a weak current flows across the Strait in the middle of W-line. The southeastward flow is driven by the set-up of water at the northern end of Hecate Strait by the wind, as noted by Crawford et al. (1988), and this return flow may carry eggs and larvae to the south, reducing the rate of their loss from the Strait. Fish eggs and larvae in the Strait tend to be concentrated

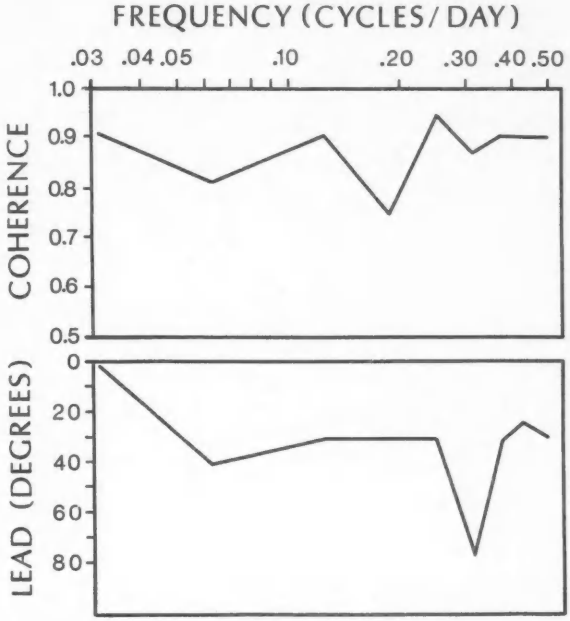

FIG. 9. Coherence (top) and phase lag (bottom) between the first mode currents and winds. Convention for arrows follows that of Fig. 1. A phase lead indicates the wind mode leads the current mode.

on the western side, putting them in position to be retained by the eddy. They seem equally abundant in the northern and southern halves, however, rather than concentrated to the south where the eddy seems most evident (Mason et al. 1981c).

The above analysis of current meter data shows that when the winds from the south increase in strength, these return flows increase in strength also, with a lag of a day or so. This type of circulation is similar to that of Lake Ontario in winter as described by Csanady (1973). The return flow to the south through M-line, observed here in both the mean and fluctuating currents, has been simulated in a barotropic model of Hecate Strait (C. Hannah, Department of Oceanography, Univ. of British Columbia, Vancouver, B.C., pers. comm.) Obviously, the flow in the south end of Hecate Strait is influenced weakly by the small opening of the Strait at the north end, and the north–south pressure gradient drives the return flow. Along W-line at mid-Strait, where the water is shallower and the central channel is narrower, the wind-forcing is felt down to the bottom and the current does not flow upwind.

Supporting data from hydrographic surveys, drifters, and thermal images show that the near-surface currents are not too different from the 50-m currents, and a near-surface return flow along the western side of Hecate Strait could be anticipated in winter.

Although the loss of larvae from the Strait may increase when these winds are stronger, the losses are not as large as they would be in a strait without a return flow, and the fraction of the larvae lost will not be strictly proportional to the wind strength.

This return flow has considerable potential to retain ichthyoplankton in the Strait. Typical flows in the Strait are $10\ \mathrm{cm \cdot s^{-1}}$ at 50-m depth in winter. Since the Strait is about 250 km long, it would take 25 d to sweep the length of Hecate Strait into Dixon Entrance. The duration of the Pacific cod's larval stage is at least 6–8 wk at 4–5°C (Rugen and Matarise 1988); they could easily be carried through the Strait. However, if one half the larvae are diverted into the eddy, which has a diameter of order 100 km and a circumference of about 300 km, they will remain in the southern Strait for 30 d before returning to their original position. Two circuits of the eddy (60 d) would keep winter-spawned larvae in the Strait, since the northward currents weaken in late March.

References

ANON. 1985. Statistical Yearbook. International North Pacific Fisheries Commission, Vancouver, B.C.

CRAWFORD, W. R., W. S. HUGGETT, M. J. WOODWARD, AND P. E. DANIEL. 1985. Summer circulation of the waters in Queen Charlotte Sound. Atmos.-Ocean. 23: 393–413.

CRAWFORD, W. R., HUGGETT, W. S., AND M. J. WOODWARD. 1988. Water transport through Hecate Strait, British Columbia. Atmos.-Ocean. 26: 301–320.

CSANADY, G. T. 1973. Wind-induced barotropic motions in long lakes. J. Phys. Oceanogr. 3: 429–438.

DODIMEAD, A. J. 1980. A general review of the Oceanography of Queen Charlotte Sound — Hecate Strait — Dixon Entrance. Can. MS Rep. Fish. Aquat. Sci. 1574: 248 p.

FARGO, J., AND S. J. WESTRHEIM. 1986. Results of the annual trawl surveys of juvenile flatfish in Hecate Strait, 1980–1985. Can. MS Rep. Fish. Aquat. Sci. 1884: 71 p.

HAIST, V., AND M. STOCKER. 1984. Stock assessments for British Columbia herring in 1983 and forecasts of the potential catch in 1984. Can. MS Rep. Fish. Aquat. Sci. 1751: 50 p.

HART, J. L. 1973. Pacific fishes of Canada. Bull. 180. Fish. Res. Board Canada. 740 p.

KETCHEN, K. S. 1956. Factors influencing the survival of the lemon sole (*Parophrys vetulus*) in Hecate Strait, British Columbia. J. Fish. Res. Board Canada 13: 647–694.

LEAMAN, J. E. 1986. Catch and effort statistics of the Canadian groundfish fishery on the Pacific coast in 1985. Can. Tech. Rep. Fish. Aquat. Sci. 1508: 80 p.

MASON, J. C., O. D. KENNEDY, AND T. H. MULLIN. 1981a. Canadian Pacific Coast Ichthyoplankton Survey. 1980. Hydrography. Part 1. Horizontal contours of temperature, salinity and sigma-T, at selected depths by monthly cruise. Can. Data Rep. Fish. Aquat. Sci. 279: 110 p.

1981b. Canadian Pacific Coast Ichthyoplankton Survey. 1980. Hydrography. Part two. Vertical contours of temperature, salinity and sigma-T, on transect lines by monthly cruise. Can. Data Rep. Fish. Aquat. Sci. 280: 77 p.

MASON, J. C., O. D. KENNEDY, AND A. C. PHILLIPS. 1981c. Canadian Pacific Coast Ichthyoplankton Survey, 1980. Ichthyoplankton Cruise. Part 3 (March 12–20). Can. Data Rep. Fish. Aquat. Sci. 277: 75 p.

MCCARTER, P. B., AND D. E. HAY. 1985. Herring survey off the Queen Charlotte Islands and in Hecate Strait, January 15–31, 1985. Can. Data Rep. Fish. Aquat. Sci. 543: 39 p.

PACIFIC OCEANOGRAPHIC GROUP. 1955. Physical and chemical data record. Hecate Project with Appendix 1. Current observations, 1955. Queen Charlotte Sound, Hecate Strait and Dixon Entrance. Joint Committee on Oceanography. 107 p.

RUGEN, W. C., AND A. C. MATARESE. 1988. Spatial and temporal distribution of Pacific cod (*Gadus macrocephalus*) larvae in the western Gulf of Alaska. NMFS/NWAFC Processed Rep. 88–18: 53 p.

THOMSON, R. E., AND R. E. WILSON. 1987. Coastal countercurrent and mesoscale eddy formation by tidal rectification near an oceanic cape. J. Phys. Oceanogr. 17: 2096–2126.

THOMSON, R. E., W. R. CRAWFORD, AND W. S. HUGGETT. 1988. Water property observations from the Northern Coastal Oceanic Dynamics Experiment (NCODE) May 1983–July 1985. Can. Data Rep. Hydrogr. Ocean Sci. 67: 6 Vol.

TYLER, A. V. (ED.) 1989. Hecate Strait project: results from four years of multispecies fisheries research. Can. Tech. Rep. Fish. Aquat. Sci. 1675: 60 p.

TYLER, A. V., AND S. J. WESTRHEIM. 1986. Effects of transport, temperature, and stock size on recruitment of Pacific cod (*Gadus macrocephalus*). INPFC Bull. 47: 175–190.

Multivariate Approach to Study Species Assemblages at Large Spatiotemporal Scales: The Community Structure of the Epibenthic Fauna of the Estuary and Gulf of St. Lawrence[1]

P.-L. Ardisson and E. Bourget

GIROQ, Département de biologie, Université Laval, Québec (Qué.) G1K 7P4 Canada

and P. Legendre

Département de sciences biologiques, Université de Montréal, C.P. 6128, Succursale A, Montréal (Qué.) H3C 3J7 Canada

Ardisson, P.-L., E. Bourget, and P. Legendre. 1990. Multivariate approach to study species assemblages at large spatiotemporal scales: the community structure of the epibenthic fauna of the Estuary and Gulf of St. Lawrence. Can. J. Fish. Aquat. Sci. 47: 1364–1377.

We investigated hierarchical organization and spatiotemporal discontinuities in species abundances in the epibenthic community of the Estuary and Gulf of St. Lawrence. Quantitative samples were obtained from 1975 to 1984, on 161 collectors (navigation buoys) moored yearly from May through November. Maximum biomass values of the dominant species, common to all regions studied, were used to assess epibenthic community structure. Numerical methods were used to characterize spatial structure and temporal variability of the dominant assemblage. Spatially constrained clustering and ordination techniques revealed six broad biogeographic zones whose limits vary yearly. However, spatially unconstrained clustering and ordination techniques showed two major sets of non-continguous localities, each characterized by a singular biotic structure. Further, spatial autocorrelation analyses showed a significant relationship between biomass and geographic distance. The resulting spatial structure of biomass was dependent on the species considered. The multidimensional Mantel technique showed an 8-yr period of variation in community structure at large (whole system, Gulf) and intermediate (North Shore plus Lower North Shore) spatial scales. The amplitude and asymmetry of this temporal cycle increased as the spatial scale decreased. In spite of the observed discontinuous spatial patterns, the temporal oscillations in community structure detected at different spatial scales suggest that the Estuary-Gulf system responds to the external input of auxiliary energy as an integrated system.

Une étude fut réalisée pour mettre en évidence l'organisation hiérarchique et les discontinuités spatiotemporelles dans les abondances d'espèces de la communauté épibenthique de l'estuaire et du golfe du Saint-Laurent. Des échantillons quantitatifs furent obtenus de 1975 à 1984 sur 161 collecteurs, mouillés de mai à novembre de chaque année. La biomasse maximale des espèces dominantes, communes à toutes les régions étudiées, fut utilisée pour évaluer la structure de la communauté épibenthique. Des méthodes numériques furent utilisées pour caractériser la structure spatiale et la variabilité temporelle de l'assemblage dominant. Des analyses de groupement et d'ordination avec contrainte spatiale ont montré six zones biogéographiques majeures dont les limites varient d'une année à l'autre. Cependant, des analyses de groupement et d'ordination sans contrainte spatiale révélèrent deux groupes majeurs de localités non continguës, chacun caractérisé par une structure biotique singulière. Par ailleurs, des analyses d'autocorrelation spatiale ont montré une relation significative entre la biomasse et la distance géographique. Le type de structure spatiale qui en résulte dépend de l'espèce considérée. Le test multidimensionnel de Mantel a mis en évidence une période de variations de 8 ans dans la structure de la communauté, et cela à différentes échelles spatiales (système Estuaire-Golfe, Golfe, et Côte Nord-Basse Côte Nord). L'amplitude et l'asymétrie de ce cycle temporel varient inversement avec l'échelle d'observation. En dépit des discontinuités observées dans les patrons spatiaux, l'oscillation temporelle dans la structure de la communauté observée à différentes échelles spatiales suggère que le système Estuaire-Golfe répond aux apports externes d'énergie auxiliaire comme un système intégré.

Received June 26, 1989
Accepted January 30, 1990
(JA212)

Reçu le 26 juin 1989
Accepté le 30 janvier 1990

One aim of community ecology is to explain the patterns of natural assemblages of organisms. Patterns can be detected by making comparisons among features of natural communities, or between natural systems and logical or theoretical models of community structure (Wiens 1984). When the first of these two approaches is considered, multivariate statistical methods allow us to analyse patterns in biotic data (species attributes/sites/times) and to relate biotic patterns to spatiotemporal environmental patterns (Field et al. 1987). In this context, understanding environmental variability and related population effects in a wide array of spatiotemporal scales has become a central point in community studies (Allen and Starr 1982; Brown 1984; Wiens 1984; Morris 1987). The spatial and temporal scales at which ecological systems are examined influence the patterns observed, the processes accounting for them as well as our perception of their stability (Legendre and Demers 1984; Brown and Maurer 1987; DeAngelis and Waterhouse 1987; Bourget 1988).

---

[1] Contribution to the program of GIROQ (Groupe Interuniversitaire de Recherches Océanographiques du Québec).

A scale-oriented approach to community structure follows logically from the hierarchical paradigm of complex ecological systems (Platt et al. 1981; Allen and Starr 1982; Ulanowicz and Platt 1985). According to this view, biotic structures are seen as a series of nested and non-nested mosaics in time and space where complexity comes from the nonlinearity and asymmetry of the interactions between biological entities and their environment. Kolasa (1989) suggests that species abundances reflect the relative size as well as the degree of fragmentation of the habitat used by a given species. In this hierarchical view, habitat fragmentation appears to increase as a function of increasing resolution. As a consequence, in hierarchical theories, processes occurring within each level of the hierarchy are considered to pertain to a higher holistic level that integrates the summary outcomes of many simultaneous processes (Ulanowicz and Platt 1985; Kolasa 1989).

Here, in order to determine the driving processes controlling the spatial and temporal patterns of variability of the marine epibenthic invertebrate community of the Estuary and Gulf of St. Lawrence, we analyse the structure of the benthic assemblages at several levels of resolution in time and space. We examine whether different levels of organization do exist in these benthic assemblages and if the entire system behaves as a continuous and stable entity. An effort was made to determine spatial patterns for single species as well as for assemblages of species. In addition to revealing spatio–temporal patterns, the complementary use of different numerical methods allowed an assessment of the appropriateness of the individual techniques used as well as the robustness of the structures revealed by each method. Patterns are interpreted in the light of the dynamics of dominant species and hydrodynamic processes. The yearly spatial structure was studied at a large scale (Estuary and Gulf). The temporal variability of the spatial structures was analysed at large and intermediate (regional) spatial scales during 10 yr, from 1975 to 1984. At these spatial and temporal scales, changes in the biomass structure of the dominant assemblage is used as the key element. Through these changes, the existence of significant discontinuities in community structure between localities and over time was revealed and consequently, biogeographic patterns were found.

Materials and Methods

Data

The spatio–temporal variations in structure of the dominant epibenthic assemblage of the Estuary and Gulf of St. Lawrence were studied from 1975 to 1984 (except in 1978 and 1979), on 161 collectors (navigation buoys) moored by Transport Canada from May through November of each year (Fig. 1). Abundance data are biomasses of the five dominant species, those common to all regions in the study. This assemblage is composed of the following sessile species: the hydroid *Obelia longissima* (Pallas), the bivalves *Hiatella arctica* (L.) and *Mytilus edulis* (L.), and the cirripedes *Semibalanus balanoides* (L.) and *Balanus crenatus* (Bruguière). Since the buoys are moored and retrieved in a short lapse of time (about 2 wk) each year, their use allowed us to obtain samples on a large spatial scale without introducing seasonal differences in the abundances of species among the regions considered. For a more detailed description of the advantages of navigation buoys as collectors, see Fradette and Bourget (1980, 1981).

Field and Laboratory Procedures

After retrieval of the buoys in November, the organisms attached to their surface were preserved due to the freezing air temperature. Shortly after the buoys arrived in the port of Québec, the attached invertebrate fauna was sampled following the methods of Fradette and Bourget (1980). Quantitative samples of 0.01 m^2 were obtained from the area of maximum biomass on each buoy, for each one of the five dominant species. The sites of maximum biomass were determined by visual inspection. Since the species distributions on the buoys are most often patchy, sampling the community in the areas of maximum biomass is the easiest way of obtaining data that are comparable among buoys. The only alternative would have been to randomly select a large number of quadrats on each buoy, which would have generated an unmanageable number of samples. Biomass was used as an indicator of abundance because, as stated by Field et al. (1982), colonial animals cannot meaningfully be counted, whereas all organisms can be expressed in units of mass.

All specimens were sorted, identified, and fixed in formalin (4%). The wet weight of each species was obtained after a 5-min drying period on blotting paper. The dry weights were calculated using the wet weight to dry decalcified weight conversion indices estimated by Fradette and Bourget (1980): *O. longissima* 0.18, *H. arctica* 0.17, *M. edulis* 0.09, *S. balanoides* 0.07, and *B. crenatus* 0.06.

Numerical Analyses

In order to identify the spatial structure of the community yearly, each year's biomass data were assembled into a multivariate data matrix (locations × species) which excluded sampling stations with zero biomass values for all species. Departures from normality were tested for each biomass variable by means of the non parametric Kolmogorov–Smirnov test, using corrected critical values calculated by Lilliefors (1967). Normality of data was achieved using the Box–Cox method (Sokal and Rohlf 1981). The asymmetric form of the Gower (1971) coefficient of similarity (S19 in Legendre and Legendre 1984) was then used to compute pairwise similarities among all stations. In addition to excluding joint absences, this similarity measure weighs all species equally in the analysis, irrespective of their absolute range of variation in the samples. From these resemblance matrices, spatially unconstrained clustering and scaling (ordination) techniques were used in conjunction with spatially constrained ones, after testing for the presence of spatial autocorrelation in the data.

Spatial autocorrelation analyses

Ecological systems are structured in space, either by forcing environmental variables or by the biological activity itself. These departures from randomness in the spatial distribution of ecological values are called spatial autocorrelation. The presence of spatial autocorrelation in data can be statistically assessed using, for instance, the Mantel test, and the shape of the spatial autocorrelation structure can be described by structure functions such as the Moran correlogram (Legendre and Fortin 1989).

We tested for the presence of spatial autocorrelation in the multivariate data by means of the Mantel test (Mantel 1967;

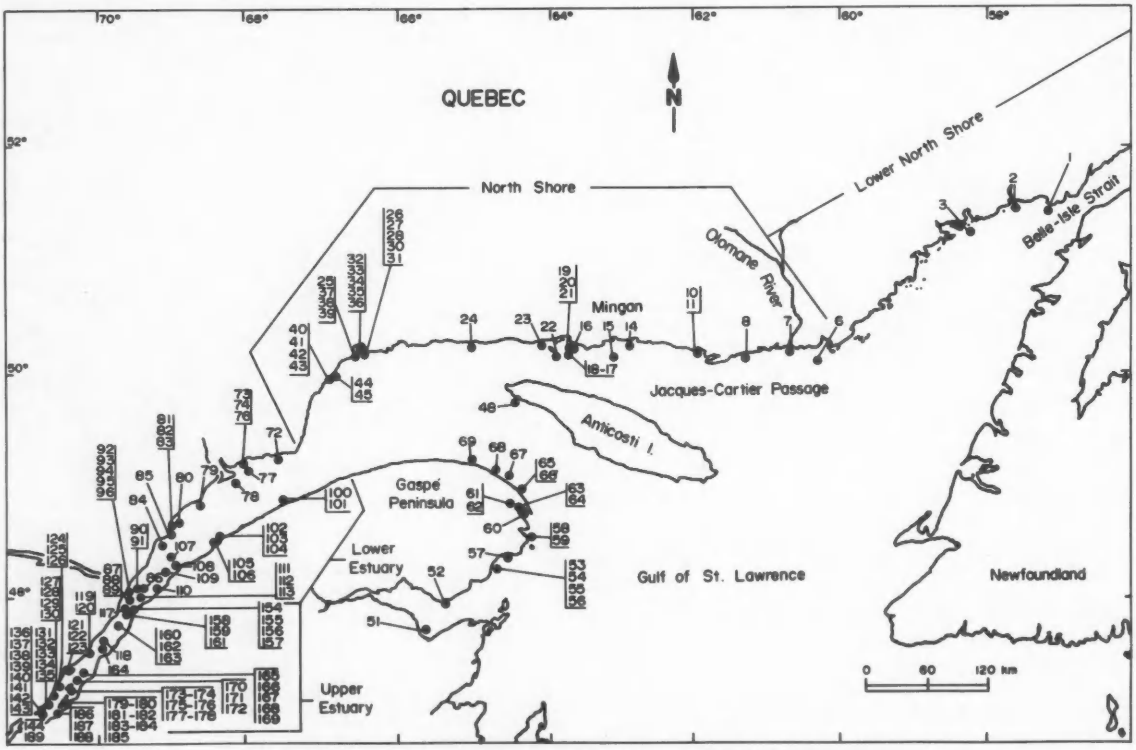

FIG. 1. Position of the sampling stations in the Estuary and Gulf of St. Lawrence.

Sokal and Thomson 1987; Legendre and Fortin 1989). Mantel tests were carried out between (1) the matrix of geographic distances among stations (buoys) and (2) matrices of similarity (converted into distances $D = 1\text{-}S$) among stations based on the species biomass data, as described above. The null hypothesis was that of independence of the distances in the two matrices. In each yearly test, the normalized Mantel statistic r was tested by randomization. In order to study the persistence of a spatial ecological structure through time, the results of the simple Mantel tests, computed on a yearly basis during the period 1975–84, were assembled in a single graph of Mantel statistics r vs. time. The overall significance of these values were tested using the Bonferroni method of correcting for multiple tests (Cooper 1968; Miller 1977).

Spatial autocorrelograms (Sokal and Oden 1978; Sokal and Thomson 1987; Legendre and Fortin 1989) were computed to demonstrate the presence of spatial patterns in the dominant species taken one by one. Moran's I coefficient was used to describe the spatial autocorrelation of the species biomass as a function of distance. Geographic distances among buoys were divided into classes for this analysis. Individual spatial autocorrelation coefficients were tested in the conventional manner, using standard errors based on the expectations of their moments (Cliff and Ord 1981). The graph of Moran's I coefficients against distances is called a correlogram. Its overall significance was tested by the Bonferroni technique (Oden 1984). Spatial autocorrelation was analyzed for each of the five dominant species, both on a yearly basis and on average values representing the overall period 1975–84. Two spatial scales were considered: the whole system, and the Estuary and Gulf regions taken separately.

Clustering and scaling analyses

UPGMA clustering (Rohlf 1963) was used to group localities with similar biotic structures. UPGMA was preferred to other agglomerative hierarchical methods because it gave the highest correlation between the original similarities and the cophenetic matrix (similarities implied by the dendrogram). Only the groups with similarities greater than 0.50 were retained for study. The matrix of Gower's distances among samples was also subjected to a principal coordinates analysis (Gower 1966). The principal coordinates method was chosen as the scaling (ordination) method instead of principal component analysis because of the existence of many zeros in the matrix entries. To determine the species contributing most to the formation of the reduced space, Kendall correlations were computed to relate the first two principal coordinate axes with the biomass of each of the dominant species in turn. The UPGMA-clustering results were plotted in the space of the first two principal coordinates to help interpret relationships among groups. Clustering and scaling analyses were carried out on a yearly basis at the large geographic scale (whole system).

The chronological clustering technique of Legendre et al. (1985) was used to identify significant discontinuities in structure in the multivariate spatial series of the dominant assemblage. Although the chronological clustering method was originally conceived as a time-constrained method, it can be used as a space-constrained method as well, provided that the spatial data form a one dimensional series (Galzin and Legendre 1987).

Space constraint, in this context, means that only those samples that are continguous along the spatial series are allowed to cluster (see Discussion: Biogeographic Patterns). The level of connectedness of the proportional-link linkage algorithm was set to 75%. In this method, a randomization test procedure is used at each clustering step to determine whether or not two objects or groups should be allowed to cluster; the statistical criterion for rejection of the null hypothesis was relaxed progressively in three steps ($\alpha = 0.15, 0.20, 0.25$) to test for successively less significant clusters. These connectedness and significance levels provided the best representation of the biotic structure at the large and intermediate spatial scales.

Because of the difficulty of establishing a sequential series of stations in two diverging directions, that would have included the Estuary and Gulf regions in the same analysis, only the spatial series of data from sampling collectors moored along the Gulf of St. Lawrence shores, ordered counter-clockwise, were submitted to this analysis. Since the sampling stations were not ordered along a real transect, but were positioned irregularly alongshore (Fig. 1), the counter-clockwise sequence was of interest at large and intermediate spatial scales but irrelevant at a scale of tens of kilometres. The theoretical model of succession upon which this spatial clustering analysis is based involves larval dispersal of benthic species, parallel to the coast, following the circulation patterns of the surface layer of the Estuary and Gulf of St. Lawrence (El–Sabh and Johannessen 1972; El-Sabh 1976). This form of clustering was applied both on a yearly basis within the period 1975–84, and on average values throughout years.

A complementary approach used to confirm the importance of the discontinuities in community structure was to perform a constrained ordination on the resemblance data matrix. Geographic information was used to constrain the output of an unconstrained scaling program, using the method proposed by Legendre (1987). The question to be answered by such a method is the following: when forced to obey the geographic contiguity constraint, do the community data still produce a gradient? In other words, is the underlying biological structure continuous, when considering the geographic arrangement of stations? This was done by computing $C = A + wB$, when A and B were, respectively, an ecological and a geographic distance matrix among stations, w was a scalar weight (ranging between 0 and 1) and C was the new spatially constrained distance matrix. A nonmetric multidimensional scaling analysis (Shepard 1962, 1966; Kruskal and Wish 1978) was then performed in the conventional manner for different values of w, and the result was selected which had the smallest value of w and in which all clusters were still internally contiguous ($w = 0.01$). This method could also be used to obtain constrained clusters from unconstrained clustering programs. Because this algebraic operation on the resemblance matrix does not change the Euclidean property of the distance matrix, principal coordinates analysis could have been used to obtain a constrained ordination. However, nonmetric multidimensional scaling (NMDS) was preferred here because, according to Gower (1966), when distances are Euclidean, NMDS permits summarization of distances in a smaller number of dimensions than principal coordinates analysis.

Once the spatial discontinuities in community structure where established, the Kruskal–Wallis one-way analysis of variance was used to test the heterogeneity of means among biogeographic zones for each of the dominant species. Since the species had been used to delineate the biogeographic zones, significant Kruskal–Wallis results have to be interpreted as measures of species contribution, and not as strict significance tests.

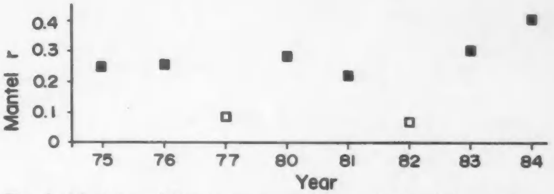

FIG. 2. Mantel statistics across years, for spatial variation patterns between two distance matrices (geographic and ecological) referring to the same collectors. The abscissa shows time in years. Ordinate: normalized Mantel's statistic r. Solid squares: Mantel tests significant at the Bonferroni-corrected probability level of ($0.05/8 = 0.00625$) for an overall significance level of 0.05 over 8 simultaneous tests. Open squares: non-significant values.

Temporal variability analysis

The spatial methods described above could, as a last resort, also reveal the temporal variability trends because the spatial structure was analyzed year by year. This would, however, produce a rather rough picture. A simpler and more elegant way to describe temporal variability is to compare pairs of similarity matrices by means of the Mantel test, where each matrix represents the structure of the dominant assemblage for a particular year. The null hypothesis tested here is the independence of the elements in the two matrices. When the output of pairwise computations among all possible combinations of resemblance matrices from different years are summarized in a square matrix form, two different analyses are then possible: (1) examination of community evolution from year to year, selecting the values on the subdiagonal that correspond to consecutive years (e.g. 1975–76, 1976–77, and so forth); or (2) examination of the overall variability structure from the period 1975 to 1984 by considering the r values of the whole matrix. Both of these avenues were investigated. (1) Single r values for consecutive years were assembled in a single graph of Mantel's statistics against time. The overall significance of these values was tested using the Bonferroni technique. (2) On the other hand, the overall matrix of Mantel statistics values, tested for overall significance using the Bonferroni technique, was subjected to a principal coordinate analysis in order to represent the yearly variability in a two-dimensional space, and to a UPGMA clusterig analysis in order to show the similarity relationships among years. Temporal variability analyses were carried out at large and intermediate (regional) scales.

Results

Spatial Autocorrelation in Data

Results of the Mantel tests (Fig. 2) showed positive and highly significant correlations between ecologic and geographic distance matrices for all years, except in 1977 and 1982. Positive correlations for particular years mean that similarity in biomass structure among sampling stations decreases as geographic distance among these same sampling stations increases, i.e. that there is a significant spatial dependency of biotic resemblance with distance.

The yearly spatial patterns of single species (not shown) were, however, highly variable and hard to characterize. Since

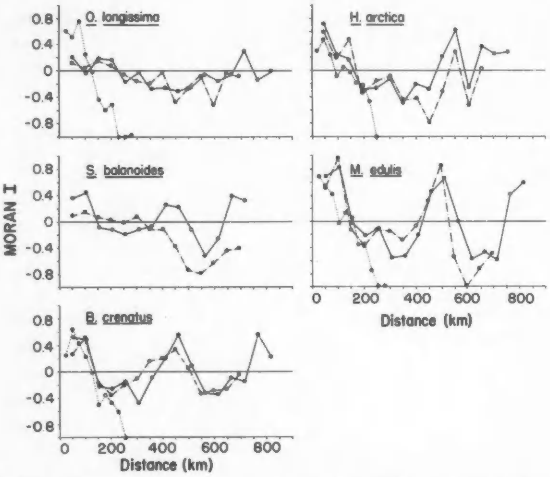

FIG. 3. Correlograms of geographic variation patterns of biomass of the five dominant epibenthic species of the Estuary and Gulf of St. Lawrence. Abscissa: distance in km. Ordinate: Moran's autocorrelation coefficient I. ——— whole system (Gulf and Estuary); – . – . – Gulf; ...... Estuary. Significant autocorrelation coefficients ($P \leq 0.05$) are indicated by solid circles. All correlograms shown are significant at the overall significance level $P = 0.05$.

no definite trends across years were observed, the spatial patterns of single species were summarized by computing correlograms on average values representing the entire period of study (Fig. 3). Rules for interpreting spatial correologrames are provided by Sokal (1979) and by Legendre and Fortin (1989). The correlogram for *Obelia longissima* (Fig. 3) showed, at the whole system scale, a weak gradient. This spatial pattern displays only the irregular decline from positive autocorrelation at 50 km to negative autocorrelation at 450 km. Likewise at the Gulf scale, only this irregular decline from positive to negative autocorrelation values was found. The correlograms for *Hiatella arctica, Semibalanus balanoides, Mytilus edulis*, and *Balanus crenatus* (Fig. 3), on the other hand, were characterized by a patchy structure both at the whole system and at the Gulf scales. Distances between patch centers are given by the distance where the second positive peak in I values occurs, as demonstrated by Legendre and Fortin (1989). Although not quite constant, that distance was approximately 400–500 km for these species. Because of the limited spatial distribution and lower abundance in the Estuary of the species that are normally dominant, only the 1983 correlograms (except for *S. balanoides*) are shown in Fig. 3 for that region. All these species showed a well-established cline from significant positive autocorrelation at 25–100 km to significant negative autocorrelation at 150–250 km. Although this method of analysis cannot show the directionality of the spatial variation pattern (for a directional spatial autocorrelation method see Oden and Sokal 1986), because of the particular configuration of the study area, the autocorrelation values for greater distances necessarily corresponds to sites located near the tips of a diagonal axis oriented northeast–southwest (see Fig. 1).

Spatial Discontinuities in Community Structure

The yearly UPGMA clusters obtained at similarity values (S) ≥ 0.57 are represented in Fig. 4. Although the scatter diagrams of stations in the reduced space formed by the first two principal coordinate axes were highly variable on a temporal basis, no trends in dispersal patterns for individual years were found. Two major groups of stations can be identified based on spatial discontinuities in the yearly biotic data. The first group (Fig. 4, A-1 to H-1), formed at $S = 0.57$–0.77, consisted mostly of stations from the Lower North Shore, the Eastern North Shore (stations 6–14), the Mingan Islands region, the Anticosti Island (one station) and the Lower and Upper Estuary. The second group (Fig. 4, A-2 to H-2) formed at $S = 0.60$–0.74, consisted mostly of stations from the Western North Shore (stations 24–45) and the Gaspé Peninsula. Except for the stations from the Lower North Shore that always grouped into the first cluster (A-1 to H-1), stations from other regions could not be entirely associated to a particular cluster during the overall period of study. Analysis of secondary clusters formed at higher similarity levels did not improve the structure outlined above. When clustering envelopes are ignored and more attention is paid to the overall dispersal of stations in the reduced space, it can be seen that stations formed a gradient along axis I whose sequence from negative to positive values was: (1) Gaspé Peninsula, (2) Western North Shore, (3) Eastern North Shore, (4) Lower Estuary, Mingan Islands region and Lower North Shore in a variable order and (5) Upper Estuary. However, only the stations from the Lower North Shore could clearly be discriminated along axis II when viewed from positive to negative values. Furthermore, during the whole period of study, the first principal axis was strongly and negatively correlated with *M. edulis* and *B. crenatus*, while the second principal axis was strongly and negatively (except in 1981, 1983, and 1984) correlated with *O. longissima* (Table 1). These correlation coefficients cannot be tested for significance because the principal coordinates are derived from these five species abundance data.

The annual spatially constrained clusters for the period 1975–84 are shown in Fig. 5. The most fundamental breaks occur at the probabilistic clustering criterion value $\alpha = 0.15$. Relaxation of the probability level from $\alpha = 0.15$–0.25 has a magnification effect that may allow finer structures to emerge. At $\alpha = 0.20$ some homogeneous clusters were split into lesser ones. For example, the cluster formed by stations 3–45 which emerged at $\alpha = 0.15$ in Fig. 5C, was partitioned in four smaller clusters when viewed at $\alpha = 0.20$. However, not all of these new clusters are of ecological interest. Clusters like 25–30, 31–41, and 42–45 in Fig. 5C were formed at a very small spatial scale whereas stations were not ordered in a real spatial sequence. Varying the clustering criterion from $\alpha = 0.20$–0.25 (not shown) essentially yielded the same clusters. At this last probability level, the singleton character of station 7 was confirmed in 1983, as well as for station 24 during 1981, 1983, and the whole period 1975–84. Group expansion tests (GET) (Legendre et al. 1985) showed that the clustering structures observed are actually a continuum that could grow in many of its parts by incorporating spatially adjacent stations. Three fundamental breaks persisted, however, throughout the years. These break points occurred between stations 23 and 25 (24 is a singleton), 45 and 69, and in 1984 between 58 and 57 (Fig. 5H). The *a posteriori* tests (Legendre et al. 1985) showed groups that would have merged in a single cluster if the spatial constraint had not existed. On the other hand, the precise location of the break points was highly variable across years (see Fig. 5, A–H). Nevertheless, the most distinct groups from these year-by-year analyses are the following: stations 1–7 (from the Belle-Isle Strait to the mouth of the Olomane river), stations 1–14 (Lower

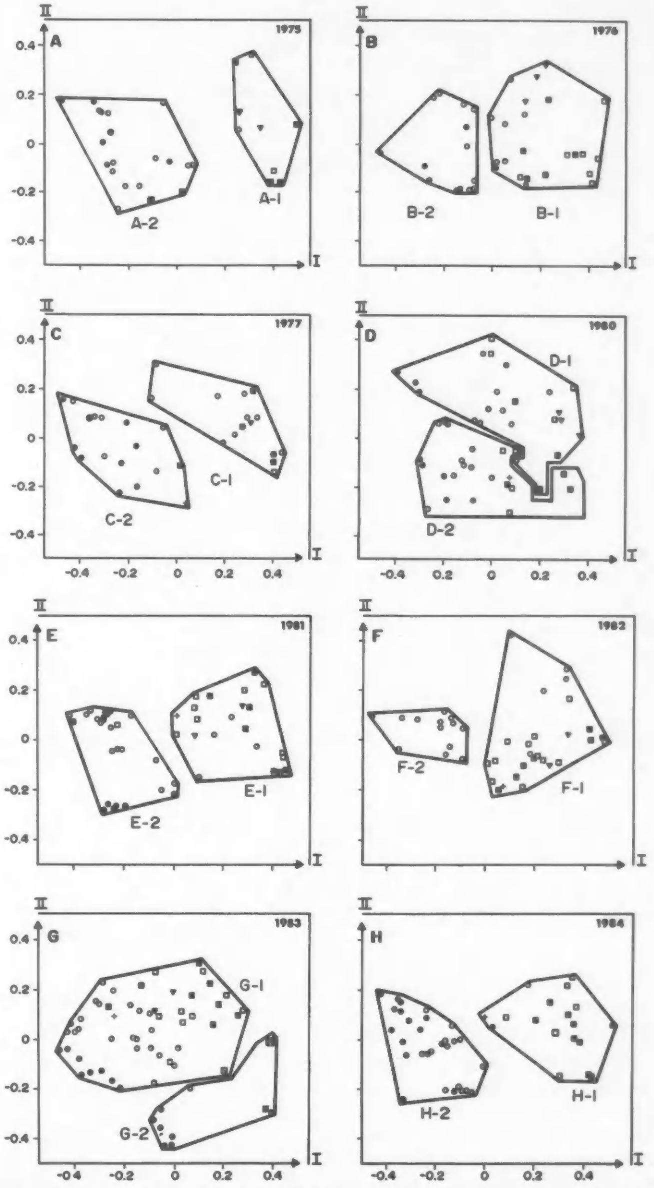

FIG. 4. Scatter diagrams of sampling sites in the reduced space formed by the first two principal coordinates of each analysis. Envelopes represent groups obtained by UPGMA clustering at $S \geqslant 0.57$. A to H are yearly analyses from 1975 to 1984 (except 1978 and 1979). Symbols represent collectors from the different sampling regions; ▼, Lower North Shore; ○, North Shore; ■, Mingan Islands; ●, Gaspé Peninsula; +, Anticosti Island; □, Lower Estuary (north coast); ⧅, Lower Estuary (south coast); ◪, Upper Estuary.

North Shore plus Eastern North Shore), stations 1–23 (from the Lower North Shore to the Mingan Islands region), stations 1–45 (Lower North Shore plus North Shore), stations 69–58 (the Northeastern Gaspé Peninsula, coalesced with stations from the Western North Shore in 1976, 1980, and 1981), and stations 57–52 (the Southeastern Gaspé Peninsula, coalesced with remaining stations of the Gaspé Peninsula in 1976–77). This picture shows a fluctuating structure that expands or shrinks by incorporating or dropping spatially-adjacent stations from one year to the next. Figure 5I, computed from average values, summarizes the representative structure for the entire period. Five major clusters are revealed: (1) stations 1–14 (Lower North Shore plus Eastern North Shore), (2) stations 15–23 (Mingan Islands region), (3) stations 25–45 (Western North Shore),

TABLE 1. Kendall correlation values between biomass of single dominant species and principal coordinate axes I and II.

	Species									
	O. longissima		*H. arctica*		*S. balanoides*		*M. edulis*		*B. crenatus*	
Year	I	II	I	II	*I*	*II*	I	II	I	II
1975	0.39	−0.77	−0.28	−0.04	−0.26	0.05	−0.77	−0.01	−0.54	0.03
1976	0.32	−0.94	−0.32	−0.13	−0.33	0.33	−0.93	−0.27	−0.84	0.21
1977	0.01	−0.56	−0.58	0.00	−0.52	0.37	−0.90	−0.02	−0.56	0.36
1980	−0.01	−0.85	−0.40	−0.17	0.14	−0.01	−0.93	−0.03	−0.40	0.39
1981	−0.41	0.63	−0.56	−0.01	−0.19	0.11	−0.82	−0.04	−0.34	−0.22
1982	−0.78	−0.19	−0.63	0.21	−0.47	0.33	−0.58	0.34	−0.44	0.56
1983	−0.68	0.32	−0.55	0.10	−0.34	0.19	−0.65	−0.36	−0.65	−0.22
1984	−0.28	0.80	−0.16	0.16	−0.14	−0.21	−0.92	0.02	−0.35	−0.02

(4) stations 69–65 (Northeastern Gaspé Peninsula and, (5) stations 63–52 (Southeastern Gaspé Peninsula). According to the Group Expansion Test (GET), when the structure created by the chronological clustering procedure is destroyed and each one of the previous groups formed are allowed, in turn, to expand, the first two clusters (1 and 2) and the last two (4 and 5) could, respectively, be merged together, reducing in this way the spatial structure to three sharply different regions representing clearly differentiated and non-overlapping subseries. Therefore, these reduced clusters are (1) stations 1–23 (Lower North shore up to the Mingan Islands), (2) stations 25–45 (Western North Shore) and (3) stations 69–52 (Gaspé Peninsula).

Spatially constrained nonmetric scaling analyses (Fig. 6) were performed in two dimensions, with a resulting stress varying between 0.043 and 0.125, depending on years. The scalar weight w chosen to constrain the starting matrix for the scaling analysis was sufficiently small ($w=0.01$) that the geographic data did not receive an undue weight in the matrix operation $C=A+wB$; it was just large enough to allow neighbouring stations to be together in the ordination. The NMDS technique, unlike spatially constrained clustering, was performed on a resemblance matrix containing all sampling stations, including the Estuary and Anticosti stations (Fig. 6, A–H). The NMDS results are in keeping with those of the spatially constrained clustering analysis. There is, however, a fundamental difference between these two techniques that may obscure the results. In the clustering analysis, the spatial constraint concerns immediate neighbours only, while in the scaling analysis the geographic constraint implies all pairwise distance relationships among stations. For that reason, drawing the constrained clusters in the constrained NMDS space would not be useful to the interpretation of relationships among clusters.

Synthesizing the constrained clustering results on average values (Fig. 5 I) and those of the constrained scaling (Fig. 6, A–H) shows that the spatial epibenthic structure during the entire period of study is characterized by six major "biogeographic zones" (Fig. 7). These are: (1) Lower North Shore plus Eastern North Shore (stations 1–14), (2) Mingan Islands (stations 15–23), (3) Western North Shore (stations 25–45), (4) Northeastern Gaspé Peninsula (stations 69–65), (5) Southeastern Gaspé Peninsula (Stations 63–52) and, (6) Lower Estuary plus Upper Estuary, from Pointe-des-Monts (station 72) to the south of Ile aux Coudres (station 171). No secondary subseries could be discriminated in the Estuary region. The Kruskal–Wallis analysis of variance showed very highly significant ($P<0.001$) heterogeneity of means among these "biogeographic zones", both for total biomass and for biomass of each of the dominant species (Table 2). This test must be read simply as an indication of the strength of the observed differences, since it is obviously improper to test a classification criterion (here: the six regions) against the very data that gave rise to it by clustering. Even with an independent classification criterion dividing the study area into regions, spatial autocorrelation in the species abundance data could have led to significant results in the analysis of variance, even in the absence of discontinuities in the data (Legendre et al. 1990).

Temporal Variability

The analyses of temporal variability of the dominant epibenthic assemblage were carried out on a set of matrices similar to the one represented in Fig. 8. These matrices were computed for each of the spatial scales examined. The graphs of Mantel statistic values across years, at large and intermediate (regional) spatial scales, are shown in Fig. 9. Mantel tests showed positive and highly significant correlations between the epibenthic biomass structure of consectuve years during the period 1975–84, at all three spatial scales considered. The degree of resemblance between consecutive years, however, was not constant throughout the period of study. Changes in resemblance seem to obey a periodic fluctuation of about 8 yr, whose amplitude increases as the spatial scale decreases. The period of study, however, was not long enough to determine the extent of the cycle of variation more precisely. The total variability of the Mantel matrices, corresponding to the same three spatial scales, is represented in Fig. 10. The dispersion pattern of years in the reduced space of the first two principal coordinate axes confirms the existence of a cycle of variation in biomass structure during this period at all three spatial scales. Dendrograms in this same figure illustrate the finer relationships of similarity among years. These results are in conformity with those of the dispersion diagrams (same figure) as well as the Mantel results in Fig. 9.

Discussion

Spatial Structure of Biomass

Overall, the spatial autocorrelation analyses (Fig. 2 and 3) showed a significant relationship between biomass and space. In the multivariate mode, the spatial affinity in community structure decreased with increasing geographic distance. A change from a coarse to a finer scale of examination resulted in a more complex picture of the spatial distribution of biomass,

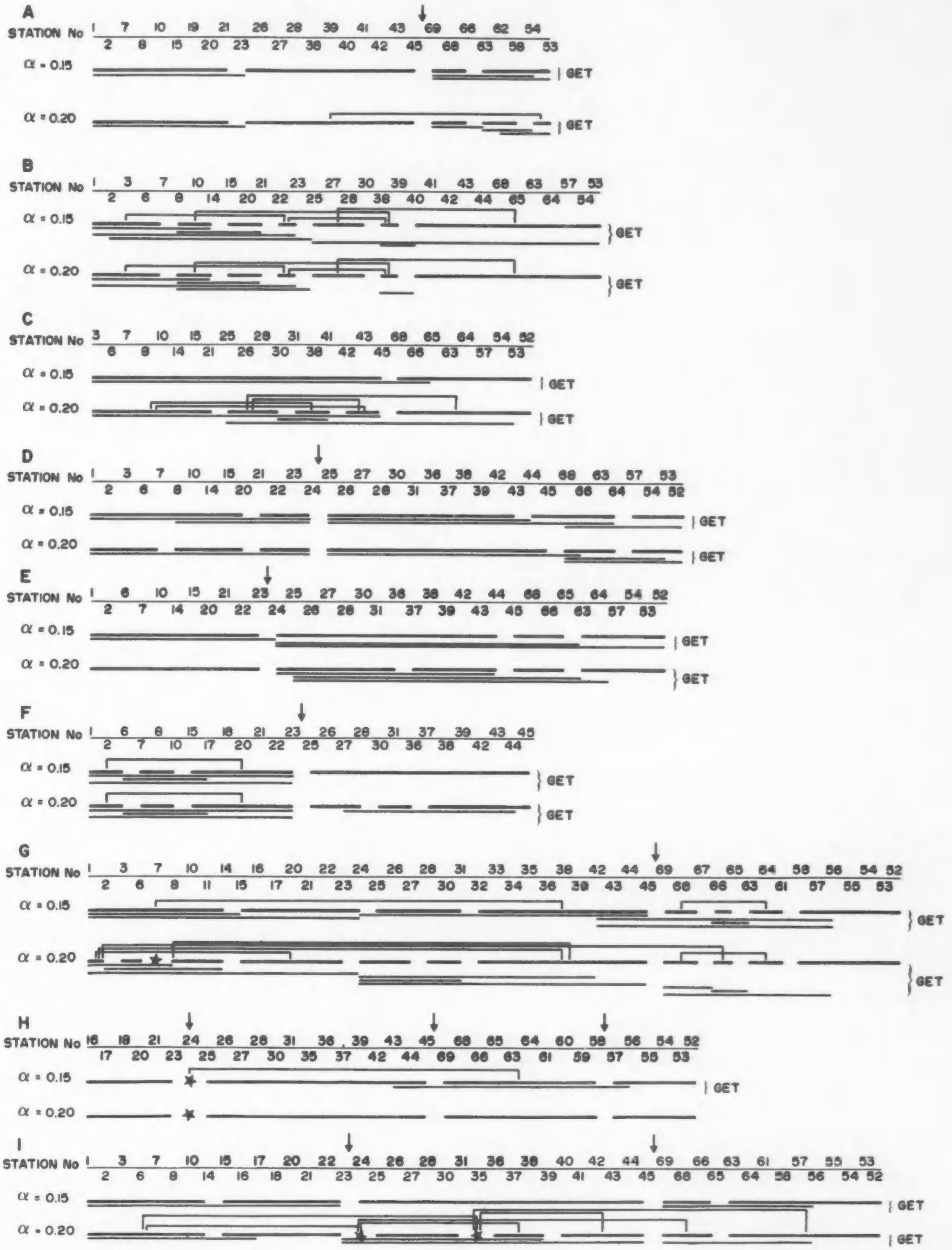

FIG. 5. Spatially constrained clustering of buoys based on the biomass data of species. Abbreviations and symbols: A to H, yearly clustering diagrams from 1975 to 1984 (except 1978 and 1979); I, clustering diagram on average biomass values for the entire period of study; heavy horizontal lines, clusters of biomass data from contiguous stations; GET, group expansion tests; horizontal brackets, *a posteriori* tests with probability of fusion greater than α; vertical arrows, most important breakpoints in the data series; stars, singletons; stations 1–3, the Lower North Shore; stations 6–45, the North Shore; stations 15–23, the Mingan island region; stations 69–52, the Gaspé Peninsula.

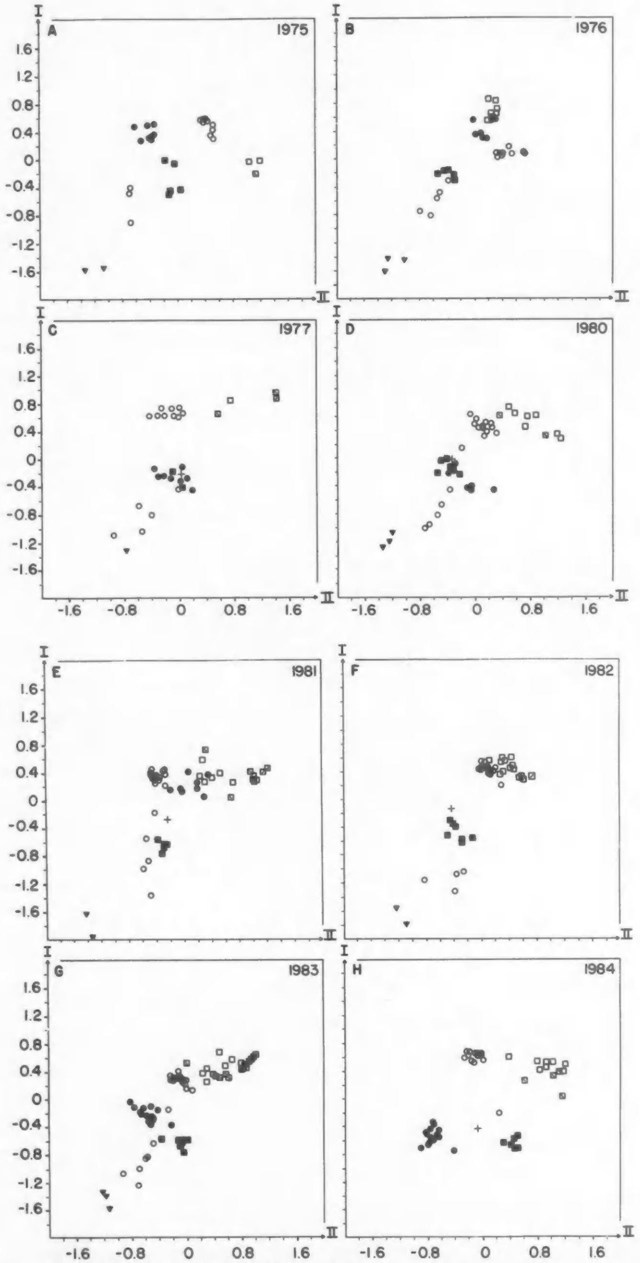

FIG. 6. Two-dimensional nonmetric multidimensional scaling of biomass data of stations. Scaling was performed on a spatially constrained resemblance matrix (Gower's index of similarity). A to H are yearly dispersal analyses from 1975 to 1984 (except 1978 and 1979). Symbols represent collectors from the different sampling regions: ▼, Lower North Shore; ○, North Shore; ■, Mingan Islands; ●, Gaspé Peninsula; +, Anticosti island; □, Lower Estuary (north coast); ⧅, Lower Estuary (south coast); ⧄, Upper Estuary.

the spatial patterns depending on species (see below). This is supported by the results of the one-way analysis of variance of means among "biogeographic zones" (Fig. 7) which indicates a significantly heterogeneous distribution of biomass throughout the study area. The existence of spatial inhomogeneities is now recognized as a more realistic

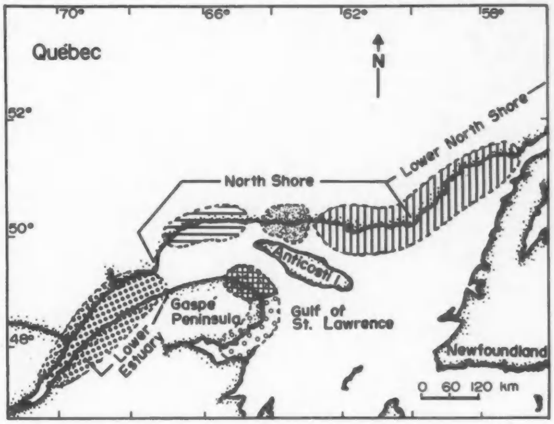

FIG. 7. Biogeographic zones during the period 1975–84 for the epibenthic fauna of the Estuary and Gulf of St. Lawrence.

ecological characteristic of species than regular or random distributions (Taylor 1984; Vance 1984; Fahrig and Paloheimo 1988a, b; Nagylaki 1988).

Trying to explain the spatial structure observed is difficult because studies of dispersal and survival of benthic larvae in the study area are lacking. Most of the quantitative studies concerning larval settlement, growth, biotic interactions, and seasonal variations of epibenthic populations in the St. Lawrence system (e.g. Archambault and Bourget 1983; Hudon et al. 1983; Brault and Bourget 1985) have been carried out at small spatio–temporal scales and did not take into account local recruitment vs. immigration–emigration processes. Hence, the crucial questions concerning larval population dynamics remain to a large extent unanswered. Certainly the presence and abundance of settling larvae is not the only factor controlling patterns. Biotic events occurring during and after settlement, such as biotic interactions among both dominant and rare epibenthic species, are also important (Buss 1980; Grosberg 1981; Brault and Bourget (1985). On the other hand, and as suggested by Sokal and Thomson (1987), the spatial patterns of biomass observed for single species may also reflect the spatial patterning of resources or other environmental factors affecting the populations. The evidence accumulated on the primary productivity and physical oceanography of the Estuary and Gulf of St. Lawrence (e.g. Lauzier et al. 1957; Steven 1974; El–Sabh 1976, 1979; Benoit et al. 1985; Therriault and Levasseur 1985; Legendre and Demers 1985) shows the physical environment to be spatially heterogeneous, resembling a mosaic of nested habitats, each one characterized by different physical and biological attributes. This suggests that the causes of patchiness are not the same from region to region and that the environmental factors are themselves patterned in space, constituting in this way a major structural force for epibenthic populations. Changes in autocorrelation values of biomass with increasing horizontal distance may then reflect the biological response of particular species to the carrying capacity of the surface layer of neighbouring localities within the limits of the study area.

As mentioned earlier, correlograms had different shapes depending on species. Two fundamental patterns emerged from them: a cline and a patchy pattern. The spatial structure of *O. longissima* at the whole system and the Gulf scales, and those of all species but *S. balanoides* at the Estuary scale, correspond to the former pattern. In contrast, the spatial structures of *H. arctica*, *M. edulis*, *S. balanoides*, and *B. crenatus* at the whole system and the Gulf scales were patchy. Correlograms also describe the change in correlation strength with increasing distance. In the Estuary area, correlation values diminished markedly in a relatively short distance (from 25–250 km). In light of the work of Therriault and Levasseur (1985), the strong slope of correlograms in the Estuary should be interpreted as resulting from a high spatial heterogeneity in carrying capacity of the environment within a relatively small area. On the basis of the spatial patterns of phytoplankton production, these authors divided the Lower Estuary into four regions, each one characterized by different values of temperature, salinity, turbidity, and nutrients. They concluded that each of these four regions was dominated by different hydrodynamic processes which have a different influence on the stability conditions of the water column. This suggests that, in this area, events occurring during and after settlement may also influence the structure of the assemblage as measured by biomass. This is quite obvious in *S. balanoides* which, although present in the Lower Estuary, was poorly represented and did not show significant spatial patterns at the time of sampling. Increasingly harsh conditions farther up the Estuary (e.g. increasing turbidity, lower salinity, highly variable nutrient content) probably reduced the growth of this species. The patchiness of *H. arctica, M. edulis, S. balanoides*, and *B. crenatus*, at the whole system and at the Gulf scales, is characterized by a patch diameter smaller than the interpatch distance. The patchiness of the biomass structure of these species could be the result of alternation of favorable and unfavorable conditions in space,

TABLE 2. Maximum average biomass values (g·0.01 m^{-2}) of dominant epibenthic species during the period 1975–84. Values in parentheses are standard deviations; n^a, number of samples per biogeographic zone.

	Biogeographic zone					
Species	Lower North Shore plus Eastern North Shore $n=8$	Mingan island region $n=6$	Western North Shore $n=16$	Northeastern Gaspé Peninsula $n=4$	Southeastern Gaspé Peninsula $n=7$	Lower Estuary to Ile aux Coudres $n=13$
O.longissima	0.37 (0.41)	1.86 (2.53)	3.35 (4.75)	5.42 (7.83)	0.60 (0.95)	1.51 (1.75)
H. arctica	0.03 (0.08)	0.08 (0.21)	0.51 (1.15)	0.12 (0.22)	0.09 (0.15)	0.10 (0.67)
M. edulis	0.95 (2.14)	0.18 (0.29)	3.30 (2.02)	9.81 (5.67)	8.91 (5.18)	0.48 (1.14)
S. balanoides	1.20 (2.61)	0.14 (0.34)	0.39 (0.67)	0.36 (0.71)	0.24 (0.86)	0.01 (0.06)
B. crenatus	0.79 (1.29)	0.10 (0.12)	1.14 (1.20)	0.75 (0.98)	1.68 (1.91)	0.19 (0.64)
Total biomass	3.63 (4.54)	2.34 (2.91)	8.90 (5.73)	17.4 (11.2)	11.7 (6.71)	2.27 (3.00)

[a]Samples obtained from collectors moored during most of the period of study (occasional buoys were discarded).

	75	76	77	80	81	82	83	84
75	1.000	0.603	0.297	0.343	0.529	0.390	0.473	0.770
76	0.603	1.000	0.434	0.499	0.411	0.320	0.403	0.461
77	0.297	0.434	1.000	0.373	0.265	0.142	0.358	0.320
80	0.343	0.499	0.373	1.000	0.396	0.387	0.432	0.428
81	0.529	0.411	0.265	0.396	1.000	0.524	0.542	0.518
82	0.390	0.320	0.142	0.387	0.524	1.000	0.578	0.506
83	0.473	0.403	0.358	0.432	0.542	0.578	1.000	0.477
84	0.770	0.461	0.320	0.428	0.518	0.506	0.477	1.000

FIG. 8. Matrix of biotic resemblance among yearly biomass structures in the Estuary and Gulf of St. Lawrence during the period 1975–84. Each value in the matrix is a Mantel statistic *r* computed between two similarity matrices comparing different years. The subdiagonal values correspond to the comparisons of consecutive years. The entire matrix is significant at the overall significance level $P<0.01$.

probably reflecting the patchiness of the physical environment itself.

Biogeographic Patterns

Clustering and scaling data on the basis of a resemblance matrix is another way of making inferences concerning community structure. Available methods, however, have different levels of model rigidity (Legendre et al. 1987). While unconstrained clustering and scaling techniques delineate spatial structures on the exclusive basis of the similarity among objects for the variables under study, regardless of the causal processes that generated them, constrained methods (e.g. time or space), by restricting the set of possible solutions to those that make sense in terms of these same constraints, delimit homogeneous regions that are more probably controlled by the same type of causal processes (Legendre 1987).

In light of the previous discussion, the spatial structures derived from unconstrained clustering and ordination analyses (Fig. 4) summarize the yearly spatial variability of biomass resulting from different but converging generating processes. The sampling sites scattered in the reduced space of the two principal coordinate axes throughout the period of study were highly variable. Yet these sites could not be entirely associated to particular clusters nor clearly discriminated along these same axes. However, when considering the main trends of variability, the clustering results, in conformity with the scaling results, showed that the stations from the Western North Shore were associated with those of the Gaspé Peninsula, both located on the left side of the first principal axis. Likewise, the collectors from the Lower North Shore, the Eastern North Shore, the Mingan Islands, Anticosti Island, and the Lower and Upper Estuary were associated to each other, and positioned on the right side of these graphs. This spatial structure, excluding the Eastern North Shore, is in keeping with the one obtained by Fradette and Bourget (1981) for the period 1975–76. In their study, these authors related the objects from the Eastern North Shore to those of the Western North Shore and the Gaspé Peninsula, even though objects 6 and 7 (4 and 5 in their study) were considered as belonging to the Lower North Shore. According to Fradette and Bourget (1981), the geographic gradient of summer surface water temperature is the factor that best explains the observed clusters. Thus, the stations located on the left side of the first principal axis, those of the North Shore (the Mingan Islands region excluded) and the Gaspé Peninsula localities, correspond to the areas of warmer summer surface water (9–16°C). Similarly, the samples located at the right of the first principal axis, those of the Lower North Shore, the Mingan Islands and the Lower Estuary localities, correspond to areas of colder summer surface water (4–14°C). These clusters are formed of similar sites coming from a set of heterogeneous localities influenced by different hydrodynamic processes (see El-Sabh 1976, 1979; Tang 1980; Dickie and Trites 1983; Bah and Legendre 1985). Two regions, the Mingan Islands and the Lower Estuary, are characterized by a common trait that

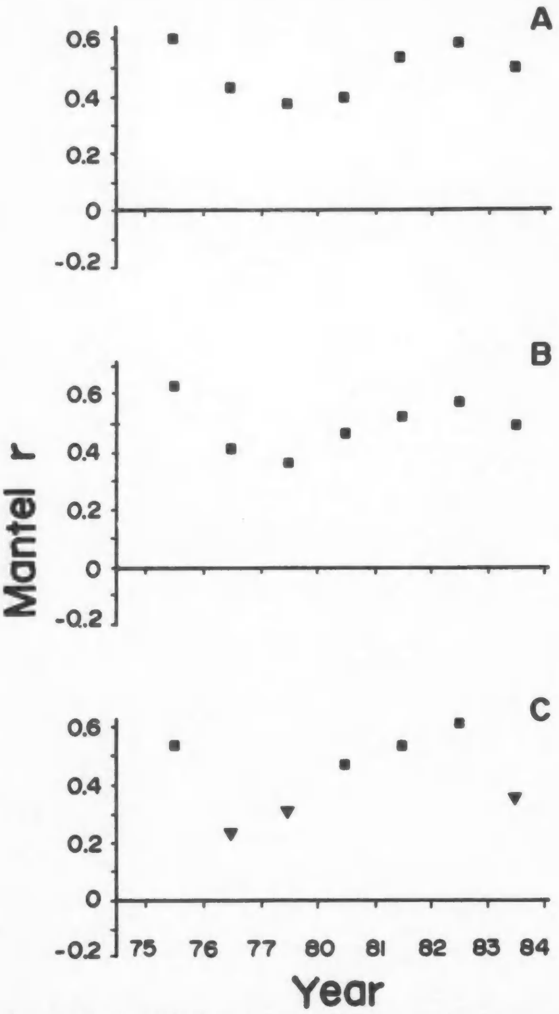

FIG. 9. Mantel statistics across years, for biotic resemblance between biomass structure of epibenthic assemblages of consecutive years during the period 1975–84 (except 1978–79), at different spatial scales. A, whole system (Gulf and Estuary); B, Gulf; C, Lower North Shore together with the North Shore. Abscissa: years. Ordinate: normalized Mantel statistic *r*. Black squares, coefficients significant at $P<0.001$. Black triangles, coefficients significant at $P\leq0.024$. The entire graphs are significant at the overall significance level $P<0.01$.

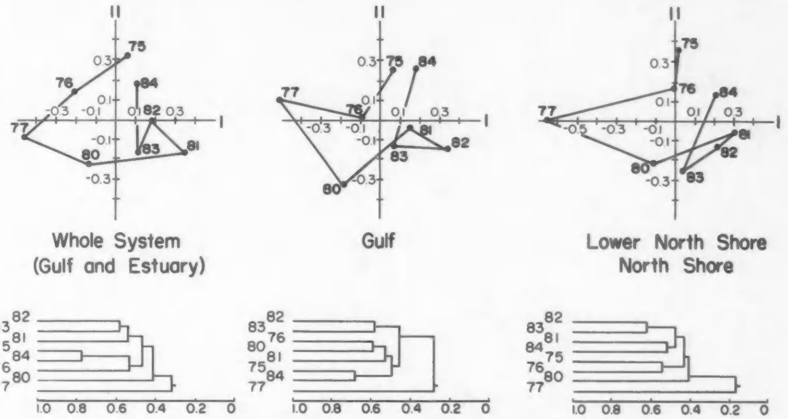

FIG. 10. UPGMA clustering and principal coordinate analysis of the normalized Mantel statistics *r*, representing the temporal variability in biomass structure of yearly epibenthic assemblages in the Estuary and Gulf of St. Lawrence during the period 1975–84 at different spatial scales. Line segments between years outline the chronological sequence. A, whole system (Gulf and Estuary); B, Gulf; C, Lower North Shore together with the North Shore. Black circles represent years in the reduced space of the first two principal axes. Dendrograms represent similarity relationships in biomass structure among years.

accounts for their similarity: the upwelling of colder, deeper waters during the summer months (Lauzier et al. 1957; Forrester 1974; Steven 1974) According to Fradette and Bourget (1980, 1981) this factor, in conjunction with other local characteristics, would be involved in the reduction of larval recruitment that is observed there. Thus, whereas in the Mingan Island region the surface dilution of larvae by upwelled waters and their subsequent offshore dispersal may be responsible for the reduced abundance of most of the species, in the Lower Estuary this effect would be obtained by the combined action of the surface dilution of larvae by upwelled waters, the loss of larvae by the downstream residual circulation, and the gradually increasing severity of the physicochemical conditions (e.g. temperature, salinity, turbidity). Moreover, the westward drift of cold water, originating partly from the Labrador current and from the episodic nearshore wind-forced upwellings in the Lower North Shore area influencing the Jacques-Cartier passage (Huntsman et al. 1954; Lauzier et al. 1957; El-Sabh 1976; Rose and Leggett 1988), can explain the affinity of the Eastern North Shore with the Lower North Shore and their inclusion into the cluster located on the right side of the first principal axis. In addition, the correlations between the two principal coordinate axes and the biomass of single species indicate that *M. edulis, B. crenatus* and *O. longissima* were the species that most contributed to the formation of the reduced space, showing in this way their preponderant role as structuring agents of the dominant assemblage.

In the presence of spatially autocorrelated data, spatially constrained clustering and scaling methods lead to a more realistic representation of the variability of biomass (Legendre et al. 1987; Legendre 1987). These analyses showed the most conspicuous discontinuities in community structure between contiguous localities. The six homogeneous "biogeographic zones" thus established (Fig. 7) characterize the average variability trends of a very resilient oscillating yearly structure. In the present study, the expression "biogeographic zone" is used only as a working concept intended to identify homogeneous areas with distinct assemblage structure of the dominant species, and not to imply differences in geographic range and species composition with increasing distance. In order to illustrate these biogeographic zones, the average biomass structure of the dominant assemblage of each zone is represented in Fig. 11. Except for the species assemblages from the Mingan Islands and the Lower and Upper Estuary which were similar both in structure and in total biomass, the species assemblages of each of the other biogeographic zones showed a singular biomass structure. The highest total biomass values of the Estuary–Gulf system during this period came from the Western North Shore and the Gaspé Peninsula zones. These results are in agreement with Steven (1974), who described this area as the region of maximum primary production in the Estuary–Gulf system. The dominant oceanographic features accounting for the nutrient richness of the surface layer of this area (Steven 1974; El-Sabh 1976) are a stationary counter-clockwise gyre, and the Gaspé Current flowing seaward along the entire length of the Gaspé coast.

Temporal Fluctuation in Biotic Resemblance

It has been shown that the yearly community structure was significantly autocorrelated during the period 1975–84, and that the strength of the correlation between years is not constant, varying in a cyclic way. What is the significance of this period of variation, and how can it be explained? At large and intermediate spatial scales, the temporal fluctuation in biotic resemblance between neighbouring years was gradual and apparently stable. Such an oscillating pattern, reflecting the change in similarity structure from one year to the next, suggests that singular biological or physical events (e.g. low density of recruiting competent larvae, or cold and strongly mixed summer surface water layer) may have a long-lasting influence on the community structure of subsequent years. However, the specific causal processes (physical and biotic) forcing the yearly community structure remain to be elucidated. From the thermo-

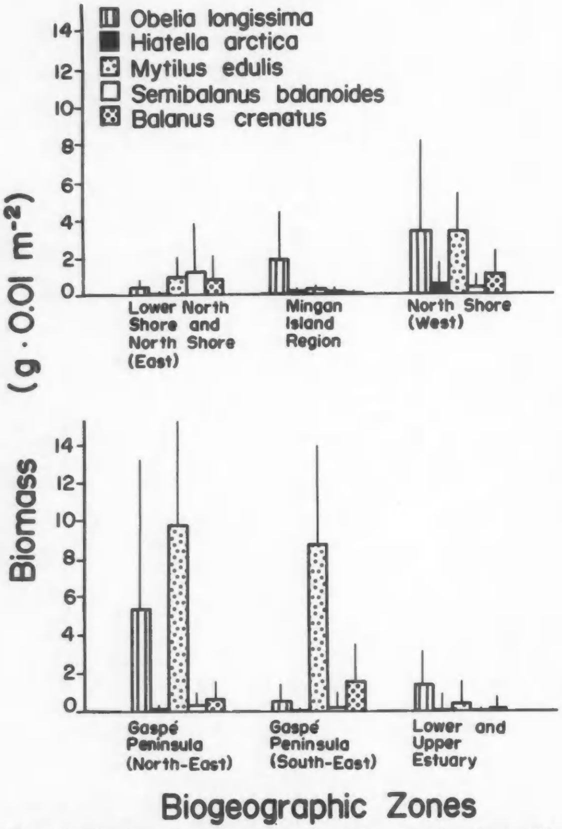

FIG. 11. Structure of the dominant epibenthic assemblage in the different biogeographic zones of the Estuary and Gulf of St. Lawrence, during the period 1975–84. Vertical bars: one standard deviation.

dynamic point of view, periodic fluctuations need an external input of energy. On continental shelves and in estuarine areas, the main sources of energy input are freshwater runoff, winds, and tides (Legendre and Demers 1985). These sources of auxiliary energy have varying periodicities and, spatially, their effects on stability and community organization are not exerted homogeneously (Platt and Denman 1975; Margalef 1979; Ulanowicz and Platt 1985). The relative weights of these driving forces at different spatio–temporal scales remain to be assessed, as well as the physical and biological mechanisms by which the variability in the energy input is transmitted to the epibenthic community inhabiting the surface water layer.

In previous sections we have emphasized the complementary use of different numerical techniques in order to reveal the spatial structure and temporal variability of observational data. This approach allowed us to overcome the shortcomings of single methods while taking advantage of the implicit and/or explicit hypotheses concerning the causal relationships among variables in each one of them. The use of different spatio–temporal scales of observation made complex patterns in community structure emerge. From this point of view the biogeographic zones thus obtained should be considered only as an abstraction helping to visualize the average structure throughout the period of study, while the year-by-year analyses represent a more realistic picture of community structure. On a yearly basis, spatial patterns resulted in a set of nested subseries that expands or shrinks from one year to the next, probably reflecting the larval population dynamics and the patterning of the environment itself. A proposal worth considering is that, in spite of these spatial discontinuities, the temporal oscillations in community structure observed at intermediate and large spatial scales suggest that the Estuary–Gulf system responds to external inputs of auxiliary energy as an integrated system. More intensive and simultaneous surveys of both biotic and physical rate processes are needed to elucidate the dynamics of the structures revealed in this study.

Acknowledgments

Financial support was provided by grants from the Natural Sciences and Engineering Research Council of Canada (NSERC) and FCAR to E.Bourget and a scholarship from the Ministère de l'Enseignement Supérieur et de la Science du Québec to P.-L.A. We thank S. Fugulin for her field and technical assistance in the initial phase of the study, Drs J. Boulva, P. Béland, and J.-C. Therriault from the Institut Maurice–Lamontagne, Fisheries and Oceans Canada, for their encouragement, and MM. L. Cardinal, L. Pépin, and R. Matte from Transport Canada for their collaboration.

References

ALLEN, T. F. H., AND T. B. STARR. 1982. Hierarchy: perspectives for ecological complexity. University of Chicago Press, Chicago, Il. 310 p.

ARCHAMBAULT, D., AND E. BOURGET. 1983. Importance du régime de dénudation sur la structure et la succession des communautés intertidales de substrat rocheux en milieu subarctique. Can. J. Fish. Aquat. Sci. 40: 1278–1292.

BAH, A., AND L. LEGENDRE. 1985. Biomasse phytoplanctonique et mélange de marée dans l'estuaire moyen du Saint-Laurent. Naturaliste Can. 112: 39–49.

BENOIT, J., M. I. EL-SABH, AND C. L. TANG. 1985. Structure and seasonal characteristics of the Gaspé current. J. Geophys. Res. 90: 3225–3236.

BOURGET, E. 1988. Barnacle larval settlement: the perception of cues at different spatial scales, p. 153–172. *In* G. Chelazzi and M. Vannini [ed.] Behavioral adaptation to intertidal life. NATO ASI Series, Vol. A151. Plenum, New York, NY.

BRAULT, S., AND E. BOURGET. 1985. Structural changes in an estuarine subtidal epibenthic community: biotic and physical causes. Mar. Ecol. Prog. Ser. 21: 63–73.

BROWN, J. H. 1984. On the relationship between abundance and distribution of species. Am. Nat. 124: 255–279.

BROWN, J. H., AND B. A. MAURER. 1987. Evolution of species assemblages: effects of energetic constraints and species dynamics on the diversification of the North American avifauna. Am. Nat. 130: 1–17.

BUSS, L. W. 1980. Bryozoan overgrowth interactions: the interdependence of competition for space and food. Nature (Lond.) 281: 475–477.

CLIFF, A. D., AND J. K. ORD. 1981. Spatial processes: Models and applications. Pion Limited, London, UK.

COOPER, D. W. 1968. The significance level in multiple tests made simultaneously. Heredity 23: 614–617.

DEANGELIS, D. L., AND J. C. WATERHOUSE. 1987. Equilibrium and nonequilibrium concepts in ecological models. Ecol. Monogr. 57: 1–21.

DICKIE, L. M., AND R. W. TRITES. 1983. The Gulf of St. Lawrence, p. 403–425. *In* B. H. Ketchum [ed.] Estuaries and enclosed seas. Elsevier, Amsterdam, The Netherlands.

EL-SABH, M. I. 1976. Surface circulation pattern in the Gulf of St. Lawrence. J. Fish. Res. Board Can. 33: 124–138.

1979. The Lower St. Lawrence Estuary as a physical oceanographic system. Naturaliste Can. 106: 55–73.

EL-SABH, M. I., AND O. M. JOHANNESSEN. 1972. Winter geostrophic circulation in the Gulf of St. Lawrence. J. Fish. Res. Board Can. 29: 595–598.

FAHRIG, L., AND J. PALOHEIMO. 1988a. Determinants of local population size in patchy habitats. Theor. Popul. Biol. 34: 194–213.

1988b. Effect of spatial arrangement of habitat patches on local population size. Ecology 69: 468–475.

FIELD, J. G., K. R. CLARKE, AND R. M. WARWICK. 1982. A practical strategy for analysing multispecies distribution patterns. Mar. Ecol. Prog. Ser. 8: 37–52.

Field, J. G., R. H. Green, F. A. de L. Andrade, E. Fresi, P. Gros, B. H. McArdle, M. Scardi, and D. Wartenberg. 1987. Numerical ecology: developments for studying the benthos, p. 485–494. *In* P. and L. Legendre [ed.] Developments in numerical ecology. NATO ASI series, Vol. G14. Springer–Verlag, Berlin.

Forrester, W. D. 1974. Internal tides in St. Lawrence Estuary. J. Mar. Res. 32: 55–66.

Fradette, P., and E. Bourget 1980. Ecology of benthic epifauna of the Estuary and Gulf of St. Lawrence: factors influencing their distribution and abundance on buoys. Can. J. Fish. Aquat. Sci. 37: 979–999.

1981. Groupement et ordination appliqués à l'étude de la répartition de l'épifaune benthique de l'estuaire maritime et du golfe du Saint–Laurent. J. Exp. Mar. Biol. Ecol. 50: 133–152.

Galzin, R., and P. Legendre.1987. The fish communities of a coral reef transect. Pacific Sci. 41: 158–165.

Gower, J. C. 1966. Some distance properties of latent root and vector methods used in multivariate analysis. Biometrika 53: 325–338.

1971. A general coefficient of similarity and some of its properties. Biometrics 27: 857–871.

Grosberg, R. K. 1981. Competitive ability influences habitat choice in marine invertebrates. Nature (Lond.) 290: 700–702.

Hudon, C., E. Bourget, and P. Legendre. 1983. An integrated study of the factors influencing the choice of the settling site of *Balanus crenatus* cyprid larvae. Can. J. Fish. Aquat. Sci. 40: 1186–1194.

Huntsman, A. G., W. B. Bailey, and H. B. Hachey. 1954. The general oceanography of the Strait of Belle Isle. J. Fish. Res. Board Can. 11: 198–260.

Kolasa, J. 1989. Ecological systems in hierarchical perspective: breaks in community structure and other consequences. Ecology 70: 36–47.

Kruskal, J. B., and M. Wish. 1978. Multidimensional scaling. Sage Publications, Beverley Hills, CA 93 p.

Lauzier, L., R. W. Trites, and H. B. Hachey. 1957. Some features of the surface layer of the Gulf of St. Lawrence. Bull. Fish. Res. Board Can. 111: 195–212.

Legendre, L., C. D. Collins, C. M. Yentsch, J. C. Bezdek, J. W. Campbell, Y. Escoufier, M. Estrada, and F. Ibanez. 1987. Numerical ecology: developments for biological oceanography and limnology, p. 521–527. *In* P. and L. Legendre [ed.] Developments in numerical ecology. NATO ASI series. Vol. G14. Springer–Verlag. Berlin.

Legendre, L., and P. Legendre. 1984. Ecologie numérique, T.2. La structure des données écologiques. 2^e édition. Collection d'écologie 13, Masson, Paris et les Presses de l'Université du Québec, P.Q. 335 p.

Legendre, L., and S. Demers. 1984. Towards dynamic biological oceanography and limnology. Can. J. Fish. Aquat. Sci. 41: 2–19.

1985. Auxiliary energy, ergoclines and aquatic biological production. Naturaliste Can. 112: 5–14.

Legendre, P. 1987. Constrained clustering, p. 289–307. *In* P. and L. Legendre [ed.] Developments in numerical ecology. NATO ASI series, Vol. G14. Springer–Verlag, Berlin.

Legendre, P., S. Dallot, and L. Legendre. 1985. Succession of species within a community:chronological clustering, with applications to marine and freshwater zooplankton. Am. Nat. 125: 257–288.

Legendre, P. and M.-J. Fortin. 1989. Spatial pattern and ecological analysis. Vegetation 80: 107–138.

Legendre, P., N. L. Oden, R. R. Sokal, A. Vaudor, and J. Kim. 1990. Approximate analysis of variance of spatially autocorrelated regional data. J. Class. 7: 53–75.

Lilliefors, H. W. 1967. The Kolmogorov–Smirnov test for normality with mean and variance unknown. J. Am. Stat. Assoc. 62: 399–402.

Mantel, N. 1967. The detection of disease clustering and a generalized regression approach. Cancer Res. 27: 209–220.

Margalef, R. 1979. The organization of space. Oikos 33: 152–159.

Miller, R. G., Jr. 1977. Developments in multiple comparisons. J. Am. Stat. Assoc. 72: 779–788.

Morris, D. W. 1987. Ecological scale and habitat use. Ecology 68: 362–369.

Nagylaki, T. 1988. The influence of spatial inhomogeneities on neutral models of geographical variation. Theor. Popul. Biol. 33: 291–310.

Oden, N. L. 1984. Assessing the significance of a spatial correlogram. Geogr. Anal. 16: 1–16.

Oden, N. L., and R. R. Sokal. 1986. Directional autocorrelation: an extension of spatial correlograms to two dimensions. Syst. Zool. 35: 608–617.

Platt, T., and K. L. Denman. 1975. Spectral analysis in ecology. Annu. Rev. Ecol. Syst. 6: 189–210.

Platt, T., K. H. Mann, and R. E. Ulanowicz. 1981. Mathematical models in biological oceanography. Monographs on oceanographic methodology 7, UNESCO Press, Paris, France, 157 p.

Rohlf, F. J. 1963. Classification of *Aedes* by numerical taxonomic methods (Diptera: Culicidae). Ann. Entomol. Soc. Am. 56: 798–804.

Rose, G. A., and W. C. Leggett. 1988. Atmosphere–ocean coupling in the northern Gulf of St. Lawrence: frequency-dependent wind-forced variations in nearshore sea temperatures and currents. Can. J. Fish. Aquat. Sci. 45: 1222–1233.

Shepard, R. N. 1962. The analysis of proximities: multidimensional scaling with an unknown distance function. Psychometrika. 27: 125–139, 219–246.

1966. Metric structures in ordinal data. J. Math. Psychol. 3: 287–315.

Sokal, R. R. 1979. Ecological parameters inferred from spatial correlograms, p. 167–196 *In* G. P. Patil and M. L. Rosenzweig, [ed.] contemporary quantitative ecology and related ecometrics. Statistical Ecology Series, Vol. 12. International Co-operative Pub. House, Fairland, MD.

Sokal, R. R., and N. L. Oden. 1978. Spatial autocorrelation in biology. 1. Methodology. Biol. J. Linn. Soc. 10: 199–228.

Sokal, R. R., and F. J. Rohlf. 1981. Biometry. The principles and practice of statistics in biological research. 2nd ed. W. H. Freeman and Co., San Francisco, CA. 859 p.

Sokal, R. R., and J. D. Thomson. 1987. Applications of spatial autocorrelation in ecology, p. 431–466. *In* P. and L. Legendre [ed.] Developments in numerical ecology. NATO ASI series, Vol. G14. Springer–Verlag, Berlin.

Steven, D. M. 1974. Primary and secondary production in the Gulf of St. Lawrence. McGill Univ., Mar. Sci. Centre MS Rep. 26. 116 p.

Tang, C. L. 1980. Mixing and circulation in the Northwestern Gulf of St. Lawrence: a study of a buoyancy-driven current system. J. Geophys. Res. 85: 2787–2796.

Taylor, L. R. 1984. Assessing and interpreting the spatial distributions of insect populations. Annu. Rev. Entomol. 29: 321–357.

Therriault, J.-C., and M. Levasseur. 1985. Control of phytoplankton production in the lower St. Lawrence estuary: light and freshwater runoff. Naturaliste Can. 112: 77–96.

Ulanowicz, R. E., and T. Platt [ed.]. 1985. Ecosystem theory for biological oceanography. Can. Bull. Fish. Aquat. Sci. 213: 260 p.

Vance, R. R. 1984. The effect of dispersal on population stability in one-species, discrete-space population growth models. Am. Nat. 123: 230–254.

Wiens, J. A. 1984. On understanding a non-equilibrium world: myth and reality in community patterns and processes, p. 439–457. *In* D. R. Strong et al. [ed.] Ecological Communities: conceptual issues and the evidence. Princeton Univ. Press, Princeton, NJ.

Phytoplankton Communities of Lakes Experimentally Acidified with Sulfuric and Nitric Acids

D. L. Findlay and S. E. M. Kasian

Department of Fisheries and Oceans, Central and Arctic Region, Freshwater Institute, 501 University Crescent, Winnipeg, Man. R3T 2N6 Canada

Findlay, D. L., and S. E. M. Kasian. 1990. Phytoplankton communities of lakes experimentally acidified with sulfuric and nitric acids. Can. J. Fish. Aquat. Sci. 47: 1378–1386.

Additions of sulfuric acid to the South Basin and nitric acid to the North Basin of Lake 302 caused major changes in the phytoplankton communities. The basins were separated by a nylon-reinforced vinyl sea curtain. In the South Basin, below pH 5.6, species composition shifted from chrysophycean dominance to one of Dinophyceae. Diatoms and cyanophytes were eliminated below pH 5.3. Phytoplankton species diversity decreased as pH decreased. Total epilimnetic biomass was unchanged, except in late fall, when entrainment of dense layers of hypolimnetic species caused increases. The assemblage in the North Basin changed immediately upon additions of HNO_3 to resemble systems experimentally fertilized with nitrogen. Chrysophycean dominance gave way to chlorophytes and dinoflagellates. Once pH decreased below 6.0, diatoms and cyanophytes were eliminated from the assemblage, as in the South Basin. Phytoplankton species diversity decreased, but total epilimnetic biomass remained unaffected.

Des additions d'acide sulfurique dans le bassin sud et d'acide nitrique dans le bassin nord du lac 302 ont entraîné des modifications importantes des communautés phytoplanctoniques. Les bassins étaient séparés par un dispositif en vinyl renforcé de nylon. Dans le bassin sud, dont le pH était inférieur à 5,6, la composition des espèces passait d'une dominance à chrysophycées à une dominance à dinophycées. Les diatomées et les cyanophycées étaient éliminées lorsque le pH était inférieur à 5,3. La diversité des espèces phytoplanctoniques diminuait lorsque le pH baissait. La biomasse épilimnétique totale ne changeait pas, sauf à la fin de l'automne, lorsque l'entraînement de couches denses des espèces de l'hypolimnion a provoqué des augmentations. L'assemblage dans le bassin nord a changé immédiatement après l'addition de HNO_3 pour ressembler à des systèmes engraissés expérimentalement à l'azote. La dominance des chrysophycées a provoqué l'effondrement des chlorophytes et des dinoflagellés. Lorsque le pH est inférieur à 6,0, les diatomées et les cyanophycées étaient éliminées de l'assemblage comme dans le bassin sud. La variété des espèces phytoplanctoniques diminuait, mais la biomasse épilimnétique totale n'était pas modifiée.

Received September 8, 1989
Accepted February 22, 1990
(JA303)

Reçu le 8 septembre 1989
Accepté le 22 février 1990

Effects of acidification on freshwater phytoplankton communities have been documented (Almer et al. 1978; Conroy et al. 1975; Kwiatkowski and Roff 1976; Yan and Stokes 1978; Dillon et al. 1979; Blouin et al. 1984; Findlay and Kasian 1986), but the early effects of acidification on phytoplankton communities are still poorly known with some conflicting results occurring. There is general agreement in the literature that species diversity declines as pH declines and that species of chrysophytes, chlorophytes, and diatoms disappear first, being replaced by dinoflagellates. However, Almer et al. (1978) and Yan and Stokes (1978) document no increase in total phytoplankton biomass as pH decreased. Conroy et al. (1975) suggested a decrease occurred as pH decreased and Findlay and Kasian (1986) reported an increase in total biomass as pH decreased. The systems which have been studied have been acidified primarily by sulfuric acid, while nitric acid inputs pose an additional and impeding threat (National Research Council Canada 1981; Norwegian State Pollution Control Authority 1987).

In 1982, a whole lake acidification experiment began on Lake 302, a small, double-basin lake at the Experimental Lakes Area (E.L.A.). The two basins were separated by inserting nylon-reinforced vinyl sea curtains in the channels on either side of an island in the narrows connecting the basins. Lake 302 South was acidified with H_2SO_4 and Lake 302 North with a similar amount of H^+ as HNO_3 to compare the effects of the two acids. Rudd et al. (1990) give details of the acidification regimes.

In this paper we present responses by phytoplankton to the Lake 302 acidification experiment from 1982 through 1986. The results from the South Basin (acidified with H_2SO_4) are compared to those from the earlier Lake 223 acidification experiment (H_2SO_4) to test if the Lake 223 results (Schindler et al. 1985; Findlay and Kasian 1986) were reproducible in a more productive system and furthermore to determine if experimental acidification elicits responses similar to those described in the existing literature for anthropogenically-acidified lakes. The results of the nitric acid additions to the North Basin of Lake 302 are compared to results both from lakes acidified with sulfuric acid and from lakes fertilized with nitrogen in non-acid forms. In addition, the results of both the sulfuric and nitric acid experiments on Lake 302 are compared to untreated, oligotrophic reference systems to assess temporal effects.

Methods

Study Site

Lake 302 is a small, slightly mesotrophic, double-basin, dimictic lake with the basins connected by two narrow channels.

TABLE 1. Morphometric features of Lake 239, Lake 302 North and South and Lakes 223, 222, 224, and 382.

Lake	Treatment	Surface area (ha)	Maximum depth (m)	Mean depth (m)	Volume $10^5 m^3$
239	Reference	56.1	30.4	10.5	59.1
302 North	HNO_3	12.8	13.8	5.7	7.3
302 South	H_2SO_4	10.9	10.6	5.1	5.5
223	H_2SO_4	27.3	14.4	7.2	19.5
222	Reference	16.4	5.8	3.7	6.0
224	Reference	25.9	27.4	11.6	30.1
382	Reference	37.1	13.1	5.7	21.1

Both basins are morphometrically similar (Table 1). The natural flow of the lake is from south to north with a single outflow situated at the north end of the North Basin. There are no distinct inflowing streams. Lake 302 is situated on the Precambrian Shield (latitude 49° 40.15′, longitude 93° 45.25′). The lake is surrounded by a pristine, unlogged, boreal forest of jack pine (*Pinus banksiana* Lamb), red pine (*Pinus resinosa* Ait.), and black spruce (*Picea mariana* (Mill.) BSP).

From 1972 to 1976 and in 1978 Lake 302 was the site of a hypolimnetic nutrient addition experiment (Schindler et al. 1980). Nutrients were injected below the thermocline into the North Basin of the lake. Because the nutrients were isolated from the euphotic zone during most of the ice-free season, eutrophying effects on the lake were slight (Schindler et al. 1980).

The basins remained partitioned until 1980, when the sea curtains were removed to allow circulation between the basins. In 1981, Lake 302 was selected for an acidification experiment, although phosphorus remained slightly elevated in the North Basin (Table 2).

In June 1981 the lake was repartitioned by the insertion of vinyl sea curtains in the two channels. The curtains were attached to the sides of the channels and were anchored on the bottom using rocks and sandbags to obtain the best possible seal. The flow from the South Basin to the North Basin was not strong enough to force water over the top of the curtain, but there was leakage. Each basin was monitored for 1 yr following curtain installation. Commencing in July 1982, the South Basin was acidified with H_2SO_4 while the North Basin was acidified with HNO_3. A target pH was chosen for the South Basin at the beginning of each ice-free season (Table 2). In 1983 and thereafter, the pH was lowered to the target level immediately after ice-out and maintained by additions of H_2SO_4 as required (usually two to three times per week). The pH of the South Basin was decreased from 6.7 in 1981 to 5.0 in 1986 (Table 2). The North Basin received similar amounts of H^+ per unit volume, using HNO_3. The pH of the North Basin decreased from 6.6 in 1981 to 5.9 in 1986 (Table 2). The pH values in the North Basin remained higher due to partial neutralization of the nitric acid by algal uptake and denitrification (Rudd et al. 1990). Details of the additions on each acidification date can be found in Cruikshank (1984, 1986).

Lake 223 is an oligotrophic, dimictic lake situated 3 km from Lake 302. It has a single inlet and outlet. The epilimnetic pH in Lake 223 was reduced from 6.7 to 5.0 (1976–81) and was held at pH 5.0 from 1981 to 1983 by epilimnetic additions of H_2SO_4 (Schindler et al. 1985). Responses of the phytoplankton community to acidification of Lake 223 have been documented, in terms of annual means by Findlay and Kasian (1986).

TABLE 2. Mean ice-free epilimnetic time weighted pH, total N, total P for Lake 302 North and South 1980–86, Lake 223 1974–83 and averages for reference lakes (222, 224, 239, and 382) 1980–86.

Lake	Year	Target pH	Time weighted epilimnetic pH	Mean epilimnetic concentration of total N, $\mu g \cdot L^{-1}$	Mean epilimnetic concentration of total P, $\mu g \cdot L^{-1}$
302N	1980		6.5	350	10.1
	1981		6.6	317	11.4
	1982		6.7	561	11.5
	1983		6.3	709	12.3
	1984		6.2	977	14.5
	1985		6.0	940	12.6
	1986		5.9	1054	9.4
302S	1980		6.6	346	7.5
	1981		6.7	321	5.2
	1982	6.3	6.2	336	7.3
	1983	5.8	5.8	332	8.3
	1984	5.5	5.6	374	12.0
	1985	5.3	5.3	414	10.7
	1986	5.0	5.0	378	7.5
223	1974		6.7	295	7.0
	1975		6.6	251	6.1
	1976		6.4	297	5.0
	1977	6.25	6.1	285	6.0
	1978	6.0	5.9	285	6.3
	1979	5.75	5.6	277	6.1
	1980	5.5	5.6	257	6.0
	1981	5.0	5.0	246	6.0
	1982	5.0	5.0	274	7.2
	1983	5.0	5.1	282	8.0
Ref	1980			341	7.1
	1981			350	8.2
	1982			358	8.4
	1983			340	8.1
	1984			329	11.3
	1985			373	9.0
	1986			333	6.1

Phytoplankton Sampling and Enumeration

Phytoplankton samples were taken in conjunction with the primary productivity measurements. An integrating sampler (Shearer 1978) was used to obtain samples from a desired stratum (epilimnion, metalimnion, or hypolimnion). For the purpose of this paper we shall be dealing only with the epilimnion, which was defined as the upper layer of uniform temperature. Each basin of Lake 302 was sampled every second week during the ice-free season from 1980 to 1986, except in 1980 when sampling commenced in mid-June.

A 125 mL aliquot was extracted and preserved in acid Lugol's solution for identification and enumeration of phytoplankton. Ten mL aliquots of Lugol's preserved samples were gravity settled for 24 h. Counts were performed on an inverted microscope at magnifications of 125×, 400×, and 1 000× (oil) with phase contrast illumination. All counts were done by the Utermöhl technique as modified by Nauwerck (1963). To aid in identification, live net samples taken with a 10 μm mesh net were examined occasionally.

Wet biomass was estimated by approximating the cell volume of each species. Estimates of cell volume for each species were obtained by measuring cells and applying the geometric formula best fitted to the shape of the cell (Vollenweider 1968). A density of 1.0 was assumed in calculating wet weight from cell volume.

Phytoplankton Species Diversity

Simpson's diversity index (D) was chosen to summarize changes in the phytoplankton community structure. This index is biased towards the more abundant species and is not sensitive to changes in rarer species. However, Washington (1984) demonstrated it to be the most suitable of presently available indices. This index is

$$D = 1 - \sum_{i=1}^{s} \frac{n_i(n_i - 1)}{n(n-1)}$$

where S = the number of species in a "sample", n = the number of individuals in a sample, and n_i = the number of individuals of species i in a sample. Species diversity (D) would be 1 in a homogeneous comunity where each species contributed equally to the total, and would be near 0 if a community with the same species was dominated by a few.

Comparison of Experimental Lakes to Reference Lakes

The four oligotrophic reference lakes chosen for comparison to the experimental lakes are: Lakes 222, 224, 239, and 382. Data do not exist for a slightly mesotrophic reference system.

To assess seasonal phytoplankton responses to treatments, average monthly biomasses in the ice-free season for the six major taxonomic groups, total phytoplankton biomass, and species diversity were calculated. Monthly means were calculated from samples taken every 2 wk. All reference lakes were included in the analysis, but to conserve space, results from only Lake 239 are presented in the figures.

Chemical Sampling and Methods

The epilimnion was sampled chemically every second week for Lake 302 and once per month for the reference lakes. Samples were taken from a single station located at the position of maximum depth of each lake. Total phosphorus (TP) and total nitrogen (TN) were measured as described by Stainton et al. (1977) and are the sums of all dissolved and suspended fractions of each nutrient. The pH values presented are ice-free, time weighted, epilimnetic values, and were measured more frequently than other parameters (D. R. Cruikshank, Freshwater Institute, Winnipeg, Man., unpubl. data).

Results

Total Phytoplankton Biomass

Total epilimnetic phytoplankton biomass in the South Basin increased as pH decreased (Fig. 1, Table 2). Increases of this magnitude were not evident in the reference lakes. The greatest increases in the South Basin occurred in September and October, when hypolimnetic blooms were entrained by fall mixing (Fig. 2). Occurrences of hypolimnetic peaks in the South Basin were documented by Fee (1976) and Fee et al. (1977), but the dominant species in 1984–86 were different and were more abundant than those previously documented.

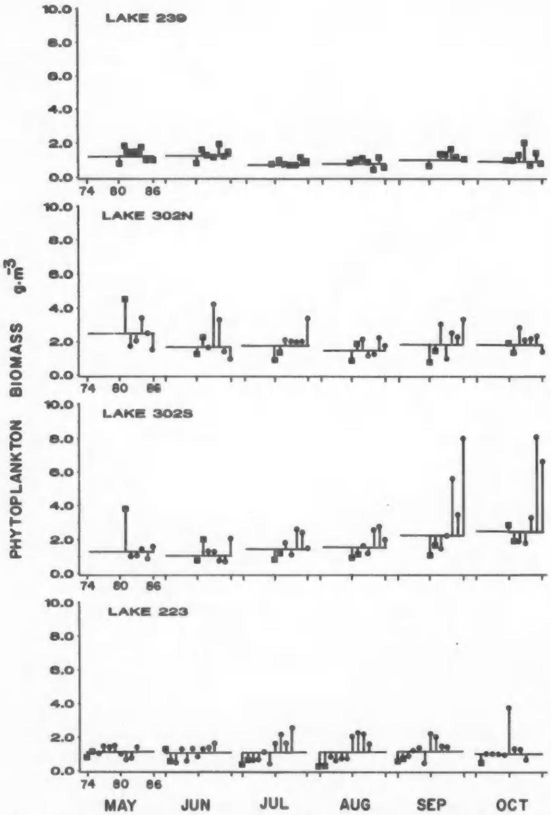

FIG. 1. Total epilimnetic mean monthly phytoplankton biomass for reference Lake 239 (1974–86). HNO_3-acidified Lake 302 North (1980–86), H_2SO_4-acidified Lake 302 South (1980–86), and H_2SO_4-acidified Lake 223 (1974–83). The horizontal lines are the long-term monthly midmeans (median of the values between the 25th and 75th percentiles). The solid dots indicate acidification years. The solid squares signify pre-acidification years.

Total epilimnetic phytoplankton biomass in the North Basin was not significantly altered by the nitric acid additions. Prior to and during acidification, biomass in the North Basin was higher than biomasses in the reference lakes due to elevated concentrations of phosphorus from the previous eutrophication experiment. During acidification, nitrogen concentrations increased 3× (Table 2). The species assemblages which developed were similar to those found in other nitrogen rich systems (Findlay and Kasian 1987).

Species Composition

Cyanophytes

The experimental and reference lakes had similar spring cyanophycean biomasses in all years, with maximums occurring in the warmer summer months (Fig. 3). In the South Basin cyanophycean biomass increased significantly in August and September 1985, at a pH level of 5.3, then disappeared below pH 5.3 (Fig. 3). A greater cyanophycean biomass increase occurred at pH levels below 5.3 in Lake 223. Cyanophytes increased in the North Basin after the first year of nitric acid additions. Subsequently, this group decreased as total nitrogen

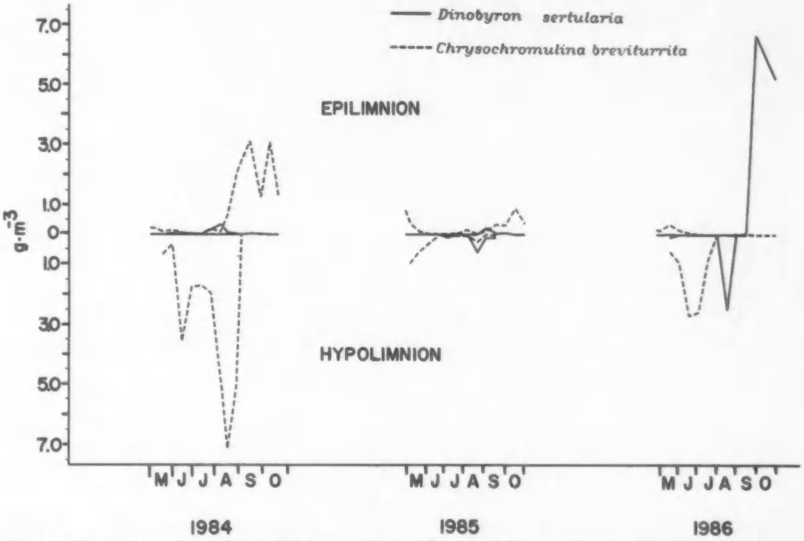

FIG. 2. Epilimnetic and hypolimnetic biomasses (g·m^{-3}) of *Dinobryon sertularia* Ehrenberg and *Chrysochromulina breviturrita* Nicholls in Lake 302 South (1984–86).

concentrations increased (Table 2) and pH decreased from 6.3 to below 6.0 (Fig. 3). During the same period (1982–86) cyanophycean abundance in Lake 239 (reference lake) remained stable. The seasonal cyanophycean pattern, indicated by the monthly midmean, for the North Basin differed from the sulfuric-acidified lakes and the reference lakes, by peaking in July instead of August (Fig. 3).

Chlorophytes

Chlorophycean biomass in the South Basin (Fig. 4), specifically *Gloeococcus Shroeterii* Lemmermann and *Oocystis submarina* var. *variabilis* Skuja, increased as pH decreased from 6.7 to 5.3. These increases occurred from June through October. Once the pH declined below 5.3 (1986), an immediate decline in chlorophycean abundance occurred. In contrast, chlorophytes in Lake 223 increased from May through July, particularly at pH levels below 5.6 (Fig. 4). In the North Basin, chlorophytes (*Scenedesmus denticulatus* Lagerheim and *S. brevispina* (G. M. Smith) Chodat) increased as nitrogen levels increased 3 × and pH decreased 0.5 units. Chlorophycean biomass in the North Basin was occasionally twice that of Lake 223 and the South Basin, and 5 × higher than the reference lakes (Fig. 4). The monthly midmean for the two basins of Lake 302, Lake 223, and the reference lakes show no particular seasonal pattern and increases attributed to experimental additions were not restricted to a specific season.

Chrysophytes

In the reference lakes and initially in the experimental lakes, chrysophytes were the predominant group. The population in the South Basin was affected to a greater degree than similar populations in the North Basin and Lake 223 (Fig. 5). Several significant episodic events occurred in the chrysophycean population in the South Basin but were not seen in the North Basin or Lake 223. At pH 5.6 (1984) a late summer bloom of *Chrysochromulina breviturrita* Nicholls occurred. This species dominated the hypolimnion during the summer months. In September it was entrained into the epilimnion during fall turnover (Fig. 2). Accompanying this bloom was a strong odor reminiscent of ''rotten cabbage''. This species and the odor have been documented in other acidified lakes (Nicholls et al. 1982). In October 1985, at a pH of 5.3, an epilimnetic bloom of the chrysophyte *Dinobryon bavaricum* Imhof occurred, constituting 7.1 g·m^{-3} of biomass (Fig. 5). This species was not prominent in the hypolimnion prior to the bloom. In September 1986 at a pH level of 5.0 *Dinobryon sertularia* Ehrenberg dominated the hypolimnion and its abundance in the epilimnion was associated with fall mixing (Fig. 2). Over the course of the nitric acid additions to the North Basin, the chrysophycean populations generally decreased both in biomass and percent contribution, particularly in mid-summer when cyanophytes and chlorophytes increased (Fig. 5). The seasonal patterns of chrysophytes in Lake 302 North and South differed from Lake 223 and the reference lakes which showed no obvious seasonal pattern. The North and South Basins had elevated spring and fall midmeans respectively.

Diatoms

Diatoms represented a small proportion of the total phytoplankton biomass in Lake 302 North and South and Lake 223, prior to acidification, in contrast to Lake 239 (Fig. 6). Populations declined even more during sulfuric and nitric acid additions. By pH 5.0 the diatom population in the South Basin had decreased to less than 0.02 g·m^{-3} (Fig. 6). This trend was also evident in Lake 223. The diatom community in the North Basin responded similarly to that in the South Basin. Diatoms diminished and eventually disappeared as pH decreased below 6.0. Although Lake 239 was unmanipulated, it too had a diminishing diatom population after 1982. Fluctuations of this magnitude have occurred previously in the long term records for this lake (unpubl. data). Although a portion of the decline in diatoms in the Lake 302 basins might be attributable to differences in climatic conditions in 1983–86, we observed a similar demise of the diatom community in acidified Lake 223, at the same pH, but 5 yr earlier. The seasonal patterns for Lakes 302 North

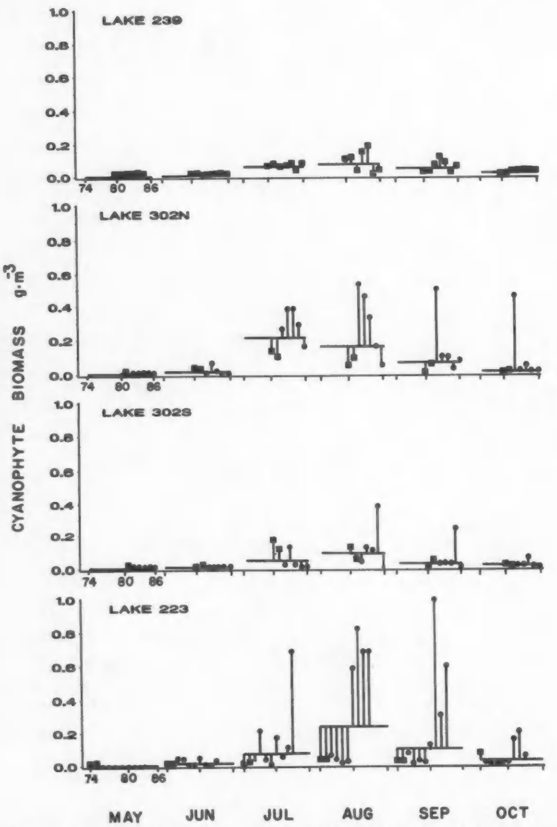

FIG. 3. Cyanophycean mean monthly biomass for reference Lake 239 (1974–86), HNO_3-acidified Lake 302 North (1980–86), H_2SO_4-acidified Lake 302 South (1980–86), and H_2SO_4-acidified Lake 223 (1974–83). The horizontal lines are the long-term monthly midmeans. The solid dots indicate acidification years. The solid squares signify pre-acidification years.

and South, 223, and 239 were unique (Fig. 6). In reference Lake 239 the maximum diatom biomass occurred in June, while in Lake 223 it occurred in May and October. The monthly midmean for the North Basin was elevated in spring and stable through the summer and fall months, while the monthly midmeans for the South Basin were stable throughout the year, except for a mid-summer depression.

Cryptophytes

Cryptophytes constituted a small proportion of the phytoplankton in Lakes 302 North, South, 223, and 239 (Fig. 7). Cryptophycean abundance in the South Basin was unaffected, except for increases occurring in September 1983 and 1984. The response of the cryptophytes in the North Basin differed from those observed in the sulfuric-acidified lakes and the reference lakes (Fig. 7). Increased cryptophytes in the North Basin occurred throughout the ice-free season. The seasonal midmean patterns for the South Basin, Lake 223, and Lake 239 were similar with slightly elevated cryptophycean abundance in spring and fall (Fig. 7). The seasonal pattern for the North Basin differed, having a large spring population.

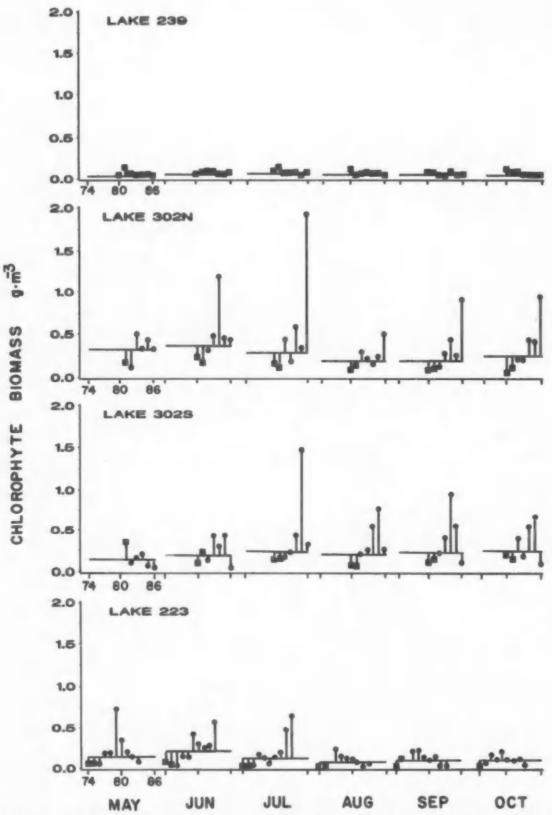

FIG. 4. Chlorophycean mean monthly biomass for reference Lake 239 (1974–86), HNO_3-acidified Lake 302 North (1980–86), H_2SO_4-acidified Lake 302 South (1980–86), and H_2SO_4-acidified Lake 223 (1974–83). The horizontal lines are the long-term monthly midmeans. The solid dots indicate acidification years. The solid squares signify pre-acidification years.

Dinoflagellates

Although the dinoflagellate population in Lake 302 North and South, and Lake 223 were dominated by the same species, the South Basin and Lake 223 displayed the most similar magnitude of response over the same pH. The dinophycean communities in the South Basin and Lake 223 increased as pH decreased (Fig. 8). During the same period, dinophycean abundance in Lake 239 increased three times as compared to a 20 × increase in the sulfuric-acidified lakes (Fig. 8). The North Basin exhibited large random fluctuations in summer and fall. Dinoflagellate biomass began to increase in the South Basin at pH 5.6 with *Gymnodinium* sp. and *Peridinium inconspicuum* Lemmerman. This increase continued as pH decreased to 5.0. Increases occurred mainly in June, September, and October. The seasonal pattern for the dinoflagellates in the experimental lakes and the reference lakes were comparable, with maximum populations occurring, on average, in the warmer summer months (Fig. 8).

Diversity

Phytoplankton species diversity in Lake 302 South and Lake 223 was strongly correlated with decreasing pH (r^2 = 0.82,

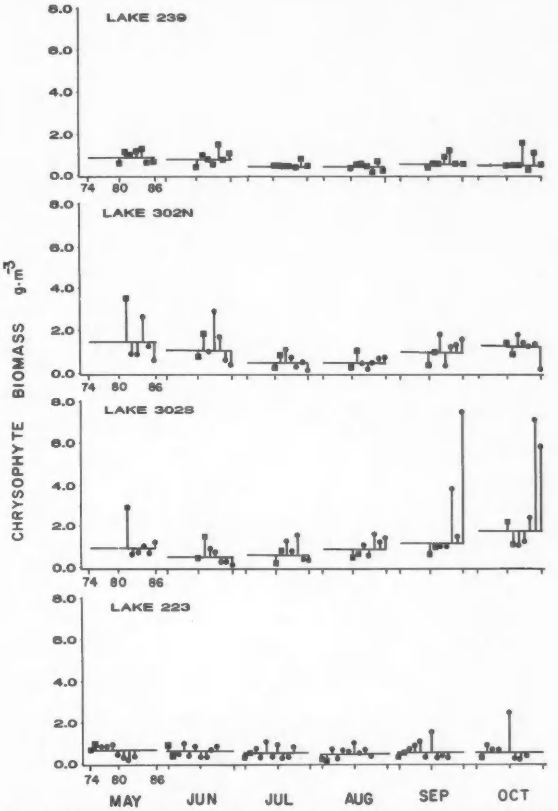

FIG. 5. Chrysophycean mean monthly biomass for reference Lake 239 (1974–86), HNO_3-acidified Lake 302 North (1980–86), H_2SO_4-acidified Lake 302 South (1980–86), and H_2SO_4-acidified Lake 223 (1974–83). The horizontal lines are the long-term monthly midmeans. The solid dots indicate acidification years. The solid squares signify pre-acidification years.

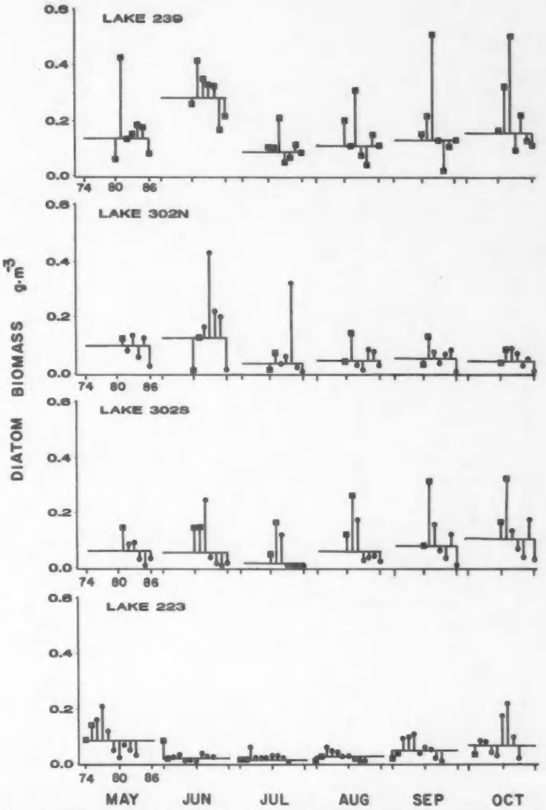

FIG. 6. Diatom mean monthly biomass for reference Lake 239 (1974–86), HNO_3-acidified Lake 302 North (1980–86), H_2SO_4-acidified Lake 302 South (1980–86), and H_2SO_4-acidified Lake 223 (1974–83). The horizontal lines are the long-term monthly midmeans. The solid dots indicate acidification years. The solid squares signify pre-acidification years.

$P = 0.0001$). There was no strong correlation with pH for the North Basin ($r^2 = 0.03$, $P = 0.708$). In the South Basin, species diversity decreased as pH decreased from 6.2 to 5.0. The decrease occurred in all months but was most pronounced in July (Fig. 9). Species diversity in the North Basin declined in June and July at pH values below 6.0. However, during the first year of nitric acid additions diversity decreased in August through October and then recovered in subsequent years. Species diversity in Lake 223 decreased at pH values below 5.6. In the reference lakes, species diversity fluctuated, but to a lesser degree than in the acidified lakes. The seasonal diversity patterns for the acidified lakes were similar to the reference lakes (Fig. 9).

Discussion

In the South Basin of Lake 302 total epilimnetic phytoplankton biomass increased slightly as pH decreased. Increased biomass is a direct response to acidification and is not due to experimental design (curtaining effect), increased nutrients, or entirely to weather conditions.

There was no obvious effect on the phytoplankton community following separation of the two basins. Prior to partitioning, both basins of Lake 302 were similar to the reference lakes in phytoplankton composition. However, both basins of Lake 302 sustained biomasses higher than the oligotrophic reference lakes and could be deemed slightly mesotrophic. Following the partitioning there was no evidence of increased biomass or changes in species composition (Figs. 1–8).

Some of the increase in phytoplankton biomass, as well as changes in species composition, were related to weather conditions. The South Basin of Lake 302 and the reference lakes are within a 10 km radius of each other and are therefore subjected to similar weather, although drainage characteristics of individual lakes differ. The pre-acidification phytoplankton community of the South Basin was initially similar to reference Lake 239 (and reference Lakes 222, 224, and 382; D. L. Findlay, unpubl. data). No increases in major nutrients were observed in the South Basin, except in 1984 and 1985 when phosphorus increased because of increased precipitation (Table 2). A similar increase in phosphorus was evident in the reference lakes. Epilimnetic biomass in the reference lakes fluctuated temporally, but increases equivalent in magnitude to those observed in the South Basin during acidification were not observed.

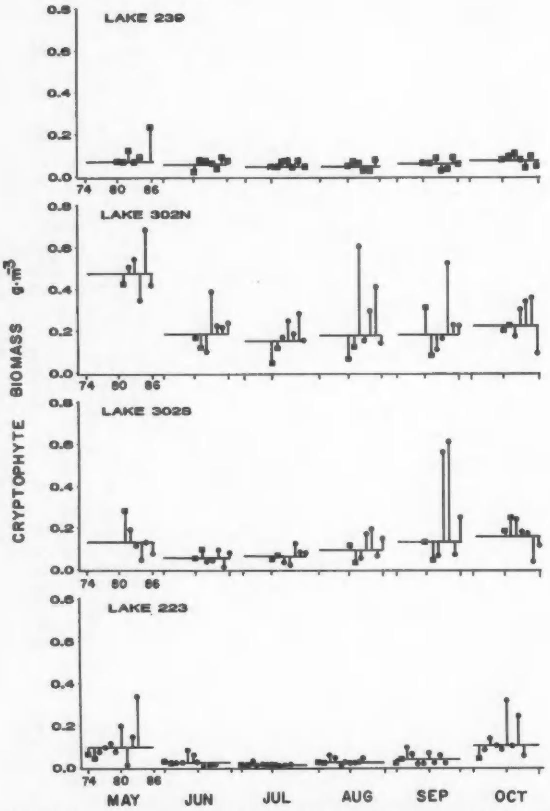

FIG. 7. Cryptophycean mean monthly biomass for reference Lake 239 (1974–86), HNO_3-acidified Lake 302 North (1980–86), H_2SO_4-acidified Lake 302 South (1980–86), and H_2SO_4-acidified Lake 223 (1974–83). The horizontal lines are the long-term monthly midmeans. The solid dots indicate acidification years. The solid squares signify pre-acidification years.

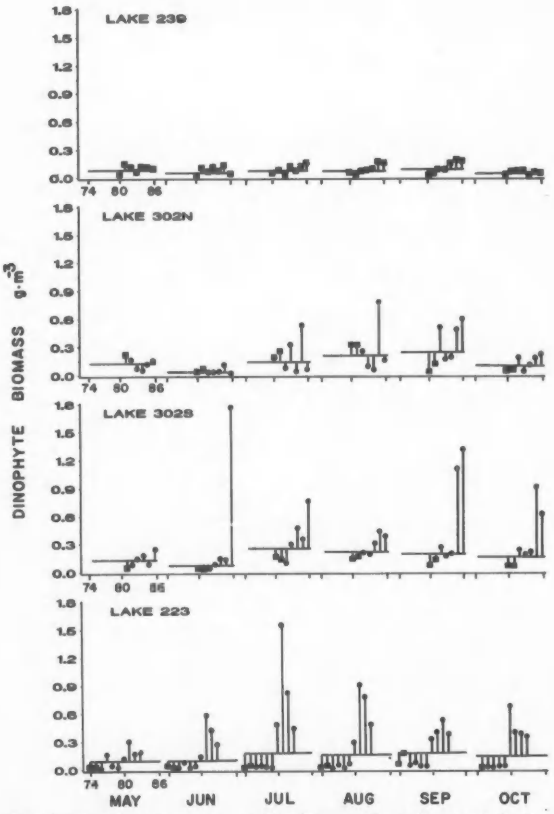

FIG. 8. Dinophycean mean monthly biomass for reference Lake 239 (1974–86), HNO_3-acidified Lake 302 North (1980–86), H_2SO_4-acidified Lake 302 South (1980–86), and H_2SO_4-acidified Lake 223 (1974–83). The horizontal lines are the long-term monthly midmeans. The solid dots indicate acidification years. The solid squares signify pre-acidification years.

Increased epilimnetic biomass in the South Basin, particularly after fall mixing, was due to entrainment of concentrated hypolimnetic blooms. Increased light transparency caused by leaching of organic material (Schindler et al. 1985; Shearer and DeBruyn 1986) at low pH's might be responsible for these exceptionally concentrated hypolimnetic blooms. Species of *Chrysochromulina breviturrita* (1984) and *Dinobryon sertularia* (1986) from the metalimnion or hypolimnion dominated these blooms (Fig. 2). Fee (1976) attributed the peaks he found in the 70's in Lake 302 South to optimal light conditions and high nutrient concentrations and O'Grady (1987), using cultures, concluded that light was a major factor in the growth of acidophilic *Chrysochromulina breviturrita*. We conclude that increased light penetration to the hypolimnion is a major factor in causing increased biomass in the South Basin of Lake 302.

Epilimnetic phytoplankton biomass in the North Basin of Lake 302 did not respond to additions of nitric acid. Biomass in this basin was slightly higher than in the South Basin because of higher phosphorus concentrations from the previous hypolimnetic eutrophication experiment (Table 2). As a result of the nitric acid additions nitrogen accumulated, but because lakes in this area are phosphorus deficient, the increased nitrogen had little effect on phytoplankton biomass.

Decreasing pH in the South Basin caused significant shifts in species composition. At pH 5.6, species composition began shifting from a chrysophycean dominated assemblage at circumneutral pH to a chlorophycean dominance at pH 5.3. Below pH 5.3, a dominant population of dinoflagellates and acidophilic chrysophycean species, such as *Chrysochromulina breviturrita*, was established. As well, diatoms and cyanophytes were eliminated from the assemblage below pH 5.3. The changes observed in phytoplankton species composition in the South Basin of Lake 302 were a direct result of acidifiction.

Changes in the phytoplankton species composition in the North Basin were more pronounced than those observed in the South Basin. Destabilization of the phytoplankton assemblage occurred immediately after HNO_3 additions commenced (1982). Nitrogen concentrations increased 1.7 × in the first year and 3.2 × over the duration of the additions with a decrease of only 0.5 pH units. Chrysophycean dominance decreased while cyanophytes, chlorophytes, and dinoflagellates increased. In contrast to Lake 302 South the dominant cyanophycean and chlorophycean species were *Scenedesmus denticulatus*, *S. brevispina*, *Oocystis submarina* var. *variabilis* (chlorophytes), and *Chroococcus limneticus* and *Synechoococcus* sp. (cyanophytes). These species are usually associated with

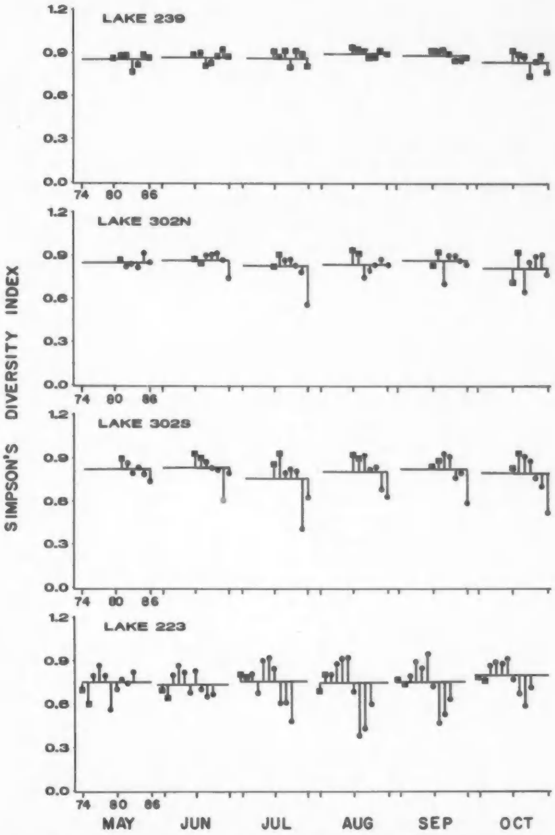

FIG. 9. Epilimnetic mean monthly species diversity for reference Lake 239 (1974–86), HNO_3-acidified Lake 302 North (1980–86), H_2SO_4-acidified Lake 302 South (1980–86), and H_2SO_4-acidified Lake 223 (1974–83). The horizontal lines are the long-term monthly midmeans. The solid dots indicate acidification years. The solid squares signify pre-acidification years.

increased nutrients, either nitrogen or nitrogen and phosphorus (Holmgren 1983; Findlay and Kasian 1987). In 1986 when pH decreased below 6.0, diatoms in the North Basin were eliminated, as in the South Basin at pH 5.3. This elimination of diatoms, coupled with decreased cyanophytes, increased dinoflagellates, and the shift in dominant chlorophytes, suggests that acidification was beginning to have an effect on the assemblage. A similar amount of H^+ added as HNO_3, in comparison to H_2SO_4, initially had a eutrophying affect on the phytoplankton composition of Lake 302 North. Only after 4 yr of acid additions did the pH finally decrease significantly.

Phytoplankton species diversity in the South Basin decreased as pH decreased. A similar decrease in species diversity occurred in the North Basin when pH declined below 6.0. The decline in species diversity in both basins was due to a decrease in species richness and an increase in abundance of a few acid tolerant species.

Acid additions to the South and North Basins of Lake 302 altered the seasonality of species composition and total phytoplankton biomass. In the South Basin prior to acidification chrysophytes predominated in spring and fall. As pH decreased, chrysophycean dominance shifted totally to the fall. In response to acidification chlorophytes and dinoflagellates increased in abundance in the summer and fall. In the North Basin chlorophytes became abundant in the early summer and the fall with no change in August. The occurrence and dominance of phytoplankton species vary temporally and it is therefore imperative to sample throughout the open-water season to understand responses of this community to acidification.

There were striking similarities between the responses of the phytoplankton communities to sulfuric acid additions in experimentally acidified Lake 223 and the South Basin, considering the different time periods of the two experiments, the trophic status of the two lakes, and the unique physical, chemical, and pre-acidification phytoplankton characteristics of each lake. Prior to acidification both lakes were dominated by chrysophytes. As pH decreased in the two lakes dominance shifted to the same major species of dinoflagellates. Decreasing pH caused the elimination of diatoms in both Lake 223 and 302 South between pH 5.6 and 5.3. Total annual phytoplankton biomass increased as pH decreased although the temporal distribution of the increases in the lakes was different. In Lake 223 biomass increased over the entire season, whereas in the South Basin the increase was mainly in the fall. Species diversity in both experimentally acidified lakes decreased as pH decreased. Overall the Lake 223 results were reproducible as shown by the Lake 302 South experiment.

The similarities of the phytoplankton community response to sulfuric acid additions in these two lakes are significant in relation to documented responses of phytoplankton communities in lakes anthropogenically acidified in other parts of Canada and Europe. Yan and Stokes (1978), Kwiatkowski and Roff (1976), Kollig and Hall (1982), and Almer et al. (1974) all documented decreasing species diversity, shifts in composition, and dominance by dinoflagellates as responses to decreasing pH. However, there is conflicting evidence for the relationship between total phytoplankton biomass and pH. Yan and Stokes (1978), Kollig and Hall (1982), and Hörnström et al. (1973) found no decrease in total biomass in experimental enclosures or Scandinavian lakes acidified by anthropogenic deposition. In contrast, Conroy et al. (1975) documented a decrease in biomass at low pH. From the Lake 223 and Lake 302 South experiment we conclude that a small to moderate increase in total biomass can be expected in small temperate lakes, at least down to pH 5.0.

The initial response of the North Basin phytoplankton community to nitric acid additions was different from lakes acidified by sulfuric acid, and in many respects resembled the response expected from eutrophied lakes. We expect that continued additions of nitric acid to the North Basin would decrease pH at an accelerated rate causing changes in the phytoplankton community similar to those in the sulfuric acidified lakes.

Since these two whole lake sulfuric acidification experiments elicit similar phytoplankton responses to lakes acidified by acid deposition, we can now predict changes which will occur in the early stages. In addition, on-going work on the controlled recovery of these lakes will allow us to characterize the responses of the phytoplankton communities and enable us to predict with confidence the expected recovery of lakes impacted by acid deposition.

Acknowledgements

E. DeBruyn and J. Shearer supplied us with phytoplankton samples in conjunction with their primary productivity program. G. Linsey and

M. Turner supplied pertinent chemical data. R. Lypka assisted with graphics programming. We appreciate the criticism provided by Dr. D. W. Schindler, Dr. K. Patalas, Dr. R. Hesslein, P. Campbell, and H. Kling during preparation of the manuscript. This work was supported by Department of Fisheries and Oceans Canada.

References

Almer, B., W. Dickson, C. Ekström, E. Hörnström, and U. Miller. 1974. Effects of acidification on Swedish lakes. Ambio 3: 30–36.

Almer, B., W. Dickson, C. Ekström, and E. Hörnström. 1978. Sulfur pollution and the aquatic ecosystem, p. 29–36. *In* J. Nriagu [ed.] Sulfur in the environment, Part 2. John Wiley and Sons, New York, NY.

Blouin, A. C., T. M. Collins, and J. J. Kerekes. 1984. Plankton of an acid stressed lake (Kejimkujik National Park, Nova Scotia, Canada). Part 2. Population dynamics of an enclosure experiment. Verh. Int. Ver. Limnol. 22: 401–405.

Conroy, N., K. Hawley, W. Keller, and C. Lafrance. 1975. Influences of the atmosphere on lakes in the Sudbury area. Atmospheric contribution to the chemistry of lake waters. J. Great Lakes Res. 2 (Suppl.): 146–165.

Cruikshank, D. R. 1984. Whole lake chemical additions in the Experimental Lakes Area, 1969–1983. Can. Data Rep. Fish. Aquat. Sci. 449: iv + 23 p.

1986. Whole lake chemical additions in the Experimental Lakes Area, 1984–1986. Can. Data Rep. Fish. Aquat. Sci. 580: iv + 10 p.

Dillon, P. J., N. D. Yan, N. A. Schneider, and N. Conroy. 1979. Acidic lakes in Ontario, Canada: characterization, extent and response to base and nutrient additions. Arch. Hydrobiol. Beih. Ergebn. Limnol. 13: 317–336.

Fee, E. J. 1976. The vertical and seasonal distribution of chlorophyll in lakes for the Experimental Lakes Area, northwestern Ontario: implications for primary production estimates. Limnol. Oceanogr. 21: 767–783.

Fee, E. J., J. A. Shearer, and D. R. Declercq. 1977. *In vivo* chlorophyll profiles from lakes in the Experimental Lakes Area, northwestern Ontario. Can. Fish. Mar. Serv. Tech. Rep. 703: vi + 136 p.

Findlay, D. L., and S. E. M. Kasian. 1986. Phytoplankton responses to acidification of Lake 223, Experimental Lakes Area, northwestern Ontario. Water Air Soil Pollut. 30: 719–726.

1987. Phytoplankton community responses to nutrient additions in Lake 226, Experimental Lakes Area, northwestern Ontario. Can. J. Fish. Aquat. Sci. 44 (Suppl. 1): 35–46.

Holmgren, S. 1983. Phytoplankton biomass and algal composition in natural, fertilized and polluted subartic lakes. Acta. Univ. Ups. Abstr. Uppsala Diss. Sci. 674: 125 p.

Hörnström, E., C. Ekström, U. Miller, and W. Dickson. 1973. Forsurningens inverkan da vastkustsioar. Information fran Sotvattens-Laboratoriet, Drottningholm. 4: 81 p.

Kollig, H. P., and T. L. Hall. 1982. The effects of acid perturbation on a controlled ecosystem. Water Air Soil Pollut. 17: 225–233.

Kwiatkowski, R. E., and J. C. Roff. 1976. Effects of acidity on the phytoplankton and primary productivity of selected northern Ontario lakes. Can. J. Bot. 54: 2546–2561.

Nauwerck, A. 1963. Die beziehungen zwischen zooplankton und phytoplankton in see Erken. Symb. Bot. Ups. 17(5): 163 p.

National Research Council of Canada. 1981. Acidification in the Canadian aquatic environment: scientific criteria for assessing the effects of acidic deposition on aquatic ecosystems. NRCC 18475.

Nicholls, K. H., J. L. Beaver, and R. H. Estabrook. 1982. Lake wide odors in Ontario and New Hampshire caused by *Chrysochromulina breviturrita* Nich. (Prymnesiophyceae). Hydrobiologia 96: 91–95.

Norwegian State Pollution Control Authority. 1987. 1000 lake survey 1986 Norway. Report 283/87, Norwegian Institute for Water Research, Oslo, Norway. 33 p.

O'Grady, K. A. 1987. Light, temperature and nitrogen interactions in two freshwater algae from lakes undergoing acidification. Ph.D. thesis, University of Western Ontario, London, Ont. 167 p.

Rudd, W. M., C. A. Kelly, D. W. Schindler, and M. A. Turner. 1990. A comparison of the acidification efficiencies of nitric and sulfuric acids by two whole-lake experiments. Limnol. Oceanogr. Vol. 35: 4. (In press).

Schindler, D. W., T. Ruszczynski, and E. J. Fee. 1980. Hypolimnion injection of nutrient effluents as a method for reducing eutrophication. Can. J. Fish. Aquat. Sci. 37: 320–327.

Schindler, D. W., K. H. Mills, D. F. Malley, D. L. Findlay, J. A. Shearer, I. J. Davies, M. A. Turner, G. A. Linsey, and D. R. Cruikshank. 1985. Long-term ecosystem stress: the effects of years of experimental acidification on a small lake. Science (Wash., DC) 228: 1395–1401.

Shearer, J. A. 1978. Two devices for obtaining water samples integrated over depth. Can. Fish. Mar. Serv. Tech. Rep. 772: iv + 9 p.

Shearer, J. A., and E. R. DeBruyn. 1986. Phytoplankton productivity responses to direct additions of sulfuric and nitric acids to the waters of a double-basin lake. Water Air Soil Pollut. 30: 695–702.

Stainton, M. P., M. J. Capel, and F. A. J. Armstrong. 1977. The chemical analysis of freshwater. 2nd ed. Can. Fish. Mar. Serv. Spec. Publ. 25: 180 p.

Vollenweider, R. A. 1968. Scientific fundamentals of the eutrophication of lakes and flowing waters, with particular reference to nitrogen and phosphorus as factors in eutrophication. Tech. Rep. O.E.C.D. Paris Das/CSI/68.27: 1–182.

Washington, H. G. 1984. Review: diversity, biotic and similarity indices. A review with special relevance to aquatic ecosystems. Water Res. 186: 653–694.

Yan N. E., and P. Stokes. 1978. Phytoplankton of an acidic lake, and its responses to experimental alteration of pH. Environ. Conserv. 5: 93–100.

Response of a Brook Trout (*Salvelinus fontinalis*) Population to a Reduction in Stream Benthos Following an Insecticide Treatment

D. P. Kreutzweiser

Forestry Canada, Forest Pest Management Institute, Box 490, Sault Ste. Marie, Ont. P6A 5M7 Canada.

Kreutzweiser, D. P. 1990. Response of a brook trout (*Salvelinus fontinalis*) population to a reduction in stream benthos following an insecticide treatment. Can. J. Fish. Aquat. Sci. 47: 1387–1401.

A forest stream was treated with permethrin to determine the response of brook trout to a reduction in the aquatic food resource following an insecticide treatment. The treatment resulted in massive invertebrate drift and significant reductions of benthos, but did not produce trout mortality or evidence of unusual behaviour. The density, population age structure, movement patterns, and condition of brook trout were not measurably affected by the permethrin treatment. The growth rates of 0+ and 1+ age-classes were significantly lower following the insecticide application than those of trout from the same age-classes of pretreatment years. This reduction in growth rate resulted in significantly smaller trout after treatment. A significant reduction in the growth of trout collected during the same period from a nearby untreated control stream indicated that unusually high summer temperatures were at least partially, if not entirely, responsible for the reduced growth rate of treated fish. Growth rates returned to or exceeded pretreatment levels by the overwinter period of the treatment year.

Un cours d'eau en forêt a été traité au perméthrine afin de déterminer la réaction de l'omble de fontaine à une réduction des ressources alimentaires aquatiques après l'application d'insecticide. Le traitement s'est soldé par une dérive massive d'invertébrés et par une réduction importante du benthos, mais n'a pas provoqué la mort de l'omble ou des comportements inhabituels. La densité, la structure de la population en fonction de l'âge, les modes de déplacement et l'état de l'omble de fontaine n'ont pas été touchés de façon mesurable par l'application de perméthrine. Le taux de croissance des classes d'âge 0+ et 1+ était significativement plus faible après l'application de l'insecticide que celui d'ombles de mêmes classes d'âge au cours des années qui ont précédé le traitement. Cette baisse du taux de croissance s'est traduite par des ombles beaucoup plus petites après l'application d'insecticide. Une diminution de la croissance des ombles prélevées pendant la même période dans un cours d'eau voisin témoin et non traité a montré que des températures estivales anormalement élevées étaient en partie responsables du moins, si non entièrement, de l'abaissement du taux de croissance des poissons exposés à l'insecticide. Les taux de croissance sont revenus au taux mesuré avant le traitement ou l'on dépassé avant la fin de la période hivernale de l'année au cours de laquelle le traitement a été appliqué.

Received March 28, 1989
Accepted February 8, 1990
(JA109)

Reçu le 28 mars 1989
Accepté le 8 février 1990

Widescale use of organochlorine insecticides in the 1950s and 1960s, including DDT and related products, to control forest insect pests commonly resulted in severe stream benthos depletions and extensive fish kills (Kerswill 1967). Because of the severe impact on fisheries and other wildlife resources, the spraying of organochlorines was discontinued by the early 1970s. Since then, environmental impact assessments of forest insecticide applications have demonstrated that currently registered insecticides, used under operational conditions in Canadian forests, do not pose a risk of acute toxicity to fish (Kingsbury 1984; Eidt et al. 1989). Some registered and candidate pesticides may cause reductions in benthos (Norris et al. 1983; Muirhead–Thomson 1987; Kreutzweiser and Kingsbury 1987), and therefore may cause secondary effects on fish populations by depleting the aquatic food resource. A few impact studies have indicated secondary effects of insecticide contamination on stream salmonids. These include emigration (Symons and Harding 1974), temporary reductions in growth rate (Sosiak 1983), and alterations in diet composition (Kingsbury and Kreutzweiser 1987), but these assessments were short-term and often poorly quantified.

With limited information available on the effects on stream fish of benthos reductions from insecticide impact, Canadian regulatory agencies have adopted a conservative approach to the registration and use of forest insecticides. During hazard evaluation of candidate pesticides, toxicity to aquatic invertebrates has been construed as detrimental to a fish population because of potential reduction in food availability. Although insecticide impact on invertebrate communities may in itself be ecologically significant, the extent to which insecticide-induced changes in food availability affect fish populations has been identified as an important question in hazard evaluation (Fairchild et al. 1989). However, the significance of benthos abundance to the density and growth of stream salmonids has not been clearly established. Symons (1971) and Elliott (1984) found that food availability was rarely a limiting factor in salmonid density, at least in the short-term. Allan (1982) and Reice and Edwards (1986) indicated that trout density in streams was not food-limited because trout predation had no regulatory effect on the benthic community. Conversely, Murphy et al. (1981), and Wilzbach et al. (1986) found that trout density and growth were positively correlated to aquatic invertebrate abundance. Despite this uncertainty, the toxicity of forest pesticides to aquatic invertebrates and the potential for secondary effects on stream fish continue to limit the registration and use of pest control products. While this approach maximizes the protection of fisheries resources, it greatly reduces the options available to forest managers for pest control.

In this study a section of stream in Ontario was treated with permethrin, a synthetic pyrethroid, to measure the response of a brook trout (*Salvelinus fontinalis*) population to an insecticide impact on benthos. The objectives of the project included: (1) assessment of the pretreatment population dynamics of brook trout in the study area; (2) treatment of the stream with a forest insecticide at a concentration sufficient to cause a disturbance of benthos without a risk of acute toxicity to fish; (3) determination of the impact of the insecticide on the composition and abundance of benthos; and (4) investigation of the effects of benthos reduction on brook trout density, movement, population age structure, growth, and production.

This experiment was not designed to simulate an aerial application of permethrin. Because the overall objective was to measure the secondary effects on trout of benthos reductions from insecticide impact, this was intentionally a high-dosage application. The insecticide concentrations and resulting impact on invertebrates were deliberately aimed at exceeding the levels normally encountered after aerial forest spraying. Insecticide concentrations from a point source, or pulse application method used in this study follow the time course of insecticide residues in streams after aerial spraying. Insecticide from inadvertent overspray, off-target aerial drift, or from runoff will enter streams over a short period of time and result in transient peak concentrations, followed by continual dissipation from dilution, degradation, or adsorption of the pesticide (Norris et al. 1983; Muirhead–Thomson 1987). Permethrin is not registered for use in aerial spraying of Canadian forests, but was selected because of previous experience and data from aquatic impact assessments of this material (Kingsbury and Kreutzweiser 1987; Kreutzweiser and Kingsbury 1987), because of current interest in permethrin as a potential forest pest control product (Helson et al. 1989), and because the high toxicity of permethrin to aquatic invertebrates (NRCC 1986) ensured a substantial disturbance of the stream invertebrate community. The results of a concomitant study of the fate and persistence of residual permethrin in the stream are presented elsewhere (Sundaram 1990).

Site Description

Icewater Creek is a third order cold-water stream in the Lake Superior watershed approximately 50 km north of Sault Ste. Marie, Ontario. The accessible 12-km portion of the creek flows through a steep-sided valley of mixed hardwoods, white spruce (*Picea glauca*), balsam fir (*Abies balsamea*), and speckled alder (*Alnus rugosa*), into the Goulais River. The brook trout population assessment was restricted to the upper reaches of Icewater Creek (9 km upstream from its junction with the Goulais River), where four discrete study sections were established: Crossover, West Branch, East Branch, and West Trib (Fig. 1). A fifth study section (East Trib) was used as an untreated control area for the measurement of trout growth. A site approximately 300 m above the injection point on East Branch was used as a control site for the benthos study.

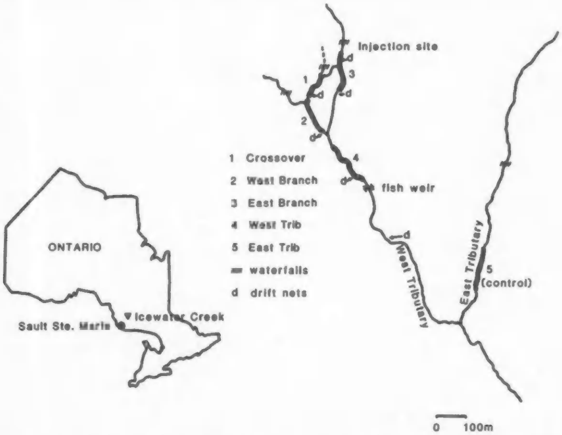

FIG. 1. Location and detail of Icewater Creek. Study sections shown in heavy black lines.

The stream is subject to extreme seasonal flow variations and environmental conditions. Most areas are completely ice and snow covered from December to the end of March, then flooded by meltwater runoff from the surrounding hills for about one month. Although early summer flash floods induced by heavy rainfall are common, water levels decline through June and July, and reach an annual low by August. Water level reductions of 70% can occur between spring runoff and early August. Riparian foliage is developed by mid-June and leaf fall occurs by mid-October. Mid-day water temperatures from May to November usually range from 6 to 20°C with extremes of 0–25°C. Dissolved oxygen remains at or near saturation, pH ranges from 6.3 to 7.0, hardness from 20 to 30 $mg\cdot L^{-1}$ $CaCO_3$, and conductivity from 19.6 to 28.1 micro $ohms\cdot cm^{-1}$. Water quality parameters were measured using a Hach kit model DR-EL/2. The average gradient through the study sections is $2.8\ m\cdot 100\ m^{-1}$. The stream bottom in the study area is approximately 50% boulder or bedrock, 30% rubble, and 20% gravel. Average widths of the study sections range from 2.8 to 7.2 m. Brook trout is the predominant fish species present, but other species occur in some sections, including blacknose dace (*Rhinichthys atratulus*), common shiner (*Notropis cornutus*), longnose dace (*Rhinichthys cataractae*), and white sucker (*Catostomus commersoni*).

Methods

Insecticide Treatment

Permethrin was injected into the stream as 50% Ambush Emulsifiable Concentrate (EC) at 0930 h on 3 June 1987. The emulsion contained 0.26% Ambush EC, 1.8% Rhodamine WT dye, and 97.94% distilled water. It was dripped into the stream at the top of a 6-m waterfall on the East Branch (Fig. 1), from a Mariott bottle calibrated to deliver 85 $mL\cdot min^{-1}$ for 15 min. This delivery rate was calculated to produce a permethrin concentration of approximately 16 $\mu g\cdot L^{-1}$ immediately below the injection site and to maintain a concentration of about 1 $\mu g\cdot L^{-1}$ for 1 h in the lower section of East Branch. These estimates of delivery rate and insecticide persistence were derived from previous injections of Rhodamine WT dye under similar stream flow conditions.

Benthic Invertebrate Sampling

The density of drifting stream invertebrates was measured to determine the initial response of benthos to the permethrin injection. Drift net locations were established at 30, 120, 220, 370, 400, 730, 1200, and 1900 m downstream from the injection point (Fig. 1). Drifting invertebrates were collected in 0.47 × 0.32 m rectangular opening nets (363 μm mesh) positioned midstream to sample from the surface to the stream bottom. Samples were collected for 5–10 min each hour from 1900 to 2400 h in the evenings of 1, 2, 3, and 4 June, immediately before and after the insecticide injection on 3 June, and every hour throughout the day of treatment. Drift samples were also collected near the mouth of East Trib to provide control data for drift density over the 4 d.

Benthos density in the treated area was measured by a standardized travelling kick method. This is a quantitative method of estimating benthos density and composition (Pollard 1981), and was used to determine post-treatment changes in the benthic invertebrate community. Six kick samples were obtained from each of the four study sections at 6 wk intervals between May and November of 1986 (pretreatment) and 1987 (post-treatment). Benthos density also was estimated from colonization of artificial substrates placed at the bottom of the East Branch study section and at the top of the West Trib section (Fig. 1). The substrates comprised 0.5 kg of 25 mm crushed rock wrapped in 8 mm mesh nylon netting, and were placed in groups of nine on the stream bottom at each location. These were collected and replaced at 6 wk intervals from May to November of 1986 and 1987. Benthos densities were also estimated by the kick method and colonization on artificial substrates at the control site in East Branch approximately 300 m above the injection site. Abundance data were analyzed at the order and family level using paired *t*-tests for repeated sampling. Changes in abundance of invertebrates between pretreatment and post-treatment samples at treated sites were compared with similar data from the corresponding months at the control site. All invertebrate samples were log transformed and tested for homogeneity of variance using an *F*-ratio (Elliott 1983).

Brook trout were not sacrificed for food habit analysis. However, other studies have shown that brook trout larger than 25 mm rely heavily on aquatic invertebrate groups such as Ephemeroptera, Plecoptera, Trichoptera, and Diptera as food sources (Ricker 1930). This dependence changes seasonally (Allan 1981) and in response to insecticide impact. Feeding habits of brook trout in streams aerially sprayed with permethrin have shifted from a pretreatment reliance on aquatic insects to almost exclusively terrestrial arthropods after the applications (Kreutzweiser and Kingsbury 1982; Kingsbury and Kreutzweiser 1987).

Experimental Design and Statistical Analysis of Brook Trout Response

Treatment effects on most parameters were determined by comparison to temporal controls. The experimental design included 3 yr pretreatment data and 1 yr post-treatment. Differences in parameters over the 4 yr were tested statistically, thus the pretreatment years functioned as temporal controls. A spatial control (East Trib) was originally included in the design, but low recapture rates (often $n < 4$ in each sampling interval and age-class) and variable density in the control precluded the use of these fish for all but measurements of mean length. Significant differences between pretreatment and post-treatment data were considered strong, although not definitive, indications of treatment effects.

Data analyses were performed on a Digital Vax 8500 computer using BMDP statistics software (Dixon 1983). Mean values were tested for significant differences at $P<0.05$ using one-way analysis of variance (ANOVA). All data sets were subjected to Levene's *F*-test (Levene 1960) for homogeneity of variance. No data transformations were performed because at least 90% of the data sets satisfied Leven's test for homogeneity of variance, and the data were considered normally distributed. When the general *F*-test (ANOVA) was significant, pairwise *t*-tests with the Bonferroni significance level for multiple comparisons (Jones 1984) were applied to determine significant differences. Differences among group means (for example, among mean lengths of an age-class over 4 yr) were considered significant at experimentwise a(alpha) = 0.05, and reported as $P<0.05$. Differences in proportional data were tested with a *G*-test of independence or chi-square, with significance at $P<0.05$. Equality of slopes in linear regressions were tested with analysis of covariance (ANCOVA) at the 5% significance level. When the ANCOVA test for parallelism was significant, a stepwise regression using dummy variables (Gujarati 1970) was used to test for differences among slopes or intercepts of linear regressions, with significance at $P<0.05$.

Fish Collection and Handling

Brook trout were sampled four times each year: spring (mid-May), early summer (late June), late summer (early August), and fall (early October), from 1984 to 1987. The trout were captured with a Smith–Root Model 12 backpack electroshocker and dip nets. Fish were anesthetized with a 3–5% solution of *t*.-amyl alcohol in stream water, weighed, measurements on fork length obtained, adipose fin-clipped, and if greater than 70 mm in length, hot branded (Groves and Novotny 1965) with a specific combination of symbols. The brands, constructed of copper and brass letter symbols mounted on wooden dowels, were heated in boiling water and applied lightly to the caudal peduncle region of the fish. All trout were returned to the stream within 25 m of their original capture site.

Trout Density

Trout were collected from within and around the study sections at each sample time for determination of age, movement, and growth, but trout density was estimated only within the discrete study sections (Fig. 1). Three to five successive electroshocker passes through the study sections (in a downstream direction) were used to collect the trout. Trout densities were estimated by a computer program based on the mean weighted likelihood estimation model of Carle and Strub (1978) and expressed as estimated number per section. Drastically fluctuating water levels precluded the use of stream volume or area as a unit of quantification. The electroshocker was inefficient in capturing young-of-the-year (0+) trout in the spring and early summer sample times and they were excluded from density estimates until the late summer period.

Trout Movement

Trout dispersion within the study area was determined by recording the capture and recapture location of marked individuals. Movement data were summarized for fish caught and recaptured within each of three periods: October to May (overwinter), May to August (spring/summer), and August to October (fall). Distance (to nearest 25 m) and direction moved were determined for each fish. Recapture intervals differed with individuals but were never less than 5 d. Upstream movement is blocked by a large waterfall at the injection point and restricted by a smaller waterfall on a first order tributary of West Branch (Fig. 1). A fish weir installed 50 m below the West Trib section (Fig. 1) in May 1987 provided data on fish movement in and out of the study area for the 1987 season.

Population Age Structure

Seasonal trends in age structure of the trout population were established by calculating percent contribution of each age-class for the total catch at each sample time. Length frequency distributions of known-age fish were used to estimate the age of other fish. The 1 + age-class was readily identified by size distribution in spring samples and 0 + (young-of-the-year) trout were easily classified in the fall. These fish were marked, and their subsequent recapture provided a size distribution of known-age fish of 0 + , 1 + , and 2 + age-classes. For each age, the mean length ± one standard deviation provided upper and lower length limits for assigning ages to the remaining fish. Trout with lengths greater than the upper limit of the 2 + age-class were grouped into 3 + + . The size distributions of known-age fish were updated each year.

Attempts at reading trout scales and otoliths were unsuccessful. Annuli were indistinguishable on scales, probably because of their small size (over 70% of the trout caught in any sampling period were less than 140 mm in length). Several projection devices were used to read scales but annuli could not be separated with any degree of certainty. Otoliths were extracted from a number of trout, but were also obscure because of their small size.

Designation of age-classes based on the size frequency of known-age fish may have introduced some bias or error. Inaccuracies in age determination could affect estimates of growth parameters based on age-groupings. However, the frequency and influence of such error was likely minimal. The age-group size limits of one standard deviation about the mean length of known-age fish did not result in overlap between age classes at any of the sample times. At least 80% of the trout from each sample time (and in many cases, 100%) fitted well within the size limits of an age-group, and the others were assigned ages based on their weight, length, or in the case of recaptures, their previous age designation. Where assigned ages were a year less or greater than the actual ages, the errors should have cancelled each other and had little combined effect. This approach to age determination was considered less prone to error than aging from scale annuli. LeCren (1974) states that more inaccuracies in the estimation of growth parameters are caused by errors in estimates of abundance than by errors in aging. It is unlikely that confirmation by scale reading would change any interpretation of results.

Growth

Growth estimates were obtained from recaptured individual fish (true growth rates) and from the mean length of captured fish at each sample time. Mean lengths were estimated for each age-group at each sample time (spring, early summer, late summer, and fall), and included both recaptured and new trout. Growth estimates from recaptured individuals were considered better measures of trout growth because the influences of migration or mortality were eliminated, and because the recaptures provided replicates of growth estimates at each sample time. Therefore, greater emphasis was placed on the assessment of growth of recaptured trout, although in some cases the low numbers of recaptures precluded statistical analysis of individual growth rates. Recaptured trout provided estimates for three recapture periods: October–May (overwinter), May–August (spring/summer), and August–October (fall). The overwinter periods are identified by the year in which the period ended, thus October–May 1985 refers to the period of October 1984–May 1985. The recapture interval was the same (within 10 d) for all fish in each period.

To provide sufficient sample sizes for statistical analysis, trout from all four treated areas were combined for growth estimates. Growth estimates for recaptured individuals included fish captured in and between the four study sections, and downstream for 300 m below the West Trib study section. Because of the inefficiency of the electroshocker in capturing young-of-the-year early in the season, growth measurements of 0 + trout were restricted to the late summer and fall samples.

Proportion of recaptured trout showing no growth — In most of the sampling periods some of the recaptured trout did not show measurable growth in length or weight. To determine if the insecticide treatment increased the number of trout that did not grow during a given period, the proportion of trout that exhibited zero growth was calculated for each recapture period and tested for differences among the 4 yr.

Daily growth rate of recaptured trout — The growth ($\mathrm{mm \cdot d^{-1}}$) of trout was calculated as

$$A = (L_j - L_i)/n$$

where A is daily growth rate, L is fork length (mm) of the fish at the beginning (i) and end (j) of the recapture period, and n is the number of days in the recapture period.

Instantaneous growth of recaptured trout — Instantaneous growth rates of recaptured fish were calculated as

$$G = (\ln W_j - \ln W_i)/n$$

where G is daily instantaneous growth rate, W is weight (g) of the fish at the beginning (i) and end (j) of the recapture period, and n is the number of days in the recapture period. The growth rates were multiplied by 10^4 to facilitate presentation of results.

Condition — The condition of the trout collected in the study sections at each sample time was determined by comparing the weights of fish of a given length using the linear relationship

$$\ln W = a + b \ln L$$

where W is weight (g) and L is length (mm) of the fish. A loss of condition was indicated by a decrease in the slope of the regression over most of the range of lengths or a decline in the elevation (intercept) of the regression line resulting from smaller weights for a given length.

Length — Differences among years in the mean lengths (mm) of each age-class of trout collected at the four sample times were tested with ANOVA and multiple comparisons tests. This provided an assessment of the effects of a reduction in growth rate on the size of trout in a given year-class.

Annual biomass and production — The mean annual biomass and annual production of brook trout from the combined treated sections were estimated for the period of May–May of succeeding years. Estimates were computed from a program developed by Garman and Waters (1983) to estimate annual production of stream fish using a size–frequency method. This method does not require cohort separation or aging, but is based on the annual summation of individual losses from one size group to the next. This was calculated from the density and size data from five sample times of each year (spring, early summer, late summer, fall, and following spring). Statistical differences in annual production estimates were determined from the overlap of 95% confidence intervals (Newman and Martin 1983). Biomass and production estimates are given in total kilograms produced in the combined treated sections. These were not converted to areal units because fluctuating water levels precluded the use of area measurements as meaningful quantifiers of trout density, and because comparisons were made among years in the same area, not among sections or streams. A single area measurement taken at "normal summer" water levels in 1986 was used to convert annual production estimates to areal units for a general comparison to other trout streams. Because concomitant area measurements were not taken with density estimates, the variance and 95% confidence intervals of production estimates could not be converted to areal units.

Results

Aquatic Invertebrates

The effects of the permethrin treatment on invertebrate drift and benthos abundance were determined in cooperation with P. K. Sibley, University of Guelph, Ontario. This work comprised part of the research for a masters thesis and is reported elsewhere (Sibley et al. 1990). Only a general summary of results is presented here. Following the insecticide injection, massive increases in the number of drifting invertebrates occurred at each site as the contaminated water reached the sampling stations. Drift increases were most pronounced in the East Branch and West Trib sections where total invertebrate drift densities ($n \cdot m^{-3}$) increased by 2 500 times the pretreatment levels, and where some groups (especially Leuctridae) increased by 20 000 times. Increases in drift were considerably smaller in the lower West Trib, Crossover, and West Branch sites, where insecticide concentrations were lower, but were still 1 000, 300, and 100 times pretreatment drift densities, respectively. Drift levels declined sharply within several hours of the application, but remained at elevated levels (up to about ten-fold) at some sites for greater than 15 h. By 36 h post-treatment, drift rates had resumed normal levels. The post-treatment invertebrate drift primarily consisted of *Leuctra tenuis, Taeniopteryx nivalis* (Plecoptera), *Baetis flavistriga, Heptagenia flavescens, Epeorus* sp. (Ephemeroptera), and *Dolophilodes distinctus* (Trichoptera). Drift rates in the control stream remained near zero during the treatment day and exhibited normal diurnal increases at dusk.

The abundance of Ephemeroptera, Plecoptera, and Trichoptera in benthos samples and artificial substrates was significantly reduced ($P<0.05$) in East Branch and West Trib following the insecticide treatment (Table 1). The insecticide impact on invertebrates in Crossover and West Branch was less pronounced, with measurable reductions (60%) only in Trichoptera abundance. By 50 d post-treatment, numbers of some taxa in East Branch and West Trib were still depressed, but with the exception of Ephemeroptera in artificial substrates, there were no significant differences between the treated and control sites (Table 1). Recovery of benthos appeared to be largely accomplished by recruitment from eggs hatching and oviposition. Samples from 50 d post-treatment and later contained substantial numbers of early instar invertebrates. Significant recolonization by invertebrate drift from upstream was unlikely. The insecticide was injected in a 6-m waterfall (one of three waterfalls in succession) which likely functioned as a barrier to invertebrate drift. Drift samples collected 2 d before the treatment 10 m below the lower falls contained several times fewer organisms than concurrent samples from further downstream (unpubl. data). Although the insecticide injection did not deplete benthos at all sites and the reductions did not persist beyond 50 d, the impact of this treatment on stream benthos was much greater than is encountered during aerial spraying of insecticides in Canadian forests (Kingsbury 1984; Kreutzweiser and Kingsbury 1987).

Trout Density

The permethrin treatment did not result in measurable reductions of brook trout numbers. In three of the four study sections, trout density in post-treatment periods (early summer to fall 1987) was comparable to or greater than density estimates for

TABLE 1. Total abundance of invertebrates in pre- and post-treatment samples from two treated sites and control. A = artificial substrates, B = benthos samples, C = East Trib (control), EB = East Branch (treated), WT = West Trib (treated), a = significantly different ($P<0.05$) from changes in control, b = not significantly different from changes in control.

Taxa	Sample type	20 d pre-			12 d post-			50 d post-		
		C	EB	WT	C	EB	WT	C	EB	WT
Ephemeroptera	B	121	106	289	950	63[a]	122[a]	1047	485[b]	681[b]
	A	134	142	188	120	16[a]	43[a]	134	26[a]	120[b]
Plecoptera	B	923	891	1088	318	121[a]	452[a]	208	152[b]	174[b]
	A	297	189	251	195	34[a]	55[a]	61	14[b]	49[b]
Trichoptera	B	50	75	93	881	23[a]	35[a]	478	175[b]	332[b]
	A	80	331	181	146	24[b]	4[a]	512	245[b]	306[b]
Diptera	B	1042	799	1092	1753	452[b]	2732[b]	847	1395[b]	1456[b]
	A	640	1205	1196	751	821[b]	1317[b]	640	1470[b]	2163[b]

[a] Adapted from Sibley et al. 1990.

TABLE 2. Density estimates (fish per section) and 95% C.I. (in parentheses) of brook trout in the four treated sections of Icewater Creek. Abundance of young-of-the-year (0+) trout not included in density estimates until late summer. Insecticide treatment occurred between spring and early summer (3 June) of 1987. Pre = pre-treatment estimate, post = post-treatment estimate.

	Spring				Early summer				Late summer				Spring			
	1984 pre	1985 pre	1986 pre	1987 pre	1984 pre	1985 pre	1986 pre	1987 post	1984 pre	1985 pre	1986 pre	1987 post	1984 pre	1985 pre	1986 pre	1987 post
Crossover 120m	23 (21–30)	32 (32–35)	18 (18–19)	19 (19–21)	20 (20–22)	12 (12–13)	15 (13–23)	24 (24–25)	15 (14–20)	33 (33–35)	5 (5–6)	39 (39–41)	18 (18–20)	18 (18–19)	16 (16–18)	35 (35–36)
West Branch 150m	23 (16–46)	25 (25–26)	26 (26–28)	19 (19–21)	36 (32–45)	27 (27–30)	22 (22–25)	39 (38–43)	17 (17–18)	82 (78–88)	26 (26–27)	93 (88–101)	23 (23–25)	36 (36–38)	24 (24–27)	38 (38–41)
East Branch 100m	32 (30–38)	45 (41–43)	38 (38–41)	26 (25–30)	46 (43–53)	32 (32–34)	43 (42–47)	34 (32–40)	37 (36–41)	43 (43–45)	42 (42–44)	25 (25–28)	54 (48–65)	32 (30–38)	16 (16–19)	36 (36–39)
West Trib 150m	28 (28–30)	18 (18–20)	35 (30–46)	34 (32–40)	34 (32–40)	24 (24–26)	42 (41–46)	35 (35–37)	34 (33–38)	71 (69–76)	55 (52–61)	72 (69–78)	38 (37–42)	17 (17–20)	28 (28–30)	35 (35–37)

the same periods in previous years (Table 2). The only instance in which the post-treatment density was lower was in East Branch during the later summer period. Because the early summer and fall density estimates of 1987 were within the range of previous years, and because the spring estimate indicated some natural decline in numbers of brook trout in East Branch, it is unlikely that the late summer density reduction resulted from the permethrin contamination. Unusually low water levels in East Branch during late summer 1987 probably contributed to the decline in numbers of trout. Ten marked trout from East Branch were found in a deep pool several metres outside the sampling area (at the base of the waterfall) on the day of the late summer 1987 sample, indicating that these fish had moved out of the East Branch fishing area to deeper water and were therefore not included in the density estimate. Trout density in East Branch returned to normal by fall, and was within the range of pretreatment values ($n = 33$, 95% C.I. = 33–35) in the spring 1988 sample.

The lack of effects on brook trout density concurs with observations that the permethrin injection did not cause fish mortality. Fish mortality in the stream was not assessed systematically, but intensive sampling activity in and around the treated areas for several days following the application did not produce any observations or evidence of dead fish. There were no observations of trout exhibiting unusual behaviour such as lethargy, surfacing, coughing, or inability to maintain position. Brook trout held in cages in the treated area from 2 d before to 2 d after the treatment also showed no evidence of unusual behaviour. Trout mortality was not expected to result from this treatment. The 24 h LC_{50} of permethrin to brook trout is 72 $\mu g \cdot L^{-1}$ (NRCC 1986). The permethrin injection was calibrated to produce an initial concentration of 16 $\mu g \cdot L^{-1}$ and to persist at near 1 $\mu g \cdot L^{-1}$ in the lower section of East Branch for 1 h. Sundaram (1990) found a peak concentration of 12 $\mu g \cdot L^{-1}$ and that residue concentrations were less than 1 $\mu g \cdot L^{-1}$ at all sites within 1 h.

Movement

The seasonal variation in trout density indicated some movement of fish in and out of the sections between sample periods. Further indication of movement was provided by the percent recapture of trout at each sample time. Although percent recaptures were generally high (median 70.5%, range 37–88%), recapture rates seldom exceeded 80%, indicating that at least 20% of the trout (excluding young-of-the-year) at each sample time were unmarked fish from other areas or had been missed on previous sample dates. The appearance of unmarked trout throughout the season indicated some degree of movement in and out of the areas. A measure of the extent of this movement was obtained from the recapture of marked individuals.

There was no evidence that the insecticide treatment induced a downstream migration of fish (possibly in avoidance of the insecticide or in search of food) or any unusual movement patterns of recaptured trout. In the pretreatment periods (October 1983–May 1987), approximately 50% of the trout recaptured at each sample period had not moved from their initial capture location (within 25 m), and up to 75% or more had not moved more than 100 m. The proportion of fish moving upstream was similar to the proportion moving downstream, with a slightly greater tendency toward upstream movement in the fall (associated with spawning activity of 2+ and older trout). These patterns continued through the postapplication periods. Because benthos recovery was essentially complete by August, and permethrin residues were rapidly diminished in the stream (Sundaram 1990), emigration in search of food or in avoidance of the insecticide would have been detected in the May–August period of 1987 (post-treatment). Figure 2 illustrates the movement of recaptured trout in the May–August periods of each year, and shows no evidence of emigration from the treated area.

Observations at the fish weir installed in the West Trib in 1987 also indicated no post-treatment downstream migration of fish. During the summer and fall of 1987, the ratio of trout moving upstream through the weir to those moving downstream was 5:1. Although the weir was impassable to fish because of low water levels for several weeks after treatment, the section of stream just above the weir was frequently electroshocked to determine if trout migrating down to the weir were being prevented from moving through. No trout were caught in this section.

Population Age Structure

There was no indication of a change in population age structure resulting from a loss or reduction of an age-class. The age composition of brook trout from the four study sections in the fall of each year is given in Table 3. Some annual variation occurred in the contribution of the four age-classes to the population structure, but the first two age-groups (0+ and 1+)

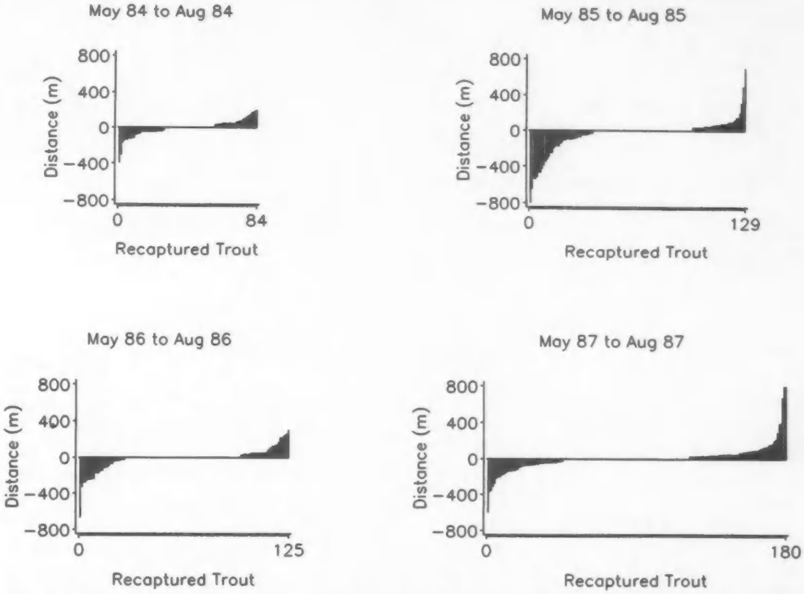

FIG. 2. Movement of recaptured brook trout collected from the treated area, May–Aug. 1984 to 1987 (post-treatment is 1987). Positive distance is upstream and negative distance is downstream. Each point along horizontal line (including 0 points) represents movement of an individual fish captured within the May–Aug. period.

TABLE 3. Percent composition of age-classes of brook trout (number of trout in parentheses) collected in October of pretreatment (1984–86) and post-treatment (1987) years from the four treated sections of Icewater Creek.

		Year			
Location	Age	1984	1985	1986	1987
Crossover	0+	67 (12)	78 (16)	56 (9)	71 (25)
	1+	27 (5)	11 (1)	31 (5)	20 (7)
	2+	6 (1)	11 (1)	13 (2)	9 (3)
	3++	0	0	0	0
West Branch	0+	43 (10)	56 (21)	54 (13)	55 (21)
	1+	30 (7)	17 (6)	38 (9)	30 (11)
	2+	17 (4)	11 (4)	4 (1)	12 (4)
	3++	10 (2)	16 (5)	4 (1)	3 (1)
East Branch	0+	70 (36)	37 (14)	19 (3)	44 (15)
	1+	23 (11)	40 (13)	62 (10)	35 (12)
	2+	5 (3)	10 (3)	19 (3)	19 (7)
	3++	2 (1)	13 (1)	0	2 (1)
West Trib	0+	49 (19)	47 (8)	43 (12)	34 (12)
	1+	43 (17)	41 (7)	36 (10)	34 (12)
	2+	4 (1)	6 (1)	11 (3)	23 (8)
	3++	4 (1)	6 (1)	10 (3)	9 (3)

comprised 75–90% of the population in every instance. A chi-square analysis of an age-class *x* year contingency table for each of the four sites indicated significant differences ($P<0.05$) in the contributions of age-groups to the population structure over the 4 yr. In three of the four sites (Crossover, West Branch, East Branch), the significant differences resulted from discrepancies between observed and expected values of pretreatment years and were therefore unrelated to the insecticide treatment.

In West Trib, the age composition in 1987 differed significantly ($P<0.05$) from pretreatment years (Table 3). To determine which age-group was contributing most to the chi-square value, each age-group was tested against the others combined using a *G*-test of independence over the 4 yr. This indicated that there were no differences among years in the proportions of 0+ or 1+ trout in the population, but the proportion of older fish was significantly higher ($P<0.05$) in 1987 than it had been in 1984 and 1985. Significant differences in the contributions of age-classes to the population structure in West Trib did not result from a post-treatment loss or reduction of an age-group.

Growth of Recaptured Trout

The results from each of the growth parameters measured are presented below in relation to the effects of the insecticide treatment, but they are summarized in general terms here. Most growth occurred in the May–August period of each year, with a marked decline in growth rates in the August–October period. Growth was reduced but still measurable in the overwinter (October–May) periods. Young age-classes (0+, 1+) grew at a greater rate than older cohorts (2+, 3++), especially during the fast growth period of May–August. Considerable variation in growth occurred within age-classes or size groups. In many instances, individuals of the same initial weight or length recaptured in the same period from the same location demonstrated differences in growth rate of up to 2–5 times.

Proportion of trout showing no growth — There were no significant differences among years in the proportions of recaptured fish that exhibited no growth in the overwinter (October–May) and summer (May–August) periods (*G*-test of independ-

TABLE 4. Comparisons among proportions of recaptured trout (from the treated area) that exhibited no growth during recapture periods. Pretreatment periods include Oct.–May 1984–87, May–Aug. 1984–86, and Aug.–Oct. 1984–86. Post-treatment periods include May–Aug. 1987, and Aug.–Oct. 1987. *G*-test of independence (Ho: proportion of non-growers is equal for all years). Underlined years are not significantly different ($P>0.05$).

Parameter	Growth period	Number of non-growers/ growers ranked highest to lowest by year			
Growth in length	Oct.–May	1987	1986	1985	
		4/28	2/16	0/8	
	May–Aug.	1984	1986	1985	1987
		0/12	0/20	0/21	0/47
	Aug.–Oct.	1987	1985	1984	1986
		18/35	4/9	1/6	1/20
Growth in weight	Oct.–May	1985	1986	1987	
		2/6	1/17	1/31	
	May–Aug.	1986	1987	1985	1984
		3/17	7/40	3/18	0/12
	Aug.–Oct.	1987	1986	1985	1984
		46/7	15/6	4/9	2/5

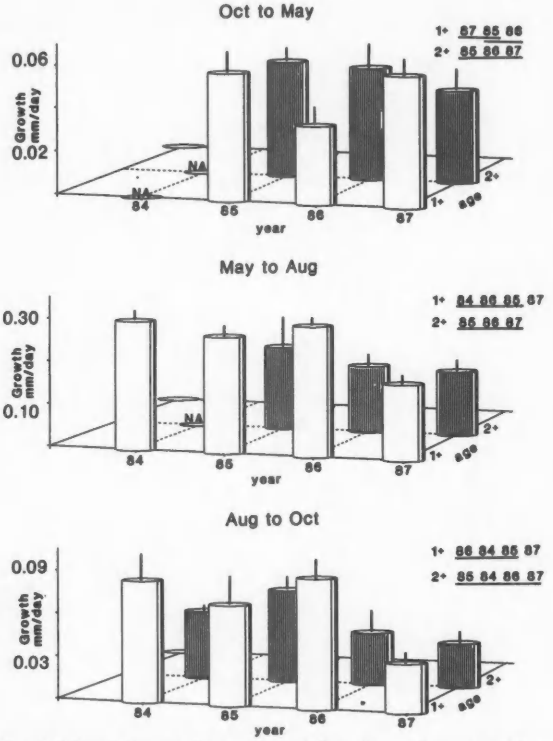

FIG. 3. Mean daily growth rates ($\mathrm{mm \cdot d^{-1}}$) and 1 SE of recaptured 1+ (open) and 2+ (shaded) brook trout from the treated area. Pretreatment periods include Oct.–May 1984–87, May–Aug. 1984–86, and Aug.–Oct. 1984–86. Post-treatment periods include May–Aug. 1987, and Aug.–Oct. 1987. Underlined years are not significantly different ($P>0.05$).

ence $P>0.05$) (Table 4). For the August–October periods, 1987 (post-treatment) showed the highest proportion of fish that did not grow. This differed significantly ($P<0.05$) only from one (growth in length) or two (growth in weight) pretreatment years. This indicates that during May–August after the insecticide treatment there was no increase in the proportion of trout that did not grow, but later in the post-treatment season, the number of trout showing no growth was greater than in pretreatment years.

Daily growth rate — Growth ($\mathrm{mm \cdot d^{-1}}$) of recaptured 1+ trout was significantly lower (pairwise *t*-tests, $P<0.05$) in the May–August and August–October periods of 1987, compared to pretreatment years (Fig. 3). Growth of 1+ fish in the overwinter period of 1986 was significantly less than 1987 (pairwise *t*-tests, $P<0.05$), but not significant from 1985 and represented natural (pretreatment) variation in growth. No significant differences (ANOVA, $P>0.05$) in the growth of 2+ trout were found in any period (Fig. 3). Limited numbers of recaptured 0+ and 3++ trout precluded analysis of variance for measurements of daily growth rate of these age-groups.

Instantaneous growth rate — The instantaneous growth rate (*G*) of 1+ trout recaptured after the insecticide treatment was significantly lower than that of pretreatment fish (Fig. 4). In the May–August period, the 1+ trout captured in 1987 showed significantly reduced growth rates (pairwise *t*-tests, $P<0.05$) from the previous years. The 1+ fish captured in the August–October period of 1987 also demonstrated reduced growth rates, but this was only significant (pairwise *t*-tests, $P<0.05$) from 1985 (Fig. 4). There were no differences (ANOVA, $P=0.13$) in the growth rates of 1+ trout during the pretreatment overwinter (October–May) periods of 1984–87.

The instantaneous growth rates of 2+ fish were not significantly reduced (ANOVA, $P=0.08$ and $P=0.11$) following the insecticide injection (Table 5). In one instance, the growth rate of 2+ trout was significantly less (pairwise *t*-tests, $P<0.05$) than other years, but this occurred in the October–May period of 1985. Sufficient numbers for analysis of 3+ fish were obtained only in the May–August periods of each year, and the growth rates of these fish did not differ (ANOVA, $P=0.97$) among years (Table 5). The limited numbers of recaptured 0+ trout did not permit an analysis of growth rates for young-of-the-year.

Growth of Trout in the Total Catch

Condition — There was no indication of a change in condition of trout collected at each sample time following the insecticide treatment. The regressions of trout weight on length for each sample time of each year were comparable (Table 6). The regression coefficients and intercepts of early summer and late summer of 1987 were slightly lower than the same sample times of pretreatment years, but these coefficients from the spring 1987 (pretreatment) sample were also marginally lower than that sample time of previous years (Table 6). This indicates that the trout were in poorer condition than previous years before the application of the insecticide. A significant difference in slopes (ANCOVA, $P<0.05$) was detected despite the similarity of regression lines. A series of stepwise regressions using dummy variables (Gujarati 1970) was used to determine which intercept or slope coefficients (which years) were contributing

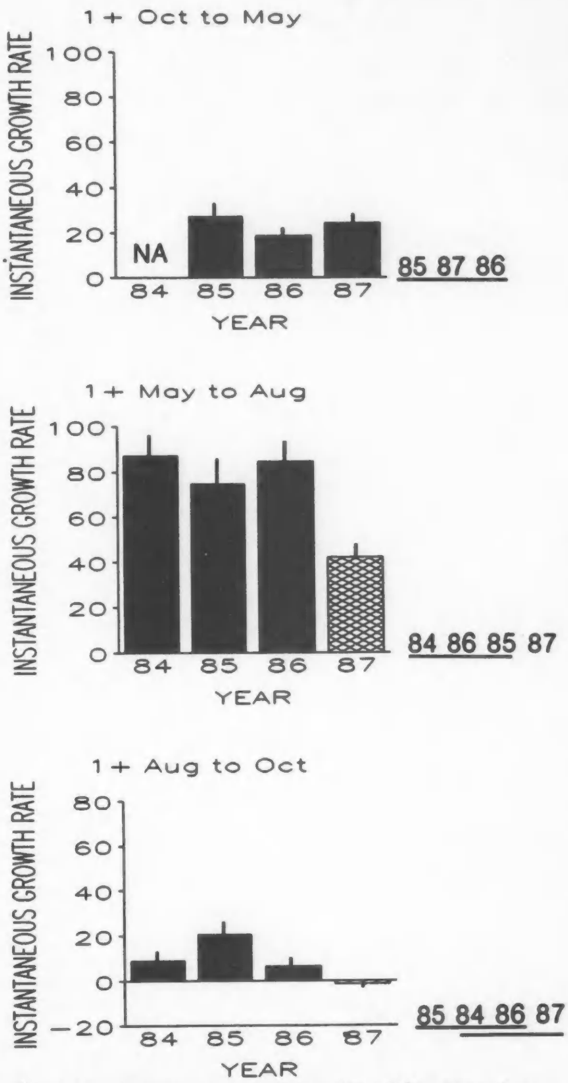

FIG. 4. Mean instantaneous growth rates ($G \times 10^4$) and 1 SE of recaptured 1+ trout from the treated area at pretreatment (solid) and post-treatment (cross-hatched) sample times. Underlined years are not significantly different ($P > 0.05$).

to the significant differences in regressions. This process was unsuccessful in elucidating year (treatment) effects because all coefficients were significantly different, including the ones from pretreatment samples. These significant differences among coefficients were detected despite their apparent similarity because of the "tightness" of the regressions ($r^2 > 0.95$), and consequently, small standard errors of the coefficients, even slight deviations from the regression would result in significant differences among slopes. The similarity in regression coefficients and intercepts indicated that there was no loss of condition in the brook trout resulting from the insecticide treatment.

TABLE 5. Mean instantaneous growth rates ($G \times 10^4$) and 1 SE (in parentheses) of 2+ and 3++ brook trout from the treated area. Pretreatment periods include Oct.–May 1984–87, May–Aug. 1984–86, and Aug.–Oct. 1984–86. Post-treatment periods include May–Aug. 1987, and Aug.–Oct. 1987. Fish recaptured in 1984 were excluded because of insufficient sample sizes. Values in rows followed by the same letter are not significantly different ($P > 0.05$).

	$G \times 10^4$		
Age/period	1985	1986	1987
2+/Oct–May	6.43a (2.6)	28.83b (7.2)	13.97b (2.0)
May–Aug	59.78a (34.2)	16.74a (6.8)	28.98a (5.9)
Aug–Oct	n.a.	−9.59a (7.6)	0.67a (2.42)
3++/May–Aug	16.69a (0.0)	14.90a (5.5)	13.90a (5.0)

Length — The mean lengths of 0+ trout captured in both the late summer and fall sample times of 1987 were significantly less (pairwise *t*-tests, $P < 0.05$) than in previous years (Fig. 5). The mean lengths of 1+ trout were also significantly smaller (pairwise *t*-tests, $P < 0.05$) in post-treatment samples than those of the same age-class collected in pretreatment years (Fig. 5). In the spring 1987 sample (pretreatment), the mean length of 1+ trout was comparable to two of the previous years and greater than the third, indicating that the reduction in size of 1+ trout did not occur until after the insecticide treatment.

There were no differences (ANOVA, $P = 0.93$) in mean lengths of 2+ trout collected in the spring sample of the 4 yr (Table 7). The mean lengths of 2+ fish from the early summer and late summer samples of 1987 were less than previous years, but these differences were not significant (ANOVA, $P = 0.83$ and $P = 0.80$). The 2+ trout in the fall 1987 sample were also smaller than previous years (Table 7), but only differed significantly (pairwise *t*-tests, $P < 0.05$) from 1984. The minimal numbers of 3+ trout (usually $n < 4$) collected at each sample time, and the possible overlap with older fish, precluded comparisons of mean lengths for this age-group.

Annual biomass and production — Annual production of brook trout in the combined study sections was less in the post-treatment year (1987–88) than in the previous 3 yr, but was significantly different (based on overlap of 95% confidence intervals, Newman and Martin 1983) from only one (1986–87) pretreatment year (Table 8). With significant reductions in post-treatment growth of 0+ and 1+ trout, lower total production for 1987 was expected. The reduced growth rate was partially offset by small post-treatment increases in density, especially later in the season (Table 2), which in turn increased biomass. The mean annual biomass was higher in the post-treatment year than in previous years (Table 8). This compensatory effect was augmented by the higher than average growth of trout in the overwinter period of October 1987–May 1988 (discussed below).

Growth of Trout in the Control Stream

The growth of brook trout in the untreated control tributary was determined by comparisons of the mean lengths of age groups over 4 yr. Low numbers of recaptures in the control stream prevented an analysis of individual growth rates. The 0+ trout collected in late summer and fall 1987 were significantly smaller (pairwise *t*-tests, $P < 0.05$) than in previous years

TABLE 6. Linear regression parameters for $\ln W = a + b \ln L$ of all trout collected from the treated area in four sampling periods. Pretreatment periods include spring 1984–87, early summer 1984–86, late summer 1984–86, and fall 1984–86. Post-treatment periods include early summer, late summer and fall 1987.

Parameters	1984	1985	1986	1987
Spring				
Number of trout (*n*)	95	116	111	102
Regression coefficient (*b*)	2.93	3.01	3.30	2.92
Intercept (*a*)	−11.2	−11.6	−12.8	−11.1
Coefficient of determination (r^2)	0.982	0.979	0.976	0.987
Early summer				
Number of trout (*n*)	96	96	191	131
Regression coefficient (*b*)	3.51	3.07	3.19	2.97
Intercept (*a*)	−13.9	−11.8	−12.2	−11.3
Coefficient of determination (r^2)	0.959	0.954	0.992	0.981
Late summer				
Number of trout (*n*)	103	239	127	229
Regression coefficient (*b*)	3.06	3.19	3.06	3.00
Intercept (*a*)	−11.8	−12.5	−11.8	−11.5
Coefficient of determination (r^2)	0.985	0.954	0.995	0.995
Fall				
Number of trout (*n*)	125	101	83	149
Regression coefficient (*b*)	3.07	3.20	2.98	3.08
Intercept (*a*)	−12.0	−12.5	−11.5	−12.0
Coefficient of determination (r^2)	0.976	0.988	0.988	0.990

(Fig. 6). Mean lengths of 1+ control fish were similar (ANOVA, $P=0.59$) in spring of each year, but were less in early summer, late summer, and fall 1987 than in previous years (Fig. 6). However, these reductions in size were not significantly different (pairwise *t*-tests, $P<0.05$) from all pretreatment years. Mean lengths of 2+ control trout did not differ significantly among years (ANOVA, $P=0.17$ and $P=0.15$) in spring and early summer, but were significantly smaller (pairwise *t*-tests, $P<0.05$) in late summer 1987 (Table 9). The limited numbers of 2+ trout in fall samples, and of 3+ fish in all sample times, prevented an assessment of the growth of these groups in the control stream.

Overwinter Growth of Trout After the Treatment

Overwinter growth of brook trout in the treated area was greater in October 1987–1988 than in the same period of pretreatment years (Table 10). The May 1988 sample yielded no fish that had not grown. Daily growth rates of 1+ and 2+ trout, and instantaneous growth rates of 1+ trout were higher than in previous years but differed significantly (pairwise *t*-tests, $P<0.05$) from only one pretreatment year. Instantaneous growth rates of 2+ fish were less than one pretreatment year (1986), but significantly higher than two pretreatment years (1985 and 1987). The condition of brook trout was comparable in May of each year. Despite the increased growth rate, the mean lengths of young trout in the May 1988 samples were still significantly lower than in pretreatment years (Table 10).

Discussion

Brook trout in Icewater Creek exhibited population age structure, density variation, and growth patterns similar to other trout streams. The longevity of trout was short, with over 75% of the population comprising 0+ and 1+ fish by the fall of each year, and with few individuals exceeding age 2+ (Hunt 1969; Hanson and Waters 1974; Flick and Webster 1975). Growth rates were higher for the first two age-classes than for older fish (Whitworth and Strange 1983), and most growth occurred in the May–August period of each year (Whitworth and Strange 1983; Canjuk et al. 1987). Marked annual variability in density and growth of trout occurred in pretreatment years (Hunt 1969; Flick and Webster 1975; Elliott 1984). The several-fold differences in growth rates that occurred among individuals of the same initial size at the beginning of a recapture period, caught at the same time from the same section of stream, has not been reported in other salmonid studies. These highly individualistic growth rates suggest "niche-specific" growth of brook trout in Icewater Creek. They imply that trout established in suitable microhabitats grow considerably faster in the same time period and under apparently similar conditions than other individuals in the same section of stream. Newman and Waters (1989) reported high temporal variation in growth of brown trout in streams, but measured population parameters within and between contiguous sections of streams, not individual growth rates. The relationship between several habitat variables and trout growth has been determined by Bowlby and Roff (1986), but their biomass comparisons were made at population levels, rather than among individuals. The variable individual growth rates of trout in Icewater Creek may indicate that natural environmental stresses are accentuated in northern Ontario streams subject to extremes in climate and topography. Schlosser (1985) submits that stochastic processes (physical or natural environmental stresses) are especially important in the establishment and success of young fish in streams. Consequently, in streams such as Icewater Creek, common in much of northern Ontario's forested areas, brook trout populations may be less stable and less productive than those in more moderate

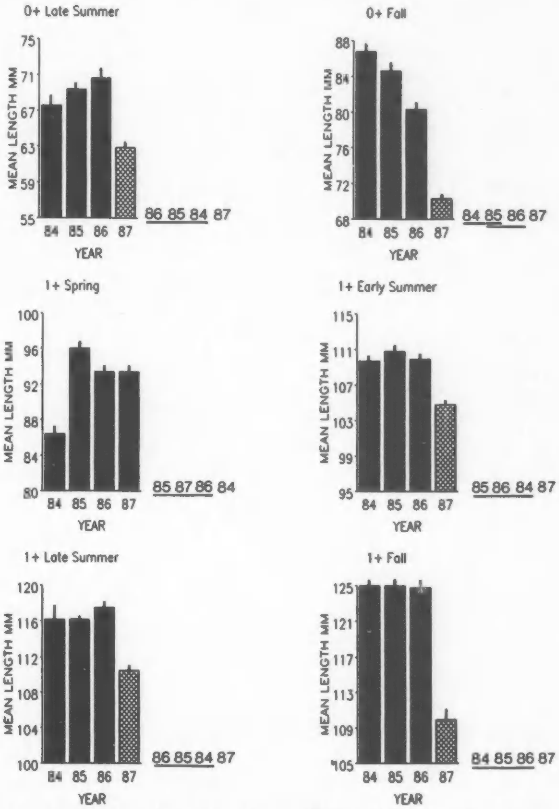

FIG. 5. Mean length (mm) and 1 SE of 0+ and 1+ brook trout collected from the treated area at pretreatment (solid) and post-treatment (cross-hatched) sample times. Underlined years are not significantly different ($P > 0.05$).

regions. When converted to common units (area measurements taken at "normal" summer water levels), annual production rates of trout in Icewater Creek ($0.7–0.9\ g \cdot m^{-2} \cdot yr^{-1}$) were less than the lowest production rates found in other trout streams (Hunt 1969; Hanson and Waters 1974; Whitworth and Strange 1983; Neves and Pardue 1983) including those ($1.5–1.6\ g \cdot m^{-2} \cdot yr^{-1}$) reported to be the lowest in North America (O'Conner and Power 1976). The variable growth and low production in streams such as Icewater Creek may make them more susceptible to effects of an insecticide perturbation.

Although there were no post-treatment changes in the density, population age structure, movement patterns, or condition of the fish, the growth of young brook trout was significantly reduced following the pesticide injection. This resulted in significant reductions in the size of post-treatment 0+ and 1+ fish compared to pretreatment years. This reduced growth of these age-groups is especially critical to the productivity of the trout community because of the high percent composition of these age-classes in the population.

The contribution of insecticide effects to this growth reduction, however, is unclear. Other factors affecting the growth of trout in 1987, especially water levels and temperature, may have been responsible for, or at least contributed to, the significant growth reductions. The 1987 field season (May–October) was unusually warm with extended periods of high temperatures and low summer rainfall. This resulted in abnormally high water temperatures in Icewater Creek for several days at a time, and the lowest recorded summer water levels (unpubl. data) in the 4 yr period. A remote weather station approximately 25 km northwest of Icewater Creek recorded the highest mean daily temperatures in June and July 1987 of the 1984–1987 period (P. W. Hazlett, Great Lakes Forestry Centre, Sault Ste. Marie, Ontario, P6A 5M7, pers. comm.). Because of repeated equipment failures, water temperatures in Icewater Creek were not continuously recorded, but numerous spot checks showed daytime water temperatures exceeded 22°C for several days through June, July, and August 1987. In the 1988 field season, hourly water temperatures in Icewater Creek were recorded and these values were regressed on air temperatures ($r^2 = 0.79$) from the remote weather station to estimate the water temperatures of 1984–1987. Mean daily temperatures calculated from these regression values for the May–August periods indicated that water temperatures in 1987 were often higher than pretreatment years, especially in the early part of the fast growth period (Fig. 7). The average summer water temperature (mean daily temperatures combined from May–August) was significantly higher in 1987 than all three previous years (ANOVA, $P < 0.01$, pairwise t-tests, $P < 0.05$).

Elliott (1975) found that the growth rate of trout was highly dependent on water temperature. Barton et al. (1985) identified water temperature as the major factor in sustaining brook trout

TABLE 7. Mean lengths (mm) and 1 SE (in parentheses) of 2+ brook trout from the treated area. Pretreatment sample times include spring 1984–87, early summer, late summer, and fall 1984–86. Post-treatment sample times include early summer, late summer, and fall 1987. Values in rows followed by the same letters are not significantly different ($P > 0.05$).

Sample time	1984	1985	1986	1987
Spring	131.7a (1.8)	133.1a (2.0)	132.9a (1.8)	133.4a (1.7)
Early summer	146.1a (3.2)	144.8a (3.7)	144.1a (1.6)	142.7a (2.2)
Late summer	149.2a (2.7)	147.0a (1.9)	146.6a (1.8)	145.8a (2.5)
Fall	155.9a (2.0	149.6ab (2.5)	153.7ab (3.1)	145.0b (2.1)

TABLE 8. Annual biomass and production of brook trout (total kg produced) in the four treated sections combined. Production estimates were calculated from May to May of succeeding years. Pretreatment periods include 1984–85, 1985–86, and 1986–87. Post-treatment period is 1987–88.

	1984–85	1985–86	1986–87	1987–88
Mean annual biomass (kg)	1.72	2.06	1.71	2.14
Production ($kg \cdot yr^{-1}$)	1.51	2.01	1.97	1.49
Variance of Production	0.0308	0.0355	0.0167	0.0135
95% C. I.	1.15–1.86	1.63–2.39	1.72–2.23	1.26–1.72

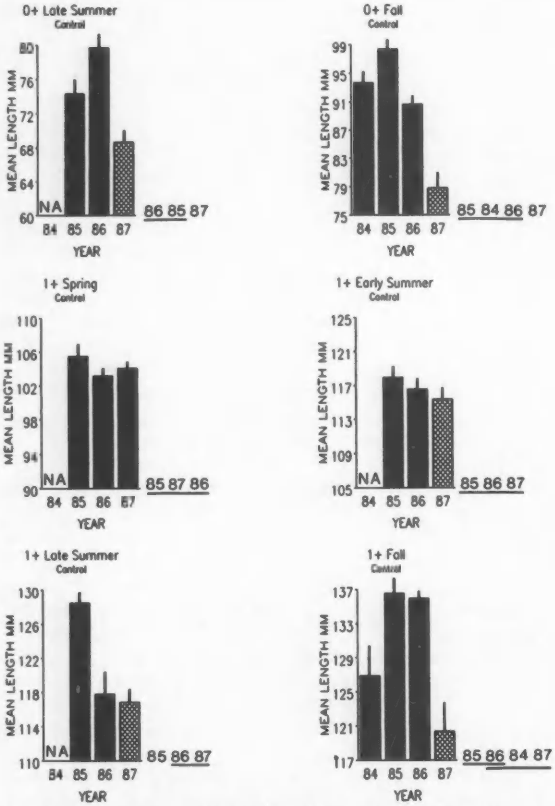

FIG. 6. Mean length (mm) and 1 SE of 0+ and 1+ brook trout collected from the control stream (East Trib) at pretreatment (solid) and post-treatment (cross-hatched) sample times. Underlined years are not significantly different ($P>0.05$).

populations, and that small increases in temperature may be important regulators of trout population success as temperatures approach critical levels. Water temperatures above 20°C are considered unsuitable and well above the optimum growth temperature of 13°C for trout (Elliott 1975; Power 1980; Barton et al. 1985). Elliott (1984) recorded significant reductions in growth of brown trout in years of drought and attributed the growth reductions to unusually high temperatures, and reductions in available space and drifting food because of the low water levels. This suggests that temperature stress and/or unusually low water levels contributed to the post-treatment growth reductions in the trout population of Icewater Creek.

TABLE 9. Mean lengths (mm) and 1 SE (in parentheses) of 2+ brook trout from the untreated control tributary (East Trib). Fish in this age-group from 1984 and from the fall of each year were excluded because of insufficient sample sizes. Values in rows followed by the same letter are not significantly different ($P>0.05$).

Sample time	1985	1986	1987
Spring	133.0a (2.1)	126.6a (2.2)	132.3a (2.2)
Early summer	136.1a (3.0)	140.3a (2.0)	143.6a (2.3)
Late summer	145.8a (1.7)	153.5b (3.4)	141.4a (2.1)

Further evidence of temperature stress affecting growth of trout during the 1987 season was given by the significant reductions in mean lengths of 0+ trout collected from the untreated control stream. There is some indication that insecticide effects may have combined with temperature stress to produce significant growth reductions in 1+ fish in the treated area. Mean lengths of post-treatment 1+ trout were significantly less than pretreatment fish, but mean lengths of control 1+ trout were not usually significant from previous years, although they were substantially reduced. However, creek temperatures from the 1988 season showed that although temperatures in the treated and control tributaries followed similar patterns, daily maximums were slightly higher (about 2°C, unpubl. data) in the treated tributary during the summer months. In periods of high temperatures, fish in the treated tributary were subject to greater temperature stress than those in the control stream. It is conceivable that negative effects on growth of the unusually high temperatures (causing temperature stress) and the low water levels (presumably reducing suitable habitat) may have been augmented by the insecticide impact on benthos. The significant growth reductions in the control stream, however, imply that the insecticide impact did not produce adverse effects over and above the natural environmental stresses. Because temperature could not be controlled or varied among streams or stream sections, temperature effects could not be separated from treatment effects. To assess the secondary effects of the insecticide impact in the absence of temperature stress would require a treatment duplication under suitable water temperatures. A treatment duplication in Icewater Creek is scheduled for 1990.

By the winter (October–May) after treatment, when water temperatures were similar to pretreatment years, growth rates of trout in the treated area were higher than they had been in previous years. This suggests some compensatory response in the growth of brook trout. Despite the increase in overwinter growth rates, the mean lengths of young brook trout in May 1988 remained significantly less than the same age-classes of pretreatment years. The recovery of benthos by late summer 1987 limited the potential for secondary effects on trout growth to the short-term, but the reduction in size of trout in these age-classes may potentially be a longer-term effect. These fish may

TABLE 10. Summary of trout growth in the overwinter (Oct.–May) periods of each year (post-treatment is Oct.–May 1988). Underlined years are not significantly different ($P>0.05$). Data from 1984 were excluded when sample sizes were insufficient for analysis.

Growth parameter	Age in May	Values ranked lowest to highest by year				
1) Proportion of zero-growth fish (non-growers/growers)	all	1988	1985	1986	1987	
		0/28	0/8	2/16	4/28	
2) Daily growth rate ($mm \cdot d^{-1}$) of recaptures	1+	1986	1985	1987	1988	
		0.037	0.061	0.062	0.066	
	2+	1987	1986	1985	1988	
		0.045	0.055	0.057	0.075	
3) Instantaneous growth ($G \times 10^4$) of recaptures	1+	1986	1987	1985	1988	
		18.86	24.37	27.21	32.17	
	2+	1985	1987	1988	1986	
		6.43	13.77	21.44	28.83	
4) Condition (regression coefficient) in May of each year	all	1987	1984	1985	1988	1986
		2.923	2.934	3.008	3.034	3.305
5) Mean length (mm) in May of each year	1+	1984	1988	1987	1986	1985
		86.4	86.6	93.4	94.4	96.0
	2+	1988	1984	1986	1985	1987
		120.1	131.7	132.9	133.1	133.4

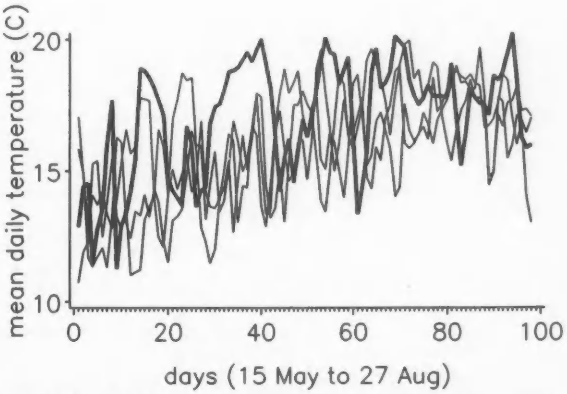

FIG. 7. Mean daily water temperatures (°C) in the West Tributary of Icewater Creek in May–Aug. of the year of treatment (heavy line) and in three previous years. Temperatures computed from regression on air temperatures (see discussion).

continue to be significantly smaller during their lifespan than trout in the same age-classes from before the treatment. On the other hand, sustained growth rates in post-treatment years may compensate for the growth reductions in 1987, and these fish may eventually reach the size of trout in their age-class from pretreatment years. Sampling of the trout population continued beyond May 1988, but these data are not analyzed.

This experiment demonstrated that an insecticide treatment of a forest stream at a concentration sufficient to cause an impact on benthos much greater than would be encountered in aerial spray operations, had a limited impact on the resident brook trout. There was no evidence of fish mortality or unusual behaviour, and no indication of post-treatment changes in trout density, population age structure, movement patterns, or condition. Annual production of trout in the treatment year was reduced but not significantly lower than pretreatment years. Although the growth rates and size of 0+ and 1+ trout in the treated area were significantly reduced, significant reductions in the size of young trout in the control stream during the same period indicated that temperature stress was at least partially, if not entirely, responsible for growth reductions of the treated fish. Significant growth reductions of fish in the untreated control stream strongly imply that the insecticide impact did not produce adverse effects on the trout population in the treated stream over and above natural environmental stresses, in this case high temperatures and low water levels.

Secondary effects on trout growth were nebulous despite catastrophic increases in invertebrate drift and significant reductions of benthos. The transient nature of insecticide impact on invertebrate communities may preclude significant secondary effects on fish. Trout populations may be sustained through periods of benthos depletion by alternate food sources and/or increased foraging efficiency on the residual invertebrate population. Kingsbury and Kreutzweiser (1987) found that brook trout fed almost exclusively on terrestrial arthropods and non-insect aquatic invertebrates after a high-dosage insecticide treatment. Cuffney et al. (1984) reported that despite a 90% reduction in stream insect biomass following a methoxychlor treatment, drift densities were similar to control levels, thus providing food resources for drift-feeding fish. Such mitigating factors may reduce the likelihood of secondary effects on fish from insecticide contamination of streams. While this experiment did not establish a clear relationship between food availability and trout viability (because alternate food sources were not excluded), it did demonstrate that an insecticide impact causing significant reduction of benthos had no measurable effects on trout density, age structure, movement, or condition, and had equivocal effects on growth of young trout.

Acknowledgements

The guidance and assistance of Peter Kingsbury in all facets of this project are greatly appreciated. Steve Holmes and Scott Capell contributed to sampling and data analysis, and Kevin Barber assisted in fish collection. Dr. D. Behmer provided many helpful suggestions for the statistical analysis, and reviewed the manuscript. Dr. L. Lockhart and an anonymous reviewer offered useful criticism on the manuscript. In each of the field seasons, technical assistance was provided by summer employees, including Tym Garside, Kelly Mick, Tarmo Poldma, Neville Rising, Pat Sarich, Dave (Bill) Thomas, Rhonda Waugh, Bryan Wisendon, and Mark Witty. The continued cooperation of the Ontario Ministry of Natural Resources in the Icewater Creek research project is appreciated.

References

Allan, J. D. 1981. Determinants of diet of brook trout (*Salvelinus fontinalis*) in a mountain stream. Can. J. Fish. Aquat. Sci. 38: 184–192.

1982. The effects of reduction in trout density on the invertebrate community in a mountain stream. Ecology 63: 1444–1455.

Barton, D. R., W. D. Taylor, and R. M. Biette. 1985. Dimensions of riparian buffer strips required to maintain trout habitat in southern Ontario streams. N. Am. J. Fish. Manage. 5: 364–378.

Bowlby, J. N., and J. C. Roff. 1986. Trout biomass and habitat relationships in southern Ontario streams. Trans. Am. Fish. Soc. 115: 503–514.

Canjuk, R. A., R. A. Currey, and G. Power. 1987. Seasonal energy budget of brook trout in streams: implications of a possible deficit in early winter. Trans. Am. Fish. Soc. 116: 817–828.

Carle, F. L., and M. R. Strub. 1978. A new method for estimating population size from removal data. Biometrics 34: 621—630.

Cuffney, T. F., J. B. Wallace, and J. R. Webster. 1984. Pesticide manipulation of a headwater stream: invertebrate responses and their significance for ecosystem processes. Freshwater Invertebr. Biol. 3: 153–171.

Dixon, W. J. 1983. BMDP statical software. University of California Press, Los Angeles, CA.

Eidt, D. C., J. E. Hollebone, W. L. Lockhart, P. D. Kingsbury, M. C. Gadsby, and W. R. Ernst. 1989. Pesticides in forestry and agriculture: Effects on aquatic habitats, p. 245–284. *In* J. A. Nriagu [ed.] Aquatic toxicology and water quality management. John Wiley and Sons, New York, NY.

Elliott, J. M. 1975. The growth rate of brown trout (*Salmo trutta*) fed on maximum rations. J. Anim. Ecol. 44(3): 805–821.

1983. Statistical analysis of samples of benthic invertebrates. Freshwater Biological Association Scientific Publication 25.

1984. Growth, size, biomass and production of young migratory trout *salmo trutta* in a lake district stream, 1966–83. J. Anim. Ecol. 53: 979–994.

Fairchild, W. L., W. R. Ernst, and V N. Mallet. 1989. Fenitrothion effects on aquatic organisms, p. 109–166. *In* W. R. Ernst, P. A. Pearce, and T. L. Pollock [ed.] Environmental effects of fenitrothion use in forestry. Environment Canada, Atlantic Region, Dartmouth, N.S.

Flick, W. A., and D. A. Webster. 1975. Movement, growth and survival in a stream population of wild brook trout (*Salvelinus fontinalis*) during a period of removal of non-trout species. J. Fish. Res. Board Can. 32: 1359–1367.

Garman, G. C., and T F) Waters. 1983. Use of the size-frequency (Hynes) method to estimate annual production of a stream fish population. Can. J. Fish. Aquat. Sci. 40: 2030–2034.

Groves, A. B., and A. J. Novotny. 1965. A thermal-marking technique for juvenile salmonids. Trans. Am. Fish. Soc. 94: 386–389.

Gujarati, D. 1970. Use of dummy variables in testing for equality between sets of coefficients in linear regressions: a generalization. Am. Stat. 24(5): 18–22.

Hanson, D. L., and T. F. Waters. 1974. Recovery of standing crop and production rate of a brook trout population in a flood-damaged stream. Trans. Am. Fish. Soc. 103: 431–439.

Helson, B. V., P. DeGroot, and J. J. Turgeon. 1989. Toxicity of insecticides to first-instar larvae of the spruce budmoth (*Zeiraphera canandensis* mut. and free.) Lepidoptera: Torticidae: laboratory and field studies. Can. Entomol. 121: 81–91.

Hunt, R. L. 1969. Effects of habitat alteration on production, standing crop and yield of brook trout in Lawrence Creek, Wisconsin, p. 281–312. *In* T. G Northcote [ed.] Symposium on salmon and trout in streams. University of British Columbia, Vancouver, B.C.

Jones, D. 1984. Use, misuse, and role of multiple comparisons procedures in ecological and agricultural entomology. Environ. Entomol. 13: 635–649.

Kerswill, C. J. 1967. Studies on effects of forest sprayings with insecticides, 1952–63, on fish and aquatic invertebrates in New Brunswick streams: introduction and summary. J. Fish. Res. Board Can. 24: 701–708.

Kingsbury, P. D. 1984. Environmental impact assessment of insecticides used in Canadian forests, p. 365–376. *In* W. Y. Garner and J. Harvey [ed.] Chemical and Biological Controls in Forestry. ACS Symposium Series, American Chemical Society, Washington, DC.

Kingsbury, P. D., and D. P. Kreutzweiser. 1987. Permethrin treatments in Canadian forests. Part 1: Impact on stream fish. Pestic. Sci. 19: 35–48.

Kreutzweiser, D. P., and P. D. Kingsbury. 1982. Recovery of stream benthos and its utilization by native fish following high dosage permethrin applications. Forest Pest Manage. Inst. Inf. Rep. FPM-X-59, Canadian Forestry Service, Sault Ste. Marie, Ont. 18 p.

1987. Permethrin treatments in Canadian forests. Part 2: Impact on stream invertebrates. Pestic. Sci. 19: 49–60.

LeCren, E. D. 1974. The effects of errors in aging in production studies, p. 221–224. *In* T. B. Bagenal [ed.] Aging of Fish. Unwin Brothers Limited, Surrey, UK.

Levene, H. 1960. Robust tests for equality of variances, p. 278–292. *In* I. Olkin [ed.] Contributions to Probability and Statistics. Standford University Press, CA.

Muirhead–Thomson, R. C. 1987. Pesticide impact on stream fauna with special reference to macroinvertebrates. Cambridge University Press, Cambridge, UK. 275 p.

Murphy, M. L., C. P. Hawkins, and N. H. Anderson. 1981. Effects of canopy modification and accumulated sediment on stream communities. Trans. Am. Fish. Soc. 110: 469–478.

Neves, R. J., and G. B. Pardue. 1983. Abundance and production of fishes in a small Appalachian stream. Trans. Am. Fish. Soc. 112: 21–26.

Newman, R. M., and F. B. Martin. 1983. Estimation of fish production rates and associated variances. Can. J. Fish. Aquat. Sci. 40: 1729–1736.

Newman, R. M., and T. F. Waters. 1989. Differences in brown trout (*Salmo trutta*) production among contiguous sections of an entire stream. Can. J. Fish. Aquat. Sci. 46: 203–213.

Norris, L. A., H. W. Lorz, and S. V. Gregory. 1983. Influence of forest and rangeland management on anadromous fish habitat in western North America: Forest chemicals. Tech. Rep. PNW-149. USDA Forest Service, Pacific Northwest Research Station, Portland, OR. 95 p.

NRCC (National Research Council of Canada). 1986. Pyrethroids: their effects on aquatic and terrestrial ecosystems. NRCC 24376, National Research Council of Canada, Ottawa, Ont. 303 p.

O'Conner, J. F., and G. Power. 1976. Production by brook trout (*Salvelinus fontinalis*) in four streams in the Matamek Watershed, Quebec. J. Fish. Res. Board Can. 33: 6–18.

Pollard, J. E. 1981. Investigator differences associated with a kicking method for sampling macroinvertebrates. J. Freshwater Ecol. 1: 215–223.

Power, G. 1980. The brook char, *Salvelinus fontinalis*, p. 140–203. *In* E. K. Balon [ed.] Charrs-trout fishes of the genus *Salvelinus*. Dr. W. Junk, The Hague, Netherlands.

Reice, S. R., and R. L. Edwards. 1986. The effect of vertebrate predation on lotic macroinvertebrate communities in Quebec, Canada. Can. J. Zool. 64: 1930–1936.

Ricker, W. E. 1930. Feeding habits of speckled trout in Ontario waters. Trans. Am. Fish. Soc. 60: 64–72.

Schlosser, I. J. 1985. Flow regime, juvenile abundance, and the assemblage structure of stream fishes. Ecology 66: 1484–1490.

Sibley, P. K., N. K. Kaushik, and D. P. Kreutzweiser. 1990. Impact of a pulse application of permethrin on the macroinvertebrate community of a headwater stream. Environ. Poll. (In press)

Sosiak, A. 1983. Fish population and growth studies, p. 81–95. *In* P. D. Kingsbury [ed.] Permethrin in New Brunswick salmon nursery streams. Forest Pest Manage. Inst. Inf. Rep. FPM-X-52, Canadian Forestry Service, Sault Ste. Marie, Ont.

Sundaram, K. M. S. 1990. Fate and short-term persistence of the insecticide permethrin in a northern Ontario (Canada) headwater stream. Pestic. Sci. (In press)

Symons, P. E. K. 1971. Behavioural adjustment of population density to available food by juvenile Atlantic salmon. J. Anim. Ecol. 40: 569–587.

Symons, P. E. K., and G. D.Harding. 1974. Biomass changes of stream fishes after spraying with the insecticide fenitrothion. FRB Tech. Rep. 432: 47 p.

WHITWORTH, W. E., AND R. J. STRANGE. 1983. Growth and production of sympatric brook and rainbow trout in an Appalachian stream. Trans. Am. Fish. Soc. 112: 469–475.

WILZBACH, M. A., K. W. CUMMINS, AND J. D. HALL. 1986. Influence of habitat manipulations on interactions between cutthroat trout and invertebrate drift. Ecology 67: 898–911.

Impact of Ice Algae on Inorganic Nutrients in Seawater and Sea Ice in Barrow Strait, NWT, Canada, During Spring

Glenn F. Cota,[1] Jeffrey L. Anning, Leslie R. Harris, W. Glen Harrison, and Ralph E. H. Smith[2]

Department of Fisheries and Oceans, Biological Sciences Branch, Bedford Institute of Oceanography, Dartmouth, N. S. B2Y 4A2 Canada

Cota, G. F., J. L. Anning, L. R. Harris, W. G. Harrison, and R. E. H. Smith. 1990. Impact of ice algae on inorganic nutrients in seawater and sea ice in Barrow Strait, NWT, Canada, during spring. Can. J. Fish. Aquat. Sci. 47: 1402–1415.

Except in "bottom ice" (lowest few centimetres) and surface waters impacted by autotrophs, the major inorganic nutrients behave conservatively in seawater and sea ice. From mid- to late spring, steep and persistent nutrient gradients were observed in the "well-mixed surface layer" with minima near the ice–water interface. Nitrate, ammonium, and phosphate are highly concentrated in heavily colonized bottom ice relative to seawater and the remainder of the ice sheet; concentrations in darkened, weakly colonized bottom ice are similar to the ice sheet. These nutrients also display strong vertical stratification over millimetre scales. Nitrate and phosphate in the bottom ice layer display strong positive relationships with chlorophyll. The accumulation of these nutrients in bottom ice must be biologically mediated and constitutes a significant sink. In contrast, silicic acid concentrations in bottom ice are close to those expected for sea ice formed from the source seawater, are only weakly related to algal biomass, and vary much less seasonally. Ice algae are apparently shocked osmotically and release their intracellular pools of dissolved nutrients. Intracellular pools of nitrate averaged 1.4–9.5% of total particulate nitrogen. Nitrient stresses, during periods of high biomass and sluggish supply, may be alleviated by pooling.

Sauf dans la "glace de fond" (les quelques centimètres de fond) et dans les eaux de surface remplies d'organismes autotrophes, les principaux éléments nutritifs inorganiques se comportent simplement dans l'eau de mer et dans la glace de mer. Du milieu jusqu'à la fin du printemps, des gradients d'éléments nutritifs abrupts et répétés ont été observés dans la couche de brassage en surface avec des minima relevés à proximité de l'interface de l'eau et de la glace. Les nitrates, les phosphates et l'ammoniac sont fortement concentrés dans la glace de fond densément colonisée par rapport à l'eau de mer et au reste de la couche de glace; les concentrations relevées dans la glace de fond plus foncée et peu colonisée sont semblables à celles de la couche de glace. Ces éléments nutritifs présentent aussi une forte stratification verticale de l'ordre du millimètre. Les nitrates et les phosphates de la couche de glace de fond présentent une forte relation positive avec la chlorophylle. L'accumulation de ces éléments nutritifs dans la glace de fond doit être réalisée par le biais d'un médiateur biologique et représente un réservoir important. Par opposition, les concentrations d'acide silicique dans la glace de fond s'approchent des concentrations prévues pour la glace de mer formée à partir de l'eau de mer de source, ne sont que faiblement liées à la biomasse des algues et varient beaucoup moins d'une saison à l'autre. Les algues contenues dans la glace subissent semble-t-il un choc osmotique et libèrent leurs réserves intracellulaires d'éléments nutritifs dissous. Les réserves intracellulaires de nitrates s'établissaient en moyenne entre 1,4 et 9,5 % de l'azote particulaire total. Des apports soudains en éléments nutritifs, pendant les périodes où la biomasse est élevée et les approvisionnements faibles, peuvent être abaissés par la constitution de réserves.

Received November 18, 1988
Accepted February 8, 1990
(J9951)

Reçu le 18 novembre 1988
Accepté le 8 février 1990

Polar environments are characterized by extreme seasonal fluctuations with extended periods of darkness and very low temperatures; these two features influence the physical environment and biological activities profoundly. The absence or near absence of light precludes significant primary productivity throughout much of the year. Except for leads and polynyas, arctic seas are normally covered with about 1–3 m of ice for 6–10 m. Most of the Arctic Ocean is covered with 2–3 m of perennial (multiyear) pack ice throughout the entire year, but throughout most of the surrounding marginal seas annual ice cover undergoes a characteristic seasonal cycle of formation and retreat.

The seasonal variations in ice cover and in water transported through the Canadian Arctic Archipelago are large (e.g. Prinsenberg and Bennett 1987). Ice cover has a late winter maximum of about $14 * 10^6$ km^2 and a minimum near half of that value in late summer (Walsh and Johnson 1979). Volume transports are lowest in winter ($0.2 * 10^6$ m$^3 \cdot$s^{-1}) but reach $1.0 * 10^6$ m$^3 \cdot$s^{-1} during late summer (Prinsenberg and Bennett 1987). Water flowing through the Archipelago is cold and relatively nutrient rich, originating from Arctic Ocean surface water (Jones and Coote 1980; Cota et al. 1987; Prinsenberg and Bennett 1987). The Archipelago is part of the polar continental shelf of North America and there are a series of restrictive shallow sills near the center of the Archipelago with maximum depths from about 85–140 m except in Smith Sound which is 250 m. The Barrow Strait region is the narrowest, central portion of the Northwest Passage (Fig. 1), and the waters flowing through the area are influenced by different factors, according to the season. In winter, surface waters lose heat and gain salt from the growing ice cover (Prinsenberg and Bennett 1987); both cooling and brine rejection promote convective mixing in surface waters. In summer, the relatively fresh melt waters from sea ice result in shallow, strongly stratified near-surface layers and phytoplankton blooms decrease or deplete nutrients in the surface mixed layer (Jones and Coote 1980; Harrison et al. 1982).

---

[1] Present address: Graduate Program in Ecology. University of Tennessee,Knoxville, TN 37996-1610 USA.

[2] Present address: Biology Department, University of Waterloo, Waterloo, Ont. N2L 3G1 Canada.

Polar seas have been greatly undersampled spatially and temporally, especially during the non-navigable, ice-covered periods when ice algae often dominate primary productivity. Furthermore, because of the relatively high concentrations in polar waters, nutrients were rarely considered to be a limiting resource for ice algal growth. However, if spring time distributions of dissolved inorganic nutrients and algal biomass in seawater and sea ice are considered, then a strong source–sink relationship is indicated and the primary source of nutrients must be the water column (Cota et al. 1987; Cota and Horne 1989). There has been numerous piecemeal observations on nutrients in sea ice or seawater, but very few comprehensive reports describing the seasonal dynamics of nutrients in ice and water (Alexander et al. 1974; Grainger 1977). These earlier works lacked sufficient spatial resolution to define nutrient gradients in the "surface mixed layer" which have a large influence on transport rates (Cota et al. 1987; Cota and Horne 1989, figure 2) and only hinted at the very pronounced gradients and accumulations of certain nutrients in bottom ice.

In this report we describe the distributions and dynamics of nutrients and algal biomass in seawater and sea ice to establish the relative importance of biological vs. physical–chemical processes in determining the observed patterns. Our data clearly illustrate that ice algal communities have a large impact on chemical distributions in the bottom few centimeters of sea ice and in surface seawater. Ice algae modify absolute concentrations and the relative abundance of certain inorganic nutrients in this biphasic interfacial system.

Methods

Seawater samples were collected with 5 L Niskin bottles and ice cores of land-fast first year sea ice were obtained with a SIPRE corer (7.62 cm I.D.) from several sites in Barrow Strait and Resolute Passage near Resolute, NWT, Canada (Fig. 1). The data presented here refer primarily to station 42 (1983; 132 m), station 3 (1984; 27 m) or station 5 (1984; 92 m) and a site very near station 5 (1985; 94 m). Data collections were limited to the spring time from April through mid-June (Cota et al. 1987; Smith et al. 1988). Seawater samples for nutrients and/or chlorophyll were collected from 5–16 depths over the water column. In 1985 we also obtained high resolution microprofiles over the top meter of the water beneath the ice from 7 depths (1, 3, 7, 15, 25, 50, and 100 cm) with a specially designed pump sampler (Cota, unpubl. data). No depth corrections have been made for drag induced "swing out" of bottles on the hydrographic wire and this may lead to errors of order ≤ 10 m, depending on wire length and current speed which may reach 30–60 $\mathrm{cm \cdot s^{-1}}$ in this area (Cota et al. 1987). Nutrient profiles were usually done during periods of slackwater when currents were weakest to minimize swing out.

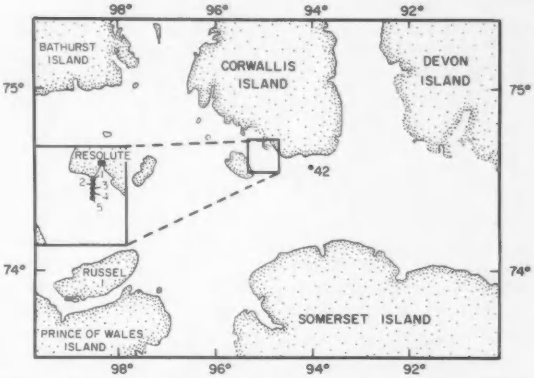

FIG. 1. Sampling locations in Barrow Strait (stn. 42) and Resolute Passage (stns. 1–5) for 1983–85 studies of ice biota.

We normally collected only the bottom few centimetres (4–5 cm) of ice cores, where there was an obvious concentration of algal pigments. We refer to this part of ice cores as "bottom ice" as opposed to the sea ice column. Complete ice cores were only taken on one occasion to obtain profiles through a 176 cm thick ice sheet. Segments 5 cm in length were sawn out from the depth intervals 0–5, 30–35, 60–65, 90–95, 120–125, 150–155, and 171–176 cm to reduce melt volumes (Cota et al. 1987). Vertical stratification in bottom ice was also examined in a few cores by shaving thin, consecutive layers (5 mm) with a knife. Ice cores for standing crops were routinely melted without dilution and we measured salinity, inorganic nutrients, chlorophyll, particulate carbon, and nitrogen. Inorganic nutrients, including nitrate (NO_3), silicic acid ($Si(OH)_4$) and phosphate (PO_4), were analyzed with standard methods (Strickland and Parsons 1972) on a Technicon autoanalyzer; ammonium (NH_4) was also determined manually in a few cases. Precision for replicate determinations was around 4–7% for NO_3 and $Si(OH)_4$ and about 12% for PO_4 and NH_4. Analyses of particulates collected on Whatman GF/F glass fiber filters were consistent with Holm–Hansen et al. (1965) for chlorophyll (CHL) and wih Sharp (1974) for particulate organic carbon and nitrogen (POC/N). Replicated measurements of CHL and POC/N had precisions between 5–11%.

Seawater salinity profiles were based on measurements with a Guildline model 8770 CTD or a Guildline Autosal model 8400 salinometer for discrete bottle samples (precisions ≈ 0.02). All melted ice core salinities were done with an American Optical refractometer (precision ≈ 0.5–1.0). All salinity measurements were referenced to standard seawater (Sagami Research Institute). In most of the cases considered herein CTD data from a discrete depth in the water column were paired with nutrient data collected with Niskin bottles in hydrocasts; paired CTD casts and hydrocasts were taken within a few hours of each other and within a horizontal distance of 100 m.

Regression analyses were conducted to examine trends in data sets and relationships between ice algal indices and environmental variables. Employing the terminology and computational techniques of Sokal and Rohlf (1981), regression parameters for both model I (predictive) and model II (functional or geometric mean, GM) relationships were computed. Symmetrical confidence intervals ($\pm 95\%$) for the slope of the model I regression coefficients are based on Sokal and Rohlf

(1981) and asymmetrical confidence limits (±95%) for the model II slope are consistent with formula 1 of Ricker (1975).

Our water column nutrient data from Resolute Passage and Barrow Strait are compared with other nutrient data selected on the basis of location and salinity characteristics from several sources, including other sites in the Northwest Passage of the Canadian Arctic Archipelago and the Arctic Ocean. The "Resolute" data of Jones and Coote (1980) represent late summer and were collected slightly "downstream" (east) of our study area in a meridonal section across Barrow Strait from the southeastern corner of Cornwallis Island during August or September, 1977. The early spring data of the Institute of Ocean Sciences (Sidney, British Columbia) were collected from April 1–15, 1982 from several locations in the western Northwest Passage which are "upstream" (west) from our study area; nutrient data were selected with salinities over 31.00 and less than 34.00 (Buckingham et al. 1985; R. A. Lake, Institute of Ocean Sciences, Sidney, British Columbia, pers. com.). We also examined data from the Arctic Ocean which were collected during April 28–May 16, 1983 over the Alpha Ridge by Jones and Anderson (1986) and by Moore et al. (1983) during April 16–May 15, 1979 over the Lomonosov Ridge near the north pole. Only data with salinities in excess of 31.00 and less than 33.10, which corresponds to surface waters above the nutrient maximum at both sites, were included in regression analyses for data from the Arctic Ocean. The open ocean data show similarities in slope, but these data are not considered in the regression line presented for the waters from the Northwest Passage (see Table 1 and Fig. 3).

Nutrient and salinity profiles collected over the entire ice sheet (i.e. "bulk ice") from this study are also compared with similar data collected from the Chukchi Sea near Barrow, Alaska in 1972 (Alexander et al. 1974) and from Frobisher Bay in the Northwest Territories, Canada during 1979–81 (Grainger and Hsiao 1982). Data from the Chukchi Sea near Barrow, Alaska are from 15–20 cm core segments taken from the top, middle, and bottom of the ice sheet. Core segments varied from 5 to over 50 cm in Grainger and Hsiao's (1982) Frobisher Bay study; in the first two samples of 1979 short 5 cm segments were sawn from the top, middle, and bottom of complete ice sheet cores, but all subsequent cores were roughly divided into thirds. Most of the ice cores from both studies were collected from March through June. Only core samples with chlorophyll values $\leq 25\ \mu g \cdot L^{-1}$ were used in these data analyses to minimize the possible influence of biologically mediated accumulations (see below); with this criterion only six observations on bottom ice segments were disqualified from the core profile data sets, leaving a total of about 90–100 observations. All three of the bottom ice segments from the complete ice cores in this study, two from Barrow, Alaska and one from Frobisher Bay, NWT were deleted.

Dilution curves for nutrient concentration vs. salinity were constructed for the combined sea ice and seawater data from our 3 yr study and the ice sheet profile data from Alexander et al. (1974) and Grainger and Hsiao (1982). Dilution lines were fitted by eye, passing the line through the origin and an unweighted average value of the three annual means for waters from the "surface mixed layer". These dilution curves represent the expected nutrient vs. salinity relationship which would result from progressive additions of deionized freshwater (or the nearly freshwater of sea ice) to full strength surface seawater.

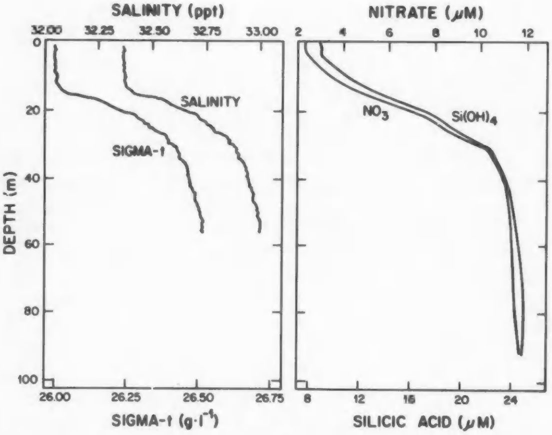

FIG. 2. Vertical profiles of salinity and density (left panel) or nitrate (NO_3) and silicic acid ($Si(OH)_4$) (right panel) from st. 5 on May 19, 1985 (after Cota and Horne 1989).

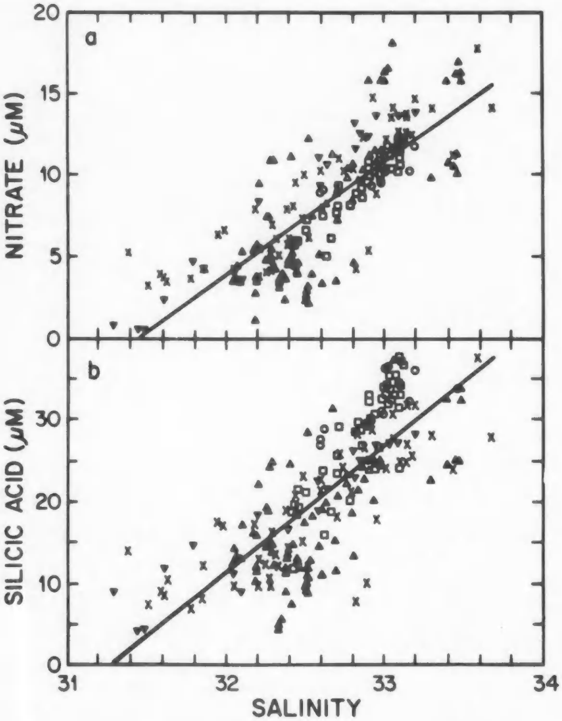

FIG. 3. Nitrate (a) or silicic acid (b) versus salinity for depths <200 m from several studies in the Northwest Passage of the Canadian Arctic Archipelago. Sites, years and symbols: Barrow Strait 1983, stn. 42 (squares), Resolute Passage 1984, stns. 3 and 5 (circles), Resolute Passage 1985, stn. 5 (triangles), Northwest Passage 1982 (diagonal crosses, x) and eastern Barrow Strait 1977 (inverted triangles). See Fig. 1, Table 1 and methods for sources.

Results

Vertical distributions of nitrate and silicic acid typically reveal structure similar to salinity and density profiles with the lowest values in the "surface mixed layer," a nutricline coincident with the pynocline and the highest values at depth in the "bottom mixed layer" (Fig. 2). However, there may be marked differences within the so-called "surface mixed layer" where there is usually very little, if any, density stratification, while nitrate and silicic acid concentrations often exhibit gradients with 1–4 mmol differences over this same interval (Fig. 2; Cota and Horne 1989). The major inorganic nutrients show a high degree of similarity in their distributions, behaving conservatively with respect to salinity, unless influenced by biological activities (e.g. Jones and Coote 1980). Significant relationships were found for nutrient–salinity data, collected from a variety of times, locations, and depths, (Fig. 3, Table 1). Only the silicic acid data from LOREX (Moore et al. 1983) appeared to be different, lying well above the other observations but with a similar slope (Table 1).

Phosphate concentrations were measured with less relative precision, and profiles displayed less discernible vertical structure in excess of analytical errors; consequently, we will not consider our phosphate data in detail. However, nutrient ratios help illustrate differences in relative abundance or fractionation between solid and liquid phases (Table 2). Because phosphate is regenerated relatively rapidly in marine systems (e.g. Harrison 1980), it is much less likely to be limiting and display the same degree of depletion.

Relatively high resolution sampling of the water column revealed several important features of the nutrient field vs. time (Fig. 4). First, there was always a pronounced nutricline for nitrate and silicic acid beween 15–30 m where concentrations increase 3–6 μM and 5–10 μM, respectively, with depth. The pycnocline and nutricline coincide within this depth interval (Fig. 2). Second, below the pycnocline nutrient concentrations are relatively constant in this and previous data sets (Cota et al. 1987), but Fig. 4 suggests that different water masses were advected through the area. Silicic acid concentrations at depth were relatively low during the first 4 d of the series and the molar ratios of NO_3:Si $(OH)_4$ were the highest (0.63–1.10) we have ever noted in the water column. These four profiles may be anomalous. About day 145 another water mass moved through our study site, characterized by elevated nutrient concentrations and more typical molar ratios of NO_3:Si $(OH)_4$ (see footnote for Table 2). The final aspect of particular note is the presence of persistent gradients across the "mixed layer" (Fig. 2) and minima (Fig. 4) near the interface. Surface waters were at or very near their freezing point and there was very little salinity or density stratification evident above about 10–12 m in CTD profiles collected during this period and the preceding 9 d (Cota and Horne 1989; E.P.W. Horne, Bedford Inst. of Oceanography, Dartmouth, N.S., unpubl. data; H. E. Welch, Freshwater Institute, Winnipeg, Man., unpubl. data). The "surface mixed layer" was defined functionally as the layer with salinity differences <0.05.

If only the "surface mixed layer" is considered, then the nitrate vs. salinity relationship displayed a Model I regression slope not significantly different from zero ($P \leqslant 0.05$) and the slope for the silicic acid relationship is barely significant ($P \leqslant 0.05$) (Fig. 5). Moreover, these relationships explain only about 4 and 9% of the variance in the data, respectively.

The differences between the ice and water environments are often very striking and remarkably consistent, between locations and different years. Salinity values in ice cores (Table 2) and within both the surface and bottom mixed layers are relatively constant; salinities within the sea ice sheet versus bottom ice (only lower few cm) are roughly 20 and 30%, respectively, of surface seawater. Nutrient levels within the ice sheet are nearly in proportion to salinity with concentrations around 20%

TABLE 1. Relationships for water column data from the Northwest Passage and the Arctic Ocean (sources in methods). Symmetrical 95% confidence limits are given for the slope of the model I (LS) regression and the approximate asymmetrical 95% confidence interval for the model II (GM) regression. Abbreviations and units are Res (Resolute), NWP (Northwest Passage), All (Arctic Ocean plus NWP), NO_3 (nitrate, μM), $Si(OH)_4$ (silicic acid, μM), PO_4 (phosphate, μM) and salinity (SAL, $g \cdot kg^{-1}$). All slopes were highly significant ($P < 0.001$).

Data set	Y, X	N	LS slope (±95% CI)	Intercept	r^2	GM slope (95% CI)
Res	NO_3, SAL	174	8.4 (±1.0)	−267.4	0.64	10.5 (9.6,11.5)
Res	$Si(OH)_4$, SAL	174	19.7 (±2.5)	−622.4	0.59	25.8 (23.4,28.4)
Res	PO_4, SAL	174	0.8 (±0.2)	−23.0	0.22	1.6 (1.4,1.9)
NWP	NO_3, SAL	247	7.1 (±0.7)	−222.0	0.64	8.8 (8.2,9.5)
NWP	$Si(OH)_4$, SAL	247	15.7 (±1.7)	−489.8	0.59	20.4 (18.8,22.1)
NWP	PO_4, SAL	247	0.5 (±0.1)	−15.3	0.19	1.2 (1.0,1.3)
All	NO_3, SAL	261	7.1 (±0.7)	−223.6	0.59	9.3 (8.6,10.1)
All[a]	$Si(OH)_4$, SAL	261	15.9 (±1.7)	−496.2	0.57	21.0 (19.4,22.7)
All	PO_4, SAL	261	0.5 (±0.1)	−15.3	0.19	1.2 (1.0,1.3)

[a](with LOREX data: $Y = 10.0X - 305.2$; $r^2 = 0.50$; $N = 290$).

TABLE 2. Environmental conditions for the ice sheet (≃ 0–155 cm), bottom ice (lowest 3–5 cm) and seawater from the "surface mixed layer" (top 10–15 m) or "bottom mixed layer" (≥50 m). Values are means ± standard deviations for the total numbers (*N*) of ice cores or seawater samples with data available. ND is no data. Sampling intervals as day of the year are given for each set of observations. Abbreviations and units as in Table 1.

Sample type	Ice sheet			Bottom ice			Surface seawater			Bottom seawater		
	1984	Barrow[a]	Frobisher[b]	1983	1984	1985	1983	1984	1985	1983	1984	1985
No. obs. (*N*)	18	46	37	31	117	96	33	68	160	38	28	60
Core vol. (ml)	≃205	—	—	201 (±14)	183 (±14)	168 (±30)	—	—	—	—	—	—
Salinity ($g \cdot kg^{-1}$)	6.8 (±1.7)	6.2 (±1.1)	4.4 (±1.7)	ND	8.9 (±1.0)	9.9 (±1.3)	32.55 (±0.06)	32.81 (±0.20)	32.34 (±0.17)	33.04 (±0.02)	33.05 (±0.14)	33.08 (±0.24)
Nitrate (μM)	1.7 (±1.3)	1.6 (±0.5)	0.5 (±0.4)	7.2 (±4.8)	10.8 (±5.1)	18.3 (±17.9)	6.8 (±0.9)	8.9 (±1.0)	4.3 (±1.1)	11.6 (±0.7)	11.6 (±0.6)	12.4 (±2.1)
Sil. acid (μM)	3.9 (±1.4)	4.2 (±1.2)	3.2 (±2.4)	6.5 (±2.2)	9.1 (±2.4)	6.9 (±3.0)	21.2 (±2.9)	28.6 (±2.3)	11.8 (±3.7)	33.4 (±2.6)	35.7 (±1.2)	25.9 (±4.4)
Phosphate (μM)	0.4 (±0.2)	0.1 (±0.1)	0.2 (±0.3)	1.7 (±1.3)	2.5 (±1.2)	4.1 (±4.9)	1.7 (±0.6)	1.2 (±0.1)	1.1 (±0.3)	1.9 (±0.7)	1.3 (±0.1)	1.6 (±0.3)
NO_3:$Si(OH)_4$ (mol:mol)	0.40 (±0.23)	0.38 (±0.13)	0.39 (±0.59)	1.1 (±0.6)	1.3 (±0.7)	2.3 (±1.5)	0.32 (±0.02)	0.31 (±0.01)	0.40[c] (±0.21)	0.35 (±0.03)	0.32 (±0.01)	0.48 (±0.05)
PO_4:NO_3 (mol:mol)	0.34 (±0.17)	0.09 (±0.12)	0.61 (±0.60)	0.24 (±0.11)	0.25 (±0.13)	0.23 (±0.15)	0.25 (±0.08)	0.13 (±0.01)	0.27 (±0.04)	0.16 (±0.05)	0.11 (±0.01)	0.12 (±0.01)
Chlorophyll ($\mu g \cdot L^{-1}$)	4.0 (±3.2)	4.4 (±5.1)	2.0 (±3.6)	297 (±344)	345 (±280)	704 (±641)	0.09 (±0.03)	0.10 (±0.12)	0.44 (±0.38)	0.03 (±0.02)	0.05 (±0.06)	0.09 (±0.06)
Day nos.	131	28–164	69–346	97–159	98–158	97–145	84–121	93–158	135–155	84–121	93–158	135–155

[a] From Alexander et al. (1974).

[b] From Grainger and Hsiao (1982).

[c] (0.31 ± 0.03 without four anamolous profiles on days 135–138).

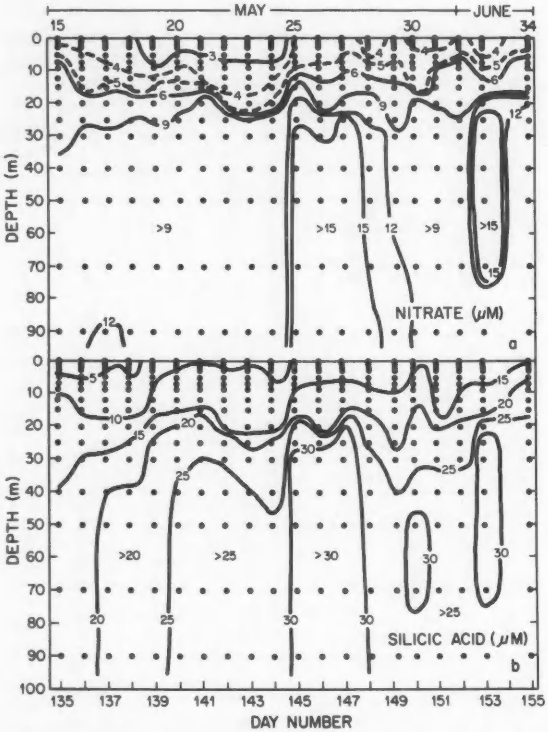

FIG. 4. Nitrate (a) and silicic acid (b) concentrations at station 5 in Barrow Passage, NWT from May 15 (day 135) to June 4 (day 155), 1985.

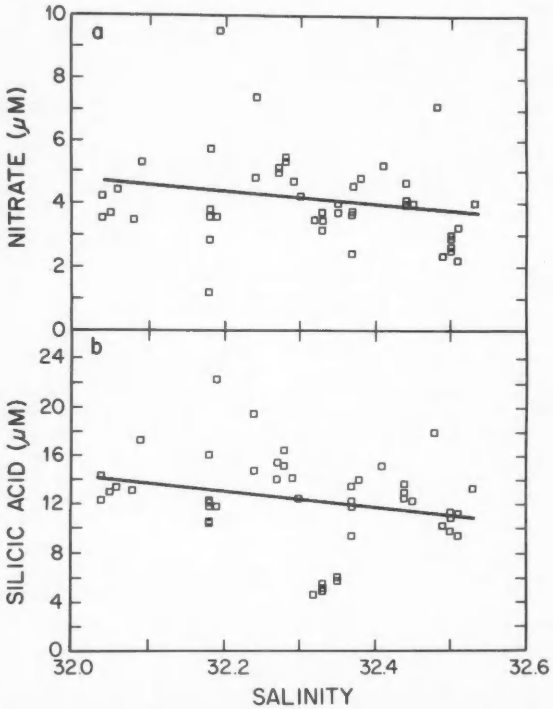

FIG. 5. Nitrate versus salinity (a) and silicic acid versus salinity (b) from the "surface mixed layer" with salinity differences less than 0.05 at station 5 in Resolute Passage, NWT from May 15 to June 4, 1985.

those of surface seawater. Average nitrate and phosphate concentrations in colonized bottom ice are normally higher than surface seawater and display the same trend in interannual variations as observed for chlorophyll concentrations in the bottom layer. However, average silicic acid concentrations in bottom ice are only about twice those within the ice sheet or approximately 30% of surface seawater values, except in 1985 when levels of ice algal biomass were highest and surface silicic acid concentrations were lowest. Nutrients within the "well-mixed" surface layer are generally abundant, well above levels normally thought to be limiting for microalgal growth, but substantial gradients are consistently present when there are large ice algal biomass accumulations.

Average molar ratios of nitrate:silicic acid (NO_3:Si $(OH)_4$) within the ice sheet were fairly consistent between the three sites ranging from 0.38 to 0.40. Average values of NO_3:Si $(OH)_4$ in bottom ice were >1.0 and followed a trend similar to algal biomass over the 3 successive yr (Table 2). Values for the same ratio in seawater wre considerably lower than in bottom ice and were relatively constant from year to year with a range from 0.31 to 0.40 above the pycnoclite and 0.32–0.48 below the pycnoclite. Average values for the molar ratio of phosphate:nitrate (PO_4:NO_3) were also relatively constant, ranging from 0.23 to 0.27, from year to year in bottom ice and in surface seawater with the exception of the ice sheet numbers and surface seawater in 1984. The mean value of phosphate:nitrate for surface seawater in 1984 was 0.13 which was similar to values below the pycnocline for all years (0.11–0.16). There was much more variability in the ice sheet data and little consistency between sites; the phosphate data are probably the least reliable of these three nutrients.

Plant biomass, averaged over the entire 1–2 m ice sheet and seasonally, was usually several times higher than in surface waters but much less concentrated than in the thin (<5 cm) bottom ice layer (Table 2). Chlorophyll within bottom ice was, on average, about two times more concentrated in 1985 than the 2 previous yr. Chlorophyll concentrations in surface seawater were normally less than 0.1–0.5 μg CHL·L^{-1} throughout our observations. Hence, chlorophyll levels were often above three orders of magnitude higher in bottom ice compared with surface seawater and much of the chlorophyll in seawater was probably derived from the ice (erosion, sinking, etc.).

The distributions of nutrients and algal biomass are weakly related, if at all, when considered over the whole ice sheet (Table 3). Ice sheet profiles at three different study sites produced comparable grand means in most cases (Table 2), but of the major inorganic nutrients only nitrate displayed a relationship with chlorophyll where the slope was significantly different than zero (Table 3). Nevertheless, all of the nutrients showed significant, positive relationships with ice salinity. The relationships for nitrate, silicic acid, phosphorus, and ammonium vs. salinity explained 42, 15, 5, and 14% of the variance in the data, respectively. However, if the Frobisher Bay data are not considered in the relationships for silicic acid and phosphate, the fits are much improved with 39 and 23% of the variances explained ($N = 64$ in both cases). The silicic acid data in Grainger and Hsiao (1982) must be considered with care, because a number of zero values were reported and these data pairs were not included in our analyses; also, their phosphate data were the most variable of the three data sets with a standard deviation greater than the mean concentration (Table 2).

The concurrent accumulation of nutrients and biomass in bottom ice was evident from our earliest time courses (Fig. 6) and point observations (Fig. 7) in 1983. Both nitrate and phosphate increased 6–8 fold over the first month, while silicic acid increased only slightly. Hence, silicic acid in the bottom ice layer was present at about the levels expected (i.e. about 30% of the concentration in the source seawater with a salinity near 32.5 and a silicic acid content around 30 μM; Cota et al. 1987), but nitrate and phosphate levels in bottom ice often equaled or exceeded concentrations in the underlying seawater by the end of the month of April. Over this same period chlorophyll (CHL) concentrations in the last few centimeters of ice increased rapidly to almost $1.2 * 10^3$ μg CHL·L^{-1} and the molar ratio of nitrate:silicic acid in bottom ice rose from about 0.3 to over 1.8. Within the time frame of the ice algal bloom these time-course data represent early through mid-season and very late season observations. In late spring (June) 1983 we also found

TABLE 3. Relationships for all ice sheet profile data with chlorophyll (CHL) < 25 μg·L^{-3} (sources in methods). Confidence intervals for slopes, abbreviations and units are the same as in Table 1. ns ≡ not significant; * $P < 0.05$; ** $P < 0.01$; *** $P < 0.001$

Data set	*Y, X*	*N*	LS slope (±95% CI)	Intercept	r^2	GM slope (95% CI)
Ice	NO_3, CHL	103	0.062** (±0.037)	0.97	0.10	0.20 (0.16,0.24)
Ice	$Si(OH)_4$, CHL	93	0.017^{ns} (±0.080)	3.78	0.002	0.39 (0.31,0.47)
Ice	PO_4, CHL	102	-0.001^{ns} (±0.009)	0.22	0.0003	−0.05 (−0.04,−0.06)
Ice	NH_4, CHL	84	0.052^{ns} (±0.086)	3.65	0.02	0.40 (0.32,0.49)
Ice	NO_3, SAL	101	0.32*** (±0.07)	−0.60	0.42	0.49 (0.42,0.57)
Ice[a]	$Si(OH)_4$, SAL	91	0.43*** (±0.21)	1.36	0.15	1.09 (0.89,1.32)
Ice[b]	PO_4, SAL	100	0.03* (±0.02)	0.06	0.05	0.12 (0.10,0.14)
1985	NH_4, SAL	84	0.41*** (±0.22)	1.60	0.14	1.09 (0.89,1.33)

[a] Without Frobisher Bay data: $Y = 0.58X + 0.45$, $r^2 = 0.39$, $N = 64$.

[b] Without Frobisher Bay data: $Y = 0.05X - 0.14$, $r^2 = 0.23$, $N = 64$.

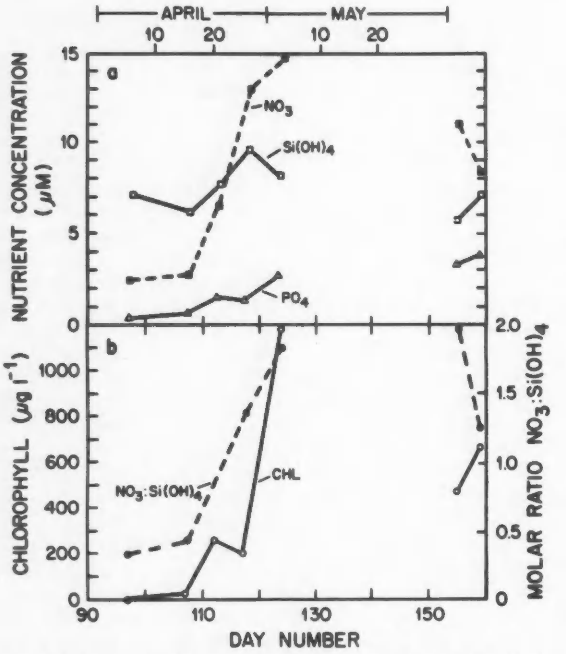

FIG. 6. Mean concentrations of nitrate (NO_3), silicic acid ($Si(OH)_4$), and phosphate (PO_4) in bottom ice under low snow in 1983 (a). Chlorophyll (CHL) concentration and the molar ratio of nitrate:silicic acid (NO_3:$Si(OH)_4$) in the same ice cores (b).

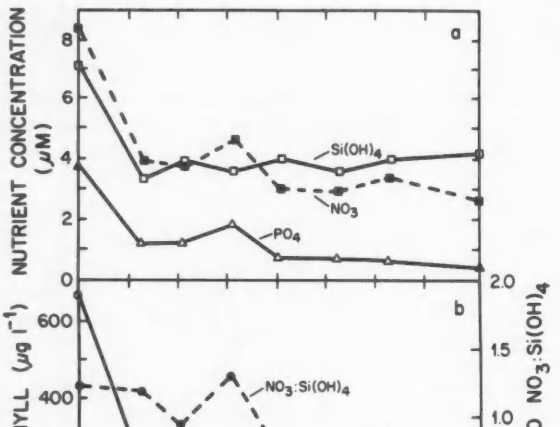

FIG. 7. Concentrations of nitrate, silicic acid and phosphate versus depth of snow cover for ice cores collected on June 6, 1983 (a). Chlorophyll and the molar ratio of nitrate:silicic acid from the same cores (b). Symbols as in Fig. 6.

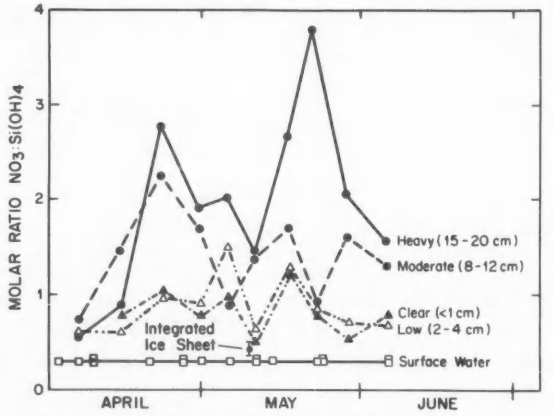

FIG. 8. Temporal changes in the molar ratio of nitrate:silicic acid from station 3 in 1984. Bottom ice from heavy (HVY),moderate (MOD), low (LOW) and no snow (CLR) cover are compared with surface seawater and a value for the entire ice sheet.

that nutrient concentrations in bottom ice paralleled levels of biomass (Fig. 7) in samples collected along a gradient of snow cover (and ambient light levels). Nutrient levels, algal biomass, and the molar ratio of nitrate:silicic acid (NO_3:$Si(OH)_4$) all decreased with increasing snow depth, which decreases the in situ growth irradiance (Smith et al. 1988). The snow cover was starting to melt rapidly during this period and snow depth decreased ca. 1 $cm \cdot d^{-1}$ for the preceding 2–4 d. Hence, snow depths in this series of observations may be underestimated by several centimeters; there were no snow-free areas (i.e. 0 cm) near our study site prior to melting.

Nutrient ratios in the ice sheet, bottom ice and surface seawater confirm that a fractionation or differential accumulation occurs between these three sites. Shortly after the onset of the ice algal bloom in 1984 molar ratios of NO_3:$Si(OH)_4$ for bottom ice populations from all snow depths were already well above those typical for surface seawater and for the integrated ice sheet (Fig. 8). Even though molar ratios of NO_3:$Si(OH)_4$ were nearly constant at 0.33 in surface seawater, they were highly variable in bottom ice and ranged from about 0.5 to almost 4 over the next 2 mo. In 1985, when biomass accumulations were greatest, values of NO_3:$Si(OH)_4$ in bottom ice were even higher and more variable than previous years (Table 2).

Except for silicic acid, nutrients in bottom ice tend to covary with algal chlorophyll biomass (Fig. 9). Pooled data from 1983–85 show that both nitrate and phosphate are more highly correlated than silicic acid. Over half the variance in the data were explained by predictive regression relationships (Table 4) for nitrate or phosphorus versus chlorophyll. The corresponding relationship for silicic acid had the lowest slope and explained only 14% of the variance. Nevertheless, all of the relationships were highly significant ($P < 0.001$). Similar analyses for nutrients v. salinity in melted ice cores revealed weak but significant relationships explaining only 3–13% of the variance (Table 4).

If algal colonization is limited or prevented, then aboslute and relative nutrient abundances in bottom ice are much reduced (Table 5). In early June, 1985 samples from an area covered with reflective "space blankets" for several weeks had much lower levels of biomass, nutrients and a molar ratio for NO_3:$Si(OH)_4$ only slightly higher than surface seawater. In

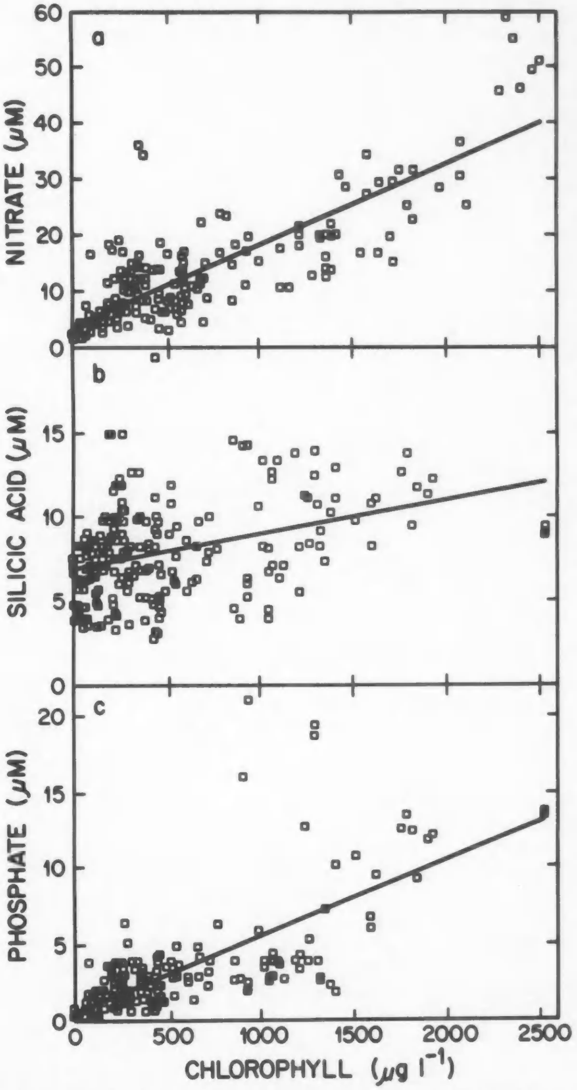

FIG. 9. Nitrate (a), silicic acid (b) and phosphate (c) cncentrations versus chlorophyll concentrations in bottom ice for all samples collected from 1983 through 1985. Lines are least square fits for a model I regression (see Table 4).

contrast, an area with moderate algal growth under low snow cover (3 cm) had much higher absolute concentrations of pigment and nutrients while the relative abundance of NO_3:$Si(OH)_4$ was over 2.0.

The vertical microdistributions of biomass and nutrients in sea ice were not examined in detail in this study, but a few observations on the concentrations in thin layers from the bottom of sea ice reveal marked differences in vertical zonation (Table 5). The bottom 5 mm of ice (i.e. 0–5 mm) usually had much higher levels of nutrients, excluding silicic acid, and chlorophyll than either the next 5 mm of ice (i.e. 5–10 mm) or the underlying seawater (Table 4). The same pattern was also true for the molar ratios of NO_3:$Si(OH)_4$.

Dissolved salts can be used as conservative tracers to distinguish water/ice masses as well as mixing ratios between them, unless the salts are involved in biogenic cycles. Dilution curves, spanning salinities from zero to undiluted surface seawater, for nutrient salts and total salts (salinity) in this two phase system illustrate the impact of biological activities on each particular nutrient (Fig. 10). Bottom ice has salinities of 6–14, and with the exception of silicic acid, nutrient levels in colonized bottom ice are generally much higher than those in seawater or within the ice sheet. Most salinity values are between 2 and 7 in the bulk ice sheet which has the lowest nutrient levels with values falling fairly close to the dilution line (Alexander et al. 1974; Grainger and Hsiao 1982; Cota et al. 1987). Water column salinities from northern Barrow Strait vary over a small range from about 32.0–33.4, but nutrient levels, can be quite variable, especially in shallow surface mixed layers where biological activities are most intense (e.g. Jones and Coote 1980; Cota et al. 1987, figures 2–5).

Dissolved reactive nitrate in bottom ice samples represents about 1–to 25% of the standing stock of particulate organic nitrogen on a molar basis (NO_3:PON) (Fig. 11). Values of NO_3:PON may also decrease over the season; there was a dramatic decrease in the ratio during mid-April, 1983 under low snow at station 42, and at all snow depths NO_3:PON declined seasonally in 1984 with values about twice as high, on average, before day 130 as those after that time. In 1985 low NO_3:PON ratios were similar to the 1983 average, but remained relatively constant over the season.

Discussion

Nutrients in Seawater

Previous observations on seawater nutrient distributions in the Arctic indicate that the three major dissolved inorganic nutrients, nitrate, silicic acid, and phosphate, are largely conservative with respect to salinity. Conservation, as indicated by a positive linear relationship between nutrients and salinity, has been noted for the ice covered surface waters of the Arctic Ocean with salinities less than about 33.1, corresponding to depths above the nutrient maximum (e.g. Moore et al. 1983; Jones and Anderson 1986). Similar observations have also been made within the Canadian Arctic Archipelago in waters deeper than about 50 m which are not impacted by summer phytoplankton blooms (Jones and Coote 1980). The data compiled here (Fig. 3 and Table 1) are consistent with the conservative behavior of nutrients in systems with little autotrophic activity, extending the seasonal and geographical generality of this result.

There are several sources of variability implicit in the nutrient and salinity data presented in Fig. 3 which exceed the routine analytical uncertainties that might be expected in paired observations from the same bottle sample. Most of our data from 1984 and 1985 represent separate CTD casts for the salinity observations and hydrocasts for the nutrient measurements. The two casts were nearly coincident in time and space, but this practice may introduce considerable noise in the paired observations because of pronounced temporal and spatial variability in the environment. There are strong diurnal tides in this region which result in large fluctuations in current speed (Cota et al. 1987; Prinsenberg and Bennett 1987) and drag induced ''swing out'' of hydrowires. Nutrient data from bottles uncorrected for depth may have been poorly matched to

TABLE 4. Relationships for bottom ice data from this 1983–85 study (see methods). Confidence intervals for slopes, abbreviations and units are consistent with Table 1. $^*P < 0.05$; $^{***} P < 0.001$

Data set	*Y, X*	*N*	LS slope (±95% CI)	Intercept	r^2	GM slope (95% CI)
83–85	NO_3, CHL	235	0.019*** (±0.002)	4.28	0.55	0.025 (0.023,0.028)
83–85	$Si(OH)_4$, CHL	236	0.002*** (±0.001)	6.90	0.14	0.006 (0.005,0.007)
83–85	PO_4, CHL	235	0.005*** (±0.001)	0.64	0.53	0.007 (0.006,0.008)
83–85	NO_3, SAL	200	3.73*** (±1.34)	−20.89	0.13	10.24 (8.98–11.67)
83–85	$Si(OH)_4$, SAL	200	0.39* (±0.31)	4.36	0.03	2.21 (1.92–2.53)
83–85	PO_4, SAL	199	0.89*** (±0.36)	−5.15	0.11	2.68 (2.35–3.06)

TABLE 5. Nutrient, salinity and chlorophyll levels in lower 5 cm of bottom ice (BI), surface seawater (SW) or a mixture of the two; values are averages of 2–3 measurements. Bottom ice samples were collected from a darkened area or regions with low snow cover (2–5 cm); bottom ice was also separated into 5 mm layers in some cores. Abbreviations as in Table 1 plus ammonium (NH_4).

Sample type (Date)	NO_3	$Si(OH)_4$	PO_4	NH_4	NO_3: $Si(OH)_4$	SAL	CHL ($\mu g \cdot L^{-1}$)
		(µM)					
BI: Darkened (3/VI/85)	1.9	4.3	1.2	—	0.44	—	28.5
BI: Low Snow (3/VI/85)	16.0	7.8	4.0	—	2.05	—	1328.8
BI: 0–5 mm (4/VI/85)	59.5	14.1	18.5	21.5	4.22	15	3623.3
BI: 5–10 mm (4/VI/85)	3.4	6.2	1.3	8.8	0.52	14	961.6
SW: Om (4/VI/85)	2.6	10.1	1.5	1.0	0.26	32	1.2
BI: 0–5 mm (2/VI/85)	45.7	14.5	12.0	15.1	3.15	13	4623.1
BI: 5–10 mm (2/VI/85)	3.9	11.7	1.4	14.9	0.33	12	760.1
SW: Om (2/VI/85)	3.0	11.6	1.4	0.2	0.26	33	0.9
BI: 0–5 mm (23/V/85)	—	—	—	9.5	—	14	4853.6
BI: 5–10 mm (23/V/85)	—	—	—	2.5	—	12	—
BI:SW (≈1:8) (23/V/85)	—	—	—	2.2	—	≈30	589.1

salinity–depth observations from the CTD and this problem would be particularly acute in regions with steep gradients. Most of our 1983 data were paired nutrient–salinity measurements from the same bottles and when these data are considered separately the fitted lines explain 92 and 80% of the variance in the relationships for nitrate vs. salinity and silicic acid vs. salinity, respectively; much of the variability in these data were associated with the pycnocline–nutriclite region (Cota et al. 1987). Other data sets with matched nutrient–salinity observations from the same bottle also display much less variability (e.g. Jones and Coote 1980; Jones and Anderson 1986). Given that the data in Fig. 3 were collected by a variety of techniques at various times, locations, and depths, some of the variance is presumably artifactual and could have been eliminated with standardization. Nevertheless, during much of the year, nutrients are largely conservative with respect to seawater salinity in the Northwest Passage except for surface waters when ice algal and phytoplankton blooms develop.

The appearance and persistence of nutrient minima (Fig. 4) and steep gradients (Fig. 2) across the "surface mixed layer" during spring tides, the periods of strongest vertical mixing, indicates intense biological activity and implies a strong source–sink relationship (Cota et al. 1987; Cota and Horne 1989). Spring tides were centered around days 141 (May 21st) and 155 (June 4th). Nutrient concentrations in surface waters were largely independent of salinity during this period (Fig. 5) when biomass and nutrient concentrations in bottom ice were high (Table 2; Cota and Horne 1989). Levels of biomass and production in the phytoplankton are very low with little in situ consumption of nutrients in the water column during the winter–spring transition (Table 2; Cota unpubl. data). Dilution of nutrients in surface waters by the melting of sea ice or terrestrial runoff should have been negligible and would be inconsistent with nearly constant salinities. Hence, the biogenic activities of the ice algae must have been responsible for the observed nutrient depletion immediately below the ice. Moreover, Smith et al. (1988) and Cota and Horne (1989) reported maximum photosynthetic activities during the spring tides corresponding to this same time series.

Nutrients in Sea Ice

Bulk ice sheet

Based upon our knowledge of sea ice formation and structure (e.g. Weeks and Ackley 1982; Maykut 1985), inorganic nutrients, like other salts, should be largely excluded from the ice matrix. Vertical profiles of inorganic nutrients through sheets or floes of sea ice suggest that nutrient salts do, in fact, behave similarly to other solutes (Alexander et al. 1974; Grainger 1977; Grainger and Hsiao 1982; Cota et al. 1987). However, sea ice studies in the Arctic which have measured both ice salinity and nutrient concentrations are scant and equivocal with little methodological consistency in sample collection between studies (Meguro et al. 1967; Alexander et al. 1974; Grainger 1977; Grainger and Hsiao 1982; Horner and Schrader 1982). For example, Meguro et al. (1967) collected irregular fragments from warm, summer (older) ice in July–August, but during spring others have examined full length ice cores or selected segments of ice cores (Alexander et al. 1974 (their

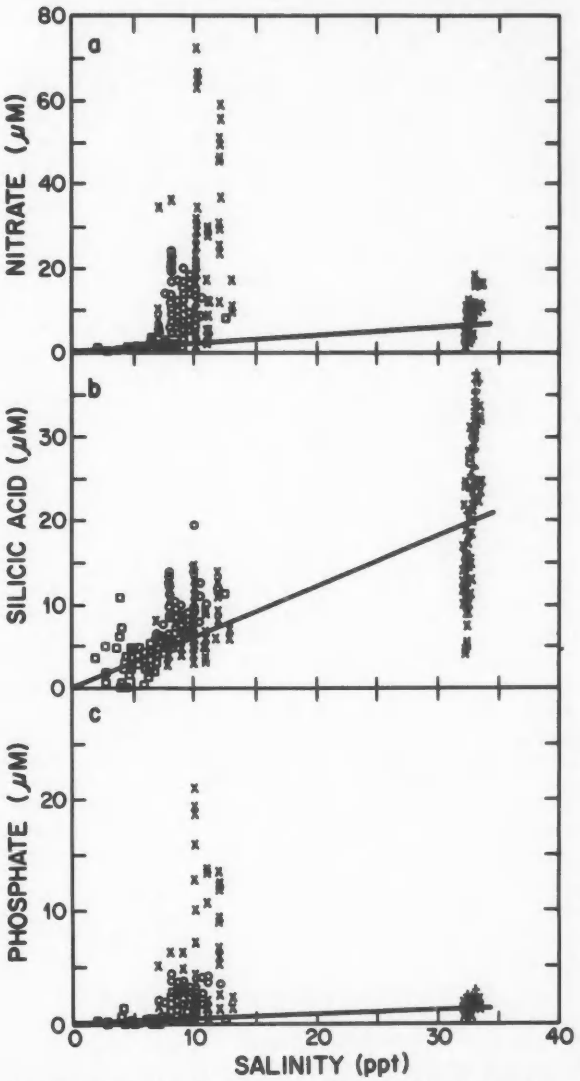

FIG. 10. Dilution lines for nitrate (a), silicic acid (b) and phosphate (c) versus salinity in sea ice column, bottom ice and seawater. Sample types and symbols: ice sheet profiles from three studies (open squares, □) or bottom ice and seawater for 1983 (vertical crosses, +), 1984 (open circles, ○) and 1985 (diagonal crosses, ×) from this study. See methods for sources.

1972 data); Grainger and Hsiao 1982; Cota et al. 1987) or the bottom portion of ice with some seawater and "interstitial waters" (Alexander et al. 1974 (their 1973 data); Horner and Schrader 1982). If standardized sampling techniques (e.g. SIPRE corer) are not employed for collections of ice cores, then it is difficult to compare and intercalibrate results which include variable amounts of seawater, "interstitial water" and sea ice (Alexander et al. 1974; Horner and Schrader 1982).

No previous studies have explicitly considered relationships between nutrients and salinity in their data, although Meguro et al. (1967) and Grainger (1977) allude to the possibility. The relationships between nutrients (including nitrate, silicic acid, phosphate, and ammonium) and salinity summarized in Table 3 are the first of their kind described for land fast annual ice in the Arctic. If one considers the bulk ice sheet in the spring when there is little, if any, algal activity within the cold (≈ −30°C to −3°C) interior ice, then all of the major dissolved inorganic nutrients appear to be conservative with respect to other salts. Tighter relationships with less variability might be obtained with consistent techniques.

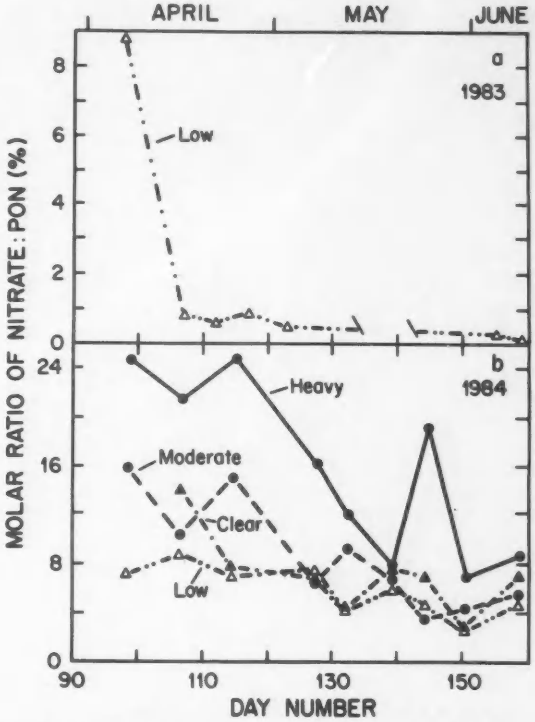

FIG. 11. Seasonal changes of the "intracellular" nitrate pool as a percentage of particulate organic nitrogen (PON) in bottom ice. Values are molar ratios of nitrogen ($N\text{-}NO_3$:N-PON). Ice algal populations were from low snow in 1983 (a) and from several snow depths in 1984 (b).

Bottom Ice Layer

Nutrients within the relatively warm bottom layer of interfacial ice (ca. skeletal ice layer (Maykut 1985)), where there is substantial algal colonization, do not appear to conform to simple physical–chemical observations and expectations. Our initial observations revealed that concentrations of nitrate and phosphate within the bottom few centimeters of sea ice increased by over fivefold during the first half of the spring ice algal bloom (ca. April), often attaining levels in excess of those in the underlying seawater (Fig. 6). In contrast, concentrations of silicic acid in bottom ice changed little over that same period and the levels were around 30% those of surface seawater, about that expected from simply freezing the source seawater. The different behavior patterns for silicic acid vs. the other nutrients were paradoxical but consistent with subsequent observations, which confirmed a positive relationship between nutrient abundance and the degree of algal colonization (Fig. 7). Furthermore, the relative abundance of dissolved nitrate and silicic acid also changes markedly over time within the bottom ice algal layer, and it is higher than the ratio for seawater (Fig. 8). Silicic acid, on the other hand, increases only slightly with increasing algal biomass and displays much more variability (Fig. 9 and Table 4). If there was conservation of nutrients in bottom ice, then stronger relationships with less variance might be expected between nutrients and ice salinity. Although the relationships for nutrients and salinity are statistically significant, they explain a much smaller fraction of the variance in the data than chlorophyll (Table 4).

The different molar ratios of NO_3:$Si(OH)_4$ in the bottom layer of sea ice compared with the ice sheet and seawater (Figs. 4–6 and Table 2) suggests that some selective accumulation must occur between these pools and that Si is most likely to be limiting. The bulk ice sheet on May 10, 1984 displayed an average value of 0.40 for the NO_3:$SI(OH)_4$ ratio while surface seawater was nearly constant at 0.31 for 2 mo (Fig. 8 and Table 2). A comparison of the water column data from this study and others revealed a significant positive relationship between NO_3:$Si(OH)_4$ ratios vs. salinity in seawater, but even at maximum depths (<200 m) values were normally below 0.50. However, even early in the ice algal blooms NO_3:$Si(OH)_4$ ratios in bottom ice were often elevated, averaging from about 1 to over 2 during the bloom period. Most of the variance in this ratio was due to fluctuations in nitrate concentrations because silicic acid levels are relatively constant and much closer to expectations based simply upon salt exclusion (Table 2).

Our nutrient data from bottom ice communities suggest that ice algae and/or other organisms in the bottom ice layer accumulate significant amounts of dissolved nutrients which are released, at least in part, when ice cores are simply melted. If ice cores are not melted in ample seawater, osmotic shocks may result from rapid reductions in ambient salinity. Garrison and Buck (1986) have shown that cell lysis may introduce bias in the composition and abundance of ice organisms, particularly flagellates and ciliates, if ice cores are not diluted prior to melting. Bates and Cota (1986) also found large differences in induced fluorescence and photosynthetic activities of ice algal suspensions which were diluted with seawater before and after melting of ice crystals. No difference was observed between chlorophyll measurements in diluted and undiluted ice samples (Cota, unpubl. data). Meguro et al. (1967) suggested that osmotic pressure, which is dependent upon the temperature and salinity of brines, may limit the vertical penetration of organisms into the ice. Ice organisms may experience a wide range of salinities in microenvironments from highly concentrated brines (e.g. 60–90) in brine channels and pockets or low salinities (ca. 10–30) in melt water lenses, but we have yet to document many microgradients and evaluate their impact upon ice organisms.

Ice–Water Interactions and Comparisons

Dilution lines (Fig. 10) help to clarify the abundance of the nutrients in the various pools of the environment and to evaluate the processes which may be responsible for their distributions. Except in shallow melt-water lenses, the salt content of the water column varies from only about 31–34 over the entire year (Prinsenberg and Bennett 1987). The large gap in the nutrient–salinity data in Fig. 10 is due to salt exclusion from the sea ice at the time of freezing. Each line passes through the origin and the mean of the annual values for the "surface mixed layer" (Table 2). Near the origin, nutrient values which fall above the line indicate nutrient accumulation in ice, and conversely, nutrient depletion is suggested by points below the line. Most of the data points (Fig. 10, open squares) for nutrients measured over the entire ice column are closest to the origin and lie relatively close to the dilution line, but the bottom ice data for nitrate and phosphate (at slightly higher, intermediate salinities) are usually well above the dilution line implying that they are highly concentrated in this thin layer (Table 2). In fact, nitrate, phosphate, and ammonium concentrations often exceed even the highest values for the water column at depth. In contrast, silicic acid may occasionally approach levels comparable with average surface seawater values, or it may also be less abundant than predicted (Fig. 10); however, it was the most variable of the nutrients when compared to chlorophyll or salinity in bottom ice (Table 4). The relatively high concentrations of nitrate, ammonium, and phosphate imply that these nutrients are actively accumulated within the colonized bottom ice layer, whereas silicic acid is usually much closer to the level expected for sea ice formed from the source seawater. Any accumulations of silicic acid are of a much smaller magnitude and are much more variable (Fig. 10).

Although there may be some unknown chemical fractionation operative in bottom ice which is selective against silicic acid compared to the other nutrients, the biogenic activities of the ice algae must be the primary mechanism responsible for the observed nutrient accumulations and the variable compositional ratios of these nutrients (Fig. 6–8). Most silicon is presumably converted into unreactive polymers and siliceous valves (Sullivan 1986), while nitrogen and phosphorus compounds are normally incorporated into particulate organic pools (Cembella et al. 1984; Wheeler 1983). Excluding silicic acid, over half of the variability in the nutrient data appears to be related to changes in ice algal biomass in the bottom ice layer (Fig. 9 and Table 4). Furthermore, the nutrient–salinity relationships for the bottom ice layer explain only a small portion of the variance in the data (Table 4), so conservation of nutrient salts can not be invoked. If physical–chemical processes were solely responsible for the accumulation of the other nutrients in this layer, then we would expect a much better relationship with salinity. However, the behavior of most nutrients in bottom ice appears to be biologically mediated with the total pool size of these nutrients varying directly with chlorophyll. The apparent layering of algal biomass and nutrients in the bottom centimeter of ice lends further support to this scenario (Table 5). Moreover, Conover et al. (1990) present high resolution microprofiles (their figure 7) 6 cm into the ice which show a strong association between chlorophyll and nitrate concentrations; in their 1986 study of concentrations of nitrate and ammonium greater than 50 μM and 10 μM were common in the ice algal layer with chlorophyll normally in excess of 5 $mg \cdot L^{-1}$ (their figure 8).

Conservation of mass requires that accumulations of nutrients in bottom ice must be offset by depletions elsewhere. We have collected very little data over the whole ice column, but the nutrient salts within the entire ice sheet are not abundant enough to account for the observed ice algal growth and these nutrient salts are dispersed through out the ice sheet, unavailable for consumption (Cota et al. 1987). Depletion of nitrate and silicic acid in the waters of the "surface mixed layer" is indicated by the existence of steep gradients (Fig. 2; Cota and Horne 1989), nutrient minima (Fig. 4) and the failure of nutrients to behave conservatively (Fig. 5). The large number of seawater observations (with relatively low salinities) falling below the dilution line in Fig. 10 also suggests a lower nutrient load in surface waters, although there was substantial interannual variation in average nutrient levels in surface waters (Table 2) and each year's data set should have its own dilution line.

Soluble Intracellular Nutrient Pools

Recent reviews by Wheeler (1983), Sullivan (1986), and Cembella et al. (1984), respectively, indicate that soluble intracellular pools of nitrogen, silicon, and phosphorus in phytoplankton are usually a small percentage of the total cellular content of these elements. However, compared with total cellular nitrogen, intracellular pool sizes range from 0 to about 30% for nitrate or from 0 to 66% for ammonium (Wheeler 1983). Intracellular pools of soluble silicon are less variable, ranging from about 5–20%; half of this soluble Si pool may be unreactive polymers, which do not form a blue silicomolybdate complex, and hence unmeasured (Sullivan 1986). Phosphorus is stored in intracellular pools by phytoplankton as soluble phosphate and as readily-hydrolyzed polyphosphates; up to 70% of the total cellular P may be in such storage forms under conditions of P-sufficiency (Cembella et al. 1984). Intracellular concentrations of nutrients may also be extremely high compared to ambient seawater (μM) concentrations with intracellular values in excess of 100 mM (Sullivan 1986). Pool sizes apparently depend upon nutrient status and, at least for nitrogen and phosphorus, they tend to be highest under nutrient replete conditions.

Our observations suggest that there is interannual, seasonal and spatial variation in the amount of nitrate pooled by ice algae (Fig. 11). Differences between 1984 vs. the other 2 yr, 1983 and 1985, were marked with most values in the second year ranging from 4 to 10% except under heavy snow, while those in the first and third years were usually below 1–2%. In the first 2 yr pool sizes declined seasonally with a large change in mid-April in 1983 followed by a gradual decrease and in 1984 decreases were nearly monotonic except under heavy snow cover which had the largest pools throughout the entire season (Fig. 11).

Phosphate and ammonium also appear to be pooled in significant quantities by the bottom ice community (Table 5; Fig. 10). Assuming an atomic ratio of 16:1 for particulate N:P in ice algae, the intracellular pool sizes are of similar magnitude as nitrate pools and may occasionally be considerably larger. If pools of soluble silicon are present in the bottom ice layer, they are on average much smaller than those for the other nutrients or they are not detected with conventional techniques. Demand for nitrogen and silicon by growing ice algal populations are roughly equal (Cota et al. 1987; Cota and Horne 1989) and the frequent occurrence of large, soluble and reactive pools of nutrients other than silicon in the bottom ice layer suggests that there is little, if any, potential for limitation by nitrogen or phosphorus. Of the three major micronutrient elements, silicon is most likely to limit ice algal populations from land fast annual sea ice in the high Arctic and Antarctic (this study, Cota and Sullivan 1990).

Nutrient Budgets

A crude balance sheet of sources, sinks, and knowledge of the relative abundances of nutrients within these pools can be instructive, even though pool sizes are approximations based upon a series of assumptions. For example, assuming an average core volume of 200 mL, N:CHL, Si:CHL, and C:CHL ratios (wt./wt.) of 5, 10, and 35 (Cota et al. 1987; Welch and Bergmann (1989) found a Si:CHL ratio (wt./wt.) of 13 ± 4 ($N = 11$)), respectively, we calculate that particulate nitrogen and biogenic silica in bottom ice in April 1983 (Fig. 6) increased to around $6 * 10^3$ $\mu g\ N \cdot L^{-1}$ and $12 * 10^3$ $\mu g\ Si \cdot L^{-1}$ or about 18.8 mmol of either N or $Si \cdot m^{-2}$ of bottom ice. Moreover, of all 3 yr, the 1983 biomass levels were the lowest and loss terms have always been ignored. Given the average concentrations and ratios of these nutrients in the ice sheet and in surface waters (Table 2), it is obvious that the major source for "new" nutrients for ice algal blooms must be the water column. There are sufficient nutrients in the top few metres of the water column, but Si gradients are steepest and Si fluxes may periodically limit production (Cota and Horne 1989). M. Gosselin (Laval Univ., Québec, P.Q., pers. comm.) has also suggested that ice algae in the offshore waters of Hudson Bay are limited primarily by their Si supply. All of the nitrate and silicate in the 1.8 m ice sheet would have been sufficient for only a small portion (≈10–30%) of the observed minimum requirement, even if it were not "locked" within the ice.

If the combined production of microalgae in sea ice and the plankton in coastal areas of the Arctic is about 40 $g\ C \cdot m^{-2} \cdot yr^{-1}$ (e.g. Subba Rao and Platt 1984; MacDonald et al. 1987), then around 11 $g\ Si \cdot m^{-2} \cdot yr^{-1}$ (or almost 410 $mmol\ Si \cdot m^{-2} \cdot yr^{-1}$) would be necessary to support diatom production. During the spring time in northern Barrow Strait, this is roughly equivalent to the amount of dissolved silicon in the top 15–25 m, depending upon mixed layer depth, ambient concentrations and gradients (Fig. 4 and Table 2). Hence, there appears to be more than ample nutrients available to support local primary productivity of that magnitude if the vertical fluxes are adequate.

Nutrient budgets have been used to assess seasonal productivity in polar marine systems by comparing nonstructured, winter profiles with those collected later in the season after algal blooms (e.g. Jennings et al. 1984). For the upper 50 m of the Beaufort Sea shelf, MacDonald et al. (1987, see their table 2) estimated a nutrient consumption of 481–679 mmol $Si \cdot m^{-2} \cdot yr^{-1}$ or 200–291 mmol $N\text{-}NO_3 \cdot m^{-2} \cdot yr^{-1}$ in consecutive years. Their results encompass winter to late summer, spanning ice algal and phytoplankton flowerings. Their study area was relatively complex with a minor input from melting sea ice and major additions of Si-rich runoff from the Mackenzie River and via winter mixing. With our conversion factors above, their Si consumption figures suggest a total production of 47–67 $g\ C \cdot m^{-2} \cdot yr^{-1}$, whereas the corresponding values for "new," nitrate-based production are 20–29 $g\ C \cdot m^{-2} \cdot yr^{-1}$. Their "new" production estimates were slightly lower at 16–23 $g\ C \cdot m^{-2} \cdot yr^{-1}$ because of different conversion factors. Similarly, Welch and Bergmann (1989) estimated that Si depletion in the 2–100 m interval was 278 $mmol \cdot m^{-2}$ from March to June near Resolute, NWT. This Si depletion is equivalent to an ice algal production of about 27 $g\ C \cdot m^{-2}$ or over 775 $mg\ CHL \cdot m^{-2}$. They stated that the observed Si removal was equivalent to only 21.4 $mg\ CHL \cdot m^{-2}$, but units (i.e. mg and mmol) were not interconverted (H. E. Welch, Freshwater Inst., Winnipeg, Man., pers. comm.). Regenerative inputs, especially in shallow systems such as the Canadian Archipelago or the Beaufort Sea shelf, and vertical mixing have not been considered as mechanisms of replenishment in these budgets so such estimates may be conservative.

Rates of export for blooms of ice algal or phytoplankton are not well known. Direct measurements of ice algal export with sediment traps are low, but other lines of evidence suggest that export may be up to half of gross production (Smith et al. 1988; Cota and Horne 1989). Estimates of gross ice algal production may be several times higher, up to 23 $g\,C\cdot m^{-2}\cdot yr^{-1}$, than previous estimates for the Arctic based on standing crops (e.g. Alexander et al. 1974; Horner and Schrader 1982; Subba Rao and Platt 1984; also see Conover et al. 1990), suggesting that much of the production may be lost from the ice during the growth season in the Arctic and the Antarctic (Smith et al. 1988; Cota and Sullivan 1990). Loss terms for algal blooms need to be carefully evaluated to improve estimates of total and "new" productivity.

In our study the magnitude of Si fluxes and the observed Si depletion in turbulent surface waters with little density stratification tend to support the higher estimates of ice algal production (Cota and Horne 1989). The silicic acid profile presented in Fig. 2 indicates a depletion of about 24 $mmol\,Si\cdot m^{-2}$ in the top 12 m (compared with an unstructured profile extrapolated from the Si level found at the base of the mixed layer), and could result in over 2 $g\,C\cdot m^{-2}$. Depletion estimates require that instantaneous measurements of standing stocks be linearly interpolated over time. However, distributions are the net result of vertical mixing, consumption and regeneration or dissolution. Mixing tends to erase gradients unless consumption by a sink were nearly equal to or greater than the rate of supply. Persistent nutrient gradients in the surface mixed layer indicate that there has been a net removal and that the rate of replenishment is probably about the same magnitude as demand by ice algae at the interface (op. cit.). The Si flux rates presented by Cota and Horne (1989) were, on average, about 5 mmol $Si\cdot m^{-2}\cdot d^{-1}$ if the last 4 d of high values are excluded from the record (or 7 $mmol\,Si\cdot m^{-2}\cdot d^{-1}$ with the four values over 10). A constant Si flux of this magnitude, which is completely utilized, could support a productivity of approximately 490 mg $C\cdot m^{-2}\cdot d^{-1}$. For a 50 d bloom of ice algae, this level of productivity represents a total production of 25 $g\,C\cdot m^{-2}$. However, a fluctuating Si supply and high levels of biomass probably result in lower realized production.

The evidence for the impact of fortnightly tidal forcing on mixing rates, nutrient fluxes, nutrient gradients, algal biomass and photophysiology (Cota et al. 1987; Smith et al. 1987; Cota and Horne 1989) are equivocal, primarily because the sampling frequencies for biological and chemical data were only 1–2 d and our observations extended for only 1.5 cycles (i.e. 21 d). With sampling frequencies of 7–10 d for chlorophyll and about 2 wk for nutrients in May, Welch and Bergmann (1989) suggest that nutrients exert little control over production and that biomass changes were not correlated with fortnightly tidal cycles. We submit that their data sets are inadequate to resolve the influence of low frequency tidal forcing. The variability of their biomass data in May (their figure 4a) is also extreme with many confidence intervals encompassing an order of magnitude or more. However, their silicic acid data do corroborate existence of nutrient minima in the surface mixed layer during May, 1985 (their figure 11) and also show considerable depletion of Si over the whole water column during the spring. The Si removal they observed is entirely consistent with our hypothesis that the ice algal community acts as a strong sink. Unless there is substantial dissolution of biogenic silica within the surface mixed layer or large vertical transports of silicic acid, then "new" production by ice algae, and later phytoplankton, could be limited by Si in this system.

Summary and Conclusions

Several lines of evidence suggest that ice algae act as a sink for nutrients and that the major source of these nutrients must be the water column. The substantial levels of demand for nutrients necessary to support the observed net growth of ice algal populations and the relative magnitudes of the sources of nutrient supply indicate that most "new" nutrients must be derived from surface waters (Cota et al. 1987). Steep and persistent nutrient gradients across the "surface mixed layer" also imply a strong source–sink relationship (Cota and Horne 1989). Depletion of nitrate and silicic acid in surface waters immediately beneath the ice results in nutrient minima even with energetic mixing during spring tides (Fig. 4), while nitrate and silicic acid in the surface layer (Fig. 5) appear to behave nonconservatively unlike the rest of the water/ice (Fig. 3, Table 3). The largest accumulations of dissolved nitrate, ammonium and phosphate in bottom ice are restricted to the lowest layers of the ice sheet which are most heavily colonized by ice algae (Fig. 6–7, Tables 2 and 5). Nutrient levels in bottom ice are not consistent with salt exclusion and often exceed those of seawater (Fig. 10). Bottom ice displays a much higher molar ratio for NO_3:$Si(OH)_4$ than the ice sheet or the water column (Fig. 8), suggesting a localized fractionation of these nutrients. Most of the variability in nutrient concentrations in bottom ice is related to the degree of ice algal colonization (Fig. 9 and Table 4; Conover et al. 1990; R. E. H. Smith unpubl. data). Ice algae appear to have measurable intracellular pools of nitrate, ammonium and phosphate throughout the spring bloom, but silicic acid pools are very small, if present at all (Figs. 10–11, Table 5). Given ample light, ice algal production may be limited by silicic acid supply rates.

Acknowledgements

This work was supported by Canadian government agencies, including the Office of Energy, Research and Development, the Department of Fisheries and Oceans, the Polar Continental Shelf Research Project, and the National Sciences and Engineering Research Council (G.F.C.). T. Siferd, P. Clement, P. Dickie, and R. Ernst provided invaluable assistance. We thank E. P. W. Horne, R. A. Lake, S. J. Prinsenberg, N. H. F. Watson, and H. E. Welch for access to unpublished data and their comments. E. Sakshaug and an anonymous reviewer improved our presentation.

References

ALEXANDER, V., R. HORNER, AND R. C. CLASBY. 1974. Metabolism of arctic sea ice organisms. University of Alaska, Inst. Mar. Sci. Rep. R74-4: 120 p.

BATES, S. S., AND G. F. COTA. 1986. Fluorescence induction and photosynthetic responses of arctic ice algae to sample preparation and salinity. J. Phycol. 22: 421–429.

BUCKINGHAM, W. R., R. A. LAKE, AND H. MELLING. 1985. Temperature and salinity measurements in the Northwest Passage: vol. 1, March–April, 1982. Can. Data Rep. Hydrogr. Ocean Sci. 39: 371 p.

CEMBELLA, A. D., N. J. ANTIA, AND P. J. HARRISON. 1984. The utilization of inorganic and organic phosphorus compounds as nutrients by eukaryotic microalgae: a multidisciplinary perspective. Part 2. CRC Crit. Rev. Microbiol. 11: 12–81.

CONOVER, R. J., G. F. COTA, W. G. HARRISON, E. P. W. HORNE, AND R. E. H. SMITH. 1990. Ice–water interactions and their effect on biological oceanography in the Arctic Archipelago, *In* C. R. Harington [ed.] Canada's Missing Dimension: Science and History in the Canadian Arctic Islands. Can. Natl. Mus. Natural Sci., Ottawa Vol. 1, p. 204–228.

COTA, G. F., AND E. P. W. HORNE. 1989. Physical control of Arctic ice algal production. Mar. Ecol. Prog. Ser. 52: 111–121.

Cota, G. F., S. J. Prinsenberg, E. B. Bennett, J. W. Loder, M. R. Lewis, J. L. Anning, N. H. F. Watson, and L. R. Harris. 1987. Nutrient fluxes during extended blooms of arctic ice algae. J. Geophys. Res. 92: 1951–1962.

Cota, G. F., and C. W. Sullivan. 1990. Photoadaptation, growth and production of bottom ice algae in the Antarctic. J. Phycol. (In press)

Garrison, D. L., and K. R. Buck. 1986. Organism losses during melting: Asorious bias in sea ice community studies. Polar Biol. 6: 237–239.

Grainger, E. H. 1977. The annual nutrient cycle in sea-ice, p. 225–300. *In* M. J. Dunbar [ed.] Polar Oceans. Arct. Inst. N. Amer.

Grainger, E. H., and S. I. C. Hsiao. 1982. A study of the ice biota of Frobisher Bay, Baffin Island 1979–1981. Can. MS. Rep. Fish. Aquat. Sci. 1647: 128 p.

Harrison, W. G. 1980. Nutrient regeneration and primary production in the sea. p 433–460. *In* P. G. Falkowski [ed.] Primary Productivity in the Sea. Plenum Press, New York, NY.

Harrison, W. G., T. Platt, and B. Irwin. 1982. Primary production and nutrient assimilation by natural phytoplankton, populations of the eastern Canadian Arctic. Can. J. Fish. Aquat. Sci. 39: 335–345.

Holm-Hansen, O., C. J. Lorenzen, R. W. Holmes, and J. D. H. Strickland. 1965. Fluorometric determination of chlorophyll. J. Cons. Int. Explor. Mer 30: 3–15.

Horner, R., and G. C. Schrader. 1982. Relative contributions of ice algae, phytoplankton and benthic algae to primary production in nearshore regions of the Beaufort Sea. Arctic 35: 485–503.

Jennings, J. C., Jr., L. I. Gordon, and D. M. Nelson. 1984, Nutrient depletion indicates high primary productivity in the Weddell Sea. Nature 308: 51–54.

Jones, E. P., and A. R. Coote. 1980. Nutrient distributions in the Canadian Archipelago: indicators of summer water mass and flow characteristics. Can. J. Fish. Aquat. Sci. 37: 589–599.

Jones, E. P., and L. G. Anderson. 1986. On the origin of the properties of the Arctic Ocean halocline. J. Geophys. Res. 91: 10759–10767.

MacDonald, R. W., C. S. Wong, and P. E. Erickson. 1987. The distribution of nutrients in the southeastern Beaufort Sea: implications for water circulation and primary production. J. Geophys. Res. 92: 2932–2952.

Maykut, G. A. 1985. The ice environment, p. 22–82. *In* R. A. Horner [ed.] Sea Ice Biota, CRC Press, Boca Raton, Fl.

Meguro, H., K. Ito, and H. Fukushima. 1967. Ice flora (bottom type): a mechanism of primary production in polar seas and the growth of diatoms in sea ice. Arctic 20: 114–133.

Moore, R. M., M. G. Lowings, and F. C. Tan. 1983. Geochemical profiles in the central Arctic Ocean: their relation to freezing and shallow circulation. J Geophys. Res. 88: 2667–2674.

Prinsenberg, S. J., and E. B. Bennett. 1987. Mixing and transports in Barrow Strait, the central part of the Northwest Passage. Cont. Shelf Res. 7: 913–935.

Ricker, W. E. 1975. A note concerning Professor Jolicoeur's comments. J. Fish. Res. Board Can. 32: 1494–1498.

Sharp, J. H. 1974. Improved analysis for "particulate" organic carbon and nitrogen from seawater. Limnol. Oceanogr. 19: 984–989.

Smith, R. E. H., P. Clement, G. F. Cota, and W. K. W. Li. 1987. Intracellular photosynthate allocation and the control of arctic marine ice algal production. J. Phycol. 23: 124–132.

Smith, R. E. H., J. Anning, P. Clement, and G. Cota. 1988. The abundance and production of ice algae in Resolute Passage, Canadian Arctic. Mar. Ecol. Prog. Ser. 48: 251–263.

Sokal, R. R., and F. J. Rohlf. 1981. Biometry. 2nd. ed., W. H. Freeman and Co., San Francisco, CA. 805 p.

Strickland, J. H., and T. R. Parsons. 1972. A practical handbook of seawater analysis. Bull. Fish. Res. Board Can. 167: 310 p.

Subba Rao, D. V., and T. Platt. 1984. Primary production of arctic waters. Polar Biol. 3: 191–201.

Sullivan, C. W. 1986. Silicification by diatoms. p. 59–89. *In* CIBA Foundation, Silicon Biochemistry. John Wiley and Sons, New York, NY.

Walsh, J. E., and C. M. Johnson. 1979. An analysis of arctic sea ice fluctuations, 1953–1977. J. Phys. Oceanogr. 9: 580–591.

Weeks, W. F., and S. F. Ackley. 1982. The growth, structure and properties of sea ice. Cold Regions Res. and Engin. Lab. Monogr. 82–1: 130 p.

Welch, H. E., and M. A. Bergmann. 1989. Seasonal development of ice algae and its prediction from environmental factors near Resolute, N.W.T., Canada, Can. J. Fish. Aquat. Sci. 46: 1793–1804.

Wheeler, P. A. 1983. Phytoplankton nitrogen metabolism, p. 309–346. *In* E. J. Carpenter and D. G. Capone [eds.] Nitrogen in the Marine Environment. Academic Press, New York, NY.

Interpretable Statistical Tests for Growth Comparisons using Parameters in the von Bertalanffy Equation[1]

Robert M. Cerrato

Marine Sciences Research Center, State University of New York, Stony Brook, NY 11794-5000 USA

Cerrato, R. M. 1990. Interpretable statistical tests for growth comparisons using parameters in the von Bertalanffy equation. Can. J. Fish. Aquat. Sci. 47: 1416–1426.

Likelihood ratio, *t*-, univariate χ^2-, and T^2-tests have been proposed to compare von Bertalanffy parameters among stocks. As commonly applied, all of these tests are approximate, with the accuracy of each dependent on the nonlinearity of the von Bertalanffy equation, sample size, and if present, the degree of heterogeneity in the error variances. An empirical comparison of these procedures shows that the likelihood ratio test often differs in outcome from the others. Analysis of the conflicting cases by confidence region comparisons and Monte Carlo simulations almost always resolved the outcome in favor of the likelihood ratio test. The parameter effects component of nonlinearity was found to be the principal factor biasing the *t*-, univariate χ^2-, and T^2-tests. Reparameterizations of the von Bertalanffy equation substantially reduced, but did not completely eliminate, conflicting outcomes. It is concluded that the likelihood ratio test is the most accurate of the procedures considered in this study, and whenever possible, it should be the approach of choice.

La méthode du rapport de vraisemblance, les épreuves de *t*-, du χ^2 à une variable et du T^2 ont été proposées afin de comparer les paramètres de von Bertalanffy entre les stocks. Toutes ces épreuves, telles qu'elles sont appliquées généralement, sont approximatives, la précision de chacune étant dépendante de la non linéarité de l'équation de von Bertalanffy, de la taille de l'échantillon, et s'il est présent, du degré d'hétérogénéité de la variance des erreurs. D'après une comparaison empirique de ces méthodes, les résultats de l'épreuve du rapport de vraisemblance diffèrent souvent des autres. Une analyse des cas contradictoires au moyen de comparaisons des régions de confiance et des simulations de Monte Carlo permet presque toujours de trancher en faveur de la méthode du rapport de vraisemblance. Les chercheurs ont trouvé que les effets des paramètres sur la composante de non linéarité étaient le principal facteur biaisant les épreuves de *t*-, du χ^2 à une variable et de T^2. Le fait d'attribuer de nouveaux paramètres à l'équation de von Bertalanffy a diminué de beaucoup les résultats contradictoires sans toutefois les éliminer complètement. Les chercheurs ont conclu que la méthode du rapport de vraisemblance est l'épreuve la plus précise des épreuves examinées dans le cadre de la présence étude, et chaque fois que cela est possible, elle devrait privilégiée.

Received November 29, 1988
Accepted February 27, 1990
(J9401)

Reçu le 29 novembre 1988
Accepté le 27 février 1990

One of the most commonly used and powerful techniques available to an investigator is to fit an appropriate model to data sets and then compare the resulting parameter estimates. Such a procedure was advocated by Rao (1958) for growth comparisons. Rao suggested that efficient comparisons are possible if the data can be reduced to a few parameters which summarize the essential aspects of growth.

The von Bertalanffy equation is useful in describing the growth of many fish and shellfish species. Given that one has an interest in comparing the estimated von Bertalanffy parameters between stocks, two general approaches are available. Most nonlinear regression programs calculate asymptotic standard errors and correlations for the parameter estimates. One approach then is to use these statistics along with the parameter estimates in hypothesis tests. For example, Kingsley (1979), Gallucci and Quinn (1979), and Misra (1980, 1986) have carried out univariate comparisons based on either the *t*- or χ^2-test. For simultaneous comparisons of two or all three of the von Bertalanffy parameters, Kingsley (1979) and Bernard (1981) have suggested a procedure based on Hotellings T^2 statistic.

The second approach, advocated by Kimura (1980), is based on likelihood ratio statistics. For reasons to be presented later, a likelihood ratio test comparing growth parameters should be more accurate or reliable than the former approach. However, it is also computationally more labor intensive, requiring multiple fits of the von Bertalanffy equation.

Both approaches are approximate ones. They are taken from linear statistical theory, and their validity when applied to the von Bertalanffy equation depends on the degree of bias and nonnormality in the parameter estimates caused by the nonlinearity of the model. In addition, both are characterized in terms of asymptotic properties for which no exact small sample theory exists. Finally, at least as commonly practiced, both approaches handle unequal and unknown error variances in an approximate way.

The approximate nature of these tests gives rise to several questions. How large must sample sizes be to use either approach? How different are their outcomes? Assuming that the likelihood ratio test is more accurate, how well does it do in light of the fact that the model is nonlinear, sample sizes are often small, and error variances in size measurements among stocks are generally unequal? Are there any practical steps that can or should be taken to improve the accuracy of either approach?

---

[1] Contribution number 696 of the Marine Sciences Research Center.

The goal of this study is to address these questions. This will be done empirically; the tests will be examined using a representative set of growth data. Methods will include assessments of nonlinear behavior based on the curvature measures of Beale (1960) and Bates and Watts (1980), comparisons of confidence regions, and Monte Carlo simulations. As will be seen, these questions can be answered for specific data sets. While it is not possible to provide a general solution to any of these questions, the methods presented here can be applied to other data sets and nonlinear models.

Materials and Methods

Characteristics of the Data and the Model

The data which will be analyzed to evaluate the performance of the tests were taken from a study by Keith (1985) of growth in the surf clam *Spisula solidissima*. In her study, Keith obtained shell height measurements from annual growth increments in cross-sectioned valves. The data set consists of surf clam samples from 16 stations in Long Island waters. Sample sizes range from 34 to 294 height measurements. All height measurements were taken at integer ages, and except for the oldest age-classes at each station, there were from 6 to 28 measurements for each age. Based on the replicated measurements and Bartlett's test (Zar 1984) with $\alpha = 0.01$, error variances were homogeneous with age at each station. However, a similar test ($\alpha = 0.01$) comparing the pooled variances of station pairs generally resulted in a significant outcome, indicating substantial heterogeneity in error variances between stations.

Given the characteristics of these data, an appropriate form of the von Bertalanffy equation can be written as

$$(1)\quad h_u = H_\infty(1 - e^{-k(t_u - t_0)}) + \epsilon_u$$
$$= f(\boldsymbol{\theta}, t_u) + \epsilon_u,$$

where h_u is the shell height at age t_u ($u = 1, \ldots, n$), H_∞ is the asymptotic maximum size, k is a growth constant, t_0 is an initial condition corresponding to the time when $h = 0$, and the ϵ_u's are assumed to be independent, identically distributed $N(0, \sigma^2)$ random variables. The von Bertalanffy equation will also be symbolically represented as $f(\boldsymbol{\theta}, t_u)$ where $\boldsymbol{\theta}$ is a three-dimensional vector of the unknown parameters.

Parameter estimates can be obtained readily by using a nonlinear least squares program such as that available in BMDP (Biomedical Computer Programs, Health Sciences Computing Facility, University of California at Los Angeles). The least squares estimate $\hat{\boldsymbol{\theta}}$ is the vector which minimizes the sum of squares of residuals

$$(2)\quad S(\boldsymbol{\theta}) = \sum_{u=1}^{n} (h_u - f(\boldsymbol{\theta}, t_u))^2,$$

where n is the sample size. Assuming that the ϵ_u are normally distributed then $\hat{\boldsymbol{\theta}}$ is also the maximum likelihood estimate of $\boldsymbol{\theta}$, and an estimate of the error variance σ^2 is

$$(3)\quad s^2 = \frac{1}{n-3} S(\hat{\boldsymbol{\theta}}).$$

Most software packages also yield asymptotic standard errors and an asymptotic correlation matrix for the parameter estimates. From these statistics, the asymptotic covariance matrix for the estimated parameters may be calculated. The asymptotic covariance matrix may also be computed directly and is given as

$$(4)\quad \boldsymbol{U} = s^2[\boldsymbol{F}'(\hat{\boldsymbol{\theta}})\boldsymbol{F}(\boldsymbol{\theta})]^{-1}$$

where $\boldsymbol{U}$ is a symmetric $p \times p$ matrix ($p = 3$), $\boldsymbol{F}(\boldsymbol{\theta})$ is an $n \times p$ matrix of partial derivatives $\frac{\partial}{\partial \theta_j} f(\boldsymbol{\theta}, t_u)$, $u = 1, \ldots, n$ and $j = 1, \ldots, p$. $\boldsymbol{F}'$ is the transpose of $\boldsymbol{F}$.

Test Procedures

We are now in a position to outline the test procedures. This outline will be brief and will be restricted to pairwise comparisons among stocks, although each procedure can be generalized for cases involving multisample tests. In keeping with the characteristics of the surf clam data, error variances will be assumed heterogeneous. It should be noted that testing for differences in normal random variables when heterogeneity is present is an example of the Behrens-Fisher problem, for which no exact solutions exist.

The multivariate T^2-test permits the simultaneous comparison of several von Bertalanffy parameters between stocks. In the two-sample case, the parameters are expressed as column vectors

$$(5)\quad \boldsymbol{\theta}_1 = \begin{pmatrix} H_{\infty_1} \\ k_1 \\ t_{0_1} \end{pmatrix} \text{ and } \boldsymbol{\theta}_2 = \begin{pmatrix} H_{\infty_2} \\ k_2 \\ t_{0_2} \end{pmatrix}$$

Defining the difference in parameter vectors as

$$(6)\quad \boldsymbol{\delta} = \boldsymbol{\theta}_1 - \boldsymbol{\theta}_2,$$

the null hypothesis

$$(7)\quad H_0\colon \boldsymbol{\delta} = \boldsymbol{0}$$

is then tested against the alternative hypothesis

$$(8)\quad H_1\colon \boldsymbol{\delta} \neq \boldsymbol{0}$$

on the basis of the estimated value

$$(9)\quad \boldsymbol{d} = \hat{\boldsymbol{\theta}}_1 - \hat{\boldsymbol{\theta}}_2.$$

The test statistic is given as

$$(10)\quad T^2 = \boldsymbol{d}'\boldsymbol{U}^{-1}\boldsymbol{d}$$

where $\boldsymbol{d}'$ is the transpose of $\boldsymbol{d}$, $\boldsymbol{U} = \boldsymbol{U}_1 + \boldsymbol{U}_2$, the $\boldsymbol{U}_i$ are the asymptotic covariance matrices for the two stocks, and $\boldsymbol{U}^{-1}$ is the inverse of $\boldsymbol{U}$. Assuming that the von Bertalanffy parameters are from a multivariate normal distribution, the quantity in equation (10) is approximately distributed as a Hotellings T^2-variable with three and f^* degrees of freedom (Mardia et al. 1979). Taking $f_i = n_i - 3$, f^* is determined (Mardia et al. 1979) by

$$(11)\quad \frac{1}{f^*} = \frac{1}{f_1}\left(\frac{\boldsymbol{d}'\boldsymbol{U}^{-1}\boldsymbol{U}_1\boldsymbol{U}^{-1}\boldsymbol{d}}{\boldsymbol{d}'\boldsymbol{U}^{-1}\boldsymbol{d}}\right)^2 + \frac{1}{f_2}\left(\frac{\boldsymbol{d}'\boldsymbol{U}^{-1}\boldsymbol{U}_2\boldsymbol{U}^{-1}\boldsymbol{d}}{\boldsymbol{d}'\boldsymbol{U}^{-1}\boldsymbol{d}}\right)^2$$

The quantity f^* will lie between the smaller of the two numbers f_1 and f_2 and their sum $f_1 + f_2$. The null hypothesis is rejected when

$$(12)\quad T^2 > T^2_\alpha(3, f^*),$$

where $T^2_\alpha(p,m)$ is defined (Mardia et al. 1979) as

$$(13)\quad \mathrm{T}^2_\alpha(p,m) = \frac{mp}{m-p+1}F^\alpha_{p,m-p+1}.$$

Here $F^{\alpha}_{p,m-p+1}$ is the upper α percentile point of the F-distribution with p and $m-p+1$ degrees of freedom.

Given the assumption of normality, the T^2-test outlined above, when based on all three von Bertalanffy parameters, is an approximate (due to heterogeneity in n_iU_i) test of the difference between the two growth curves. The T^2-test may also be used for bivariate (e.g. $H_{\infty i}$ and k_i only) and univariate comparisons. To do this, the unwanted rows in $\boldsymbol{\theta}_i$, and the corresponding rows and columns in $\boldsymbol{U}_i$, are deleted. The test statistic is then compared with $T^2_\alpha(p,m)$ where p is the reduced dimension of the test. For univariate comparisons, $p=1$ and equation (13) becomes

$$(14)\quad T^2_\alpha(1,m)=F^\alpha_{1,m}=(t_{\alpha/2,m})^2,$$

where $t_{\alpha/2,m}$ is a Student t-variable with m degrees of freedom. Additionally, equations (10) and (11), respectively, reduce to

$$(15)\quad T^2 = \frac{(\hat{\theta}_{j1}-\hat{\theta}_{j2})^2}{(u_{jj1}+u_{jj2})}$$

$$(16)\quad \frac{1}{\hat{f}} = \frac{1}{f_1}\left(\frac{u_{jj1}}{u_{jj1}+u_{jj2}}\right)^2 + \frac{1}{f_2}\left(\frac{u_{jj2}}{u_{jj1}+u_{jj2}}\right)^2$$

where u_{jj1} and u_{jj2} represent the jth diagonal element in the asymptotic covariance matrix $\boldsymbol{U}$ for each of the two stocks. That is, $\sqrt{u_{jj1}}$ and $\sqrt{u_{jj2}}$ are the asymptotic standard errors of the parameter estimate in each stock. Thus, the T^2-test as formulated for the univariate case is simply the squared version of the commonly used, two-sided, t-test for unknown and unequal variances.

Before proceeding, several comments need to be made regarding Bernard's (1981) formulation of the T^2-test. First, Bernard based his test on n_i-1 rather than n_i-3 degrees of freedom. As in any regression situation, the degrees of freedom should be decreased by the number of parameters being estimated. Secondly, in the process of pooling his covariance matrices and computing T^2, Bernard essentially reduced the pooled matrix by a factor proportional to the sample size. Asymptotic covariance matrices for the parameter estimates are calculated from cross products of standard errors, so further reductions are not appropriate. Finally, Bernard assumes a common covariance structure. That is, he assumes that the n_iU_i are equal, and he pools the two matrices. The procedure formulated here, while approximate, does not make a similar assumption and is the multivariate equivalent of the t-test for unknown, unequal variances.

The procedure for the univariate χ^2-test is given in Rao (1973). Assuming that the asymptotic distribution of $\sqrt{n_i}\,(\hat{\theta}_{ji}-\theta_{ji})$ is normal as $n_i\to\infty$, the test statistic for the two sample case is

$$(17)\quad H = \sum_{i=1}^{2}\frac{(_{ij}-(\hat{\theta}^2_{ji}-\hat{\Theta}_{ji})^2}{u_{jji}}$$

where

$$(18)\quad \hat{\Theta} = \frac{\sum\limits_{i=1}^{2}\dfrac{\theta_{ji}}{u_{jji}}}{\sum\limits_{i=1}^{2}\dfrac{1}{u_{jji}}}$$

With two samples, the quantity H in equation (17) is distributed as a χ^2 random variable with one degree of freedom as $n_1+n_2\to\infty$. The null hypothesis is rejected at the α level of significance when

$$(19)\quad H>\chi^2_\alpha(1).$$

The likelihood ratio test comparing two growth curves is given as follows. The null hypothesis (Kimura 1980) is

H_ω: The parameter vectors $\boldsymbol{\theta}_1$ and $\boldsymbol{\theta}_2$
satisfy some set of q linear constraints of the form

$$(20)\quad \theta_{j1} = \theta_{j2}\quad j=1,2,\text{ and/or }3.$$

For two stocks with $q=3$, for example, the linear constraints are $H_{\infty1}=H_{\infty2}$, $k_1=k_2$, and $t_{01}=t_{02}$. This is to be tested against the alternative hypothesis (Kimura 1980)

H_Ω: The parameters vectors $\boldsymbol{\theta}_1$ and $\boldsymbol{\theta}_2$ possibly satisfy no linear constraints, i.e.

$$(21)\quad \theta_{j1} \neq \theta_{j2}\quad j=1,2,\text{ and/or }3.$$

For two stocks with unequal error variances, the weighted sum of squares of residuals is defined as

$$(22)\quad S'(\boldsymbol{\theta}_1,\sigma^2_1,\boldsymbol{\theta}_2,\sigma^2_2) = \sum_{i=1}^{2}\sum_{u=1}^{n_i}\frac{1}{\sigma^2_i}(\mathrm{h}_{ui}-f(\boldsymbol{\theta}_i,\ t_{ui}))^2$$

where h_{ui} is the uth observation from the ith sample. The joint likelihood function under either hypothesis is

$$(23)\quad L(\boldsymbol{\theta}_1,\sigma^2_1,\boldsymbol{\theta}_2,\sigma^2_2) = (2\pi\sigma^2_1)^{-n_1/2}\,(2\pi\sigma^2_2)^{-n_2/2}\,e^{-S'(\boldsymbol{\theta}_1,\ \sigma^2_1,\boldsymbol{\theta}_2,\ \sigma^2_2)/2}$$

The maximum likelihood estimates for σ^2_1 and σ^2_2 are obtained by taking the partial derivatives of the log of the likelihood function with respect to σ^2_1 or σ^2_2 and setting the resulting equations to zero. These estimates are

$$(24)\quad \hat{\sigma}^2_i = S(\boldsymbol{\theta}_i)\,/n_i\quad \mathrm{i}=1,2\,,$$

where $S(\boldsymbol{\theta}_i)$ is the sum of squares of residuals for the ith sample. vBecause of the unequal variances, the maximum likelihood estimates $\hat{\sigma}^2_1$ and $\hat{\sigma}^2_2$ under either the null or alternative hypothesis are obtained by minimizing S'. In practice, this must be done using an iteratively reweighted least squares procedure. In the case of the null hypothesis, the minimization is carried out subject to the q linear constraints.

The likelihood ratio is given as

$$(25)\quad \Lambda = \frac{L(\hat{\boldsymbol{\theta}}_{1\omega},\hat{\sigma}^2_{1\omega},\hat{\boldsymbol{\theta}}_{2\omega},\hat{\sigma}^2_{2\omega})}{L(\hat{\boldsymbol{\theta}}_{1\Omega},\hat{\sigma}^2_{1\Omega},\hat{\boldsymbol{\theta}}_{2\Omega},\hat{\sigma}^2_{2\Omega})} = \left(\frac{\hat{\sigma}^2_{1\omega}}{\hat{\sigma}_{1\Omega}}\right)^{-n_1/2}\left(\frac{\hat{\sigma}^2_{2\omega}}{\hat{\sigma}^2_{2\Omega}}\right)^{-n_2/2}$$

where the subscripts ω and Ω are used to distinguish the estimates obtained under the null and alternative hypothesis, respectively. Under the null hypothesis, the test statistic $-2\log(\Lambda)$ converges asymptotically to a $\chi^2(q)$ distribution (Kendall and Stuart 1967). The null hypothesis is rejected at the α level of significance when

$$(26)\quad -2\log(\Lambda) > \chi^2_\alpha(q).$$

Alternatively, Gallant (1975a) showed that $\Lambda^{-2/n}$ converges asymptotically to a random variable whose distribution under the null hypothesis is a function of the F-distribution. The null hypothesis is rejected at the α level of significance when

$$\text{(27)}\quad \Lambda^{-2/n} > \left(1 + \frac{q}{f_1 + f_2} F^{\alpha}_{q,f_1+f_2}\right)$$

where $f_i = n_i - 3$.

Before proceeding, several comments are again warranted. When the error variances are homogeneous (i.e. $\sigma_1^2 = \sigma_2^2 = \sigma^2$), $\Lambda^{-2/n} = \hat{\sigma}^2_{\omega}/\hat{\sigma}^2_{\Omega}$ and expression (27) can be rewritten as (Gallant 1975a)

$$\text{(28)}\quad \frac{(S(\hat{\boldsymbol{\theta}}_{1\omega}, \hat{\boldsymbol{\theta}}_{2\omega}) - S(\hat{\boldsymbol{\theta}}_{1\Omega}, \hat{\boldsymbol{\theta}}_{2\Omega}))/q}{S(\hat{\boldsymbol{\theta}}_{1\Omega}, \hat{\boldsymbol{\theta}}_{2\Omega}) \,/\, (f_1 + f_2)} > F^{\alpha}_{q,f_1+f_2}$$

where S is the sum of squares of residuals for both samples. This is the test procedure advocated by Ratkowsky (1983) and is equivalent in form to the F-test used in linear regression. Expression (27) results in a more conservative test than expression (26) since, by putting the critical values in equivalent terms, one finds that

$$\text{(29)}\quad n \log \left(1 + \frac{q}{f_1 + f_2} F^{\alpha}_{q,f_1+f_2}\right) > \chi^2_{\alpha}(q).$$

Expression (29) approaches equality as $n \rightarrow \infty$.

Analysis Methods

The basic strategy of this study was to compare the outcomes of each test procedure applied to the surf clam data sets. Several methods were then used to analyze the statistical properties of the parameter estimates and to resolve disagreements in the test outcomes. These included calculating the nonlinearity measures of Beale (1960) and Bates and Watts (1980), comparing confidence regions, and Monte Carlo simulations. Each will be described briefly here.

The sample space is taken to be n-dimensional, and a given data set, say n measurements of shell height, can be represented as a single point ($\boldsymbol{h}$) in this space. The solution locus for a model is a p-dimensional subspace of this sample space. It is generated by evaluating the model for the set of n independent variables over all possible combinations of parameter values. The least squares estimate is that combination of parameter values $\hat{\boldsymbol{\theta}}$ which provides a point on the solution locus lying closest to $\boldsymbol{h}$.

When the model is truely linear in $\boldsymbol{\theta}$, the solution locus is planar. This will be referred to as the tangent plane. When the model is nonlinear in $\boldsymbol{\theta}$, the solution locus is curved. The tangent plane, generated from a first order Taylor series expansion of the model, represents a linear approximation of the solution locus in the neighborhood of $\hat{\boldsymbol{\theta}}$.

Bates and Watts (1980) proposed two measures, the maximum intrinsic curvature (Γ^N) and the maximum parameter affects curvature (Γ^T), to assess the degree of curvature of the solution locus relative to the tangent plane for a given "model–experimental design–parameterization combination". The maximum intrinsic curvature Γ^N measures the maximum curvature of the solution locus in a direction normal to the tangent plane. It assesses a property of the solution locus which is invariant under reparameterization of the model. The maximum parameter effects curvature Γ^T measures the maximum degree of twisting, lack of parallelism, and unequal scaling in the parameter curves of the solution locus projected onto the tangent plane (Bates and Watts 1981). These tangential nonlinearity effects are caused by the specific model parameterization and may be altered by nonlinear transformations of the parameters.

Beale's (1960) measures N_{ϕ} and N_{θ} also assess the curvature of the solution locus. N_{ϕ}, the intrinsic nonlinearity of the model, is invariant under reparameterizations. The difference $N_{\theta} - N_{\phi}$ represents the parameter-dependent component of nonlinearity, and this difference can be reduced by reparameterization of the model. Bates and Watts (1980) prove that N_{ϕ} and $(N_{\theta} - N_{\phi})$ are equal to one-quarter of the mean square intrinsic and parameter effects curvatures, respectively. Investigators (e.g. Ratkowsky 1983, 1986; Cook and Goldberg 1986) have shown a preference for Bates and Watts' measures because their conceptual framework is more readily interpreted in geometric terms, and because the mean square curvatures of Beale can mask very localized but severe departures from linearity. In the present study, Beale's measures will be calculated only where required.

All of the measures are zero for a linear model, and larger values indicate greater departures from linearity. Both Beale (1960) and Bates and Watts (1980) set conditions for the validity of the tangent plane approximation to the solution locus. Beale states that the linear approximation is "satisfactory" if N_{ϕ} and N_{θ} are less than $0.01/F^{\alpha}_{p,n-p}$. Bates and Watts suggest comparing their measures to $1/\sqrt{F^{\alpha}_{p,n-p}}$, but in discussing a set of examples, they use the more conservative value of $1/2\sqrt{F^{\chi}_{p,n-p}}$. Ratkowsky (1983) also suggests the latter value. When the particular model–experimental design–parameterization combination fulfills the criteria, it exhibits what Ratkowsky has termed "close-to-linear" behavior. That is, the tangent plane closely approximates the solution locus.

The effect of a nonlinear model on the statistical properties of the parameter estimates were also examined by comparing the differences in three confidence regions generated under different assumptions. The confidence regions are

$$\text{(30)}\quad (\boldsymbol{\theta} - \hat{\boldsymbol{\theta}})'\boldsymbol{F}'(\hat{\boldsymbol{\theta}})\boldsymbol{F}(\hat{\boldsymbol{\theta}})\,(\boldsymbol{\theta} - \hat{\boldsymbol{\theta}}) \leqslant \frac{pS(\hat{\boldsymbol{\theta}})}{n-p} F^{\alpha}_{p,n-p}$$

$$\text{(31)}\quad S(\boldsymbol{\theta}) - S(\hat{\boldsymbol{\theta}}) \leqslant \frac{pS(\hat{\boldsymbol{\theta}})}{n-p} F^{\alpha}_{p,n-p}$$

$$\text{(32)}\quad S(\boldsymbol{\theta}) - S(\hat{\boldsymbol{\theta}}) \leqslant \frac{pS(\hat{\boldsymbol{\theta}})}{n-p} F^{\alpha}_{p,n-p} \begin{cases} 1 + \dfrac{n}{n-1} N_{\phi} & \text{for } p = 1 \\ 1 + \dfrac{n(p+2)}{(n-p)p} N_{\phi} & \text{for } p > 1 \end{cases}$$

Expression (30) is based on the assumption that the linearized form of the von Bertalanffy equation is valid around $\hat{\boldsymbol{\theta}}$, and consequently, that the nonlinearity effects are negligible. Note that this expression is obtained by inverting a one-sample T^2-test. A one-sample likelihood ratio test can also be inverted (Gallant 1975b), and this results in expression (31). Because the bias in $S(\hat{\boldsymbol{\theta}})$ depends only on the intrinsic nonlinearity in the model (Ratkowsky 1983), expression (31) produces a confidence region which accounts for the parameter effects curvature. Expression (32) accounts for both the intrinsic and parameter effects curvature but in an approximate way. Beale (1960) showed that this confidence region is conservative and has an associated probability greater than or equal to $1 - \alpha$.

TABLE 1. Estimates of the von Bertalanffy parameters for each station. Also given are estimates of the error variance (s^2) based on equation (3).

Station	n	H_∞ (mm)	k (yr)$^{-1}$	t_0 (yr)	s^2
1	113	73.12	0.643	0.415	18.08
2	128	62.38	0.574	−0.028	27.74
3	123	67.76	0.433	−0.241	25.04
4	166	62.77	0.579	−0.007	15.38
5	150	64.95	0.665	0.084	13.37
6	142	72.37	0.568	0.128	39.28
7	162	69.14	0.492	−0.032	28.69
8	187	76.88	0.589	0.145	13.42
9	150	85.89	0.743	0.029	13.73
10	294	116.81	0.324	0.150	62.26
11	236	114.77	0.384	0.318	31.23
12	48	96.94	0.305	0.180	50.22
13	135	118.72	0.257	0.243	43.19
14	43	85.88	0.560	0.280	80.28
15	34	83.33	0.649	0.470	29.49
16	126	96.16	0.288	0.046	49.19

Finally, the distributional properties of selected statistics were examined by Monte Carlo methods. In particular, empirical distributions of the likelihood ratio test statistic, generated by bootstrapping (Efron 1982) the surf clam data, can account for the biases associated with sample size and unequal error variances. Additionally, since bias in the $\hat{\sigma}_i^2$ is independent of the parameter effects curvature, the only bias which cannot be resolved by Monte Carlo simulation is due to the intrinsic curvature of the model. If Γ^N is small under both the null and alternative hypotheses, then the numerical solutions for the likelihood ratio test would be almost unbiased and can serve as a standard for evaluating the reliability of the various test procedures.

Results

The von Bertalanffy equation was fitted to the surf clam data for each stock using an iterative Gauss–Newton algorithm. The program yielded estimates for the parameters, their asymptotic standard errors, and an asymptotic correlation matrix. Sample sizes, parameter estimates, and residual mean squares for each of the 16 stations are listed in Table 1. While not strictly valid for nonlinear models, both Draper and Smith (1966) and Kimura (1980) suggest carrying out a standard F-test in order to obtain an approximate assessment of lack of fit of the model. Pure error estimates of σ^2 were obtained from the replicated observations. In the present case, the results for each stock were nonsignificant at the 0.01 level, indicating no lack of fit.

Table 2 provides a comparison of the nonlinearity measures with the appropriate criterion values for each of the surf clam data sets ($\alpha = 0.01$). N_θ and Γ^T for each station exceed the criteria. It may be concluded from this result that substantial parameter effects curvature is present, and that the tangent plane does not closely approximate the solution locus in the neighborhood of $\hat{\theta}$. In contrast, N_ϕ and Γ^N for each data set are less than their respective criteria. Thus, the intrinsic curvature of the solution locus is small.

TABLE 2. Nonlinearity measures for each station compared with criterion values based on the F-distribution.

Station	N_θ	N_ϕ	$\frac{0.01}{F}$	Γ^T	Γ^N	$\frac{1}{2\sqrt{F}}$
1	0.0276	0.000208	0.00252	0.714	0.0645	0.251
2	0.147	0.000678	0.00254	1.665	0.1164	0.252
3	0.574	0.000439	0.00253	3.345	0.0936	0.252
4	0.0731	0.000238	0.00256	1.179	0.0690	0.253
5	0.0422	0.000242	0.00255	0.890	0.0696	0.253
6	0.114	0.000457	0.00255	1.466	0.0956	0.253
7	0.138	0.000338	0.00256	1.626	0.0822	0.253
8	0.0133	0.000128	0.00257	0.494	0.506	0.254
9	0.0293	0.000177	0.00255	0.742	0.0594	0.253
10	0.00590	0.000154	0.00260	0.320	0.0552	0.255
11	0.00348	0.00101	0.00258	0.244	0.0449	0.254
12	0.588	0.00103	0.00235	3.377	0.1434	0.243
13	0.0101	0.000172	0.00255	0.424	0.0587	0.252
14	0.259	0.00209	0.00232	2.187	0.2047	0.241
15	0.132	0.000744	0.00232	1.574	0.1220	0.236
16	0.188	0.000533	0.00254	1.910	0.1033	0.252

Five hypotheses were tested: a univariate test on each parameter estimate, a bivariate test of H_∞ and k, and a simultaneous test of all three parameter estimates. Combinations of all possible pairs of the 16 data sets resulted in 120 comparisons for each hypothesis. All tests were carried out at the 0.01 level of significance. The multivariate comparisons tended to have a higher number of significant outcomes than the univariate tests. Overall, however, about 65% of the comparisons were significant.

Outcomes for the two versions of the likelihood ratio test (expressions (26) and (27)) were identical. Results for the univariate χ^2-test were almost identical to the t-test (i.e. univariate T^2), differing in only three of the 360 univariate comparisons. However, the comparison between the likelihood ratio and T^2-tests resulted in a substantial number of conflicting outcomes. The two test procedures differed in 24 of the 600 cases analyzed. This represented 4% of the total number of comparisons. For the remainder of the study, therefore, attention was restricted to the T^2 and likelihood ratio procedures, bearing in mind that the t- and T^2-tests are identical for univariate comparisons, and the fact that there was little difference between the outcomes of the t- and univariate χ^2-tests.

A listing of the 24 cases where the likelihood ratio and T^2-tests differed is given in Table 3. All but two data sets (stations 4 and 5) were involved in at least one of these cases. The outcomes for the univariate tests were evenly distributed, with the likelihood ratio test rejecting the null hypothesis in half of the cases and with the T^2-test significant in the other half. The likelihood ratio test was significant and the T^2-test nonsignificant in all of the multivariate cases.

Comparing this listing with the information in Tables 1 and 2, several trends are evident. Data sets with the six smallest sample sizes (stations 15, 14, 12, 1, 3, and 16) were involved in 22 of the 24 cases. Four of these data sets (stations 12, 3, 14, and 16) also had the largest maximum parameter effects curvatures. These four stations alone represent 18 of the 24 cases where disagreements occurred.

Conservative confidence regions, presented in Table 3 for the univariate cases and in Figs. 1 and 2 for the multivariate cases, were compared in an attempt to resolve the conflicting outcomes. This was possible to do unambiguously in eight of the cases, when either complete overlap of the conservative confidence regions occurred, or they were completely separated. The outcome supported the likelihood ratio test result in each case (Table 3).

TABLE 3. Detailed listing of all cases in which the T^2 and the likelihood ratio (LR) tests of the von Bertalanffy parameters disagreed. Also given are 99% linear, likelihood, and conservative confidence regions for each station. The last column in this table shows the outcome supported by either a comparison of conservative confidence regions or Monte Carlo analysis. ns = nonsignificant; * = significant.

Hypothesis/Stations		Test Outcomes		99% Confidence regions			
		T^2	LR	Linear	Likelihood	Conservative	Confirmation
H_0: $H_{\infty 1}=H_{\infty 2}$	3	*	ns	60.11/74.60	61.87/77.88	61.86/77.91	LR[a]
	8			75.31/78.40	75.34/78.48	75.34/78.48	
	6	*	ns	67.89/76.53	68.48/77.57	68.48/77.57	LR[b]
	8			75.31/78.40	75.34/78.48	75.34/78.48	
	8	ns	*	75.31/78.40	75.34/78.48	75.34/78.48	LR[a]
	12			75.54/115.70	82.08/122.98	82.07/123.02	
	10	*	ns	114.55/119.01	114.60/119.12	114.60/119.12	LR[b]
	12			75.54/115.70	82.08/122.98	82.07/123.02	
	12	*	ns	75.54/115.70	82.08/122.98	82.07/123.02	LR[a]
	13			115.28/122.06	115.46/122.27	115.46/122.27	
	8	ns	*	75.31/78.40	75.34/78.48	75.34/78.48	LR[b]
	14			75.73/94.81	77.48/100.26	77.46/100.31	
	9	ns	*	84.09/87.64	84.14/87.85	84.14/87.85	LR[b]
	16			85.82/105.69	86.80/110.23	86.80/110.27	
H_0: $k_1=k_2$	1	*	ns	0.526/0.759	0.530/0.769	0.530/0.769	T^{2b}
	3			0.259/0.607	0.271/0.616	0.271/0.616	
	3	ns	*	0.259/0.607	0.271/0.616	0.271/0.616	LR[b]
	13			0.223/0.291	0.224/0.292	0.224/0.292	
	13	ns	*	0.223/0.291	0.224/0.292	0.224/0.292	LR[a]
	14			0.246/0.874	0.283/0.954	0.283/0.955	
	11	*	ns	0.350/0.417	0.351/0.419	0.351/0.419	LR[b]
	16			0.203/0.373	0.199/0.390	0.199/0.390	
H_0: $t_{01}=t_{02}$	3	ns	*	−0.676/0.194	−0.779/0.107	−0.779/0.107	LR[b]
	8			0.009/0.281	−0.002/0.269	−0.002/0.269	
	2	ns	*	−0.382/0.326	−0.495/0.279	−0.496/0.279	LR[b]
	11			0.187/0.449	0.177/0.441	0.177/0.441	
	3	ns	*	−0.676/0.194	−0.779/0.107	−0.779/0.107	LR[b]
	13			−0.009/0.495	−0.034/0.473	−0.035/0.473	
	8	*	ns	0.009/0.281	−0.002/0.269	−0.002/0.269	LR[b]
	15			0.200/0.740	0.117/0.683	0.117/0.683	
	15	*	ns	0.200/0.740	0.117/0.683	0.117/0.683	LR[b]
	16			−0.283/0.374	−0.384/0.348	−0.384/0.348	
H_0: $H_{\infty 1}=H_{\infty 2}$	3	ns	*		See Fig. 1a		LR[b]
$k_1=k_2$	7						
	12	ns	*		See Fig. 1b		LR[b]
	15						
H_0: $H_{\infty 1}=H_{\infty 2}$	1	ns	*		See Fig. 2a		LR[b]
$k_1=k_2$	6						
$t_{01}=t_{02}$	3	ns	*		See Fig. 2b		LR[b]
	7						
	12	ns	*		See Fig. 2c		LR[a]
	14						
	12	ns	*		See Fig. 2d		LR[a]
	15						
	14	ns	*		See Fig. 2e		LR[a]
	16						
	15	ns	*		See Fig. 2f		LR[a]
	16						

[a] Confirmed by comparing conservative confidence regions.
[b] Confirmed by Monte Carlo analysis.

For the remaining 16 conflicts, Monte Carlo analysis was used to generate an empirical distribution and a nonparametric critical value for the likelihood ratio test statistic. In each case, 1000—2000 bootstrapped data sets were created. Γ^N was also calculated for the original maximum likelihood estimates under both the null and alternative hypothesis, and it was found in each case that this curvature measure never exceeded the criterion value. Monte Carlo results supported the outcome of the parametric likelihood ratio test in 15 of the 16 instances (Table 3). In the one exception (a test of k differences for stations 1 and 3), the value of $-2\log(\Lambda)$ was 6.63, and the outcome of the parametric likelihood ratio test was marginally nonsignificant since $\chi^2_{0.01}(1)=6.63$.

Thus, the conflicts were overwhelmingly resolved in favor of the likelihood ratio test. By examining the linear, likelihood, and conservative confidence regions in Table 3 and Figs. 1–2, it is possible to identify conditions under which conflicts between the two test procedures occurred, and why they were resolved in favor of the likelihood ratio test. First note that the differences between the likelihood and conservative confidence regions are negligible, while both are clearly distinguishable from the linear confidence regions. This result can be directly related to the relative sizes of the curvature measures as stated earlier.

For each surf clam data set, the distributions of both $\hat{H}_\infty$ and $\hat{k}$ were positively skewed (confirmed by Monte Carlo analysis). As a result, the endpoints of the one dimensional likelihood and conservative confidence intervals were shifted in a positive direction relative to the linear confidence regions which are based on the normal distribution. The degree to which this occurred depended on the size of the parameter effects curvature. In all of the cases for which the one dimensional likelihood ratio test of $\hat{H}_\infty$ or $\hat{k}$ was significant, the station with the larger value of Γ^T also had a parameter estimate which exceeded that of the other station. The overall effect of this orientation and positive skewness was to decrease the overlap in the likelihood and conservative confidence intervals relative to the linear intervals. In all of the cases for which the one-dimensional likelihood ratio test of $\hat{H}_\infty$ or $\hat{k}$ was nonsignificant, the station with the larger value of Γ^T also had a parameter estimate which was less than that of the other station. Thus the degree of overlap in the likelihood and conservative confidence intervals for the two stations was increased relative to the linear intervals. A similar interpretation was found for the one dimensional t_0 cases, except that its empirical distribution was negatively skewed, and the relative position of the parameter estimate of the station with the largest Γ^T was reversed. The multivariate cases could not be completely resolved in terms of the relative positions of the estimates and the size of Γ^T. However, the orientation and skewing of the confidence regions is strikingly similar in all of the cases.

The parameter effects component of nonlinearity is, therefore, clearly implicated in creating the conflicting test outcomes. The T^2-test, which assumes that the parameters are jointly normal, is in effect evaluating the degree of overlap in the linear confidence regions (which are not accurate). On the other hand, the likelihood ratio test is a function of the $\hat{\sigma}_i^2$, the distributions of which are not affected by the parameter effects curvature.

Improving the Reliability of the Tests

T^2-Test

It was stated earlier that the tangent plane approximation to the solution locus and the parameter effects component of nonlinearity depend on the specific algebraic form of the model. Both may be altered by reparameterization. Ratkowsky (1983) discusses the benefits gained by reducing Γ^T. These include two which can improve the reliability of the T^2-test: (1) a reduction in the bias of the parameter estimates, and (2) a joint distribution of the estimates which more closely approximates normality. In this section, the effects of reparameterizations on the outcome of the T^2-test will be examined.

Several reparameterizations were considered:

(33) $h=\frac{\omega}{k}(1-e^{-k(t-t_0)})$ Gallucci and Quinn (1979)

(34) $h=H_\infty-(H_\infty-H_0)e^{-kt}$

(35) $h=H_\infty-\beta\rho^t$ Misra (1980)

(36) $H=\frac{\omega}{k}-\beta e^{-kt}$

(37) $h=h_1+(h_M-h_1)\frac{1-\kappa^{t-1}}{1-\kappa^{M-1}}$

Schnute and Fournier (1980)

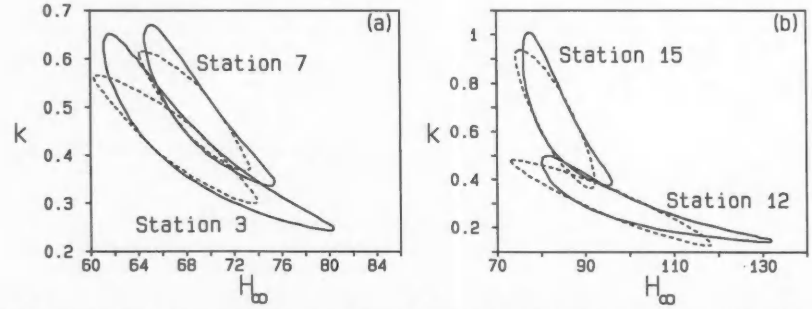

FIG. 1. Bivariate 99% linear, likelihood, and conservative confidence regions for the two cases where the simultaneous tests of (H_∞,k) disagreed. Confidence regions were generated by projections. Dashed lines represent linear confidence regions. It was not possible to visually distinguish the difference between the likelihood and conservative confidence regions (expressions (31) and (32)), and both are representated by solid lines. Refer to Table 3 for additional information.

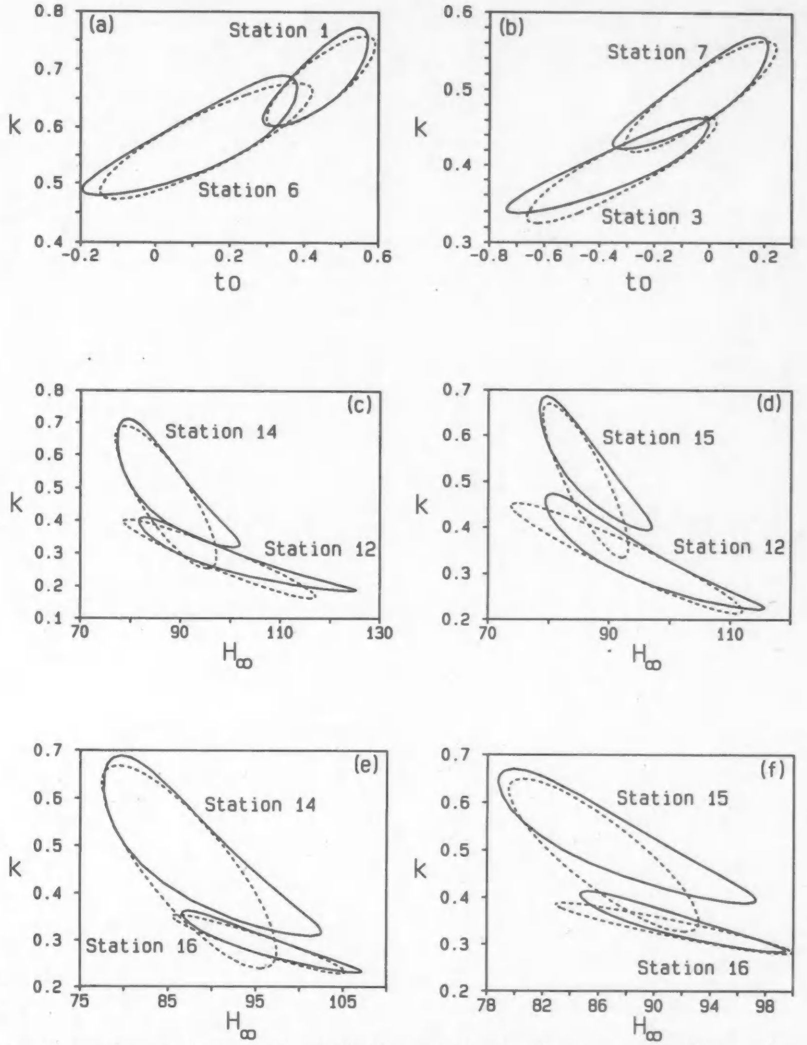

FIG. 2. Two dimensional cross sections of 99% linear, likelihood, and conservative confidence regions for the six cases where the simultaneous tests of (H_∞, k, t_0) disagreed. Sections were generated by holding the third parameter constant. Values of this parameter were chosen to show areas of maximum overlap between the station pairs. Dashed lines represent linear confidence regions. It was not possible to visually distinguish the difference between the likelihood and conservative confidence regions, and both are represented by solid lines. See Table 3 for additional information. (a) $H_\infty = 72$ mm. (b)$H_\infty = 69$ mm. (c) $t_0 = 0.10$ yr. (d) $t_0 = 0.28$ yr. (e) $t_0 = 0.06$ yr. (f) $t_0 = 0.26$ yr.

$$(38)\quad h = h_1 + (h_M - h_1)\frac{1 - \left(\dfrac{h_M - h_{(M+1)/2}}{h_{(M+1)/2} - h_1}\right)^{\frac{2(t-1)}{(M-1)}}}{1 - \left(\dfrac{h_M - h_{(M+1)/2}}{h_{(M+1)/2} - h_1}\right)^{2}}$$

The latter two equations make use of what Ross (1978) has termed expected-value transformations with the parameters h_i equal to the expected size at age i. In both equations M is the age of the oldest individuals in the data set. For equation (38), M must be odd when ages are integers, and so M is the oldest odd age in the data set. While expression (38) is more complex than any of the other reparameterizations, Ratkowsky (1986) for equation (37) and Bates and Watts (1981) have shown that expected-value transformations tend to considerably reduce the parameter effects component of nonlinearity.

Values of Γ^T calculated for each reparameterization are listed in Table 4. In general, all of the reparameterizations reduced the maximum parameter effects curvature to levels below that of the original von Bertalanffy equation. The expected-value function (equation (38)) had the greatest reductions in Γ^T, with values lower than any other model in 11 of the 16 data sets and

TABLE 4. Maximum parameter effects curvatures (Γ^T) for equations (33)–(38) compared with criterion values based on the F-distribution.

Station	(33)	(34)	(35)	(36)	(37)	(38)	$\frac{1}{2\sqrt{F}}$
1	0.405	0.467	0.391	0.358	0.128	0.132	0.251
2	0.982	0.929	0.666	0.652	0.320	0.192	0.252
3	1.330	2.186	1.573	1.488	0.161	0.032	0.252
4	0.668	0.675	0.480	0.466	0.162	0.148	0.253
5	0.579	0.469	0.419	0.374	0.196	0.144	0.253
6	0.804	0.900	0.643	0.612	0.201	0.185	0.253
7	0.797	1.029	0.724	0.660	0.175	0.145	0.253
8	0.333	0.274	0.231	0.204	0.117	0.135	0.254
9	0.531	0.344	0.396	0.317	0.117	0.139	0.253
10	0.231	0.192	0.154	0.121	0.142	0.224	0.255
11	0.179	0.147	0.113	0.102	0.106	0.195	0.254
12	0.935	2.798	2.245	2.309	0.446	0.289	0.243
13	0.255	0.297	0.252	0.165	0.164	0.160	0.252
14	1.285	1.386	1.049	0.960	0.420	0.251	0.241
15	0.803	1.088	0.858	0.822	0.183	0.060	0.236
16	0.593	1.513	1.238	1.093	0.464	0.233	0.252

with Γ^T meeting the criteria for 14 of the 16 stations. As was found by Ratkowsky (1986), the model of Schnute and Fournier (1980) was also well behaved. Values of Γ^T met the criteria for 12 of the 16 data sets, and this parameterization had the smallest maximum parameter effects curvature in three cases. Curiously, a third model, equation (36), had the lowest values of Γ^T for the two largest data sets. Although only four of the 16 stations met the criteria for this model, it was generally better behaved than expressions (33)–(35).

Based on the reductions in Γ^T, T^2-tests of parameters in equations (36)–(38) should prove to be more reliable than those of the original von Bertalanffy parameters. The obvious choice for a multivariate test of all parameters is the expected-value function (equation (38)). It should be noted that this test has one extra computational step not required for the original von Bertalanffy parameters; the comparison must be carried out at a common value of M. Thus, the parameters and the asymptotic covariance matrix for one of the two stocks being compared must be transformed if the M values do not match.

Of the possible parameter subset comparisons among stocks, several involving expressions (36)–(38) are amenable to a biological interpretation. For example, a bivariate test of ω and k in equation (36) is equivalent to comparing size-specific differences in growth rate among stocks since

$$(39) \quad \frac{dh}{dt} = \omega - kh.$$

For univariate tests, both h_1 and κ are biologically meaningful. The latter parameter is the expected fractional reduction in annual incremental growth (Schnute and Fournier 1980) and is analogous to comparing k in the original von Bertalanffy equation ($\kappa = e^{-k}$).

A third univariate test, that of h_M differences, would seem at first to be reasonable since it would compare the expected maximum sizes among stocks. However, the surf clam samples were taken in distinctly different habitats, and the oldest age-class M varies widely among the data sets. If the test of h_M is carried out at a common M, the parameter estimate for one stock needs to be transformed to that of the younger stock (to avoid extrapolation). The test is then no longer a comparison of expected maximum sizes. On the other hand, if the test is carried out directly on the untransformed h_M values from each data set, then one is comparing parameter estimates from two essentially different models. Neither alternative appears to be particularly suitable for the surf clam data. For other instances where the oldest age-classes in the stocks are more comparable, a univariate test of h_M differences may be meaningful.

With the same approach as before, four hypotheses were examined: univariate tests with h_1 and κ, a bivariate test of ω and k, and a simultaneous test of all three parameter estimates in expression (38). As anticipated, comparisons between the likelihood ratio and T^2-tests yielded fewer conflicts. Test results differed in only five of 480 cases (three for h_1 comparisons, one for κ, and one for the multivariate test of the parameters in equation 38). Monte Carlo simulations supported the outcome of the likelihood ratio test in all five instances. Additionally, four of these cases involved at least one data set with a large maximum parameter effects curvature. Thus, while reparameterizations improved the reliability of the T^2-test, incorrect outcomes were still not completely eliminated.

Likelihood Ratio Test

It is clear that the likelihood ratio test is the most reliable of the procedures considered in this study. Box (1971) derived an expression for estimating the bias in an arbitrary function of the parameter estimates. Using this expression, it can be shown analytically, and Ratkowsky (1983) illustrates by example, that expected biases in predicted values of the dependent variable are invariant under reparameterization. As a result, the likelihood ratio test statistic, since it is a function of the $\hat{\sigma}_i^2$ which in turn involve only the observed and predicted values of the dependent variable, is not biased by the parameter effects component of nonlinearity.

A direct consequence of this invariance is that likelihood ratio tests of parameter sets or subsets in reparameterizations which are 1:1 transformations of one another yield identical outcomes. Therefore, a multivariate test of (H_∞, k, t_0) yields the identical outcome as a test of $(h_1, h_{(M+1)/2}, h_M)$. A bivariate test of ω and k ($\omega = H_\infty k$) is equivalent to a bivariate test of H_∞ and k. And, as a final example, likelihood ratio tests of k and κ will produce the same result. In the context of likelihood ratio tests, the only compelling reason to select a parameterization with a low Γ^T is a practical one; it is computationally more efficient to do so. Parameterizations with low Γ^T require less accurate initial values and will converge to the least squares estimate in fewer iterations (Ratkowsky 1983).

It should not be implied from the statements made so far that the likelihood ratio test, using either expression (26) or (27), is free from bias. In particular, small sample sizes and unequal error variances both contribute to biasing these two procedures. Additionally, even though their outcomes were identical for the comparisons made in this study, the two test procedures are not exactly equivalent. In fact, it was already noted that expression (27) results in larger critical values and is, therefore, more conservative.

One particularly appropriate assessment of the accuracy of the two likelihood ratio test procedures is to compare the nominal probability of a Type I error to Monte Carlo results. Two examples of this are presented in Fig. 3. These examples were chosen such that the critical value from Monte Carlo analysis was greater than (Fig. 3a) and less than (Fig. 3b) that of the asymptotic χ^2-test in expression (26). They also illustrate differences related to sample size. In Fig. 3a, the combined sample size is 82 observations, and the difference between the two test

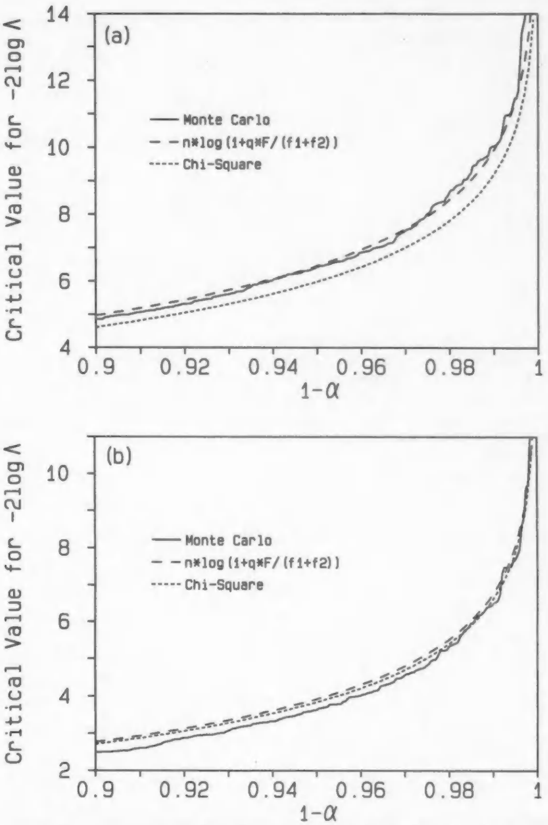

FIG. 3. Examples comparing the cumulative distribution functions of the likelihood ratio tests in equations (26) and (27) to Monte Carlo results. (a) $q=2$ and $n=82$. (b) $q=1$ and $n=310$.

procedures is clearly evident. For a nominal 0.01 test, the Monte Carlo estimate of a Type I error was 0.017 for the asymptotic χ^2-test and 0.011 for the test involving the F-distribution (expression (27)). At combined sample sizes above 300 observations, there is little difference in critical values between the two test procedures (Fig. 3b). The probability of a Type I error was 0.009 for both tests in this example.

Overall, based on the Monte Carlo results for all of the cases listed in Table 3, departures from a nominal 0.01 test were small, with Type I errors averaging 0.011 and ranging from 0.007 to 0.018 for the asymptotic χ^2-test. With the F-test, Type I errors averaged 0.009 and ranged from 0.005 to 0.017. For a significance level of 0.05, the departures from the nominal value were slightly greater due to a shallower slope in the cumulative distribution curves (see Fig. 3). Monte Carlo estimates of Type I errors averaged 0.054 and ranged from 0.041 to 0.067 for the asymptotic χ^2-test. The average was 0.051 and the range was 0.041 to 0.063 for the F-test. These results indicate that the significance level of both likelihood ratio test procedures is reasonably accurate. However, for combined sample sizes less than 300 observations, the more conservative test using expression (27) is preferable, since it is less likely to produce a Type I error which is greater than the nominal value.

Conclusions

In this study, various statistical procedures which have been proposed to compare parameters in the von Bertalanffy equation were examined in detail. The analysis was empirical and made use of a specific set of growth data obtained by Keith (1985). The likelihood ratio test was found to differ from the t-, univariate χ^2-, and T^2-tests of the original von Bertalanffy parameters in about 4% of the outcomes examined. Therefore, it is clear that the test approaches should not be regarded as equivalent.

Confidence region comparisons and Monte Carlo simulations were used to analyze these conflicting outcomes. Disagreements were overwhelmingly resolved in favor of the likelihood ratio test. The parameter effects component of nonlinearity was the major factor implicated in biasing the t-, T^2, and presumably, the univariate χ^2-tests. Two conditions, notable skewness in the distribution of at least one set of estimated parameters coupled with a specific geometric orientation of the estimates being compared, were common to all of the conflicting cases. Since these conditions are specifically tied to the characteristics of the data, no general statement regarding the frequency which conflicts occur can be made.

In relation to the sample sizes considered in this study, the number of inaccurate outcomes for the t- and T^2-tests is, however, surprising. Sample sizes greater than 30 observations are considered to be ''large'' samples in many statistical applications. For the von Bertalanffy equation, the criteria for negligible parameter effects curvature was violated in all of the data sets. Sample sizes in excess of 300 measurements would have been required to produce acceptably low curvature measures. Assuming that the nonlinearity criteria are a suitable means of assessing the distributional properties of the estimates, then even a procedure as simple as a t-test, when applied to the von Bertalanffy parameters, requires larger sample sizes than one would generally expect.

An examination of a number of reparameterizations of the von Bertalanffy equation showed that the maximum parameter effects curvature can be reduced considerably. However, none of the alternate models reduced Γ^T enough to meet the criteria for all 16 data sets. Despite its complexity, the expected-value function in equation (38) was the best behaved of the alternate models with acceptable values of Γ^T for all but two of the smallest samples ($n=43$ and 48). Comparisons between the T^2- and likelihood ratio tests involving the three best behaved reparameterizations produced substantially fewer conflicting cases. Of the few disagreements which did occur, almost all were attributable to the parameter effects curvature and all were resolved by Monte Carlo analysis in favor of the likelihood ratio test.

In contrast to the other procedures, the likelihood ratio test is not biased by the parameter effects component of nonlinearity. As a result, tests of parameter sets or subsets which are 1:1 transformations of one another will always yield identical outcomes. Bias due to the intrinsic curvature of the model is still present (as it is for the other procedures), but analyses presented in this study suggest that its contribution is small. Bias related to the combined effects of sample size and unequal error variances was evaluated for both forms of the likelihood ratio test (expressions (26) and (27)) by comparing the nominal Type I error probabilities to Monte Carlo results. Both forms of the test were found to be reasonably accurate, but the more conservative F-test was preferable when combined sample sizes were less than 300 observations.

Under most circumstances, therefore, the likelihood ratio test should be the approach of choice. Unfortunately, it does require the raw growth data, a condition rarely satisfied when comparisons include results from the published literature. In this one exception, an investigator has no choice but to use a T^2- or t-test. There are, however, several steps which can be taken to guard against inaccurate outcomes.

If the parameter estimates, the error variance, and the number of observations in each age-class are provided, sufficient information exists to calculate both the asymptotic standard errors and the nonlinearity measures. The approach is straightforward in this case. The maximum parameter effects curvature can be evaluated, and accuracy of the comparisons can always be improved by selecting an appropriate reparameterization.

Instead of the number of observations in each age-class, if only the asymptotic covariance matrix is provided, the options open to the investigator are more limited. Reparameterizations are still possible but curvature measures cannot be calculated. Comparisons using parameter sets or subsets which are 1:1 transformations of one another can be carried out for several parameterizations. Substantial parameter effects curvature is indicated if the outcomes under different parameterizations disagree. A very labor intensive procedure could also be attempted to qualitatively assess the parameter effects curvature. Linear confidence regions can be generated with expression (30) for several reparameterizations. The resulting ellipsoids can then be transformed back into the original (H_∞,k,t_0) parameter space. The parameter effects curvature is small if the set of confidence regions closely resemble one another. In any event, an investigator in this situation should consider T^2- or t-tests only when no other alternatives are available. Sample sizes should be very large, models with expected-value transformations are the safest alternatives, and the test results should be clearly reported as approximations.

Acknowledgments

I with to thank the referees for their careful review of the manuscript, and their constructive suggestions for improving the approach.

References

BATES, D. M., AND D. G. WATTS. 1980. Relative curvature measures of nonlinearity (with discussion). J. R. Statist. Soc. B 42(1): 1–25.

1981. Parameter transformations for improved approximate confidence regions in nonlinear least squares. Ann. Stat. 9: 1152–1167..

BEALE, E M. L. 1960. Confidence regions in non-linear estimation (with discussion). J. R. Statist. Soc. B 22(1): 41–88.

BERNARD, D. R. 1981. Multivariate analysis as a means of comparing growth in fish. Can. J. Fish. Aquat. Sci. 38: 233–236.

BOX, M. J. 1971. Bias in nonlinear estimation. J. R. Statist. Soc. B 32(2): 171–201.

COOK, R. D., AND M. L. GOLDBERG. 1986. Curvatures for parameter subsets in nonlinear regression. Ann. Stat. 14(4): 1399–1418.

DRAPER, N. R., AND H. SMITH. 1986. Applied regression analysis. John Wiley and Sons, New York, NY. 407 p.

EFRON, B. 1982. The jacknife, the bootstrap, and other resampling plans. Society for Industrial and Applied Mathematics, Philadelphia, PA. 92 p.

GALLANT, A. R. 1975a. The power of the likelihood ratio test of location in nonlinear models. J. Am.Stat. Assoc. 70: 198–203.

1975b. Nonlinear regression. Am. Stat. 29(2): 73–81.

GALLUCCI, V. F., AND T. J. QUINN II. 1979. Reparameterizing, fitting, and testing a simple growth model. Trans. Am. Fish. Soc. 108: 14–25.

KEITH, D. L. 1985. Age, morphometric variation, and growth rate of the Atlantic surf clam, *Spisula solidissima*, from Long Island waters, M. S. thesis, Marine Sciences Research Center, State University of New York, Stony Brook, NY. 145 p.

KENDALL, M. G., AND A. STUART. 1967. The advanced theory of statistics. Vol. 2. Inference and relationship. 2nd ed. Hafner Publishing Co., N.Y. 690 p.

KIMURA, D. K. 1980. Likelihood methods for the von Bertalanffy growth curve. Fish. Bull. 77(4): 765–776.

KINGSLEY, M. C. S. 1979. Fitting the von Bertalanffy growth equation to polar bear age–weight data. Can. J. Zool. 57: 1020–1025.

MARDIA, K. V., J. T. KENT, AND J. M. BIBBY. 1979. Multivariate analysis. Academic Press, London 521 p.

MISRA, R. K. 1980. Statistical comparisons of several growth curves of the von Bertalanffy type. Can. J. Fish. Aquat. Sci. 37: 920–926.

1986. Fitting and comparing several growth curves of the generalized von Bertalanffy type. Can. J. Fish. Aquat. Sci. 43: 1656–1659.

RAO, C. R. 1958. Some statistical methods for comparison of growth curves. Biometrics 14: 1–17.

1973. Linear statistical inference and its applications. John Wiley and Sons, New York, NY.

RATKOWSKY, D. A. 1983. Nonlinear regression modeling: a unified practical approach. Marcel Dekker, New York, NY. 276 p.

1986. Statistical properties of alternative parameterizations of the von Bertalanffy growth curve. Can. J. Fish. Aquat. Sci. 43: 742–747.

ROSS, G. J. S. 1978. Exact and approximate confidence regions for functions of parameters in non-linear models. *In* Corstein and J. Hermans [ed.] COMPSTAT 78, Third Symposium on Computation. Physica-Verlag, Vienna.

SCHNUTE, J., AND D. FOURNIER. 1984. A new approach to length–frequency analysis: growth structure. Can. J. Fish. Aquat. Sci. 37: 1337–1351.

ZAR, J. H. 1984. Biostatistical analysis. 2nd ed. Prentice-Hall, Englewood Cliffs, NJ. 718 p.

Variation in Lake Water Temperature in the Nanticoke Region of Long Point Bay, Lake Erie, during the Open-Water Season

T. G. Dunstall

Ontario Hydro Research Division, 800 Kipling Ave., Toronto, Ont. M8V 5S4 Canada

D. W. Lawler and R. Farooqui

Ontario Hydro Design and Development Division — Generation, 700 University Ave., Toronto, Ont. M5G 1X6 Canada

and G. T. Haymes

Ontario Hydro Research Division, 800 Kipling Ave., Toronto, Ont., M8V 5S4 Canada

Dunstall, T. G., D. W. Lawler, R. Farooqui, and G. T. Haymes. 1990. Variation in lake water temperature in the Nanticoke region of Long Point Bay, Lake Erie, during the open-water season. Can. J. Fish. Aquat. Sci. 47: 1427–1433.

Lake water temperature on the north shore of Long Point Bay near Nanticoke (Lake Erie) over the years 1971–83 varied considerably during the lake warming cycle. Upwellings, resulting in temperature drops of 5–10°C over a 2–3 d period, were common from mid-May to mid-August. Warmer surface waters returned within 6 d (usually 3 d) following summer upwellings. In spring, the recovery times were variable but typically lasted longer, up to 25 d. Temperature fluctuations that exceeded 5°C but lasted less than 48 h were also frequent during the lake warming cycle. The progressive deepening of the epilimnion to the 12-m depth of Long Point Bay and the associated increase in the heat content of the Bay resulted in a stable temperature regime by mid-August. Diurnal heating and cooling of surface waters, by as much as 4°C, was apparent under calm conditions. Mean April–November temperatures varied by more than 2°C, reflecting annual variation in atmospheric warming.

De 1971 à 1983, la température de l'eau du lac sur la rive nord de la baie Longue Pointe près de Nanticoke (lac Erié), a varié énormément pendant le cycle de réchauffement du lac. Des remontées d'eau froide, attribuables à des chutes de température de 5 à 10°C pendant 2 ou 3 jours, étaient courantes de la mi-mai à la mi-août. Les eaux de surface redevenaient plus chaudes en 6 jours (habituellement 3) après des remontées d'eau froide estivales. Au printemps, le temps de rétablissement était variable mais il était en général plus long, pouvant atteindre 25 jours. Des variations de température supérieures à 5°C, mais de moins de 48 h, étaient également fréquentes pendant le cycle de réchauffement du lac. L'enfoncement progressif de l'épilimnion jusqu'à la profondeur de 12 m de la baie Longue Pointe et la hausse associée à la chaleur de la Baie ont produit un régime de température stable dès la mi-août. Le réchauffement et le refroidissement diurnes des eaux de surface, de 4°C, étaient évidents par temps calme. La variation des températures moyennes d'avril à novembre était supérieure à 2°C, ce qui traduit une variation annuelle du réchauffement atmosphérique.

Received November 18, 1988
Accepted February 8, 1990
(J9949)

Reçu le 18 novembre 1988
Accepté le 8 février 1990

Although dynamic physical processes can be expected to influence components of the aquatic environment, many studies, particularly those concerned with the effects of anthropogenic activity, assume that a degree of environmental homogeneity exists in space and over short periods of time. This assumption often leads to an inability to distinguish anthropogenic effects from natural variability. One approach to this problem is to determine the normal, or non-stressed, condition and then examine deviations from this condition and the physical forces that contribute to these deviations. Natural events, which can have profound effects on the environment are considered to be unusual if they are perceived to be infrequent. However, whether or not an event is perceived to be unusual often depends on the duration of the particular study (Lewin 1986). Long-term studies are valuable in understanding the significance of the extent and causes of natural heterogeneity and should be an essential part of environmental impact assessment.

Meteorological conditions directly influence water movement in large lakes and associated temperature changes, including the abrupt temperature excursions that result from upwellings (Boyce 1974). In large lakes upwellings are common within 8–10 km of shore, in a region defined as the coastal boundary layer (Csanady 1984). In the nearshore region of Long Point Bay (Lake Erie) near Nanticoke, water movement is mainly responsive to wind stress and shore parallel currents predominate, with net water transport directed to the east (Kohli and Farooqui 1980). Ekman–type upwellings occur when these nearshore waters are displaced both alongshore and offshore, being replaced by cooler, hypolimnetic water (Csanady 1977; Simons 1978; Simons and Schertzer 1987). Warm surface water returns to the nearshore area (downwelling) when conditions

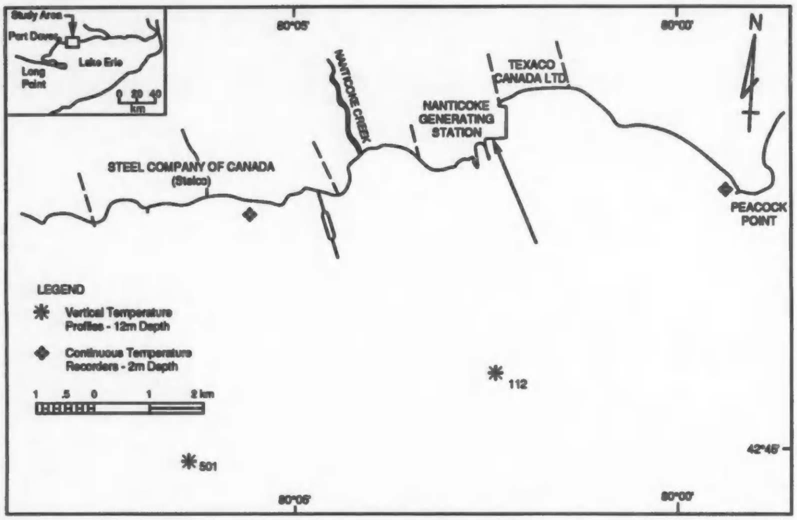

FIG. 1. Temperature measurement locations in the Nanticoke region of Long Point Bay, 1971–83.

change. Vertical mixing, induced by upwelling–downwelling events, affect nutrient levels and the distributions and productivity of biota within the nearshore euphotic zone (Schleske et al. 1971; Yaguchi 1977; Evans 1981; Heufelder et al. 1982).

In this paper we test the hypothesis that homogeneity within the nearshore environment is often transitory. The analyses are based on continuous measurements of nearshore water temperatures taken in the area of Nanticoke, over the years 1971–83. The extent and causes of annual, seasonal, and daily variations in natural lake water temperatures were examined for the open-water period.

The goal of our study was to determine the influence of industrial activity at Nanticoke on the aquatic environment (Haymes and Dunstall 1989). The long-term data that formed the basis for our analyses consisted of measurements of physical, chemical and biological variables[1]. In a companion paper (Dunstall et al. 1990) we test the hypothesis that physical forces contribute to short-term variability among biological and chemical components of the nearshore environment.

Materials and Methods

The study area was located on the north shore of Long Point Bay, Lake Erie, near the town of Nanticoke (Ontario, Canada) (Fig. 1). Long Point Bay, bordered to the south and to the west by Long Point, is relatively shallow with depth increasing gradually offshore. Industrial development along the shoreline includes a steel mill, a fossil-fired electric generating station and an oil refinery.

Water temperatures were recorded continuously at several nearshore locations from the Stelco site to Peacock Point during the open-water seasons from 1971 to 1983 (Fig. 1). The predominance of westerly winds results in lake currents being directed mainly to the east. The water to the west of the generating station is seldom affected by the generating station's thermal plume (Kohli and Farooqui 1980; Burchat 1984). Thus, continuous temperature readings taken at the 2-m depth near Stelco, 3.7 km west of the generating station outfall, were used to describe ambient near-shore conditions. The effect of Nanticoke generating station on lake water temperature has been described by Arden and Farooqui (1981).

Temperatures were recorded as an analog trace on pressure-sensitive paper using single channel Rustrak temperature recorders. Data were abstracted at hourly intervals from the analog strip charts using a Gradicon digitizing system and were transferred to a computer for storage in Standard Time Series format. Overall accuracy was considered to be ± 0.5°C. Occasional missing data for the Stelco site were supplemented with temperature records from other near-shore locations, primarily Peacock Point, which was affected to only a limited extent by the generating station (Lawler 1985).

Upwellings were considered to be persistent events, being defined as a sustained decrease in daily mean water temperatures of $\geq$ 5°C over a 2 to 3-d period. Declines in daily mean temperatures of 6°C or more over 2 d were considered to represent major upwelling events. Temperature data were also examined to identify transient temperature fluctuations. These were defined as differences of 5°C or more between minimum and maximum hourly temperatures that occurred within a 2-d period, and included abrupt (i.e. 1 d) upwelling–downwelling events. Fluctuations exceeding 5°C were also a component of many of the upwellings that lasted longer than 2 d.

Thermal structure of Long Point Bay was determined from vertical temperature profiles taken at the two deepest sampling sites (bottom depth 12-m), located approximately 4 km from shore (Fig. 1). These profiles were taken at 2 wk intervals during the open-water seasons, from 1971–83, using a Yellow Springs Instrument (YSI) thermistor probe.

Hourly wind speed and direction data for the Long Point meteorological station and mean monthly air temperature data for the Port Dover meteorological station were obtained from the Atmospheric Environment Service, Toronto, Ontario.

---

[1] Complete set of tabular data is available, at a nominal charge, from the Depository of Unpublished Data, CISTI, National Research Council of Canada, Ottawa, Canada, K1A 0S2

TABLE 1. Nearshore water temperature conditions in the Nanticoke region of Long Point Bay, 1971–83.

	Upwelling events[a]		No. of times temperature changed ≥5°C in 48 h	Onset of Thermal[b] Stability	Mean temperatures (°C)		
Year	Total	Major			Lake water (Apr.–Nov.)	Air (Apr.–Nov.)	Lake water[c] (Jan.–Feb.)
1971	8	3	41	Aug. 17	13.9	13.7	
72	1	1	34	Aug. 12	12.8	12.6	
73	2	1	27	Aug. 12	14.4	14.3	
74	1	0	22	Aug. 7	13.2	13.1	
75	2	0	34	Aug. 3	14.5	14.2	1.3
76	2	1	22	Aug. 1	13.0	12.8	1.1
77	1	0	28	July 4	13.9	13.9	1.3
78	3	3	32	Aug. 20	13.6	13.2	1.6
79	4	3	37	Aug. 18	13.8	13.2	1.5
80	0	0	27	July 11	13.9	13.5	1.3
81	2	0	15	July 14	14.0	13.6	1.6
82	2	0	42	Aug. 17	13.4	13.2	1.4
83	4	3	41	Aug. 9	15.1	13.6	2.0
Means	2.5	1.2	31	Aug. 4	13.8	13.5	1.5

[a] Upwelling defined as a temperature drop of ≥5°C in a 3-d period. A major event is a change ≥6°C in a 2-d period.
[b] Date of last upwelling or temperature fluctuation during warming cycle.
[c] Winter lake water temperature for GS intake cooling water; 1975–83.

Results

Thirty-two upwellings, including 15 major events, occurred during the 13-yr period (Table 1). Up to three major upwelling events occurred in a given year. The total number of upwellings per year varied from eight during 1971, to none during 1980. These 2 yr exemplify the differences among years in the relative stability of lake water temperature.

Upwelling occurred on 28 occasions during the lake warming cycle, from mid-May to mid-August (Fig. 2). All major upwelling events occurred during this period. On four occasions upwellings resulted in temperature decreases of more than 9°C over a 2-d period: May 30–June 1, 1972 and 1978, July 4–6, 1973, and July 16–18, 1971. Four upwellings occurred between late September and mid-October but these events were not followed by a return to warmer lake water temperatures.

The meteorological conditions that preceded an upwelling typically followed two patterns. In both cases winds from the south-west quadrant with speeds of 25–70 km·h^{-1} persisted for at least 1 d prior to upwelling. Thirteen upwellings occurred when winds continued to prevail from the southwest quadrant. These events occurred during spring warming (May–early July) or fall cooling (September–October). The remaining upwelling events occurred following a shift in the origin of the strong winds, from the southwest quadrant to the northwest quadrant (Fig. 3). This pattern accounted for all nine summer upwellings that were recorded after the first week of July. However, it should be noted that these wind patterns did not always generate an upwelling.

The time required for surface water to recover to within 10% of the pre-upwelling temperatures, varied from 3–25 d for the 15 upwellings which occurred during the spring. Summer recovery periods were shorter, averaging 3 d, with a range of 1–6 d (Fig. 4). Longer recovery periods, following both spring and summer upwellings, resulted from a persistence of moderate to strong winds with the same westerly component that initiated the upwelling. Seven upwelling events were followed by winds that remained strong, but the origin of the winds had shifted to the north-northeast. Winds from this sector also delayed the return of warm waters to the nearshore zone. The relatively long recovery period of 6 d for the summer upwelling shown in Fig. 3 appeared to result from the persistence of moderate winds from the south to southwest and subsequently from the northeast. In contrast, recovery periods of short duration occurred when wind velocity diminished and the source of the winds became variable, but with a tendency to rotate in a clockwise direction.

Short-term temperature fluctuations (i.e. $<$ 48 h), like upwellings, were most frequent during the lake warming cycle (Fig. 2). Changes in lake water temperatures of 10–16°C were recorded within a 48 h period but these were relatively uncommon, comprising only 6% of the total number of fluctuations. The remainder of the fluctuations represented temperature changes of 5–10°C. The most pronounced 48-h fluctuations generally occurred at the onset of upwellings. Fluctuations were most frequent during 1971, 1982, and 1983 (Table 1). In all years, however, there was considerable temperature instability as identified by these short-term fluctuations.

Towards the peak of the lake warming cycle, surface temperatures (2-m depth) became relatively stable and upwellings or short-term temperature fluctuations rarely occurred (Fig. 2). The onset of thermal stability in Long Point Bay varied con-

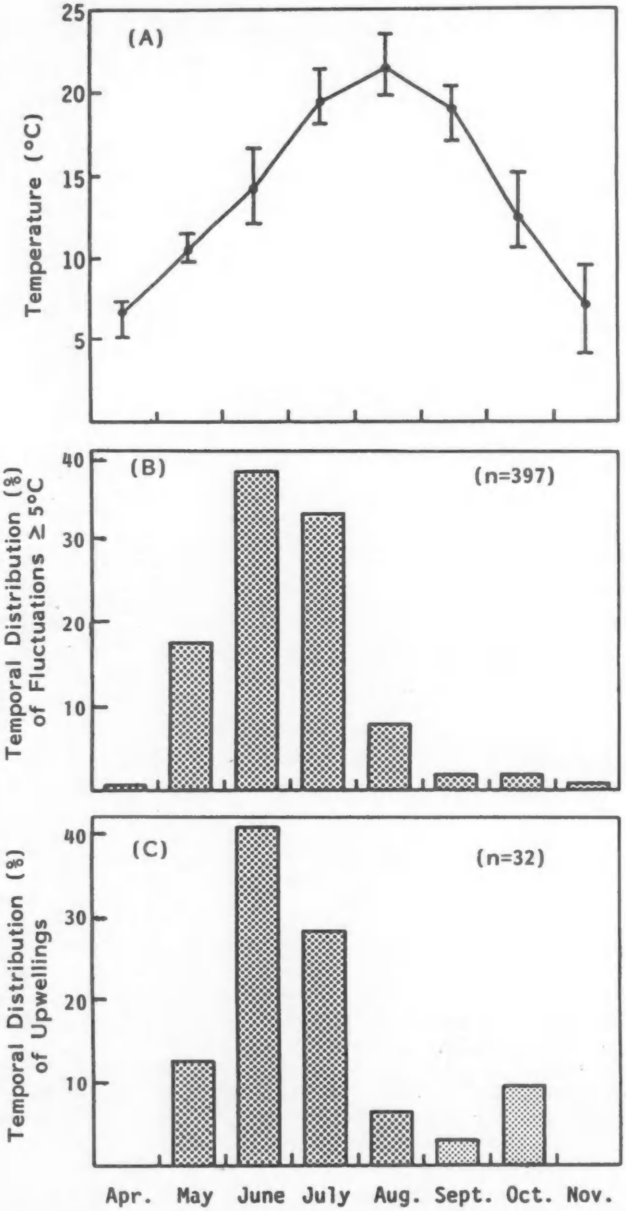

FIG. 2. Mean monthly temperatures (vertical bars = range) at the 2-m depth of Long Point Bay for the years 1971–83 (A), frequency of temperature fluctuations ⩾ 5°C in a 48 h period (B) and frequency of upwellings (C) defined as a change in daily mean temperature ⩾ 5°C within a 3-d period. (Light stipple indicates upwellings that were not followed by temperature recovery.)

siderably among years with the earliest and latest dates being July 4 (1977) and August 20 (1978) (Table 1).

The depth of the epilimnion (below which temperature decreased by more than 1°C·m^{-1}), as determined from offshore vertical temperature profiles to the 12-m depth, was variable from May through July (Fig. 5A). During this period steep temperature gradients at a depth of 1–2 m were not uncommon, indicating that unstable thermal conditions existed at this time of the year. By August the minimum depth of the epilimnion was 8 m. In nearly half the profiles taken during August, iso-

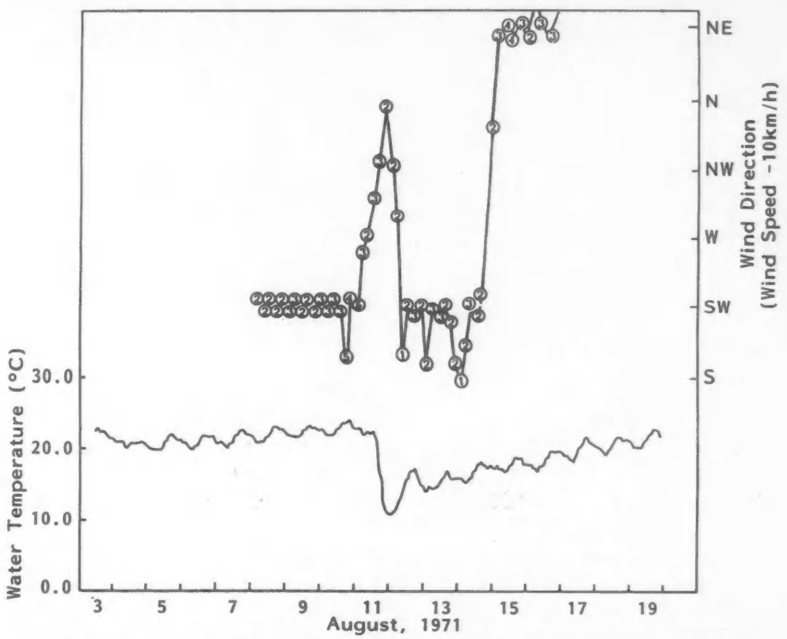

FIG. 3. Chronology of a lake upwelling event at Nanticoke displaying hourly lake water temperatures for 3–19 August, 1971 (lower graph), and wind speed (rounded to tens of km) and direction averaged over 4-h intervals (upper graph).

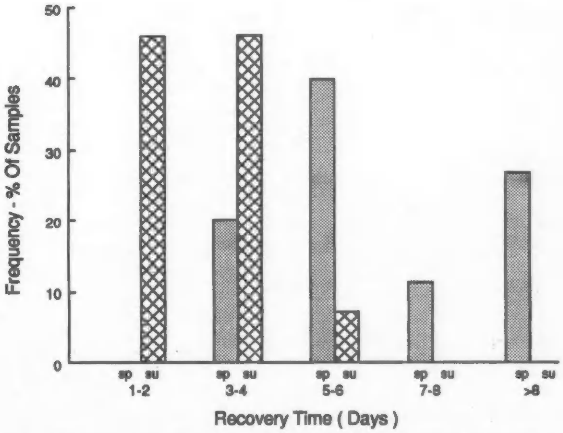

FIG. 4. Interval in days between peak upwelling and recovery of lake surface waters to within 10% of pre-upwelling temperatures for the spring (shaded) and the summer (cross-hatched).

thermal conditions existed in Long Point Bay (Fig. 5B). The heat content (MJ·m^{-2}) of Long Point Bay (to the 12–m depth) was also greatest in August, and followed the same pattern as the mean monthly temperatures derived from the 2–m continuous recorders (Fig. 2A). There was, however, a continued decrease in the occurrence of pronounced temperature gradients (> 1°C·m^{-1}) within Long Point Bay into October.

Diurnal variation in surface water temperatures was often evident from May to August, being detectable when winds were relatively calm (Fig. 3). This daily warming–cooling cycle approximated a sine curve with a period of 24 h. Minimum daily lake water temperatures occurred at dawn (approximately 0600 h) while maximum temperatures were recorded at about 1800 h. The amplitude of temperature change was 1–4°C, but more commonly varied between 1.5 and 3.0°C.

Mean April–November surface water temperature (2-m depth) for the 13 y of study was 13.8°C. The lowest and highest annual mean temperatures (April–November) were 12.8°C (1972) and 15.1°C (1983), respectively (Table 1). Although seasonal temperature patterns in 1971 and 1980 were quite different, mean April–November temperatures for these 2 y were identical (Table 1).

Mean April–November water temperatures were positively correlated to mean air temperatures for the same period ($r = 0.800$). Relatively warm surface water temperatures were recorded during 1983 although air temperatures were only average. This warm lake temperature in 1983 was partly due to the preceding winter which was one of the mildest in recent history (Assel et al. 1984) (Table 1). The water temperature to air temperature relationship improved if the extent of lake warming above the winter base temperature (mean January–February temperature) was used in the regression ($r = 0.851$):

$$\text{Water Temperature} = 1.00(\text{Air Temperature}) + 0.300 \qquad (n = 13)$$

Discussion

The nearshore waters in the Nanticoke region of Long Point Bay are subject to frequent variations in temperature during the lake warming cycle, from mid-May to mid-August. Tempera-

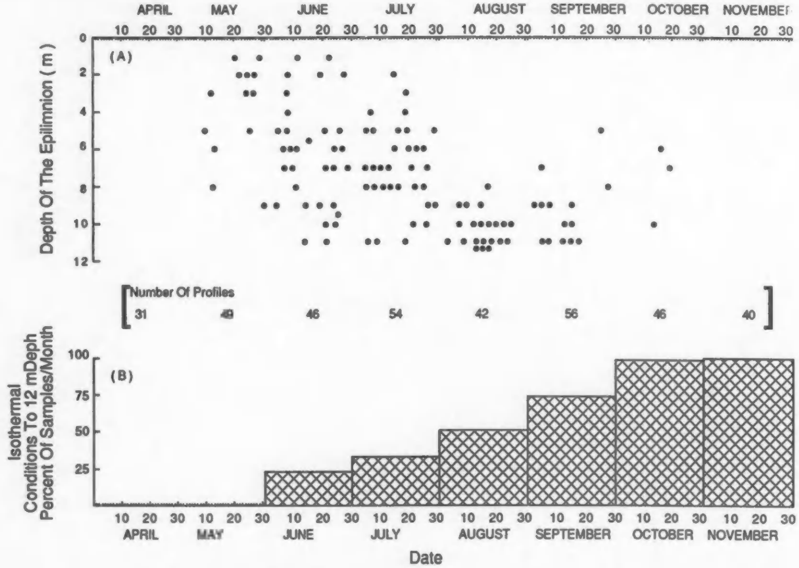

FIG. 5. Results of vertical temperature profiles for the years 1971–83 indicating the presence of a temperature gradient (> 1°C per m) within the 12-m depth (A), and frequency of profile measurements in which Long Point Bay was isothermal to the 12-m depth (B).

ture excursions due to upwellings and to short-term temperature fluctuations, both of which are wind-induced, are common at this time of the year. However, the number of upwellings that occurred in a given year varied, ranging from zero to eight over the years 1971–83.

Warm epilimnetic waters occupy Long Point Bay by mid-August, although there are occasional intrusions of the thermocline into the Bay, between the bottom (12-m depth) and the 8-m depth. As the lake warms, wind-induced turbulence contributes to the rate and overall extent to which the epilimnion deepens. Associated with this mixing is an increase in the stability imparted to the lake surface stratum as the heat content of the lake increases. The epilimnion in the Eastern Basin of Lake Erie usually extends beyond the 15-m depth by mid-August and pronounced stratification exists in deeper offshore regions of the lake (Burns 1976; Kerman et al. 1977; Lam et al. 1983). After mid-August, but prior to fall cooling, the energy associated with even the most severe winds fails to result in the total displacement of the warm surface waters within the relatively shallow reaches of Long Point Bay. However, the strong winds responsible for initiating upwelling also tend to be less frequent and less sustained in mid-summer. Ivey and Patterson (1984) similarly reported the absence of upwellings in the Central Basin of Lake Erie during the period of strong thermal stratification.

The importance of wind direction in initiating upwelling was related to the thermal stability of Long Point Bay. The initial set-up of east-directed currents by winds from the southwest quadrant was often sufficient to result in Ekman-type upwelling during the early stages of the lake warming cycle or in the fall. In the summer, however, upwelling occurred when the source of the strong winds shifted from the southwest to northwest quadrants. This shift results in substantial direct stress being applied to surface waters in an offshore direction. It should be noted however, that upwelling did not result from all occurrences of wind patterns that fit the above two descriptions. In addition to local wind conditions, upwellings can propagate into the region from disturbances at other points around the lake (Simons and Schertzer 1987).

The time taken for warmer surface water to return to the nearshore zone was also related to thermal stability. The short recovery times, typically 2–4 d, in the summer suggests that distinct water masses are replaced during both upwelling and downwelling. Thus, there is a rapid return to the stable energy condition represented by thermal stratification, once the winds that propagated the upwelling subside. Longer recovery periods typical of spring upwellings occur at a time when the lake is weakly stratified, suggesting a gradual mixing of water masses following upwelling.

Longer recovery periods following both spring and summer upwellings resulted from the persistence of winds that had initiated the upwelling. A more rapid return to ambient temperatures tended to be associated with the movement of a high pressure system into the region, identified by a substantial decrease in wind strength and by a clock-wise rotation in wind direction. The downwelling process did not result from a reversal in the direction of strong winds.

The nearshore environments of large lakes are dynamic systems, influenced by meterological conditions. In this study we have characterized the natural variability in lake water temperature within Long Point Bay. Abrupt temperature changes, resulting from upwellings and related short-term temperature fluctuations, occur frequently and irregularly but only during the period of lake warming. This temporal pattern is attributed to the development of thermal stability within the Eastern Basin of Lake Erie and to the relatively shallow topography of Long Point Bay. Less pronounced temperature changes result from the daily warming and cooling of lake surface waters and from annual variations in atmospheric warming. Understanding the sources and extent of natural variability in the physical environment, which is influenced to a considerable extent by wind-induced mass water movements, is an essential first step in attempting to determine the natural or anthropogenic factors that affect other components of the aquatic environment.

Acknowledgements

Studies related to the industrial development at Nanticoke were conducted under the guidance of the Nanticoke Environmental Committee. Technical and financial resources for these studies were provided by the Ontario Ministry of Natural Resources, Ontario Ministry of the Environment, Ontario Hydro, Stelco and Texaco. Irene Cord provided valuable assistance in the analysis of the data.

References

ARDEN, R. S., AND R. FAROOQUI. 1981. Water temperature in Nanticoke – Long Point Bay region of Lake Erie. J. Great Lakes Res. 7: 337–344.

ASSEL, R. A., C. R. SNIDER, AND R. LAWRENCE. 1984. Great Lakes winter weather and ice conditions for 1982–83. Great Lakes Environ. Res. Lab. Rep. 55: 35 p.

BOYCE, F. M. 1974. Some aspects of Great Lakes physics of importance to biological and chemical processes. J. Fish. Res. Board Can. 31: 689–730.

BURCHAT, W. L. 1984. Nanticoke thermal generating station thermal plume field investigations, 1975–1983. Ontario Hydro Des. Devel. Div. 84512.

BURNS, N. M. 1976. Temperature, oxygen and nutrient distribution patterns in Lake Erie, 1970. J. Fish. Res. Board Can. 33: 485–511.

CSANADY, G. T. 1984. Milestones of research on the physical limnology of the Great Lakes. J. Great Lakes Res. 10: 114–125.

1977. Intermittent "full" upwelling in Lake Ontario. J. Geophys. Res. 82: 397–419.

DUNSTALL, T. C., J. C. H. CARTER, B. P. MONROE, G. T. HAYMES, R. R. WEILER, AND G. J. HOPKINS. 1990. Influence of upwellings, storms, and generating station operation on water chemistry and plankton in the Nanticoke region of Long Point Bay, Lake Erie. Can. J. Fish. Aquat. Sci. 47: 1434–1445.

EVANS, M. S. 1981. Distribution of zooplankton populations within and adjacent to a thermal plume. Can. J. Fish. Aquat. Sci. 38: 441–448.

HAYMES, G. T., AND T. G. DUNSTALL. 1989. The influence of industrialization on the aquatic environment of Long Point Bay, Lake Erie, in the vicinity of Nanticoke — 1968 to 1983. Report of the Nanticoke Environmental Committee.

HEUFELDER, G. R., D. J. JUDE, AND F. J. TESAR. 1982. Effects of upwelling on local abundance and distribution of larval alewife (*Alosa pseudoharengus*) in eastern Lake Michigan. Can. J. Fish. Aquat. Sci. 39: 1531–1537.

IVEY, G. N., AND J. C. PATTERSON. 1984. A model of the vertical mixing in Lake Erie. Limnol. Oceanogr. 29: 553–563.

KERMAN, M., D. HYDE, AND J. BULL. 1977. Limnological observations from the Eastern and Central Basin of Lake Erie, May to November, 1977. Limnological observations from the Eastern and Central Basin of Lake Erie, May to November, 1977. Environment Canada. Canada Center Inland Waters Report.

KOHLI, B., AND R. FAROOQUI. 1980. Nanticoke water movements, 1967–1978. Ont. Min. Environ. Rep. March 1980. 68 p.

LAM, D. C. K., W. M. SCHERTZER, AND A. S. FRASER. 1983. Simulation of Lake Erie water quality responses to loading and weather variations. Environ. Can. Sci. Ser. 134.

LAWLER, D. W. 1985. Lake Erie water temperatures in the vicinity of Nanticoke TGS — A post-operational summary, 1979–1983. Ontario Hydro Des. Devel. Div. Rep. 85154.

LEWIN, R. 1986. How unusual are unusual events? Science (Wash., DC) 233: 1385.

SCHLESKE, C. L., E. F. STOERMER, AND L. E. FELDT. 1971. Nutrients, phytoplankton productivity and species composition as influenced by upwelling in Lake Michigan. p. 102–113. *In* Proc. 14th Conf. Great Lakes Res. Internat. Assoc. Great Lakes Res.

SIMONS, T. J. 1978. Generation and propagation of downwelling fronts. J. Phys. Oceanogr. 8: 571–581.

SIMONS, T. J., AND W. M. SCHERTZER. 1987. Stratification, currents, and upwelling in Lake Ontario, summer 1982. Can. J. Fish. Aquat. Sci. 44: 2047–2058.

YAGUCHI, E. M. 1977. Nutrients and productivity as indicators of thermal effluent–upwelling interactions in Lake Michigan. J. Great Lakes Res. 3: 57–64.

Influence of Upwellings, Storms, and Generating Station Operation on Water Chemistry and Plankton in the Nanticoke Region of Long Point Bay, Lake Erie

T. G. Dunstall and J. C. H. Carter,[1]

Ontario Hydro Research Division, 800 Kipling Ave., Toronto, Ont. M8V 5S4 Canada

B. P. Monroe,

Ontario Ministry of Natural Resources, Whitney, Ont. K0J 2M0 Canada

G. T. Haymes,

Ontario Hydro Research Division, 800 Kipling Ave., Toronto, Ont. M8V 5S4 Canada

R. R. Weiler,

Ontario Ministry of the Environment, 135 St. Clair Ave., Toronto, Ont. M4V 1P5 Canada

and G. J. Hopkins

Ontario Ministry of the Environment, Box 213, Rexdale, Ont. M9W 5L1 Canada

Dunstall, T. G., J. C. H. Carter, B. P. Monroe, G. T. Haymes, R. R. Weiler, and G. J. Hopkins. 1990. Influence of upwellings, storms, and generating station operation on water chemistry and plankton in the Nanticoke region of Long Point Bay, Lake Erie. Can. J. Fish. Aquat. Sci. 47: 1434–1445.

Storms and upwellings resulted in significant alterations to the aquatic environment in the Long Point Bay region of Lake Erie, contributing to short-term variability in water chemistry and plankton. Both storms and upwellings resulted in nutrient enrichment (filtered reactive phosphorus, total inorganic nitrogen, reactive silicates and organic nitrogen) in lake surface waters during the period of lake warming, prior to mid-August. Storms and upwellings also differentially affected the distributions of specific zooplankton taxa in the lake surface stratum. The most prominent effect was the increased abundance of *Diacyclops bicuspidatus thomasi* during upwellings, particularly towards shore. The once-through cooling process of the generating station also affected zooplankton distributions, most notably that of *D. bicuspidatus thomasi*, with a nearshore increase in abundance that was similar to the influence exerted by upwelling.

Des tempêtes et des remontées d'eau froide ont modifié énormément le milieu aquatique de la région de la baie Longue Pointe du lac Erié, favorisant la variabilité à court terme des propriétés chimiques de l'eau et du plancton. Ces deux phénomènes ont entraîné un enrichissement en éléments nutritifs (phosphore réactif filtré, azote inorganique total, silicates réactifs et azote organique) dans les eaux de surface du lac pendant la période de réchauffement du lac, avant la mi-août. Ils ont également touché de façon différente les répartitions des taxons zooplanctoniques spécifiques dans la strate superficielle du lac. L'effet le plus important a été l'abondance accrue de *Diacyclops bicuspidatus thomasi* pendant les remontées d'eau froide, notamment vers le littoral. Le processus de refroidissement continu de la centrale électrique a aussi modifié les répartitions du zooplancton, plus particulièrement celle de *D. bicuspidatus thomasi*, avec une augmentation de l'abondance pré-côtière qui était semblable à l'influence exercée par les remontées d'eau froide.

Received 18 November 1988
Accepted Feburary 8, 1990
(J9950)

Reçu le 18 novembre 1988
Accepté le 8 février 1990

Nearshore environment of large lakes is a dynamic system, subject to continually changing conditions that result from wind-forced mass water movements (Boyce 1974). Upwellings and storms are prominent disturbances that generate the mass transport of water. Upwellings occur when nearshore waters are displaced both along-shore and offshore, being replaced by cooler, deeper, hypolimnetic water (Csanady 1977; Simons and Schertzer 1987). Upwellings are followed by the return of warm surface (epilimnetic) water into the nearshore region when wind conditions change. Strong winds associated with storms can generate extensive vertical mixing. The frequency of upwellings and storms varies seasonally, with lake thermal structure influencing both the occurrence and extent of displacement or mixing (Boyce 1974). At times when wind

---

[1] Deceased.

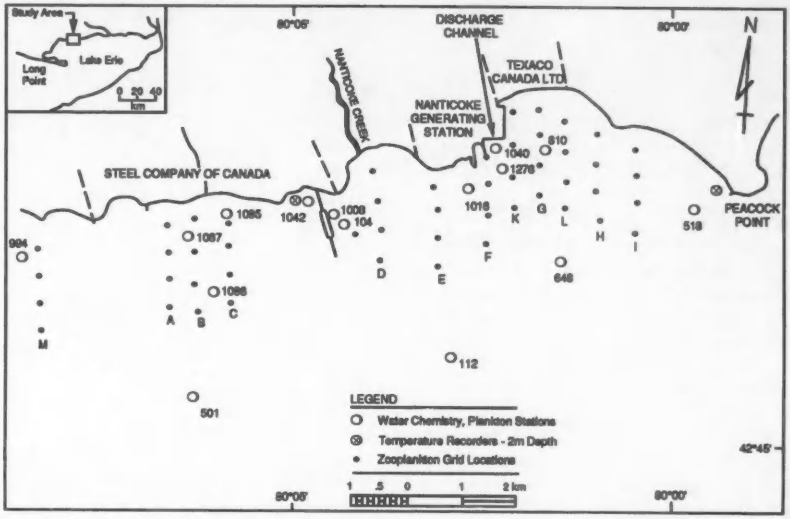

FIG. 1. Location of sampling stations for temperature, water chemistry, and biological monitoring in the Nanticoke region of Long Point Bay, 1969–83.

conditions are quiescent a relatively stable environment can be expected.

It has been suggested that upwelling replenishes surface waters with nutrients thereby serving to maximize potential biological productivity of large lakes (Blanton and Winklhofer 1972; Ragotzkie 1974). In Lake Michigan upwelling resulted in elevated nearshore levels of nitrate and silica and contributed to variability in the concentrations of these nutrients (Schelske et al. 1971). Higher phytoplankton densities, primarily diatoms, and higher primary production rates were also observed following upwelling. Yaguchi (1977) reported higher phytoplankton densities during upwelling, although the contribution of diatoms was reduced and primary production following upwelling declined. The effects of upwelling in Lake Ontario were transitory, with nearshore surface waters being displaced by upwelling but returning at the end of each event (Haffner et al. 1984). Evans (1981) described the change in zooplankton distribution resulting from an upwelling which was characterized by a shoreward increase in abundance. The effects of storm activity on chemical and biological variables within the nearshore environment of the Great Lakes have received little or no attention.

In this paper we test the hypothesis that the mass transport of water that results from upwellings and storms is a major contributor to short-term variability among plankton and chemical variables in the nearshore aquatic environment of Long Point Bay near Nanticoke (Lake Erie). Upwellings and related short-term temperature fluctuations that result in the vertical transport of water, are common features of this region during the lake warming cycle (Dunstall et al. 1990). Over longer periods, normal seasonal patterns and anthropogenic activities contribute to observed variability (Scavia et al. 1986).

The overall goal of our study was to determine the effects of industrial development at Nanticoke on the aquatic environment. Physical, chemical, and biological components of the aquatic environment were closely studied over the years 1969–83 (Haymes and Dunstall 1989). In addition to the long-term studies, a more intensive spatial sampling program allowed for the characterization of zooplankton spatial distributions. Identification of the environmental conditions that contributed to short-term variability and spatial distribution patterns of the study variables provided a framework upon which the effects of industrialization could be assessed. We describe localized changes in zooplankton distributions that result from the relocation of generating station cooling water.

Materials and Methods

Study Area

Sampling stations were located within an area of approximately 10 km × 4 km on the north shore of Long Point Bay, Lake Erie, near the town of Nanticoke (Ontario, Canada). Centred within this area is the Nanticoke industrial complex with a lake frontage of approximately 7 km. Stations located 0.5–4.0 km from shore were sampled for water chemistry, phytoplankton and zooplankton (Fig. 1). Water temperatures at the 2-m depth were recorded continuously at two stations.

Ontario Hydro's Nanticoke Thermal Generating Station is located in the middle of the industrial complex. This station is an eight unit, 4040 MW coal-fired facility that commenced partial operation in 1972 and reached full capacity in 1978. Water used for once-through cooling is drawn through two submerged intakes located at the 10-m depth, 550 m offshore. Each of the condenser units, when operating, passes cooling water at the rate of 11 $m^3 \cdot s^{-1}$. During the study, tempering pumps were used to mix ambient temperature water with condenser cooling water prior to discharge to the lake, thereby maintaining effluent temperatures within established regulations. Maximum water usage by Nanticoke TGS, at full load, is 154 $m^3 \cdot s^{-1}$.

Texaco's oil refinery is located to the east of the generating station and Stelco's steel mill is to the west. Use of air cooling and the recycling of waste waters has reduced total water usage to about 2% and 8%, respectively, of that used by conventional facilities. Process waters from both industries, that must be released to avoid build-up of dissolved solids, are treated prior to discharge. Stelco releases enter the lake via Centre Creek while Texaco releases are discharged through a diffuser located within the generating station's thermal plume. The Texaco refinery commenced operation in 1978 and Stelco began operating in 1980.

Long-Term Studies

Samples were taken approximately every 2 wk from mid-April to mid-November, during the years 1969–83. The total number of zooplankton, phytoplankton, or water chemistry samples per year ranged from 7–20 per station. Zooplankton and chemistry samples were taken near the surface and from mid-depth or near the bottom. Zooplankton samples were collected with a 10-L Juday trap equipped with a 76-μm mesh screen. Grab samples of lake water for chemical analyses were taken using a plastic Van Dorn bottle, and were subsequently processed using standard procedures (Ontario Ministry of the Environment 1975, 1981, and 1983). Phytoplankton samples were photic zone composites taken with a weighted 1-L narrow-neck bottle (Hopkins and Lea 1982). Not all stations and depths were sampled in all years.

Prior to 1974 zooplankton were identified to genus. Subsequently, all crustacean zooplankton (except *Chydorus*) were identified to species. In earlier years, no distinction was made between the cladocerans, *Bosmina* and *Eubosmina*. Taxonomic texts used in the identifications included Wilson (1959), Yeatman (1959), Brooks (1957, 1959) and Deveey and Deveey (1971). Abundances of individual taxa are given as numbers per litre.

Continuous temperature records for 1971–83 from the Stelco site, which is removed from the influence of the generating station's thermal plume (Fig. 1), made it possible to identify the occurrence of upwellings (Dunstall et al. 1990). Samples considered to be taken during an upwelling included those collected within 2 d prior to or following peak upwelling, which included periods of decreasing and increasing temperatures. An upwelling was defined as a decline in mean daily temperatures of ≥ 5°C over a 2 to 3-day period. Abrupt upwellings (short-term temperature fluctuations) also occur in the vicinity of Nanticoke as indicated by relatively rapid temperature changes. On these occasions mean daily temperatures remained relatively constant although the difference between maximum and minimum hourly temperatures within a 48-h period exceeded 5°C. Samples taken during these periods were also identified.

Wind data provided by the Atmospheric Environment Services (Downsview, Ontario) for the Long Point weather station, enabled the identification of samples that had been taken within 1–5 d following a storm. Winds exceeding 40 $km \cdot h^{-1}$ that originated from the ENE to SSE direction were used to define storm events. Storms from this direction have the greatest effect on the nearshore waters within the confines of Long Point Bay. This demarcation also enabled a distinction between storms and upwellings; the latter resulting from strong winds that have a westerly component (Dunstall et al. 1990).

Bi-weekly samples taken from the near-surface stratum over the years 1971–83 were therefore assigned to the upwellings, short-term temperature fluctuations, and post-storm categories. All remaining samples were considered to be taken at times when lake conditions were relatively stable. Samples were also grouped according to habitat (nearshore vs. offshore sampling stations) and season: early spring (April 1–May 15), late spring (May 16–June 30), early summer (July 1–August 15), late summer (August 16–September 30) and fall (October 1–November 30). Specific habitats and seasons were considered since both are likely to contribute to variability among plankton and chemical variables (Heathcote et al. 1981). Comparison of variables between stable and upwelling conditions and between stable and storm conditions were made for each location–season grouping. Samples taken on days characterized by short-term temperature fluctuations were excluded from these analyses since the source of this water (epilimnetic or upwelled) was unknown.

TABLE 1. Stations and years for water chemistry and plankton samples collected in the Nanticoke region of Long Point Bay.

Location	Station	Chemistry/ Phytoplankton	Zooplankton
Offshore	112	1971–78, 1980	1971–80
	501	1971–79, 1981–83	1971–78
Nearshore	1016	1971–78	1971–80
	994	1971–78, 1980–83	1981–83
	810	1971	1971

Variables included in the analyses of upwellings and storms included turbidity, filtered reactive phosphorus (FRP), total inorganic nitrogen (TIN; nitrate + nitrite + ammonia), reactive silicates, total Kjeldahl nitrogen (TKN), chlorophyll *a* (+ pheophytin) and densities of phytoplankton, rotifers, cladocerans, cyclopoid copepods, copepod nauplii, and calanoid copepods[2]. Turbidity was measured using formazin turbidity units (FTU) while FRP, TIN, reactive silicates, and TKN concentrations were determined colourimetrically (Ontario Ministry of Environment 1975, 1981, and 1983). To normalize the distributions of the variables, all data were transformed using natural logarithms with a value of one being added to plankton counts prior to transformation. Comparisons of sample groups were made using appropriate *t*-tests for equal or unequal variances.

The sampling stations included in the offshore and near-shore designations and the years for which data were available are shown in Table 1. Station 1016, located immediately south of Nanticoke TGS, was included as part of the nearshore location because it was considered to be removed from the main influence of the generating station. Although wind and current directions are mainly to the east (Kohli and Farooqui 1980), the generating station did have a limited effect on station 1016 during 1975–80. Station 810 was included as part of the nearshore location for the 1 yr (1971) that it was sampled prior to operation of the generating station. Both the offshore and nearshore locations were considered to be within the region that is normally subject to upwelling activity.

During July 19–27, 1979, one nearshore (810) and one offshore (501) station were repeatedly sampled for water chemistry. This sampling program fortuitously coincided with an upwelling, and enabled an examination of resulting water chemistry changes.

Grid Sampling

A zooplankton sampling grid was used on seven occasions during 1981–83. Intensive sampling (within a single day) over a large area contiguous to the Nanticoke development provided a "point-in-time" picture of zooplankton distribution.

---

[2] Complete set of tabular data is available, at a nominal charge, from the Depository of Unpublished Data, CISTI, National Research Council of Canada, Ottawa, Ont. K1A 0S2 Canada

Samples were taken using a 27-L Schindler–Patalas trap in the immediate station outfall area and along a series of up to 12 transects (A to M) located perpendicular to shore. A 64-μm mesh was attached to the trap except on the first collection date (June 17, 1981). The larger mesh size (158 μm) used on this date would have largely precluded rotifers from the catch. Samples were taken at the 1-m depth; 0.3, 1.0, 1.5, and 2.0 km from shore (Fig. 1). The total number of grid stations were 44 in 1981, 45 in 1982, and 49 in 1983. Samples were also taken at the 3-m depth from the 33 stations closest to the generating station (east of transect D) in 1982–83.

Results

Temporal and Spatial Variability

Consideration of seasonal patterns among chemical and plankton variables facilitates an understanding of the factors contributing to short-term variability. Seasonal patterns were similar in nearshore and offshore waters for all variables, and only data for the latter location are presented.

Turbidity was high in early spring, decreased into early summer, and then increased into the fall. Coincidentally, the seasonal pattern for chlorophyll was similar to that of turbidity, with lowest levels occurring in early summer even though mean phytoplankton abundance varied only slightly over the open-water period (Fig. 2a, 2f, 2g). FRP concentrations were highest in early spring and in the fall and lowest during the intervening periods (Fig. 2b). Concentrations of TIN were lowest and those of reactive silicates were highest in late summer (Fig. 2c, 2d). TKN levels tended to be highest in late spring (Fig. 2e).

Considerable seasonal variability occurred among zooplankton (Fig. 2h–2l). The seasonal abundance of the most abundant rotifers, *Keratella* spp. and *Polyarthra* spp., which together accounted for 75% of total rotifer numbers, varied between years although greatest abundance generally occurred in late spring and in late summer. Crustacean zooplankton abundance peaked in early summer. Abundance of the cladocerans *Bosmina* and *Eubosmina* (mostly *B. longirostris*) was highest from mid-June to mid-July, while densities of *Daphnia galeata mendota* and *D. retrocurva* usually peaked during July or August. These three species accounted for over 99% of the total cladoceran numbers. The cyclopoid copepod, *Diacyclops bicuspidatus thomasi*, was the most abundant crustacean zooplankton in the vicinity of Nanticoke reaching maximum densities in early summer. Copepod nauplii were generally abundant in late spring although numerous minor abundance peaks were typical from May to September. The abundance of calanoid copepods was low in the spring and relatively high during the remainder of the open water period, peaking in late summer.

In addition to temporal variability, vertical gradients in zooplankton densities occurred within the study region. Mean densities of crustacean zooplankton for the open-water period tended to be lower in surface waters than were densities in mid-depth or bottom strata (Fig. 3a). Rotifer densities tended to be lowest near the surface and highest in the mid-depth stratum (Fig. 3b).

Short-Term Variability (Within Seasons)

The frequency of occurrence of upwellings and storms that were directed into Long Point Bay varied considerably during the five seasonal periods (Table 2). Upwellings and related short-term temperature fluctuations were largely confined to the late spring and early summer. Samples taken under these conditions accounted for approximately 59% and 28%, respectively, of the total number of samples collected in each period. Furthermore, samples collected within 5 d following storms accounted for approximately 12% of the total number of samples taken during each of these two periods. In early spring,

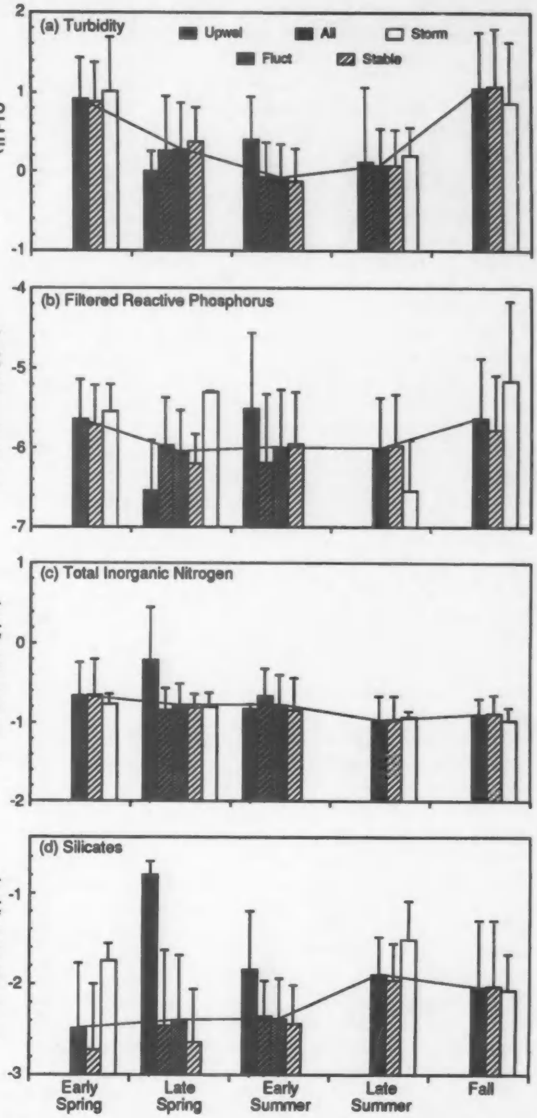

FIG. 2. Temporal patterns for chemical and biological variables in the Nanticoke region of Long Point Bay based on offshore samples collected within each of five seasonal periods during the years 1969–83. Shown are means (vertical bars) and standard deviations for all samples and for samples subdivided into upwelling, short-term temperature fluctuation, stable condition and storm categories.

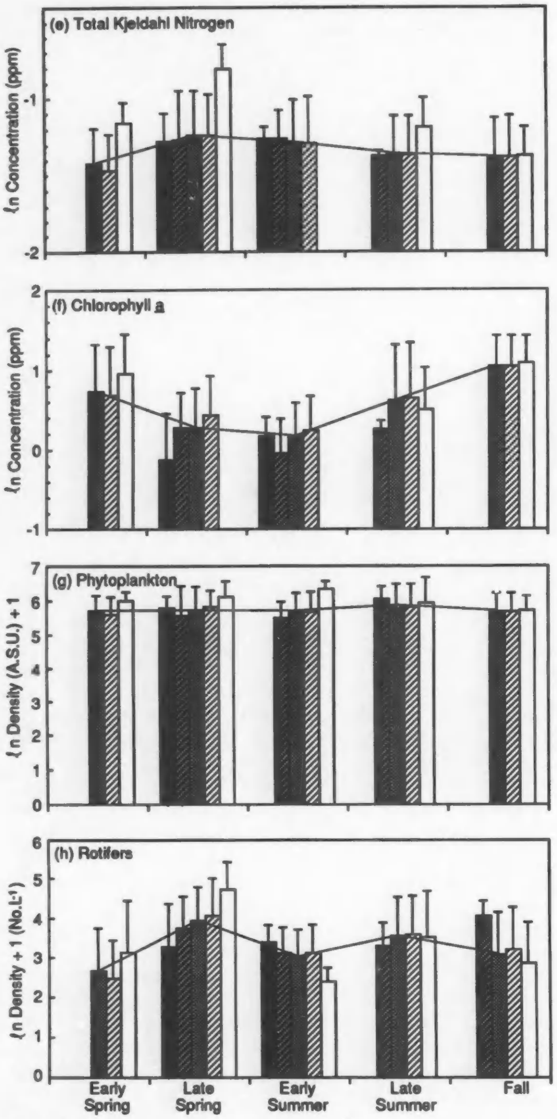

FIG. 2. (*Continued.*)

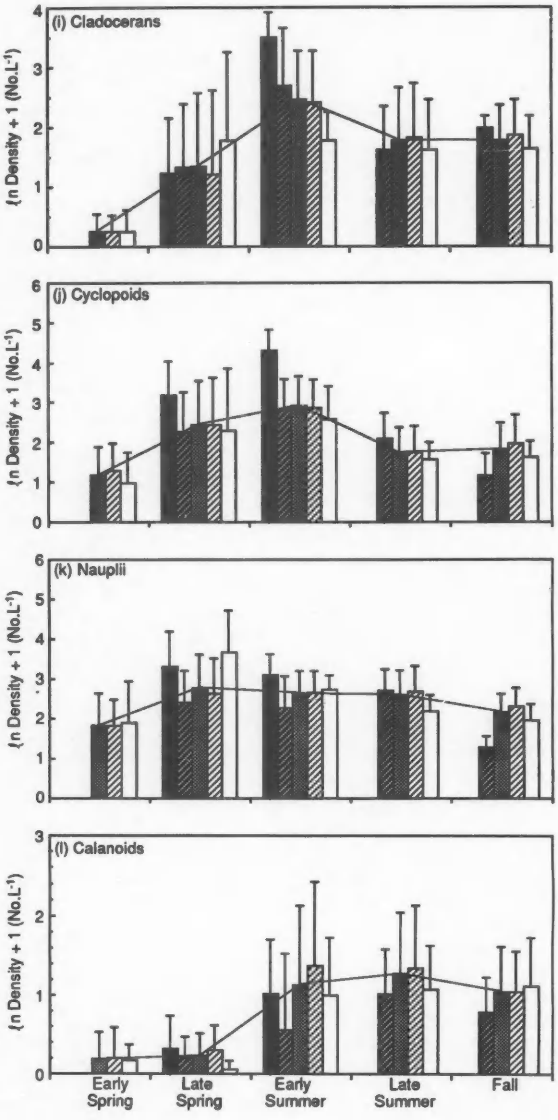

FIG. 2. (*Concluded.*)

late summer, and fall between 20 and 30% of the samples were collected within 5 d following storm activity.

Storm effects — Increased concentrations of FRP, reactive silicates, and TKN and changes to plankton composition were apparent following storms. In early spring, storms resulted in increased turbidity in nearshore waters and higher concentrations of reactive silicates and TKN in offshore waters. Late spring storms also resulted in an increase in TKN offshore and increased concentrations of FRP at both nearshore and offshore locations. Mean post-storm phytoplankton abundances tended to be higher than levels during stable lake conditions from early spring to early summer (Table 3, Fig. 2g). Post-storm chlorophyll levels were also higher than levels during stable conditions during early spring, although the differences were not significant. It should be noted that there were no post-storm turbidity, chlorophyll, or silicate data for late spring and no post-storm chemical data for early summer.

Higher concentrations of reactive silicates in offshore waters followed storms that occurred in late summer. Storms in the fall resulted in increased filtered reactive phosphorus concentrations in both offshore and nearshore waters. Increases in FRP were most noticeable in November samples, with post-storm phosphorus concentrations being three to seven times higher than those in other November samples taken during stable lake conditions.

TABLE 2. Categorization of water chemistry (including phytoplankton) and zooplankton samples collected from the Nanticoke region of Long Point Bay during 1971–83 by lake conditions and seasonal time intervals.

Time block	Sample type	Number of samples	Lake conditions			
			Stable	Upwelling	Post-storm	Fluctuation
Early spring	Chem	78	67	1	9	1
	Zoo	68	46	0	20	2
Late spring	Chem	98	26	11	11	50
	Zoo	111	31	14	18	48
Early summer	Chem	111	69	2	10	30
	Zoo	109	64	7	15	23
Late summer	Chem	129	102	0	27	0
	Zoo	129	90	2	30	7
Fall	Chem	152	107	0	45	0
	Zoo	139	90	3	42	4

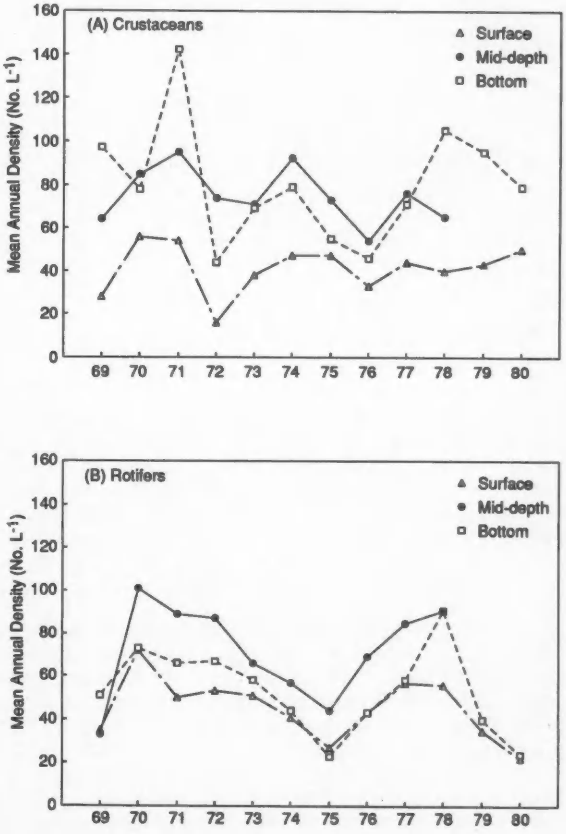

FIG. 3. Mean annual densities of (A) crustacean zooplankton and (B) rotifers at offshore sampling stations for surface (△- -△), mid-depth (●—●) and bottom (□- - -□) strata.

The effects of storms on zooplankton were distinctly different in the spring as opposed to the summer–fall periods. (Fig. 2h–2l). In the spring, densities of rotifers, cladocerans, and nauplii tended to be higher and densities of calanoid copepods lower in post-storm waters as compared to their respective densities under stable lake conditions. Significant differences existed for rotifers and calanoids in early and late spring and for copepod nauplii in late spring (Table 3).

Densities of all zooplankton groups tended to be lower following summer and fall storms but significant reductions in densities were evident only at offshore stations (Fig. 2h–2l; Table 3). Post-storm densities were significantly lower for rotifers and cladocerans (primarily *B. longirostris*) in early summer, copepod nauplii in late summer, and for cyclopoid copepods and copepod nauplii in the fall.

Upwelling effects — Upwellings resulted in increased concentrations of nutrients although enrichment of specific nutrients (FRP, TIN, reactive silicates) was not consistent during all upwellings (Table 3). In late spring, TIN concentrations were generally two to four times higher, and silica concentrations two to eight times higher in upwelled samples compared to levels during stable lake conditions (Fig. 2c,2d). Increased reactive silicate concentrations were also apparent in early summer. Although upwellings resulted in nutrient enrichment, chlorophyll levels decreased in offshore surface waters during late spring upwellings. It should be noted that limited data prevented the evaluation of upwellings on water chemistry at the nearshore stations during early summer.

Some of the observed changes in water chemistry based on classification of individual samples were evident in the sequential sampling that led up to upwelling on July 27, 1979. Nearshore lake water temperature at station 810 had decreased by 6–7°C between July 25 and 27, to 16–17°C. The decline in offshore (station 501) temperature over the same period was approximately 4°C. After July 27 lake water temperate increased by 1–2°C per day, returning to 22°C by July 31.

Concentrations for chemical variables leading up to and including full upwelling on July 27 were compared to con-

TABLE 3. Influence of storms and upwellings on water chemistry and plankton. Shown are significant differences (t-test; $P<0.10$)[a] between samples taken during stable lake conditions and samples taken within 5 d following storms or samples taken during upwellings. Sample sizes indicated in brackets (No. stable samples/storm or upwelling samples.)

Period	Variable	Storm[b]		Upwelling[c]	
		Nearshore	Offshore	Nearshore	Offshore
Early spring	Silicates	ID[D]	+(14/2)	ID	ID
	TKN	NC[E]	++(28/3)	ID	ID
	Turbidity	++(18/3)	NC	ID	ID
	Phyto	+(20/4)	+(19/5)	ID	ID
	Rotifers	++(19/8)	+(27/12)	ID	ID
	Calanoids	−−(19/8)	NC	ID	ID
Late spring	FRP	++(4/3)	++(13/2)	NC	NC
	TIN	NC	NC	++(4/2)	++(14/3)
	Silicates	ID	ID	NC	++(10/2)
	TKN	NC	++(16/2)	NC	NC
	Chlorophyll	ID	ID	NC	−−(18/6)
	Rotifers	+(13/9)	+(18/9)	NC	−(18/7)
	Cyclopoids	NC	NC	++(13/7)	NC
	Nauplii	++(13/9)	++(18/9)	++(13/7)	+(18/7)
	Calanoids	NC	−−(18/9)	+(13/7)	NC
Early summer	Silicates	NC	NC	ID	+(18/2)
	Phyto	NC	++(35/4)	ID	ID
	Rotifers	NC	−−(36/8)	NC	NC
	Cladocerans	NC	−−(36/8)	NC	++(36/4)
	Cyclopoids	NC	NC	++(28/3)	++(36/4)
Late summer	Silicates	NC	+(29/3)	ID	ID
	Nauplii	NC	−−(48/9)	ID	ID
Fall	FRP	++(19/15)	++(43/12)	ID	ID
	Cyclopoids	NC	−−(52/22)	ID	ID
	Nauplii	NC	−−(52/22)	ID	ID

[a] +, − $0.05 < P < 0.10$; ++, −− $P \leqslant 0.05$.

[b] Storms defined as sustained winds >40 $\mathrm{km \cdot h^{-1}}$ from the ENE to SSE quadrant.

[c] Upwellings defined as a temperature decrease >5°C over a 2 to 3–d period.

[d] Insufficient data (<2 events).

[e] No significant change.

centrations based on all other samples collected during 1979 (Fig. 4). In nearshore waters the concentrations of FRP, TIN, and TKN reached their highest levels during the height of upwelling, exceeding annual mean concentrations by 1.7 to 5.5 times. FRP concentration was also higher offshore during upwelling but the extent of this increase was less pronounced. There were no appreciable changes in turbidity or silica levels during this upwelling.

Increased abundance of cyclopoid copepods, copepod nauplii and cladocerans was common following upwellings at Nanticoke (Table 3, Fig. 2i–2k). Although only data for offshore stations have been shown, upwellings generally had the greatest influence on zooplankton at the nearshore stations. Significantly higher mean densities of cyclopoid copepods (mainly *D. bicuspidatus thomasi*) occurred following upwelling at the nearshore locations during late spring and at both the nearshore and offshore locations in early summer. Copepod nauplii were significantly more abundant in upwelled samples during late spring. Mean densities of cladocerans, mainly *Bosmina longirostris*, were significantly higher in offshore waters during early summer upwellings. Decreased abundance of rotifers following upwellings was indicated during late spring (Table 3).

Grid sampling provided detailed spatial representation of zooplankton distributions during two upwellings. A minor upwelling was in progress on June 17, 1981, with water temperature decreasing towards shore (Fig. 5a). Relatively high densities of *D. bicuspidatus thomasi* (adults and juveniles) occurred in nearshore waters, particularly in front of the generating station (E), a location that was outside the influence of the discharge plume, and in the Centre Creek area (A–C) (Fig. 5b).

A more intensive upwelling event occurred during grid sampling on July 6, 1983. Lake water temperature had dropped 9°C between July 4 and 6. On the date of sampling, temperatures decreased from west to east and, in the western half of the study area, decreased towards shore (Fig. 6a). Extending west of the generating station to Center Creek, and east towards Peacock Point, copepod densities at the 1-m depth were relatively high within 1 km of shore (Fig. 6b). This distribution was associated with the region of greatest upwelling activity. Nearshore sampling stations on transect H appeared to be a focal point of upwelling, characterized by high densities of *D. bicuspidatus thomasi*. Higher densities of copepods towards shore was also apparent at the 3-m depth in the region between transects D and

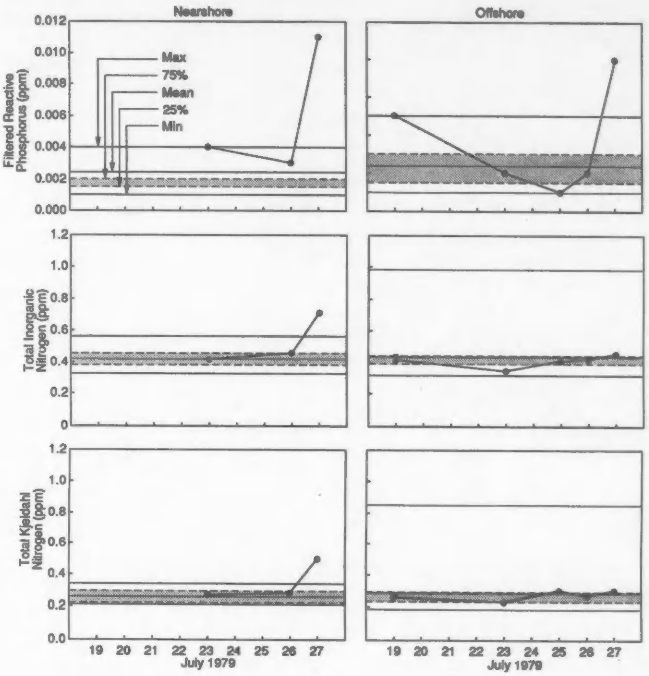

FIG. 4. Concentrations of selected chemical variables at Nanticoke prior to and during upwelling in July, 1979. Horizontal lines represent maximum, mean and minimum concentrations and shaded areas are the 25th–75th percentile ranges based on 15 and 20 measurements (1979) for nearshore (810) and offshore (501) stations, respectively, but excluding individual values shown for the upwelling period.

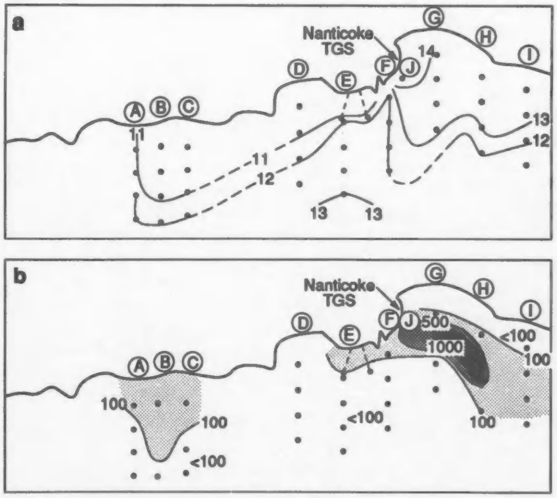
a
Nanticoke TGS
A
B
C
D
E
F
G
H
I
J
14
11
11
12
13
12
13
13
b
Nanticoke TGS
500
1000
<100
100
100
<100
100
100
<100

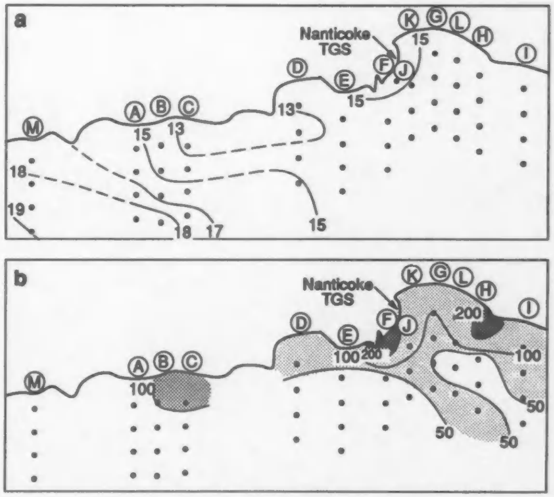
a
Nanticoke TGS
A
B
C
D
E
F
G
H
I
J
K
L
M
15
15
13
13
15
15
18
19
18
17
15
b
Nanticoke TGS
200
200
100
100
100
50
50
50

FIG. 5. Grid studies at the 1-m depth on June 17, 1981, showing (a) isotherms in °C and (b) densities of *D. bicuspidatus thomasi* copepodites + adults (No·L^{-1}). Wind on 17/6/81 was from the W to SW at 22.4 km·h^{-1} (800–1600 h); cooling water flow = 98 m^3·s^{-1}.

FIG. 6. Grid studies at the 1-m depth on July 6, 1983, showing (a) isotherms in °C and (b) densities of *D. bicuspidatus thomasi* copepodites + adults (No·L^{-1}). Wind on 6/7/83 was from the N at 17.5 km·h^{-1} (800–1600 h); cooling water flow = 68 m^3·s^{-1}.

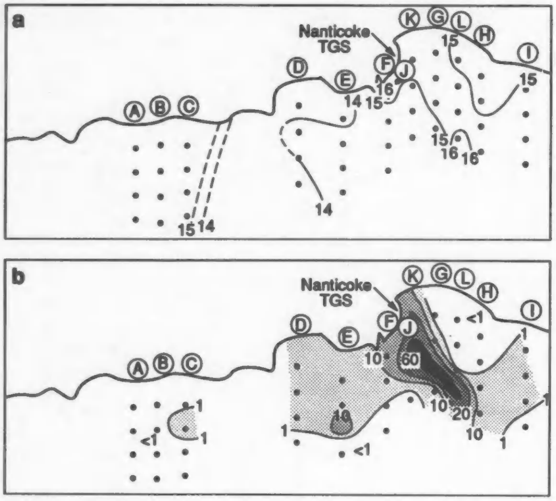

FIG. 7. Grid studies at the 1-m depth on June 11, 1982, showing (a) isotherms in °C and (b) densities of *D. bicuspidatus thomasi* copepodites + adults (No·L^{-1}). Wind on 11/6/82 was from E to S at 7 km·h^{-1} (800–1600 h); cooling water flow = 127 m^3·s^{-1}.

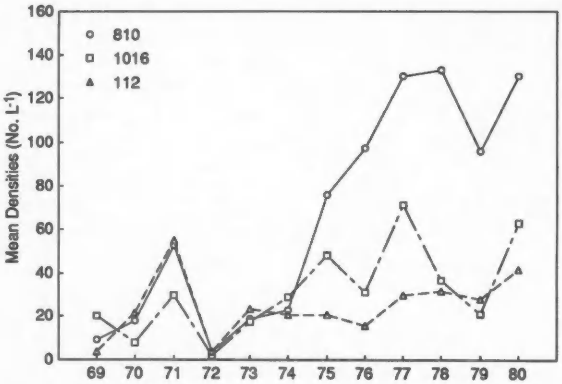

FIG. 8. Mean densities of cyclopoid copepods (adults and copepodites) in the surface stratum at increasing distances from the generating station outfall during early summer (July 1–August 5), based on two to four collections at each of three sites sampled from 1969–83. Stations 810 (circles) proximal to the discharge; station 1016 (squares) west of the discharge centre-line; station 112 (triangles) offshore.

TABLE 4. Zooplankton distribution patterns during grid studies in the Nanticoke region of Long Point Bay.

Date	Taxa	Distribution
June 17, 1981[a]	*D. b. thomasi*	Higher densities towards shore Higher densities in GS[b] plume
	Copeopd Nauplii	Higher densities in GS plume
August 25, 1981	All	Random
November 3, 1981	All	Random
June 11, 1982	*D. b. thomasi*	Higher densities in GS plume
	Copeopd Nauplii	Higher densities in GS plume
	Keratella spp.	Higher densities in GS plume
August 4, 1982	*D. b. thomasi*	Higher densities in GS plume
	Daphnia spp.	Higher densities in GS plume
July 6, 1983[a]	*D. b. thomasi*	Higher densities in GS plume Higher densities towards shore
	Copeopod Nauplii	Higher densities towards shore
	Keratella spp.	Higher densities towards shore
August 18, 1983	All	Random

[a] Dates on which grid sampling coincided with upwellings.
[b] GS – Generating Station.

I (data not shown). Densities of *Keratella* spp. and copepod nauplii at both the 1-m and 3-m depths also increased towards shore in the region east of the generating station (transects K to I), and this too was related to upwelling (Table 4). *B. longirostris* was most abundant to the southeast of the generating station and offshore on the D and E transects, removed from the nearshore region where upwelling activity was most pronounced.

Generating station effects — Once-through cooling had a marked influence on zooplankton distribution on each of the four dates on which grid sampling was conducted, prior to mid-August. Higher densities of *D. bicuspidatus thomasi* (adults and juveniles) occurred in the discharge area on all four of these dates, while densities of copepod nauplii, *Daphnia* spp., and the rotifer, *Keratella* spp., were occasionally higher (Table 4). Changes in zooplankton distributions on these dates generally extended beyond the area delineated by the thermal plume. Prior to mid-August, the generating station thermal plumes tend to be relatively small due to temperature stratification that exists between lake surface waters and the intake depth (10 m). The addition of tempering water to effluent condenser cooling water further minimizes the temperature difference between the water discharged to the lake and the ambient surface waters. Alterations in zooplankton distributions on these four dates, however, clearly occurred in the same regions as the thermal plumes and extended from the generating station in the same direction as predicted from wind conditions on these dates (Burchat 1984).

In addition to the influence of upwelling, once-through cooling resulted in increased densities of *D. bicuspidatus thomasi* in the station outfall area on June 17, 1981 and July 6, 1983. The area of higher *D. bicuspidatus thomasi* abundance on June 17 extended to the east beyond the sampling grid and well beyond the area in which the thermal plume was indicated (Fig. 5). The effect of the generating station on the distribution of this species was much less pronounced on July 6, being confined to the immediate discharge area (Fig. 6). The limited once-through cooling effect on July 6 was attributed in part to a cooling water flow that was only 44% of capacity.

The distribution of *D. bicuspidatus thomasi* on June 11, 1982 was related only to operation of the generating station since there was no upwelling activity, but occurred during the period when pronounced vertical temperature gradients exist within Long Point Bay. The wind on June 11 was from the east to south quadrant, which characteristically produces a split plume configuration, with alongshore movement of water to both the east and west from the point of discharge (Burchat 1984). The distribution of *D. bicuspidatus thomasi* at the 1-m depth had the shape of this plume configuration (Fig. 7b). Highest cyclopoid densities were apparent to the southwest of the generating station outfall. Station C2 likely represented the western extent of the "biological plume," which was expected to be large in area based on a high cooling water flow rate (82% of capacity). The split in the plume is apparent offshore on the F and K transects. Distributions of this species at the 3-m depth on June 11 (and also on August 4, 1982) indicated that these organisms were being vertically entrained from deeper stratum into the overlying plume (data not shown). Increased densities of copepod nauplii and rotifers on June 11 (and *Daphnia* spp. on August 4) were also evident in surface waters in the vicinity of the generating station discharge (Table 4).

In the three grid studies conducted after mid-August (Table 4), zooplankton distributions tended to be heterogeneous throughout the Nanticoke region, although occasional inshore-offshore density gradients were apparent throughout the grid area. Vertical temperature gradients tend to be small, and isothermal conditions often exist, in Long Point Bay at this time of the year. Thus the generating station thermal plumes in the late summer and fall are large compared to those in the period prior to mid-August.

Among the zooplankton, a persistent change in distribution that could be attributed to generating station operation was only evident for *D. bicuspidatus thomasi* adults and copepodites and only in early summer (Fig. 8). From 1969 to 1974, copepod densities were similar at each of three sites located at various distances offshore from the generating station outfall. During these years the highest mean copepod densities occurred in 1971, a year of exceptionally frequent upwelling (Dunstall et al. 1990). A substantial increase in copepod densities occurred close to the discharge (site 810) in the operational years, 1975–80. (Although Nanticoke TGS began operation in 1972, little energy was produced during April–November prior to 1975). At site 1016, to the west of the main body of water influenced by the station (given prevailing westerly winds), and offshore at site 112, early summer copepod densities were generally 2–4 times lower than those at site 810 during the years of station operation. It also appears that copepod densities at site 1016 had increased during 1975–80 and, except for 1979, were found in higher densities than at site 112. Early summer copepod densities at site 112 remained relatively constant in both the pre-operational and operational years. Although late spring cyclopoid copepod densities near the discharge were generally higher than, or comparable to, densities at the other sites, no consistent pattern was apparent during 1975–80.

Discussion

Lake conditions in the Nanticoke region of Long Point Bay were frequently subject to changes induced by storm and upwelling activity. Storms and upwellings were major contributors to short-term variability among chemical and biological variables, particularly during the lake warming cycle. Closely related to upwellings were occasions in which temperature fluctuations of shorter duration occurred. However, because of the abruptness of temperature change, the source of the water (epilimnetic or upwelled) that was sampled on these occasions was unknown. Samples taken at times of stable lake conditions accounted for only 27% and 61% of the total number of samples collected in late spring and early summer, respectively.

The frequency of upwellings, related short-term temperature fluctuations, and storms suggests there is a near continuous vertical mixing in the spring when the lake is weakly stratified. Gradual mixing of upwelled water and displaced surface waters can occur in the spring (Dunstall et al. 1990). Storms at this time of the year would facilitate deep vertical mixing.

Spring storms contributed to increases in turbidity and nutrient concentrations (FRP, reactive silicates, organic nitrogen) in near-surface waters. Resuspension of lake sediments deposited since the previous growing season and watershed runoff could also have resulted from these spring storms. Upwellings at this time of the year also result in nutrient enrichment (FRP, TIN, reactive silicates), with greatest increases in concentrations towards shore.

Under stable lake conditions during both the spring and early summer, nutrients supporting phytoplankton growth would become depleted within the photic zone. The increase in phytoplankton abundance, and possibly chlorophyll, following storms between April and mid-August suggest the possibility of increased primary production as a result of increased nutrient availability. Although upwellings could also contribute to increased nutrient levels and productivity in the spring, it is unlikely that upwellings have a similar effect in the summer. Upwellings occur in Long Point Bay up to mid-August but become less frequent as the lake stratifies and the epilimnion deepens. By early summer, distinct surface and upwelled water masses are displaced during upwellings and subsequent downwellings (Dunstall et al. 1990). Increased productivity as a result of summer upwellings is unlikely because of this displacement, a situation that is similar to that described for Lake Ontario by Haffner et al. (1984).

The epilimnion continues to deepen into August and isothermal conditions come to exist in Long Point Bay. At this point upwellings cease to occur. Development of a well defined thermal structure would also limit vertical mixing resulting from storms to within the epilimnion. Gradual depletion of nutrients would therefore occur within the photic zone in summer, with limited replenishment of surface waters from deeper strata. The lowest concentrations of the nutrients that support phytoplankton growth generally occur during late summer in the vicinity of Nanticoke. Relatively stable conditions persist within Long Point Bay in late summer and early fall, prior to fall turnover. The increase in filtered reactive phosphorus concentrations following fall storms is attributed to lake turnover.

The influence of storms and upwellings on zooplankton densities in surface waters was related to the vertical distributions of specific taxa. Rotifer abundance increased following spring storms and decreased during late spring upwellings. This was consistent with the fact that rotifers tend to be most abundant at mid-depth in Long Point Bay and suggests that rotifer densities were lowest in the deeper strata that was subject to displacement during upwellings.

In the spring, densities of copepod nauplii, and possibly cladocerans, in near-surface waters were lowest during stable lake conditions and increased as a result of both storm and upwelling activity. Increased cladoceran abundance in early summer occurred only during upwellings indicating that individuals from this group were present in greater densities in deeper strata following the onset of thermal stratification.

Cyclopoid copepod (primarily *Diacyclops bicuspidatus thomasi*, adults and copepodites) and calanoid copepod abundance increased following upwellings, but densities were reduced (calanoids) or unchanged (cyclopoids) following spring or early summer storms. The increase in abundance of these two groups therefore resulted from the displacement of surface water with water from a deeper stratum that was not subject to storm-induced vertical mixing. A return to relatively low copepod densities occurred during stable lake conditions.

The decrease in post-storm zooplankton abundance at the offshore locations in the summer and fall suggests that within the epilimnion zooplankton densities tend to be highest in surface waters. Higher densities could also be associated with the lake bottom at this time of the year possibly accounting for the fact that post-storm zooplankton densities were unchanged at the nearshore sampling stations.

At Nanticoke, changes in zooplankton distribution resulting from once-through cooling are related to the relocation of cooling water from the 10-m intake depth to the lake surface, and to the upward movement of organisms from a deeper stratum due to plume entrainment. Plume currents are directed away from shore and could enhance the upward vertical movement of water in a manner analogous to the offshore winds which lead to upwelling. The changes observed as a result of once-through cooling are, however, confined to the open-water period prior to mid-August, a time when steep thermal gradients are common within Long Point Bay (Dunstall et al. 1990). A similar vertical displacement of zooplankton, including *D. bicuspidatus thomasi*, was mediated by the submerged discharge diffusers at the Donald C. Cook Nuclear Generating Station on Lake Michigan (Evans 1981). In contrast, altered zooplankton distributions near Lennox Generating Station, Lake Ontario, were associated with the direct relocation of cooling water from the hypolimnion (21-m intake depth) to the lake surface (Dunstall et al. 1985). In each case the changes observed were consistent with *D. bicuspidatus thomasi*'s preference for a benthic habitat and their concentration in deeper offshore hypolimnetic waters (Barton and Carter 1982).

Higher zooplankton densities in the generating station discharge area might also suggest that increased productivity has occurred in this area. An increase in production could result from nutrient enrichment, facilitated by the relocation of cooling water from a deeper stratum, or from the local elevation in lake water temperature. Increased nutrient concentrations are possible during the period of lake warming and could sustain localized increases in primary and secondary production. The possibility of a temperature influence on productivity seem unlikely. Increases in zooplankton abundance in the generating station discharge area occurred only during the lake warming cycle and the heat input to the lake via plumes is minimal at this time of the year. Once isothermal conditions become established within Long Point Bay, usually by mid-August, upwelling becomes rare and the generating station exerts little or no influence on the distribution and abundance of zooplankton.

Apart from the changes in zooplankton distributions that resulted from once-through cooling, industrialization at Nanticoke had no other observable effects. To the contrary, trends in zooplankton populations over the years 1969–83 indicated a general improvement in the trophic status of this region of Lake Erie. There was an overall decrease in cladoceran abundance over the study period. *B. longirostris*, the dominant cladoceran from 1969–80, shared dominance with *D. galaeta mendotae* or *D. retrocurva* from 1981–83. The abundance of the rotifer, *Keratella* spp. declined over the 15-yr study period. *Chromogaster* spp., a rotifer that was recorded from Lake Erie in the early 1900's (Burkholder 1929a, b) had reappeared in the Long Point Bay region in 1982–83. The calanoid copepods, especially *Diaptomus* spp., increased in actual and relative abundance over the study period. The apparent lack of change in cyclopoid abundance between 1969 and 1983 may have been related in part to increased local abundance of this group resulting from operation of the generating station. There was also no trend over time in overall phytoplankton abundance in the Nanticoke region even though filtered reactive phosphorus levels had decreased.

Mass water movements related to storm and upwelling activity contributed to short-term variability among water chemistry and plankton variables in Long Point Bay. This was particularly evident during the period of lake warming. A continual state of flux perhaps best describes ''normal'' conditions at this time of the year. Identification of the causes and extent of natural variation among study variables aided the detection of changes superimposed on this aquatic system as a result of industrial development. The main effects of this development on water chemistry and plankton were related to the once-through cooling process of the thermal electric generating station which resulted in localized displacement of lake surface waters with water drawn from a deeper stratum.

Acknowledgements

Studies related to the industrial development at Nanticoke were conducted under the guidance of the Nanticoke Environmental Committee, to which technical and financial resources were provided by the Ontario Ministry of Natural Resources, Ontario Ministry of the Environment, Ontario Hydro, Stelco, and Texaco. Mr. R. MacGregor contributed to the zooplankton program during the latter part of the study. Dr. S. A. Bartlett assisted with aspects of the data analyses and Dr. D. R. Barton provided valuable comments on the manuscript.

References

Barton, D. R., and J. C. H. Carter. 1982. Shallow-water epilithic invertebrate communities of eastern Georgian Bay, Ontario, in relation to exposure to wave action. Can. J. Zool. 60: 984–993.

Blanton, J. O., and A. R. Winklhofer. 1972. Physical processes affecting the hypolimnion of the Central Basin of Lake Erie. Project Hypo. Can. Centre Inland Waters 6: 9–37.

Boyce, F. M. 1974. Some aspects of Great Lakes physics of importance to biological and chemical processes. J. Fish. Res. Board Can. 31: 689–730.

Brooks, J. L. 1959. Cladocera. p. 587–656. *In* W. T. Edmondson [ed.] Freshwater Biology. John Wiley and Sons, New York, NY.

1957. The systematics of North American *Daphnia*. Mem. Conn. Acad. Arts Sci. 13: 1–180.

Burchat, W. L. 1984. Nanticoke thermal generating station — thermal plume field investigations 1975–1983. Ont. Hydro Design Dev. Div. Rep. 84512: 28 p.

Burkholder, P. R. 1929a. Microplankton studies of Lake Erie. N.Y. State Conserv. Dept., Suppl. to Ann. Rep. 18: 60–66.

1929b. Microplankton studies of Lake Erie. p. 73–93. *In* C. J. Fish [ed.] Preliminary report on the co-operative survey of Lake Erie, season of 1928. Bull. Buffalo Soc. Nat. Sci. 14.

Csanady, G. T. 1977. Intermittent "full" upwelling in Lake Ontario. J. Geophys. Res. 82: 379–419.

Deevey, E. S., and G. B. Deevey. 1971. The American species of *Eubosmina* Seigo (Crustacea, Cladocera). Limnol. Oceanogr. 16: 201–218.

Dunstall, T. G., G. T. Haymes, and J. K. Kwik. 1985. Influence of a thermal electric generating station on water chemistry and distribution of plankton. J. Great Lakes Res. 11: 530–539.

Dunstall, T. G., D. W. Lawler, R. Farooqui, and G. T. Haymes. 1990. Variation in lake water temperature in the Nanticoke region of Long Point Bay, Lake Erie, during the open-water season. Can. J. Fish. Aquat. Sci. 47: 1427–1433.

Evans, M. S. 1981. Distribution of zooplankton populations within and adjacent to a thermal plume. Can. J. Fish. Aquat. Sci. 38: 441–448.

Haffner, G. D., M. L. Yallop, P. D. N. Hebert, and M. Griffiths. 1984. Ecological significance of upwelling events in Lake Ontario. J. Great Lakes Res. 10: 28–37.

Haymes, G. T., and T. G. Dunstall. 1989. The influence of industrialization on the aquatic environment of Long Point Bay, Lake Erie, in the vicinity of Nanticoke — 1968–83. Report of the Nanticoke Environmental Committee.

Heathcote, I. W., R. R. Weiler, and J. W. Tanner. 1981. Lake Erie nearshore water chemistry at Nanticoke, Ontario, 1969–78. J. Great Lakes Res. 7: 130–135.

Hopkins, G. J., and C. Lea. 1982. A ten-year study of phytoplankton biomass and composition in the Nanticoke region of Long Point Bay, Lake Erie. J. Great Lakes Res. 8: 428–438.

Kohli, B., and R. Farooqui. 1980. Nanticoke water movements, 1967–78. Ont. Min. Environ. Rep. 68 p.

Ontario Ministry of the Environment. 1983. Handbook of analytical methods for environmental samples. Ont. Min. Environ. Lab. Serv., Appl. Res. Branch. Toronto, Ont. 2 Vol.

1981. Outlines of analytical methods. Ont. Min. Environ. Lab. Serv. Branch. Toronto, Ont. 246 p.

1975. Outline of analytical methods; a guide to the occurrence, significance, sampling and analysis of chemical parameters in water. Ont. Min. Environ. Lab. Serv. Branch. Toronto, Ont. 98 p.

Ragotzkie, R. A. 1974. Vertical motions along the north shore of Lake Superior. p. 456–461. *In* Proc. 17th Conf. Great Lakes Res. Internat. Assoc. Great Lakes Res.

Scavia, D., G. L. Fahnenstiel, M. S. Evans, D. J. Jude, and J. T. Lehman. 1986. Influence of salmonine predation and weather on long-term water quality trends in Lake Michigan. Can. J. Fish. Aquat. Sci. 43: 435–443.

Schelske, C. L., E. F. Stoermer, and L. E. Feldt. 1971. Nutrients, phytoplankton productivity and species composition as influenced by upwelling in Lake Michigan. p. 102–113. *In* Proc. 14th Conf. Great Lakes Res. Internat. Assoc. Great Lakes Res.

Simons, T. J., and W. M. Schertzer. 1987. Stratification, currents, and upwelling in Lake Ontario, summer, 1982. Can. J. Fish. Aquat. Sci. 44: 2047–2058.

Wilson, M. S. 1959. Free-living Copepoda: Calanoida. p. 735–794. *In* W. T. Edmondson [ed.] Freshwater biology. John Wiley and Sons, New York, NY.

Yagushi, E. M. 1977. Nutrients and productivity as indicators of thermal effluent upwelling interactions in Lake Michigan. J. Great Lakes Res. 3: 57–64.

Yeatman, H. C. 1959. Free-living Copepoda: Cyclopoida. p. 795–815. *In* W. T. Edmondson [ed.] Freshwater biology. John Wiley and Sons, New York, NY.

Effect of Fluoride Complexation on Aluminum Toxicity Towards Juvenile Atlantic Salmon (*Salmo salar*)

Kevin J. Wilkinson, Peter G. C. Campbell,[1] and Pierre Couture

Université du Québec, INRS-Eau, C. P. 7500, Ste-Foy, Québec, G1V 4C7 Canada

Wilkinson, K. J., P. G. C. Campbell, and P. Couture. 1990. Effect of fluoride complexation on aluminum toxicity towards juvenile Atlantic salmon (*Salmo salar*) Can. J. Fish. Aquat. Sci. 47: 1446–1452.

In 7-d semistatic bioassays, fluoride complexation attenuated Al toxicity to juvenile Atlantic salmon (*Salmo salar;* age 1 +) and the accumulation of Al in gill tissue, but not to the extent predicted by the free-ion model of metal toxicity. Bioaccumulation and toxicity persisted even in the presence of an excess of the complexing ligand. An equilibrium model, involving the formation of a mixed ligand complex (F–Al–L-gill) at the gill surface, is proposed to explain this residual toxicity (L-gill = ligand at the gill surface). Exposure to Al, or to a combination of Al and F, led to a decrease in the plasma sodium levels even for sublethal conditions. Aluminum concentrations as low as 2 μM adversely affected the salmon. The similarity of the osmo-regulatory response to the H^+-ion, to Al^{3+}, and to $Al(F)_x$ suggested that the mechanism of toxicity in the presence of fluoride did not differ markedly from that observed by previous workers for salmonid species exposed to moderately acidic media containing Al but without added fluoride.

Dans une série d'expériences semi-statiques (durée = 7 j), la complexation de l'aluminium inorganique par les fluorures a réduit sa toxicité et sa bioaccumulation (branchiale) chez les tacons (âge 1 +) du saumon atlantique (*Salmo salar*). Cependant, cette atténuation s'est avérée moins importante que celle prédite en fonction du modèle de l'ion libre. Un modèle des interactions entre l'aluminium et les branchies, impliquant la formation de complexes mixtes (F–Al–L-branchie) à la surface de la branchie, a été élaboré pour expliquer cette toxicité résiduelle (L-branchie = ligand à la surface des branchies). L'aluminium seul, toute comme la combinaison aluminium + fluorures, a provoqué une diminution du Na plasmatique, même à des conditions sous-létales. Des concentrations en Al aussi faibles que 2 μM ont adversement affecté le saumon. En milieu acide, le mécanisme de toxicité de l'aluminium en présence de fluorures ressemble à la réponse osmorégulatrice déjà documentée chez les salmonidés en absence de fluorures.

Received August 22, 1989
Accepted January 30, 1990
(JA284)

Reçu le 22 août 1989
Accepté le 30 janvier 1990

Episodic acidification of running waters and the accompanying geochemical mobilization of aluminum have often been reported during spring snowmelt (Johannessen et al. 1980; Driscoll et al. 1980; Lachance et al. 1983; Hansen and Campbell 1987). The drop in pH leads not only to marked increases in dissolved aluminum concentrations but also to important modifications of the speciation of this element. In their studies of a small New England stream, Driscoll et al. (1980) noted an increased proportion of fluoro-aluminum complexes, $Al(F)_x$, during this critical period of low pH. Similarly, for three Atlantic salmon rivers on the Quebec North Shore, levels of dissolved inorganic Al increased by a factor of ≥ 3 during the spring pH depression (attaining values of ≈ 2.4 μM); up to 60% of this aluminum was present as $Al(F)_x$ species (Hansen and Campbell 1987; Campbell et al. 1989).

Elevated aluminum concentrations have been associated with an aggravated toxic response for several aquatic species under acid conditions (NRCC 1986), notably salmonid fish (Cronan and Schofield 1979; Henriksen et al. 1984). However, despite their obvious geochemical importance, there is little information available regarding the toxicity of aluminum–fluoride complexes to aquatic biota. Examination of the available literature reveals conflicting results: reported effects of fluoride complexation on Al toxicity range from complete suppression (barley seedlings — *Hordeum vulgare*: Cameron et al. 1986) through partial mitigation (white sucker fry — *Catostomus commersoni*: Driscoll et al. 1980) to unaltered toxicity (amphibian eggs — *Bufo americanus*, *Rana sylvatica*: Clark and LaZerte 1985).

For metals commonly linked to anthropogenic activities (e.g. Cd, Cu, Pb, Zn), the aquo-ion activity (M^{Z+}) has often proven to be the best predictor of metal availability towards aquatic biota (Nelson et al. 1981; Petersen 1982; Sunda and Huntsman 1983; Pagenkopf 1983). Simple models involving the surface complexation of metals at the biological interface have been developed to explain these results (M^{Z+} + L-cell $\leftrightarrow$ M^{Z+}–L-cell: Morel 1983; Pagenkopf 1983). In such "free-ion" toxicity models, the surface complex is represented by M^{Z+}–L-cell, where L-cell = a cellular ligand and the biological response is proportional to the concentration of surface complexes, [M^{Z+}–L-cell].

$$\text{biological response } \alpha \ [M^{Z+}\text{–L-cell}] = K\ [\text{L-cell}]\ [M^{Z+}]$$

By analogy one might hypothesize that the toxic response of aquatic biota to dissolved aluminum would be best predicted on the basis of concentrations of the Al aquo-ion, i.e. Al^{3+} (Cameron et al. 1986; Kinraide and Parker 1989).

The goal of this study was to determine the effect of fluoride complexation on the biological response of an acid-sensitive

---

[1] Author to whom correspondence should be addressed.

Table 1. Nominal experimental conditions.[a]

Experiment[b,c]	[A1] (µM)	[F⁻] (µM)	pH
A	9	0–12	4.5
B	0–12	0–11	4.5
C	0–12	0–11	4.9
$D_{i,ii}$	0–11	0	4.5
E	0–11	7	4.5
F	0–11	18	4.5

[a] Average measured concentrations are presented in the text and figures; summary data for all runs are available on request (Wilkinson et al. 1989).

[b] In experiments B and C, the nominal sum of $Al(OH)_n$ and Al^{3+} was constant (1.4 µM).

[c] Subscripts (*i, ii*) for experiment D refer to the size difference of fish run under identical experimental conditions. See Materials and Methods for futher details.

species of economic importance, *Salmo salar*. Experimental variables were chosen to reflect conditions that prevail in Atlantic salmon rivers on the Quebec North Shore during the spring snow-melt period (e.g. pH 4.9–5.5, dissolved [A1] 5–8 µM, inorganic [A1] 0.8–4 µM, total [F⁻] ≈ 1.5 µM; Campbell et al. 1989). As the free-ion model of toxicity is widely used to predict the bioaccumulation and toxicity of metals in aquatic systems, our experiments were also designed to test the adequacy of this model as it applies to aluminum in the presence of fluoride ion.

Materials and Methods

General

Juvenile Atlantic salmon (*Salmo salar*; age 1+) were exposed to various aluminum, fluoride, and hydrogen-ion concentrations (Table 1) in a series of semistatic experiments (water renewal every 12 h). The salmon were obtained from the provincial fish hatchery in L'Anse Pleureuse, Québec. Small individuals (parr stage: 5.9 ± 2.2 g; x ± SD) were used for experiments A, D_{ii}, and F, while larger individuals (smolt stage: 30.3 ± 9.0 g; x ± SD) were tested in experiments B, C, D_i, and E. Fish (8–10 per chamber; chamber vol. = 64 L) were exposed to synthetic Shield water (Table 2: Van Coillie et al. 1983) during a 2-d progressive acidification–acclimation period, after which Al-containing test waters (with or without fluoride) were employed. The chambers were kept at 9–11°C in an enclosed environmental chamber with a 16 h photoperiod.

The water temperature varied only slightly (10 ± 1°C) during the exposure period. Dissolved oxygen (10 ± 2 mg·L⁻¹) as well as major ion concentrations (mean ± SD of all experiments: [Ca] = 45 ± 2 µM, [Mg] = 59 ± 2 µM, N = 18) were maintained constant for the duration of each experiment. Greater than 90% of the pH readings were within ± 0.1 units of the nominal pH value (SD = 0.06).

In designing toxicological experiments with aluminum one must consider the particular chemical properties of the element: low solubility at neutral pH; slow precipitation/dissolution kinetics; tendency to adsorb on available surfaces; ability to form metastable polynuclear species in solution — see Burrows (1977). The exposure conditions in the present experiments were chosen to avoid the formation of polynuclear or particulate species and to maintain the aluminum in an inorganic mononuclear state. Indeed, >90% of the Al added to the exposure media could be accounted for as dissolved inorganic monomeric Al, as determined by the ion-exchange/catechol violet procedure of Rogeberg and Henriksen (1985) — method described below. No monomeric organic aluminum could be detected after filtration and subsequent passage of the filtrate through the cation exchange column. Frequent water renewal assured that the concentration of aluminum in solution remained reasonably constant (± 10%), a condition essential to the equilibrium modeling approach.

TABLE 2. Nominal concentrations of major ions in the artificial media (adapted from Van Coillie et al. 1983)[a].

Component	Concentration (mg·L⁻¹)	Concentration (µM)
$NaHCO_3$	12.0	143
$CaSO_4 \cdot 2H_2O$	7.5	44
$MgSO_4$	7.5	62
KCl	0.5	7

[a] Measured [Na] = 128 ± 15 µM, [Ca] = 45 ± 2 µM, [Mg] = 59 ± 2 µM, [K] = 9 ± 1 µM.

Solution Chemistry

The synthetic exposure media were allowed to age 24 h to ensure solution equilibrium prior to addition of fish. To minimize organic complexation of the aluminum by fish excretory products, the exposure media were renewed every 12 h and fish were not fed after transfer to the acclimation chambers (64 L each). Nitric acid (Aristar grade) and sodium hydroxide (Reagent grade) were used to adjust the pH. Fluoride was added as the sodium salt (NaF, Reagent grade). Since variations in the concentration of Na in solution could in principle affect plasma Na levels (see below), care was taken to minimize this potential artifact; where feasible, $NaHCO_3$ concentrations were lowered slightly to ensure equivalent Na concentrations (within experimental error: ± 9 µM) in the experimental chambers.

Total aluminum concentrations in the exposure media were determined by graphite furnace atomic absorption spectrophotometry (unfiltered samples: total Al). Aluminum speciation in solution was determined (4× daily) on filtered samples (0.4 µm Nuclepore filters) with an automated method involving cation-exchange and the colorimetric determination of monomeric Al with pyrocatechol-violet (total dissolved Al, dissolved inorganic Al and organic-bound Al; Rogeberg and Henriksen 1985). The distribution of Al among the different inorganic monomeric forms was calculated from the values for exchangeable monomeric Al, pH, and total fluoride, with the aid of the MINEQL chemical equilibrium model (Westall et al. 1976). Updated formation constants were used as summarized in Neville and Campbell (1988).

Fluoride was determined potentiometrically with a fluoride selective electrode (Orion Model No. 940909) in the presence of appropriate buffers: commercial TISAB II (Fisher Scientific: total fluoride) and prepared TISAB without the cyclohexylenediaminetetraacetic acid (free fluoride). When detectable, levels of free fluoride compared favorably with theoretical values as obtained with inorganic aluminum concentrations and equilibrium calculations (MINEQL). Representative results from experiment F are presented in Table 3.

Major ion concentrations (Ca, Mg, Na, K) in the synthetic media were determined by plasma emission spectrophotometry.

TABLE 3. Measured and calculated free fluoride concentrations for Experiment F.

Experimental chamber	Measured free $[F^-]$ (μM)	Calculated free $[F^-]$ (μM)
1	14.4	14.2
2	12.0	12.8
3	11.6	11.6
4	10.8	10.1
5	9.0	9.0
6	7.5	7.5
7	6.7	6.8
8	6.0	6.0
9	5.0	5.0
10	3.9	4.5

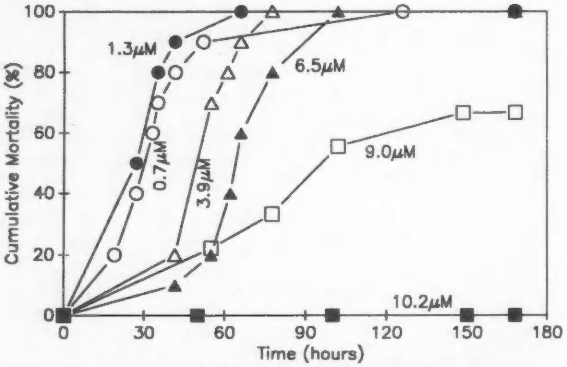

FIG. 1. Cumulative mortality (%) of juvenile Atlantic salmon parr (experiment A) – pH 4.5, inorganic monomeric [Al] = 8.7 ± 1.0 μM and variable $[F]_T$ (0.7–10.2 μM, as indicated).

Response of *Salmo salar*

Mortality was judged to be upon cessation of gill opercular movement. Fish surviving to the end of an experiment were anesthetized with MS-222 (ethyl 3-aminobenzoate methanesulfonic acid) and the gills were then removed and bisected. One gill half was soaked for 15 min in 10^{-3} M Na_2EDTA (ethylenediamine-tetraacetic acid, disodium salt) to remove adsorbed Al (see Schenck et al. 1988) and subsequently blotted (GF-C filter paper) to remove mucus adhering to the gill surface. Both gill segments were subsequently stored at −20°C, then lyophylized (−50°C, 13 Pa) and subjected to microwave nitric acid digestion (Bastille et al. 1989). Gill aluminum concentrations were measured by plasma emission and graphite furnace spectrophotometry.

At the end of each experiment, blood samples (10–60 μL) were removed by caudal puncture from surviving fish, previously anesthetized. After centrifugation (7000 rpm), the plasma was decanted, weighed (due to the extremely small volumes), and frozen for later dilution with HCl (BDH Ultrapure grade) and demineralized water. Plasma sodium concentrations were determined by atomic emission spectrophotometry.

Results

Toxicity Tests

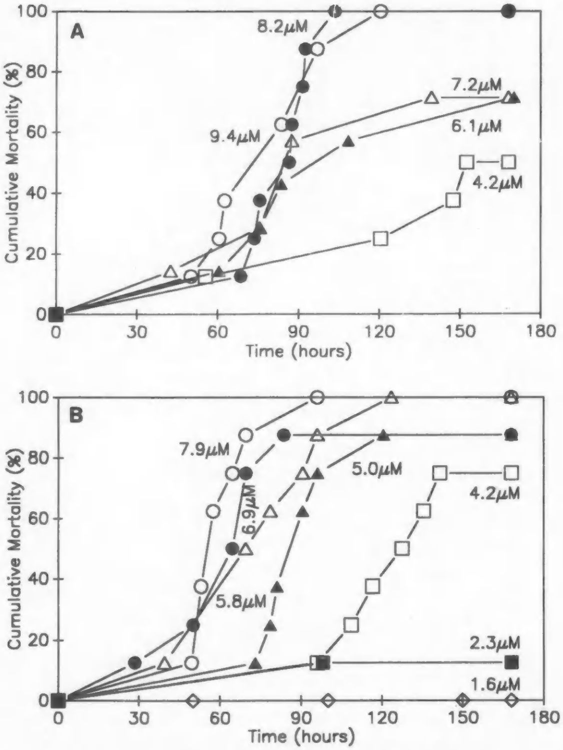

FIG. 2. (A) Cumulative mortality (%) of juvenile Atlantic salmon smolt (experiment B) – pH 4.5, $\Sigma\,[Al^{3+}]+[Al(OH)_n]$ = 1.3 ± 0.1 μM and variable $[AlF_x]$ (4.2–9.4 μM, as indicated). (B) Cumulative mortality (%) of juvenile Atlantic salmon smolt (experiment C) – pH 4.9, $\Sigma\,[Al^{3+}]+[Al(OH)_n]$ = 1.4 ± 0.1 μM and variable $[AlF_x]$ (1.6–7.9 μM, as indicated).

For a constant inorganic aluminum concentration (8.7 ± 1.0 μM), the toxic effect of aluminum was attenuated as the fluoride concentration increased from 0.7 to 10.2 μM (experiment A — Fig. 1). Just such a monotonic response, i.e. diminished toxicity as the concentration of Al^{3+} is reduced, would be predicted from the free-ion model for metal toxicity. Indeed, speciation calculations on the test solutions indicated that the free Al^{3+} concentration decreased from 6.1 μM (68% of the total inorganic species) to 0.4 μM (5% of the total) as the fluoride concentration increased.

Experiments B (pH 4.5) and C (pH 4.9) were designed to test further the adequacy of the free-ion model. Here, using equilibrium calculations, we maintained the concentration of the free Al^{3+} ion and its hydroxy-complexes constant while increasing both the aluminum and fluoride concentrations (i.e. $[Al(F)_x]$ increases, $[Al^{3+}]$ and $[Al(OH)_n]$ remain constant). If fluoro-Al species do not contribute to aluminum toxicity, the cumulative mortality curves should be independent of the fluoride concentrations. As can be seen in Fig. 2A and 2B, *this is clearly not the case*. The rise in mortality as $Al(F)_x$ concentrations increase is substantial proof of the toxicity of $Al(F)_x$ species. Note also that there is an apparent pH effect; for comparable concentrations of Al^{3+}, $Al(OH)_n$ and $Al(F)_x$, mortality appears to occur earlier at the higher pH. In control runs (no added Al or F, pH = 6.3) fish did not demonstrate significant mortality.

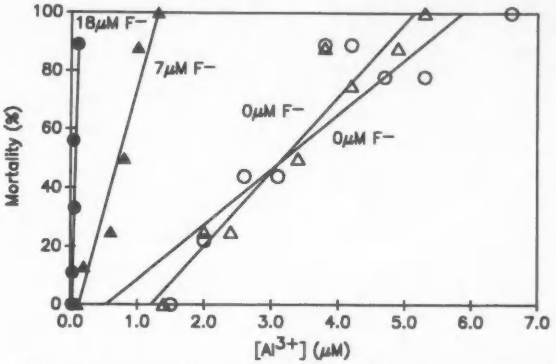

FIG. 3. Mortality curves: Salmon mortality after 7 d as a function of free ion (Al^{3+}) concentrations. Open symbols, (Δ,○), experiments ($D_{i,ii}$) in which no fluoride was added. Closed triangles (▲), 6.6 ± 0.2 μM added fluoride (experiment E). Closed circles (●), 18.2 ± 0.2 μM added fluoride (experiment F). See Table 1 for experimental conditions.

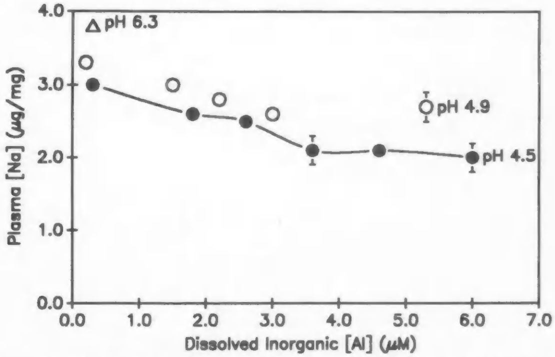

FIG. 4. Variation of plasma sodium concentrations as a function of dissolved inorganic aluminum for experiments B (pH 4.5: ●) and C (pH 4.9: ○) as well as control fish (pH 6.3:Δ). Means ± standard errors are presented; *n* varies between 3 and 8. Note that $\Sigma\ [Al^{3+}] + [Al(OH)_n]$ was held constant; increases in $[Al]_{inorganic}$ along the *X*-axis thus correspond to increases in $[AlF_x]$.

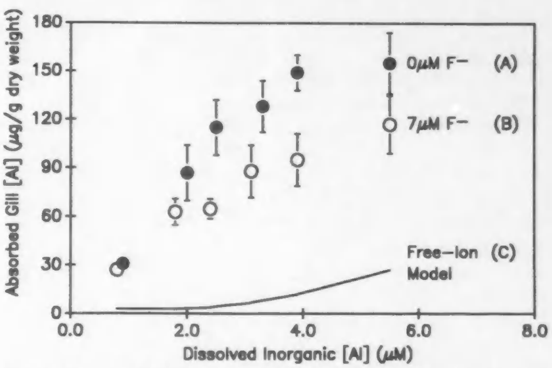

FIG. 5. Absorbed gill aluminum (7 d) as a function of inorganic monomeric aluminum concentrations (pH 4.5: experiments D_i and E) for fish that did not succumb to experimental conditions. Closed circles (● — curve A), treatments without added fluoride. Open circles (○ — curve B), 6.6 ± 0.2 μM added fluoride. Means ± standard errors are presented; *n* varies between 3 and 9. Curve C corresponds to expected absorbed aluminum concentrations based on the simple free-ion model, calibrated with respect to the experimental curve obtained in the absence of fluoride (experiment D_i — curve A).

In another series of experiments, fish were exposed to increasing aluminum concentrations with or without added fluoride. The mortality diagram (Fig. 3: experiments D_i, D_{ii}, E and F) provides additional evidence confirming the failure of $[Al^{3+}]$ to predict the toxic response to aluminum in the presence of fluoride. Indeed, our results demonstrate that although fluoride mitigates aluminum toxicity, appreciable toxicity persists even in the presence of an excess of the complexing ligand. Such a response does not agree with the free-ion model of metal toxicity.

Plasma Sodium Concentrations

Plasma sodium levels were examined for surviving fish. Results from experiments B and C are presented in Fig. 4. Sodium concentrations (μg $Na \cdot mg^{-1}$ plasma) as measured on day 7 decreased up to 33% as a function of the dissolved inorganic aluminum concentration. At both pH 4.5 and 4.9, increases in inorganic aluminum resulted in significant decreases in plasma sodium concentrations (ANOVA — unbalanced design, $P \leq 0.05$). Note that any experimental artifacts attributable to the incremental NaF addition (which resulted in slight increases in [Na] in the exposure media as the concentrations of AlF_x increased) would have yielded a trend opposite to that observed in Fig. 4.

At a given pH, all plasma sodium levels were significantly different (one way ANOVA, $P \leq 0.05$) from their pH controls (circles at the extreme left of Fig. 4 — no added aluminum). The effect of decreasing pH was also evident; plasma sodium concentrations at pH 4.5 were consistently less than those at pH 4.9. Control values (no added aluminum) decreased significantly as the pH decreased from 6.3 (Δ) through 4.9 (○) to 4.5 (●) (ANOVA — unbalanced design, $P \leq 0.05$).

Aluminum Bioaccumulation

As anticipated, the levels of absorbed gill aluminum (i.e. Al remaining after EDTA extraction) varied as a function of the dissolved inorganic Al concentration. Results from two experiments, with (6.6 ± 0.2 μM F) and without added fluoride, showed that absorbed gill aluminum concentrations determined for fish surviving at the end of the 7-d period increased as a function of dissolved [Al] (Fig. 5).

Discussion

The results of the present research clearly demonstrate the attenuating effect of fluoride complexation on the toxicity of inorganic Al toward juvenile Atlantic salmon. Despite this attenuation, the residual toxicity of Al in the presence of fluoride ion is greater than can be explained by the concentrations of the free Al^{3+} ion and its hydroxo-complexes. The following discussion deals with this unexpected residual toxicity: we first consider the physiological response of the fish to aluminum in the presence of fluoride, as well as their bioaccumulation of Al under these conditions, and then examine the relation between toxicity and solution chemistry.

Plasma Sodium

For salmonid fish held in moderately acidic media, it is well established that increased aluminum levels result in decreases in plasma salt concentrations similar to those observed at low pH (Muniz and Leivestad 1980; Neville 1985; Rosseland et al. 1986; Booth et al. 1988). In contrast, for circumneutral solutions (pH 6.3) containing low aluminum concentrations (2.8 μM inorganic Al), Neville (1985) found that the osmoregulatory response of rainbow trout (*Oncorhynchus mykiss*) was not affected as compared to control fish, yet substantial mortality occurred. The acute response under these conditions was attributed to impaired oxygen exchange. In the present experiments, plasma sodium levels were followed to determine if the mechanism of Al toxicity in the presence of fluoride and the H^+-ion involved osmoregulatory perturbation.

Plasma sodium was found to decrease as a function of increased aluminum concentrations at pH 4.5 and 4.9 (Fig. 4: experiments B and C). Since the concentrations of Al^{3+} and the corresponding hydroxo-species were kept constant in these experiments, the observed decreases in plasma sodium can be attributed to increases in fluoro-Al species. The similarity of the osmoregulatory response to the H^+-ion, to Al^{3+}, and to $Al(F)_x$ suggests that the mechanism of toxicity in the presence of fluoride does not differ markedly from that observed by previous workers for salmonid species exposed to aluminum alone in moderately acidic media (Fivelstad and Leivestad 1984; Neville 1985; Wood and McDonald 1987).

Al Bioaccumulation

As demonstrated in Fig. 5, bioaccumulation in gill tissue among survivors (t = 7 d) increased towards a plateau as a function of dissolved aluminum (0→6 μM) both in the absence and presence of added fluoride (6.6 ± 0.2 μM). As anticipated, curve B obtained in the presence of fluoride lies below that obtained in the experiment without fluoride. However, this reduction in Al bioaccumulation was much less than would have been predicted on the basis of changes in free Al^{3+} concentrations (curve C). For example, at pH 4.5, for an inorganic aluminum concentration of 2 μM, the free Al^{3+} concentration decreased by ≈97% (1.4–0.04 μM) in the presence of 7 μM F, yet gill aluminum (corrected by subtracting background gill [Al] as measured in control fish) was reduced by only ≈30% (see Fig. 5). The parallel with the mortality results is striking: fluoride addition decreases both Al toxicity and its accumulation in the gills, but in both cases the attenuation is much less than would be predicted if the response were a simple function of $[Al^{3+}]$.

Relation of Toxicity and Solution Chemistry

The free-ion model has successfully explained the toxicity of such divalent metals as Cd, Cu, and Zn to various aquatic organisms (Nelson et al. 1981; Petersen 1982; Pagenkopf 1983; Sunda and Huntsman 1983). However, as seen in Fig. 2A, 2B, and 3, the concentration of Al^{3+} does not provide a consistent indication of the biological response of *Salmo salar* in the presence of different concentrations of fluoride ion.

As a result of the failure of the simple free-ion model to predict the increases in salmon mortality for increasing $Al(F)_x$ concentrations, we searched for certain empirical relations that might be useful to predict the toxic response as a function of solution chemistry. Following the approach of Fivelstad and Leivestad (1984), the data for all experiments among similar fish sizes were pooled and multiple regression analyses were performed with percent mortality (7 d) as the dependent variable and the various inorganic aluminum species (Al^{3+}, $AlOH^{2+}$, $Al(OH)^{2+}$, AlF^{2+}, etc.) as predictors. The best prediction of fish mortality was obtained as a function of the species Al^{3+} and AlF^{2+} (Table 4 and Fig. 6).

TABLE 4. Percent salmon mortality as explained by various inorganic aluminum species at pH 4.5 (coefficients of determination, r^2). Predictors are derived from a least squares multiple regression analysis of aluminum toxicity as a function of the inorganic aluminum species. $p<0.01$ was used as criterion for selection of individual elements. Colinear variables were eliminated (i.e., $Al(OH)^{2+}$ and $Al(OH)_2{}^+$).

Predictor employed	smolt	parr
Al^{3+} (or $Al(OH)^{2+}$ or $Al(OH)_2{}^+$)	0.69	0.72
AlF^{2+}	0.61	0.35
$AlF_2{}^+$	0.04	0.15
Al^{3+} and AlF^{2+}	0.93[a]	0.83[b]

[a] Predicted mortality = $16.3[Al^{3+}] + 10.3[AlF^{2+}]$, N = 22, SE of estimation = 17.6 (Experiments B, D_i, E).

[b] Predicted mortality = $15.5[Al^{3+}] + 7.2[AlF^{2+}]$, N = 18, SE of estimation = 28.0 (Experiments A, D_{ii}, F).

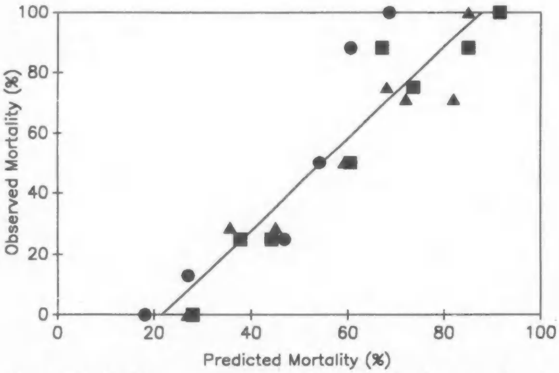

FIG. 6. Predicted versus observed (7 d) mortality for experiments B (▲), D_i (●), and E (■). Observed = 1.5 · Predicted − 33; r^2=0.93. Predicted mortality was calculated from the equation in Table 4 (footnote a).

Modeling Trials

To explain the toxicity results (i.e. the need to include Al^{3+} and AlF^{2+} in the predictive model), we adapted the aluminum toxicity model proposed by Neville and Campbell (1988). Implicit in the model are a number of assumptions:

1) The fish gills are the site of the toxic action of aluminum (NRCC 1986).
2) The interaction of Al with the gill surface can be represented in terms of the formation of X–Al–L-gill surface complexes (Pagenkopf 1983), where L-gill = a cellular ligand and X = H_2O, HO, or F.

$$\begin{tikzcd} Al^{3+} \arrow[drr, leftrightarrow] \arrow[dd, leftrightarrow] & & \\ & & X-Al-L\text{-gill} \\ AlX_n \arrow[urr, leftrightarrow] & & \end{tikzcd}$$

3) For modeling purposes, the gill surface sites can be treated

as ligands in solution with discrete formation constants and the total Al concentration in solution can be considered constant.

4) Equilibrium is rapidly established among Al species in solution, and between the solution and the gill surface ("rapid" = faster than the expression of the biological response).
5) The toxic response is proportional to the concentration of surface complexes, [X–Al–L-gill].

$$\text{biological response} \propto [\text{X–Al–L-gill}]$$

The fourth assumption merits close scrutiny. If it is assumed that the gill surface is in equilibrium with the various monomeric Al species in solution, and that this equilibrium precedes the expression of the biological response, it follows that the identity of the Al form(s) reacting with the gill surface is of no significance — *no one species can be considered more (or less) toxic than another*. The solution equilibrium assumption is acceptable provided the solubility limit for $Al(OH)_3(s)$ is not exceeded; equilibrium among the various monomeric aluminum species (Al^{3+}, $AlOH^{2+}$, $Al(OH)_2{}^{+}$, AlF^{2+}, ...) is known to be attained rapidly (Baes and Mesmer 1976; Plankey et al. 1986). As well, the frequent water renewal (twice daily) assured reasonably stable total aluminum concentrations.

In addition to the solution equilibria involving Al and its hydroxo- and fluoro-complexes, the following reactions are considered in the model (charges on the gill surface complexes are omitted for simplicity):

$$\begin{array}{llll}
Al^{3+} + \text{L-gill} & \leftrightarrow & \text{Al–L-gill} & (1)\ \log K_1 = 6.5 \\
Al^{3+} + OH^{-} + \text{L-gill} & \leftrightarrow & \text{HO–Al–L-gill} & (2)\ \log K_2 = 14.5 \\
 & & & \\
H^{+} + \text{L-gill} & \leftrightarrow & \text{H–L-gill} & (3)\ \log K_3 = 4.5 \\
2H^{+} + \text{L-gill} & \leftrightarrow & H_2\text{–L-gill} & (4)\ \log K_4 = 9.1 \\
 & & & \\
Ca^{2+} + \text{L-gill} & \leftrightarrow & \text{Ca–L-gill} & (5)\ \log K_5 = 3.7 \\
 & & & \\
Al^{3+} + F^{-} + \text{L-gill} & \leftrightarrow & \text{F–Al–L-gill} & (6)\ \log K_6 = 13.5
\end{array}$$

The interaction of aluminum with the gill surface is represented by reactions (1) and (2), which yield, respectively, an Al-gill complex and a mixed ligand hydroxo-Al-gill species. Reactions (3) and (4) correspond to the competition of H^{+}-ions for metal binding sites on the gill surface (Campbell and Stokes 1985), whereas reaction (5) accounts for the protection afforded by moderate calcium concentrations (Wood et al. 1988).

The combination of reactions 1–5 corresponds to the modified free-ion model proposed by Neville and Campbell (1988). Indeed, values assigned to the various equilibrium constants are the same as those used in the earlier application (reactions 3, 4, 5) or have been slightly modified (reactions 1, 2) to account for the results obtained in the absence of fluoride (experiment D). However, when applied to experiments B or C, this model failed to predict the observed toxic response. As $[Al]_T$ and $[F]_T$ increase in a given experiment, calculated values for both {Al–L-gill} and {HO–Al-gill} remain constant, yet cumulative mortality increases (see Fig. 2A). To simulate this increase in mortality, it proved necessary to add to the model a mixed ligand fluoro-Al-gill complex (i.e. reaction 6). Note that mathematically the concentration of this species, (F–Al–L-gill), is proportional to the concentration of $[AlF^{2+}]$ in solution (equation 10, where $K_{67} = K_6 \div K_7$).

$$\begin{array}{llll}
Al^{3+} + F^{-} & \leftrightarrow & AlF^{2+} & (7)\ \log K_7 = 7.0 \\
[AlF^{2+}] & = & K_7\,[Al^{3+}]\,[F^{-}] & (8) \\
\{\text{F–Al–L-gill}\} & = & K_6\,[Al^{3+}]\,[F^{-}]\,[\text{L-gill}] & (9) \\
 & = & K_{67}\,[AlF^{2+}]\,[\text{L-gill}] & (10)
\end{array}$$

The model is thus compatible with the results of the regression analysis.

To our knowledge, the existence of mixed fluoro-aluminum complexes involving organic ligands has not been verified by physical methods. Some precedent does exist, however — the formation of $Al(OH)_mF_nL_p$ mixed complexes has recently been invoked to explain the solubility of aluminum in the presence of fluoride (Sanjuan and Michard 1987) and the kinetics of aluminum fluoride complexation in acidic waters in the presence of fulvic acid (Plankey and Patterson 1988). Similarly, mixed hydroxo species, (HO–Al–L,L′, where L = salicylate, pyrocatechol, or 1,2-dihydroxy-naphthalene-4-sulfonate) have been postulated for in vitro systems (Marklund et al. 1986). Given the apparent role of mixed complexes in aluminum toxicity, there is a strong incentive to demonstrate the existence of such (F–Al–L.....) species at biological surfaces. Work in this area is currently underway.

Conclusion

The free-ion model of metal toxicity does not account adequately for the toxicity of aluminum to Atlantic salmon in the presence of fluoride. Toxicological data indicate the formation of a mixed ligand complex, (F–Al–L-gill), at the gill surface. Even in the presence of excess fluoride, gill tissue accumulates Al (though to a lesser extent than when exposed to inorganic aluminum without the added ligand); the resulting perturbation of the salmon's osmoregulatory system will, if initially severe enough, lead to death.

Acknowledgements

Funding for this research was provided by Fisheries and Oceans Canada (Research Subvention Programme + DSS Contract No. FP707-7-2356/01-XSK) and by the Natural Sciences and Engineering Research Council of Canada. Partial student support (KJW) from the Québec Fonds pour la Formation de Chercheurs et l'Aide à la Recherche (FCAR) is also gratefully acknowledged. The fish bioassays were performed in the Environment Canada laboratories in Longueuil, Québec with fish supplied by le ministère du Loisir, Chasse et Pêche du Québec (MLCP). C. Blaise (Environment Canada), S. Thorne (Environment Canada), and G. Walsh (Fisheries and Oceans Canada) provided valuable advice and assistance. We also thank the staff of the fish hatchery at L'Anse Pleureuse and those of the Maurice Lamontagne Institute. We are grateful to J. C. Auclair, R. L. Hare, W. O. Nelson, C. M. Neville, and G. Walsh for useful comments on the manuscript.

References

BAES, C. F., AND R. E. MESMER. 1976. The Hydrolysis of Cations, John Wiley and Sons Ltd., New York, NY. p. 317–381.

BASTILLE, C., S. ST-PIERRE, AND B. DUBREUIL. 1989. Digestion de matière biologique par four à micro-ondes, méthode DIG 050.1, Manuel des méthodes de laboratoire, INRS-Eau. Available from INRS-Eau, C.P. 7500, Ste-Foy, QC, G1V 4C7.

BOOTH, C. E., D. G. MCDONALD, B. P. SIMONS, AND C. M. WOOD. 1988. Effects of aluminum and low pH on net ion fluxes and ion balance in brook trout (*Salvelinus fontinalis*). Can. J. Fish. Aquat. Sci. 45: 1563–1574.

BURROWS, W. D. 1977. Aquatic aluminum: chemistry, toxicology, and environmental prevalence. CRC Crit. Rev. Environ. Control 7: 167–216.

Cameron, R. C., G. S. P. Ritchie, and A. D. Robson. 1986. Relative toxicities of inorganic aluminum complexes to barley. Soil Sci. Soc. Am. J. 50: 1231–1236.

Campbell, P. G. C., and P. M. Stokes. 1985. Acidification and toxicity of metals to aquatic biota. Can. J. Fish. Aquat. Sci. 42: 2034–2049.

Campbell, P. G. C., B. Dubreuil, and H. J. Hansen. 1989. Comportement géochimique de l'aluminium dans quelques rivières à saumon de la Côte-Nord (golfe du Saint-Laurent). Rapp. Tech. Can. Sci. Halieut. Aquat. 1697: x + 80 p.

Clark, K. L., and B. D. LaZerte. 1985. A laboratory study of the effects of aluminum and pH on amphibian eggs and tadpoles. Can. J. Fish. Aquat. Sci. 42: 1544–1551.

Cronan, C. S., and C. L. Schofield. 1979. Aluminum leaching response to acid precipitation: effects on high-elevation watersheds in the Northeast. Science (Wash., DC) 204: 304–306.

Driscoll, C. T., J. P. Baker, J. J. Bisogni, and C. L. Schofield. 1980. Effect of aluminum speciation on fish in acidified waters. Nature (Lond.) 284: 161–164.

Fivelstad, S., and H. Leivestad. 1984. Aluminum toxicity to Atlantic salmon (*Salmo salar* L.) and brown trout (*Salmo trutta* L): mortality and physiological response. Inst. Freshwater Res. Drottningholm 61: 69–77.

Hansen, H. J., and P. G. C. Campbell. 1987. Aluminum speciation in rivers on the Canadian Precambrian Shield (Côte-Nord du St-Laurent, Québec) during snowmelt, p. 372–379. *In* R. Perry, R. M. Harrison, J. N. B. Bell, and J. N. Lester [ed.] Acid Rain: scientific and technical advances. Selper Ltd., London, UK.

Henriksen, A., O. K. Skogheim, and B. O. Rosseland. 1984. Episodic changes in pH and aluminium speciation kill fish in a Norwegian salmon river. Vatten 40: 255–260.

Johannessen, M., A. Skartveit, and R. F. Wright. 1980. Streamwater chemistry before, during and after snowmelt, p. 224–225. *In* D. Drablos and A. Tollan [ed.] Ecological Impact of Acidic Precipitation, SNSF Project, Norway.

Kinraide, T. B., and D. R. Parker. 1989. Assessing the phytotoxicity of mononuclear hydroxy-aluminum. Plant Cell Environ. 12: 479–487.

Lachance, M., D. Brouard, R. Van Coillie, and J. D. Dutil. 1983. Composition chimique des eaux de la rivière Sainte–Marguerite en période de fonte. Water Pollut. Res. J. Can. 18: 85–102.

Marklund, E., S. Sjöberg, and L.-O. Ohman. 1986. Equilibrium and structural studies of silicon (IV) and aluminium (III) in aqueous solution. 14. Speciation and equilibria in the aluminium (III)–lactic acid-OH^- system. Acta Chem. Scand. A40: 367–373.

Morel, F. M. M. 1983. Principles of Aquatic Chemistry, p. 300–308, John Wiley and Sons Ltd., New York, NY.

Muniz, I. P., and H. Leivestad. 1980. Toxic effects of aluminum on the brown trout, *Salmo trutta* L., p. 320–321. *In* D. Drablos and A. Tollan [ed.], Ecological Impact of Acidic Precipitation, SNSF Project, Norway.

Nelson, P. O., A. K. Chung, and M. C. Hudson. 1981. Factors affecting the fate of heavy metals in the activated sludge process. J. Water Pollut. Control Fed. 53: 1323–1333.

Neville, C. M. 1985. Physiological response of juvenile rainbow trout, *Salmo gairdneri*, to acid and aluminum — prediction of field responses from laboratory data. Can. J. Fish. Aquat. Sci. 42: 2004–2019.

Neville, C. M., and P. G. C. Campbell. 1988. Possible mechanisms of aluminum toxicity in a dilute, acidic environment to fingerlings and older life stages of salmonids. Water Air Soil Pollut. 42: 311–327.

NRCC. (National Research Council of Canada). 1986. Aluminum in the Canadian Environment. National Research Council of Canada, Associate Committee on Scientific Criteria for Environmental Quality, NRCC Rep. 24759: 331 p.

Pagenkopf, G. K. 1983. Gill surface interaction model for trace-metal toxicity to fishes: role of complexation, pH, and water hardness. Environ. Sci. Technol. 17: 342–347.

Petersen, R. 1982. Influence of copper and zinc on the growth of a freshwater alga, *Scenedesmus quadricauda*: the significance of chemical speciation. Environ. Sci. Technol. 16: 443–447.

Plankey, B. J., and H. H. Patterson. 1988. Effect of fulvic acid on the kinetics of aluminum fluoride complexation in acidic waters. Environ. Sci. Technol. 22: 1454–1459.

Plankey, B. J., H. H. Patterson, and C. S. Cronan. 1986. Kinetics of aluminum fluoride complexation in acidic waters. Environ. Sci. Technol. 20: 160–165.

Rogeberg, E. J. S., and A. Henriksen. 1985. An automatic method for fractionation and determination of aluminum species in fresh-waters. Vatten 41: 48–53.

Rosseland, B. O., O. K. Skogheim, F. Kroglund, and E. Hoell. 1986. Mortality and physiological stress of year classes of landlocked and migratory Atlantic salmon, brown trout and brook trout in acid aluminum-rich soft water. Water Air Soil Pollut. 30: 751–756.

Sanjuan, B., and G. Michard. 1987. Aluminum hydroxide solubility in aqueous solutions containing fluoride ions at 50°C. Geochim. Cosmochim. Acta 51: 1823–1831.

Schenck, R. C., A. Tessier, and P. G. C. Campbell. 1988. The effect of pH on iron and manganese uptake by a green alga. Limnol. Oceanogr. 33: 538–550.

Sunda, W. G., and S. A. Huntsman. 1983. Effect of competitive interactions between manganese and copper on cellular manganese and growth in estuarine and oceanic species of the diatom *Thalassiosira*. Limnol. Oceanogr. 28: 924–934.

Van Coillie, R., C. Thellen, P. G. C. Campbell, and Y. Vigneault. 1983. Effets toxiques de l'aluminium chez les salmonidés en relation avec des conditions physico-chimiques acides. Rapp. Tech. Can. Sci. Halieut. Aquat. 1237: ix + 88 p.

Westall, J. C., J. L. Zachary, and F. M. M. Morel. 1976. MINEQL, a computer program for the calculation of the chemical equilibrium composition of aqueous systems, Massachusetts Institute of Technology, Dept. Civil Eng., Tech. Rep. 18: 91 p.

Wilkinson, K. J., P. G. C. Campbell, and P. Couture. 1989. Biodisponibilité des fluoro-complexes d'aluminium chez des juvéniles du saumon atlantique, *Salmo salar*. INRS-Eau, rapport scientifique 266: 101 p. (Available from INRS-Eau, C.P. 7500, Ste-Foy, QC, G1V 4C7.)

Wood, C. M., and D. G. McDonald. 1987. The physiology of acid/aluminum stress in trout. Ann. Soc. R. Zool. Belg. 117: 399–410.

Wood, C. M., R. C. Playle, B. P. Simons, G. G. Goss, and D. G. McDonald. 1988. Blood gases, acid-base status, ions, and hematology in adult brook trout (*Salvelinus fontinalis*) under acid/aluminum exposure. Can. J. Fish. Aquat. Sci. 45: 1575–1586.

An Errors-In-Variables Bias Model with an Application to Salmon Hatchery Data

J. T. Schnute, T. J. Mulligan, and B. R. Kuhn

Department of Fisheries and Oceans, Pacific Biological Station, Nanaimo, B.C. V9R 5K6 Canada

Schnute, J. T., T. J. Mulligan, and B. R. Kuhn. 1990. An errors-in-variables bias model with an application to salmon hatchery data. Can. J. Fish. Aquat. Sci. 47: 1453–1467.

This paper presents an errors-in-variables (EV) model for assessing differences between two measurements of the same phenomenon, where each measurement is subject to error. The model, equivalent to a classical EV model, specifically includes parameters associated with the relative bias between the two measurements. We derive a complete statistical theory for this errors-in-variables bias (EVB) model, including analytical formulas for confidence intervals that are exact when the error lies in one variable alone and approximate otherwise. The model is used to compare two methods of estimating the number of salmon that return to their hatchery of origin. One method involves direct counting, while the other is based on fish marked with coded wire tags (CWTs). We conclude that, for coho (*Oncorhynchus kisutch*) and chinook (*Oncorhynchus tshawytscha*) hatcheries in British Columbia, Canada, estimates from CWTs are, on average, 22% lower than comparable counting estimates.

Les auteurs du présent article présente un modèle d'erreurs dans les variables pour évaluer les écarts entre deux mesures du même phénomène, lorsque chaque mesure est sujette à erreur. Le modèle, équivalent à un modèle classique d'erreurs dans les variables, comprend expressément des paramètres associés aux biais relatifs entre les deux mesures. Une théorie statistique complète a été élaborée pour ce modèle de biais des erreurs dans les variables, comprenant des formules d'analyse pour les intervalles de confiance qui sont exacts lorsque l'erreur se situe au niveau d'une seule variable et s'en approche. Le modèle est utilisé pour comparer deux méthodes d'estimation du nombre de saumons qui reviennent à leur écloserie d'origine. Une méthode comprend le dénombrement direct, tandis que l'autre est fondée sur le marquage des poissons au moyen de fils métalliques codés. Les auteurs concluent que, dans le cas des écloseries du coho (*Oncorhynchus kisutch*) et de quinnat (*Oncorhynchus tshawytscha*) en Colombie-Britannique (Canada), les estimations effectuées à partir de fils métalliques codés, sont en moyenne 22% plus faibles que les estimations comparables effectuées par dénombrement.

Received March 10, 1989
Accepted February 8, 1990
(JA095)

Reçu le 16 mars 1989
Accepté le 8 février 1990

Analysis of fishery data often involves comparing two measurements of the same phenomenon. For example, absolute stock biomass might be estimated from a model of catch and effort data or from a hydroacoustic survey. Similarly, the number of fish in a tank might be estimated from a mark-recovery experiment or from a direct visual count. Such independent measurements often disagree markedly, and, due to uncertainties in both methods, it may be impossible to make a rational choice between them.

This paper presents a model for comparing such measurements and, in particular, for estimating the relative bias between them. Motivation for the work comes from a problem of considerable interest in operating hatcheries for Pacific salmon. Within a hatchery, two independent measurements of the total number of returning fish are possible. One results from a direct count. The second comes from analysis of marked fish recovered in the hatchery returns. Since juveniles released from the hatchery are marked at a known rate, the number of marks among returning adults theoretically provides an estimate of the total population.

In this case, as in most measures of fish populations, both methods are subject to numerous sources of error. For example, direct counts may be difficult, especially with large numbers of fish. On the other hand, marked fish may experience different mortality from unmarked fish, and they may be difficult to detect among the returning adults. Furthermore, if the object of the exercise is to count fish of hatchery origin, then both methods are subject to the problem of straying. Fish not of hatchery origin may be counted in the observed run, and hatchery fish may return to other tributaries of the stream. Marked and unmarked fish could conceivably exhibit different straying patterns, thus biasing estimates from the marks.

Such complexities typically make it impossible to assess the full extent of error in either measurement. The data are left to speak for themselves. Comparisons can, however, be based on a series of paired measurements. For example, returns to hatcheries over several years, or even returns to several hatcheries, can be estimated by both methods. The data then consist of a set of points (x_i, y_i), $i = 1, \ldots, n$, where x_i and y_i represent the two measurements in each of n different settings.

In this paper, we suppose that the two measurements are sufficiently compatible to exhibit a linear trend when the points (x_i, y_i) are plotted. Consider three possibilities for the trend line. First, it may coincide with the 45° line where $x = y$. In this case, the measurements agree. Notice, however, that they may still be incorrect if they share the same bias relative to the true (but unknown) measure. Second, the trend line may be parallel to the line $x = y$, but above or below it. In this case there is constant relative bias between the two measures, i.e. a bias not dependent on x or y. Third, the trend line may not be parallel to the 45° line. In this case, not only is there a relative bias between the two measures, but it varies systematically with x and y.

Each scenario has practical implications for the measuring process. The ideal first case corresponds to compatible measurements. In the second, some process consistently distinguishes the two measurements. For example, due to tagging mortality, the marked to unmarked ratio among fish leaving a hatchery may be consistently overestimated. In the third case, the discrepancy between the measurements varies as the magnitude increases. This might happen, for example, if the ability to detect marks in a salmon run declines steadily with increasing run size.

Incidentally, nothing is lost in this discussion if we suppose that a transformation is required to obtain a linear relationship between x_i and y_i, or to stabilize the variance of points (x_i, y_i) around the trend line. For example, in the hatchery data we find that a log transform makes the trend appear linear, with a homogeneous scatter about the apparent trend line. This is reasonable intuitively because salmon runs vary by orders of magnitude, so that a logarithmic scale seems appropriate. In general, we regard x_i and y_i as transformed values of the raw data, where a transformation is chosen to achieve linearity and homoscedasticity.

An essential feature of the data described here is that both variates are subject to error. Consequently, an errors-in-variables (EV) model is required for the analysis. In the model here (a reformulation of the classical EV model), the relative bias between the two measurement methods is identified as a specific parameter. Subsequent likelihood estimation methods give both an estimate of the bias and an associated confidence interval. Hypothesis tests can be used to assign statistical probability to the three scenarios discussed above. Furthermore, if the data are divided into subsets, such as returns to different hatcheries, then statistical comparisons among subsets can be made by methods similar to classical analysis of variance.

As with all EV models, parameter estimation cannot proceed without knowledge of the relative error between the two measurement methods. (For a geometrically motivated proof of this point, see Schnute 1987, p. 161–166.) Normally, it is sufficient to know λ, the ratio of error variances, from information outside the data being analyzed. In the data sets we examine, even this information is not available. Consequently, we devise graphical methods to assess simultaneously the results for all possible values of λ. We show that λ is more important in some contexts than in others. For example, the estimate of bias turns out to be independent of λ, although a corresponding confidence interval generally does depend on λ.

No exact method is known for determining confidence intervals for parameters in EV models. By contrast, when all error is known to be in one variate, then classical regression theory provides a standard technique based on the F-distribution. Here we devise a method for EV models that naturally extends the exact results from regression theory, and we use simulations to verify the scope and validity of our procedure. It includes analytical formulas for confidence intervals that are exact when the error lies in one variable alone and approximate otherwise. As far as we know, our method is new, although similar ideas are discussed by Fuller (1987, p. 33–34).

In summary, our paper has two main components. First, we present an EV model that can be used to assess the relative bias between two linearly related measurements of the same phenomenon. Second, we apply the model to estimated returns of coho (*Oncorhynchus kisutch*) and chinook (*Oncorhynchus tshawytscha*) salmon to hatcheries in British Columbia, Canada. We compare estimates based on direct counts with those based on fish marked with coded wire tags (CWTs).

Section 1 of the paper presents the EV model used for bias estimation. This new EVB (errors-in-variable bias) model differs from a classical EV model in several respects. In particular, a new parameter represents the mean relative bias between the two measurement methods. Section 2 derives the likelihood function for the EVB model and gives explicit formulas for maximum likelihood estimates of all model parameters. Likelihood methods are also used in Section 3 to obtain a method of computing confidence regions for the parameters. As discussed above, this new method extends classical linear regression theory, where the extension is approximate when both measurements are made with error. Section 4 examines the special case when the trend line is parallel to the 45° line and shows that the analysis simplifies considerably.

To illustrate an application of the EVB model, Section 5 analyses data from all major chinook and coho salmon returns to British Columbia hatcheries. The data span six hatcheries, with up to 14 different return years per hatchery. We break our discussion into three parts. First (Section 5A), we give a brief description of hatchery operation and data collection. Second (Section 5B), we provide a sample analysis based on one data set. In particular, we show how to represent parameter estimates and confidence regions graphically for all values of λ. Finally (Section 5C), we use results from 17 data sets to make statistical comparisons among them. Overall, we find a pronounced relative bias between counts of observed hatchery returns and estimates from CWTs. On average, the latter are approximately 22% lower than the former.

We defer all significant mathematical proofs, such as derivations of maximum likelihood estimates, to appendices. Also, where possible, we compile equations into tables. To distinguish equations in the text from those in tables, we use parentheses and brackets. For example, (2.5) and [2.5] indicate the fifth equation in Section 2 and Table 2, respectively.

1. EV Bias Model

In this section we begin by presenting the classical EV model for two observations x and y. We then reformulate the model to address the context in which both x and y are intended to measure the same quantity. Our formulation involves a new set of parameters, equivalent to those in the EV model, that pertain to the relative bias between the two measurements. We refer to this new model as an errors-in-variables bias (EVB) model to distinguish it from the classical formulation.

The classical EV model describes data (x_i, y_i), $i = 1, \ldots, n$, where both x_i and y_i are presumed to contain error. Corresponding true, but unobserved, points (X_i, Y_i) are assumed to lie exactly on a straight line. The model consists of the three equations

$$(1.1) \quad x_i = X_i + \sigma\delta_i ,$$

$$(1.2) \quad y_i = Y_i + \tau\epsilon_i ,$$

$$(1.3) \quad Y_i = \alpha + \beta X_i ,$$

where δ_i and ϵ_i are independent normal variates with mean 0 and variance 1. Here α and β are the intercept and slope, respectively, of the trend line. Equation (1.3) states that points

TABLE 1. Parameters of the EV model that can be defined in terms of the $n+3$ independent parameters α, β, σ, $X_1, \ldots, X_n$. The variance ratio λ is presumed known. The parameters $\overline{X}$ and $\overline{Y}$ are the respective means of the parameters X_i and Y_i $(i, \ldots, n)$.

[1.1] $Y_i = \alpha + \beta X_i$

[1.2] $B_i = Y_i - X_i$

[1.3] $B = \frac{1}{n} \sum_{i=1}^{n} B_i$

[1.4] $\tau^2 = \lambda \sigma^2$

[1.5] $\nu^2 = \sigma^2 + \tau^2$

[1.6] $V_X = \frac{1}{n} \sum_{i=1}^{n} (X_i - \overline{X})^2$

[1.7] $V_Y = \frac{1}{n} \sum_{i=1}^{n} (Y_i - \overline{Y})^2$

[1.8] $V_B = \frac{1}{n} \sum_{i=1}^{n} (B_i - B)^2$

[1.9] $V = V_X + V_Y$

[1.10] $\Omega^2 = \nu^2/V$

(X_i, Y_i) lie exactly on this line. Also, by (1.1)–(1.2), the measurement error variances in x_i and y_i are σ^2 and τ^2, respectively.

Kendall and Stuart (1979, chapter 29) refer to (1.1)–(1.3) as a "functional" EV model. It contains $n+4$ independent parameters, α, β, σ, τ, and $X_i, \ldots, X_n$, where n represents the number of pairs of observations (x_i, y_i). As is well known (op. cit., p. 408–410), consistent likelihood estimates for the parameters can be obtained only when additional information is available about the error structure from sources external to the data being analyzed. In particular, it is sufficient to know

$$\lambda = \frac{\tau^2}{\sigma^2}, \tag{1.4}$$

the ratio of error variances. With the constraint (1.4), the number of parameters in the EV model is reduced to $n+3$. Thus, τ is determined by σ when λ is given.

Some features of this EV model deserve mention here. First, the model is parametrically nonlinear, since (1.3) includes products βX_i of the parameters. Second, (1.3) determines the parameters Y_i in terms of the remaining parameters α, β, and X_i. Third, the number of parameters increases with the number of observations, since each pair of observations (x_i, y_i) is associated with an unknown parameter X_i. Finally, there are $2n$ individual observations $(x_1, \ldots, x_n, y_1, \ldots, y_n)$; consequently, estimates could, in principal, be obtained for the $n+3$ parameters if $2n \geqslant n+3$, i.e. $n \geqslant 3$.

Table 1 lists definitions of various additional parameters that can be expressed in terms of the model's $n+3$ independent parameters $(\alpha, \beta, \sigma, X_1, \ldots, X_n)$. Note that [1.1] is the same as (1.3); it is included here to emphasize that the parameter Y_i is determined by α, β, and X_i. The parameter B_i in [1.2] represents the relative bias between the two true (but unobserved) measurements X_i and Y_i. Furthermore, the parameter B in [1.3] provides an index of the overall bias, namely the mean of the individual bias parameters B_i. The definition [1.4], consistent with (1.4), emphasizes that τ is determined by σ when λ is given. The parameter ν^2 in [1.5] represents the total error variance associated with both observations x_i and y_i. Other parameters of interest include the variances V_X, V_Y, and V_B defined by [1.6]–[1.8]. The parameter V in [1.9] represents the variance due to the scatter of points (X_i, Y_i) along the line (1.3). This can be compared with the total variance ν^2 due to measurement error, as suggested by the definition of Ω in [1.10]. Thus, for example, Ω will be small when the measurement error is small in comparison with the scatter of points along the line $Y = \alpha + \beta X$.

TABLE 2. Relationships among parameters implied by the formulas in Table 1.

[2.1] $\alpha = B + (1-\beta)\overline{X}$

[2.2] $Y_i = B + \overline{X} + \beta(X_i - \overline{X})$

[2.3] $B_i = B + (\beta - 1)(X_i - \overline{X})$

[2.4] $\sigma^2 = \frac{1}{1+\lambda} \cdot \nu^2$

[2.5] $\tau^2 = \frac{\lambda}{1+\lambda} \cdot \nu^2$

[2.6] $V_B = (\beta - 1)^2 V_X$

[2.7] $V_Y = \beta^2 V_X$

[2.8] $V = (1+\beta^2) V_X$

[2.9] $\Omega^2 = \frac{1+\lambda}{1+\beta^2} \cdot \frac{\sigma^2}{V_X}$

Table 2 shows various relationships that exist among the independent parameters of the EV model and those defined in Table 1. Specifically, [2.1] shows that α can be expressed in terms of B, β, and $\overline{X}$, the mean of X_i $(i = 1, \ldots, n)$. Similarly, given λ, [2.4]–[2.5] show that σ and τ are determined by ν. These relationships allow us to express the EV model (1.1)–(1.3) in the equivalent form

$$x_i = X_i + \sqrt{\frac{1}{1+\lambda}}\, \nu \delta_i, \tag{1.5}$$

$$y_i = Y_i + \sqrt{\frac{\lambda}{1+\lambda}}\, \nu \epsilon_i, \tag{1.6}$$

$$Y_i = B + \overline{X} + \beta\,(X_i - \overline{X}). \tag{1.7}$$

Model (1.5)–(1.7) is the EVB model mentioned in the first paragraph of this section. It involves $n+3$ parameters $(B, \beta, \nu, X_1, \ldots, X_n)$ that are equivalent to those of the EV model (1.1)–(1.3), where Tables 1 and 2 provide the formulae needed to convert from one set of parameters to the other.

A fundamental premise in constructing the EVB model is that X_i and Y_i are measurements of the same phenomenon. Since they share the same measurement units, it makes sense to compute the difference $Y_i - X_i$ in [1.2] and the sum $\sigma^2 + \tau^2$ in [1.5]. Furthermore, by (1.4), λ is dimensionless; consequently, the quantity $1 + \lambda$ that appears in (1.5), (1.6), and Table 2 is meaningful. By contrast, in the classical EV model, X_i and Y_i typically correspond to separate phenomena and may have different measurement units. Thus, it may be impossible to attribute meaning to parameters such as B and ν in that context.

Equation [2.3] shows that B_i is a linear function of X_i; more generally, the bias B_X for a given X depends linearly on X:

(1.8) $B_X = B + (\beta - 1)(X - \bar{X})$.

This equation, together with (1.7), allows us to give analytic definition to the three scenarios for a trend line discussed in the introduction. They correspond, respectively, to the following three hypotheses for the parameters B and β:

(1.9a) H_1: $B = 0$, $\beta = 1$;

(1.9b) H_2: $B \neq 0$, $\beta = 1$;

(1.9c) H_3: $B \neq 0$, $\beta \neq 1$.

If H_1 is true, then from (1.7) the trend line is the 45° line $Y_i = X_i$, and from (1.8) the bias B_X is 0 for every X. Thus, the first scenario is equivalent to H_1. Similarly, under H_2, $Y_i = B + X_i$ and $B_X = B \neq 0$. Thus, the trend line is parallel to the 45° line, but not coincident with it, as in the second scenario. Finally, H_3 describes the general case when the trend line is not parallel to the 45° line. Indeed, from (1.8), H_3 implies systematic dependence between B_X and X, as in the third scenario.

We conclude this section with a final remark about the EVB model. Notice that the parameter B represents only the *relative* bias between two measurements. As we have discussed in the introduction, consistent measurements may still share a common bias relative to the true (but unknown) quantity of interest. The EVB model recognizes that only relative bias is estimable from the observations alone. Nevertheless, statistical statements about B and β can be made in a framework that acknowledges error in both measurement methods.

2. Parameter Estimation

In this section we present the likelihood function for the EVB model and obtain analytical expressions for maximum likelihood estimates of all model parameters, including those defined in Table 1. Some of these estimates are not consistent (i.e. do not converge in probability to the true values as $n \rightarrow \infty$), and we obtain corrected, consistent estimates where possible. Finally, we minimize the negative log likelihood with respect to all parameters except one or both of B and β. Our analytical results form the basis of a theory of confidence regions developed in the next section.

The EVB model likelihood, expressed as a function of the parameters $(B, \beta, \nu, X_1, \ldots, X_n)$, is given by

$$(2.1)\quad L = \left[\frac{(1+\lambda)}{2\pi\sqrt{\lambda}\,\nu^2}\right]^n \prod_{i=1}^{n} \exp\left\{-\frac{1+\lambda}{2\nu^2}(x_i - X_i)^2 - \frac{1+\lambda}{2\lambda\nu^2}\left[y_i - B - \bar{X} - \beta(X_i - \bar{X})\right]^2\right\}.$$

Thus, L consists of a product of normal likelihoods associated with δ_i and ϵ_i in (1.5)–(1.6). Our analysis is based on the negative log likelihood (except for a constant)

$$(2.2)\quad \ell(B, \beta, \nu, X_1, \ldots, X_n) = -\ln(L) - n \cdot \ln\left[\frac{\pi\sqrt{\lambda}}{1+\lambda}\right] - n.$$

Analytic expressions for the maximum likelihood parameter estimates can be obtained by minimizing $\ell(B, \beta, \nu, X_1, \ldots, X_n)$. These are given in Table 3, along with estimates of other useful parameters from Table 1. Here $\bar{x}$ and $\bar{y}$ denote the means of the respective observations, and the quantities

$$(2.3)\quad m_{ij} = \frac{1}{n}\sum_{k=1}^{n}\left[x_k - \bar{x}\right]^i\left[y_k - \bar{y}\right]^j$$

represent sample moments. Appendix A provides proof of the estimates [3.1]–[3.7].

TABLE 3. Maximum likelihood parameter estimates for the EVB model, where m_{ij} is given by (2.3). Carets (^) indicate maximum likelihood estimates, and tildes (~) indicate estimates corrected for consistency.

[3.1] $\hat{B} = \bar{y} - \bar{x}$

[3.2] $\hat{\beta} = \dfrac{m_{02} - \lambda m_{20} + \sqrt{(m_{02} - \lambda m_{20})^2 + 4\lambda m_{11}^2}}{2m_{11}}$

[3.3] $\hat{X}_i = x_i + \dfrac{\hat{\beta}}{\hat{\beta}^2 + \lambda}\left[(y_i - \bar{y}) - \hat{\beta}(x_i - \bar{x})\right]$

[3.4] $\hat{Y}_i = y_i - \dfrac{\lambda}{\hat{\beta}^2 + \lambda}\left[(y_i - \bar{y}) - \hat{\beta}(x_i - \bar{x})\right]$

[3.5] $\hat{\nu}^2 = \dfrac{1}{2}\left[\dfrac{1 + \lambda}{\hat{\beta}^2 + \lambda} \cdot (m_{02} - 2\hat{\beta}\mathrm{m}_{11} + \hat{\beta}^2 m_{20})\right]$

[3.6] $\hat{V} = \dfrac{1 + \hat{\beta}^2}{(\lambda + \hat{\beta}^2)^2} \cdot (\lambda^2 m_{20} + 2\lambda\hat{\beta} m_{11} + \hat{\beta}^2 m_{02})$

[3.7] $\hat{\Omega}^2 = \dfrac{\hat{\nu}^2}{\hat{V}}$

[3.8] $\tilde{\nu}^2 = 2\hat{\nu}^2$

[3.9] $\tilde{V} = \dfrac{1 + \hat{\beta}^2}{\hat{\beta}} \cdot m_{11}$

[3.10] $\tilde{\Omega}^2 = \dfrac{\tilde{\nu}^2}{\tilde{V}}$

Note that $\hat{B}$ is the only estimate independent of λ in Table 3. Furthermore, $\hat{B}$ involves only the means $\bar{x}$ and $\bar{y}$, while $\hat{\beta}$ and the remaining estimates depend on second order moments. It can be shown (Appendix B) that $\hat{B}$ and $\hat{\beta}$ are consistent estimates of B and β, respectively. By contrast, $\hat{\nu}^2$ converges in probability to $\nu^2/2$ as $n \rightarrow \infty$. Thus, the estimate $\tilde{\nu}^2$ in [3.8] is consistent for ν^2. This agrees with an analogous result for classical EV models discussed by Kendall and Stuart (1979, p. 411). Similarly, although $\hat{V}$ and $\hat{\Omega}$ are not consistent for V and Ω, the adjusted estimates $\tilde{V}$ and $\tilde{\Omega}$ are. Proofs of [3.8]–[3.10] are given in Appendix B.

Since B and β are the parameters of principal interest, it is sometimes convenient to treat the others as nuisance parameters. In this context, the following three functions are of statistical interest:

$$(2.4)\quad \ell_1(B, \beta) = \min_{\nu, X_1, \ldots, X_n} \ell(B, \beta, \nu, X_1, \ldots, X_n),$$

$$(2.5)\quad \ell_2(B) = \min_{\beta, \nu, X_1, \ldots, X_n} \ell(B, \beta, \nu, X_1, \ldots, X_n),$$

$$(2.6)\quad \ell_3(\beta) = \min_{B, \nu, X_1, \ldots, X_n} \ell(B, \beta, \nu, X_1, \ldots, X_n),$$

TABLE 4. Explicit representations of the function ℓ_h ($h = 1,2,3$) defined by (2.4)–(2.6).

[4.1] $$\ell_1(B,\beta) = n\cdot\ln\left[(\bar{y} - \bar{x} - B)^2 + \frac{1+\lambda}{\beta^2+\lambda}\cdot(m_{02} - 2\beta m_{11} + \beta^2 m_{20})\right]$$

[4.2] $$\ell_2(B) = n\cdot\ln\left[(\bar{y} - \bar{x} - B)^2 + \frac{1+\lambda}{\hat{\beta}^2+\lambda}\cdot(m_{02} - 2\hat{\beta} m_{11} + \hat{\beta}^2 m_{20})\right]$$

[4.3] $$\ell_3(\beta) = n\cdot\ln\left[\frac{1+\lambda}{\beta^2+\lambda}\cdot(m_{02} - 2\beta m_{11} + \beta^2 m_{20})\right]$$

Essentially, these three functions contain all statistical information available on the parameters B and β. Their definitions imply the relationships

(2.7) $\ell_2(B) = \ell_1(B, \hat{\beta})$,

(2.8) $\ell_3(\beta) = \ell_1(\hat{B}, \beta)$.

Furthermore, as shown in Table 4 (and derived in Appendix A), the functions ℓ_h ($h = 1,2,3$) can be expressed analytically in terms of the data, i.e. in terms of $\bar{x}$, $\bar{y}$, and m_{ij} ($i+j = 2$). In the next section we use these functions to obtain approximate confidence regions for B and/or β.

3. Confidence Regions

When $\lambda = 0$ or $\lambda = \infty$, the EVB model (1.5)–(1.7) reduces to a conventional regression model with error in only one variable. In these two cases, classical theory can be used to construct confidence intervals for the model parameters. For example, when $\lambda = \infty$, error is confined to the y-variable, the estimates $(\hat{B}, \hat{\beta})$ are binormally distributed, and standard tests based on the F-distribution lead to a confidence region for (B, β). Unfortunately, for values of λ in the open interval $(0, \infty)$, the exact distribution of $(\hat{B}, \hat{\beta})$ cannot be represented analytically. Furthermore, since the number of model parameters increases with the number of observations, asymptotic results (such as likelihood ratio tests) cannot be assumed to apply automatically.

Various ad hoc methods have been devised for constructing confidence regions when $\lambda > 0$. For example, Schnute (1984) notes that the variate

$$z_i(\beta) = y_i - \beta x_i$$

is normal at the true value of β. Thus, a test of normality leads to a confidence interval for β, where a value of β is accepted if and only if the sequence $\{z_i(\beta)\}$ appears normal. A more sensitive test due to Creasy (1956) is discussed by Kendall and Stuart (1979, p. 411–413) and modified by Fuller (1987, p. 44–48). None of these tests, however, reduce to classical regression theory as $\lambda \rightarrow 0$ or $\lambda \rightarrow \infty$.

In this paper we take a different approach by starting with results from regression theory, extending them formally to the EVB model, and verifying their validity with simulation. Although our methods are approximate for λ in $(0, \infty)$, the approximations appear legitimate for the data considered here. Furthermore, an immediate consequence of this approach is that our results are identical to those from the exact theory when $\lambda = 0$ or $\lambda = \infty$.

We begin with a discussion of ordinary regression in the context of the simple model

(3.1) $y_i = \alpha + \beta x_i + \tau\epsilon_i$

for n observations (x_i, y_i). This is the same as (1.1)–(1.3) with $\sigma = 0$ and $\lambda = \infty$. Let $L(\alpha, \beta, \tau)$ denote the likelihood function for (3.1); similarly, let

(3.2) $\ell(\alpha, \beta) = -2\cdot\min_{\tau}\{\ln[L(\alpha,\beta,\tau)]\} - n\cdot\ln(4\pi^2/n) - n$

be twice the negative log likelihood (except for a constant), minimized with respect to τ. Then it can be shown (Appendix C) that

(3.3) $\ell(\Theta) = n\cdot\ln[S(\Theta)]$,

where $\Theta = (\alpha, \beta)$ is the vector of regression parameters and

(3.4a) $S(\Theta) = \sum_{i=1}^{n} (y_i - \alpha - \beta x_i)^2$

is the sum of squares of model residuals. Incidentally, a short calculation shows that $S(\Theta)$ can be expressed in terms of data moments as

(3.4b) $S(\Theta) = (\bar{y} - \alpha - \beta\bar{x})^2 + (m_{02} - 2\,\beta m_{11} + \beta^2 m_{20})$.

In general, regression models typically lead to a likelihood function of the form (3.3), where $\Theta = (\theta_1, \ldots, \theta_k)$ is a k-dimensional parameter vector and $S(\Theta)$ is a sum of squares of residuals. The maximum likelihood estimate $\hat{\Theta}$ corresponds to the minima of both $\ell(\Theta)$ and $S(\Theta)$, and confidence regions for Θ can be obtained from the fact that a variance ratio is known to be F-distributed. To be precise,

(3.5) $$\frac{n-k}{k}\cdot\frac{S(\Theta) - S(\hat{\Theta})}{S(\hat{\Theta})} \sim F(k, n-k),$$

where Θ in (3.5) is the true (but unknown) parameter vector, $F(k, n-k)$ refers to the F-distribution with k and $n-k$ degrees of freedom, and (following statistical convention) the symbol "$\sim$" means "is distributed as." Combining (3.3) and (3.5) shows that

(3.6) $$\ell(\Theta) - \ell(\hat{\Theta}) \sim n\cdot\ln\left[1 + \frac{k}{n-k}\,F(k, n-k)\right].$$

Consequently, the boundary of a p-level confidence region for Θ is determined by the equation

(3.7) $$\ell(\Theta) = \ell(\hat{\Theta}) + n\cdot\ln\left[1 + \frac{k}{n-k}\,F_p\,(k, n-k)\right],$$

where $0 \leq p \leq 1$ and F_p denotes the upper p-level cutoff point of the cumulative F-distribution.

The functions ℓ_h ($h = 1, 2, 3$) in Table 4 are all formally analogous to ℓ in (3.3), provided that $S(\Theta)$ is suitably defined as the argument of the logarithm function in each case. Notice,

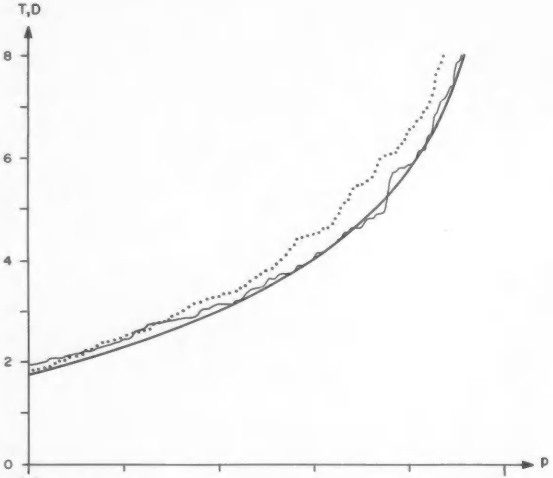

FIG. 1. Simulated and exact distributions (3.6) for the function $\ell_1(B,\beta)$ in [4.1]. The simulations are based on model (1.5)–(1.7) with $n = 10$, $B = -0.3$, $\beta = 0.9$, $X_i = i$ ($i = 1, \ldots, 10$), $\lambda = 1$, and either $\nu = 1$ or $\nu = 2$. The heavy curve indicates the theoretical value T in (3.8) as a function of the cumulative probability p. The light curve represents the cumulative distribution of the difference D in (3.9) for 300 simulations with $\nu = 1$. The dotted curve similarly corresponds to the distribution of D for 300 simulations with $\nu = 2$.

in particular, the similarity between $\ell(\alpha, \beta)$ in (3.3)–(3.4) and $\ell_1(B, \beta)$ in [4.1] as $\lambda \rightarrow \infty$. This similarity is present in spite of the fact that ℓ in (3.3) comes from *twice* the negative log likelihood for a regression model, while the functions ℓ_h ($h = 1, 2, 3$) in [4.1]–[4.3] come from the negative log likelihood itself for an EVB model. We conclude that, to extend regression theory continuously to an EV model, it is necessary to compare the EV log likelihood with twice the regression log likelihood. Intuitively, this extension is correct because the EV likelihood is a product of normal densities from two variates (such as δ_i and ϵ_i in (1.5)–(1.6)), while the regression likelihood is associated with only a single variate (such as ϵ_i in (3.1)). Thus, the EV log likelihood has twice as many terms as the regression log likelihood.

If, indeed, the functions in Table 4 can be used as legitimate extensions from regression theory, then each of them should conform to the distribution (3.6). We can test this conjecture by simulation. For example, Fig. 1 shows simulated and exact results for $\ell_1(B, \beta)$ in a model with $n = 10$, based on the parameters $B = -0.3$, $\beta = 0.9$, $X_i = i$ ($i = 1, \ldots, 10$), $\lambda = 1$, and either $\nu = 1$ or $\nu = 2$. We use two values of ν to test sensitivity to the model's noise level. The heavy curve in Fig. 1 represents the right side of (3.6), i.e. the theoretical value

$$(3.8) \quad T = 10 \cdot \ln[1 + (2/8) \cdot F_p(2, 8)],$$

as a function of p. Note that $k = 2$ here, since $\ell_1(B, \beta)$ depends on two parameters. The light curve in Fig. 1 represents the cumulative distribution of the difference

$$(3.9) \quad D = \ell_1(B, \beta) - \ell_1(\hat{B}, \hat{\beta})$$

from the left side of (3.6), based on 300 simulations with $\nu = 1$. To be precise, each simulation involves three steps. First, for $i = 1, \ldots, 10$, generate normal random variables (δ_i, ϵ_i), and then determine points (x_i, y_i) from (1.5)–(1.7). Second, use the resulting 10 points to compute ($\hat{B}$, $\hat{\beta}$) from [3.1]–[3.2]. Third, calculate the difference D in (3.9), using the true values $(B, \beta) = (-0.3, 0.9)$ and the estimate ($\hat{B}$, $\hat{\beta}$). The resulting 300 differences D are then sorted in ascending order, so that the proportion of differences less than or equal to the jth difference D_j is $p_j = j/300$. The light curve in Fig. 1 shows the cumulative plot, D_j vs. p_j, when $\nu = 1$. The dotted curve shows a similar plot for 300 simulations with $\nu = 2$.

For low values of p, the observed difference D in Fig. 1 is close to the theoretical value T when $\nu = 1$ or $\nu = 2$. At higher p, D remains close to T when $\nu = 1$, but D rises distinctively above T when $\nu = 2$. As a result of many tests over a wide range of parameter values, we conclude that the distribution (3.6) is legitimate for ℓ_1 (B, β) as long as the noise level ν is small compared with the scatter of points (X_i, Y_i) along the line (1.7). The variance V in [1.9] provides an overall measure of this scatter, and we can summarize our conclusions by stating that (3.6) appears valid as long as

$$(3.10) \quad \Omega < 0.3,$$

where $\Omega = \nu/\sqrt{V}$ as in [1.10]. Furthermore, this limitation applies when $\lambda = 1$, the case considered in Fig. 1. As λ moves toward the extreme values 0 or ∞, (3.6) remains valid for values of Ω larger than 0.3. Indeed, at the extremes when $\lambda = 0$ or $\lambda = \infty$, (3.6) is an exact result of regression theory for all values of the model parameters.

We have also performed similar tests of (3.6) for the functions $\ell_2(B)$ and $\ell_3(\beta)$ in [4.2]–[4.3]. Note that $k = 1$ in these cases, each of which involves only one parameter. Our results again indicate the validity of (3.6), given the restriction (3.10).

The practical significance of (3.6) is that it implies equation (3.7) for parameter confidence regions. In particular, (3.7) leads to analytic formulas that describe confidence regions for B and/or β. These are listed in Table 5. For example, by applying (3.7) to $\ell_1(B, \beta)$, one can derive (Appendix C) the joint confidence region [5.1] for (B, β). Similarly, the confidence intervals [5.2]–[5.3] for B and β can be obtained (Appendix C) by applying (3.7) to $\ell_2(B)$ and $\ell_3(\beta)$, respectively.

To apply [5.1] with a specified confidence level p, note that, in general, two values of $B(\beta)$ are determined by a given value of β. These determine the upper and lower boundaries of a p-level confidence region plotted in (B, β) space. Obviously, the quantity under the radical in [5.1] must be positive for the function $B(\beta)$ to be real. Typically, this quantity is positive only for a finite β-range, and values of β for which it is 0 determine extreme points on the contour. In between, the resulting contour is oval shaped. The application of [5.2] or [5.3] is more straightforward, since each formula gives the two end points of a confidence interval.

In summary, the results in Table 5, obtained by analogy with regression theory, describe confidence regions for the EVB model parameters (B,β) that are approximate when $0<\lambda<\infty$ and exact when $\lambda = 0$ or $\lambda = \infty$. The approximations are legitimate over the entire λ-range, subject to the restriction (3.10).

4. The Special Case $\beta = 1$

The special case $\beta = 1$ has particular importance for the EVB model. From a practical point of view, as discussed in the introduction and in connection with (1.8)–(1.9), the bias is constant when $\beta = 1$. From a theoretical and numerical point of view, we show in this section that both the model and its

TABLE 5. Formulas for determining p-level confidence regions for the parameters B and/or β. These are approximate for $0 < \lambda < \infty$ and exact for $\lambda = 0$ or $\lambda = \infty$.

$$[5.1] \quad B(\beta) = \hat{B} \pm \sqrt{\tilde{\nu}^2 \left[1 + \frac{2}{n-2} \cdot F_p\,(2,n-2)\right] - \frac{1+\lambda}{\beta^2+\lambda} \cdot (m_{02} - 2\beta m_{11} + \beta^2 m_{20})}$$

$$[5.2] \quad B = \hat{B} \pm \tilde{\nu} \sqrt{\frac{1}{(n-1)} \cdot F_p(1,n-1)}$$

$$[5.3a] \quad \beta = \frac{A_1 \pm \sqrt{A_1^2 - A_0 A_2}}{A_2}$$

$$[5.3b] \quad A_0 = m_{02} - \frac{\lambda}{1+\lambda} \cdot \tilde{\nu}^2 \left[1 + \frac{1}{n-1} \cdot F_p(1,n-1)\right]$$

$$[5.3c] \quad A_1 = m_{11}$$

$$[5.3d] \quad A_2 = m_{20} - \frac{1}{1+\lambda} \cdot \tilde{\nu}^2 \left[1 + \frac{1}{n-1} \cdot F_p(1,n-1)\right]$$

analysis simplify considerably. Furthermore, this simplicity provides an opportunity to check our results in a special case.

To see how the model itself simplifies when $\beta = 1$, let

$$(4.1) \quad b_i = y_i - x_i$$

be the observed bias at the point (x_i, y_i). From (1.7), note that $Y_i = B + X_i$ when $\beta = 1$; consequently, subtracting (1.5) from (1.6) gives

$$(4.2) \quad b_i = B + \nu\eta_i\,,$$

where

$$\eta_i = \sqrt{\frac{\lambda}{1+\lambda}}\,\epsilon_i - \sqrt{\frac{1}{1+\lambda}}\,\delta_i\,.$$

Since δ_i and ϵ_i are independent normal variates with mean 0 and variance 1, it follows that η_i is normal with mean 0 and variance

$$\frac{\lambda}{1+\lambda} + \frac{1}{1+\lambda} = 1.$$

Thus, when $\beta = 1$, the variates b_i in (4.1)–(4.2) are normal with mean B and variance ν^2, independent of λ.

Just as λ disappears from the model in (4.1)–(4.2), it also cancels in various model results when $\beta = 1$. For example, note that [3.5], [4.1], [4.2], [4.3], and [5.1] all contain the expression $(1+\lambda)/(\beta^2+\lambda)$, which reduces to 1 when $\beta = 1$. In particular, [3.5] and [3.8] show that

$$(4.3) \quad \tilde{\nu}^2 = m_{02} - 2m_{11} + m_{20}.$$

Thus, the EVB model estimate of ν does not depend on λ when $\beta = 1$.

We have already mentioned that $\hat{B}$ in [3.1] does not depend on λ. In general, however, confidence intervals for B computed from [5.2] do vary with λ. This happens because the calculation involves $\tilde{\nu}$, which from [3.5] and [3.8] generally depends on λ. Because of (4.3), this dependency is absent when $\beta = 1$.

Since the EVB model implies (4.1)–(4.2) when $\beta = 1$, analysis of the parameter B in this case should reduce to conventional statistics for a normal distribution. To check this, note first that [3.1] is the usual estimate for B since

$$\bar{b} = \bar{y} - \bar{x}.$$

Second, since

$$m_{02} - 2m_{11} + m_{20} = \frac{1}{n}\sum_{i=1}^{n} (b_i - \bar{b})^2,$$

$\tilde{\nu}^2$ in (4.3) is the conventional maximum likelihood variance estimate. Finally, [5.2] is equivalent to

$$(4.4) \quad B = \hat{B} \pm \frac{\nu'}{\sqrt{n}}\; t_p(n-1),$$

where $t_p(n-1)$ is the p-level cut-off for Student's t-statistic with $n-1$ df and

$$\nu' = \sqrt{\frac{n}{n-1}}\,\tilde{\nu}$$

is the usual bias corrected estimate for ν. Note that (4.4) defines conventional confidence intervals for the mean of a normal distribution. Incidentally, we have used the fact that $t_p(n-1)$ is the square root of $F_p(1, n-1)$.

The model (4.1)–(4.2) offers a simple alternative to the EVB model, and might be used in contexts where it is certain that $\beta = 1$. The advantage of the full EVB model is that it does not require $\beta = 1$; indeed, it provides a statistical test of that hypothesis. Furthermore, the full model gives estimates of the true points (X_i, Y_i) corresponding to the observations (x_i, y_i). These estimates generally depend on λ, even when $\beta = 1$. Finally, given the high noise levels common in fishery data, both parameters B and β may have considerable interest when comparing two methods of measurement.

5. Example

As described in the introduction, we illustrate the EVB model's application by comparing two methods of measuring numbers of adult salmon returning to various hatcheries in British Columbia, Canada. One method involves direct counting, while the other is based on marked fish. We present our example in three parts. Section 5A provides background material on hatchery operation and data collection. Section 5B uses data from one hatchery to exemplify the model analysis. Finally, Section 5C applies the model to data from various hatcheries and uses the results to make statistical comparisons among them.

5A. Data Description

Data for our example relate to chinook and coho salmon reared in British Columbia hatcheries. These species have a remarkable ability to return to their natal freshwater rearing sites. Thus, salmon returning to a hatchery typically come from stocks released there. To track fish throughout their life cycle, a fraction of juveniles are marked before their release from the hatchery.

The most common marking method involves the use of binary coded wire tags (CWTs). These are small enough to be inserted into the nose cartilage of young salmon before they migrate to salt water. Since the CWT is not visible by external examination, a secondary mark (usually removal of the adipose fin) is used to enable recognition among adults. The CWT possesses the advantages of being both relatively easy to apply and capable of delineating a large number of unique tag codes.

An analysis of CWT data requires notation for various quantities of interest. Suppose that a particular hatchery and species is selected. For a given tag code t, let R_t be the number of (marked and unmarked) fish released from the hatchery, including a group of T_t tagged fish. Suppose that, in a subsequent year i, O_{it} of these tagged fish are observed among returns to the hatchery. On the basis of the original proportion of marked fish, these observed recoveries represent

$$(5.1)\quad E_{it} = \frac{R_t}{T_t} O_{it}$$

fish from the original population. The quantity E_{it} is termed the expanded number of recoveries.

The returns in year i typically include fish with several different tag codes. If A represents the set of all tag codes recovered among returning adults in year i, then the total

$$(5.2)\quad E_i = \sum_{t \in A} E_{it}$$

is the number of fish in the run that can be explained on the basis of marked fish. We wish to compare E_i with H_i, the number estimated from a visual count of returning adults in year i. These estimates should be comparable, since all groups of juveniles released from the hatchery contain a proportion of marked fish.

Information on the release and recovery of CWT-marked salmon from British Columbia is stored in a database maintained by the Canadian Department of Fisheries and Oceans (Kuhn et al. 1988). Fields in this database include the quantities O_{it}, R_t, T_t, and H_i defined above. Accesss programs (Kuhn 1988) allow the user to determine tag codes relevant to a specific hatchery and recovery year (set A in (5.2)), so that both E_i and H_i for selected hatcheries and recovery years can be easily obtained.

TABLE 6. Hatcheries and recovery years for data used in the analysis. The table lists years for which tag recoveries are available in the database. Within each combination of hatchery and species, any year i is excluded from the analysis if $O_i < 20$, where O_i represents the total number (5.3) of observed tags from all tag codes recovered in year i.

	Coho		Chinook	
Hatchery	Available	Excluded	Available	Excluded
Big Qualicum	1973–86		1973–86	
Capilano	1973–86		1973–86	
Chilliwack	1982–86		1982–86	1982
Puntledge	1978–86		1974–86	1974
Quinsam	1976–86		1977–86	1977–78
Robertson Creek	1974–86	1980–81	1977–86	

From data available in the database, we selected all British Columbia hatcheries with at least five return years that included marked fish (Table 6). Six hatcheries were selected by this criterion, each of which releases both chinook and coho salmon. We wanted to exclude combinations of hatchery, species, and recovery year for which the number of recovered tags was small. Thus, for each hatchery-species combination, we considered the total number of observed recoveries in each year i, that is,

$$(5.3)\quad O_i = \sum_{t \in A} O_{it}\ ,$$

where A is the set of tag codes relevant to the combination. We excluded from our analysis any year i for which $O_i < 20$, and the resulting six exclusions are also listed in Table 6.

We began our analysis with exploratory plots of the data sets in Table 6. We found that log-transformed data

$$(5.4)\quad (x_i, y_i) = (\ln H_i, \ln E_i)$$

generally appeared to follow a linear trend with homogeneous variance. Consequently, we based all EVB model analyses on the transformed data (5.4).

5B. Sample Analysis

In this section, by way of illustration, we restrict our attention to a single species from one hatchery. We choose data on chinook salmon from the Puntledge River Hatchery because the resulting parameter estimates are considerably affected by the choice of λ. As shown in Fig. 2, most points (x_i, y_i) in the data set fall below the line $y = x$. Thus, since $\hat{B} = \bar{y} - \bar{x}$, casual inspection suggests that there should be a negative bias. It also appears that a straight line through the data may have a slope greater than 1. Formulas from Table 3 give the following estimates:

$\hat{B}$	$\hat{\beta}$			$\tilde{\nu}$		
	$\lambda = 0$	$\lambda = 1$	$\lambda = \infty$	$\lambda = 0$	$\lambda = 1$	$\lambda = \infty$
−0.29	1.57	1.48	1.30	0.20	0.23	0.28

As mentioned in Section 3, $\hat{B}$ is independent of λ. Note, however, that $\hat{\beta}$ decreases and $\tilde{\nu}$ increases as λ goes from 0 to ∞. Therefore, an opinion of the source of error (in x_i, y_i, or both) affects our estimates of the slope β and the total variance ν^2 of random error. We discuss this point further in Section 5C below.

The joint confidence region for B and β from [5.1] similarly depends on λ (Fig. 3). For $\lambda = \infty$, this confidence region is elliptical, a familiar shape from regression analysis. By contrast, for $\lambda = 0$, the contour is decidedly teardrop shaped. For $\lambda = 1$, the shape of the contour is intermediate between those

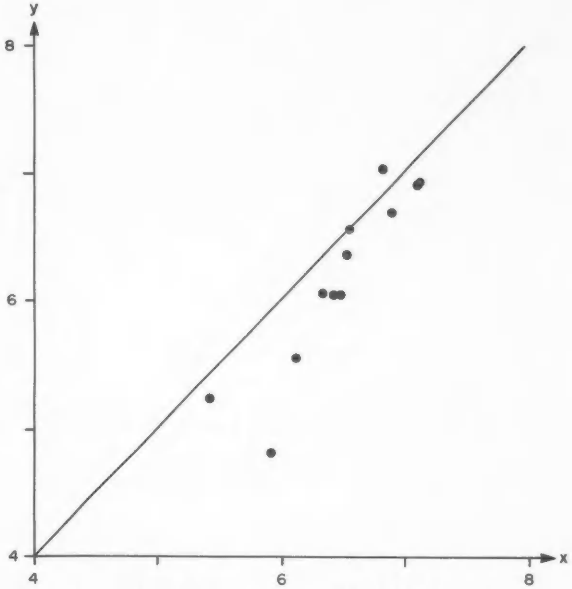

FIG. 2. Scatter plot of $y_i = \ln(E_i)$ vs. $x_i = \ln(H_i)$ for chinook returns to Puntledge hatchery, 1975–86. E_i and H_i refer to return estimates based on marked fish and visual counts, respectively. The line $y = x$ is shown for reference. Most points lie below this line, and the estimated bias $\hat{B} = \bar{y} - \bar{x}$ is negative.

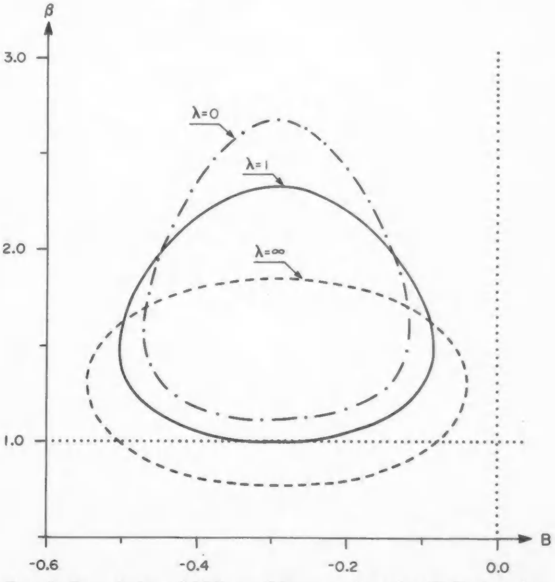

FIG. 3. Boundaries of 95% confidence regions for (B,β), based on chinook data from Puntledge hatchery. Three curves are computed from [5.1] with $\lambda = 0$ (–·–), $\lambda = 1$ (———), and $\lambda = \infty$ (---). Light dotted lines indicate the special values $B = 0$ and $\beta = 1$.

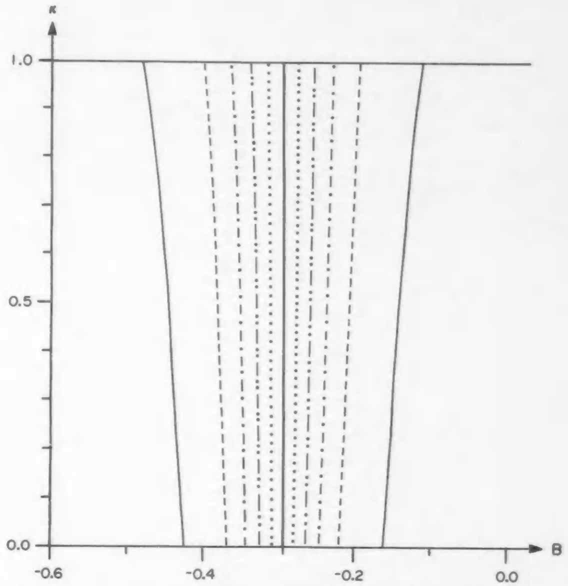

FIG. 4. Confidence intervals for B, based on chinook data from Puntledge hatchery. The width of each interval depends on the p-level and on κ, where κ is related to λ by (5.5). The heavy line at the diagram center indicates the estimate $\hat{B}$, which is independent of κ. The outer light lines represent left and right boundaries of a 95% confidence interval for B, which is narrowest when $\kappa = 0$ ($\lambda = 0$) and broadest when $\kappa = 1$ ($\lambda = \infty$). The remaining lines similarly indicate confidence intervals with $p = 19\%$ (···), $p = 38\%$ (–··–), $p = 57\%$ (-·-), and $p = 76\%$ (---), where these p-levels correspond to regular fractions of 95%.

for the extreme values of λ. The contour's asymmetry when $\lambda = 0$ comes from the fact that, in this case, we are regressing x on y, rather than the customary y on x. Since $1/\beta$ is the slope of this alternative regression, the teardrop shaped contour for $\lambda = 0$ in (B,β) space corresponds to an elliptical contour in $(B,1/\beta)$ space.

Notice that the major and minor axes of the contours of Fig. 3 are oriented parallel to the B and β axes. The reason for this is apparent from [4.1]. The argument of the logarithm in $\ell_1(B,\beta)$ is the sum of two quadratic terms, one containing only B and the other only β. Because $B\beta$ cross product terms are absent, the major and minor axes of the confidence region are parallel to the B and β axes themselves.

Confidence intervals for either B or β alone can also be obtained using [5.2]–[5.3]. Since these intervals depend on λ, it is desirable to plot them for all positive values of λ. To do so, we use the transformation

$$(5.5) \quad \kappa = \frac{2}{\pi}\tan^{-1}(\lambda).$$

Given (5.5), κ goes from 0 to 1 as λ goes from 0 to ∞; also $\kappa = 0.5$ when $\lambda = 1$. Fig. 4 demonstrates that the confidence interval around $\hat{B}$ is symmetric for the entire range of κ. By contrast, the confidence interval around $\hat{\beta}$ (Fig. 5) is symmetric for $\kappa = 1$ ($\lambda = \infty$) and becomes increasingly asymmetric as κ approaches 0 ($\lambda = 0$). This asymmetry corresponds to the effect discussed above in connection with the teardrop shapes of Fig. 3. It is also apparent from Fig. 5 that $\hat{\beta}$ depends on κ (i.e. on λ). Confidence intervals for both B and β depend on κ. The narrowest interval for B corresponds to $\kappa = 0$, while the interval for β is narrowest when $\kappa = 1$.

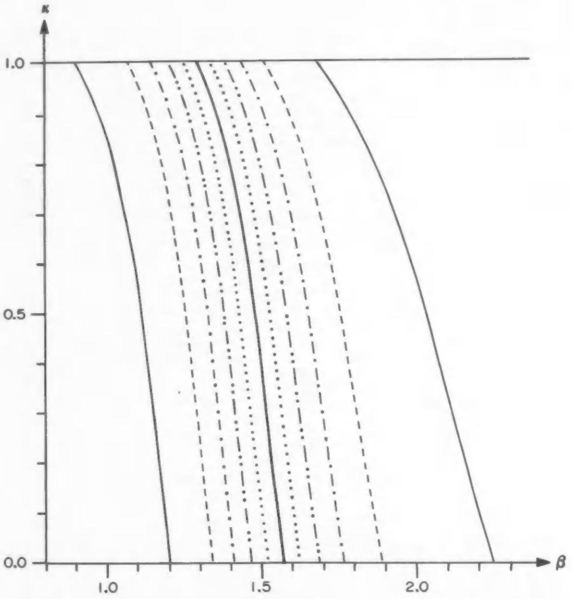

FIG. 5. Confidence intervals for β, based on chinook data from Puntledge hatchery. As in Fig. 4, the width of each interval depends on p and κ. The heavy curve at the center indicates the estimate $\hat{\beta}$, which varies with κ. The outer light lines represent left and right boundaries of a 95% confidence interval for β, which is broadest when κ = 0 (λ = 0) and narrowest when κ = 1 (λ = ∞). The remaining lines similarly indicate confidence intervals with $p = 19\%$ (···), $p = 38\%$ (-··-), $p = 57\%$ (-·-), and $p = 76\%$ (---).

Both Figs. 4 and 5 demonstrate that lower p-level contours are spaced at closer intervals than higher p-level contours. In other words, the "valley" portrayed by these contours is V-shaped with the valley sides becoming steeper near the bottom. By contrast, the valley becomes almost flat near the top because, as the required confidence level p approaches 1, the confidence interval widens at an increasing rate.

We have examined Puntledge chinook data to illustrate a detailed application of the EVB model. Figs. 2–5 illustrate four key steps in the analysis: an exploratory plot of the data (Fig. 2), an examination of $B\beta$ confidence contours for several values of λ (Fig. 3), a diagram representing confidence intervals for B across the entire λ-range (Fig. 4), and a similar diagram for β confidence intervals (Fig. 5). With these steps in mind, it is now appropriate to consider the results of such analyses on the remaining data sets listed in Table 6.

5C. Comparative analyses

If we were to complete the above analysis for each of the 12 data sets (six hatcheries and two species) listed in Table 6, the result would be a set of 12×4 = 48 figures. Furthermore, if we also considered data sets formed by grouping various hatcheries and species, the results would proliferate even further. In this section, we describe methods of comparative analysis designed to portray similarities and differences among such data groups. We apply these methods to 17 groups (the 12 in Table 6, plus two subgroups, and three combined groups) and conclude that, on average, CWT estimates of hatchery returns are about 22% lower than comparable counting estimates. We end the paper with a discussion of mechanisms that might account for this bias.

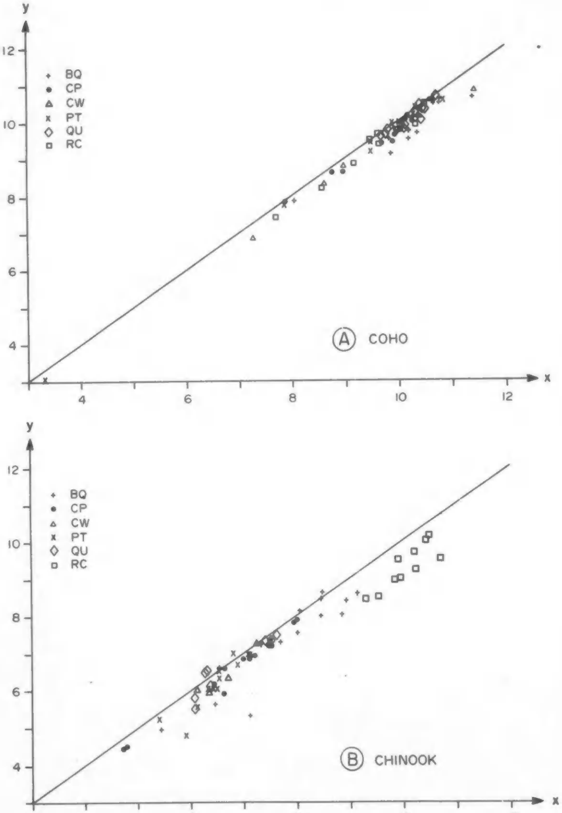

FIG. 6. (A) Scatter plot of $y_i = \ln(E_i)$ vs. $x_i = \ln(H_i)$ for coho returns to various hatcheries in various years, as listed in Table 6. E_i and H_i refer to return estimates based on marked fish and visual counts, respectively. Symbols indicate hatcheries as follows: Big Qualicum (+), Capilano (·), Chilliwack (triangle), Puntledge (×), Quinsam (diamond), and Robertson Creek (square). (B) Similar plot for chinook returns listed in Table 6.

We begin with plots of the data for all hatcheries combined. Figures for coho (Fig. 6A) and chinook (6B) are similar, except that the coho data are more tightly clustered. Both panels of Fig. 6 show a remarkable linearity among observed points (x_i, y_i) over the entire range 3–11.5. Since x and y are logarithmic variables this corresponds to fish counts in the range e^3–$e^{11.5}$ (i.e. 20–10^5). Another striking feature in both panels is that the majority of points lie below the line $y = x$. Specifically, only 10 of the total 126 observed points lie above this reference line.

Table 7 lists 17 data sets of particular interest. These include the 12 in Table 6, as well as three combined groups: all coho, all chinook, and both species combined. We isolate Robertson Creek chinook data as a special case. Close scrutiny of Fig. 6B reveals that the 10 data points for this hatchery appear to lie in two distinct groups (four points close to the line $y = x$ and six points more distant) associated with different trend lines. Points in the first group come from the years 1977–80, while those from the second come from 1981–86. A possible explanation for this break in the data trend is that the hatchery installed a

TABLE 7. Estimates $\hat{B}$ and $\hat{\beta}$ for 17 data groups, where negative values $\hat{B}$ indicate that counts based on marked fish are lower than visual counts. Group codes use a two-part notation, where the first and second parts identify the hatchery and species, respectively. Hatchery codes include "BQ" (Big Qualicum), "CP" (Capilano), "CW" (Chilliwack), "PT" (Puntledge), "QU" (Quinsam), "RC" (Robertson Creek), "R1" (Robertson Creek, return years 1977–80), and "R2" (Robertson Creek, return years 1981–86). Species codes are "CO" (coho salmon) and "CH" (chinook salmon). The code "*" designates combined groups as follows: "*-CO" (groups 1–6), "*-CH" (groups 8–12), "*-*" (groups 1–6 and 8–12). Since data on Robertson Creek chinook have rather distinct characteristics, they are excluded from the combined analyses.

				$\hat{\beta}$		
Group	Code	n	$\hat{B}$	$\lambda = 0$	$\lambda = 1$	$\lambda = \infty$
1	BQ-CO	14	−0.34	1.021	0.966	0.917
2	CP-CO	14	−0.21	1.035	1.022	1.008
3	CW-CO	5	−0.37	0.974	0.969	0.965
4	PT-CO	9	−0.11	1.020	1.018	1.017
5	QU-CO	11	−0.16	1.025	0.972	0.925
6	RC-CO	11	−0.21	1.081	1.070	1.057
7	*-CO	64	−0.23	1.015	1.004	0.993
8	BQ-CH	14	−0.40	1.268	1.180	1.068
9	CP-CH	14	−0.23	1.064	1.054	1.043
10	CW-CH	4	−0.18	1.278	1.231	1.164
11	PT-CH	12	−0.29	1.570	1.478	1.301
12	QU-CH	8	−0.15	1.175	1.113	1.040
13	*-CH	52	−0.28	1.135	1.079	1.018
14	*-*	116	−0.25	1.033	1.022	1.011
15	RC-CH	10	−0.73	1.544	1.388	1.141
16	R1-CH	4	−0.40	1.143	1.122	1.096
17	R2-CH	6	−0.95	0.848	0.832	0.821

new fishway between the 1980 and 1981 chinook returns. Thus, in Table 7, we identify groups 16 and 17 as cases worthy of separate consideration.

As might be anticipated from Fig. 6, all 17 estimates $\hat{B}$ in Table 7 are negative, ranging from -0.11 (group 4) to -0.95 (group 17). In the present context, $B = \ln(E) - \ln(H)$, where E is a CWT estimate and H is a direct count; that is,

$$(5.6) \quad E - H = (e^{B} - 1)H.$$

Based on (5.6), we refer to the quantity

$$(5.7) \quad f = e^{B} - 1$$

as the fractional bias between E and H. For example, when $B = -0.11$, the fractional bias is -0.10; i.e. E is 10% lower than H. Thus, the fractional bias associated with estimates $\hat{B}$ in Table 7 ranges from -10% to -61%. Note, however, that the three lowest values $\hat{B}$ are associated with groups 15–17, i.e. with Robertson Creek chinook. If we exclude these cases as non-representative, then the fractional bias ranges more narrowly from -10% to -33%. Since $\hat{B} = -0.25$ for group 14 (the combination of the remaining representative groups), we estimate the overall fractional bias to be -22%.

Incidentally, note that (5.7) defines a parameter f equivalent to the parameter B. Thus, a confidence interval for B determines a corresponding confidence interval for f. Unlike intervals for B, however, intervals for f are not generally symmetric about the estimate. This difference is due to the fact that the relationship (5.7) is nonlinear.

As discussed in Section 2, the estimate $\hat{B}$ does not depend on λ. For the remaining parameters, we provide estimates at the three reference values $\lambda = 0$, $\lambda = 1$, and $\lambda = \infty$. Table 7 illustrates a general feature of EV models that $\hat{\beta}$ decreases as λ increases. (For a geometric explanation of this feature, see Schnute 1987, pages 161–166). Furthermore, the variability of $\hat{\beta}$ across the λ-range provides a rough measure of error in the data, where $\hat{\beta}$ is independent of λ if and only if the data lie precisely on a straight line.

Estimates $\hat{\beta}$ in Table 7 range from 0.82 (group 17, $\lambda = \infty$) to 1.57 (group 11, $\lambda = 0$), where the majority of estimates lie between 0.9 and 1.1. Estimates for coho are both closer to 1.0 and less variable than those for chinook. The variation in $\hat{\beta}$ as a function of λ is greater in some cases than others. For example, $\hat{\beta}$ is almost independent of λ in the combined coho group 7. This is consistent with the highly linear scatter of data points in Fig. 6A. By contrast, the estimate $\hat{\beta}$ for group 11 (the group considered in detail in section 5B) varies considerably with λ, as might be anticipated from the dispersion of data points in Fig. 2.

Similar features of the model are illustrated by the effect on $\hat{\beta}$ of combining groups. For example, $\hat{\beta}$ is generally more dependent on λ for individual chinook groups 8–12 than for the combined group 13. This occurs because, as shown in Fig. 6B, the range of data for all hatcheries combined is much larger than that for any single hatchery. Thus, the line for the combined group is better determined than that for the component groups. By contrast, $\hat{\beta}$ is more variable for the combined group 15 than for either of the component groups 16 and 17. This is consistent with our earlier discussion showing that groups 16 and 17 appear to be associated with distinct trend lines in Fig. 6B.

The estimates in Table 8 reinforce patterns evident in Table 7. In particular, $\tilde{\nu}$ is generally smaller for coho than for chinook. Thus, lower noise levels are associated with less dependency of $\hat{\beta}$ on λ. The low noise levels in groups 16 and 17 once more corroborate the linear trends discussed for these small data sets. Perhaps the quantity of greatest interest in Table 8 is $\tilde{\Omega}$, since this measures noise in relation to scatter of the data. Notice that low values of $\tilde{\Omega}$ are associated with the combined groups 7 and 14, as might be expected from the overall linearity of data portrayed in Fig. 6.

Another reason for considering $\tilde{\Omega}$ is the criterion (3.10) for the legitimacy of our confidence interval approximations. Recall that the critical value 0.3 in (3.10) applies primarily when $\lambda = 1$, since the approximations become exact as λ tends to 0 or ∞. Fortunately, when $\lambda = 1$, most estimates $\tilde{\Omega}$ fall below 0.3; the sole exception is group 15, which we have already identified as an anomalous case.

Tables 7 and 8 allow us to compare bias and variance as sources of measurement error. Curiously, $\hat{B}$ and $\tilde{\nu}$ are roughly equal in magnitude for most cases, particularly for the combined group 14 in which $\tilde{\nu}$ varies from 0.25 to 0.26 (depending on λ) and $\hat{B} = -0.25$. When interpreting this result, it is important to remember that B measures relative (as opposed to absolute) bias.

Our discussion so far has focused on the estimates in Tables 7 and 8. Figures 7–9 portray confidence regions similar to those illustrated earlier in Figs. 3–5 for Puntledge chinook (group 11). In the present context, for the sake of easy comparative analysis, we reduce the level of detail available for each group. For example, Figs. 7 and 8 show confidence intervals for all 17 groups simultaneously, but only when $p = 95\%$ and $\lambda = 0$ or ∞. These figures can be compared with Figs. 4–5, which involve multiple values of p and the entire λ-range. Similarly,

TABLE 8. Estimates $\tilde{\nu}$ and $\tilde{\Omega}$ for the 17 data groups described in Table 7.

			$\tilde{\nu}$			$\tilde{\Omega}$		
Group	Code	n	$\lambda = 0$	$\lambda = 1$	$\lambda = \infty$	$\lambda = 0$	$\lambda = 1$	$\lambda = \infty$
1	BQ-CO	14	0.228	0.227	0.221	0.235	0.234	0.227
2	CP-CO	14	0.119	0.121	0.122	0.115	0.116	0.117
3	CW-CO	5	0.136	0.134	0.132	0.068	0.067	0.066
4	PT-CO	9	0.106	0.107	0.108	0.034	0.034	0.035
5	QU-CO	11	0.101	0.101	0.098	0.230	0.230	0.224
6	RC-CO	11	0.119	0.124	0.128	0.103	0.106	0.110
7	*-CO	64	0.173	0.173	0.173	0.106	0.106	0.106
8	BQ-CH	14	0.416	0.456	0.484	0.268	0.295	0.315
9	CP-CH	14	0.137	0.141	0.145	0.098	0.100	0.103
10	CW-CH	4	0.127	0.141	0.155	0.193	0.214	0.238
11	PT-CH	12	0.196	0.231	0.280	0.244	0.292	0.360
12	QU-CH	8	0.216	0.230	0.239	0.233	0.249	0.259
13	*-CH	52	0.312	0.327	0.335	0.224	0.236	0.242
14	*-*	116	0.254	0.257	0.259	0.102	0.103	0.104
15	RC-CH	10	0.212	0.248	0.282	0.323	0.385	0.447
16	R1-CH	4	0.047	0.049	0.052	0.136	0.144	0.152
17	R2-CH	6	0.081	0.073	0.067	0.137	0.124	0.114

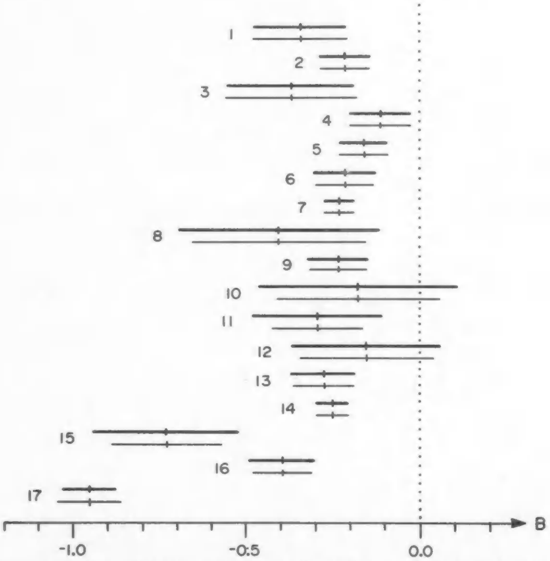

FIG. 7. 95% confidence intervals for B when $\lambda = 0$ (light line) and $\lambda = \infty$ (heavy line). Intervals are shown for each of the 17 groups cited in Table 7. A tick mark at the center of each interval indicates the estimate $\hat{B}$. The vertical dotted line at $B = 0$ accentuates the fact that most intervals are entirely negative.

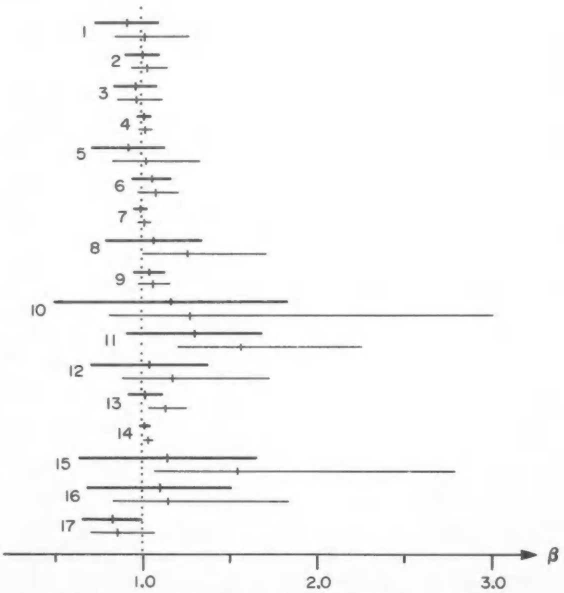

FIG. 8. 95% confidence intervals for β when $\lambda = 0$ (light line) and $\lambda = \infty$ (heavy line). Intervals are shown for each of the 17 cases cited in Table 7. A tick mark inside each interval indicates the estimate $\hat{\beta}$. The vertical dotted line shows that most intervals do not allow us to reject the hypothesis $\beta = 1$.

like Fig. 3, the panels of Fig. 9 represent 95% confidence regions for the coho (Fig. 9A) and chinook (Fig. 9B) data sets, but only when $\lambda = 1$.

Inspection of Figs. 7–9 reveals several key features of the 17 data sets cited in Table 7. In general, these figures add rigor to the discussion above because confidence intervals can be used to detect statistical differences. The next six paragraphs summarize some of the main points.

1) Irrespective of the value of λ, 95% confidence intervals for B (Fig. 7) allow us to reject the hypothesis $B = 0$ in all but two cases, groups 10 and 12. Even in these cases, most of the confidence interval lies below $B = 0$. Thus, Fig. 7 gives statistical validity to our claim that B is negative.

2) On the other hand, Fig. 8 shows that, in most cases we cannot reject the value $\beta = 1$. Therefore, we have no consistent evidence of a difference in measurement efficiency between the two measurement methods. This conclusion is, however, somewhat dependent on λ, as illustrated by groups 8, 11, 13, 14, 15, and 17.

3) The parameters B and β are better determined by some data sets than others. For example, Figs. 7 and 8 show that B

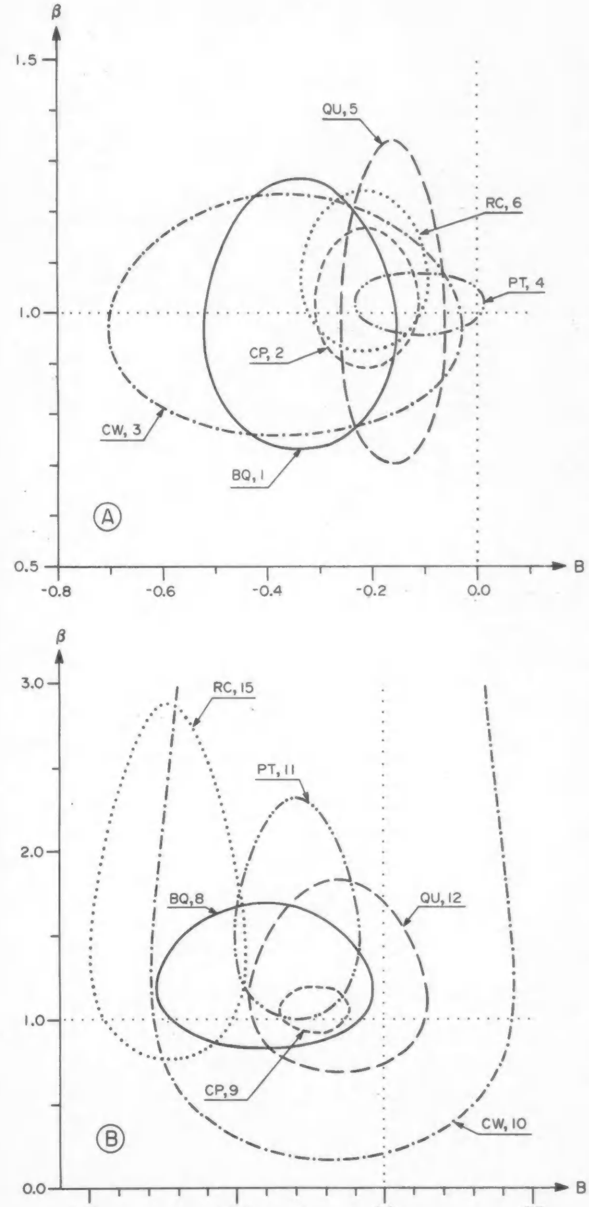

FIG. 9. (A) Boundaries of 95% confidence regions for (B,β), based on coho data from the six hatcheries listed in Table 6. In each case, it is assumed that $\lambda = 1$. Various curve types correspond to hatcheries as follows: Big Qualicum (——), Capilano (---), Chilliwack (-·-), Puntledge (-···-), Quinsam (— —), and Robertson Creek (···). Contours are labelled with the hatchery code and group number from Table 7. Light dotted lines indicate the special values $B = 0$ and $\beta = 1$. (B) Similar plots, based on chinook data from these hatcheries.

and β are best determined for the combined groups 7 and 14, as anticipated from the visual evidence of Fig. 6. By contrast, Figs. 7–9 all indicate that the parameters for group 10 are the least well defined. This is primarily due to the small sample size ($n = 4$) and moderate noise level ($\tilde{\nu} > 1.2$) shown in Table 8.

4) Both B and β are much better defined by groups 16 and 17 than by the combined group 15. In particular, Fig. 7 provides statistical evidence that groups 16 and 17 have different values of B. Once more, this confirms the visual observation that these groups correspond roughly to lines at different distances from the line $y = x$.

5) In general, Fig. 9 shows that B and β are better determined for coho than for chinook. Note the difference in scales of the axes in Figs. 9A and 9B.

6) Group 17 stands out as a distinct outlier in Fig. 7. To some extent, group 15 is also an outlier (as can also be seen in Fig. 9B); however, since group 15 is a combination of groups 16–17 and since group 16 is similar to the others, any abnormality of group 15 is due primarily to the influence of group 17.

In summary, we conclude that CWT estimates are lower than corresponding counting estimates for coho and chinook returns to hatcheries in British Columbia. We find no compelling evidence that this bias is greatly influenced by hatchery or species, with the exception of Robertson Creek chinook. For the remaining cases combined, the CWT estimates are approximately 22% lower than the counting estimates. Furthermore, this systematic component of error is roughly as large as the random component present in one or both of the methods of measurement.

Although our analysis does not identify mechanisms responsible for the observed bias, we can suggest several potential causes. These might include aspects of fish behaviour and biology, such as (1) a higher mortality or a greater propensity for straying among fish marked with CWTs, (2) shedding of CWTs by tagged fish, and (3) straying of wild fish into the hatchery. Additional causes may be related to operational difficulties in the hatchery, such as (4) underestimating total fish or overestimating tagged fish at the time of release or (5) failing to detect tags or overestimating total returns at the time of recovery. Specialized experiments to identify one or more of these causes might well be considered an essential component of salmon tagging programs in British Columbia.

Acknowledgements

We are indebted to staff members of the Canadian Department of Fisheries and Oceans, Pacific Region, for assembling the database on marked Pacific salmonids. The research here would have been impossible without their efforts, which are documented briefly by Kuhn et al. (1988, p. 52–53). We also received stimulation, encouragement, and advice from colleagues on the International Working Group on Mark Recovery Statistics, organized by the Pacific Salmon Commission. Finally, we are grateful to P. Macdonald, G. Evans, and an anonymous reviewer for suggestions leading to an improved presentation.

References

CREASY, M. A. 1956. Confidence limits for the gradient in the linear functional relationship. J. R. Statist. Soc. (Ser. B) 18: 65–70.

FULLER, W. A. 1987. Measurement error models. John Wiley and Sons, New York, NY. 440 p.

KENDALL, M., AND A. STUART. 1979. The advanced theory of statistics, Vol. 2: Inference and relationship 4th ed. MacMillan Publ. Co. Inc., New York, NY. 738 p.

KUHN, B. R. 1988. The MRP-Reporter program: a data extraction and reporting tool for the Mark Recovery Program database. Can. Tech. Rep. Fish. Aquat. Sci. 1625: 145 p.

KUHN, B. R., L. LAPI, AND J. M. HAMER. 1988. An introduction to the Canadian database on marked Pacific salmonids. Can. Tech. Rep. Fish. Aquat. Sci. 1649: 56 p.

SCHNUTE, J. 1984. Linear mixtures: a new approach to bivariate trend lines. J. Am. Statist. Soc. 79: 1–8.

1987. Data uncertainty, model ambiguity, and model identification. Nat. Res. Model. 2: 159–212.

Appendix A. Likelihood Estimates

This appendix derives the likelihood estimates [3.1]–[3.7] and the functions ℓ_h $(h = 1,2,3)$ in [4.1]–[4.3]. The main step in these proofs is to obtain [4.1] by minimizing ℓ in (2.2) with respect to X_i $(i=1,\ldots,n)$ and ν. Once this is complete, the remaining results can be obtained readily.

To begin, notice from (2.1)–(2.2) that

$$\text{(A.1)}\quad \ell = n\cdot\ln(2\nu^2) - n + \frac{1+\lambda}{2\nu^2}\cdot[S_1 + (1/\lambda)S_2]\ ,$$

where

$$\text{(A.2)}\quad S_1 = \sum_{i=1}^{n}(X_i - x_i)^2,$$

$$\text{(A.3)}\quad S_2 = \sum_{i=1}^{n}[\beta X_i - y_i + (1-\beta)\,\overline{X} + B]^2.$$

It follows from the definitions (A.2)–(A.3) that

$$\text{(A.4)}\quad \partial S_1/\partial X_j = 2(X_j - x_j),$$

$$\text{(A.5)}\quad \partial S_2/\partial X_j = 2\beta[\beta X_j - y_j + (1-\beta)\overline{X} + B] + 2(1-\beta)[\overline{X} - \bar{y} + B],$$

where (A.5) uses the fact that $\partial\overline{X}/\partial X_j = 1/n$.

To minimize ℓ with respect to X_j, we use the equation

$$\text{(A.6a)}\quad \partial\,\ell/\partial X_j = 0,$$

which, by (A.1), (A.4), and (A.5), is equivalent to

$$\text{(A.6b)}\quad \lambda(X_j - x_j) + (B + \overline{X} - \bar{y}) + \beta[\beta(X_j - \overline{X}) - (y_j - \bar{y})] = 0.$$

Furthermore, if (A.6b) is true for $j = 1, \ldots, n$, then averaging over j shows that

$$\lambda(\overline{X} - \bar{x}) + (B + \overline{X} - \bar{y}) = 0,$$

which is equivalent to

$$\text{(A.7)}\quad \overline{X} = \bar{x} + (\bar{y} - \bar{x} - B)/(1+\lambda) = 0.$$

One can use (A.7) to eliminate $\overline{X}$ from (A.6b). Solving the resulting equation for X_j gives (after some algebra)

$$\text{(A.8)}\quad X_i' = x_i + \frac{\bar{y} - \bar{x} - B}{1+\lambda} + \frac{\beta}{\beta^2+\lambda}\cdot[(y_i - \bar{y}) - \beta\,(x_i - \bar{x})].$$

where we replace the index j by i. In (A.8) and the remainder of this appendix, we use the apostrophe to denote maximum likelihood estimates for specified (B,β). Indeed, it is evident in (A.8) that X_i' depends only on the data and the parameters (B, β).

It is similarly possible to obtain the estimate Y_i'. Substituting (A.7)–(A.8) into (1.7) gives (again, after some algebra)

$$\text{(A.9)}\quad Y_i' = y_i - \frac{\lambda(\bar{y} - \bar{x} - B)}{1+\lambda} - \frac{\lambda}{\beta^2+\lambda}\cdot[(y_i - \bar{y}) - \beta(x_i - \bar{x})].$$

Another way to obtain (A.9) from (A.8) is by symmetry, since the EVB model is invariant under the transformations $x \longleftrightarrow y$, $B \longleftrightarrow -B$, $\beta \longleftrightarrow 1/\beta$, and $\lambda \longleftrightarrow 1/\lambda$.

The next step involves computing S_1' and S_2' from (A.2)–(A.3). Notice first that

$$\text{(A.10)}\quad S_2 = \sum_{i=1}^{n}(Y_i - y_i)^2$$

from (1.7) and (A.3). Also, it can readily be verified that

$$\text{(A.11a)}\quad \sum_{i=1}^{n}[(y_i - \bar{y}) - \beta(x_i - \bar{x})] = 0,$$

$$\text{(A.11b)}\quad \sum_{i=1}^{n}[(y_i - \bar{y}) - \beta(x_i - \bar{x})]^2 = n(m_{02} - 2\beta m_{11} + \beta^2 m_{20}).$$

Substituting (A.8) into (A.2) and taking account of (A.11) gives

$$\text{(A.12a)}\quad S_1' = n\left(\frac{1}{1+\lambda}\right)^2(\bar{y} - \bar{x} - B)^2 + n\left(\frac{\beta}{\beta^2+\lambda}\right)^2(m_{02} - 2\beta m_{11} + \beta^2 m_{20}).$$

Similarly, (A.9)–(A.11) show that

$$\text{(A.12b)}\quad S_2' = n\left(\frac{\lambda}{1+\lambda}\right)^2(\bar{y} - \bar{x} - B)^2 + n\left(\frac{\lambda}{\beta^2+\lambda}\right)^2(m_{02} - 2\beta m_{11} + \beta^2 m_{20}).$$

Furthermore, if we define

$$\text{(A.13)}\quad S = S_1 + (1/\lambda)S_2,$$

then it follows from (A.12) that

$$\text{(A.14)}\quad S' = \frac{n}{1+\lambda}\cdot(\bar{y} - \bar{x} - B)^2 + \frac{n}{\beta^2+\lambda}\cdot(m_{02} - 2\beta m_{11} + \beta^2 m_{20}).$$

To obtain the estimate ν', we use the equation

$$\text{(A.15a)}\quad \partial\ell/\partial\nu = 0,$$

which, from (A.1) and (A.13), is equivalent to

$$\text{(A.15b)}\quad (2n/\nu) - [(1+\lambda)/\nu^3]S = 0.$$

Solving (A.15b) for ν gives

$$\text{(A.16)}\quad \nu'^2 = [(1+\lambda)/(2n)]S',$$

since S' is the estimate of S for specified (B, β). Thus, from (A.1), (A.13), and (A.16)

$$\ell' = n\cdot\ln[(1+\lambda)\,(S'/n)],$$

that is, from (A.14)

$$\text{(A.17)}\quad \ell' = \mathrm{n}\cdot\ln\left[(\bar{y} - \bar{x} - B)^2 + \frac{1+\lambda}{\beta^2+\lambda}\cdot(m_{02} - 2\beta m_{11} + \beta^2 m_{20})\right].$$

Note that, by (A.6a) and (A.15a), ℓ' here is the same as $\ell_1(B,$

β) in (2.4). Thus, (A.17) proves [4.1], the first main result of this appendix.

To minimize $\ell_1(B, \beta)$, we use the equations $\partial\ell/\partial B = 0$ and $\partial\ell/\partial\beta = 0$, which are equivalent to

(A.18) $\bar{y} - \bar{x} - B = 0,$

(A.19) $m_{11}\beta^2 + (\lambda m_{20} - m_{02})\beta - \lambda m_{11} = 0,$

respectively. The estimate $\hat{B}$ in [3.1] is immediate from (A.18), and $\hat{\beta}$ in [3.2] results from solving the quadratic equation (A.19). A short proof (not given here) shows that the "+" sign in front of the radical in [3.2] corresponds to the minimum of ℓ_1, while a "$-$" sign corresponds to the maximum.

Substituting ($\hat{B}$, $\hat{\beta}$) into (A.8)–(A.9) gives the estimates [3.3]–[3.4] for $\hat{X}_i$ and $\hat{Y}_i$. Similarly, combining [3.1], [3.2], (A.14), and (A.16) gives the estimate [3.5] for ν^2. Furthermore, summing both sides of [3.3] and taking account of (A.11a) gives

(A.20) $\hat{\bar{X}} = \bar{x}.$

Thus, from [3.3] and (A.20),

(A.21) $\hat{X}_i - \hat{\bar{X}} = \dfrac{1}{\hat{\beta}^2 + \lambda} \cdot [\lambda(x_i - \bar{x}) + \hat{\beta}\,(y_i - \bar{y})]^2.$

Summing the squares of both sides of (A.21) gives

(A.22) $\hat{V}_X = (\hat{\beta}^2 + \lambda)^{-2}\,(\lambda^2 m_{20} + 2\lambda\hat{\beta} m_{11} + \hat{\beta}^2 m_{02})$

from the definition [1.6] of V_X. Combining [2.8] and (A.22) proves [3.6]. Finally, [3.7] is simply a consequence of the definition [1.10] of Ω.

Having obtained the estimates [3.1]–[3.7] in Table 3 and expression [4.1] for ℓ_1 in Table 4, it remains only to derive [4.2]–[4.3] for ℓ_2 and ℓ_3. These follow immediately from [4.1], since definitions (2.5)–(2.6) imply that $\ell_2(B) = \ell_1\,(B, \hat{\beta})$ and $\ell_3(\beta) = \ell_1\,(\hat{B}, \beta)$.

Appendix B. Consistency

This appendix proves the consistency of ($\hat{B}$, $\hat{\beta}$) and shows that the corrected estimates [3.8]–[3.10] are consistent. To begin, notice from (1.5) and [2.4] that

$$m_{20} = \frac{1}{n}\sum_{i=1}^{n} [X_i + \sigma\delta_i - \bar{X} - \sigma\bar{\delta}]^2$$

$$= V_X + \frac{2\sigma}{n}\sum_{i=1}^{n} (X_i - \bar{X})\delta_i + \frac{\sigma^2}{n}\sum_{i=1}^{n} (\delta_i - \bar{\delta})^2;$$

consequently,

(B.1) $E(m_{20}) = V_X + [(n-1)/n]\sigma^2.$

Similarly, one can show that

(B.2) $E(m_{11}) = \beta V_X,$

(B.3) $E(m_{02}) = \beta^2 V_X + [(n-1)/n]\lambda\sigma^2.$

Assume that, as $n \to \infty$, the mean $\bar{X}$ and variance V_X have a finite limit. Then the moments m_{ij} converge in probability to their expected values as $n \to \infty$. If we denote the limit of m_{ij} by M_{ij}, then it follows from (B.1)–(B.3) that

(B.4) $M_{20} = V_X + \sigma^2,$

(B.5) $M_{11} = \beta V_X,$

(B.6) $M_{02} = \beta^2 V_X + \lambda\sigma^2.$

Formally substituting M_{ij} for m_{ij} in [3.2] gives $\hat{\beta} = \beta$, thus proving that $\hat{\beta}$ is consistent. Similarly, one can show that $\tilde{\nu}$, $\tilde{V}$, and $\tilde{\Omega}$ in [3.8]–[3.10] are consistent. Finally, $\hat{B}$ is consistent since $E(\bar{x}) = E(\bar{X} + \sigma\bar{\delta}) = \bar{X}$, $E(\bar{y}) = \bar{Y}$, and $E(\hat{B}) = \bar{Y} - \bar{X} = B$.

Appendix C. Confidence Regions

This appendix proves the formulas for confidence regions in Table 5. A key step in these proofs is the fact that

(C.1) $\ell_1(\hat{B}, \hat{\beta}) = n\cdot\ln(\tilde{\nu}^2),$

as can be seen from [3.1], [3.5], [3.8], and [4.1]. Notice also that $\ell_2(\hat{B}) = \ell_1(\hat{B}, \hat{\beta})$ and $\ell_3(\hat{\beta}) = \ell_1(\hat{B}, \hat{\beta})$.

To obtain [5.1], apply (3.7) to $\ell_1(B,\beta)$; this gives

(C.2) $\ell_1\,(B, \beta)$

$$= \ell_1\,(\hat{B}, \hat{\beta}) + n\cdot\ln\left[\,1 + \frac{2}{n-2}\cdot F_p\,(2, n-2)\right].$$

Taking account of the expression [4.1] for $\ell_1(B,\beta)$ and (C.1) for $\ell_1(\hat{B},\hat{\beta})$, one can use straightforward algebra to solve for B in (C.2). The result is [5.1]. In similar fashion, [5.2] and [5.3] can be obtained from

(C.3) $\ell_2\,(B) = \ell_2\,(\hat{B}) + n\cdot\ln\left[\,1 + \dfrac{1}{n-1}\cdot F_p\,(1, n-1)\right],$

(C.4) $\ell_3\,(\beta) = \ell_3\,(\hat{\beta}) + n\cdot\ln\left[\,1 + \dfrac{1}{n-1}\cdot F_p\,(1, n-1)\right],$

respectively. Note in particular that (C.4) leads to a quadratic equation in β with coefficients [5.3b]–[5.3d].

Phosphorus and Nitrogen Limitation of Phytoplankton Growth in the Freshwaters of North America: A Review and Critique of Experimental Enrichments

James J. Elser, Erich R. Marzolf, and Charles R. Goldman

Division of Environmental Studies, University of California–Davis, Davis, CA 95616 USA

Elser, J. J., E. R. Marzolf, and C. R. Goldman. 1990. Phosphorus and nitrogen limitation of phytoplankton growth in the freshwaters of North America: a review and critique of experimental enrichments. Can. J. Fish. Aquat. Sci. 47: 1468–1477.

While phosphorus is generally considered to be the primary nutrient limiting algal growth in lakes, limitation of algal growth by nitrogen has been observed in freshwater. It is also commonly observed that the most pronounced phytoplankton responses to enrichment occur when both N and P are added together. This led us to re-evaluate nitrogen's status as a secondary nutrient in freshwater through a systematic literature search. In our survey of enrichment bioassays, we found considerable deficiencies in the degree to which investigators have applied sufficient replication, performed and reported statistical tests, and assessed seasonal and spatial differences in algal nutrient limitation. Given these limitations, however, we found that combined N + P enrichment enhanced algal growth much more frequently and more substantially than did addition of N or P singly. On average, the frequency and degree of algal response did not differ for P vs. N enrichment. From our review of whole-lake fertilizations, we concluded that the roles of N and P in constraining algal growth at the whole-lake scale have not been completely separated. However, examination of the distribution between treatments (+ N, + P, + N, and P) of lake-years in which substantial algal growth response occurred indicated that combined N and P enrichment was required to consistently produce substantial algal growth response. A more important role than has previously been recognized for N as a limiting nutrient in freshwaters is indicated. We suggest that greater attention should be given to both P and N in the future.

Bien que le phosphore soit considéré en général comme le principal élément nutritif limitant la croissance des algues dans les lacs, on a remarqué que l'azote limitait la croissance des algues dans les eaux douces. On a observé généralement aussi que les réactions les plus marquées du phytoplancton à l'enrichissement se produisent lorsque l'azote (N) et le phosphore (P) sont ajoutés ensemble. Suite à ces observations, nous avons réévalué l'état de l'azote comme élément nutritif secondaire en eau douce par le biais d'une recherche systématique dans la littérature. Dans le cadre de nos études sur les essais biologiques d'enrichissement, nous avons relevé des lacunes importantes au niveau du nombre de répétitions des essais effectuées par les chercheurs, des épreuves statistiques effectuées et de la déclaration des résultats, et de l'évaluation des écarts saisonniers et spatiaux au niveau de la limitation des éléments nutritifs des algues. Compte tenu de ces limites, toutefois, nous avons observé qu'un enrichissement combiné en N et P augmentait la croissance des algues beaucoup plus souvent et beaucoup plus substantiellement que l'addition de N ou de P seul. En moyenne, la fréquence et le degré de réaction des algues ne différaient pas pour l'enrichissement en P par rapport à l'enrichissement en N. D'après nos études sur la fertilisation d'un lac dans son ensemble, nous avons conclu que les rôles de N et du P en limitant la croissance des algues à l'échelle de tout un lac n'ont pas été complètement séparés. Toutefois, l'étude de la répartition entre les traitements (+ N, + P, + N et P) du lac pendant les années au cours desquelles il y a eu une importante croissance des algues a montré qu'un enrichissement combiné à l'azote et au phosphore était nécessaire pour produire régulièrement une croissance importante des algues. L'azote en tant qu'élément nutritif limitant en eau douce mérite un rôle plus important que celui qui était prévu. Une plus grande attention devrait être accordée au phosphore et à l'azote dans l'avenir.

Received September 5, 1989
Accepted February 8, 1990
(JA297)

Reçu le 5 septembre 1989
Accepté le 8 février 1990

Study of the dynamics and effects of chemical nutrients in lakes has been one of the central themes of modern limnology (Goldman and Horne 1983; Wetzel 1983; Schindler 1988). Insights from these studies have produced some of the field's greatest practical successes — the recovery and prevention of culturally eutrophied lakes. The discovery of relatively strong empirical relationships between P loading rates and lake trophic status (Vollenweider 1976), along with experimental confirmation of P's primary role in promoting algal growth in a series of whole-lake nutrient addition studies in some Canadian lakes (Schindler 1975, 1977), firmly established P as the central focus of biogeochemical and ecological studies in freshwater (Hecky and Kilham 1988). Concurrently, in the marine sciences, the emphasis on N as a limiting nutrient was increasing, resulting in a conventional view which assumes that freshwater systems are primarily limited by P while marine systems are N-limited.

While it is clear that P is of great importance as a limiting nutrient in freshwater ecosystems, many studies indicate that N can be both a primary limiting nutrient as well as a secondary nutrient which can enhance the effect of added P. In some lakes only addition of N can produce enhanced algal growth rates, as in Lake Tahoe (Goldman 1981). Short-term enrichment experiments commonly demonstrate that much greater algal growth is achieved when both N and P are added together than when either is added alone (e.g. Elser and Kimmel 1985; others). In other systems, unexpected changes in the nature of nutrient limitation can be produced by changes in the organisms responsible for nutrient recycling, indicating close proximity of P- and N-limitation in these lakes (Elser et al. 1988). Finally, on the larger scale, ecological and geochemical constraints on N_2-fixation many prevent some lakes from drawing on the vast atmospheric N_2 reserve (as occurred in the whole-lake experiments of Schindler) and thus N-limitation on the ecosystem scale may result (Howarth and Cole 1985; Wurtsbaugh 1988).

The possibility that N-limitation of algal growth in freshwater systems (at least over shorter ecological, rather than biogeochemical, time scales) may be more prevalent than is generally believed motivated us to seek a way to evaluate the relative importance of N vs. P in constraining algal growth in a wide variety of lakes. The degree to which limited nutrient availability reduces or potentially reduces algal growth rates below their maximum may be assessed in a number of ways, each of which provides insights into processes operating at certain time scales and which suffers from some limitations. We have classified approaches into three categories: physiological studies, experimental studies, and ecosystem studies.

In physiological studies, metabolic symptoms of nutrient deficiency are assayed. These symptoms may be generalized responses to nutrient limitation, as in protein:carbohydrate ratios (Healey 1979) or specific signs of limitation by a given nutrient (such as alkaline phosphatase activity as an indicator of P-limitation, Pettersson 1980). These techniques are quite sensitive but may suffer from limitations resulting from short-term transient responses not indicative of the overall growth status of the community (Healey 1979). In addition, results of physiological studies obtained with different methods by different investigators may not be comparable and a limited set of widely accepted indicators has not yet come into use for a wide variety of lakes, making the multi-lake comparisons that we desired problematic.

Experimental studies are generally of two kinds: those that use single-species algal cultures in filtered lake water (the "Algal assay procedure: bottle test"; EPA 1971) and those that use the natural phytoplankton assemblage present when the lake is sampled (Goldman 1978). While maximizing replicability and experimental control, the use of cultured algal species (often the usually exotic species *Selenastrum capricornatum*) provides little insight into how complex natural assemblages adapted to the nutrient supply conditions of their native habitat would respond to changes in N or P availability. In recent years, nutrient enrichment experiments which employ intact phytoplankton communities have come into wide use (Goldman 1978). In such experiments, samples of lake water containing phytoplankton are subdivided into experimental treatments which receive varying amounts of chemical nutrients (or are unenriched) and incubated for a period of time. Community response variables such as chlorophyll concentration or primary productivity (measured with the ^{14}C method) are commonly monitored, although in vivo chlorophyll fluorescence, algal cell counts, or particulate matter measurements are sometimes used. Enrichment bioassays can provide somewhat misleading indications of the extent of in situ growth limitation by isolating the algal assemblage from external sources of nutrients and by altering the physical, chemical and biological environment during incubation (Elser and Kimmel 1986). However, such experiments appear capable of assessing imbalances in the relative availability of major limiting nutrients. In studies in which both bioassay and physiological data are available, similar conclusions about the nature of nutrient limitation in the lake have been drawn from both approaches (Elser et al. 1988), although short-term assessments (time-scale of hours) of response to nutrient amendments can yield misleading results (Lean and Pick 1981). We chose to focus on algal responses in longer-term experiments in this study because of the wide use of such enrichment bioassays (time-scale of days) and the possibility of objectively comparing responses between lakes.

Ecosystem studies, in which nutrient additions are made to real lakes, have also produced convincing evidence for the importance of P as a primary limiting nutrient in lake ecosystems (Schindler 1988). Whole-lake studies maximize realism by incorporating all of the complex causal pathways operating in whole ecosystems and are of sufficient duration to permit longer-term ecosystem responses to occur, e.g., invasion of CO_2 across the lake–air interface or proliferation of N_2-fixing organisms. However, whole-lake experiments are difficult to interpret (Hurlbert 1984) and logistic constraints have prevented widespread application of this approach. We have chosen, therefore, to make a simple qualitative survey of whole-lake enrichments involving nitrogen and phosphorus.

This paper reports the results of surveys of the aquatic biology literature designed to distinguish the role of N and P in constraining algal growth in lakes and to evaluate the degree of their interaction. Our main focus is on short-term (<1 m) nutrient enrichment bioassays employing natural phytoplankton assemblages because these experiments have been most widely applied and are amenable to quantitative comparisons between different systems and methods. We also summarize the protocols and outcomes of whole-lake nutrient addition experiments to assess whether such experiments have adequately separated the roles of N and P in limiting algal growth in whole ecosystems. We restricted our search to studies of North American lakes for three reasons. First, the paradigm of P as the dominant limiting factor in freshwater was developed largely by North American limnologists studying lakes at temperate latitudes, making a review of North American studies most relevant for purposes of confirming or contradicting this paradigm. Considering that N is thought to be of greater importance in limiting phytoplankton growth in tropical systems (e.g. Melack et al. 1982; Vincent et al. 1984; others), this restriction then is a conservative one with respect to the role of P as a limiting factor in the lakes of the world. Second, we felt that methods would be less heterogeneous among studies if we constrained our review to a single geographic area. Finally, by limiting our systematic review to North American lakes we made the laborious task of locating and summarizing relevant studies more manageable.

Methods

Survey of Enrichment Bioassays

A systematic search of papers published in major limnological and ecological journals between 1968 and 1988 was conducted; the journals searched are listed in Table 1. Additional studies were found by examining the reference

TABLE 1. Limnological journals systematically searched for studies of nutrient limitation using nutrient enrichment bioassays.

Journal	Volumes searched	Years
Archiv fur Hydrobiologie	68–113	1970–88
Archiv fur Hydrobiologie (supplement)	42–72	1972–86
Canadian Journal of Fisheries and Aquatic Sciences	30–41	1973–84
Freshwater Biology	9–15	1979–85
Hydrobiologia	35–168	1970–88
Journal of Great Lakes Research	1–13	1975–87
Journal of Plankton Research	1–10	1979–88
Limnology and Oceanography	15–33	1970–88
Oikos	25–46	1974–86
Verh. Int. Ver. Limnol.	17–24	1968–88

sections of papers located during the systematic literature search. Criteria for selection of a study were as follows:

1) The lake or reservoir was located in North America.

2) The study involved nutrient enrichment experiments with intact native phytoplankton communities.

3) The experimental design assessed single-nutrient effects (N vs. P), single vs. combined enrichment effects (N or P vs. N+P), or, the best case, all single and combined effects (a factorial design: N vs. P, N vs. N+P, P vs. N+P).

4) Enough data were presented that the frequency and/or magnitude of enrichment responses could be obtained, either directly from explicitly presented data or from examination of figures.

Morphometric and water quality parameters, experimental program and protocol, and degree of response to nutrient enrichment were examined in each study meeting the criteria (Table 2). Lake area, maximum depth, and mean depth of each lake were recorded when presented or obtained from other sources where possible. Lake trophic state was estimated either by the average chlorophyll concentration in the lake when the enrichment study was conducted or by the average initial chlorophyll concentration of the experimental treatments themselves.

Several aspects of the sampling program and experimental protocol were recorded and considered. The duration of the study (number of weeks between the first experiment reported and the last), the number of dates on which enrichment experiments were performed, and the total number of experiments conducted (this differs from the previous number for studies in which more than one sampling station was monitored) were noted. Aspects of experimental protocol

TABLE 2. Parameters recorded for each lake and study included in the literature survey of nutrient enrichment bioassays.

Variable	Units	Explanation
Area	km^2	area of lake
Z_{max}	m	maximum depth
Z_{mn}	m	mean depth
Chorophyll concentration	µg/L	avg. chlorophyll concentration of ambient or initial water samples during study period
Duration of study	wk	time between first and last experiments
Number of sampling dates	#	number of dates when samples were taken for enrichment experiments
Number of experiments	#	total number of experiments run (differs from number of dates only when more than 1 sampling station within a lake was sampled
Volume of experimental container	L	–
Number of replicates per treatment	#	–
Experimental design	—	full factorial design; +P and +N+P treatments; +N treatments only
P-added	µg/L	P enrichment over ambient levels
N-added	µg/L	N enrichment over ambient levels
Form of N added	—	NO_3 only; NH_4 only; NO_3 and NH_4 together
Statistical tests	—	were responses tested for statistical significance?
Response variable	—	chlorophyll; carbon fixation; cell volume; fluorescence
Response time	d	time after start of experiment when relative response was reported or interpolated
P-fraction	—	fraction of experiments in a lake in which addition of P alone produced "significant" increase in algal growth (see text for discussion of "significant" responses)
N-fraction	—	fraction of experiments in which addition of N alone produced "significant" increase in algal growth
NP-fraction	—	fraction of experiments in which addition of N+P together produced "significant" increase in algal growth
P-response (sig.)	ratio	mean relative growth response to P-enrichment for experiments in which response was significant (i.e. ratio of response variable in P-treatment to control treatment)
N-response (sig.)	ratio	mean relative growth response to N-enrichment for experiments in which response was significant
NP-response (sig.)	ratio	mean relative growth response to N+P-enrichment for experiments in which response was significant
P-response (all)	ratio	mean relative growth response to P-enrichment, all experiments
N-response (all)	ratio	mean relative growth response to N-enrichment, all experiments
NP-response (all)	ratio	mean relative growth response to N+P-enrichment, all experiments
Synergism fraction	—	fraction of experiments in which significantly greater growth occurred when N and P were added simultaneously than in single nutrient enrichments
Synergism response	ratio	mean relative degree of synergistic response (ratio of response variable in N+P treatment to its value in the larger of the P or N treatments)

recorded were the duration of the experiments (mean duration was recorded for studies in which the duration varied considerably between experiments), the volume of the experimental container, the number of replicates used for treatments, the response variable monitored (usually chorophyll concentration or total C-fixation rates, but also in vivo chlorophyll fluorescence and cell counts), the molar concentrations of added N and/or P, the form in which N was added (i.e. NH_4 vs. NO_3), the experimental design, and whether the authors applied inferential statistics to evaluate enrichment responses.

The relative response of phytoplankton communities to enrichment by N and/or P was assessed in a number of ways. First we quantitatively examined the responses of phytoplankton in each experiment presented. By calculating the percentage of experiments responding to a given treatment as well as the ratio of treatment values to control values, we placed community responses to N or P on relative scales, facilitating comparison of studies performed in different lakes using different methods and different response variables. Because the degree of response to a treatment is likely to be a function of the amount of time that the sample is allowed to respond to that treatment, we attempted to assess responses that occurred after a period of 4–7 d, the most common experimental duration, and interpolated where necessary for experiments which proceeded for longer periods. The time period at which response estimates were made was recorded.

We calculated the degree of response to a given treatment (+N, +P, and/or +N+P) for each experiment in each study as the ratio of the mean response value in a treatment to its mean value in the unenriched control. Then we recorded the fraction of all experiments in a lake in which the phytoplankton responded significantly to enrichment by N, by P, and/or by N+P. We considered a response significant if the relative response to a treatment was greater than 1.25 in studies in which no inferential statistics were applied. Next, we calculated the mean relative responses to N, to P, and/or to N+P (as calculated above) for each lake, both for all experiments conducted and for all experiments for which a "significant" response was observed. Finally, for each experiment in each lake, we calculated the ratio of the response to N+P enrichment to the response to single nutrient enrichment (N or P, whichever was greatest) in order to assess the frequency and degree to which N and P enrichment behaved synergistically when performed in combination in these lakes. We estimated the degree of synergism as the mean of this ratio when all experiments in a lake were pooled. We also recorded the fraction of experiments in a lake in which combined N+P enrichment produced a greater response (1.25× when inferential statistics were not applied) than enrichment with either nutrient added singly.

Survey of Whole-Lake Experiments

The literature search for whole lake fertilizations was accomplished by an expanding search of references for whole-lake fertilization experiments, beginning with references from the ELA and British Columbia lake enrichment programs. References were gathered from both journals and government documents.

Data were tabulated as a response for each fertilized year; thus, data units are lake-years. Studies were excluded from consideration for a variety of reasons (such as studies that used organic forms of fertilizer, that involved fish ponds, that fertilized under ice or to the hypolimnion, or that presented insufficient chlorophyll data). A response was arbitrarily designated as "significant" if a doubling in annual or seasonal chlorophyll concentration occurred, compared to unfertilized conditions (either a similar "control" lake or data from unfertilized years). Bare Lake response was analyzed on the basis of cell counts and total cell volume, because chlorophyll data were not published (Nelson and Edmondson 1955). No attempt was made to assess the degree of response on the basis of the magnitude of change in chlorophyll. Each lake-year was categorized as either receiving inorganic nitrogen (N), phosphorus (P), or both (N+P). The molar N:P ratio was noted for each fertilization. The proportion of added fertilizer to natural loading ranged from less than one to several times natural loading. Kennedy Lake results were reported for two separate arms which received different treatments (Stockner and Shortreed 1988). Lakes varied in the number of fertilized years, from a minimum of two to a maximum of 10. For Lakes 227 and 226 (Experimental Lakes Area), responses were assumed to remain significant during 1977 and 1978, although no data for those years were reported. However, Schindler (1980) presented the average chlorophyll concentration for all but the first year of fertilization for those lakes. Based on this long-term average and the previous years' response, we judged that the lake responded significantly in the last 2 y.

Results and Discussion

Survey of Enrichment Bioassays

A total of 62 lakes from 34 published studies met our criteria.

Characteristics of the study lakes

Because four of the Laurentian Great Lakes were included, surveyed lakes covered an enormous morphometric range. Mean lake area was 3004 km^2, reflecting the contribution of lakes Erie, Huron, Michigan, and Ontario. When the Great Lakes were excluded mean lake area was 137 km^2. Average values of maximum depth and mean depth for the data were 59.7 and 25.7 m, respectively (or 46.4 and 22 m when these Great Lakes were excluded). Lake trophic state, as indicated by average chlorophyll concentrations, also covered a wide range, with chlorophyll values of 0.54 μg/L in Lake St. Clair to 35.9 μg/L in eutrophic Clear Lake (mean: 7.26 μg/L).

Sampling intensities and experimental protocol

A considerable proportion of the lakes was sampled on a single date (48%). As a result, the mean number of dates on which samples were taken was 3.7, but when single-experiment studies were excluded, the mean number of sampling dates increased to 6.0. Only 32% of the lakes were sampled on more than four dates, indicating that the seasonality of nutrient availability in many of these lakes has not been thoroughly characterized. Study duration varied from 1 wk (for studies with just one experiment) to 114 wk (means: 13.3 wk). When single-experiment studies were excluded, this average increased to 24.1 wk. Clearly a large number of nutrient limitation studies fail to attempt to characterize seasonal variation in limitation by N and/or P, although such variation can be substantial and of considerable ecological importance (e.g. Lehman and Sandgren 1978; Elser et al. 1988).

Even fewer studies characterized spatial variation in nutrient limitation within lakes: only 10 of the 62 lakes were sampled

TABLE 3. Summarized algal responses to nitrogen and phosphorus in nutrient enrichment bioassay
2 and in the text. A total of 60 lakes is included.

Lake	P-fraction	N-fraction	NP-fraction	P-response (sign.)	N-response (sign.)	NP-response (sign.)
Big Soda	0	0	1	—	—	1.45
Washington	1	1	1	2	2.3	5.8
Melton Hill	0.6	0	0.7	2.42	—	3.1
Norris	0.7	0	0.8	1.87	—	2.42
Watts Bar	0.9	0	0.9	1.61	—	1.83
Peter	0.11	0	1	1.7	—	5.8
Paul	0.11	0.11	1	1.3	1.7	4.8
Tuesday	0.11	0.67	1	1.7	2	4.6
Sammamish	0	0	1	—	—	1.97
Mirror	0	0	1	—	—	2.2
Jackson	1	0.5	1	3.03	4.95	10.01
Erie	0.71	0.28	1	2.42	1.29	2.84
O'Woods	1	—	1	1.4	—	6.6
Crystal	1	0	1	2.26	—	2.26
Crater	0	0.33	0.33	—	2	2.05
Tahoe	0	0.25	0.25	—	1.5	1.8
Egg	0.25	0.75	1	2.09	1.73	2.49
Huron	0.78	0.33	1	3	1.57	15.1
Placid	0	—	1	—	—	3.32
Francis	1	—	1	4.5	—	6
Annie	0	—	1	—	—	15
Brainard	0.6	0	0.6	—	—	—
Shadow Mountain	0	0.43	0.57	—	—	—
Grand	0	0.25	0.38	—	—	—
Monarch	0.33	0.33	0.33	—	—	—
Estes	0.167	0.17	0.33	—	—	—
Green Mountain	0.143	0	0.28	—	—	—
Dillon	0.143	0	0.43	—	—	—
Granby	0	0.38	0.5	—	—	—
Lobstick	1	1	1	5.15	1.62	3.6
Risher	0	0	1	—	—	1.4
Shagawa	1	1	1	7	3.9	19.9
Long	0	1	1	—	6	10.75
Amisk	1	0	1	5	—	7.33
Island	0	0	1	—	—	7.5
Narrow	1	0	1	7.94	—	8.23
Mohave	0.5	0	1	1.95	—	1.95
L302	1	1	1	1.26	1.26	1.86
L81	1	0	1	1.29	—	2.06
L132	1	1	1	1.7	1.3	2.1
L239	0	0	0	—	—	—
L161	1	1	1	1.48	1.3	1.4
Michigan	1	0	1	2.75	—	2.32
L227	1	—	1	2.28	—	2.28
Meretta	1	1	1	2.67	1.44	1.89
Ontario	0	1	1	—	1.8	6.8
Skaha	0.5	0.5	0.5	7.25	15	10.2
Kalamalka	0.5	0.5	1	1.25	1.28	6.07
Osoyoos	1	1	1	3.17	2.05	4.41
Wood	0.5	1	1	1.56	2.36	1.62
Okanagan	0.33	0.17	1	2.09	2	3.42
Vaseaux	1	1	1	2.1	3.7	3
Chautauqua	0.4	0.3	0.87	2.09	1.56	2.9
Kennedy	0.33	0.67	1	1.5	2.84	10.6
China	0.31	0.38	0.86	1.79	1.78	2.55
St. Clair	0.22	0	—	1.59	—	—
Toolik	0.083	0.83	0.91	1.27	1.46	1.75
Cheat	1	0	1	2.31	—	3.49
East Canyon	0	0.5	1	—	2.15	4.05
Great Salt	0.25	1	1	1.3	1.71	3.55
Bear	0.17	0.83	1	1.25	2.8	9.84
Clear	0.2	0.5	—	2	2.23	—

bioassays for lakes obtained in the literature survey. Explanation for the variables is given in Table

sponse n.)	P-response (all)	N-response (all)	NP-response (all)	Synergism fraction	Synergism response	Citation
45	1.2	1.4	1.45	0	—	Axler et al. (1978)
8	2	2.3	5.8	1	2.52	Edmondson (1972)
1	1.85	1	2.47	0.5	1.65	Elser and Kimmel (1985)
42	1.61	1	2.14	0.4	1.48	Elser and Kimmel (1985)
83	1.55	1	1.75	0.2	1.46	Elser and Kimmel (1985)
8	1.25	1.19	5.8	1	4	Elser et al. (1988)
8	0.87	1.22	4.8	1	3.9	Elser et al. (1988)
6	1.07	1.7	4.6	1	2.5	Elser et al. (1988)
97	1.14	1.29	1.97	1	1.53	Emery et al. (1973)
2	1.09	1.09	2.2	1	2	Gerhart (1975)
01	3.03	2.77	5.95	0.5	2.1	Glooschenko and Alvis (1973)
84	2	1.14	2.84	0.71	1.57	Hartig and Wallen (1984)
6	1.4	—	6.6	1	4.7	Havens and DeCosta (1984)
26	2.26	1	2.26	0	—	Jordan and Bender (1973)
05	1.07	1.5	1.8	0.33	1.5	Lane and Goldman (1984)
8	1.03	1.21	1.34	0	—	Lane and Goldman (1984)
49	1.36	1.68	2.49	1	1.41	Lehman (1979)
1	1.25	2.6	15.1	0.89	5.8	Lin and Schelske (1981)
32	1	—	3.32	1	3.32	McDiffett (1980)
5	4.5	—	6	1	1.33	McDiffett (1980)
5	1.1	—	15	1	15	McDiffett (1980)
—	—	—	—	—	—	Morris and Lewis (1988)
—	—	—	—	—	—	Morris and Lewis (1988)
—	—	—	—	—	—	Morris and Lewis (1988)
—	—	—	—	—	—	Morris and Lewis (1988)
—	—	—	—	—	—	Morris and Lewis (1988)
—	—	—	—	—	—	Morris and Lewis (1988)
—	—	—	—	—	—	Morris and Lewis (1988)
—	—	—	—	—	—	Morris and Lewis (1988)
6	5.15	1.62	3.6	0.5	2.1	Ostrofsky and Duthie (1975)
4	1	1	1.4	1	1.4	Polisini et al. (1970)
9	7	3.9	19.9	0.5	4.31	Powers et al (1972)
75	1.1	6	10.75	1	1.79	Prepas and Trimbee (1988)
33	5	2.67	7.33	1	1.47	Prepas and Trimbee (1988)
5	2	2	7.5	1	3.75	Prepas and Trimbee (1988)
23	7.94	1.59	8.23	0	—	Prepas and Trimbee (1988)
95	1.61	0.98	1.73	0	—	Priscu et al. (1982)
86	1.26	1.26	1.86	1	1.48	Sakamoto (1971)
06	1.29	0.95	2.06	1	1.6	Sakamoto (1971)
1	1.7	1.3	2.1	1	1.3	Sakamoto (1971)
—	0.98	1.02	1.06	0	—	Sakamoto (1971)
4	1.48	1.3	1.4	0	—	Sakamoto (1971)
32	2.75	0.93	2.32	0	—	Schelske et al. (1978)
28	2.28	—	2.28	0	—	Schindler et al. (1971)
.89	2.67	1.44	1.89	0	—	Schindler et al. (1971)
.8	1.2	1.8	1	6.8	3.8	Sridharan and Lee (1977)
.2	3.87	8.1	5.5	0	—	Stockner and Northcote (1974)
.07	1.12	0.82	6.07	1	4.76	Stockner and Northcote (1974)
.41	3.17	2.05	4.41	0.5	1.7	Stockner and Northcote (1974)
.62	1.2	2.36	1.62	0	—	Stockner and Northcote (1974)
.42	1.78	0.82	3.42	0.83	3.32	Stockner and Northcote (1974)
3	2.1	3.7	3	0	—	Stockner and Northcote (1974)
.9	1.51	1.23	2.65	0.47	2.5	Storch and Dietrich (1979)
.6	1.15	2.26	10.6	1	5.6	Suttle and Harrison (1988)
.55	1.15	1.25	2.31	0.42	2.28	Thurlow et al. (1975)
—	1.15	1.07	—	—	—	Wallen (1979)
.75	1.02	1.42	1.69	0.45	1.32	Whalen and Alexander (1986)
.49	2.31	1	3.49	1	1.51	Wilcox and DeCosta (1982)
.05	1.7	1.07	4.05	1	2.17	Wurtsbaugh (1988)
.55	1.22	1.71	3.55	0.5	2.75	Wurtsbaugh (1988)
.84	1.1	2.48	9.84	1	6.45	Wurtsbaugh (1988)
—	0.74	1.73	—	—	—	Wurtsbaugh and Horne (1983)

at more than one site. Spatial variation in the degree of nutrient limitation can be considerable in large systems, such as reservoirs where longitudinal differences in physical and chemical conditions arise from riverine inflow (Elser and Kimmel 1985). However, spatial variation in nutrient limitation is probably unimportant in the smaller lakes which comprise the majority of our sample. Also, it is unlikely that spatial or seasonal variation in N/P limitation introduces any systematic bias in our assessment of the frequency and degree of N and/or P limitation of algal growth in these bioassays.

On average, experimental replication was surprisingly low in these studies: the mean number of replicates per treatment was 2.31. Although the majority of studies employed manageable experimental containers (vessels less than 5 L were used in 65% of study lakes in which vessel volume was reported), in nine study lakes only a single replicate was used while in 17 lakes two replicates were used. Lack of replication precludes statistical analysis while low replication ($N=2$) weakens the ability to detect significant responses, reducing confidence in the validity of conclusions (i.e. the probability of Type II error is high). A surprisingly high percentage of studies failed to present the results of statistical analysis: 47% of all studies and 12% of studies where replicates were stated to have been used. This overall lack of statistical rigor present in this set of studies necessitated our decision to arbitrarily classify a relative response value of >1.25 as "significant" for studies which lacked statistical analyses.

NO_3 or a mixture of NO_3 and NH_4 was used as a nitrogen source in N-enrichments in 62% of the lakes. Average molar concentrations of added N and P were 46.3 μM and 2.63 μM respectively. The average molar N:P ratio was 31.1.

Responses to N and P in enrichment bioassays

Eighty-two percent of the lake studies employed a full factorial design, facilitating the separation of the effects of N and P added singly and in combination. Chlorophyll was the most common response variable, employed in 63% of the study lakes, with carbon fixation the second most common (24%). Dates on which responses were assessed or interpolated varied, with a mean value of 6.8 d (range: 1–17 d).

Data relating to the frequency and degree of algal response to N, P, and/or N + P enrichment in each lake are presented in Table 3 and an explanation of response variables is presented in Table 2. Simultaneous enrichment of N and P nearly always produced a significant growth response in these lakes: the mean value fraction of experiments in a lake which showed significant growth response to combined N + P enrichment was 0.86 (Fig. 1A). Single nutrient enrichment produced responses much less frequently: 0.47 of experiments for P vs. 0.40 for N (Fig. 1A). The mean fraction of experiments responding to N + P was higher ($P<0.05$) than both the fraction of experiments responding to N alone and the fraction of experiments responding to P alone. The mean fraction of experiments responding to P alone was not significantly different from the mean fraction of experiments responding to N alone ($P \gg 0.05$). Low frequency of detectable algal response to single nutrient enrichment relative to the combined enrichment is consistent with a view that both N and P are in relatively short supply, such that enrichment of one nutrient without the other produces only a brief growth enhancement until depletion of the other nutrient occurs. When both N and P are added, enhanced algal growth can be sustained and produce substantial and detectable responses.

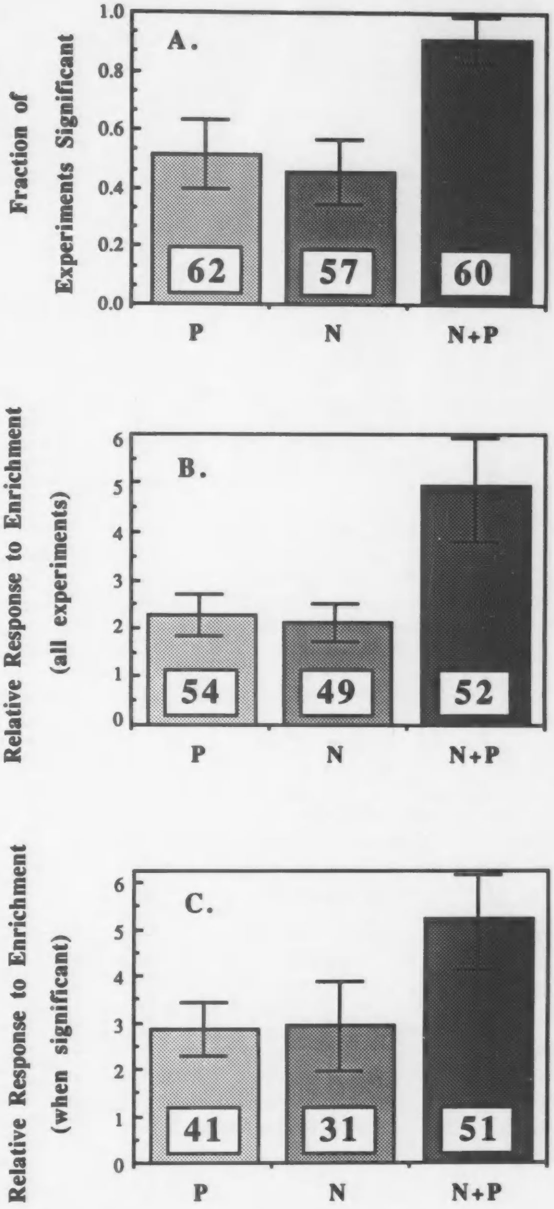

FIG. 1. Results of literature survey of studies using nutrient enrichment bioassays to study N and P limitation of algal growth. (A) Mean (over all lakes) of the frequency with which a nutrient enrichment treatment resulted in "significant" algal growth response in a given lake (columns 2–4 in Table 3). (B) Mean (over all lakes) of the relative response (ratio of treatment to control) to nutrient enrichment treatment, for all experiments in a given lake (columns 8–10 in Table 3). (C) Mean (over all lakes) of relative response to nutrient enrichment treatment, for experiments in which growth response was "significant" (columns 5–7 in Table 3). P-addition = P, N-addition = N, N + P-addition = N + P. Value on each bar indicates the number of lakes reflected in that mean. Error bars represent 95% confidence limits.

TABLE 4. Whole-lake fertilization studies included in the literature review.

Lake	Citation(s)
ELA 226SW	Schindler (1980); Fee (1979), Schindler and Fee (1974); Schindler et al. (1973)
ELA 227	Schindler (1980); Fee (1979); Schindler and Fee (1974); Schindler et al. (1973); Schindler et al. (1971)
ELA 261	Schindler (1980); Fee (1979)
ELA 303	Schindler (1980); Fee (1979)
ELA 304	Schindler (1980); Fee (1979); Schindler (1975)
Kennedy L.	Stockner and Shortreed (1988)
L. Maryjo	Smith et al. (1984)
L. Hope	Smith et al. (1984)
L. Lejeune	Smith et al. (1984)
L. Far	Welch et al. (1989)
L. Jade	Welch et al. (1989)
L. P+N	Welch et al. (1989)
Great Central L.	LeBrassuer et al. (1978)
L. Bare	Nelson and Edmondson (1955)
L. Hobitan	Hardy et al. (1986)

Combined nutrient enrichment also produced considerably stronger growth responses than enrichment by N or P alone. Mean relative growth response, measured as the ratio of the response variable in a treatment to its value in the control, to N+P enrichment was 4.61 vs. 1.97 for P and 1.79 for N when all experiments are considered (Fig. 1B). N+P response differed significantly from both single enrichment responses, which did not differ from each other. Similar patterns were observed when only experiments having significant responses were considered: 4.91 for the ratio of the N+P treatment to control, 2.54 for P, and 2.60 for N (Fig. 1C). Considerably larger growth responses occurred when N and P were added together, indicating that, while instantaneous growth may have been more limited by one nutrient or the other, total algal biomass production on these time scales was commonly limited by the availability of both N and P.

The relative importance of combined vs. single nutrient enrichment was reflected in the frequency and magnitude of synergistic effects of combined N and P enrichment. On average, combined N+P enrichment produced significantly greater growth than the higher of the single N or P treatments in 61% of the experiments. The average magnitude of this synergism was 2.95 (ratio of response variable in the N+P treatment to its values in the higher of the single N or P treatments). The frequency and magnitude of synergistic effects emphasize the interplay between N and P availability in constraining algal growth in these lakes.

These results can be compared with those of the multi-lake comparative study of potential nutrient limitation reported by Miller et al. (1974). Miller et al. employed the EPA Bottle Test (using *Selenastrum capricornatum*) and sampled 49 lakes throughout the continental United States. In contrast to our results, they found phosphorus to be stimulatory to algal growth much more frequently than nitrogen: phosphorus was limiting in 72% of the lakes sampled, while nitrogen was limiting in only 16%. While it is problematic to compare the two studies explicitly, the apparent balance between N and P limitation when assayed for the mixed phytoplankton community suggests that the mixed physiological requirements of a multi-species assemblage may closely equilibrate with the N and P supply regime of a given lake, while a single-species assay such as the EPA test primarily reflects potential imbalances between ambient nutrient availability and the specific physiological requirements of *S. capricornatum* itself. Miller et al. (1974) also reported that the frequency of N-limitation increased with increasing lake trophic status. No such trend was apparent in our data when we correlated the frequency or degree of N vs. P limitation with lake trophic status as indicated by chlorophyll concentration.

Survey of Whole-Lake Fertilizations

Twelve studies of 15 lakes met the criteria of the literature survey (Table 4). Some authors (e.g. Schindler 1980) excluded the first year of fertilization due to a lag in response following a change in nutrient loading. However, we have not excluded these years from consideration because in only one instance did a lake not respond significantly during the first year and then respond significantly in the second (Hobitan, Hardy et al. 1986). In this case, the second year was the only one of four which had a significant response. In total, 80 lake-years were included in the analysis (Table 5). The range of fertilizer molar N:P ratios was 5–35 with a year-weighted mean of 12.3.

More than 60% of the lake-years were fertilized with N+P. Of the lake-years receiving only N or P, only two lake-years were found to have higher chlorophyll content than under unfertilized conditions. Both resulted from P addition. A χ^2 test was used to assess whether the lake-year responses were distributed as would be predicted by the ratio of each treatment to the total and by the observed frequency of total significant vs. non-significant responses (Table 5). We rejected the hypothesis that the data were distributed among treatments as predicted by the treatment ratios ($P<0.001$). The largest factors contributing to the χ^2 resulted from the disproportionate distribution of N+P lake-years to significant relative to non-significant cells.

The limited number of studies involving single-nutrient fertilization and the lack of studies comparing N+P treatments to both single nutrient treatments (i.e. factorial in design) indicates that the effects of N and P on lake phytoplankton have probably not been separated adequately on the whole-lake scale. However, the whole lake data do provide support on a larger scale for the dual importance of N and P in constraining phytoplankton growth in this sample of North American lakes. Substantial algal responses to whole-lake fertilization occur consistently when both N and P are added. Only two of 31 lake-years which received only a single nutrient responded substantially. Fee (1979), in an assessment of whole-lake fertilizations at ELA, also observed that combined N and P addition produced the greatest whole-lake response and concluded that both elements were in short supply relative to phytoplankton metabolic requirements. Despite the ability of lake ecosystems to draw on atmospheric N_2 reserves, as demonstrated in the whole-lake fertilization experiments of Schindler (1977) and Persson et al. (1977), constraints on N_2 fixation may prevent sufficient ecosystem compensation in many lakes, at least over the time scales encompassed by these whole-lake fertilizations. This speculation is supported by the frequency with which significant responses to N were observed in nutrient enrichment bioassays. Fertilization with sufficiently high levels of added P may need to be sustained for longer periods of time than the periods encompassed by many of these studies in order to permit N_2-fixing blue–green algae to proliferate and increase N-inputs to the system.

TABLE 5. Distribution of lake-years among categories based on treatment and the occurrence of significant algal response. At the bottom of each category are values for the observed and expected (brackets) number of lake-years for that category, based on the observed distribution of lake-years among treatment and significance categories (see row and column totals).

	N fertilization alone	P fertilization alone	P + N fertilization	Row totals
Significant response	0 [7.17]	82 L. Maryjo (1) 76 ELA 261 (1) 2 [8.71]	72 Great Central L. (1) 69–78 ELA 227 (10) 73–78 ELA 226NE (6) 75–76 ELA 303 71–72, 75–76 ELA 304 (4) 79–81 L. P + N (3) 50–53 L. Bare (4) 81 L. Hobitan (1) L. Kennedy 78, 80–84 Clayoquot Arm (6) 80, 85 Main Arm (2) 39 [25.11]	41
No significant response	73–78 ELA 226SW (6) 73–74 ELA 304 (2) Kennedy Lake 85 Clayoquot Arm (1) 78, 81–84 Main Arm (5) 14 [6.83]	80–82 L. Hope (3) 80–81 L. Maryjo (2) 79–81 L. Fair (3) 79–82 L. Lejeune (4) 73–75 ELA 261 (3) 15 [8.29]	70–71, 73 Great Central L. (3) 79–80 L. Jade (2) 80, 82–83 L. Hobitan (3) Kennedy L. 79 Clayoquot Arm (1) 79 Main Arm (1) 10 [23.89]	39
Column totals	14	17	49	80

Conclusions and Recommendations

The summarized methodological data for nutrient enrichment bioassays presented above may serve as guidelines for investigators planning to conduct studies involving nutrient enrichment experiments. We urge experimenters to implement factorial designs which evaluate the separate and interactive roles of N and P, in addition to other nutrients, in constraining algal growth under the conditions of incubation. We also strongly suggest that greater efforts be made to characterize the seasonal and spatial variation in algal nutrient limitation, as such efforts have been limited in the past. Increased rigor in replication and reporting of statistical tests will also greatly improve the confidence which can be placed on any given experimental study. Finally, in the case of whole-lake enrichment experiments, we suggest that the roles of N and P in constraining algal growth at the ecosystem scale have not been completely separated. Important insights may yet be derived from a multi-lake approach which can overcome the substantial logistical constraints involved in separating the effects of N and P added singly from their effects when added in combination.

Little support can be found in these results for the conventional wisdom that P is the predominant primary limiting nutrient in freshwater, with N functioning largely as a secondary limiting factor in special situations. Both P and N were potentially limiting to algal growth in these lakes and considerable interaction occurred when N and P were added in combination. Increased efforts should be made by limnologists to characterize the important processes involved in both N and P fluxes in lakes. For example, phytoplankton ecologists should evaluate both N and P kinetics in studies of alga–nutrient relations in a system, while zooplankton ecologists should quantify both N-recycling and P-recycling when evaluating zooplankton nutrient regeneration in lake ecosystems. The outcome of resource-based competition between phytoplankton species is driven by relative abilities to obtain various nutrients, in addition to the relative rates at which those nutrients are supplied (Tilman 1982). Thus, a more complete understanding of the dynamics of phytoplankton seasonal succession will be enhanced by a more thorough characterization of relative availabilities of all major limiting nutrients in lake ecosystems.

Our review, however, does not imply that continued focus on P as a means of controlling and reducing lake eutrophication is unwarranted. In wastewater treatment, technological reduction of P-levels can be much easier to achieve than elimination of N (Wetzel 1983). In addition, efforts to reduce P-inputs from non-point sources will also tend to reduce N-inputs as well, as in limitations on fertilizer use within watersheds or in attempts to limit watershed disturbance and development. Finally, to the degree that some lakes can respond to N-reduction by increasing N_2-fixation, P-reduction will generally be a more reliable means to achieve lower algal standing stocks in the long term.

Acknowledgements

Partial support for the authors during this research was provided by NSF grants BSR-8705170 to C. R. Goldman and BSR-8801084 to J. J. Elser and C. R. Goldman. J. J. Elser was supported by a University of California–Davis graduate fellowship throughout. We thank the various scientists who sent preprints or otherwise assisted in the assembly of these review data. We are grateful to C. Marzolf, R. Marzolf, C. Suttle, and an anonymous reviewer for comments that improved the paper.

References

AXLER, R. P., R. M. GERSBERG, AND L. J. PAULSON. 1978. Primary productivity in meromictic Big Soda Lake, Nevada. Great Basin Nat. 38: 187–192.

EDMONDSON, W. T. 1972. Nutrients and phytoplankton in Lake Washington. p. 173–188. *In* Likens, G. E. [ed.] Nutrients and eutrophication: the limiting nutrient controversy. Allen Press, Inc., Lawrence, KS.

ELSER, J. J., M. M. ELSER, N. A. MACKAY, AND S. R. CARPENTER. 1988. Zooplankton-mediated transitions between N and P limited algal growth. Limnol. Oceanogr. 33: 1–14.

Elser, J. J., and B. L. Kimmel. 1985. Nutrient availability for phytoplankton production in a multiple-impoundment series. Can. J. Fish. Aquat. Sci. 42: 1359–1370.

1986. Alteration of phytoplankton phosphorus status during enrichment experiments: implications for interpreting nutrient enrichment bioassays. Hydrobiologia 133: 217–222.

Emery, R. M., C. E. Moon, and E. B. Welch. 1973. Enriching effects of urban runoff on the productivity of a mesotrophic lake. Water Res. 7: 1505–1516.

Environmental Protection Agency (epa), National Eutrophication Research Program. 1971. Algal assay program: bottle test.

Fee, E. J. 1979. A relation between lake morphometry and primary productivity and its use in interpreting whole-lake eutrophication experiments. Limnol. Oceanogr. 24: 401–416.

Gerhart, D. Z. 1975. Nutrient limitation in a small oligotrophic lake in New Hampshire. Verh. Internat. Ver. Limnol. 19: 1013–1022.

Glooschenko, W. A., and C. Alvis. 1973. Changes in species composition of phytoplankton due to enrichment by N, P, and Si of water from a North Florida lake. Hydrobiologia 42: 285–294.

Goldman, C. R. 1978. The use of natural phytoplankton assemblages in bioassay. Mitt. Int. Ver. Limnol. 21: 364–371.

Goldman, C. R. 1981. Lake Tahoe: two decades of change in a nitrogen-deficient oligotrophic lake. Verh. Internat. Verein. Limnol. 21: 45–70.

Goldman, C. R., and A. J. Horne. 1983. Limnology. McGraw Hill Publ. Co., New York, NY. 484 p.

Hardy, F. J., K. S. Shortreed, and J. G. Stockner. 1986. Bacterioplankton, phytoplankton, and zooplankton communities in a British Columbia coastal lake before and after nutrient reduction. Can. J. Fish. Aquat. Sci. 43: 1504–1514.

Havens, K. E., and J. DeCosta. 1984. The effects of acidification and phosphorus addition on phytoplankton biomass and productivity in a circumneutral lake receiving acid precipitation. Arch. Hydrobiol. 69: 443–476.

Healey, F. P. 1979. Short-term responses of nutrient-deficient algae to nutrient addition. J. Phycol. 15: 289–299.

Hecky, R. E., and P. Kilham. 1988. Nutrient limitation of phytoplankton in freshwater and marine environments: a review of recent evidence on the effects of enrichment. Limnol. Oceanogr. 33: 796–822.

Howarth, R. W., and J. J. Cole. 1985. Molybdenum availability, nitrogen limitation, and phytoplankton growth in natural waters. Science (Wash. DC) 229: 653–655.

Hurlbert, S. H. 1984. Pseudoreplication and the design of ecological field experiments. Ecol. Monogr. 54: 187–211.

Jordan, R. A., and M. E. Bender. 1973. Stimulation of phytoplankton growth by mixtures of phosphate, nitrate, and organic chelators. Water Res. 7: 189–195.

Lane, J. L., and C. R. Goldman. 1984. Size-fractionation of natural phytoplankton communities in nutrient bioassay studies. Hydrobiologia 118: 219–223.

Lean, D. R. S., and F. R. Pick. 1981. Photosynthetic response of lake plankton to nutrient enrichment: a test for nutrient limitation. Limnol. Oceanogr. 26: 1001–1019.

LeBrassuer, R. J., C. D. McAllister, W. E. Barraclough, O. D. Kennedy, J. Manzer, D. Robinson and K. Stephen. 1978. Enhancement of sockeye salmon (*Oncorhynchus nerka*) by lake fertilization in Great Central Lake: Summary Report. J. Fish. Res. Board Can. 35: 1580–1596.

Lehman, J. T. 1979. Physical and chemical factors affecting the seasonal abundance of *Asterionella formosa* Hass. in a small temperate lake. Arch. Hydrobiol. 87: 274–303.

Lehman, J. T., and C. D. Sandgren. 1978. Documenting a seasonal change from phosphorus to nitrogen limitation in a small temperate lake, and its impact on the population dynamics of *Asterionella*. Verh. Int. Ver. Limnol. 20: 375–380.

Lin, C. K., and C. L. Schelske. 1981. Seasonal variation of potential nutrient limitation to chlorophyll production in southern Lake Huron. Can. J. Fish. Aquat. Sci. 38: 1–9.

McDiffett, W. F. 1980. Limnological characteristics of several lakes on the Lake Wales ridge, south–central Florida. Hydrobiologia 71: 137–145.

Melack, J. M., P. Kilham, and T. R. Fisher. 1982. Responses to phytoplankton to experimental fertilization with ammonium and phosphate in an African soda lake. Oecologia 52: 321–326.

Miller, W. E., T. E. Maloney, and J. C. Greene. 1974. Algal productivity in 49 lake waters as determied by algal assays. Water Res. 8: 667–679.

Morris, D. P., and W. M. Lewis. 1988. Phytoplankton nutrient limitation in Colorado mountain lakes. Freshwater Biol. 20: 315–327.

Nelson, P. R., and W. T. Edmondson. 1955. Limnological effects of fertilizing Bare Lake, Alaska. Fishery Bulletin of the Fish and Wildlife Service. 56: 413–436.

Ostrofsky, M. L., and H. C. Duthie. 1975. Primary productivity, phytoplankton and limiting nutrient factors in Labrador lakes. Int. Rev. Gesamten Hydrobiol. 60: 145–158.

Persson, G., S. K. Holmgren, M. Jansson, A. Lundgren, B. Nyman, D. Solander, and C. Anell. 1977. Phosphorus and nitrogen and the regulation of lake ecosystems: experimental approaches in subarctic Sweden. p. 1–19. *In* Proceedings from Circumpolar Conference on Northern Ecology, Ottawa, Canada.

Pettersson, K. 1980. Alkaline phosphatase activity and algal surplus phosphorus as phosphorus-deficiency indicators in Lake Erken. Arch. Hydrobiol. 89: 54–87.

Polisini, J. M., C. E. Boyd, and B. Didgeon. 1970. Nutrient limiting factors in an oligotrophic South Carolina pond. Oikos 21: 344–347.

Powers, C. F., D. W. Schults, K. W. Malueg, R. M. Brice, and M. D. Schuldt. 1972. Algal responses to nutrient additions in natural waters. II. Field experiments. p. 141–154. *In* Likens, G. E. [ed.] Nutrients and eutrophication: the limiting nutrient controversy. Allen Press, Inc., Lawrence, KS.

Prepas, E. E., and A. M. Trimbee. 1988. Evaluation of indicators of nitrogen limitation in deep prairie lakes with laboratory bioassays and limnocorrals. Hydrobiologia 159: 269–276.

Priscu, J. C., J. Verduin, and J. E. Deacon. 1982. Primary productivity and nutrient balance in a lower Colorado River reservoir. Arch. Hydrobiol. 94: 1–23.

Sakamoto, M. 1971. Chemical factors involved in the control of phytolankton production in the Experimental Lakes Area, Northwestern Ontario. J. Fish. Res. Board Can. 28: 203–213.

Schelske, C. L., E. D. Rothman, and M. S. Simmons. 1978. Comparison of bioassay procedures for growth-limiting nutrients in the Laurentian Great Lakes. Mitt. Int. Ver. Limnol. 21: 65–80.

Schindler, D. W. 1975. Whole-lake eutrophication experiments with phosphorus, nitrogen and carbon. Verh. Int. Ver. Limnol. 19: 3221–3231.

1977. Evolution of phosphorus limitation in lakes. Science (Wash., DC) 195: 260–262.

1980. The effect of fertilization with phosphorus and nitrogen versus phosphorus alone on eutrophication of experimental lakes. Limnol. Oceanogr. 25: 1149–1152.

1988. Experimental studies of chemical stressors on whole lake ecosystems. Verh. Int. Ver. Limnol. 23: 11–41.

Schindler, D. W., F. A. J. Armstrong, S. K. Holmgren, and G. J. Brunskill. 1971. Eutrophication of Lake 227, Experimental Lakes Area, northwestern Ontario, by addition of phosphate and nitrate. J. Fish. Res. Board Can. 28: 1763–1782.

Schindler, D. W., and E. J. Fee. 1974. Experimental Lakes Area: whole-lake experiments in eutrophication. J. Fish. Res. Board Can. 31: 937–953.

Schindler, D. W., J. Kalff, H. E. Welch, G. J. Brunskill, H. Kling, and N. Kritsch. 1974. Eutrophication in the high Arctic: Meretta Lake, Cornwallis Island (75°N Lat.). J. Fish. Res. Board Can. 31: 647–662.

Schindler, D. W., H. Kling, R. V. Schmidt, J. Prokopowich, V. E. Frost, R. A. Reid, and M. Capel. 1973. Eutrophication of Lake 227 by addition of phosphate and nitrate: the second, third, and fourth years of enrichment, 1970, 1971, and 1972. J. Fish. Res. Board Canada. 30: 1415–1440.

Smith, V. H., F. H. Rigler, O. Choulik, M. Diamond, S. Griesbach, and D. Skraba. 1984. Effects of phosphorus fertilization on phytoplankton biomass and phosphorus retention in subarctic Quebec lakes. Verh. Int. Ver. Limnol. 22: 376–382.

Sridharan, N., and G. F. Lee. 1977. Algal nutrient limitation in Lake Ontario and tributary waters. Water Res. 11: 849–858.

Stockner, J. G., and T. G. Northcote. 1974. Recent limnological studies of Okanagan Basin lakes and their contribution to comprehensive water resource planning. J. Fish. Res. Board Can. 31: 955–976.

Stockner, J. G., and K. S. Shortreed. 1988. Response of *Anabaena* and *Synechococcus* to manipulation of nitrogen: phosphorus ratios in a lake fertilization experiment. Limnol. Oceanogr. 33: 1348–1361.

Storch, T. A., and G. A. Dietrich. 1979. Seasonal cycling of algal nutrient limitation in Chautauqua Lake, New York. J. Phycol. 15: 399–405.

Suttle, C. A., and P. J. Harrison. 1988. Ammonium and phosphate uptake rates, N:P supply ratios, and evidence for N and P limitation in some oligotrophic lakes. Limnol. Oceanogr. 33: 186–202.

Thurlow, D. L., R. B. Davis, and D. R. Sasseville. 1975. Primary productivity, phytoplankton populations, and nutrient bioassays in China Lake, Maine, U.S.A. Verh. Int. Ver. Limnol. 19: 1029–1036.

Tilman, D. 1982. Resource competition and community structure. Princeton, NJ. 296 p.

Vincent, W. F., W. Wurtsbaugh, C. L. Vincent, and P. J. Richerson. 1984. Seasonal dynamics of nutrient limitation in a tropical high-altitude lake (Lake Titicaca, Peru–Bolivia): application of physiological bioassays, Limnol. Oceanogr. 29: 540–552.

VOLLENWEIDER, R. A. 1976. Advances in defining critical loading levels of phosphorus in lake eutrophication. Mem. Ist. Ital. Idrobiol. 33: 53–83.

WALLEN, D. G. 1979. Nutrients limiting phytoplankton production in ice-covered Lake St. Clair. J. Great Lakes Res. 5: 91–98.

WELCH, H. E., J. A. LEGAULT, AND H. J. KLING. 1989. Phytoplankton, nutrients, and primary production in fertilized and natural lakes at Saqvaqjuac, N.W.T. Can. J. Fish. Aquat. Sci. 46: 90–107.

WETZEL, R. G. 1983. Limnology. Saunders. 767 p.

WHALEN, S. C., AND V. ALEXANDER. 1986. Chemical influences on ^{14}C and ^{15}N primary production in an Arctic Lake. Polar Biol. 5: 211–219.

WILCOX, G., AND J. DECOSTA. 1982. The effect of phosphorus and nitrogen addition on the algal biomass and species composition of an acidic lake. Arch. Hydrobiol. 94: 393–424.

WURTSBAUGH, W. A. 1988. Iron, molybdenum, and phosphorus limitation of N_2 fixation maintains nitrogen deficiency of plankton in the Great Salt Lake drainage (Utah, USA.). Verh. Int. Ver. Limnol. 23: 121–130.

WURTSBAUCH, W. A., AND A. J. HORNE. 1983. Iron in eutrophic Clear Lake, California: its importance for algal nitrogen fixation and growth. Can. J. Fish. Aquat. Sci. 40: 1419–1429.

OBITUARY/NÉCROLOGIE

Dr. W. E. (Wally) Johnson

1923–1989

The fisheries science and management community lost a dynamic personality with the sudden death at age 66 of Dr. Wally Johnson, in Vancouver, British Columbia, on September 14, 1989. Wally was unique among fisheries scientists. Those who met him never forgot him. He was alive with ideas and his energy was boundless. His accomplishments as a scientist and as an administrator will influence our science long after we are gone.

Wally was born June 10, 1923, in Osseo, Wisconsin, U.S.A. After serving in the U.S. Army from 1942 to 1946, he attended the University of Wisconsin. Under the supervision of Dr. Arthur Hasler, he completed his Ph.D. studies in 1954. He accepted in that year a U.S. National Science Foundation postdoctoral fellowship to work at the Pacific Biological Station and a year later was hired as a full time scientist. Within a few years of arriving in Nanaimo, Wally made his decision to stay in Canada and he became a Canadian citizen.

Wally was strongly influenced by the world-renowned Dr. Bill Ricker. He first met Dr. Ricker as a student and it was this meeting that attracted him to Nanaimo where Dr. Ricker worked. They became close friends as well as colleagues. Both played in the Nanaimo symphony orchestra. Wally used to delight in telling one of his favorite stories about how Dr. Ricker asked the conductor of the orchestra what instrument he needed, then went home and learned how to play it in about six months. Later in life Wally's musical talents were enjoyed by others while he extemporaneously performed with a jazz band in Hong Kong while on one of his many trips to Southeast Asia.

In the late 1950's and early 1960's Wally spent most of his time at Babine Lake on the Skeena River system studying the production of juvenile sockeye salmon. He loved his work and he loved the lake. He also had great respect and fondness for the local native Indians. Wally always expected his research would benefit both native and non-native fishermen on the Skeena. It is interesting that throughout his career this desire to apply fisheries science to management issues for the benefit of man never left him.

In 1961 he married Gerd–Elise Larsen after the field season at Babine Lake, and they promptly left for the lake the next spring to get there before the lake turned over. Gerd and Wally built a cottage at Babine and returned to it many times. The "cottage" could rival a resort in size, reflecting that Wally always did everything on a grand scale. His association with the Babine area resulted in world-class research publications that brought him an award from the American Fisheries Society, and came to fruition in a ten million dollar project aimed at increasing sockeye salmon production through use of manmade spawning channels.

During the days at Babine, Wally developed a fondness for hunting. He would hike up into the mountains to seek mountain goats and prowl the lowlands around the lake for moose. On one occasion while cruising down the lake in the company of Dr. A. W. (Alf) Needler, a former Director of the Pacific Biological Station and Deputy Minister of Fisheries for Canada, a moose was spotted on the shoreline. Both Wally and Alf raised their rifles and fired simultaneously. The argument was never settled as to whose bullet felled the moose.

It was only a matter of time before a person of Wally's calibre would be asked to become involved in research management.

He was never afraid to express his views on science, on management, or any other topic even if they were contrary to accepted opinion. He was a man of wit and vision and never afraid of taking risks.

Early in 1965 he was called to Ottawa to assist the former Fisheries Research Board with the planning of a new freshwater fisheries research institute. There is little doubt that the clarity of his thinking and his pragmatic approach to science greatly contributed to the establishment of the Freshwater Institute in Winnipeg. As its first Director, Wally had total freedom to recruit the research staff, an opportunity he used to the full. Later in his career he liked to remind over zealous bureaucrats of these marvelous times, when things were readily accomplished without the benefit of their ministrations.

A number of scientists now in the Canada Department of Fisheries and Oceans was hired either directly or indirectly as a result of the establishment of the Freshwater Institute. As always, Wally shot for the stars. He wanted the best people he could find and he got them, whether from North America or abroad. Wally had that rare gift of getting people to do just about anything he asked of them. A combination of respect and charm or, if that didn't work, a good joke and a drink of scotch had you working evenings and weekends. The Institute's staff was stimulated by him and the formative years of the Institute were times of great excitement.

The lure of the west coast was, however, never stilled. Wally accepted the directorship of the Pacific Biological Station in 1973. Twenty-four years after his first visit, he was back, married with three children.

In addition to being a Director of two of Canada's prominent fisheries and aquatic sciences research laboratories, Wally was deeply involved with a CIDA (Canadian International Development Agency) project in Thailand. He was responsible for the establishment and construction of the National Inland Fisheries Institute in Bangkok and became influential in many aspects of fisheries development in that country. He was revered by the Thais. For his assistance and contributions in fisheries research and development, he received from the King of Thailand the highest civilian award available to a foreigner. Recently, the library at the Inland Fisheries Institute in Bangkok was named the *W. E. Johnson Library*.

Wally moved from Director of the Pacific Biological Station to Director General of the Pacific Region after four years. It was a turbulent time in the late 1970's and Wally met the challenges head-on. The extension of coastal states' fisheries jurisdiction, the salmon enhancement program, declining salmon stocks, and a herring fishery that seemed headed for disaster were some of the major issues to confront Wally in his new post. Wally made decisions. He provided direction. Staff and fishermen knew that if he gave you his word "you could take it to the bank." As Director General the challenges took their toll and in 1980 Wally accepted an Order-in-Council appointment to become the first head of FORAC (Fisheries and Oceans Research Advisory Council). Reporting directly to the Minister, he formed a council of the best fisheries advisors in the country. The council provided recommendations to the Minister of Fisheries and Oceans similar to the function of the old Fisheries Research Board but without its independence. Wally was a particular favourite of the Minister of Fisheries, again, because of his experience and his incisive logic.

Wally retired in 1985 and subsequently accepted a position as a contractor to coordinate the Northern Fisheries Project in Thailand, his second home. Forced by an illness to return home after two years, Wally was at once appointed as the Canadian member of the first Canadian-U.S. Free Trade Panel, dealing with the controversial Canadian landing requirement for Pacific coast salmon and herring.

Before the Panel finished its work and with Wally already planning his return to Thailand, he died of a heart attack while strolling in his garden as he loved to do.

In all his tasks Wally has been an intrepid scientific leader in a field where much controversy prevails. In his private life he was a devoted parent and husband. To those who knew him only professionally it might come as a surprise to learn that he was an accomplished handyman, able to fix plumbing or set his hands at any small but necessary task at home. He designed his house in Nanaimo, he was an accomplished musician, a basketball player, a passionate gardener, and a person with whom you could easily converse. For his contributions to fisheries in Canada and abroad, he was awarded the Order of Canada in 1988.

Our Department and our Government will miss Dr. Johnson, and his contributions to fisheries in Canada will long be valued. It is rare to find someone of such vitality. All who knew Wally will remember him with great fondness.

R. J. Beamish
and
L. Margolis
Biological Sciences Branch
Pacific Biological Station
Nanaimo, B.C.

ANNOUNCEMENTS/AVIS

Canadian Conference for Fisheries Research (CCFFR)

University of Guelph
Guelph, Ontario
January 3–4, 1991

Announcement of Conference
and Call for Papers

This conference will be held in Guelph, Ontario, January 3 and 4, 1991.

The major themes of the conference will be:

1. **Biodiversity at or Below the Species Level**

   (Convenors: Moira Ferguson, John Leatherland, and Glen van der Kraak)

   Topics:

   a) Biodiversity at the species level: disappearing taxa or the fate of non-exploited fishes;

   b) Quantifying biodiversity below the species level: stock identification, stock definition, etc.;

   c) Maintaining biodiversity: technology used for gene bank development, value of gene banks, hatchery breeding programmes;

   d) Increasing biodiversity: stock choice, habitat restoration;

   e) Decreasing biodiversity: effect of stock transplantation, effect on endemics, etc.;

   f) Manipulating biodiversity: use of triploids, sex manipulation, transgenic studies, etc.

2. Sustainable Fisheries

(Convenors: W. Jack Christie, David L. G. Noakes)

Topics:

a) Sustainable by and to whom? Assessing costs and benefits;

b) Environmentally sustainable fisheries;

c) Politically sustainable fisheries; and

d) Economically sustainable fisheries.

Conférence Canadienne sur la recherche sur les pêches (CCRP)

Université de Guelph
Guelph, Ontario
les 3 et 4 janvier 1991

Avis de conférence et
demande d'articles

Cette conférence aura lieu les 3 et 4 janvier 1991 à Guelph, Ontario.

La conférence portera sur les principaux thèmes suivants :

1. **La biodiversité au niveau de l'espèce ou de la sous-espèce**

   (Responsables : Moira Ferguson, John Leatherland et Glen van der Kraak)

   Sujets :

   a) La biodiversité au niveau spécifique : les taxons en disparition ou le destin des espèces non exploitées;

   b) La quantification de la biodiversité au niveau infra-spécifique : l'identification des stocks, la définition d'un stock, etc.;

   c) La conservation de la biodiversité : les techniques utilisées pour la création de la banque de gènes, la valeur de ces banques, les programmes de reproduction en écloserie;

   d) L'augmentation de la biodiversité : le choix de stock, la restauration des habitats;

   e) La réduction de la biodiversité : l'incidence de la transplantation de stock, l'incidence sur les espèces endémiques, etc.;

   f) La manipulation de la biodiversité : l'utilisation d'individus triploïdes, la manipulation génétique, les études transgéniques, etc.

2. Rendement des pêches à l'équilibre

(Responsables : W. Jack Christie, David L. G. Noakes)

Sujets :

a) Qui en sera responsable et qui en bénéficiera? Une évaluation des coûts et des avantages;

b) Des pêches viables au niveau environnemental;

c) Des pêches viables au niveau politique;

d) Des pêches viables au niveau économique.

While papers on other themes may be submitted, authors are encouraged to adhere to the above themes as much as possible.

Deadline for abstracts is August 30, 1990. They should be typed (maximum 200 words, single spaced) and nature of presentation (oral/poster) indicated. A high quality of copy is required, suitable for photographic reproduction.

Abstracts should be addressed to:
Dr. Eugene K. Balon
Department of Zoology
University of Guelph
Guelph, Ontario N1G 2W1
Tel. (519) 824-4120, ext. 3978

New Perspectives for Watershed Management: Balancing Long-Term Sustainability with Cumulative Environmental Change

November 27–29, 1990

University of Washington campus, Seattle, WA

Sponsored by the Center for Streamside Studies, University of Washington and the College of Forestry, Oregon State University. Contact: *Continuing Education, College of Forest Resources, AR-10, University of Washington, Seattle, WA 98195 (206)543-0867.*

Posters are solicited for topics related to the research and management activities of watershed management issues, including range utilisation, urbanization, old growth harvest, maintenance of biodiversity, and long-term productivity of agricultural and forested lands. Submit two copies of a 200-word abstract, by September 1, 1990, to *George Ice, Technical Poster Coordinator, NCASI, P.O. Box 458, Corvallis, OR 97339.*

On peut présenter des études sur d'autres thèmes quoiqu'on encourage les chercheurs à s'en tenir autant que possible aux thèmes susmentionnés.

La date limite d'envoi de résumés a été fixée au 30 août 1990. La résumé doit être dactylographié (200 mots au maximum, simple interligne) et l'on doit préciser le genre de présentation) présentation orale/affiche). Une copie de très bonne qualité est requise pour faciliter la reproduction photographique.

Veuillez faire parvenir votre résumé à :
Dr Eugene K. Balon
Département de Zoologie
Université de Guelph
Guelph (Ontario) N1G 2W1
Tel. (519) 824-4120, poste 3978

New Perspectives for Watershed Management : Balancing Long-Term Sustainability with Cumulative Environmental Change

Du 27 au 29 novembre 1990,
campus de l'université de Washington, Seattle, WA.

Parrainé par le Center for Streamside Studies de l'université de Washington et le college of Forestry de l'université d'État de l'Orégon. Pour renseignements : *Continuing Education, College of Forest Resources, AR-10, University of Washington, Seattle, WA 98195 (206) 543-0867.*

Des affiches sont demandées pour des travaux de recherche et de gestion ayant trait à la gestion des bassins versants et comprenant notamment l'utilisation des terres, l'urbanisation, la récolte des peuplements âgés, le maintien de la biodiversité et la productivité à long terme des terres agricoles et boisées. Deux exemplaires d'un résumé de 200 mots doivent être présentés, avant le 1er septembre 1990, à *George Ice, Technical Poster Coordinator, NCASI, P.O. Box 458, Corvallis, OR 97339.*

Hydrobiologia

Editor-in-Chief

H.J. Dumont, *Ghent, Belgium*

Hydrobiologia publishes original articles in the fields of fundamental limnology and marine biology.
A wide range of papers are published, including ecology, physiology, biogeography, methodology and taxonomy. Applied (technological) papers are also published, provided they are of general interest and not solely technical in nature. Occasional very long papers and reviews are published at the invitation of the Editors, as are the proceedings of relevant, specialized symposia.

Subscription Information
ISSN 0018–8158
1990, Volumes 185–205 (63 issues)
Subscription rate: Dfl. 5691.00/
US$2656.50 *incl. postage/handling*

Subscribers also receive the issues of the **Journal of Applied Phycology** included in their subscription.

P.O. Box 322, 3300 AH Dordrecht, The Netherlands
P.O. Box 358, Accord Station, Hingham, MA 02018-0358, U.S.A.

Journal Highlight

KLUWER ACADEMIC PUBLISHERS

Reviews/Synthèses

Elser, J. J., E. R. Marzolf, and C. R. Goldman. Phosphorus and nitrogen limitation of phytoplankton growth in the freshwaters of North America: a review and critique of experimental enrichments **1468–1477**

Obituary/Nécrologie

Beamish, R. J., and L. Margolis. W. E. (Wally) Johnson, 1923–1989 **1478–1479**

Announcements/Avis **1480–1481**

Canadian Journal of Fisheries and Aquatic Sciences

Journal canadien des sciences halieutiques et aquatiques

Volume 47, No. 7, July 1990

Volume 47, nº 7, juillet 1990

Li, W. K. W. Particles in "particle-free" seawater: growth of ultraphytoplankton and implications for dilution experiments **1258–1268**

Dillon, P. J., R. D. Evans, and L. A. Molot. Retention and resuspension of phosphorus, nitrogen, and iron in a central Ontario Lake **1269–1274**

Shields, J. D., R. K. Okazaki, and A. M. Kuris. Brood mortality and egg predation by the nemertean, *Carcinonemertes epialti,* on the yellow rock crab, *Cancer anthonyi,* in southern California **1275–1281**

Jolly, G. M., and I. Hampton. A stratified random transect design for acoustic surveys of fish stocks **1282–1291**

Danzmann, R. G., G. J. Van Der Kraak, T. T. Chen, and D. A. Powers. Metabolic effects of bovine growth hormone and genetically engineered rainbow trout growth hormone in rainbow trout (*Oncorhynchus mykiss*) reared at a high temperature **1292–1301**

Bernard, F. R., and D. J. Noakes. Pumping rates, water pressures, and oxygen use in eight species of marine bivalve molluscs from British Columbia **1302–1306**

Stevens, B. G. Temperature-dependent growth of juvenile red king crab (*Paralithodes camtschatica*), and its effects on size-at-age and subsequent recruitment in the eastern Bering Sea **1307–1317**

Smith, M. E., B. J. Wyskowski, C. M. Brooks, C. T. Driscoll, and C. C. Cosentini. Relationships between acidity and benthic invertebrates of low-order woodland streams in the Adirondack Mountains, New York **1318–1329**

Phillips, B. F. Estimating the density and mortality of juvenile western rock lobsters (*Panulirus cygnus*) in nursery reefs **1330–1338**

Silver, P. A., and J. S. Hamer. Use of extant populations of scaled chrysophytes for the inference of lakewater pH **1339–1347**

Smith, R. E. H., W. G. Harrison, L. R. Harris, and A. W. Herman. Vertical fine structure of particulate matter and nutrients in sea ice of the high arctic **1348–1355**

Crawford, W. R., A. V. Tyler, and R. E. Thomson. A possible eddy retention mechanism for ichthyoplankton in Hecate Strait **1356–1363**

Ardisson, P.-L., E. Bourget, and P. Legendre. Multivariate approach to study species assemblages at large spatiotemporal scales: the community structure of the epibenthic fauna of the Estuary and Gulf of St. Lawrence **1364–1377**

Findlay, D. L., and S. E. M. Kasian. Phytoplankton communities of lakes experimentally acidified with sulfuric and nitric acids **1378–1386**

Kreutzweiser, D. P. Response of a brook trout (*Salvelinus fontinalis*) population to a reduction in stream benthos following an insecticide treatment **1387–1401**

Cota, G. F., J. L. Anning, L. R. Harris, W. G. Harrison, and R. E. H. Smith. Impact of ice algae on inorganic nutrients in seawater and sea ice in Barrow Strait, NWT, Canada, during spring **1402–1415**

Cerrato, R. M. Interpretable statistical tests for growth comparisons using parameters in the von Bertalanffy equation **1416–1426**

Dunstall, T. G., D. W. Lawler, R. Farooqui, and G. T. Haymes. Variation in lake water temperature in the Nanticoke region of Long Point Bay, Lake Erie, during the open-water season **1427–1433**

Dunstall, T. G., J. C. H. Carter, B. P. Monroe, G. T. Haymes, R. R. Weller, and G. J. Hopkins. Influence of upwellings, storms, and generating station operation on water chemistry and plankton in the Nanticoke region of Long Point Bay, Lake Erie **1434–1445**

Wilkinson, K. J., P. G. C. Campbell, and P. Couture. Effect of fluoride complexation on aluminum toxicity towards juvenile Atlantic salmon (*Salmo salar*) **1446–1452**

Schnute, J. T., T. J. Mulligan, and B. R. Kuhn. An errors-in-variables bias model with an application to salmon hatchery data **1453–1467**

(Continued)

© Minister of Supply and Services Canada 1990
Ministre des Approvisionnements et Services Canada 1990

CJFSDX47(7) 1258–1481 (1990)
ISSN 0706-652X

Subscription rates/Abonnements

Canada: Institutional/Collectif $200; Personal/Personnel $75
Other countries/Autres pays : Institutional/Collectif $240; Personal/Personnel $90
Single issue/Par numéro : $13.95 (Canada); $16.75 (Other countries/Autres pays)